HANDBOOK ON PHYSICAL PROPERTIES OF SEMICONDUCTORS

Volume 3

II-VI Compound Semiconductors

Edited by
Sadao Adachi

HANDBOOK ON PHYSICAL PROPERTIES OF SEMICONDUCTORS

VOLUME 3

II-VI Compound Semiconductors

HANDBOOK ON PHYSICAL PROPERTIES OF SEMICONDUCTORS

VOLUME 3

II-VI Compound Semiconductors

Sadao Adachi
Department of Electronic Engineering
Gunma University
Kiryu-shi, Gunma 376-8515
Japan

KLUWER ACADEMIC PUBLISHERS
NEW YORK, BOSTON, DORDRECHT, LONDON, MOSCOW

eBook ISBN: 1-4020-7821-8
Print ISBN: 1-4020-7820-X

©2004 Kluwer Academic Publishers
New York, Boston, Dordrecht, London, Moscow

Print ©2004 Kluwer Academic Publishers
Boston

All rights reserved

No part of this eBook may be reproduced or transmitted in any form or by any means, electronic, mechanical, recording, or otherwise, without written consent from the Publisher

Created in the United States of America

Visit Kluwer Online at: http://kluweronline.com
and Kluwer's eBookstore at: http://ebooks.kluweronline.com

To

Kōya

CONTENTS

Preface xxxiii

Acknowledgments xxxv

Contents of Other Volumes xxxvii

1 Magnesium Oxide (MgO) 1

1.1 Structural Properties / 1
1.1.1 Ionicity / 1
1.1.2 Elemental Isotopic Abundance and Molecular Weight / 1
1.1.3 Crystal Structure and Space Group / 2
1.1.4 Lattice Constant and Its Related Parameters / 2
1.1.5 Structural Phase Transition / 2
1.1.6 Cleavage Plane / 3
1.2 Thermal Properties / 3
1.2.1 Melting Point and Its Related Parameters / 3
1.2.2 Specific Heat / 4
1.2.3 Debye Temperature / 5
1.2.4 Thermal Expansion Coefficient / 6
1.2.5 Thermal Conductivity and Diffusivity / 6
1.3 Elastic Properties / 7
1.3.1 Elastic Constant / 7
1.3.2 Third-Order Elastic Constant / 9

1.3.3 Young's Modulus, Poisson's Ratio, and Similar / 9
1.3.4 Microhardness / 10
1.3.5 Sound Velocity / 10
1.4 Phonons and Lattice Vibronic Properties / 11
1.4.1 Phonon Dispersion Relation / 11
1.4.2 Phonon Frequency / 12
1.4.3 Mode Grüneisen Parameter / 13
1.4.4 Phonon Deformation Potential / 13
1.5 Collective Effects and Related Properties / 13
1.5.1 Piezoelectric Constant / 13
1.5.2 Fröhlich Coupling Constant / 13
1.6 Energy-Band Structure: Energy-Band Gaps / 13
1.6.1 Basic Properties / 13
1.6.2 E_0-Gap Region / 15
1.6.3 Higher-Lying Direct Gap / 15
1.6.4 Lowest Indirect Gap / 16
1.6.5 Conduction-Valley Energy Separation / 16
1.6.6 Direct–Indirect-Gap Transition Pressure / 16
1.7 Energy-Band Structure: Electron and Hole Effective Masses / 17
1.7.1 Electron Effective Mass: Γ Valley / 17
1.7.2 Electron Effective Mass: Satellite Valley / 17
1.7.3 Hole Effective Mass / 17
1.8 Electronic Deformation Potential / 17
1.8.1 Intravalley Deformation Potential: Γ Point / 17
1.8.2 Intravalley Deformation Potential: High-Symmetry Points / 17
1.8.3 Intervalley Deformation Potential / 17
1.9 Electron Affinity and Schottky Barrier Height / 18
1.9.1 Electron Affinity / 18
1.9.2 Schottky Barrier Height / 18
1.10 Optical Properties / 18
1.10.1 Summary of Optical Dispersion Relations / 18
1.10.2 The Reststrahlen Region / 19
1.10.3 At or Near the Fundamental Absorption Edge / 20
1.10.4 The Interband Transition Region / 22
1.10.5 Free-Carrier Absorption and Related Phenomena / 22
1.11 Elastooptic, Electrooptic, and Nonlinear Optical Properties / 22
1.11.1 Elastooptic Effect / 22
1.11.2 Linear Electrooptic Constant / 23
1.11.3 Quadratic Electrooptic Constant / 23
1.11.4 Franz–Keldysh Effect / 23
1.11.5 Nonlinear Optical Constant / 23
1.12 Carrier Transport Properties / 23
1.12.1 Low-Field Mobility: Electrons / 23
1.12.2 Low-Field Mobility: Holes / 23
1.12.3 High-Field Transport: Electrons / 23
1.12.4 High-Field Transport: Holes / 23
1.12.5 Minority-Carrier Transport: Electrons in *p*-Type Materials / 23
1.12.6 Minority-Carrier Transport: Holes in *n*-Type Materials / 23

1.12.7 Impact Ionization Coefficient / 24

2 Zincblende Magnesium Sulphide (β-MgS) 25

2.1 Structural Properties / 25
2.1.1 Ionicity / 25
2.1.2 Elemental Isotopic Abundance and Molecular Weight / 25
2.1.3 Crystal Structure and Space Group / 26
2.1.4 Lattice Constant and Its Related Parameters / 26
2.1.5 Structural Phase Transition / 27
2.1.6 Cleavage Plane / 27
2.2 Thermal Properties / 27
2.2.1 Melting Point and Its Related Parameters / 27
2.2.2 Specific Heat / 27
2.2.3 Debye Temperature / 27
2.2.4 Thermal Expansion Coefficient / 27
2.2.5 Thermal Conductivity and Diffusivity / 27
2.3 Elastic Properties / 28
2.3.1 Elastic Constant / 28
2.3.2 Third-Order Elastic Constant / 28
2.3.3 Young's Modulus, Poisson's Ratio, and Similar / 28
2.3.4 Microhardness / 29
2.3.5 Sound Velocity / 29
2.4 Phonons and Lattice Vibronic Properties / 30
2.4.1 Phonon Dispersion Relation / 30
2.4.2 Phonon Frequency / 30
2.4.3 Mode Grüneisen Parameter / 30
2.4.4 Phonon Deformation Potential / 30
2.5 Collective Effects and Related Properties / 30
2.5.1 Piezoelectric Constant / 30
2.5.2 Fröhlich Coupling Constant / 30
2.6 Energy-Band Structure: Energy-Band Gaps / 31
2.6.1 Basic Properties / 31
2.6.2 E_0-Gap Region / 31
2.6.3 Higher-Lying Direct Gap / 32
2.6.4 Lowest Indirect Gap / 32
2.6.5 Conduction-Valley Energy Separation / 32
2.6.6 Direct–Indirect-Gap Transition Pressure / 32
2.7 Energy-Band Structure: Electron and Hole Effective Masses / 32
2.7.1 Electron Effective Mass: Γ Valley / 32
2.7.2 Electron Effective Mass: Satellite Valley / 33
2.7.3 Hole Effective Mass / 33
2.8 Electronic Deformation Potential / 34
2.8.1 Intravalley Deformation Potential: Γ Point / 34
2.8.2 Intravalley Deformation Potential: High-Symmetry Points / 34
2.8.3 Intervalley Deformation Potential / 34
2.9 Electron Affinity and Schottky Barrier Height / 34
2.9.1 Electron Affinity / 34
2.9.2 Schottky Barrier Height / 35

2.10 Optical Properties / 35
2.10.1 Summary of Optical Dispersion Relations / 35
2.10.2 The Reststrahlen Region / 35
2.10.3 At or Near the Fundamental Absorption Edge / 35
2.10.4 The Interband Transition Region / 35
2.10.5 Free-Carrier Absorption and Related Phenomena / 35
2.11 Elastooptic, Electrooptic, and Nonlinear Optical Properties / 35
2.11.1 Elastooptic Effect / 35
2.11.2 Linear Electrooptic Constant / 35
2.11.3 Quadratic Electrooptic Constant / 35
2.11.4 Franz–Keldysh Effect / 35
2.11.5 Nonlinear Optical Constant / 35
2.12 Carrier Transport Properties / 36
2.12.1 Low-Field Mobility: Electrons / 36
2.12.2 Low-Field Mobility: Holes / 36
2.12.3 High-Field Transport: Electrons / 36
2.12.4 High-Field Transport: Holes / 36
2.12.5 Minority-Carrier Transport: Electrons in *p*-Type Materials / 36
2.12.6 Minority-Carrier Transport: Holes in *n*-Type Materials / 36
2.12.7 Impact Ionization Coefficient / 36

3 Zincblende Magnesium Selenide (β-MgSe) 37

3.1 Structural Properties / 37
3.1.1 Ionicity / 37
3.1.2 Elemental Isotopic Abundance and Molecular Weight / 37
3.1.3 Crystal Structure and Space Group / 38
3.1.4 Lattice Constant and Its Related Parameters / 38
3.1.5 Structural Phase Transition / 39
3.1.6 Cleavage Plane / 39
3.2 Thermal Properties / 39
3.2.1 Melting Point and Its Related Parameters / 39
3.2.2 Specific Heat / 39
3.2.3 Debye Temperature / 39
3.2.4 Thermal Expansion Coefficient / 39
3.2.5 Thermal Conductivity and Diffusivity / 39
3.3 Elastic Properties / 40
3.3.1 Elastic Constant / 40
3.3.2 Third-Order Elastic Constant / 40
3.3.3 Young's Modulus, Poisson's Ratio, and Similar / 40
3.3.4 Microhardness / 41
3.3.5 Sound Velocity / 41
3.4 Phonons and Lattice Vibronic Properties / 42
3.4.1 Phonon Dispersion Relation / 42
3.4.2 Phonon Frequency / 42
3.4.3 Mode Grüneisen Parameter / 42
3.4.4 Phonon Deformation Potential / 42
3.5 Collective Effects and Related Properties / 43
3.5.1 Piezoelectric Constant / 43

3.5.2 Fröhlich Coupling Constant / 43
3.6 Energy-Band Structure: Energy-Band Gaps / 43
3.6.1 Basic Properties / 43
3.6.2 E_0-Gap Region / 44
3.6.3 Higher-Lying Direct Gap / 45
3.6.4 Lowest Indirect Gap / 45
3.6.5 Conduction-Valley Energy Separation / 45
3.6.6 Direct–Indirect-Gap Transition Pressure / 45
3.7 Energy-Band Structure: Electron and Hole Effective Masses / 45
3.7.1 Electron Effective Mass: Γ Valley / 45
3.7.2 Electron Effective Mass: Satellite Valley / 46
3.7.3 Hole Effective Mass / 46
3.8 Electronic Deformation Potential / 47
3.8.1 Intravalley Deformation Potential: Γ Point / 47
3.8.2 Intravalley Deformation Potential: High-Symmetry Points / 48
3.8.3 Intervalley Deformation Potential / 48
3.9 Electron Affinity and Schottky Barrier Height / 48
3.9.1 Electron Affinity / 48
3.9.2 Schottky Barrier Height / 48
3.10 Optical Properties / 48
3.10.1 Summary of Optical Dispersion Relations / 48
3.10.2 The Reststrahlen Region / 48
3.10.3 At or Near the Fundamental Absorption Edge / 48
3.10.4 The Interband Transition Region / 49
3.10.5 Free-Carrier Absorption and Related Phenomena / 49
3.11 Elastooptic, Electrooptic, and Nonlinear Optical Properties / 49
3.11.1 Elastooptic Effect / 49
3.11.2 Linear Electrooptic Constant / 49
3.11.3 Quadratic Electrooptic Constant / 49
3.11.4 Franz–Keldysh Effect / 49
3.11.5 Nonlinear Optical Constant / 50
3.12 Carrier Transport Properties / 50
3.12.1 Low-Field Mobility: Electrons / 50
3.12.2 Low-Field Mobility: Holes / 50
3.12.3 High-Field Transport: Electrons / 50
3.12.4 High-Field Transport: Holes / 50
3.12.5 Minority-Carrier Transport: Electrons in *p*-Type Materials / 50
3.12.6 Minority-Carrier Transport: Holes in *n*-Type Materials / 50
3.12.7 Impact Ionization Coefficient / 50

4 Zincblende Magnesium Telluride (β-MgTe) 51

4.1 Structural Properties / 51
4.1.1 Ionicity / 51
4.1.2 Elemental Isotopic Abundance and Molecular Weight / 51
4.1.3 Crystal Structure and Space Group / 52
4.1.4 Lattice Constant and Its Related Parameters / 52
4.1.5 Structural Phase Transition / 53
4.1.6 Cleavage Plane / 53

4.2 Thermal Properties / 53
4.2.1 Melting Point and Its Related Parameters / 53
4.2.2 Specific Heat / 53
4.2.3 Debye Temperature / 53
4.2.4 Thermal Expansion Coefficient / 53
4.2.5 Thermal Conductivity and Diffusivity / 53
4.3 Elastic Properties / 54
4.3.1 Elastic Constant / 54
4.3.2 Third-Order Elastic Constant / 54
4.3.3 Young's Modulus, Poisson's Ratio, and Similar / 54
4.3.4 Microhardness / 55
4.3.5 Sound Velocity / 55
4.4 Phonons and Lattice Vibronic Properties / 56
4.4.1 Phonon Dispersion Relation / 56
4.4.2 Phonon Frequency / 56
4.4.3 Mode Grüneisen Parameter / 56
4.4.4 Phonon Deformation Potential / 56
4.5 Collective Effects and Related Properties / 56
4.5.1 Piezoelectric Constant / 56
4.5.2 Fröhlich Coupling Constant / 56
4.6 Energy-Band Structure: Energy-Band Gaps / 57
4.6.1 Basic Properties / 57
4.6.2 E_0-Gap Region / 58
4.6.3 Higher-Lying Direct Gap / 59
4.6.4 Lowest Indirect Gap / 59
4.6.5 Conduction-Valley Energy Separation / 59
4.6.6 Direct–Indirect-Gap Transition Pressure / 59
4.7 Energy-Band Structure: Electron and Hole Effective Masses / 60
4.7.1 Electron Effective Mass: Γ Valley / 60
4.7.2 Electron Effective Mass: Satellite Valley / 60
4.7.3 Hole Effective Mass / 60
4.8 Electronic Deformation Potential / 61
4.8.1 Intravalley Deformation Potential: Γ Point / 61
4.8.2 Intravalley Deformation Potential: High-Symmetry Points / 61
4.8.3 Intervalley Deformation Potential / 61
4.9 Electron Affinity and Schottky Barrier Height / 61
4.9.1 Electron Affinity / 61
4.9.2 Schottky Barrier Height / 62
4.10 Optical Properties / 62
4.10.1 Summary of Optical Dispersion Relations / 62
4.10.2 The Reststrahlen Region / 62
4.10.3 At or Near the Fundamental Absorption Edge / 62
4.10.4 The Interband Transition Region / 63
4.10.5 Free-Carrier Absorption and Related Phenomena / 63
4.11 Elastooptic, Electrooptic, and Nonlinear Optical Properties / 63
4.11.1 Elastooptic Effect / 63
4.11.2 Linear Electrooptic Constant / 63
4.11.3 Quadratic Electrooptic Constant / 63

4.11.4 Franz–Keldysh Effect / 63
4.11.5 Nonlinear Optical Constant / 63
4.12 Carrier Transport Properties / 63
4.12.1 Low-Field Mobility: Electrons / 63
4.12.2 Low-Field Mobility: Holes / 63
4.12.3 High-Field Transport: Electrons / 64
4.12.4 High-Field Transport: Holes / 64
4.12.5 Minority-Carrier Transport: Electrons in *p*-Type Materials / 64
4.12.6 Minority-Carrier Transport: Holes in *n*-Type Materials / 64
4.12.7 Impact Ionization Coefficient / 64

5 Zinc Oxide (ZnO) 65

5.1 Structural Properties / 65
5.1.1 Ionicity / 65
5.1.2 Elemental Isotopic Abundance and Molecular Weight / 65
5.1.3 Crystal Structure and Space Group / 66
5.1.4 Lattice Constant and Its Related Parameters / 66
5.1.5 Structural Phase Transition / 66
5.1.6 Cleavage Plane / 67
5.2 Thermal Properties / 67
5.2.1 Melting Point and Its Related Parameters / 67
5.2.2 Specific Heat / 68
5.2.3 Debye Temperature / 68
5.2.4 Thermal Expansion Coefficient / 68
5.2.5 Thermal Conductivity and Diffusivity / 69
5.3 Elastic Properties / 71
5.3.1 Elastic Constant / 71
5.3.2 Third-Order Elastic Constant / 72
5.3.3 Young's Modulus, Poisson's Ratio, and Similar / 72
5.3.4 Microhardness / 73
5.3.5 Sound Velocity / 73
5.4 Phonons and Lattice Vibronic Properties / 73
5.4.1 Phonon Dispersion Relation / 73
5.4.2 Phonon Frequency / 74
5.4.3 Mode Grüneisen Parameter / 74
5.4.4 Phonon Deformation Potential / 75
5.5 Collective Effects and Related Properties / 75
5.5.1 Piezoelectric Constant / 75
5.5.2 Fröhlich Coupling Constant / 75
5.6 Energy-Band Structure: Energy-Band Gaps / 76
5.6.1 Basic Properties / 76
5.6.2 E_0-Gap Region / 77
5.6.3 Higher-Lying Direct Gap / 81
5.6.4 Lowest Indirect Gap / 81
5.6.5 Conduction-Valley Energy Separation / 82
5.6.6 Direct–Indirect-Gap Transition Pressure / 82
5.7 Energy-Band Structure: Electron and Hole Effective Masses / 82
5.7.1 Electron Effective Mass: Γ Valley / 82

5.7.2 Electron Effective Mass: Satellite Valley / 83
5.7.3 Hole Effective Mass / 83
5.8 Electronic Deformation Potential / 84
5.8.1 Intravalley Deformation Potential: Γ Point / 84
5.8.2 Intravalley Deformation Potential: High-Symmetry Points / 84
5.8.3 Intervalley Deformation Potential / 84
5.9 Electron Affinity and Schottky Barrier Height / 85
5.9.1 Electron Affinity / 85
5.9.2 Schottky Barrier Height / 85
5.10 Optical Properties / 86
5.10.1 Summary of Optical Dispersion Relations / 86
5.10.2 The Reststrahlen Region / 87
5.10.3 At or Near the Fundamental Absorption Edge / 88
5.10.4 The Interband Transition Region / 91
5.10.5 Free-Carrier Absorption and Related Phenomena / 92
5.11 Elastooptic, Electrooptic, and Nonlinear Optical Properties / 92
5.11.1 Elastooptic Effect / 92
5.11.2 Linear Electrooptic Constant / 93
5.11.3 Quadratic Electrooptic Constant / 93
5.11.4 Franz–Keldysh Effect / 94
5.11.5 Nonlinear Optical Constant / 94
5.12 Carrier Transport Properties / 95
5.12.1 Low-Field Mobility: Electrons / 95
5.12.2 Low-Field Mobility: Holes / 97
5.12.3 High-Field Transport: Electrons / 97
5.12.4 High-Field Transport: Holes / 97
5.12.5 Minority-Carrier Transport: Electrons in *p*-Type Materials / 97
5.12.6 Minority-Carrier Transport: Holes in *n*-Type Materials / 97
5.12.7 Impact Ionization Coefficient / 97

6 Wurtzite Zinc Sulphide (α-ZnS) 99

6.1 Structural Properties / 99
6.1.1 Ionicity / 99
6.1.2 Elemental Isotopic Abundance and Molecular Weight / 99
6.1.3 Crystal Structure and Space Group / 100
6.1.4 Lattice Constant and Its Related Parameters / 100
6.1.5 Structural Phase Transition / 100
6.1.6 Cleavage Plane / 100
6.2 Thermal Properties / 101
6.2.1 Melting Point and Its Related Parameters / 101
6.2.2 Specific Heat / 101
6.2.3 Debye Temperature / 101
6.2.4 Thermal Expansion Coefficient / 101
6.2.5 Thermal Conductivity and Diffusivity / 102
6.3 Elastic Properties / 102
6.3.1 Elastic Constant / 102
6.3.2 Third-Order Elastic Constant / 103
6.3.3 Young's Modulus, Poisson's Ratio, and Similar / 103

6.3.4 Microhardness / 104
6.3.5 Sound Velocity / 104
6.4 Phonons and Lattice Vibronic Properties / 105
6.4.1 Phonon Dispersion Relation / 105
6.4.2 Phonon Frequency / 105
6.4.3 Mode Grüneisen Parameter / 105
6.4.4 Phonon Deformation Potential / 105
6.5 Collective Effects and Related Properties / 106
6.5.1 Piezoelectric Constant / 106
6.5.2 Fröhlich Coupling Constant / 106
6.6 Energy-Band Structure: Energy-Band Gaps / 106
6.6.1 Basic Properties / 106
6.6.2 E_0-Gap Region / 108
6.6.3 Higher-Lying Direct Gap / 109
6.6.4 Lowest Indirect Gap / 110
6.6.5 Conduction-Valley Energy Separation / 110
6.6.6 Direct–Indirect-Gap Transition Pressure / 110
6.7 Energy-Band Structure: Electron and Hole Effective Masses / 110
6.7.1 Electron Effective Mass: Γ Valley / 110
6.7.2 Electron Effective Mass: Satellite Valley / 111
6.7.3 Hole Effective Mass / 111
6.8 Electronic Deformation Potential / 111
6.8.1 Intravalley Deformation Potential: Γ Point / 111
6.8.2 Intravalley Deformation Potential: High-Symmetry Points / 112
6.8.3 Intervalley Deformation Potential / 112
6.9 Electron Affinity and Schottky Barrier Height / 112
6.9.1 Electron Affinity / 112
6.9.2 Schottky Barrier Height / 112
6.10 Optical Properties / 113
6.10.1 Summary of Optical Dispersion Relations / 113
6.10.2 The Reststrahlen Region / 114
6.10.3 At or Near the Fundamental Absorption Edge / 115
6.10.4 The Interband Transition Region / 117
6.10.5 Free-Carrier Absorption and Related Phenomena / 117
6.11 Elastooptic, Electrooptic, and Nonlinear Optical Properties / 117
6.11.1 Elastooptic Effect / 117
6.11.2 Linear Electrooptic Constant / 118
6.11.3 Quadratic Electrooptic Constant / 118
6.11.4 Franz–Keldysh Effect / 118
6.11.5 Nonlinear Optical Constant / 118
6.12 Carrier Transport Properties / 119
6.12.1 Low-Field Mobility: Electrons / 119
6.12.2 Low-Field Mobility: Holes / 120
6.12.3 High-Field Transport: Electrons / 120
6.12.4 High-Field Transport: Holes / 121
6.12.5 Minority-Carrier Transport: Electrons in *p*-Type Materials / 121
6.12.6 Minority-Carrier Transport: Holes in *n*-Type Materials / 121
6.12.7 Impact Ionization Coefficient / 121

7 Cubic Zinc Sulphide (β-ZnS) 123

7.1 Structural Properties / 123
7.1.1 Ionicity / 123
7.1.2 Elemental Isotopic Abundance and Molecular Weight / 123
7.1.3 Crystal Structure and Space Group / 124
7.1.4 Lattice Constant and Its Related Parameters / 124
7.1.5 Structural Phase Transition / 124
7.1.6 Cleavage Plane / 125
7.2 Thermal Properties / 126
7.2.1 Melting Point and Its Related Parameters / 126
7.2.2 Specific Heat / 126
7.2.3 Debye Temperature / 127
7.2.4 Thermal Expansion Coefficient / 128
7.2.5 Thermal Conductivity and Diffusivity / 129
7.3 Elastic Properties / 129
7.3.1 Elastic Constant / 129
7.3.2 Third-Order Elastic Constant / 130
7.3.3 Young's Modulus, Poisson's Ratio, and Similar / 130
7.3.4 Microhardness / 131
7.3.5 Sound Velocity / 131
7.4 Phonons and Lattice Vibronic Properties / 132
7.4.1 Phonon Dispersion Relation / 132
7.4.2 Phonon Frequency / 133
7.4.3 Mode Grüneisen Parameter / 134
7.4.4 Phonon Deformation Potential / 134
7.5 Collective Effects and Related Properties / 134
7.5.1 Piezoelectric Constant / 134
7.5.2 Fröhlich Coupling Constant / 135
7.6 Energy-Band Structure: Energy-Band Gaps / 135
7.6.1 Basic Properties / 135
7.6.2 E_0-Gap Region / 136
7.6.3 Higher-Lying Direct Gap / 140
7.6.4 Lowest Indirect Gap / 141
7.6.5 Conduction-Valley Energy Separation / 141
7.6.6 Direct–Indirect-Gap Transition Pressure / 141
7.7 Energy-Band Structure: Electron and Hole Effective Masses / 142
7.7.1 Electron Effective Mass: Γ Valley / 142
7.7.2 Electron Effective Mass: Satellite Valley / 142
7.7.3 Hole Effective Mass / 142
7.8 Electronic Deformation Potential / 143
7.8.1 Intravalley Deformation Potential: Γ Point / 143
7.8.2 Intravalley Deformation Potential: High-Symmetry Points / 146
7.8.3 Intervalley Deformation Potential / 146
7.9 Electron Affinity and Schottky Barrier Height / 147
7.9.1 Electron Affinity / 147
7.9.2 Schottky Barrier Height / 147
7.10 Optical Properties / 147
7.10.1 Summary of Optical Dispersion Relations / 147

7.10.2 The Reststrahlen Region / 148
7.10.3 At or Near the Fundamental Absorption Edge / 150
7.10.4 The Interband Transition Region / 154
7.10.5 Free-Carrier Absorption and Related Phenomena / 154
7.11 Elastooptic, Electrooptic, and Nonlinear Optical Properties / 154
7.11.1 Elastooptic Effect / 154
7.11.2 Linear Electrooptic Constant / 155
7.11.3 Quadratic Electrooptic Constant / 156
7.11.4 Franz–Keldysh Effect / 156
7.11.5 Nonlinear Optical Constant / 157
7.12 Carrier Transport Properties / 158
7.12.1 Low-Field Mobility: Electrons / 158
7.12.2 Low-Field Mobility: Holes / 159
7.12.3 High-Field Transport: Electrons / 159
7.12.4 High-Field Transport: Holes / 160
7.12.5 Minority-Carrier Transport: Electrons in *p*-Type Materials / 160
7.12.6 Minority-Carrier Transport: Holes in *n*-Type Materials / 160
7.12.7 Impact Ionization Coefficient / 160

8 Zinc Selenide (ZnSe) 161

8.1 Structural Properties / 161
8.1.1 Ionicity / 161
8.1.2 Elemental Isotopic Abundance and Molecular Weight / 161
8.1.3 Crystal Structure and Space Group / 162
8.1.4 Lattice Constant and Its Related Parameters / 162
8.1.5 Structural Phase Transition / 162
8.1.6 Cleavage Plane / 163
8.2 Thermal Properties / 163
8.2.1 Melting Point and Its Related Parameters / 163
8.2.2 Specific Heat / 164
8.2.3 Debye Temperature / 165
8.2.4 Thermal Expansion Coefficient / 166
8.2.5 Thermal Conductivity and Diffusivity / 167
8.3 Elastic Properties / 168
8.3.1 Elastic Constant / 168
8.3.2 Third-Order Elastic Constant / 169
8.3.3 Young's Modulus, Poisson's Ratio, and Similar / 169
8.3.4 Microhardness / 170
8.3.5 Sound Velocity / 170
8.4 Phonons and Lattice Vibronic Properties / 171
8.4.1 Phonon Dispersion Relation / 171
8.4.2 Phonon Frequency / 172
8.4.3 Mode Grüneisen Parameter / 173
8.4.4 Phonon Deformation Potential / 174
8.5 Collective Effects and Related Properties / 174
8.5.1 Piezoelectric Constant / 174
8.5.2 Fröhlich Coupling Constant / 174

8.6 Energy-Band Structure: Energy-Band Gaps / 175
8.6.1 Basic Properties / 175
8.6.2 E_0-Gap Region / 176
8.6.3 Higher-Lying Direct Gap / 180
8.6.4 Lowest Indirect Gap / 182
8.6.5 Conduction-Valley Energy Separation / 183
8.6.6 Direct–Indirect-Gap Transition Pressure / 184
8.7 Energy-Band Structure: Electron and Hole Effective Masses / 184
8.7.1 Electron Effective Mass: Γ Valley / 184
8.7.2 Electron Effective Mass: Satellite Valley / 185
8.7.3 Hole Effective Mass / 185
8.8 Electronic Deformation Potential / 186
8.8.1 Intravalley Deformation Potential: Γ Point / 186
8.8.2 Intravalley Deformation Potential: High-Symmetry Points / 189
8.8.3 Intervalley Deformation Potential / 190
8.9 Electron Affinity and Schottky Barrier Height / 191
8.9.1 Electron Affinity / 191
8.9.2 Schottky Barrier Height / 191
8.10 Optical Properties / 192
8.10.1 Summary of Optical Dispersion Relations / 192
8.10.2 The Reststrahlen Region / 193
8.10.3 At or Near the Fundamental Absorption Edge / 195
8.10.4 The Interband Transition Region / 199
8.10.5 Free-Carrier Absorption and Related Phenomena / 200
8.11 Elastooptic, Electrooptic, and Nonlinear Optical Properties / 200
8.11.1 Elastooptic Effect / 200
8.11.2 Linear Electrooptic Constant / 202
8.11.3 Quadratic Electrooptic Constant / 202
8.11.4 Franz–Keldysh Effect / 202
8.11.5 Nonlinear Optical Constant / 203
8.12 Carrier Transport Properties / 205
8.12.1 Low-Field Mobility: Electrons / 205
8.12.2 Low-Field Mobility: Holes / 206
8.12.3 High-Field Transport: Electrons / 207
8.12.4 High-Field Transport: Holes / 208
8.12.5 Minority-Carrier Transport: Electrons in *p*-Type Materials / 208
8.12.6 Minority-Carrier Transport: Holes in *n*-Type Materials / 208
8.12.7 Impact Ionization Coefficient / 209

9 Zinc Telluride (ZnTe) 211

9.1 Structural Properties / 211
9.1.1 Ionicity / 211
9.1.2 Elemental Isotopic Abundance and Molecular Weight / 211
9.1.3 Crystal Structure and Space Group / 212
9.1.4 Lattice Constant and Its Related Parameters / 212
9.1.5 Structural Phase Transition / 212
9.1.6 Cleavage Plane / 213

9.2 Thermal Properties / 214
9.2.1 Melting Point and Its Related Parameters / 214
9.2.2 Specific Heat / 214
9.2.3 Debye Temperature / 216
9.2.4 Thermal Expansion Coefficient / 216
9.2.5 Thermal Conductivity and Diffusivity / 218
9.3 Elastic Properties / 218
9.3.1 Elastic Constant / 218
9.3.2 Third-Order Elastic Constant / 219
9.3.3 Young's Modulus, Poisson's Ratio, and Similar / 219
9.3.4 Microhardness / 220
9.3.5 Sound Velocity / 221
9.4 Phonons and Lattice Vibronic Properties / 221
9.4.1 Phonon Dispersion Relation / 221
9.4.2 Phonon Frequency / 222
9.4.3 Mode Grüneisen Parameter / 223
9.4.4 Phonon Deformation Potential / 224
9.5 Collective Effects and Related Properties / 224
9.5.1 Piezoelectric Constant / 224
9.5.2 Fröhlich Coupling Constant / 225
9.6 Energy-Band Structure: Energy-Band Gaps / 225
9.6.1 Basic Properties / 225
9.6.2 E_0-Gap Region / 226
9.6.3 Higher-Lying Direct Gap / 230
9.6.4 Lowest Indirect Gap / 233
9.6.5 Conduction-Valley Energy Separation / 233
9.6.6 Direct–Indirect-Gap Transition Pressure / 234
9.7 Energy-Band Structure: Electron and Hole Effective Masses / 234
9.7.1 Electron Effective Mass: Γ Valley / 234
9.7.2 Electron Effective Mass: Satellite Valley / 234
9.7.3 Hole Effective Mass / 235
9.8 Electronic Deformation Potential / 236
9.8.1 Intravalley Deformation Potential: Γ Point / 236
9.8.2 Intravalley Deformation Potential: High-Symmetry Points / 238
9.8.3 Intervalley Deformation Potential / 239
9.9 Electron Affinity and Schottky Barrier Height / 240
9.9.1 Electron Affinity / 240
9.9.2 Schottky Barrier Height / 240
9.10 Optical Properties / 241
9.10.1 Summary of Optical Dispersion Relations / 241
9.10.2 The Reststrahlen Region / 242
9.10.3 At or Near the Fundamental Absorption Edge / 243
9.10.4 The Interband Transition Region / 246
9.10.5 Free-Carrier Absorption and Related Phenomena / 247
9.11 Elastooptic, Electrooptic, and Nonlinear Optical Properties / 247
9.11.1 Elastooptic Effect / 247
9.11.2 Linear Electrooptic Constant / 248
9.11.3 Quadratic Electrooptic Constant / 249

9.11.4 Franz–Keldysh Effect / 249
9.11.5 Nonlinear Optical Constant / 249
9.12 Carrier Transport Properties / 250
9.12.1 Low-Field Mobility: Electrons / 250
9.12.2 Low-Field Mobility: Holes / 251
9.12.3 High-Field Transport: Electrons / 252
9.12.4 High-Field Transport: Holes / 253
9.12.5 Minority-Carrier Transport: Electrons in *p*-Type Materials / 253
9.12.6 Minority-Carrier Transport: Holes in *n*-Type Materials / 253
9.12.7 Impact Ionization Coefficient / 253

10 Cubic Cadmium Sulphide (*c*-CdS) 255

10.1 Structural Properties / 255
10.1.1 Ionicity / 255
10.1.2 Elemental Isotopic Abundance and Molecular Weight / 255
10.1.3 Crystal Structure and Space Group / 256
10.1.4 Lattice Constant and Its Related Parameters / 256
10.1.5 Structural Phase Transition / 256
10.1.6 Cleavage Plane / 257
10.2 Thermal Properties / 257
10.2.1 Melting Point and Its Related Parameters / 257
10.2.2 Specific Heat / 258
10.2.3 Debye Temperature / 258
10.2.4 Thermal Expansion Coefficient / 258
10.2.5 Thermal Conductivity and Diffusivity / 258
10.3 Elastic Properties / 258
10.3.1 Elastic Constant / 258
10.3.2 Third-Order Elastic Constant / 258
10.3.3 Young's Modulus, Poisson's Ratio, and Similar / 259
10.3.4 Microhardness / 260
10.3.5 Sound Velocity / 260
10.4 Phonons and Lattice Vibronic Properties / 260
10.4.1 Phonon Dispersion Relation / 260
10.4.2 Phonon Frequency / 260
10.4.3 Mode Grüneisen Parameter / 261
10.4.4 Phonon Deformation Potential / 261
10.5 Collective Effects and Related Properties / 261
10.5.1 Piezoelectric Constant / 261
10.5.2 Fröhlich Coupling Constant / 261
10.6 Energy-Band Structure: Energy-Band Gaps / 261
10.6.1 Basic Properties / 261
10.6.2 E_0-Gap Region / 263
10.6.3 Higher-Lying Direct Gap / 264
10.6.4 Lowest Indirect Gap / 264
10.6.5 Conduction-Valley Energy Separation / 265
10.6.6 Direct–Indirect-Gap Transition Pressure / 265
10.7 Energy-Band Structure: Electron and Hole Effective Masses / 265
10.7.1 Electron Effective Mass: Γ Valley / 265

10.7.2 Electron Effective Mass: Satellite Valley / 266
10.7.3 Hole Effective Mass / 266
10.8 Electronic Deformation Potential / 267
10.8.1 Intravalley Deformation Potential: Γ Point/ 267
10.8.2 Intravalley Deformation Potential: High-Symmetry Points / 268
10.8.3 Intervalley Deformation Potential / 268
10.9 Electron Affinity and Schottky Barrier Height / 268
10.9.1 Electron Affinity / 268
10.9.2 Schottky Barrier Height / 268
10.10 Optical Properties / 268
10.10.1 Summary of Optical Dispersion Relations / 268
10.10.2 The Reststrahlen Region / 269
10.10.3 At or Near the Fundamental Absorption Edge / 269
10.10.4 The Interband Transition Region / 270
10.10.5 Free-Carrier Absorption and Related Phenomena / 271
10.11 Elastooptic, Electrooptic, and Nonlinear Optical Properties / 271
10.11.1 Elastooptic Effect / 271
10.11.2 Linear Electrooptic Constant / 271
10.11.3 Quadratic Electrooptic Constant / 271
10.11.4 Franz–Keldysh Effect / 271
10.11.5 Nonlinear Optical Constant / 271
10.12 Carrier Transport Properties / 272
10.12.1 Low-Field Mobility: Electrons / 272
10.12.2 Low-Field Mobility: Holes / 272
10.12.3 High-Field Transport: Electrons / 272
10.12.4 High-Field Transport: Holes / 272
10.12.5 Minority-Carrier Transport: Electrons in *p*-Type Materials / 272
10.12.6 Minority-Carrier Transport: Holes in *n*-Type Materials / 272
10.12.7 Impact Ionization Coefficient / 272

11 Wurtzite Cadmium Sulphide (*w*-CdS) 273

11.1 Structural Properties / 273
11.1.1 Ionicity / 273
11.1.2 Elemental Isotopic Abundance and Molecular Weight / 273
11.1.3 Crystal Structure and Space Group / 274
11.1.4 Lattice Constant and Its Related Parameters / 274
11.1.5 Structural Phase Transition / 274
11.1.6 Cleavage Plane / 275
11.2 Thermal Properties / 275
11.2.1 Melting Point and Its Related Parameters / 275
11.2.2 Specific Heat / 276
11.2.3 Debye Temperature / 276
11.2.4 Thermal Expansion Coefficient / 277
11.2.5 Thermal Conductivity and Diffusivity / 277
11.3 Elastic Properties / 278
11.3.1 Elastic Constant / 278
11.3.2 Third-Order Elastic Constant / 279
11.3.3 Young's Modulus, Poisson's Ratio, and Similar / 279

11.3.4 Microhardness / 280
11.3.5 Sound Velocity / 280
11.4 Phonons and Lattice Vibronic Properties / 281
11.4.1 Phonon Dispersion Relation / 281
11.4.2 Phonon Frequency / 281
11.4.3 Mode Grüneisen Parameter / 282
11.4.4 Phonon Deformation Potential / 282
11.5 Collective Effects and Related Properties / 283
11.5.1 Piezoelectric Constant / 283
11.5.2 Fröhlich Coupling Constant / 283
11.6 Energy-Band Structure: Energy-Band Gaps / 284
11.6.1 Basic Properties / 284
11.6.2 E_0-Gap Region / 285
11.6.3 Higher-Lying Direct Gap / 289
11.6.4 Lowest Indirect Gap / 290
11.6.5 Conduction-Valley Energy Separation / 290
11.6.6 Direct–Indirect-Gap Transition Pressure / 291
11.7 Energy-Band Structure: Electron and Hole Effective Masses / 291
11.7.1 Electron Effective Mass: Γ Valley / 291
11.7.2 Electron Effective Mass: Satellite Valley / 292
11.7.3 Hole Effective Mass / 292
11.8 Electronic Deformation Potential / 293
11.8.1 Intravalley Deformation Potential: Γ Point / 293
11.8.2 Intravalley Deformation Potential: High-Symmetry Points / 293
11.8.3 Intervalley Deformation Potential / 294
11.9 Electron Affinity and Schottky Barrier Height / 294
11.9.1 Electron Affinity / 294
11.9.2 Schottky Barrier Height / 294
11.10 Optical Properties / 295
11.10.1 Summary of Optical Dispersion Relations / 295
11.10.2 The Reststrahlen Region / 296
11.10.3 At or Near the Fundamental Absorption Edge / 298
11.10.4 The Interband Transition Region / 302
11.10.5 Free-Carrier Absorption and Related Phenomena / 303
11.11 Elastooptic, Electrooptic, and Nonlinear Optical Properties / 303
11.11.1 Elastooptic Effect / 303
11.11.2 Linear Electrooptic Constant / 304
11.11.3 Quadratic Electrooptic Constant / 304
11.11.4 Franz–Keldysh Effect / 304
11.11.5 Nonlinear Optical Constant / 305
11.12 Carrier Transport Properties / 305
11.12.1 Low-Field Mobility: Electrons / 305
11.12.2 Low-Field Mobility: Holes / 307
11.12.3 High-Field Transport: Electrons / 308
11.12.4 High-Field Transport: Holes / 309
11.12.5 Minority-Carrier Transport: Electrons in *p*-Type Materials / 309
11.12.6 Minority-Carrier Transport: Holes in *n*-Type Materials / 309
11.12.7 Impact Ionization Coefficient / 309

12 Cubic Cadmium Selenide (*c*-CdSe) 311

12.1 Structural Properties / 311
12.1.1 Ionicity / 311
12.1.2 Elemental Isotopic Abundance and Molecular Weight / 311
12.1.3 Crystal Structure and Space Group / 312
12.1.4 Lattice Constant and Its Related Parameters / 312
12.1.5 Structural Phase Transition / 312
12.1.6 Cleavage Plane / 313
12.2 Thermal Properties / 313
12.2.1 Melting Point and Its Related Parameters / 313
12.2.2 Specific Heat / 314
12.2.3 Debye Temperature / 314
12.2.4 Thermal Expansion Coefficient / 314
12.2.5 Thermal Conductivity and Diffusivity / 314
12.3 Elastic Properties / 314
12.3.1 Elastic Constant / 314
12.3.2 Third-Order Elastic Constant / 315
12.3.3 Young's Modulus, Poisson's Ratio, and Similar / 315
12.3.4 Microhardness / 316
12.3.5 Sound Velocity / 316
12.4 Phonons and Lattice Vibronic Properties / 316
12.4.1 Phonon Dispersion Relation / 316
12.4.2 Phonon Frequency / 317
12.4.3 Mode Grüneisen Parameter / 317
12.4.4 Phonon Deformation Potential / 317
12.5 Collective Effects and Related Properties / 317
12.5.1 Piezoelectric Constant / 317
12.5.2 Fröhlich Coupling Constant / 317
12.6 Energy-Band Structure: Energy-Band Gaps / 318
12.6.1 Basic Properties / 318
12.6.2 E_0-Gap Region / 319
12.6.3 Higher-Lying Direct Gap / 321
12.6.4 Lowest Indirect Gap / 321
12.6.5 Conduction-Valley Energy Separation / 322
12.6.6 Direct–Indirect-Gap Transition Pressure / 322
12.7 Energy-Band Structure: Electron and Hole Effective Masses / 322
12.7.1 Electron Effective Mass: Γ Valley / 322
12.7.2 Electron Effective Mass: Satellite Valley / 323
12.7.3 Hole Effective Mass / 323
12.8 Electronic Deformation Potential / 324
12.8.1 Intravalley Deformation Potential: Γ Point / 324
12.8.2 Intravalley Deformation Potential: High-Symmetry Points / 325
12.8.3 Intervalley Deformation Potential / 325
12.9 Electron Affinity and Schottky Barrier Height / 325
12.9.1 Electron Affinity / 325
12.9.2 Schottky Barrier Height / 325
12.10 Optical Properties / 325
12.10.1 Summary of Optical Dispersion Relations / 325

12.10.2 The Reststrahlen Region / 326
12.10.3 At or Near the Fundamental Absorption Edge / 326
12.10.4 The Interband Transition Region / 327
12.10.5 Free-Carrier Absorption and Related Phenomena / 327
12.11 Elastooptic, Electrooptic, and Nonlinear Optical Properties / 327
12.11.1 Elastooptic Effect / 327
12.11.2 Linear Electrooptic Constant / 327
12.11.3 Quadratic Electrooptic Constant / 327
12.11.4 Franz–Keldysh Effect / 327
12.11.5 Nonlinear Optical Constant / 327
12.12 Carrier Transport Properties / 328
12.12.1 Low-Field Mobility: Electrons / 328
12.12.2 Low-Field Mobility: Holes / 328
12.12.3 High-Field Transport: Electrons / 328
12.12.4 High-Field Transport: Holes / 328
12.12.5 Minority-Carrier Transport: Electrons in *p*-Type Materials / 328
12.12.6 Minority-Carrier Transport: Holes in *n*-Type Materials / 328
12.12.7 Impact Ionization Coefficient / 328

13 Wurtzite Cadmium Selenide (*w*-CdSe) 329

13.1 Structural Properties / 329
13.1.1 Ionicity / 329
13.1.2 Elemental Isotopic Abundance and Molecular Weight / 329
13.1.3 Crystal Structure and Space Group / 330
13.1.4 Lattice Constant and Its Related Parameters / 330
13.1.5 Structural Phase Transition / 330
13.1.6 Cleavage Plane / 331
13.2 Thermal Properties / 331
13.2.1 Melting Point and Its Related Parameters / 331
13.2.2 Specific Heat / 331
13.2.3 Debye Temperature / 332
13.2.4 Thermal Expansion Coefficient / 333
13.2.5 Thermal Conductivity and Diffusivity / 333
13.3 Elastic Properties / 333
13.3.1 Elastic Constant / 333
13.3.2 Third-Order Elastic Constant / 334
13.3.3 Young's Modulus, Poisson's Ratio, and Similar / 334
13.3.4 Microhardness / 335
13.3.5 Sound Velocity / 335
13.4 Phonons and Lattice Vibronic Properties / 335
13.4.1 Phonon Dispersion Relation / 335
13.4.2 Phonon Frequency / 335
13.4.3 Mode Grüneisen Parameter / 336
13.4.4 Phonon Deformation Potential / 336
13.5 Collective Effects and Related Properties / 336
13.5.1 Piezoelectric Constant / 336
13.5.2 Fröhlich Coupling Constant / 336

13.6 Energy-Band Structure: Energy-Band Gaps / 337
13.6.1 Basic Properties / 337
13.6.2 E_0-Gap Region / 338
13.6.3 Higher-Lying Direct Gap / 341
13.6.4 Lowest Indirect Gap / 343
13.6.5 Conduction-Valley Energy Separation / 343
13.6.6 Direct–Indirect-Gap Transition Pressure / 343
13.7 Energy-Band Structure: Electron and Hole Effective Masses / 344
13.7.1 Electron Effective Mass: Γ Valley / 344
13.7.2 Electron Effective Mass: Satellite Valley / 345
13.7.3 Hole Effective Mass / 345
13.8 Electronic Deformation Potential / 345
13.8.1 Intravalley Deformation Potential: Γ Point / 345
13.8.2 Intravalley Deformation Potential: High-Symmetry Points / 346
13.8.3 Intervalley Deformation Potential / 346
13.9 Electron Affinity and Schottky Barrier Height / 346
13.9.1 Electron Affinity / 346
13.9.2 Schottky Barrier Height / 347
13.10 Optical Properties / 347
13.10.1 Summary of Optical Dispersion Relations / 347
13.10.2 The Reststrahlen Region / 348
13.10.3 At or Near the Fundamental Absorption Edge / 350
13.10.4 The Interband Transition Region / 353
13.10.5 Free-Carrier Absorption and Related Phenomena / 353
13.11 Elastooptic, Electrooptic, and Nonlinear Optical Properties / 354
13.11.1 Elastooptic Effect / 354
13.11.2 Linear Electrooptic Constant / 354
13.11.3 Quadratic Electrooptic Constant / 354
13.11.4 Franz–Keldysh Effect / 354
13.11.5 Nonlinear Optical Constant / 355
13.12 Carrier Transport Properties / 355
13.12.1 Low-Field Mobility: Electrons / 355
13.12.2 Low-Field Mobility: Holes / 356
13.12.3 High-Field Transport: Electrons / 357
13.12.4 High-Field Transport: Holes / 357
13.12.5 Minority-Carrier Transport: Electrons in *p*-Type Materials / 357
13.12.6 Minority-Carrier Transport: Holes in *n*-Type Materials / 357
13.12.7 Impact Ionization Coefficient / 357

14 Cadmium Telluride (CdTe) 359

14.1 Structural Properties / 359
14.1.1 Ionicity / 359
14.1.2 Elemental Isotopic Abundance and Molecular Weight / 359
14.1.3 Crystal Structure and Space Group / 360
14.1.4 Lattice Constant and Its Related Parameters / 360
14.1.5 Structural Phase Transition / 360
14.1.6 Cleavage Plane / 361

14.2 Thermal Properties / 362
14.2.1 Melting Point and Its Related Parameters / 362
14.2.2 Specific Heat / 362
14.2.3 Debye Temperature / 364
14.2.4 Thermal Expansion Coefficient / 365
14.2.5 Thermal Conductivity and Diffusivity / 366
14.3 Elastic Properties / 367
14.3.1 Elastic Constant / 367
14.3.2 Third-Order Elastic Constant / 368
14.3.3 Young's Modulus, Poisson's Ratio, and Similar / 368
14.3.4 Microhardness / 369
14.3.5 Sound Velocity / 369
14.4 Phonons and Lattice Vibronic Properties / 369
14.4.1 Phonon Dispersion Relation / 369
14.4.2 Phonon Frequency / 370
14.4.3 Mode Grüneisen Parameter / 371
14.4.4 Phonon Deformation Potential / 372
14.5 Collective Effects and Related Properties / 372
14.5.1 Piezoelectric Constant / 372
14.5.2 Fröhlich Coupling Constant / 372
14.6 Energy-Band Structure: Energy-Band Gaps / 373
14.6.1 Basic Properties / 373
14.6.2 E_0-Gap Region / 374
14.6.3 Higher-Lying Direct Gap / 378
14.6.4 Lowest Indirect Gap / 382
14.6.5 Conduction-Valley Energy Separation / 383
14.6.6 Direct–Indirect-Gap Transition Pressure / 383
14.7 Energy-Band Structure: Electron and Hole Effective Masses / 383
14.7.1 Electron Effective Mass: Γ Valley / 383
14.7.2 Electron Effective Mass: Satellite Valley / 384
14.7.3 Hole Effective Mass / 384
14.8 Electronic Deformation Potential / 385
14.8.1 Intravalley Deformation Potential: Γ Point / 385
14.8.2 Intravalley Deformation Potential: High-Symmetry Points / 387
14.8.3 Intervalley Deformation Potential / 387
14.9 Electron Affinity and Schottky Barrier Height / 387
14.9.1 Electron Affinity / 387
14.9.2 Schottky Barrier Height / 388
14.10 Optical Properties / 389
14.10.1 Summary of Optical Dispersion Relations / 389
14.10.2 The Reststrahlen Region / 390
14.10.3 At or Near the Fundamental Absorption Edge / 392
14.10.4 The Interband Transition Region / 394
14.10.5 Free-Carrier Absorption and Related Phenomena / 395
14.11 Elastooptic, Electrooptic, and Nonlinear Optical Properties / 395
14.11.1 Elastooptic Effect / 395
14.11.2 Linear Electrooptic Constant / 396
14.11.3 Quadratic Electrooptic Constant / 396

14.11.4 Franz–Keldysh Effect / 396
14.11.5 Nonlinear Optical Constant / 397
14.12 Carrier Transport Properties / 398
14.12.1 Low-Field Mobility: Electrons / 398
14.12.2 Low-Field Mobility: Holes / 399
14.12.3 High-Field Transport: Electrons / 399
14.12.4 High-Field Transport: Holes / 400
14.12.5 Minority-Carrier Transport: Electrons in *p*-Type Materials / 400
14.12.6 Minority-Carrier Transport: Holes in *n*-Type Materials / 401
14.12.7 Impact Ionization Coefficient / 401

15 Cubic Mercury Sulphide (β-HgS) 403

15.1 Structural Properties / 403
15.1.1 Ionicity / 403
15.1.2 Elemental Isotopic Abundance and Molecular Weight / 403
15.1.3 Crystal Structure and Space Group / 404
15.1.4 Lattice Constant and Its Related Parameters / 404
15.1.5 Structural Phase Transition / 404
15.1.6 Cleavage Plane / 405
15.2 Thermal Properties / 405
15.2.1 Melting Point and Its Related Parameters / 405
15.2.2 Specific Heat / 405
15.2.3 Debye Temperature / 405
15.2.4 Thermal Expansion Coefficient / 406
15.2.5 Thermal Conductivity and Diffusivity / 406
15.3 Elastic Properties / 406
15.3.1 Elastic Constant / 406
15.3.2 Third-Order Elastic Constant / 406
15.3.3 Young's Modulus, Poisson's Ratio, and Similar / 406
15.3.4 Microhardness / 407
15.3.5 Sound Velocity / 407
15.4 Phonons and Lattice Vibronic Properties / 408
15.4.1 Phonon Dispersion Relation / 408
15.4.2 Phonon Frequency / 408
15.4.3 Mode Grüneisen Parameter / 408
15.4.4 Phonon Deformation Potential / 408
15.5 Collective Effects and Related Properties / 409
15.5.1 Piezoelectric Constant / 409
15.5.2 Fröhlich Coupling Constant / 409
15.6 Energy-Band Structure: Energy-Band Gaps / 409
15.6.1 Basic Properties / 409
15.6.2 E_0-Gap Region / 410
15.6.3 Higher-Lying Direct Gap / 411
15.6.4 Lowest Indirect Gap / 411
15.6.5 Conduction-Valley Energy Separation / 412
15.6.6 Direct–Indirect-Gap Transition Pressure / 412
15.7 Energy-Band Structure: Electron and Hole Effective Masses / 412
15.7.1 Electron Effective Mass: Γ Valley / 412

15.7.2 Electron Effective Mass: Satellite Valley / 412
15.7.3 Hole Effective Mass / 412
15.8 Electronic Deformation Potential / 414
15.8.1 Intravalley Deformation Potential: Γ Point / 414
15.8.2 Intravalley Deformation Potential: High-Symmetry Points / 414
15.8.3 Intervalley Deformation Potential / 414
15.9 Electron Affinity and Schottky Barrier Height / 415
15.9.1 Electron Affinity / 415
15.9.2 Schottky Barrier Height / 415
15.10 Optical Properties / 415
15.10.1 Summary of Optical Dispersion Relations / 415
15.10.2 The Reststrahlen Region / 415
15.10.3 At or Near the Fundamental Absorption Edge / 416
15.10.4 The Interband Transition Region / 416
15.10.5 Free-Carrier Absorption and Related Phenomena / 417
15.11 Elastooptic, Electrooptic, and Nonlinear Optical Properties / 417
15.11.1 Elastooptic Effect / 417
15.11.2 Linear Electrooptic Constant / 417
15.11.3 Quadratic Electrooptic Constant / 417
15.11.4 Franz–Keldysh Effect / 417
15.11.5 Nonlinear Optical Constant / 417
15.12 Carrier Transport Properties / 418
15.12.1 Low-Field Mobility: Electrons / 418
15.12.2 Low-Field Mobility: Holes / 418
15.12.3 High-Field Transport: Electrons / 418
15.12.4 High-Field Transport: Holes / 418
15.12.5 Minority-Carrier Transport: Electrons in *p*-Type Materials / 418
15.12.6 Minority-Carrier Transport: Holes in *n*-Type Materials / 418
15.12.7 Impact Ionization Coefficient / 418

16 Mercury Selenide (HgSe) 419

16.1 Structural Properties / 419
16.1.1 Ionicity / 419
16.1.2 Elemental Isotopic Abundance and Molecular Weight / 419
16.1.3 Crystal Structure and Space Group / 420
16.1.4 Lattice Constant and Its Related Parameters / 420
16.1.5 Structural Phase Transition / 420
16.1.6 Cleavage Plane / 421
16.2 Thermal Properties / 421
16.2.1 Melting Point and Its Related Parameters / 421
16.2.2 Specific Heat / 421
16.2.3 Debye Temperature / 422
16.2.4 Thermal Expansion Coefficient / 422
16.2.5 Thermal Conductivity and Diffusivity / 423
16.3 Elastic Properties / 424
16.3.1 Elastic Constant / 424
16.3.2 Third-Order Elastic Constant / 424
16.3.3 Young's Modulus, Poisson's Ratio, and Similar / 425

16.3.4 Microhardness / 426
16.3.5 Sound Velocity / 426
16.4 Phonons and Lattice Vibronic Properties / 426
16.4.1 Phonon Dispersion Relation / 426
16.4.2 Phonon Frequency / 427
16.4.3 Mode Grüneisen Parameter / 427
16.4.4 Phonon Deformation Potential / 428
16.5 Collective Effects and Related Properties / 428
16.5.1 Piezoelectric Constant / 428
16.5.2 Fröhlich Coupling Constant / 428
16.6 Energy-Band Structure: Energy-Band Gaps / 428
16.6.1 Basic Properties / 428
16.6.2 E_0-Gap Region / 429
16.6.3 Higher-Lying Direct Gap / 432
16.6.4 Lowest Indirect Gap / 434
16.6.5 Conduction-Valley Energy Separation / 435
16.6.6 Direct–Indirect-Gap Transition Pressure / 435
16.7 Energy-Band Structure: Electron and Hole Effective Masses / 435
16.7.1 Electron Effective Mass: Γ Valley / 435
16.7.2 Electron Effective Mass: Satellite Valley / 435
16.7.3 Hole Effective Mass / 435
16.8 Electronic Deformation Potential / 437
16.8.1 Intravalley Deformation Potential: Γ Point / 437
16.8.2 Intravalley Deformation Potential: High-Symmetry Points / 437
16.8.3 Intervalley Deformation Potential / 437
16.9 Electron Affinity and Schottky Barrier Height / 437
16.9.1 Electron Affinity / 437
16.9.2 Schottky Barrier Height / 438
16.10 Optical Properties / 438
16.10.1 Summary of Optical Dispersion Relations / 438
16.10.2 The Reststrahlen Region / 439
16.10.3 At or Near the Fundamental Absorption Edge / 440
16.10.4 The Interband Transition Region / 441
16.10.5 Free-Carrier Absorption and Related Phenomena / 441
16.11 Elastooptic, Electrooptic, and Nonlinear Optical Properties / 441
16.11.1 Elastooptic Effect / 441
16.11.2 Linear Electrooptic Constant / 441
16.11.3 Quadratic Electrooptic Constant / 441
16.11.4 Franz–Keldysh Effect / 441
16.11.5 Nonlinear Optical Constant / 442
16.12 Carrier Transport Properties / 442
16.12.1 Low-Field Mobility: Electrons / 442
16.12.2 Low-Field Mobility: Holes / 443
16.12.3 High-Field Transport: Electrons / 443
16.12.4 High-Field Transport: Holes / 443
16.12.5 Minority-Carrier Transport: Electrons in *p*-Type Materials / 443
16.12.6 Minority-Carrier Transport: Holes in *n*-Type Materials / 443
16.12.7 Impact Ionization Coefficient / 443

17 Mercury Telluride (HgTe) 445

17.1 Structural Properties / 445
17.1.1 Ionicity / 445
17.1.2 Elemental Isotopic Abundance and Molecular Weight / 445
17.1.3 Crystal Structure and Space Group / 446
17.1.4 Lattice Constant and Its Related Parameters / 446
17.1.5 Structural Phase Transition / 446
17.1.6 Cleavage Plane / 447
17.2 Thermal Properties / 447
17.2.1 Melting Point and Its Related Parameters / 447
17.2.2 Specific Heat / 448
17.2.3 Debye Temperature / 449
17.2.4 Thermal Expansion Coefficient / 449
17.2.5 Thermal Conductivity and Diffusivity / 450
17.3 Elastic Properties / 452
17.3.1 Elastic Constant / 452
17.3.2 Third-Order Elastic Constant / 452
17.3.3 Young's Modulus, Poisson's Ratio, and Similar / 453
17.3.4 Microhardness / 454
17.3.5 Sound Velocity / 454
17.4 Phonons and Lattice Vibronic Properties / 454
17.4.1 Phonon Dispersion Relation / 454
17.4.2 Phonon Frequency / 455
17.4.3 Mode Grüneisen Parameter / 455
17.4.4 Phonon Deformation Potential / 456
17.5 Collective Effects and Related Properties / 456
17.5.1 Piezoelectric Constant / 456
17.5.2 Fröhlich Coupling Constant / 456
17.6 Energy-Band Structure: Energy-Band Gaps / 456
17.6.1 Basic Properties / 456
17.6.2 E_0-Gap Region / 457
17.6.3 Higher-Lying Direct Gap / 459
17.6.4 Lowest Indirect Gap / 461
17.6.5 Conduction-Valley Energy Separation / 461
17.6.6 Direct–Indirect-Gap Transition Pressure / 461
17.7 Energy-Band Structure: Electron and Hole Effective Masses / 462
17.7.1 Electron Effective Mass: Γ Valley / 462
17.7.2 Electron Effective Mass: Satellite Valley / 462
17.7.3 Hole Effective Mass / 462
17.8 Electronic Deformation Potential / 464
17.8.1 Intravalley Deformation Potential: Γ Point / 464
17.8.2 Intravalley Deformation Potential: High-Symmetry Points / 465
17.8.3 Intervalley Deformation Potential / 465
17.9 Electron Affinity and Schottky Barrier Height / 465
17.9.1 Electron Affinity / 465
17.9.2 Schottky Barrier Height / 465
17.10 Optical Properties / 466
17.10.1 Summary of Optical Dispersion Relations / 466

17.10.2 The Reststrahlen Region / 467
17.10.3 At or Near the Fundamental Absorption Edge / 468
17.10.4 The Interband Transition Region / 469
17.10.5 Free-Carrier Absorption and Related Phenomena / 470
17.11 Elastooptic, Electrooptic, and Nonlinear Optical Properties / 470
17.11.1 Elastooptic Effect / 470
17.11.2 Linear Electrooptic Constant / 470
17.11.3 Quadratic Electrooptic Constant / 470
17.11.4 Franz–Keldysh Effect / 470
17.11.5 Nonlinear Optical Constant / 470
17.12 Carrier Transport Properties / 470
17.12.1 Low-Field Mobility: Electrons / 470
17.12.2 Low-Field Mobility: Holes / 472
17.12.3 High-Field Transport: Electrons / 472
17.12.4 High-Field Transport: Holes / 472
17.12.5 Minority-Carrier Transport: Electrons in *p*-Type Materials / 472
17.12.6 Minority-Carrier Transport: Holes in *n*-Type Materials / 472
17.12.7 Impact Ionization Coefficient / 472

PREFACE

The progress made in physics and technology of semiconductors depends mainly on three families of materials: the group-IV elemental, III–V, and II–VI compound semiconductors. Almost all II–VI compound semiconductors crystallize either in the zincblende or wurtzite structure. The first research papers on II–VI compound semiconductors date back to the middle of the nineteenth century. In the ensuring hundred years extensive literature has been accumulated as much research and development works are being carried out on these compound semiconductors. At present, the II–VI compound semiconductors are widely used as photodetectors, x-ray sensors and scintillators, phosphors in lighting, displays, etc. New applications are continuously being proposed. Thus, it seems to timely bring together the most up-to-date information on the material and semiconducting properties of II–VI compound semiconductors.

The aim throughout has been to present in convenient form as large amount of accurate, reliable, and up-to-date information on the physical properties of II-VI compound semiconductors for a variety of basic research and device applications. The data on the physical properties of each semiconductor are organized in the same way in order to facilitate searching for information. The physical properties considered in this book can be classified into 12 groups: (1) structural properties; (2) thermal properties; (3) elastic properties; (4) phonons and lattice vibronic properties; (5) collective effects and related properties; (6) energy-band structure:

energy-band gaps; (7) energy-band structure: electron and hole effective mass; (8) electronic deformation potential; (9) electron affinity and Schottky barrier height; (10) optical properties; (11) elastooptic, electrooptic, and nonlinear optical properties; and (12) carrier transport properties.

The extensive bibliography is included for those who wish to find additional information if required. I hope that the book will aid many who want to know various properties of those semiconductor materials in the course of their work. The reader will also find the series books "Group-IV Semiconductors" and "III–V Compound Semiconductors" useful in order to find the needed information quickly on these practically important semiconductors.

ACKNOWLEDGMENTS

The author wishes to thank the editors and authors of the following journals, symposium papers, and books for permission to reproduce previously published figures: *Academic Press* for Figs. 14.12.1 and 16.12.2; *Appl. Phys. Lett.* for Figs.5.10.7, 5.11.3, 6.12.1, 8.10.3, 8.12.3, 8.12.6, 8.12.7, 14.10.3, and 14.12.4; *Brit. J. Appl. Phys.* for Figs. 6.12.4, 7.12.5, 11.12.7, and 11.12.8; *Can. J. Phys.* for Fig. 7.10.4; *Eur. Phys. J.* for Fig. 8.10.11; *INSPEC* (*IEE*) for Figs. 8.10.8, 11.10.8, 11.10.9, and 12.10.3; *Int. J. Electron.* for Fig. 11.12.6; *J. Appl. Phys.* for Figs. 6.11.1, 6.12.3, 7.6.3, 7.11.2, 7.12.1, 7.12.4, 8.6.3, 8.10.4, 8.12.1, 8.12.5, 9.6.3, 9.11.3, 11.6.3, 11.10.5, 14.4.1, 14.4.2, 16.7.1, 17.4.1, and 17.4.2; *J. Chem. Phys.* for Figs. 7.4.1, 7.4.2, 9.4.1, and 9.4.2; *J. Cryst. Growth* for Fig. 15.4.1; *J. Opt. Soc. Am.* for Figs. 7.10.6, 8.10.6, and 14.10.5; *J. Phys. Chem. Solids* for Figs. 1.4.1, 1.4.2, 5.12.1, 5.12.2, 8.1.1, 9.6.2, 14.11.1, and 17.12.1; *J. Phys.: Condens. Matter* for Fig. 4.6.1; *J. Phys. D: Appl. Phys.* for Fig. 9.12.1; *J. Phys. Soc. Jpn* for Figs. 7.11.1, 9.11.1, 9.11.2, 11.11.1, 11.11.3, 11.12.1, 11.12.3, and 14.12.2; *Jpn. J. Appl. Phys.* for Figs. 7.11.3 and 8.11.3; *North-Holland Publishing Company* for Figs. 8.2.1, 9.2.1, 10.2.1, 11.2.1, 11.12.4, 12.2.1, 13.2.1, 14.2.1, 16.2.1, and 17.2.1; *Opt. Mater.* for Figs. 11.10.10 and 14.10.8; *Phys. Rev.* for Figs. 1.2.1, 1.6.1, 1.6.2, 5.1.1, 5.6.1, 5.6.2, 5.10.5, 5.11.1, 5.11.2, 6.6.1, 6.6.2, 6.10.4, 7.1.1, 7.2.2, 7.6.2, 7.6.4, 7.10.3, 7.10.7, 7.10.8, 7.11.4, 8.2.3, 8.6.1, 8.6.2, 8.10.7, 8.11.1, 8.11.2, 8.11.4, 9.1.1, 9.2.3, 9.6.1, 9.10.3, 9.10.5, 9.10.6, 9.10.8, 9.11.4, 9.11.5, 10.6.1, 10.6.2,

10.10.4, 11.6.1, 11.6.2, 11.10.4, 12.1.1, 12.4.1, 12.6.1, 12.6.2, 13.6.1–13.6.3, 13.10.8, 14.4.3, 14.6.1, 14.6.2, 14.10.6, 14.10.9, 14.12.3, 15.10.3, 16.6.4, 16.6.5, 16.10.4–16.10.6, 16.12.1, 17.10.3, 17.10.4, and 17.10.8; *Phys. Scripta* for Figs. 1.10.3, 16.4.1, and 16.4.2; *Phys. Status Solidi* for Figs. 8.4.1–8.4.3, 8.12.9, 9.12.3, 11.10.7, 13.10.5, 14.1.1, 15.7.1, 15.10.1, 15.10.2, 15.12.1, 16.2.4, 16.6.1, 16.10.3, 17.2.3, 17.6.1, 17.10.5, 17.10.6, and 17.12.3; *Physica* for Fig. 11.7.1; *Proc. Phys. Soc.* for Fig. 11.12.5; *Proc. Roy. Soc.* for Fig. 13.10.6; *Semicond. Sci. Technol.* for Figs. 2.6.1, 3.6.1, 3.10.1, and 9.12.5; *Solid State Commun.* for Figs. 5.4.1, 5.6.3, 8.6.4, 8.10.9, 8.11.5, 9.6.4, 11.4.1, and 13.12.3; *Sov. Phys. Semicond.* for Figs. 13.12.1 and 17.12.2; *Sov. Phys. Solid State* for Fig. 13.11.1; and *W. A. Benjamin Inc.* for Fig. 11.12.2.

CONTENTS OF OTHER VOLUMES

HANDBOOK ON PHYSICAL PROPERTIES OF SEMICONDUCTORS I
Group-IV Semiconductors

Sadao Adachi, Author

1 Diamond (C)
2 Silicon (Si)
3 Germanium (Ge)
4 Gray Tin (α-Sn)
5 Cubic Silicon Carbide (3C-SiC)
6 Hexagonal Silicon Carbide (2H-, 4H-, 6H-SiC, etc.)
7 Rhombohedral Silicon Carbide (15R-, 21R-, 24R-SiC, etc.)

HANDBOOK ON PHYSICAL PROPERTIES OF SEMICONDUCTORS II
III–V Compound Semiconductors

Sadao Adachi, Author

1 Cubic Boron Nitride (*c*-BN)
2 Hexagonal Boron Nitride (*h*-BN)
3 Boron Phosphide (BP)
4 Boron Arsenide (BAs)
5 Wurtzite Aluminum Nitride (*w*-AlN)
6 Cubic Aluminum Nitride (*c*-AlN)
7 Aluminum Phosphide (A1P)
8 Aluminum Arsenide (AlAs)
9 Aluminum Antimonide (AlSb)
10 Wurtzite Gallium Nitride (α-GaN)
11 Cubic Gallium Nitride (β-GaN)
12 Gallium Phosphide (GaP)
13 Gallium Arsenide (GaAs)
14 Gallium Antimonide (GaSb)
15 Indium Nitride (InN)
16 Indium Phosphide (InP)
17 Indium Arsenide (InAs)
18 Indium Antimonide (InSb)

Chapter 1

Magnesium Oxide (MgO)

1.1 STRUCTURAL PROPERTIES

1.1.1 Ionicity

Table 1.1.1 *Phillips's ionicity f_i for MgO [1.1].*

f_i
0.841

[1.1] J. C. Phillips, *Bonds and Bands in Semiconductors* (Academic, New York, 1973).

1.1.2 Elemental Isotopic Abundance and Molecular Weight

- **Isotopic abundance**

Table 1.1.2 *Isotopic abundance in percent for magnesium and oxygen [1.2].*

Isotope	% nat. abundance	Isotope	% nat. abundance
^{24}Mg	78.99	^{16}O	99.762
^{25}Mg	10.00	^{17}O	0.038
^{26}Mg	11.01		

[1.2] D. R. Lide, *CRC Handbook of Chemistry and Physics,* 78th Edition (CRC Press, Boca Raton, 1997).

• **Molecular weight**

Table 1.1.3 *Molecular (average atomic) weight M for MgO.*

M (amu)
40.3044

1.1.3 Crystal Structure and Space Group

Table 1.1.4 *Crystal structure and its space and pint groups for MgO.*

Crystal structure	Space group	Point group
Rocksalt (Cubic)	$Fm3m$	O_h^5

1.1.4 Lattice Constant and Its Related Parameters

• **Lattice constant, near-neighbor distance, etc.**

Table 1.1.5 *Lattice constant (a), near-neighbor distance (d), unit cube volume* (a^3)*, and molecular density* (d_M) *for MgO at 300 K.*

Parameter	Value
Lattice constant a (Å)	4.203 [1.3]
d (Cation–Anion) (Å)	2.1015*
Unit cube volume a^3 (10^{-23} cm^3)	7.425*
Molecular density d_M (10^{22} cm^{-3})	5.387*

[1.3] K. Hirata, K. Moriya, and Y. Waseda, *J. Mater. Sci.* **12,** 838 (1977).
*Calculated.

• **Crystal density**

Table 1.1.6 *Crystal density g for MgO at 300 K.**

g (g/cm^3)
3.606

*Calculated using a=4.203 Å.

1.1.5 Structural Phase Transition

Table 1.1.7 *Structural phase transition in MgO at high pressures.*

Structure	Transition pressure (GPa)
Rocksalt ($Fm3m$)	Normal pressure
	No phase transition up to 227 GPa [1.4]

[1.4] T. S. Duffy, R. J. Hemley, and H. Mao, *Phys. Rev. Lett.* **74**, 1371 (1995).

1.1.6 Cleavage Plane

Table 1.1.8 *Crystallographic plane most readily cleaved for MgO [1.5].*

Cleavage plane
(100)

[1.5] See, e.g., J. J. Gilman, *J. Appl. Phys.* **31,** 2208 (1960).

- **Surface energy**

Table 1.1.9 *Experimental surface energy for MgO (in J/m^2).*

Plane	Surface energy (J/m^2)	Comment
(100)	1.2	T=77 K [1.6]

[1.6] J. J. Gilman, *J. Appl. Phys.* **31,** 2208 (1960).

1.2 THERMAL PROPERTIES

1.2.1 Melting Point and Its Related Parameters

Table 1.2.1 *Melting point T_m and its pressure derivative dT_m/dp for MgO.*

Parameter	Value
Melting point T_m (K)	3040±100 [2.1]
	3250±20 [2.2]
Pressure coefficient dT_m/dp (°C/kbar)	+3.6 [2.1]

[2.1] A. Zerr and R. Boehler, *Nature* **371**, 506 (1994).
[2.2] C. Ronchi and M. Sheindlin, *J. Appl. Phys.* **90**, 3325 (2001).

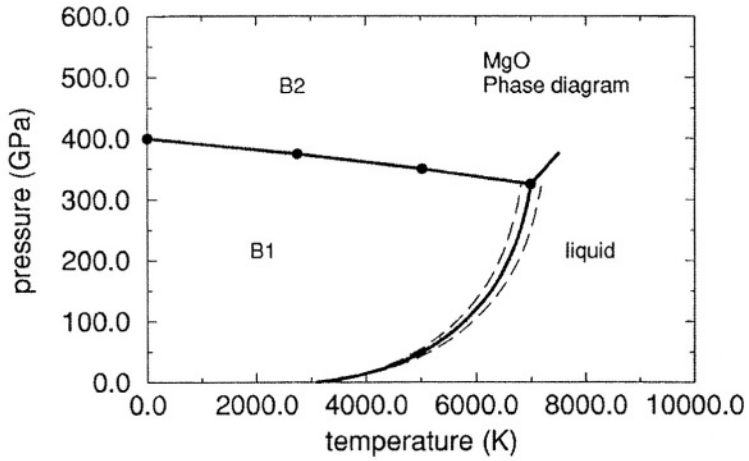

Fig. 1.2.1 Theoretical phase diagram of MgO. B1=NaC1 (six coordinated) structure; B2=CsCl (eight coordinated) structure. [From A. Strachan, T. Çağin, and W. A. Goddard III, *Phys. Rev. B* **60**, 15084 (1999).]

1.2.2 Specific Heat

Table 1.2.2 *Experimental specific heat C_p (at constant pressure) for MgO [2.3].*

Temperature (K)	C_p (J/g K)	Temperature (K)	C_p (J/g K)
4	0.00000728	140	0.404
6	0.0000247	150	0.452
7	0.0000395	160	0.509
8	0.0000599	170	0.543
9	0.0000849	180	0.593
10	0.000118	190	0.626
15	0.000396	200	0.664
20	0.000948	210	0.672
25	0.00190	220	0.729
30	0.00340	230	0.760
40	0.00914	240	0.788
50	0.0206	250	0.814
60	0.0400	260	0.841
70	0.0697	270	0.862
80	0.109	280	0.885
90	0.157	290	0.907
100	0.205	300	0.928
110	0.253	310	0.945
120	0.305	320	0.962
130	0.355		

[2.3] E. Gmelin, *Z. Naturf.* **24a**, 1794 (1969).

Table 1.2.3 *Experimental specific heat C_p (at constant pressure) for MgO [2.4].*

Temperature (K)	C_p (J/g K)	Temperature (K)	C_p (J/g K)
300	0.928	1100	1.276
400	1.061	1200	1.289
500	1.130	1300	1.301
600	1.173	1400	1.312
700	1.204	1500	1.323
800	1.227	1600	1.334
900	1.246	1700	1.346
1000	1.262	1800	1.358

[2.4] See, D. G. Isaak, O. L. Anderson, and T. Goto, *Phys. Chem. Miner.* **16,** 704 (1989).

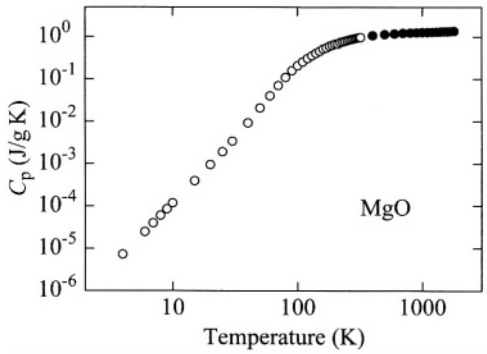

Fig. 1.2.2 Specific heat C_p (at constant pressure) versus temperature for MgO. The experimental data are taken from E. Gmelin [*Z. Naturf.* **24a**, 1794 (1969); open circles] and from D. G. Isaak, O. L. Anderson, and T. Goto [*Phys. Chem. Miner.* **16,** 704 (1989); solid circles].

1.2.3 Debye Temperature

Table 1.2.4 *Calorimetric Dbye temperature θ_D for MgO [2.5].*

Temperature (K)	θ_D (K)	Temperature (K)	θ_D (K)
0	945	100	743
5	944	110	743
10	943	120	747
15	940	140	753
20	936	160	757
30	913	180	757
40	880	200	758
50	835	220	758
60	803	240	758
70	778	260	757
80	760	280	752
90	747	300	745

[2.5] E. Gmelin, *Z. Naturf.* **24a**, 1794 (1969).

Table 1.2.5 *Debye temperature θ_D for MgO obtained from elasticity data [2.6].*

Temperature (K)	θ_D (K)	Temperature (K)	θ_D (K)
300	945	1100	875
400	937	1200	866
500	928	1300	857
600	920	1400	847
700	911	1500	838
800	902	1600	828
900	894	1700	820
1000	885	1800	811

[2.6] D. G. Isaak, O. L. Anderson, and T. Goto, *Phys. Chem. Miner.* **16**, 704 (1989).

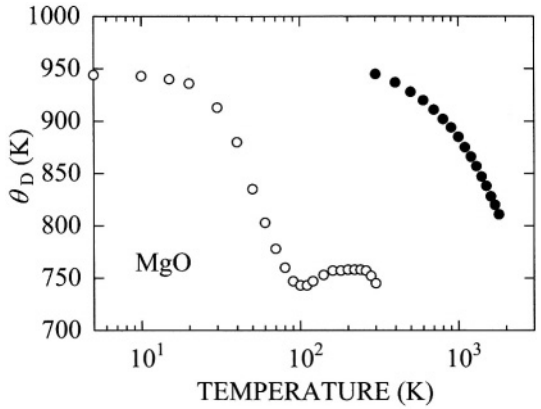

Fig. 1.2.3 Debye temperature θ_D for MgO. The data are obtained calorimetrically by E. Gmelin [*Z. Naturf.* **24a**, 1794 (1969); open circles] and from elasticity data by .D. G. Isaak, O. L. Anderson, and T. Goto [*Phys. Chem. Miner.* **16**, 704 (1989); solid circles].

1.2.4 Thermal Expansion Coefficient

Table 1.2.6 *Thermal expansion coefficient α_{th} for MgO [2.7].*

Temperature (K)	α_{th} (10^{-6} K^{-1})	Temperature (K)	α_{th} (10^{-6} K^{-1})
20	0.012	250	9.3
25	0.022	275	10.0
30	0.039	300	10.5
35	0.065	400	11.8
65	0.59	500	12.7
70	0.76	600	13.3
80	1.15	700	14.0
90	1.65	800	14.5
100	2.2	900	14.8
125	3.7	1000	15.0
150	5.0	1100	15.2
200	7.6	1200	15.3

[2.7] G. K. White and O. L. Anderson, *J. Appl. Phys.* **37**, 430 (1966).

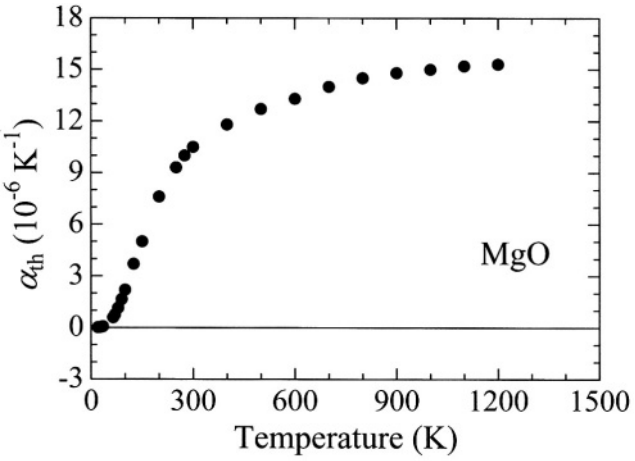

Fig. 1.2.4 Thermal expansion coefficient α_{th} versus temperature for MgO. The experimental data are taken from G. K. White and O. L. Anderson [*J. Appl. Phys.* **37**, 430 (1966)].

1.2.5 Thermal Conductivity and Diffusivity

Table 1.2.7 *Thermal conductivity K for MgO.* Thermal diffusivity can be calculated from a relation $D=K/(C_p \cdot g)$, where C_p is the specific heat at constant pressure and g is the crystal density.*

Temperature (K)	*K* (W/cm K)	Temperature (K)	*K* (W/cm K)
0.4	0.0008	27	21.0
0.5	0.0015	30	20.5
0.6	0.0026	35	19.2
0.7	0.0040	40	17.0
0.8	0.0060	45	14.3
0.9	0.0081	50	12.0
1	0.011	60	8.3
1.5	0.037	70	5.8
2	0.09	100	1.65

Table 1.2.7 *Continued.*

Temperature (K)	K (W/cm K)	Temperature (K)	K (W/cm K)
3	0.32	150	0.97
4	0.8	200	0.70
5	1.6	300	0.52
6	2.5	400	0.40
7	3.6	500	0.30
8	4.7	600	0.24
9	6.1	700	0.20
10	7.4	800	0.18
15	13.5	900	0.16
20	18.5	1000	0.15
25	20.7	1200	0.14

*The experimental data are taken for $T \leq 70$ K from D. S. Kupperman, G. Kurz, and H. Weinstock [*J. Low Temp. Phys.* **10,** 193 (1973)] and for $T \geq 100$ K from N. N. Kovalev, A. V. Petrov, and O. V. Sorokin [*Sov. Phys.– Solid State* **13,** 232 (1971)].

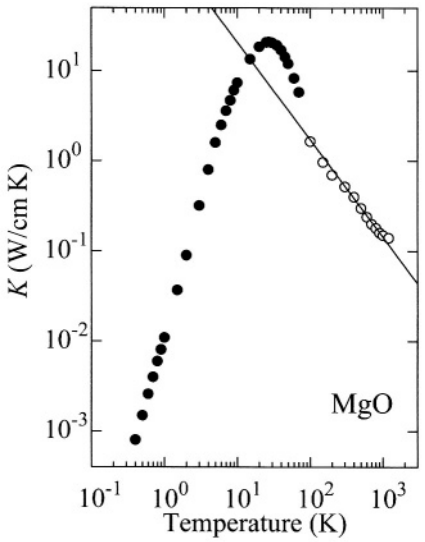

Fig. 1.2.5 Thermal conductivity K for MgO. The experimental data are taken for $T \leq 70$ K from D. S. Kupperman, G. Kurz, and H. Weinstock [*J. Low Temp. Phys.* **10,** 193 (1973); solid circles] and for $T \geq 100$ K from N. N. Kovalev, A. V. Petrov, and O. V. Sorokin [*Sov. Phys.– Solid State* **13,** 232 (1971); open circles]. The solid line represents the calculated result of $K = AT^n$ with $A = 250$ W/cm K$^{-0.08}$ and $n = -1.08$.

1.3 ELASTIC PROPERTIES

1.3.1 Elastic Constant

- **Room-temperature value and its temperature and pressure derivatives**

Table 1.3.1 *Elastic constant and its temperature and pressure derivatives for MgO at 300 K.*

Parameter	Value
Stiffness (10^{11} dyn/cm^2) [3.1]	
C_{11}	29.4
C_{12}	9.3
C_{44}	15.5

Table 1.3.1 *Continued.*

Parameter	Value
Compliance (10^{-13} cm^2/dyn) [3.1]	
S_{11}	4.01
S_{12}	–0.96
S_{44}	6.47
dC_{ij}/dT (10^7 dyn/cm^2 K) [3.2]	
C_{11}	–58.5
C_{12}	+7.5
C_{44}	–12.6
dC_{ij}/dp [3.1]	
C_{11}	9.38
C_{12}	1.94
C_{44}	1.15

[3.1] *Numerical Data and Functional Relationships in Science and Technology,* edited by K.-H. Hellwege and A. M. Hellwege, Landolt–Börnstein, New Series, Group III, Vol. 11 (Springer, Berlin, 1979).
[3.2] D. G. Isaak, O. L. Anderson, and T. Goto, *Phys. Chem. Minerals* **16,** 704 (1989).

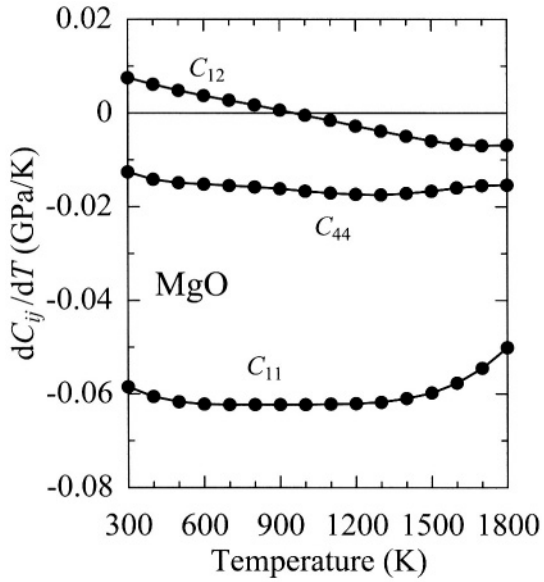

Fig. 1.3.1 Temperature derivative of the elastic stiffness constant versus temperature for MgO. The experimental data are taken from D. G. Isaak, O. L. Anderson, and T. Goto [*Phys. Chem. Minerals* **16,** 704 (1989)].

● **Pressure dependence**

Table 1.3.2 *Pressure variation of the elastic stiffness constant in MgO at 300 K [3.3].*

$$C_{ij}(p) = C_{ij}(0)+ap+bp^2$$

C_{ij}	$C_{ij}(0)$ (GPa)	a	b
C_{11}	297.9	9.05	–0.045
C_{12}	95.8	1.34	–0.001
C_{44}	154.4	0.84	+0.003

[3.3] S. V. Sinogeikin and J. D. Bass, *Phys. Rev. B* **59**, R14141 (1999).

1.3.2 Third-Order Elastic Constant

Table 1.3.3 *Third-order elastic constant of MgO [3.4].*

Modulus	Value (10^{12} dyn/cm^2)
C_{111}	–49.0
C_{112}	–0.95
C_{123}	–0.69
C_{144}	+1.13
C_{166}	–6.59
C_{456}	+1.47

[3.4] *Numerical Data and Functional Relationships in Science and Technology,* edited by K.-H. Hellwege and A. M. Hellwege, Landolt–Börnstein, New Series, Group III, Vol. 11 (Springer, Berlin, 1979).

1.3.3 Young's Modulus, Poisson's Ratio, and Similar

- **Young's modulus**

Table 1.3.4 *Young's modulus Y for MgO at 300K.**

Crystallographic plane	Y (10^{12} dyn/cm^2)
(100) plane	
[001] direction	2.49
[011] direction	3.18
(110) plane	
[001] direction	2.49
[111] direction	3.51
(111) plane	3.18

*Calculated using S_{11}=4.01, S_{12}= –0.96, and S_{44}=6.47 (all in 10^{-13} cm^2/dyn).

- **Poisson's ratio**

Table 1.3.5 *Poisson's ratio P for MgO at 300 K.**

Crystallographic plane	P
(100) plane	
m=[010], n=[001]	0.239
m=[011], n=[$0\bar{1}1$]	0.029
(110) plane	
m=[001], n=[$1\bar{1}0$]	0.239
m=[$\bar{1}11$], n=[$1\bar{1}\bar{2}$]	0.134
(111) plane	0.213

*Calculated using S_{11}=4.01, S_{12}= –0.96, and S_{44}=6.47 (all in 10^{-13} cm^2/dyn).

• **Bulk modulus, shear modulus, etc.**

Table 1.3.6 *Bulk modulus, B_u, pressure derivative of B_u, dB_u/dp, shear modulus, C_s, isotropy factor, A, linear compressibility, C_o, Caucy ratio, C_a, and Born ratio, B_o, for MgO at 300 K.*

Parameter	Value
B_u (10^{12} dyn/cm^2)	1.60 [3.5]
dB_u/dp	4.0±0.1 [3.6], [3.7]
C_s (10^{12} dyn/cm^2)	1.01 [3.5]
A	0.648 [3.5]
C_o (10^{-13} cm^2/dyn)	2.08 [3.5]
C_a	0.600 [3.5]
B_o	0.916 [3.5]

[3.5] Calculated using C_{11}=29.4, C_{12}=9.3, and C_{44}=15.5 (all in 10^{11} dyn/cm^2).
[3.6] T. S. Duffy, R. J. Hemley, and H. Mao, *Phys. Rev. Lett.* **74**, 1371 (1995).
[3.7] S. V. Sinogeikin and J. D. Bass, *Phys. Rev. B* **59**, R14141 (1999).

1.3.4 Microhardness

Table 1.3.7 *Knoop hardness H for MgO (in GPa).*

(001)		(110)			Slip system	Ref.
<100>	<110>	<001>	<1$\bar{1}$1>	<1$\bar{1}$0>		
4.0	8.0				{110}, <1$\bar{1}$0>	[3.8]
4.0	7.8	4.2	9.3	8.1	{110}, <1$\bar{1}$0>	[3.9]

[3.8] F. P. Bowden and C. A. Brookes, *Proc. Roy. Soc. London A* **295**, 244 (1966).
[3.9] C. A. Brookes, J. B. O'Neill, and B. A. W. Redfern, *Proc. Roy. Soc. London A* **322**, 73 (1971).

1.3.5 Sound Velocity

Table 1.3.8 *Sound velocity propagating in MgO at 300 K.* LA=longitudinal acoustic; TA1, TA2=transverse acoustic.*

Propagation direction	Mode	Sound velocity (10^5 cm/s)
[100]	LA	9.03
[100]	TA1, TA2	6.56
[110]	LA	9.83
[110]	TA1	5.28
[110]	TA2	6.56
[111]	LA	10.1
[111]	TA1, TA2	5.74

*Calculated using C_{11}=2.94×10^{12} dyn/cm^2, C_{12}=9.3×10^{11} dyn/cm^2, C_{44}=1.55×10^{12} dyn/cm^2, and g=3.606 g/cm^3.

1.4 PHONONS AND LATTICE VIBRONIC PROPERTIES

1.4.1 Phonon Dispersion Relation

- **Dispersion curve**

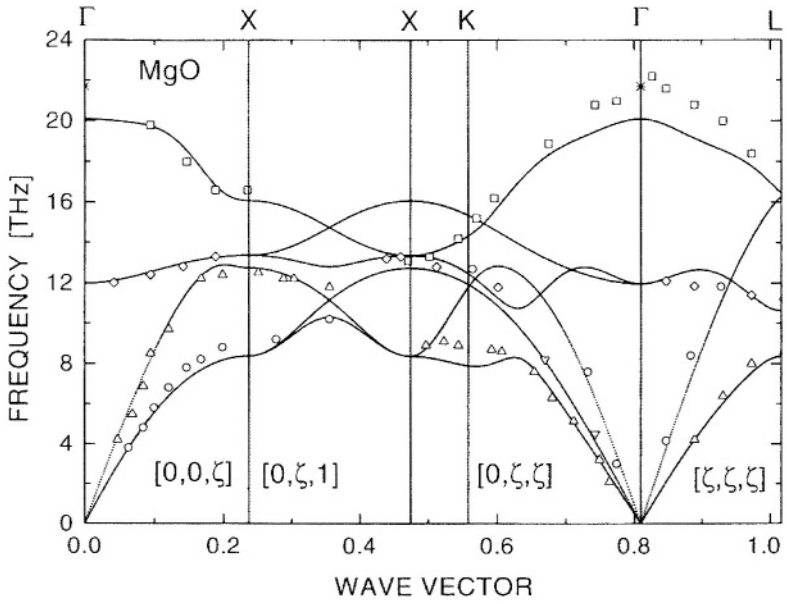

Fig. 1.4.1 Calculated phonon dispersion curves for MgO. The symbols represent the experimental data. [From K. Parlinski, J. Łażewski, and Y. Kawazoe, *J. Phys. Chem. Solids* **61,** 87 (2000).]

- **Phonon density of states**

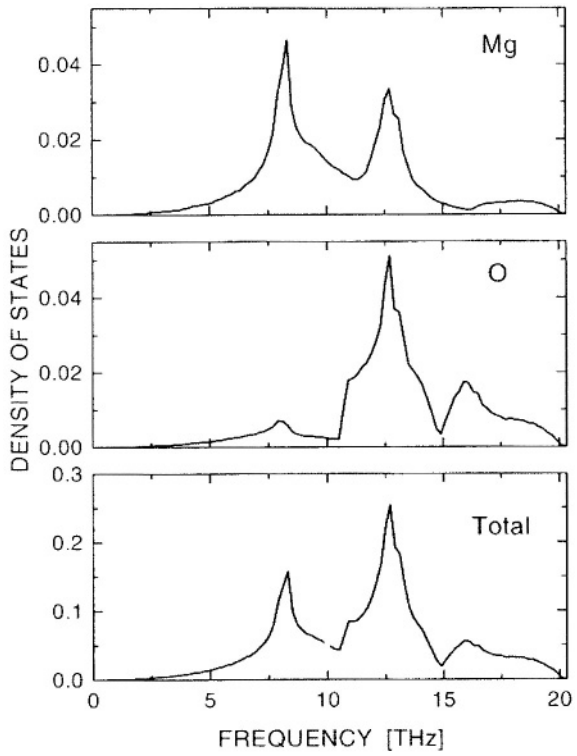

Fig. 1.4.2 Phonon density of states for Mg, O atoms and total density of states for MgO. The distributions are normalized to 1/6, 1/6, and 1, respectively. [From K. Parlinski, J. Łażewski, and Y. Kawazoe, *J. Phys. Chem. Solids* **61,** 87 (2000).]

1.4.2 Phonon Frequency

• Room-temperature value

Table 1.4.1 *Long-wavelength (q→0) and zone-boundary phonon frequencies for MgO.*

Critical point	Phonon	Phonon frequency (cm^{-1})				
		a	b	c	d	e
Γ	TO	401	398		402	405.5±0.5
	LO	725	740		718	
X	TA		306			
	LA		434	443.3±6.7		
	TO		422			
	LO		520	554.0±6.7		
L	TA		296	287		
	LA		519			
	TO		341	367		
	LO		684			

[a] J. R. Jasperse, A. Kahan, J. N. Plendl, and S. S. Mitra, *Phys. Rev.* **146,** 526 (1966).
[b] J.-P. Mon, in *Light Scattering Spectra of Solids,* edited by G. B. Wright (Springer, Berlin, 1969), p. 121.
[c] M. J. L. Sangster, G. Peckham, and D. H. Saunderson, *J. Phys. C: Solid State Phys.* **3**, 1026 (1970).
[d] J. B. Bates and M. H. Brooker, *J. Phys. Chem. Solids* **32**, 2403 (1971).
[e] S. Cunsolo, P. Dore, S. Lupi, P. Maselli, and C. P. Varsamis, *Infrared Phys.* **33**, 539 (1992).

• Temperature dependence

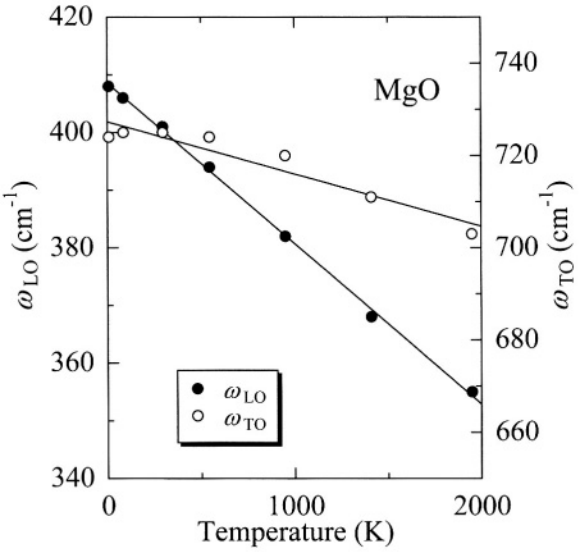

Fig. 1.4.3 Temperature dependence of the long-wavelength (*q*→0) phonon frequency in MgO. The experimental data are taken from J. R. Jasperse, A. Kahan, J. N. Plendl, and S. S. Mitra [*Phys. Rev.* **146,** 526 (1966)].

• Temperature and/or pressure coefficient

Table 1.4.2 *Linear temperature coefficient $d\omega_q/dT$ of the long-wavelength (q→0) phonon frequency in MgO.**

Coefficient	Phonon	Value (10^{-2} cm^{-1}/K)
$d\omega_q/dp$	TO	−2.8
	LO	−1.1

*Estimated from data by J. R. Jasperse, A. Kahan, J. N. Plendl, and S. S. Mitra [*Phys. Rev.* **146,** 526 (1966)].

1.4.3 Mode Grüneisen Parameter

Table 1.4.3 *Theoretical mode Grüneisen parameter for the long-wavelength ($q \to 0$) phonons in MgO [4.1].*

Critical point	Phonon	Mode Grüneisen parameter	
		Rigid ion	Polarizable ion
Γ	TO	3.03	3.90
	LO	1.64	1.42

[4.1] J. R. Jasperse, A. Kahan, J. N. Plendl, and S. S. Mitra, *Phys. Rev.* **146**, 526 (1966).

1.4.4 Phonon Deformation Potential

No detailed data are available for MgO.

1.5 COLLECTIVE EFFECTS AND RELATED PROPERTIES

1.5.1 Piezoelectric Constant

No detailed data are available for MgO.

1.5.2 Fröhlich Coupling Constant

No detailed data are available for MgO.

1.6 ENERGY-BAND STRUCTURE: ENERGY-BAND GAPS

1.6.1 Basic Properties

- **Electronic energy-band structure**

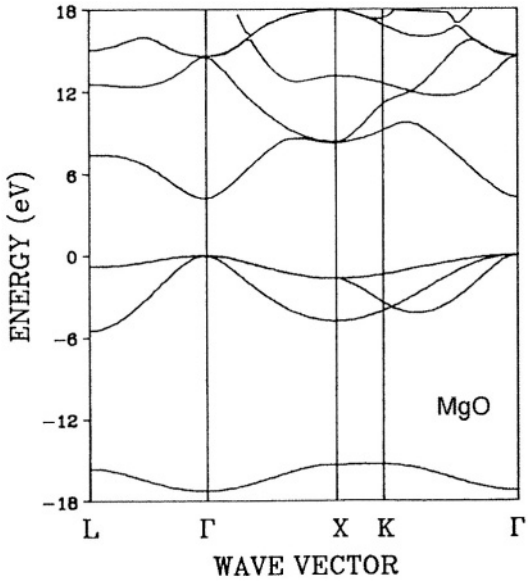

Fig. 1.6.1 Electronic energy-band structure of MgO as calculated by the first-principles orthogonalized linear combination of atomic orbitals method. [From Y.-N. Xu and W. Y. Ching, *Phys. Rev. B* **43**, 4461 (1991).]

• **Electronic density of states**

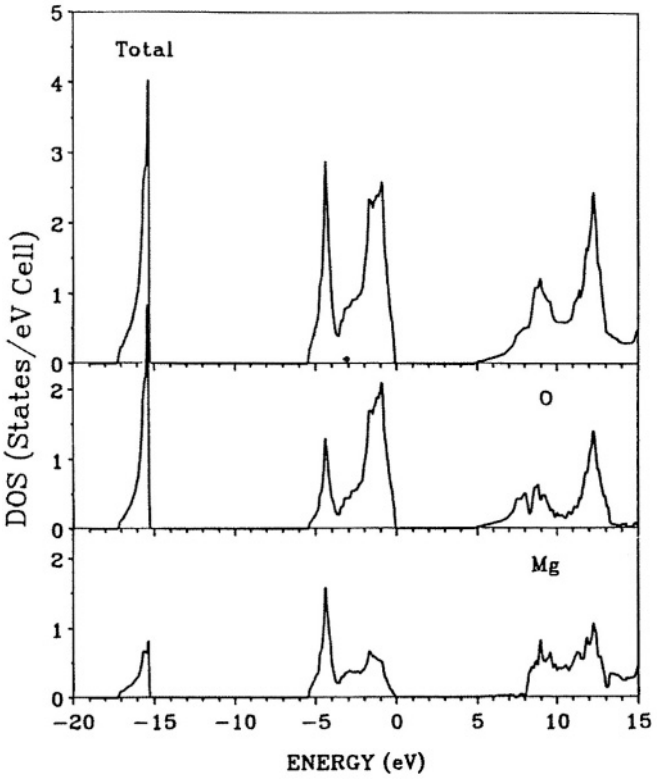

Fig. 1.6.2 Calculated total density of states (DOS) for MgO and partial DOS for O and Mg atoms. [From Y.-N. Xu and W. Y. Ching, *Phys. Rev. B* **43**, 4461 (1991).]

• **Energy eigenvalue**

Table 1.6.1 *Energy eigenvalues at the Γ, X, and L points for the valence and first few conduction bands of MgO [6.1].*

Critical point	Level	Value (eV)	
		Calc.	Exper.
Γ	Γ_{15}^{v}	0.00	0.00
	Γ_{1}^{c}	5.2	7.77–7.833
	$\Gamma_{25'}^{c}$	15.7	
X	$X_{4'}^{v}$	–4.3	
	$X_{5'}^{v}$	–1.5	
	X_{3}^{c}	9.0	
	X_{1}^{c}	9.6	
	X_{5}^{c}	13.7	
L	L_{2}^{v}	–4.9	
	L_{3}^{v}	–0.8	
	$L_{2'}^{c}$	8.1	
	$L_{3'}^{c}$	12.9	
	L_{1}^{c}	16.4	

[6.1] U. Schönberger and F. Aryasetiawan, *Phys. Rev. B* **52**, 8788 (1995).

1.6.2 E_0-Gap Region

- **Temperature dependence**

Table 1.6.2 *E_0-gap energy for MgO determined at various temperatures.*

Temperature (K)	E_0 (eV)	Ref.
77	7.77±0.01	[6.2]
85	7.833±0.020	[6.3]
100	7.65*	[6.4]
292	7.6*	[6.5]
300	7.55*	[6.4]
	7.9±0.1	[6.6]
400	7.45*	[6.4]
Recommended T=300 K value: 7.8 eV		

[6.2] D. M. Roessler and W. C. Walker, *Phys. Rev.* **159,** 733 (1967).
[6.3] R. C. Whited, C. J. Flaten, and W. C. Walker, *Solid State Commun.* **13,** 1903 (1973).
[6.4] J. L. Freeouf, *Phys. Rev. B* **7**, 3810 (1973).
[6.5] R. H. French, *Phys. Scripta* **41,** 404 (1990).
[6.6] M. W. Williams and E. T. Arakawa, *J. Appl. Phys.* **38,** 5272 (1967).
*Excitonic energy gap.

Table 1.6.3 *Spin-orbit-splitoff energy Δ_0 for MgO.**

Δ_0 (eV)	Comment
0.022±0.006	T=85 K [6.7]

[6.7] R. C. Whited, C. J. Flaten, and W. C. Walker, *Solid State Commun.* **13**, 1903 (1973).
*Note that Δ_0 may not vary with temperature if one supposes the valence-band rigidity of the II–VI compounds.

- **Temperature and/or pressure coefficient**

Table 1.6.4 *Linear temperature coefficient of the E_0-gap energy for MgO.*

Coefficient	Value	Comment
dE_0/dT (10^{-4} eV/K)	–9.2 *	T=292–1573 K [6.8]

[6.8] R. H. French, *Phys. Scripta* **41**, 404 (1990).
*Excitonic energy gap.

1.6.3 Higher-Lying Direct Gap

- **Theoretical and experimental values**

Table 1.6.5 *Theoretically and experimentally obtained higher-lying direct-gap energies for MgO.*

Band gap	Theoretical (eV)	Experimental (eV)
E_1 ($L_3^v \rightarrow L_2^c$)	11.48 [6.9]	10.8 (T=300 K, [6.13])
	15.56 [6.10]	11.0 (T=300 K, [6.14])
	8.9 [6.11]	11.0 (T=300 K, [6.15])
	9.37 [6.12]	

Table 1.6.5 *Continued.*

Band gap	Theoretical (eV)	Experimental (eV)
E_2 ($X_5^v \rightarrow X_3^c, X_1^c$)	15.79 [6.9]	13.3 (T=300 K, [6.13])
	17.56 [6.10]	13.2 (T=300 K, [6.14])
	10.5, 11.1 [6.11]	13.45 (T=300 K, [6.15])
	11.06 [6.12]	
E_1' ($L_3^v \rightarrow L_3^c$)	13.7 [6.11]	16.8 (T=300 K, [6.13])
		17.0 (T=300 K, [6.14])
		17.6 (T=300 K, [6.15])

[6.9] R. Pandey, J. E. Jaffe, and A. B. Kunz, *Phys. Rev. B* **43**, 9228 (1991).
[6.10] T. Kotani, *Phys. Rev. B* **50**, 14816 (1994).
[6.11] U. Schönberger and F. Aryasetiawan, *Phys. Rev. B* **52**, 8788 (1995).
[6.12] T. Kotani and H. Akai, *Phys. Rev. B* **54**, 16502 (1996).
[6.13] D. M. Roessler and W. C. Walker, *Phys. Rev.* **159**, 733 (1967).
[6.14] M. W. Williams and E. T. Arakawa, *J. Appl. Phys.* **38,** 5272 (1967).
[6.15] J. L. Freeouf, *Phys. Rev. B* **7**, 3810 (1973).

1.6.4 Lowest Indirect Gap

- **Theoretical value**

Table 1.6.6 *Lowest indirect-gap energy for MgO.*

Band gap	Value (eV)	Ref.
E_g^L ($\Gamma_{15}^v \rightarrow L_2^c$)	8.1	[6.16]
	8.80	[6.17]
E_g^X ($\Gamma_{15}^v \rightarrow X_3^c, X_1^c$)	9.0, 9.6	[6.16]
	9.87	[6.17]

[6.16] U. Schönberger and F. Aryasetiawan, *Phys. Rev. B* **52**, 8788 (1995).
[6.17] T. Kotani and H. Akai, *Phys. Rev. B* **54**, 16502 (1996).

1.6.5 Conduction-Valley Energy Separation

Table 1.6.7 *Conduction-valley energy separation ΔE_g estimated from theoretical E_0, E_g^X, and E_g^L values for MgO.*

ΔE_g (eV)		Ref.
$L_2^c - \Gamma_1^c$	$X_3^c - \Gamma_1^c$	
2.9	3.8	[6.18]
2.85	3.92	[6.19]

[6.18] U. Schönberger and F. Aryasetiawan, *Phys. Rev. B* **52**, 8788 (1995).
[6.19] T. Kotani and H. Akai, *Phys. Rev. B* **54**, 16502 (1996).

1.6.6 Direct–Indirect–Gap Transition Pressure

No detailed data are available for MgO.

1.7 ENERGY-BAND STRUCTURE: ELECTRON AND HOLE EFFECTIVE MASSES

1.7.1 Electron Effective Mass: Γ Valley

- **Theoretical value**

Table 1.7.1 *Theoretically obtained electron effective mass m_e^{Γ} at the Γ valley for MgO.*

m_e^{Γ}/m_0	Technique
0.35	Linear combination of atomic orbital method [7.1]

[7.1] Y.-N. Xu and W. Y. Ching, *Phys. Rev. B* **43**, 4461 (1991).

1.7.2 Electron Effective Mass: Satellite Valley

No detailed data are available for MgO.

1.7.3 Hole Effective Mass

- **Band mass, cyclotron mass, etc.**

Table 1.7.2 *Theoretically obtained band masses (m_{HH}, m_{LH}) in MgO [7.2].*

Mass	Value (m_0)
m_{HH} ([001] direction)	1.60
([011] direction)	1.80, 4.10
([111] direction)	2.77
m_{LH} ([001] direction)	0.35
([011] direction)	0.32
([111] direction)	0.31

[7.2] Linear combination of atomic orbital method [Y.-N. Xu and W. Y. Ching, *Phys. Rev. B* **43**, 4461 (1991)].

1.8 ELECTRONIC DEFORMATION POTENTIAL

1.8.1 Intravalley Deformation Potential: Γ Point

No detailed data are available for MgO.

1.8.2 Intravalley Deformation Potential: High-Symmetry Points

No detailed data are available for MgO.

1.8.3 Intervalley Deformation Potential

No detailed data are available for MgO.

1.9 ELECTRON AFFINITY AND SCHOTTKY BARRIER HEIGHT

1.9.1 Electron Affinity

Table 1.9.1 *Electron affinity χ_s for MgO.*

χ_s (eV)	Comment
−4 ~ +1	(see [9.1])
Negative value (−2.5)	[9.1]

[9.1] A. M. Stoneham and M. M. D. Ramos, *J. Solid State Chem.* **106**, 2 (1993).

1.9.2 Schottky Barrier Height

No detailed data are available for MgO.

1.10 OPTICAL PROPERTIES

1.10.1 Summary of Optical Dispersion Relations

- **$\varepsilon(E)$ and n^*(E) spectra**

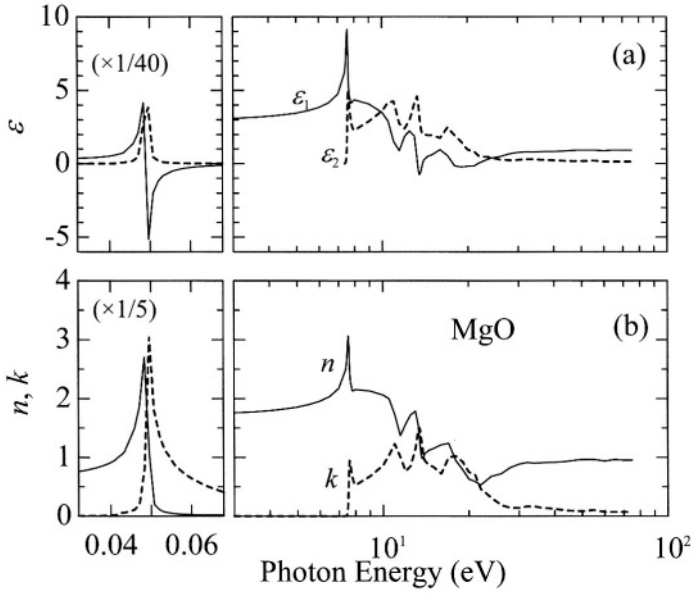

Fig. 1.10.1 (a) Complex dielectric-constant [$\varepsilon(E)=\varepsilon_1(E)+i\varepsilon_2(E)$] and (b) complex refractive-index spectra [$n^*(E)=n(E)+ik(E)$] for MgO at 300 K. The numerical data are taken from tabulation by S. Adachi [*Optical Constants of Crystalline and Amorphous Semiconductors: Numerical Data and Graphical Information* (Kluwer Academic, Boston, 1999)].

- **$\alpha(E)$ and $R(E)$ spectra**

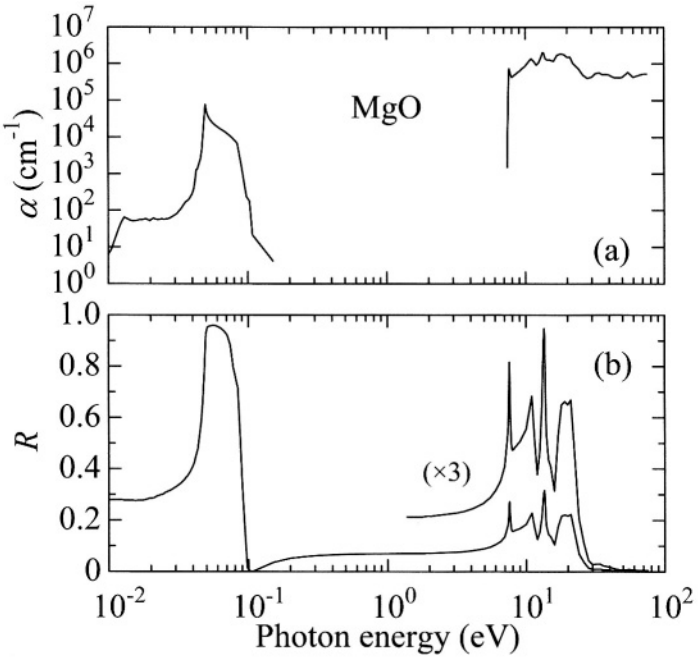

Fig. 1.10.2 (a) Absorption [$\alpha(E)$] and (b) normal-incidence reflectivity spectra [$R(E)$] for MgO at 300 K. The numerical data are taken from tabulation by S. Adachi [*Optical Constants of Crystalline and Amorphous Semiconductors: Numerical Data and Graphical Information* (Kluwer Academic, Boston, 1999)].

1.10.2 The Reststrahlen Region

- **Static and high-frequency dielectric constants**

Table 1.10.1 *Room-temperature static and high-frequency dielectric constants ε_s and ε_∞ for MgO.*

ε_s	ε_∞	Ref.
	2.99*	[10.1]
9.64	3.01	[10.2]
	2.944*	[10.3]
9.958		[10.4]
9.833±0.001		[10.5]
9.830		[10.6]
	3.3	[10.7]
9.8	3.1	Mean value

[10.1] R. E. Stephens and I. H. Malitson, *J. Res. Natl. Bur. Stand.* **49**, 249 (1952).
[10.2] J. R. Jasperse, A. Kahan, J. N. Plendl, and S. S. Mitra, *Phys. Rev.* **146**, 526 (1966).
[10.3] I. M. Boswarva, *Phys. Rev. B* **1**,1698 (1970).
[10.4] R. A. Bartels and P. A. Smith, *Phys. Rev. B* **7**, 3885 (1973).
[10.5] J. Fontanella, C. Andreen, and D. Shuele, *J. Appl. Phys.* **45**, 2852 (1974).
[10.6] M. Wintersgill, J. Fontanella, C. Andreen, and D. Schuele, *J. Appl. Phys.* **50,** 8259 (1979).
[10.7] S. Cunsolo, P. Dore S. Lupi, P. Maselli, and C. P. Varsamis, *Infrared Phys.* **33**, 539 (1992).
* $\varepsilon_\infty = n_\infty^2$.

Table 1.10.2 *Linear temperature and pressure coefficients of the static (ε_s) and high-frequency dielectric constants (ε_∞) for MgO near 300 K and normal pressure.*

Coefficient	Value	Ref.
$d\varepsilon_s/dT$ (10^{-4} K^{-1})	9.4	[10.8]
	9.8	[10.9]
	9.9	[10.10]
$d\varepsilon_s/dp$ (GPa^{-1})	–0.179	[10.9]
$d\varepsilon_\infty/dT$ (10^{-4} K^{-1})		
$d\varepsilon_\infty/dp$ (GPa^{-1})		

[10.8] Estimated from data by J. R. Jasperse, A. Kahan, J. N. Plendl, and S. S. Mitra [*Phys. Rev.* 146, 526 (1966)].
[10.9] R. A. Bartels and P. A. Smith, *Phys. Rev. B* **7**, 3885 (1973).
[10.10] Estimated from data by M. Wintersgill, J. Fontanella, C. Andreen, and D. Schuele [*J. Appl. Phys.* **50,** 8259 (1979)].

- **Reststrahlen parameter**

Table 1.10.3 *A set of the reststrahlen parameters for MgO [10.11].*

$$\varepsilon(\omega) = \varepsilon_\infty + \sum_i \frac{S_i^2}{\omega_i^2 - \omega^2 - i\omega\gamma_i}$$

ε_∞	ω_i (cm^{-1})		S_i (cm^{-1})		γ_i (cm^{-1})		Comment
	i=1	i=2	i=1	i=2	i=1	i=2	
3.3	406.5±0.5	655±2	1094±4	88±3	9.5±0.3	85±2	T=20 K
3.3	406*	654.5*	1095*	93*	9.8±0.5	86*	T=60 K
3.3	406*	654.0*	1096*	97*	11.5±0.5	88*	T=100 K
3.3	406*	653.5*	1097*	102*	13.5±0.5	90*	T=150 K
3.3	405.5±0.5	652±2	1100±4	116±3	16.7±0.3	95±2	T=295 K

[10.11] S. Cunsolo, P. Dore S. Lupi, P. Maselli, and C. P. Varsamis, *Infrared Phys.* **33**, 539 (1992).
*Fixed.

1.10.3 At or Near the Fundamental Absorption Edge

- **Free-exciton binding energy and related parameters**

Table 1.10.4 *Free-exciton binding (Rydberg) energy G for MgO.*

G (meV)	Comment
80	T=77 K [10.12]
145±20	T=85 K [10.13]

[10.12] D. M. Roessler and W. C. Walker, *Phys. Rev.* **159,** 733 (1967).
[10.13] R. C. Whited, C. J. Flaten, and W. C. Walker, *Solid State Commun.* **13,** 1903 (1973).

Table 1.10.5 *Free-exciton parameters (G=binding energy; a_B=1st-orbital Bohr radius; μ=reduced mass) at the fundamental absorption edge of MgO.*

G (meV)	a_B (Å)	μ (m_0)	Comment
145	16 *	0.102 *	Direct exciton

*Calculated using ε_∞=3.1.

- **Refractive index**

Table 1.10.6 *Refractive index n near the fundamental absorption edge of MgO at 300 K [10.14].*

E (eV)	λ (μm)	n	E (eV)	λ (μm)	n
1.38	0.898	1.724	4.13	0.300	1.804
1.46	0.849	1.725	4.96	0.250	1.853
1.55	0.800	1.726	5	0.248	1.858
1.65	0.751	1.728	5.5	0.225	1.901
1.77	0.700	1.729	6	0.207	1.958
1.91	0.649	1.732	6.5	0.191	2.039
2.07	0.599	1.735	7	0.177	2.176
2.25	0.551	1.739	7.4	0.168	2.494
2.48	0.500	1.744	7.45	0.166	2.603
2.76	0.449	1.751	7.48	0.166	2.701
3.1	0.400	1.762	7.5	0.165	2.793
3.54	0.350	1.770			

[10.14] See, S. Adachi, *Optical Constants of Crystalline and Amorphous Semiconductors: Numerical Data and Graphical Information* (Kluwer Academic, Boston, 1999).

- **Refractive index: Temperature dependence**

Table 1.10.7 *Temperature coefficient of the refractive index $n^{-1}(dn/dT)$ in the long-wavelength limit for MgO [10.15].*

$\frac{1}{n}\frac{dn}{dT}$ (10^{-5} K^{-1})
1.4

[10.15] R. E. Stephens and I. H. Malitson, *J. Res. Natl. Bur. Stand.* **49**, 249 (1952).

- **Refractive index: Pressure dependence**

Table 1.10.8 *Pressure coefficient of the refractive index $n^{-1}(dn/dp)$ in the long-wavelength limit for MgO [10.16].*

$\frac{1}{n}\frac{dn}{dp}$ (10^{-12} Pa^{-1})	Ref.
−1.0	[10.16]
−1.58	[10.17]

[10.16] R. M. Waxler and C. E. Weir, *J. Res. Natl. Bur. Stand. A* **69**, 325 (1965).
[10.17] K. Vedam and E. D. D. Schmidt, *Phys. Rev.* **146,** 548 (1966).

- **Fundamental absorption edge: Temperature dependence**

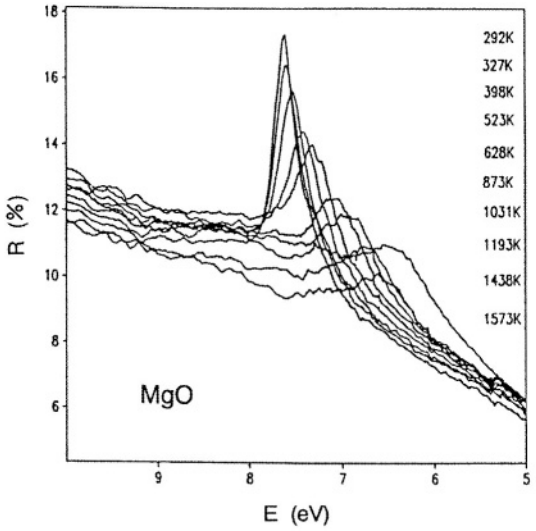

Fig. 1.10.3 Fundamental reflectivity spectra R at the $\Gamma_{15}\rightarrow\Gamma_{15}$ exciton region of MgO at temperatures between 292 and 1573 K. [From R. H. French, *Phys. Scripta* **41**, 404 (1990).]

1.10.4 The Interband Transition Region

- **Fundamental optical spectra**

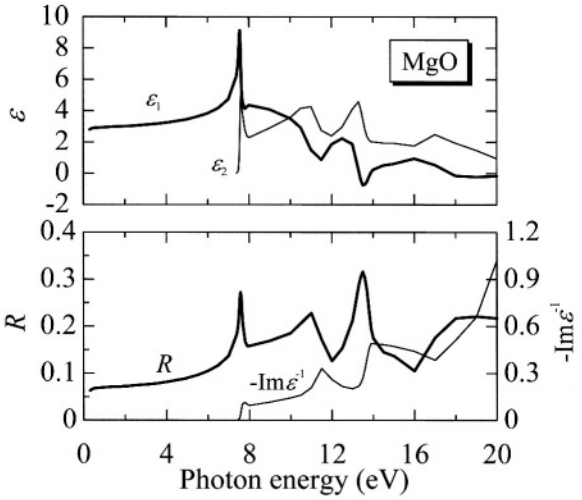

Fig. 1.10.4 Complex dielectric function, $\varepsilon(E)=\varepsilon_2(E)+i\varepsilon_2(E)$, fundamental reflectivity, $R(E)$, and energy-loss function, $-\mathrm{Im}\varepsilon^{-1}(E)$, for MgO at 300 K. The experimental data are taken from tabulation by S. Adachi [*Optical Constants of Crystalline and Amorphous Semiconductors: Numerical Data and Graphical Information* (Kluwer Academic, Boston, 1999)].

1.10.5 Free-Carrier Absorption and Related Phenomena

No detailed data are available for MgO.

1.11 ELASTOOPTIC, ELECTROOPTIC, AND NONLINEAR OPTICAL PROPERTIES

1.11.1 Elastooptic Effect

- **Photoelastic constant**

Table 1.11.1 *Photoelastic constant p_{ij} in the static limit ($E\rightarrow 0$ eV) for MgO.*

$p_{11}-p_{12}$	p_{44}
–0.257	–0.096

1.11.2 Linear Electrooptic Constant

No detailed data are available for MgO.

1.11.3 Quadratic Electrooptic Constant

No detailed data are available for MgO.

1.11.4 Franz–Keldysh Effect

No detailed data are available for MgO.

1.11.5 Nonlinear Optical Constant

- **Third-order nonlinear optical susceptibility**

Table 1.11.2 *Third-order nonlinear optical susceptibility* $\chi^{(3)}_{ijkl}(-3\omega;\omega,\omega,\omega)$ *in the static limit* $(\hbar\omega \to 0\ eV)$ *for MgO.*

$\lvert\chi^{(3)}_{ijkl}\rvert$ $(10^{-13}$ esu)*		Comment.
$\lvert\chi^{(3)}_{1111}\rvert$	$\lvert\chi^{(3)}_{1212}\rvert$	
0.40	0.21	Calc. [11.1]
0.294	0.142	Exper. (see [11.1])

[11.1] W. Y. Ching, F. Gan, and M.-Z. Huang, *Phys. Rev. B* **52**, 1596 (1995).

*1 $m^2/V^2 = 9\times10^8/4\pi$ esu.

1.12 CARRIER TRANSPORT PROPERTIES

1.12.1 Low-Field Mobility: Electrons

Since MgO is an insulator with a band gap of ≥7 eV, its electrical characterization has been limited to high resistivity measurement [see, e.g., C. M. Osburn and R. W. Vest, *J. Am. Ceram. Soc.* **54**, 428 (1971)].

1.12.2 Low-Field Mobility: Holes

No detailed data are available for MgO.

1.12.3 High-Field Transport: Electrons

No detailed data are available for MgO.

1.12.4 High-Field Transport: Holes

No detailed data are available for MgO.

1.12.5 Minority-Carrier Transport: Electrons in *p*-Type Materials

No detailed data are available for MgO.

1.12.6 Minority-Carrier Transport: Holes in *n*-Type Materials

No detailed data are available for MgO.

1.12.7 Impact Ionization Coefficient

No detailed data are available for MgO.

Chapter 2

Zincblende Magnesium Sulphide (β-MgS)

2.1 STRUCTURAL PROPERTIES

2.1.1 Ionicity

Table 2.1.1 *Phillips's ionicity f_i for β-MgS [1.1].*

f_i
0.786

[1.1] J. C. Phillips, *Bonds and Bands in Semiconductors* (Academic, New York, 1973).

2.1.2 Elemental Isotopic Abundance and Molecular Weight

- **Isotopic abundance**

Table 2.1.2 *Isotopic abundance in percent for magnesium and sulfur [1.2].*

Isotope	% nat. abundance	Isotope	% nat. abundance
^{24}Mg	78.99	^{32}S	95.02
^{25}Mg	10.00	^{33}S	0.75
^{26}Mg	11.01	^{34}S	4.21
		^{36}S	0.02

[1.2] D. R. Lide, *CRC Handbook of Chemistry and Physics,* 78th Edition (CRC Press, Boca Raton, 1997).

• **Molecular weight**

Table 2.1.3 *Molecular (average atomic) weight M for β-MgS.*

M (amu)
56.371

2.1.3 Crystal Structure and Space Group

Table 2.1.4 *Crystal structure and its space and pint groups for β-MgS.*

Crystal structure	Space group	Point group
Zincblende (Cubic)	$F\bar{4}3m$	T_d

2.1.4 Lattice Constant and Its Related Parameters

• **Lattice constant**

Table 2.1.5 *Lattice constant a for β-MgS at 300 K.*

a (Å)	Ref.
5.62	[1.3]
5.59	[1.4]

[1.3] H. Okuyama, K. Nakano, T. Miyajima, and K. Akimoto, *J. Cryst. Growth* **117**, 139 (1992); H. Okuyama, Y. Kishita, and A. Ishibashi, *Phys. Rev. B* **57**, 2257 (1998).
[1.4] K. Uesugi, T. Obinata, I. Suemune, H. Kumano, and J. Nakahara, *Appl. Phys. Lett.* **68**, 844 (1996); I. Suemune, T. Obinata, K. Uesugi, H. Suzuki, H. Kumano, H. Nashiki, and J. Nakahara, *J. Cryst. Growth* **170**, 480 (1997)..

• **Lattice constant, near-neighbor distance, etc.**

Table 2.1.6 *Lattice constant (a), near-neighbor distance (d), unit cube volume (a^3), and molecular density (d_M) for β-MgS at 300 K.*

Parameter	Value
Lattice constant a (Å)	5.62
d (Cation–Anion) (Å)	2.43*
d (Cation–Cation) (Å)	3.97*
Unit cube volume a^3 (10^{-22} cm^3)	1.78*
Molecular density d_M (10^{22} cm^{-3})	2.25*

*Calculated.

• **Crystal density**

Table 2.1.7 *Crystal density g for β-MgS at 300 K.**

g (g/cm^3)
2.11

*Calculated using a=5.62 Å.

2.1.5 Structural Phase Transition

Theoretically, a phase transition B3 (zincblende)→B1 (rocksalt) is obtained to occur at around 1 GPa [A. Lichanot, A. Dargelos, C. Larrieu, and R. Oriando, *Solid State Commun.* **90**, 189 (1994)].

2.1.6 Cleavage Plane

Table 2.1.8 *Crystallographic plane most readily cleaved for β-MgS.**

Cleavage plane
(100)

*Expected.

2.2 THERMAL PROPERTIES

2.2.1 Melting Point and Its Related Parameters

Table 2.2.1 *Melting point T_m and its related parameter for MgS.*

Parameter	Value
Melting point T_m (K)	2783* [2.1]
Entropy of fusion ΔS_m (cal/mol K)	16.49* [2.1]

[2.1] J. A. Van Vechten, *Phys. Rev. B* **7**, 1479 (1973).
*Theoretical value.

2.2.2 Specific Heat

No detailed data are available for β-MgS.

2.2.3 Debye Temperature

No detailed data are available for β-MgS.

2.2.4 Thermal Expansion Coefficient

No detailed data are available for β-MgS.

2.2.5 Thermal Conductivity and Diffusivity

No detailed data are available for β-MgS.

2.3 ELASTIC PROPERTIES

2.3.1 Elastic Constant

• Room-temperature value

Table 2.3.1 *Elastic stiffness and compliance constants for β-MgS at 300 K.*

Parameter	Value
Stiffness (10^{11} dyn/cm^2) [3.1]	
C_{11}	8.88
C_{12}	5.53
C_{44}	3.87
Compliance (10^{-12} cm^2/dyn) [3.2]	
S_{11}	2.16
S_{12}	–0.83
S_{44}	2.58

[3.1] Estimated from a C_{ij}–a (lattice constant) relation.
[3.2] Calculated from C_{ij} values.

2.3.2 Third-Order Elastic Constant

No detailed data are available for β-MgS.

2.3.3 Young's Modulus, Poisson's Ratio, and Similar

• Young's modulus

Table 2.3.2 *Young's modulus Y for β-MgS at 300 K.**

Crystallographic plane	Y (10^{11} dyn/cm^2)
(100) plane	
[001] direction	4.63
[011] direction	7.63
(110) plane	
[001] direction	4.63
[111] direction	9.73
(111) plane	7.63

*Calculated using S_{11}=2.16, S_{12}= –0.83, and S_{44}=2.58 (all in 10^{-12} cm^2/dyn).

• Poisson's ratio

Table 2.3.3 *Poisson's ratio P for β-MgS at 300 K.**

Crystallographic plane	P
(100) plane	
m=[010], n=[001]	0.383
m=[011], n=[0$\bar{1}$1]	–0.016
(110) plane	
m=[001], n=[1$\bar{1}$0]	0.383
m=[1$\bar{1}$1], n=[11$\bar{2}$]	0.255

Table 2.3.3 *Continued.*

Crystallographic plane	*P*
(111) plane	0.416

*Calculated using S_{11}=2.16, S_{12}= –0.83, and S_{44}=2.58 (all in 10^{-12} cm^2/dyn).

• Bulk modulus, shear modulus, etc.

Table 2.3.4 *Bulk modulus, B_u, shear modulus, C_s, isotropy factor, A, linear compressibility, C_o, Caucy ratio, C_a, and Born ratio, B_o, for β-MgS at 300 K [3.3].*

Parameter	Value
B_u (10^{11} dyn/cm^2)	6.65
C_s (10^{11} dyn/cm^2)	1.68
A	0.433
C_o (10^{-13} cm^2/dyn)	5.02
C_a	1.43
B_o	1.17

[3.3] Calculated using C_{11}=8.88, C_{12}=5.53, and C_{44}=3.87 (all in 10^{11} dyn/cm^2).

Table 2.3.5 *Bulk modulus, B_u, and its pressure derivative, dB_u/dp, for β-MgS.*

B_u (GPa)	dB_u/dp	Comment
60.4		Calc. [3.4]
57.5	3.7	Calc. [3.5]
78.96	3.75	Calc. [3.6]

[3.4] A. Lichanot, A. Dargelos, C. Larrieu, and R. Orlando, *Solid State Commun.* **90**, 189 (1994).
[3.5] S.-G. Lee and K. J. Chang, *Phys. Rev. B* **52**, 191 (1995).
[3.6] G. Kalpana, B. Palanivel, R. M. Thomas, and M. Rajagopalan, *Physica B* **222**, 223 (1996).

2.3.4 Microhardness

No detailed data are available for β-MgS.

2.3.5 Sound Velocity

Table 2.3.6 *Sound velocity propagating in β-MgS at 300 K.* LA=longitudinal acoustic; TA1, TA2=transverse acoustic.*

Propagation direction	Mode	Sound velocity (10^5 cm/s)
[100]	LA	6.49
[100]	TA1, TA2	4.28
[110]	LA	7.24
[110]	TA1	2.82
[110]	TA2	4.28
[111]	LA	7.48
[111]	TA1, TA2	3.38

*Calculated using C_{11}=8.88×10^{11} dyn/cm^2, C_{12}=5.53×10^{11} dyn/cm^2, C_{44}=3.87×10^{11} dyn/cm^2, and *g*=2.11 g/cm^3.

2.4 PHONONS AND LATTICE VIBRONIC PROPERTIES

2.4.1 Phonon Dispersion Relation

No detailed data are available for β-MgS.

2.4.2 Phonon Frequency

• Room-temperature value

Table 2.4.1 *Long-wavelength ($q \to 0$) and zone-boundary phonon frequencies for β-MgS [4.1].*

Critical point	Phonon	Phonon frequency (cm^{-1})
Γ	TO	327±6
	LO	425±1
X	TA	
	LA	
	TO	
	LO	
L	TA	
	LA	
	TO	
	LO	

[4.1] D. Wolverson, D. M. Bird, C. Bradford, K. A. Prior, and B. C. Cavenett, *Phys. Rev. B* **64**, 113203 (2001).

2.4.3 Mode Grüneisen Parameter

No detailed data are available for β-MgS.

2.4.4 Phonon Deformation Potential

No detailed data are available for β-MgS.

2.5 COLLECTIVE EFFECTS AND RELATED PROPERTIES

2.5.1 Piezoelectric Constant

No detailed data are available for β-MgS.

2.5.2 Fröhlich Coupling Constant

No detailed data are available for β-MgS.

2.6 ENERGY-BAND STRUCTURE: ENERGY-BAND GAPS

2.6.1 Basic Properties

- **Electronic energy-band structure**

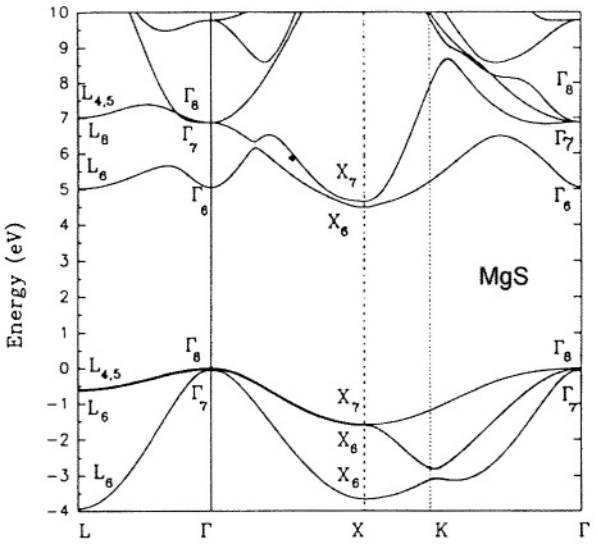

Fig. 2.6.1 Electronic energy-band structure of β-MgS as calculated by an empirical pseudopotential method. [From K. L. Teo, Y. P. Feng, M. F. Li, T. C. Chong, and J. B. Xia, *Semicond. Sci. Technol.* **9**, 349 (1994).]

- **Energy eigenvalue**

Table 2.6.1 *Energy eigenvalues at the Γ, X, and L points for the valence band in β-MgS [6.1].*

Critical point	Level	Value (eV)
Γ	Γ_6^v (Γ_1^v)	−11.5
	Γ_7^v (Γ_{15}^v)	−0.098
	Γ_8^v	0.00
X	X_6^v (X_1^v)	−11.0
	X_6^v (X_3^v)	−3.88
	X_6^v (X_5^v)	−1.41
	X_7^v	−1.37
L	L_6^v (L_1^v)	−11.2
	L_6^v (L_1^v)	−3.81
	L_6^v (L_3^v)	−0.56
	$L_{4,5}^v$	−0.50

[6.1] Q. Guo, H. C. Poon, Y. P. Feng, and C. K. Ong, *Semicond. Sci. Technol.* **10**, 677 (1995).

2.6.2 E_0-Gap Region

- **Temperature dependence**

Table 2.6.2 *E_0-gap (excitonic) energy for β-MgS determined at various temperatures.*

Temperature (K)	E_0 (eV)	Comment
10	4.53	$Zn_{1-x}Mg_xS$ ($x \rightarrow 1.0$) [6.2]
300	4.45±0.2	$Zn_{1-x}Mg_xS$ ($x \rightarrow 1.0$) [6.3]

[6.2] K. Ichino, K. Ueyama, M. Yamamoto, H. Kariya, H. Miyata, H. Misasa, M. Kitagawa, and H. Kobayashi, *J. Appl. Phys.* **87**, 4249 (2000).
[6.3] H. Okuyama, Y. Kishita, and A. Ishibashi, *Phys. Rev. B* **57**, 2257 (1998).

Table 2.6.3 *Spin–orbit–splitoff energy Δ_0 for β-MgS.* *

Δ_0 (eV)
0.07

*Since this quantity is primarily determined by the anion atomic spin–orbit splitting, it is assumed to have the nearly same value as that for β-ZnS. It is also noted that Δ_0 may not vary with temperature if one supposes the valence-band rigidity of the II–VI compounds.

2.6.3 Higher-Lying Direct Gap

No detailed data are available for β-MgS.

2.6.4 Lowest Indirect Gap

- **Theoretical value**

Table 2.6.4 *Lowest indirect-gap energy for β-MgS.*

Band gap	Value (eV)	Ref.
$E_g^X(\Gamma_8^v \rightarrow X_6^c)$	3.7	[6.4]

[6.4] G. Kalpana, B. Palanivel, R. M. Thomas, and M. Rajagopalan, *Physica B* **222**, 223 (1996).

2.6.5 Conduction-Valley Energy Separation

No detailed data are available for β-MgS.

2.6.6 Direct–Indirect-Gap Transition Pressure

No detailed data are available for β-MgS.

2.7 ENERGY-BAND STRUCTURE: ELECTRON AND HOLE EFFECTIVE MASSES

2.7.1 Electron Effective Mass: Γ Valley

Table 2.7.1 *Electron effective mass m_e^Γ at the Γ valley for β-MgS.*

m_e^Γ/m_0
0.225 *

*Estimated from a plot of E_0 versus m_e^Γ for a number of the group-IV, III–V, and II–VI semiconductors in the cubic structure (see figure, below).

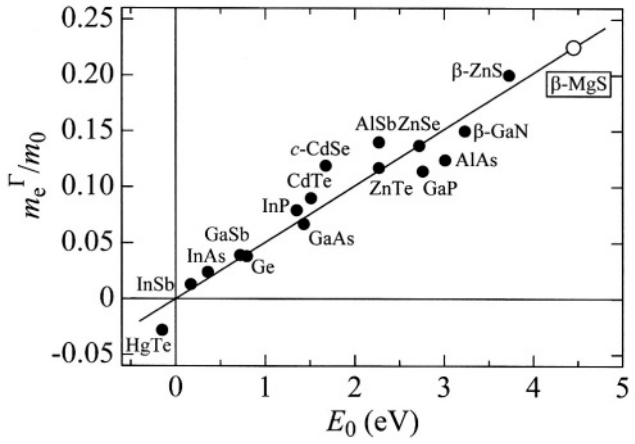

Fig. 2.7.1 Electron effective mass m^Γ_e/m_0 versus E_0 for a number of the group-IV, III–V, and II–VI semiconductors in the cubic structure. From this plot, we can estimate m^Γ_e value for β-MgS to be $0.225m_0$.

2.7.2 Electron Effective Mass: Satellite Valley

No detailed data are available for β-MgS.

2.7.3 Hole Effective Mass

- **Luttinger's valence-band parameter**

Table 2.7.2 *Luttinger's valence-band parameter γ_i for β-MgS (in $\hbar^2/2m_0$).*

γ_1	γ_2	γ_3
2.62	0.38	0.91

*Estimated from a plot of E_0 versus γ_i for some cubic group-IV, III–V, and II–VI semiconductors (see figure, below).

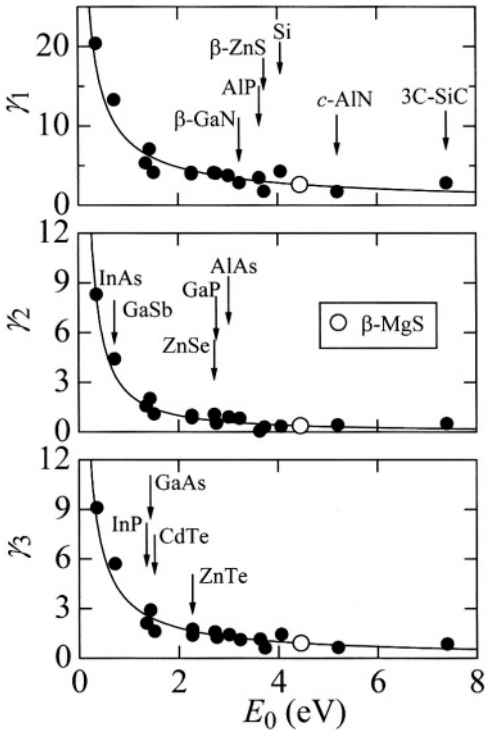

Fig. 2.7.2 Luttinger's valence-band parameter γ_i versus E_0 for a number of the group-IV, III–V, and II–VI semiconductors in the cubic structure. From this plot, we can estimate γ_i values for β-MgS to be γ_1=2.62, γ_2=0.38, and γ_3=0.91 (in $\hbar^2/2m_0$).

• **Band mass, cyclotron mass, etc.**

Table 2.7.3 *Band (m_{HH}, m_{LH}), density-of-states heavy-hole (m_{HH}*), averaged light-hole (m_{LH}*), and spherically-averaged heavy-hole (m_{HH}^s) and light-hole masses (m_{LH}^s) in β-MgS.**

Mass	Value (m_0)
m_{HH} ([001] direction)	0.54
m_{LH} ([001] direction)	0.30
m_{HH} ([111] direction)	1.25
m_{LH} ([111] direction)	0.23
m_{HH}*	0.93
m_{LH}*	0.25
m_{HH}^s	0.82
m_{LH}^s	0.25

*Calculated using a set of the Luttinger's parameters, γ_1=2.62, γ_2=0.38, and γ_3=0.91.

• **Spin–orbit–splitoff hole effective mass**

Table 2.7.4 *Spin–orbit–splitoff hole effective mass m_{SO} for β-MgS.*

m_{SO}/m_0
0.38

*Obtained from the Luttinger's parameter (m_{SO}=1/γ_1).

2.8 ELECTRONIC DEFORMATION POTENTIAL

2.8.1 Intravalley Deformation Potential: Γ Point

• **Optical-phonon deformation potential**

Table 2.8.1 *Optical-phonon deformation potential d_0 at the Γ-valence band of β-MgS.*

d_0 (eV)	Comment
15.2	Calc. [8.1]

[8.1] L. Brey, N. E. Christensen, and M. Cardona, *Phys. Rev. B* **36**, 2638 (1987).

2.8.2 Intravalley Deformation Potential: High-Symmetry Points

No detailed data are available for β-MgS.

2.8.3 Intervalley Deformation Potential

No detailed data are available for β-MgS.

2.9 ELECTRON AFFINITY AND SCHOTTKY BARRIER HEIGHT

2.9.1 Electron Affinity

No detailed data are available for β-MgS.

2.9.2 Schottky Barrier Height

No detailed data are available for β-MgS.

2.10 OPTICAL PROPERTIES

2.10.1 Summary of Optical Dispersion Relations

No detailed data are available for β-MgS.

2.10.2 The Reststrahlen Region

No detailed data are available for β-MgS.

2.10.3 At or Near the Fundamental Absorption Edge

No detailed data are available for β-MgS.

2.10.4 The Interband Transition Region

No detailed data are available for β-MgS.

2.10.5 Free-Carrier Absorption and Related Phenomena

No detailed data are available for β-MgS.

2.11 ELASTOOPTIC, ELECTROOPTIC, AND NONLINEAR OPTICAL PROPERTIES

2.11.1 Elastooptic Effect

No detailed data are available for β-MgS.

2.11.2 Linear Electrooptic Constant

No detailed data are available for β-MgS.

2.11.3 Quadratic Electrooptic Constant

No detailed data are available for β-MgS.

2.11.4 Franz–Keldysh Effect

No detailed data are available for β-MgS.

2.11.5 Nonlinear Optical Constant

No detailed data are available for β-MgS.

2.12 CARRIER TRANSPORT PROPERTIES

2.12.1 Low-Field Mobility: Electrons

No detailed data are available for β-MgS.

2.12.2 Low-Field Mobility: Holes

No detailed data are available for β-MgS.

2.12.3 High-Field Transport: Electrons

- **LO-phonon-scattering-limited electron saturation drift velocity**

Table 2.12.1 *Calculated LO-phonon-scattering-limited electron saturation drift velocity $v_{e,sat}$ in the lowest-conduction-band valley α for β-MgS at 300 K.**

$$v_{e,sat}^{\alpha} = \left(\frac{8\hbar\omega_{LO}}{3\pi m_c^{\alpha}} \right)^{1/2}$$

Valley	$v_{e,sat}$ (10^7 cm/s)
Γ	1.9

*Calculated with $m_c^{\Gamma} = 0.225 m_0$ and $\omega_{LO} = 425$ cm^{-1}.

2.12.4 High-Field Transport: Holes

No detailed data are available for β-MgS.

2.12.5 Minority-Carrier Transport: Electrons in *p*-Type Materials

No detailed data are available for β-MgS.

2.12.6 Minority-Carrier Transport: Holes in *n*-Type Materials

No detailed data are available for β-MgS.

2.12.7 Impact Ionization Coefficient

No detailed data are available for β-MgS.

Chapter 3

Zincblende Magnesium Selenide (β-MgSe)

3.1 STRUCTURAL PROPERTIES

3.1.1 Ionicity

Table 3.1.1 *Phillips's ionicity f_i for β-MgSe [1.1].*

f_i
0.790

[1.1] J. C. Phillips, *Bonds and Bands in Semiconductors* (Academic, New York, 1973).

3.1.2 Elemental Isotopic Abundance and Molecular Weight

- **Isotopic abundance**

Table 3.1.2 *Isotopic abundance in percent for magnesium and selenium [1.2].*

Isotope	% nat. abundance	Isotope	% nat. abundance
^{24}Mg	78.99	^{74}Se	0.89
^{25}Mg	10.00	^{76}Se	9.36
^{26}Mg	11.01	^{77}Se	7.63
		^{78}Se	23.78
		^{80}Se	49.61
		^{82}Se	8.73

[1.2] D. R. Lide, *CRC Handbook of Chemistry and Physics,* 78th Edition (CRC Press, Boca Raton, 1997).

• **Molecular weight**

Table 3.1.3 *Molecular (average atomic) weight M for β-MgSe.*

M (amu)
103.27

3.1.3 Crystal Structure and Space Group

Table 3.1.4 *Crystal structure and its space and pint groups for β-MgSe.*

Crystal structure	Space group	Point group
Zincblende (Cubic)	$F\bar{4}3m$	T_d

3.1.4 Lattice Constant and Its Related Parameters

• **Lattice constant**

Table 3.1.5 *Lattice constant a for β-MgSe at 300 K.*

a (Å)	Ref.
5.873	[1.3]
5.89	[1.4]
5.91	[1.5]
5.91	[1.6]
5.96	[1.7]
5.908	[1.8]
5.91	Recommended

[1.3] S.-G. Lee and K. J. Chang, *Phys. Rev. B* **52**, 1918 (1995).
[1.4] H. Okuyama, K. Nakano, T. Miyajima, and K. Akimoto, *J. Cryst. Growth* **117**, 139 (1992).
[1.5] B. Jobst, D. Hommel, U. Lunz, T. Gerhard, and G. Landwehr, *Appl. Phys. Lett.* **69**, 97 (1996).
[1.6] F. Firszt, S. Łęgowski, H. Męczyńska, H. L. Oczkowski, W. Osińska, J. Szatkowski, W. Paszkowicz, and Z. M. Spolnik, *J. Cryst. Growth* **159**, 167 (1996).
[1.7] F. Jiang, Q. Liao, G. Fan, C. Xiong, X. Peng, C. Pan, and N. Liu, *J. Cryst. Growth* **183**, 289 (1998).
[1.8] I. Miotkowski, R. Vogelgesang, H. Alawadhi, M. J. Seong, A. K. Ramdas, S. Miotkowska, and W. Paszkowicz, *J. Cryst. Growth* **203**, 51 (1999).

• **Lattice constant, near-neighbor distance, etc.**

Table 3.1.6 *Lattice constant (a), near-neighbor distance (d), unit cube volume (a^3), and molecular density (d_M) for β-MgSe at 300 K.*

Parameter	Value
Lattice constant a (Å)	5.91
d (Cation–Anion) (Å)	2.56*
d (Cation–Cation) (Å)	4.18*
Unit cube volume a^3 (10^{-22} cm^3)	2.06*
Molecular density d_M (10^{22} cm^{-3})	1.94*

*Calculated.

● **Crystal density**

Table 3.1.7 *Crystal density g for β-MgSe at 300 K.**

g (g/cm^3)
3.32

*Calculated using a=5.91 Å.

3.1.5 Structural Phase Transition

No detailed data are available for β-MgSe.

3.1.6 Cleavage Plane

Table 3.1.8 *Crystallographic plane most readily cleaved for β-MgSe.**

Cleavage plane
(100)

*Expected.

3.2 THERMAL PROPERTIES

3.2.1 Melting Point and Its Related Parameters

Table 3.2.1 *Melting point T_m and its related parameter for MgSe.*

Parameter	Value
Melting point T_m (K)	~1560 (see [2.1])
Entropy of fusion ΔS_m (cal/mol K)	16.48* [2.1]

[2.1] J. A. Van Vechten, *Phys. Rev. B* **7**, 1479 (1973).
*Theoretical value.

3.2.2 Specific Heat

No detailed data are available for β-MgSe.

3.2.3 Debye Temperature

No detailed data are available for β-MgSe.

3.2.4 Thermal Expansion Coefficient

No detailed data are available for β-MgSe.

3.2.5 Thermal Conductivity and Diffusivity

No detailed data are available for β-MgSe.

3.3 ELASTIC PROPERTIES

3.3.1 Elastic Constant

• Room-temperature value

Table 3.3.1 *Elastic stiffness and compliance constants for β-MgSe at 300 K.*

Parameter	Value
Stiffness (10^{11} dyn/cm^2) [3.1]	
C_{11}	7.58
C_{12}	4.86
C_{44}	3.17
Compliance (10^{-12} cm^2/dyn) [3.2]	
S_{11}	2.64
S_{12}	−1.03
S_{44}	3.15

[3.1] Estimated from a C_{ij}–a (lattice constant) relation.
[3.2] Calculated from C_{ij} values.

3.3.2 Third-Order Elastic Constant

No detailed data are available for β-MgSe.

3.3.3 Young's Modulus, Poisson's Ratio, and Similar

• Young's modulus

Table 3.3.2 *Young's modulus Y for β-MgSe at 300 K.**

Crystallographic plane	Y (10^{11} dyn/cm^2)
(100) plane	
[001] direction	3.79
[011] direction	6.28
(110) plane	
[001] direction	3.79
[111] direction	8.04
(111) plane	6.28

*Calculated using S_{11}=2.64, S_{12}=−1.03, and S_{44}=3.15 (all in 10^{-12} cm^2/dyn).

• Poisson's ratio

Table 3.3.3 *Poisson's ratio P for β-MgSe at 300 K.**

Crystallographic plane	P
(100) plane	
m=[010], n=[001]	0.390
m=[011], n=[0$\bar{1}$1]	−0.011
(110) plane	
m=[001], n=[1$\bar{1}$0]	0.390
m=[1$\bar{1}$1], n=[11$\bar{2}$]	0.267

Table 3.3.3 *Continued.*

Crystallographic plane	P
(111) plane	0.428

*Calculated using S_{11}=2.64, S_{12}= −1.03, and S_{44}=3.15 (all in 10^{-12} cm^2/dyn).

- **Bulk modulus, shear modulus, etc.**

Table 3.3.4 *Bulk modulus, B_u, shear modulus, C_s, isotropy factor, A, linear compressibility, C_o, Caucy ratio, C_a, and Born ratio, B_o, for β-MgSe at 300K [3.3].*

Parameter	Value
B_u (10^{11} dyn/cm^2)	5.77
C_s (10^{11} dyn/cm^2)	1.36
A	0.429
C_o (10^{-13} cm^2/dyn)	5.78
C_a	1.53
B_o	1.16

[3.3] Calculated using C_{11}=7.58, C_{12}=4.86, and C_{44}=3.17 (all in 10^{11} dyn/cm^2).

Table 3.3.5 *Bulk modulus, B_u, and its pressure derivative, dB_u/dp, for β-MgSe.*

B_u (GPa)	dB_u/dp	Comment
58	2.89	Calc. [3.4]
47.0	4.0	Calc. [3.5]
64.75	3.87	Calc. [3.6]
47.8	4.04	Calc. [3.7]
48.0		Calc. (see [3.8])

[3.4] R. Pandey and A. Sutjianto, *Solid State Commun.* **91**, 269 (1994).
[3.5] S.-G. Lee and K. J. Chang, *Phys. Rev. B* **52**, 191 (1995).
[3.6] G. Kalpana, B. Palanivel, R. M. Thomas, and M. Rajagopalan, *Physica B* **222**, 223 (1996).
[3.7] P. E. Van Camp, V. E.Van Doren, and J. L. Martins, *Phys. Rev. B* **55**, 775 (1997).
[3.8] M.Wörz, E. Griebl, Th. Reisinger, R. Flierl, B. Haserer, T. Semmler, T. Frey, and W. Gebhardt, *Phys. Status Solidi B* **202**, 805 (1997).

3.3.4 Microhardness

No detailed data are available for β-MgSe.

3.3.5 Sound Velocity

Table 3.3.6 *Sound velocity propagating in β-MgSe at 300 K.* LA=longitudinal acoustic; TA1, TA2=transverse acoustic.*

Propagation direction	Mode	Sound velocity (10^5 cm/s)
[100]	LA	4.78
[100]	TA1, TA2	3.09
[110]	LA	5.32
[110]	TA1	2.02
[110]	TA2	3.09

Table 3.3.6 *Continued.*

Propagation direction	Mode	Sound velocity (10^5 cm/s)
[111]	LA	5.49
[111]	TA1, TA2	2.43

*Calculated using C_{11}=7.58×10^{11} dyn/cm^2, C_{12}=4.86×10^{11} dyn/cm^2, C_{44}=3.17×10^{11} dyn/cm^2, and g=3.32 g/cm^3.

3.4 PHONONS AND LATTICE VIBRONIC PROPERTIES

3.4.1 Phonon Dispersion Relation

No detailed data are available for β-MgSe.

3.4.2 Phonon Frequency

- **Room-temperature value**

Table 3.4.1 *Long-wavelength ($q \to 0$) and zone-boundary phonon frequencies for β-MgSe.*

Critical point	Phonon	Phonon frequency (cm^{-1})	
		a	b
Γ	TO	237	237
	LO	340	340
X	TA		
	LA		
	TO		
	LO		
L	TA		
	LA		
	TO		
	LO		

[a]D. Huang, C. Jin, D. Wang, X. Liu, J. Wang, and X. Wang, *Appl. Phys. Lett.* **67**, 3611 (1995).
[b]M. Kozielski, M. Szybowicz, F. Firszt, S. Legowski, H. Meczynska, J. Szatkowski, and W. Paszkowicz, *Cryst. Res. Technol.* **34**, 699 (1999).

3.4.3 Mode Grüneisen Parameter

No detailed data are available for β-MgSe.

3.4.4 Phonon Deformation Potential

No detailed data are available for β-MgSe.

3.5 COLLECTIVE EFFECTS AND RELATED PROPERTIES

3.5.1 Piezoelectric Constant

No detailed data are available for β-MgSe.

3.5.2 Fröhlich Coupling Constant

No detailed data are available for β-MgSe.

3.6 ENERGY-BAND STRUCTURE: ENERGY-BAND GAPS

3.6.1 Basic Properties

- **Electronic energy-band structure**

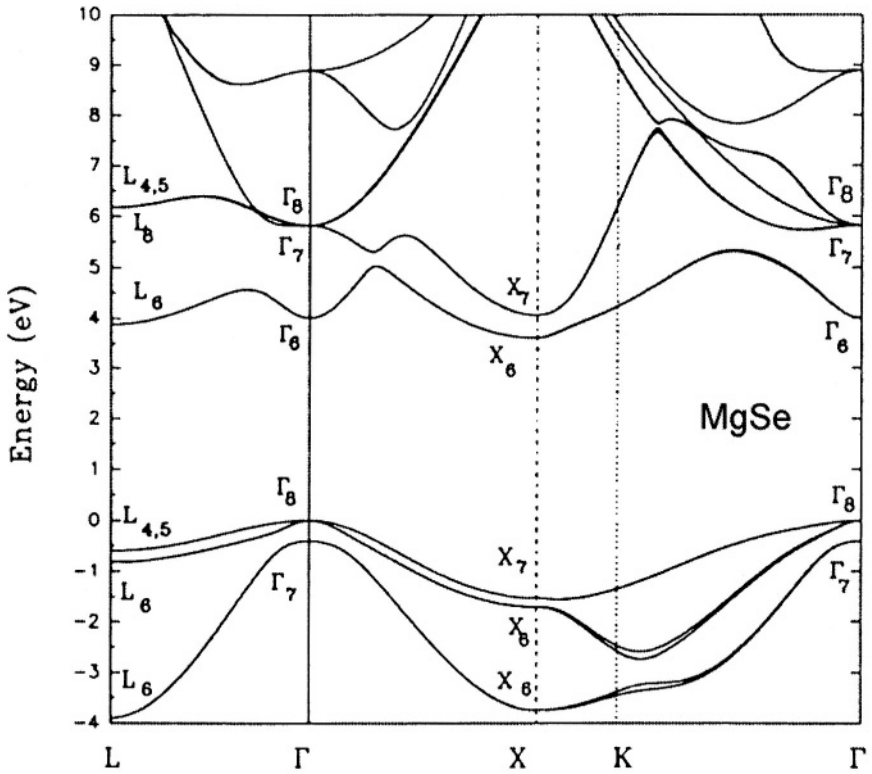

Fig. 3.6.1 Electronic energy-band structure of β-MgSe as calculated by an empirical pseudopotential method. [From K. L. Teo, Y. P. Feng, M. F. Li, T. C. Chong, and J. B. Xia, *Semicond. Sci. Technol.* **9**, 349 (1994).]

• **Energy eigenvalue**

Table 3.6.1 *Energy eigenvalues at the Γ, X, and L points for the valence band in β-MgSe [6.1].*

Critical point	Level	Value (eV)
Γ	Γ_6^v (Γ_1^v)	−11.7
	Γ_7^v (Γ_{15}^v)	−0.403
	Γ_8^v	0.00
X	X_6^v (X_1^v)	−11.5
	X_6^v (X_3^v)	−3.52
	X_6^v (X_5^v)	−1.19
	X_7^v	−1.01
L	L_6^v (L_1^v)	−11.5
	L_6^v (L_1^v)	−3.42
	L_6^v (L_3^v)	−0.41
	$L_{4,5}^v$	−0.17

[6.1] Q. Guo, H. C. Poon, Y. P. Feng, and C. K. Ong, *Semicond. Sci. Technol.* **10**, 677 (1995).

3.6.2 E_0-Gap Region

• **Temperature dependence**

Table 3.6.2 *E_0-gap (excitonic) energy for β-MgSe determined at various temperatures.*

Temperature (K)	E_0 (eV)	Comment
0	3.839	$Zn_{1-x}Mg_xSe$ ($x \rightarrow 1.0$) [6.2]
	3.781*	$Zn_{1-x}Mg_xSe$ ($x \rightarrow 1.0$) [6.2]
300	3.674	$Zn_{1-x}Mg_xSe$ ($x \rightarrow 1.0$) [6.2]
	3.616*	$Zn_{1-x}Mg_xSe$ ($x \rightarrow 1.0$) [6.2]
	4.0	$Zn_{1-x}Mg_xSe$ ($x \rightarrow 1.0$) [6.3]
	4.05	[6.4]
	4.0	Recommended (T=300 K)

[6.2] R. Pässler, F. Blaschta, E. Griebl, K. Papagelis, B. Haserer, T. Reisinger, S. Ves, and W. Gebhardt, *Phys. Status Solid B* **204,** 685 (1997).
[6.3] B. Jobst, D. Hommel, U. Lunz, T. Gerhard, and G. Landwehr, *Appl. Phys. Lett.* **69**, 97 (1996).
[6.4] M. Th. Litz, K. Watanabe, M. Korn, H. Ress, U. Lunz, W. Ossau, A. Waag, G. Landwehr, Th. Walter, B. Neubauer, D. Gerthsen, U. Schüssler, *J. Cryst. Growth* **159**, 54 (1996).
*n=1 exciton peak energy.

Table 3.6.3 *Spin–orbit–splitoff energy Δ_0 for β-MgSe.**

Δ_0 (eV)
0.42

*Since this quantity is primarily determined by the anion atomic spin–orbit splitting, it is assumed to have the nearly same value as that for ZnSe. It is also noted that Δ_0 may not vary with temperature if one supposes the valence-band rigidity of the II–VI compounds.

3.6.3 Higher-Lying Direct Gap

• Room-temperature value

Table 3.6.4 *Higher-lying direct-gap energies for β-MgSe obtained from $Zn_{1-x}Mg_xSe$ values using an extrapolation ($x \to 1.0$).*

Band gap	Value (eV)	
	a	b
E_1	5.251	5.84
$E_1+\Delta_1$	5.628	6.21
Δ_1	0.377	0.37

[a]K. J. Kim, M. H. Lee, J. H. Bahng, C. Y. Kwak, and E. Oh, *Solid State Commun.* **105**, 17 (1998).
[b]H. Lee, I.-Y. Kim, J. Powell, D. E. Aspnes, S. Lee, F. Peiris, and J. K. Furdyna, *J. Appl. Phys.* **88**, 878 (2000).

3.6.4 Lowest Indirect Gap

• Theoretical value

Table 3.6.5 *Lowest indirect-gap energy for β-MgSe.*

Band gap	Value (eV)	Ref.
$E_g^X(\Gamma_8^v \to X_6^c)$	3.3	[6.5]
	6.422	[6.6]
$E_g^L(\Gamma_8^v \to L_6^c)$	5.159	[6.6]

[6.5] G. Kalpana, B. Palanivel, R. M. Thomas, and M. Rajagopalan, *Physica B* **222**, 223 (1996).
[6.6] F. Benkabou, H. Aourag, M. Certier, and T. Kobayashi, *Superlatt. Microstruct.* **30**, 9 (2001).

3.6.5 Conduction-Valley Energy Separation

No detailed data are available for β-MgSe.

3.6.6 Direct-Indirect-Gap Transition Pressure

No detailed data are available for β-MgSe.

3.7 ENERGY-BAND STRUCTURE: ELECTRON AND HOLE EFFECTIVE MASSES

3.7.1 Electron Effective Mass: Γ Valley

Table 3.7.1 *Electron effective mass m_e^Γ at the Γ valley for β-MgSe.*

m_e^Γ/m_0
0.20 *

*Estimated from a plot of E_0 versus m_e^Γ for a number of the group-IV, III–V, and II–VI semiconductors in the cubic structure (see figure, below).

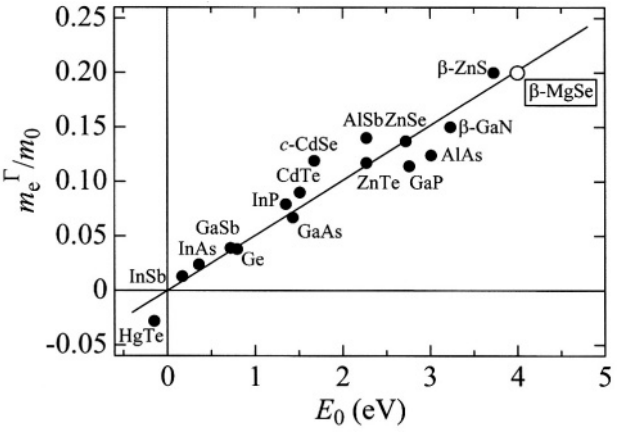

Fig. 3.7.1 Electron effective mass m^Γ_e/m_0 versus E_0 for a number of the group-IV, III–V, and II–VI semiconductors in the cubic structure. From this plot, we can estimate m^Γ_e value for β-MgSe to be $0.20m_0$.

3.7.2 Electron Effective Mass: Satellite Valley

No detailed data are available for β-MgSe.

3.7.3 Hole Effective Mass

- **Luttinger's valence-band parameter**

Table 3.7.2 *Luttinger's valence-band parameter γ_i for β-MgSe (in $\hbar^2/2m_0$).*

γ_1	γ_2	γ_3
2.84	0.43	1.00

*Estimated from a plot of E_0 versus γ_i for some cubic group-IV, III–V, and II–VI semiconductors (see figure, below).

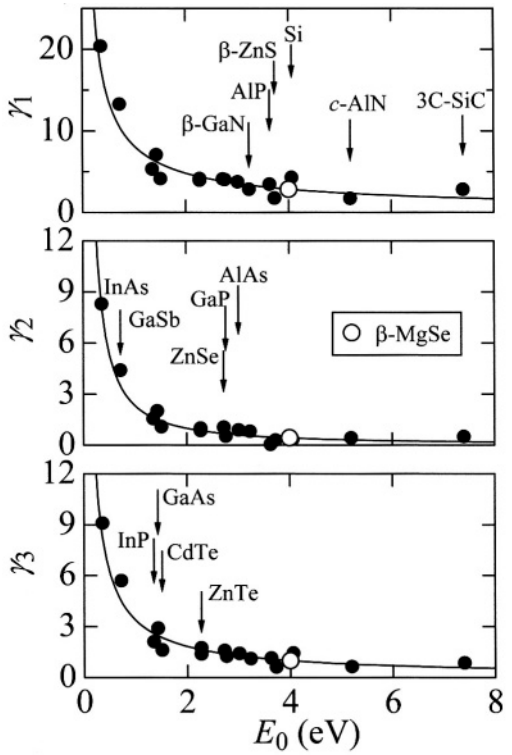

Fig. 3.7.2 Luttinger's valence-band parameter γ_i versus E_0 for a number of the group-IV, III–V, and II–VI semiconductors in the cubic structure. From this plot, we can estimate γ_i values for β-MgSe to be γ_1=2.84, γ_2=0.43, and γ_3=1.00 (in $\hbar^2/2m_0$).

• **Band mass, cyclotron mass, etc.**

Table 3.7.3 *Band (m_{HH}, m_{LH}), density-of-states heavy-hole (m_{HH}*), averaged light-hole (m_{LH}*), and spherically-averaged heavy-hole (m_{HH}^s) and light-hole masses (m_{LH}^s) in β-MgSe.**

Mass	Value (m_0)
m_{HH} ([001] direction)	0.51
m_{LH} ([001] direction)	0.27
m_{HH} ([111] direction)	1.19
m_{LH} ([111] direction)	0.21
m_{HH}*	0.88
m_{LH}*	0.23
m_{HH}^s	0.77
m_{LH}^s	0.23

*Calculated using a set of the Luttinger's parameters, γ_1=2.84, γ_2=0.43, and γ_3=1.00.

• **Spin–orbit–splitoff hole effective mass**

Table 3.7.4 *Spin-orbit-splitoff hole effective mass m_{SO} for β-MgSe.*

m_{SO}/m_0
0.35

*Obtained from the Luttinger's parameter ($m_{SO}=1/\gamma_1$).

3.8 ELECTRONIC DEFORMATION POTENTIAL

3.8.1 Intravalley Deformation Potential: Γ Point

• **Valence band**

Table 3.8.1 *Γ-valence-band deformation potentials a, b, and d for β-MgSe.*

Deformation potential (eV)			Comment
a	*b*	*d*	
−1.0	−1.27		Extrapolated (see [8.1])

[8.1] M. Wörz, E. Griebl, Th. Reisinger, R. Flierl, B. Haserer, T. Semmler, T. Frey, and W. Gebhardt, *Phys. Status Solidi B* **202**, 805 (1997).

• **E_0 gap**

Table 3.8.2 *Hydrostatic deformation potential a_0^Γ for the E_0 gap of β-MgSe.*

a_0^Γ (eV)	Comment
−4.2	Extrapolated (see [8.2])

[8.2] M. Wörz, E. Griebl, Th. Reisinger, R. Flierl, B. Haserer, T. Semmler, T. Frey, and W. Gebhardt, *Phys. Status Solidi B* **202**, 805 (1997).

3.8.2 Intravalley Deformation Potential: High-Symmetry Points

No detailed data are available for β-MgSe.

3.8.3 Intervalley Deformation Potential

No detailed data are available for β-MgSe.

3.9 ELECTRON AFFINITY AND SCHOTTKY BARRIER HEIGHT

3.9.1 Electron Affinity

No detailed data are available for β-MgSe.

3.9.2 Schottky Barrier Height

No detailed data are available for β-MgSe.

3.10 OPTICAL PROPERTIES

3.10.1 Summary of Optical Dispersion Relations

No detailed data are available for β-MgSe.

3.10.2 The Reststrahlen Region

- **Static and high-frequency dielectric constants**

Table 3.10.1 *Static and high-frequency dielectric constants ε_s and ε_∞ for β-MgSe.*

ε_s	ε_∞	Ref.
7.8*	3.8	[10.1]

[10.1] D. Huang, C. Jin, D. Wang, X. Liu, J. Wang, and X. Wang, *Appl. Phys. Lett.* **67**, 3611 (1995).
*Calculated from Lyddane–Sachs–Teller relationship.

3.10.3 At or Near the Fundamental Absorption Edge

- **Free-exciton binding energy and related parameters**

Table 3.10.2 *Free-exciton binding (Rydberg) energy G for β-MgSe.*

G (meV)	Comment
57.3	$Zn_{1-x}Mg_xSe$ ($x \rightarrow 1.0$) [10.2]

[10.2] R. Pässler, F. Blaschta, E. Griebl, K. Papagelis, B. Haserer, T. Reisinger, S. Ves, and W. Gebhardt, *Phys. Status Solidi B* **204**, 685 (1997).

Table 3.10.3 *Free-exciton parameters (G=binding energy; a_B=1st-orbital Bohr radius; μ=reduced mass) at the fundamental absorption edge of β-MgSe.**

G (meV)	a_B (Å)	μ (m_0)	Comment
57.3	33*	0.061*	Direct exciton

*Calculated using ε_∞=3.8.

- **Fundamental absorption edge**

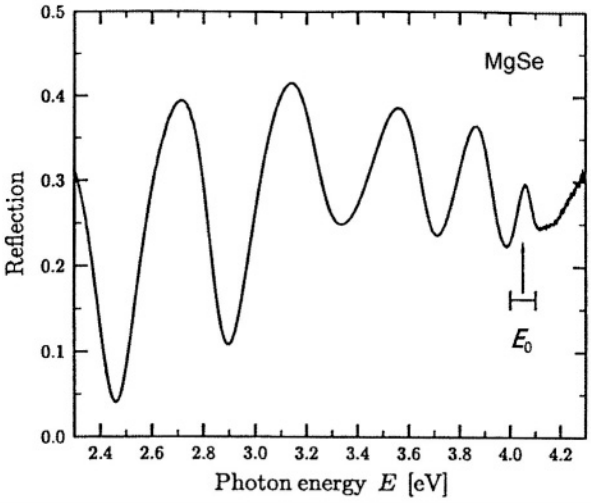

Fig. 3.10.1 Fundamental reflectivity spectrum of β-MgSe at 300 K. The sample measured was grown on (100)GaAs substrate by molecular beam epitaxy. The lowest-direct-band-gap energy of E_0=4.05 eV was determined from the onset of the interference fringes. [From U. Lunz, C. Schumacher, J. Nürnberger, K. Schüll, A. Gerhard, U. Schüssler, B. Jobst, W. Faschinger, and G. Landwehr, *Semicond. Sci. Technol.* **12,** 970 (1997).]

3.10.4 The Interband Transition Region

No detailed data are available for β-MgSe.

3.10.5 Free-Carrier Absorption and Related Phenomena

No detailed data are available for β-MgSe.

3.11 ELASTOOPTIC, ELECTROOPTIC, AND NONLINEAR OPTICAL PROPERTIES

3.11.1 Elastooptic Effect

No detailed data are available for β-MgSe.

3.11.2 Linear Electrooptic Constant

No detailed data are available for β-MgSe.

3.11.3 Quadratic Electrooptic Constant

No detailed data are available for β-MgSe.

3.11.4 Franz–Keldysh Effect

No detailed data are available for β-MgSe.

3.11.5 Nonlinear Optical Constant

No detailed data are available for β-MgSe.

3.12 CARRIER TRANSPORT PROPERTIES

3.12.1 Low-Field Mobility: Electrons

No detailed data are available for β-MgSe.

3.12.2 Low-Field Mobility: Holes

No detailed data are available for β-MgSe.

3.12.3 High-Field Transport: Electrons

- **LO-phonon-scattering-limited electron saturation drift velocity**

Table 3.12.1 *Calculated LO-phonon-scattering-limited electron saturation drift velocity $v_{e,sat}$ in the lowest-conduction-band valley α for β-MgSe at 300 K.**

$$v_{e,sat}^{\alpha} = \left(\frac{8\hbar\omega_{LO}}{3\pi m_c^{\alpha}} \right)^{1/2}$$

Valley	$v_{e,sat}$ (10^7 cm/s)
Γ	1.8

*Calculated with $m_c^{\Gamma} = 0.20 m_0$ and $\omega_{LO} = 340$ cm^{-1}.

3.12.4 High-Field Transport: Holes

No detailed data are available for β-MgSe.

3.12.5 Minority-Carrier Transport: Electrons in *p*-Type Materials

No detailed data are available for β-MgSe.

3.12.6 Minority-Carrier Transport: Holes in *n*-Type Materials

No detailed data are available for β-MgSe.

3.12.7 Impact Ionization Coefficient

No detailed data are available for β-MgSe.

Chapter 4

Zincblende Magnesium Telluride (β-MgTe)

4.1 STRUCTURAL PROPERTIES

4.1.1 Ionicity

Table 4.1.1 *Phillips's ionicity f_i for β-MgTe [1.1].*

f_i
0.554

[1.1] J. C. Phillips, *Bonds and Bands in Semiconductors* (Academic, New York, 1973).

4.1.2 Elemental Isotopic Abundance and Molecular Weight

- **Isotopic abundance**

Table 4.1.2 *Isotopic abundance in percent for magnesium and tellurium [1.2].*

Isotope	% nat. abundance	Isotope	% nat. abundance
^{24}Mg	78.99	^{120}Te	0.096
^{25}Mg	10.00	^{122}Te	2.603
^{26}Mg	11.01	^{123}Te	0.908
		^{124}Te	4.816
		^{125}Te	7.139
		^{126}Te	18.95
		^{128}Te	31.69
		^{130}Te	33.80

[1.2] D. R. Lide, *CRC Handbook of Chemistry and Physics,* 78th Edition (CRC Press, Boca Raton, 1997).

- **Molecular weight**

Table 4.1.3 *Molecular (average atomic) weight M for β-MgTe.*

M (amu)
151.91

4.1.3 Crystal Structure and Space Group

Table 4.1.4 *Crystal structure and its space and pint groups for β-MgTe.*

Crystal structure	Space group	Point group
Zincblende (Cubic)	$F\bar{4}3m$	T_d

4.1.4 Lattice Constant and Its Related Parameters

- **Lattice constant**

Table 4.1.5 *Lattice constant a for β-MgTe at 300 K.*

a (Å)	Ref.
6.420±0.005	[1.3]
6.423	[1.4]
6.419±0.001	[1.5]

[1.3] J. M. Hartmann, J. Cibert, F. Kany, H. Mariette, M. Charleux, P. Alleysson, R. Langer, and G. Feuillet, *J. Appl. Phys.* **80**, 6257 (1996).
[1.4] S.-J. Chung, Y. Kwon, C.-S. Yoon, B.-H. Kim, D. Cha, C.-D. Kim, W.-T. Kim, and C. U. Hong, *J. Phys. Chem. Solids* **60**, 799 (1999).
[1.5] E. Dynowska, E. Janik, J. Bąk-Misiuk, J. Domagala, T. Wojtowicz, and J. Kossut, *J. Alloys Compounds* **286**, 276 (1999).

- **Lattice constant, near-neighbor distance, etc.**

Table 4.1.6 *Lattice constant (a), near-neighbor distance (d), unit cube volume (a^3), and molecular density (d_M) for β-MgTe at 300 K.*

Parameter	Value
Lattice constant a (Å)	6.42
d (Cation–Anion) (Å)	2.78*
d (Cation–Cation) (Å)	4.54*
Unit cube volume a^3 (10^{-22} cm^3)	2.65*
Molecular density d_M (10^{22} cm^{-3})	1.51*

*Calculated.

- **Crystal density**

Table 4.1.7 *Crystal density g for β-MgTe at 300 K.**

g (g/cm^3)
3.81

*Calculated using a=6.42 Å.

4.1.5 Structural Phase Transition

No detailed data are available for β-MgTe.

4.1.6 Cleavage Plane

Table 4.1.8 *Crystallographic plane most readily cleaved for β-MgTe.**

Cleavage plane
(110)

*Expected.

4.2 THERMAL PROPERTIES

4.2.1 Melting Point and Its Related Parameters

Table 4.2.1 *Melting point T_m and its related parameter for MgTe.*

Parameter	Value
Melting point T_m (K)	>1300 (see [2.1])
Entropy of fusion ΔS_m (cal/mol K)	16.60* [2.1]

[2.1] J. A. Van Vechten, *Phys. Rev. B* **7**, 1479 (1973).
*Theoretical value.

4.2.2 Specific Heat

No detailed data are available for β-MgTe.

4.2.3 Debye Temperature

No detailed data are available for β-MgTe.

4.2.4 Thermal Expansion Coefficient

No detailed data are available for β-MgTe.

4.2.5 Thermal Conductivity and Diffusivity

No detailed data are available for β-MgTe.

4.3 ELASTIC PROPERTIES

4.3.1 Elastic Constant

• Room-temperature value

Table 4.3.1 *Elastic stiffness and compliance constants for β-MgTe at 300 K.*

Parameter	Value
Stiffness (10^{11} dyn/cm^2) [3.1]	
C_{11}	5.28
C_{12}	3.66
C_{44}	1.93
Compliance (10^{-12} cm^2/dyn) [3.2]	
S_{11}	4.38
S_{12}	−1.79
S_{44}	5.18

[3.1] Estimated from a C_{ij}–a (lattice constant) relation.
[3.2] Calculated from C_{ij} values.

4.3.2 Third-Order Elastic Constant

No detailed data are available for β-MgTe.

4.3.3 Young's Modulus, Poisson's Ratio, and Similar

• Young's modulus

Table 4.3.2 *Young's modulus Y for β-MgTe at 300K.**

Crystallographic plane	Y (10^{11} dyn/cm^2)
(100) plane	
[001] direction	2.28
[011] direction	3.86
(110) plane	
[001] direction	2.28
[111] direction	5.02
(111) plane	3.86

*Calculated using S_{11}=4.38, S_{12}=−1.79, and S_{44}=5.18 (all in 10^{-12} cm^2/dyn).

• Poisson's ratio

Table 4.3.3 *Poisson's ratio P for β-MgTe at 300 K.**

Crystallographic plane	P
(100) plane	
m=[010], n=[001]	0.409
m=[011], n=[0$\bar{1}$1]	−0.000
(110) plane	
m=[001], n=[1$\bar{1}$0]	0.409
m=[1$\bar{1}$1], n=[1$\bar{1}\bar{2}$]	0.299

Table 4.3.3 *Continued.*

Crystallographic plane	P
(111) plane	0.461

*Calculated using S_{11}=4.38, S_{12}= −1.79, and S_{44}=5.18 (all in 10^{-12} cm^2/dyn).

- **Bulk modulus, shear modulus, etc.**

Table 4.3.4 *Bulk modulus, B_u, shear modulus, C_s, isotropy factor, A, linear compressibility, C_o, Caucy ratio, C_a, and Born ratio, B_o, for β-MgTe at 300K [3.3].*

Parameter	Value
B_u (10^{11} dyn/cm^2)	4.20
C_s (10^{11} dyn/cm^2)	0.810
A	0.420
C_o (10^{-13} cm^2/dyn)	7.94
C_a	1.90
B_o	1.13

[3.3] Calculated using C_{11}=5.28, C_{12}=3.66, and C_{44}=1.93 (all in 10^{11} dyn/cm^2).

Table 4.3.5 *Bulk modulus, B_u, and its pressure derivative, dB_u/dp, for β-MgTe.*

B_u (GPa)	dB_u/dp	Comment
37.6		Calc. [3.4]
38.0	3.96	Calc. [3.5]

[3.4] B. Freytag, *J. Phys.: Condens. Matter* **6**, 9875 (1994).
[3.5] P. E. Van Camp, V. E.Van Doren, and J. L. Martins, *Phys. Rev. B* **55**, 775 (1997).

4.3.4 Microhardness

No detailed data are available for β-MgTe.

4.3.5 Sound Velocity

Table 4.3.6 *Sound velocity propagating in β-MgTe at 300 K.* LA= longitudinal acoustic; TA1, TA2=transverse acoustic.*

Propagation direction	Mode	Sound velocity (10^5 cm/s)
[100]	LA	3.72
[100]	TA1, TA2	2.25
[110]	LA	4.10
[110]	TA1	1.46
[110]	TA2	2.25
[111]	LA	4.22
[111]	TA1, TA2	1.76

*Calculated using C_{11}=5.28×10^{11} dyn/cm^2, C_{12}=3.66×10^{11} dyn/cm^2, C_{44}=1.93×10^{11} dyn/cm^2, and g=3.81 g/cm^3.

4.4 PHONONS AND LATTICE VIBRONIC PROPERTIES

4.4.1 Phonon Dispersion Relation

No detailed data are available for β-MgTe.

4.4.2 Phonon Frequency

• Room-temperature value

Table 4.4.1 *Long-wavelength (q→0) and zone-boundary phonon frequencies for β-MgTe.*

Critical point	Phonon	Phonon frequency (cm^{-1})
Γ	TO	235 [4.1]
		235 [4.2]
	LO	320 [4.1]
		292 [4.2]
X	TA	
	LA	
	TO	
	LO	
L	TA	
	LA	
	TO	
	LO	

[4.1] S. Nakashima, T. Fukumoto, A. Mitsuishi, and K. Itoh, *J. Phys. Soc. Jpn* **35,** 1437 (1973).
[4.2] E. Oh, C. Parks, I. Miotkowski, M. D. Sciacca, A. J. Mayur, and A. K. Ramdas, *Phys. Rev. B* **48**, 15040 (1993).

4.4.3 Mode Grüneisen Parameter

No detailed data are available for β-MgTe.

4.4.4 Phonon Deformation Potential

No detailed data are available for β-MgTe.

4.5 COLLECTIVE EFFECTS AND RELATED PROPERTIES

4.5.1 Piezoelectric Constant

No detailed data are available for β-MgTe.

4.5.2 Fröhlich Coupling Constant

No detailed data are available for β-MgTe.

4.6 ENERGY-BAND STRUCTURE: ENERGY-BAND GAPS

4.6.1 Basic Properties

- **Electronic energy-band structure/density of states**

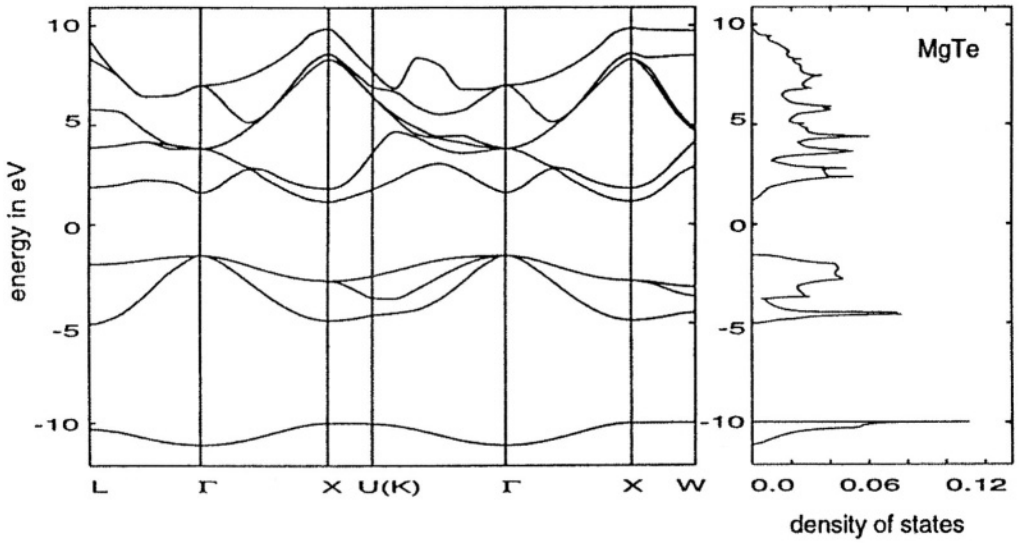

Fig. 4.6.1 Electronic energy-band structure and density of states for β-MgTe as calculated with the local-density approximation. [From B. Freytag, *J. Phys.: Condens. Matter* **6**, 9875 (1994).]

- **Energy eigenvalue**

Table 4.6.1 *Energy eigenvalues at the Γ, X, and L points for the valence band in β-MgTe [6.1].*

Critical point	Level	Value (eV)
Γ	Γ_6^v (Γ_1^v)	–9.5
	Γ_7^v (Γ_{15}^v)	
	Γ_8^v	0.0
X	X_6^v (X_1^v)	–8.5
	X_6^v (X_3^v)	–3.3
	X_6^v, X_7^v (X_5^v)	–1.3
L	L_6^v (L_1^v)	–8.7
	L_6^v (L_1^v)	–3.5
	L_6^v, $L_{4,5}^v$ (L_3^v)	–0.5

[6.1] B. Freytag, *J. Phys.: Condens. Matter* **6**, 9875 (1994).

4.6.2 E_0-Gap Region

- **Temperature dependence**

Table 4.6.2 *E_0-gap (excitonic) energy for β-MgTe determined at various temperatures.*

Temperature (K)	E_0 (eV)	Comment
1.8	3.356	$Cd_{1-x}Mg_xTe$ ($x\rightarrow1.0$) [6.2]
4.2	3.191*	$Zn_{1-x}Mg_xTe$ ($x\rightarrow1.0$) [6.3]
10	3.20	$Cd_{1-x}Mg_xTe$ ($x\rightarrow1.0$) [6.4]
300	3.25	$Cd_{1-x}Mg_xTe$ ($x\rightarrow1.0$) [6.2]
	3.07*	$Zn_{1-x}Mg_xTe$ ($x\rightarrow1.0$) [6.3]
	3.5	$Cd_{1-x}Mg_xTe$ ($x\rightarrow1.0$) [6.5]
	3.49	[6.6]
	3.189	$Cd_{1-x}Mg_xTe$ ($x\rightarrow1.0$) [6.7]
	3.49	$Hg_{1-x}Mg_xTe$ ($x\rightarrow1.0$) [6.8]
	3.4	Mean value (T=300 K)

[6.2] M. Luttmann, F. Bertin, and A. Chabli, *J. Appl. Phys.* **78**, 3387 (1995).
[6.3] S.-J. Chung, Y. Kwon, C.-S. Yoon, B.-H. Kim, D. Cha, C.-D. Kim, W.-T. Kim, and C. U. Hong, *J. Phys. Chem. Solids* **60**, 799 (1999).
[6.4] E. Oh, C. Parks, I. Miotkowski, M. D. Sciacca, A. J. Mayur, and A. K. Ramdas, *Phys. Rev. B* **48**, 15040 (1993).
[6.5] J. M. Hartmann, J. Cibert, F. Kany, H. Mariette, M. Charleux, P. Alleysson, R. Langer, and G. Feuillet, *J. Appl. Phys.* **80**, 6257 (1996).
[6.6] M. Th. Litz, K. Watanabe, M. Korn, H. Ress, U. Lunz, W. Ossau, A. Waag, G. Landwehr, Th. Walter, B. Neubauer, D. Gerthsen, U. Schüssler, *J. Cryst. Growth* **159**, 54 (1996).
[6.7] S. G. Choi, Y. D. Kim, S. D. Yoo, D. E. Aspnes, I. Miotkowski, and A. K. Ramdas, *Appl. Phys. Lett.* **71**, 249 (1997).
[6.8] S. Oehling, U. Lunz, H. Heinke, G. Plahl, C. R. Becker, and G. Landwehr, *J. Cryst. Growth* **159**, 1157 (1996).
*n=1 exciton peak energy.

Table 4.6.3 *Spin–orbit–splitoff energy Δ_0 for β-MgTe.**

Δ_0 (eV)
0.95

*Since this quantity is primarily determined by the anion atomic spin–orbit splitting, it is assumed to have the nearly same value as that for ZnTe. It is also noted that Δ_0 may not vary with temperature if one supposes the valence-band rigidity of the II–VI compounds.

- **Temperature and/or pressure coefficient**

Table 4.6.4 *Linear temperature coefficient of the E_0-gap energy for β-MgTe.*

Coefficient	Value	Ref.
dE_0/dT (10^{-4} eV/K)	–4.5±0.3	[6.9]

[6.9] D. Barbier, B. Montegu, and A. Laugier, *Solid State Commun.* **28**, 525 (1978).

4.6.3 Higher-Lying Direct Gap

- **Room-temperature value**

Table 4.6.5 *Higher-lying direct-gap energies for* β-$MgTe$ *obtained from* $Cd_{1-x}Mg_xTe$ *values using an extrapolation* $(x \rightarrow 1.0)$ *[6.10].*

Band gap	Value (eV)
E_1	4.255
$E_1+\Delta_1$	4.673
Δ_1	0.418
E_2	5.156
E_0'	5:327

[6.10] S. G. Choi, Y. D. Kim, S. D. Yoo, D. E. Aspnes, I. Miotkowski, and A. K. Ramdas, *Appl. Phys. Lett.* **71,** 249 (1997).

4.6.4 Lowest Indirect Gap

- **Theoretical value**

Table 4.6.6 *Lowest indirect-gap energy for* β-$MgTe$.

Band gap	Value (eV)	Ref.
E_g^L ($\Gamma_8^v \rightarrow L_6^c$)	2.71	[6.11]
E_g^X ($\Gamma_8^v \rightarrow X_6^c$)	3.46	[6.11]

[6.11] B. Freytag, *J. Phys.: Condens. Matter* **6**, 9875 (1994).

4.6.5 Conduction-Valley Energy Separation

Table 4.6.7 *Theoretically obtained conduction-valley energy separation* ΔE_g *for* β-$MgTe$ *[6.12].*

ΔE_g	Value (eV)
Γ_6^c–X_6^c	0.66
L_6^c–X_6^c	0.75
L_6^c–Γ_6^c	0.09

[6.12] B. Freytag, *J. Phys.: Condens. Matter* **6**, 9875 (1994).

4.6.6 Direct–Indirect-Gap Transition Pressure

No detailed data are available for β-MgTe.

4.7 ENERGY-BAND STRUCTURE: ELECTRON AND HOLE EFFECTIVE MASSES

4.7.1 Electron Effective Mass: Γ Valley

Table 4.7.1 *Electron effective mass m_e^Γ at the Γ valley for β-MgTe.*

m_e^Γ/m_0
0.17 *

*Estimated from a plot of E_0 versus m_e^Γ for a number of the group-IV, III–V, and II–VI semiconductors in the cubic structure (see figure, below).

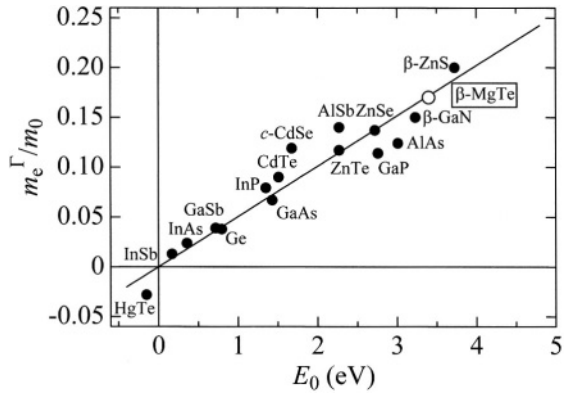

Fig. 4.7.1 Electron effective mass m^Γ_e/m_0 versus E_0 for a number of the group-IV, III–V, and II–VI semiconductors in the cubic structure. From this plot, we can estimate m^Γ_e value for β-MgTe to be $0.17m_0$.

4.7.2 Electron Effective Mass: Satellite Valley

No detailed data are available for β-MgTe.

4.7.3 Hole Effective Mass

- **Luttinger's valence-band parameter**

Table 4.7.2 *Luttinger's valence-band parameter γ_i for β-MgTe (in $\hbar^2/2m_0$).*

γ_1	γ_2	γ_3
3.21	0.52	1.15

*Estimated from a plot of E_0 versus γ_i for some cubic group-IV, III–V, and II–VI semiconductors (see figure, below).

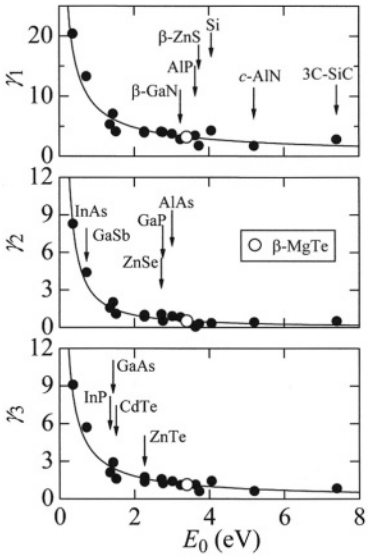

Fig. 4.7.2 Luttinger's valence-band parameter γ_i versus E_0 for a number of the group-IV, III–V, and II–VI semiconductors in the cubic structure. From this plot, we can estimate γ_i values for β-MgTe to be γ_1=3.21, γ_2=0.52, and γ_3=1.15 (in $\hbar^2/2m_0$).

• **Band mass, cyclotron mass, etc.**

Table 4.7.3 *Band (m_{HH}, m_{LH}), density-of-states heavy-hole (m_{HH}*), averaged light-hole (m_{LH}*), and spherically-averaged heavy-hole (m_{HH}^s) and light-hole masses (m_{LH}^s) in* β-MgTe.*

Mass	Value (m_0)
m_{HH} ([001] direction)	0.46
m_{LH} ([001] direction)	0.24
m_{HH} ([111] direction)	1.10
m_{LH} ([111] direction)	0.18
m_{HH}*	0.80
m_{LH}*	0.20
m_{HH}^s	0.71
m_{LH}^s	0.20

*Calculated using a set of the Luttinger's parameters, γ_1=3.21, γ_2=0.52, and γ_3=1.15.

• **Spin–orbit–splitoff hole effective mass**

Table 4.7.4 *Spin–orbit–splitoff hole effective mass m_{SO} for β-MgTe.*

m_{SO}/m_0
0.31

*Obtained from the Luttinger's parameter ($m_{SO}=1/\gamma_1$).

4.8 ELECTRONIC DEFORMATION POTENTIAL

4.8.1 Intravalley Deformation Potential: Γ Point

No detailed data are available for β-MgTe.

4.8.2 Intravalley Deformation Potential: High-Symmetry Points

No detailed data are available for β-MgTe.

4.8.3 Intervalley Deformation Potential

No detailed data are available for β-MgTe.

4.9 ELECTRON AFFINITY AND SCHOTTKY BARRIER HEIGHT

4.9.1 Electron Affinity

No detailed data are available for β-MgTe.

4.9.2 Schottky Barrier Height

No detailed data are available for β-MgTe.

4.10 OPTICAL PROPERTIES

4.10.1 Summary of Optical Dispersion Relations

No detailed data are available for β-MgTe.

4.10.2 The Reststrahlen Region

- **Static and high-frequency dielectric constants**

Table 4.10.1 *Static and high-frequency dielectric constants ε_s and ε_∞ for β-MgTe.*

ε_s	ε_∞	Ref.
6.9	3.7	[10.1]
7.0	4.5*	[10.2]

[10.1] S. Nakashima, T. Fukumoto, A. Mitsuishi, and K. Itoh, *J. Phys. Soc. Jpn* **35**, 1437 (1973).
[10.2] E. Oh, C. Parks, I. Miotkowski, M. D. Sciacca, A. J. Mayur, and A. K. Ramdas, *Phys. Rev. B* **48**, 15040 (1993).
*Calculated from Lyddane–Sachs–Teller relationship.

4.10.3 At or Near the Fundamental Absorption Edge

- **Refractive index**

Table 4.10.2 *Sellmeier equation for the refractive-index dispersion of β-MgTe.*

$$n^2(\lambda) = a + \frac{b\lambda^2}{\lambda^2 - c^2}, \quad \lambda \text{ in } \mu\text{m}$$

Parameter			Comment
a	b	c	
3.007	2.253	0.315	T=300 K [10.3]
4.677	1.059	0.294	T=4 K [10.4]

[10.3] M. Luttmann, F. Bertin, and A. Chabli, *J. Appl. Phys.* **78**, 3387 (1995).
[10.4] R. André and Le Si Dang, *J. Appl. Phys.* **82**, 5086 (1997).

Table 4.10.3 *Empirical expression for the refractive-index dispersion of β-MgTe [10.5].*

$$n^2(\lambda) = a + \frac{bE^2}{1-(E/c)^2}, \quad E < c$$

Parameter			Comment
a	b	c	
2.90	0.058	4.34	T=300 K
3.48	0.089	4.70	T=77 K

[10.5] M.-J. Lugauer, F. Fischer, T. Litz, A. Waag, D. Hommel, and G. Landwehr, *Semicond. Sci. Technol.* **9,**1567(1994).

4.10.4 The Interband Transition Region

No detailed data are available for β-MgTe.

4.10.5 Free-Carrier Absorption and Related Phenomena

No detailed data are available for β-MgTe.

4.11 ELASTOOPTIC, ELECTROOPTIC, AND NONLINEAR OPTICAL PROPERTIES

4.11.1 Elastooptic Effect

No detailed data are available for β-MgTe.

4.11.2 Linear Electrooptic Constant

No detailed data are available for β-MgTe.

4.11.3 Quadratic Electrooptic Constant

No detailed data are available for β-MgTe.

4.11.4 Franz–Keldysh Effect

No detailed data are available for β-MgTe.

4.11.5 Nonlinear Optical Constant

No detailed data are available for β-MgTe.

4.12 CARRIER TRANSPORT PROPERTIES

4.12.1 Low-Field Mobility: Electrons

No detailed data are available for β-MgTe.

4.12.2 Low-Field Mobility: Holes

No detailed data are available for β-MgTe.

4.12.3 High-Field Transport: Electrons

• LO-phonon-scattering-limited electron saturation drift velocity

Table 4.12.1 *Calculated LO-phonon-scattering-limited electron saturation drift velocity $v_{e,sat}$ in the lowest-conduction-band valley α for β-MgTe at 300K.**

$$v_{e,sat}^{\alpha} = \left(\frac{8\hbar\omega_{LO}}{3\pi m_c^{\alpha}} \right)^{1/2}$$

Valley	$v_{e,sat}$ (10^7 cm/s)
Γ	1.8

*Calculated with $m_c^{\Gamma} = 0.17 m_0$ and $\omega_{LO} = 292$ cm^{-1}.

4.12.4 High-Field Transport: Holes

No detailed data are available for β-MgTe.

4.12.5 Minority-Carrier Transport: Electrons in *p*-Type Materials

No detailed data are available for β-MgTe.

4.12.6 Minority-Carrier Transport: Holes in *n*-Type Materials

No detailed data are available for β-MgTe.

4.12.7 Impact Ionization Coefficient

No detailed data are available for β-MgTe.

Chapter 5

Zinc Oxide (ZnO)

5.1 STRUCTURAL PROPERTIES

5.1.1 Ionicity

Table 5.1.1 *Phillips's ionicity f_i for ZnO [1.1].*

f_i
0.616

[1.1] J. C. Phillips, *Bonds and Bands in Semiconductors* (Academic, New York, 1973).

5.1.2 Elemental Isotopic Abundance and Molecular Weight

- **Isotopic abundance**

Table 5.1.2 *Isotopic abundance in percent for zinc and oxygen [1.2].*

Isotope	% nat. abundance	Isotope	% nat. abundance
^{64}Zn	48.6	^{16}O	99.762
^{66}Zn	27.9	^{17}O	0.038
^{67}Zn	4.1		
^{68}Zn	18.8		
^{70}Zn	0.6		

[1.2] D. R. Lide, *CRC Handbook of Chemistry and Physics,* 78th Edition (CRC Press, Boca Raton, 1997).

• **Molecular weight**

Table 5.1.3 *Molecular (average atomic) weight M for ZnO.*

M (amu)
81.39

5.1.3 Crystal Structure and Space Group

Table 5.1.4 *Crystal structure and its space and pint groups for ZnO.*

Crystal structure	Space group	Point group
Wurtzite (Hexagonal)	$P6_3mc$	C_{6v}^4

5.1.4 Lattice Constant and Its Related Parameters

• **Lattice constant and molecular density**

Table 5.1.5 *Lattice constant (a, c) and molecular density (d_M) for ZnO at 300 K.*

Parameter	Value
Lattice constant a (Å)	3.2495 [1.3]
c (Å)	5.2069 [1.3]
Molecular density d_M (10^{22} cm^{-3})	4.2004*

[1.3] D. F. Croxall, R. C. C. Ward, C. A. Wallace, and R. C. Kell, *J. Cryst. Growth* **22**, 117 (1974).
*Calculated.

• **Crystal density**

Table 5.1.6 *Crystal density g for ZnO at 300 K.**

g (g/cm^3)
5.6768

*Calculated using a=3.2495 Å and c=5.2069Å.

5.1.5 Structural Phase Transition

Table 5.1.7 *Structural phase transition in ZnO at high pressures.*

Structure	Transition pressure (GPa)
Wurtzite ($P6_3mc$)	Normal pressure
Rocksalt (NaCl)	10 [1.4]
	9.0 [1.5]
	8.0±0.3 [1.6]
	8.7±0.5 [1.7]
	9.1±0.2 [1.8]

[1.4] C. H. Bates, W. B. White, and R. Roy, *Science* **137**, 993 (1962).
[1.5] J. C. Jamieson, *Phys. Earth Planet. Inter.* **3**, 201 (1970).
[1.6] S. C. Yu, I. L. Spain, and E. F. Skelton, *Solid State Commun.* **25**, 49 (1978).
[1.7] H. Karzel, W. Potzel, M. Köfferlein, W. Schiessl, M. Steiner, U. Hiller, G. M. Kalvius, D. W. Mitchell, T. P. Das, P. Blaha, K. Schwarz, and M. P. Pasternak, *Phys. Rev. B* **53**, 11425 (1996).
[1.8] S. Desgreniers, *Phys. Rev. B* **58**, 14102 (1998).

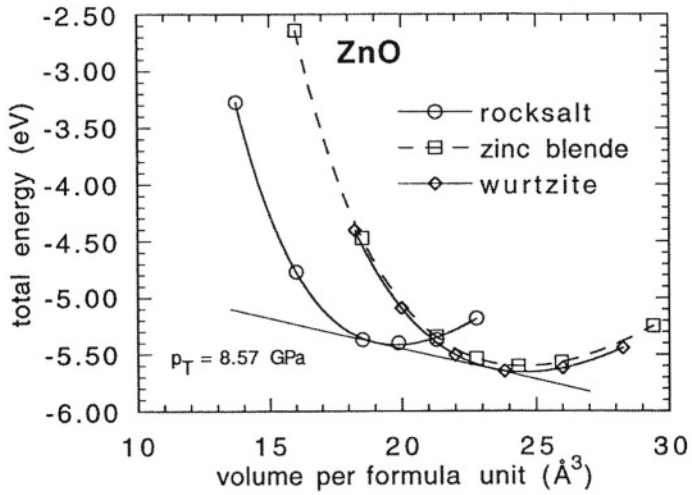

Fig. 5.1.1 Theoretical total energy versus volume for ZnO. The zero of energy is the sum of total energies of an isolated Zn and an isolated O atom, calculated with the atomic limit of the basis set of these atoms. [From J. E. Jaffe and A. C. Hess, *Phys. Rev. B* **48**,7903 (1993).]

5.1.6 Cleavage Plane

Table 5.1.8 *Crystallographic plane most readily cleaved for ZnO.*

Cleavage plane
$(11\bar{2}0)$, $(10\bar{1}0)$

- **Surface energy**

Table 5.1.9 *Surface energy for ZnO (in J/m^2).*

Plane		Comment
(0001)	$(000\bar{1})$	
1.95	0.96	Calc. [1.9]

[1.9] B. N. Oshcherin, *Phys. Status Solidi A* **34**, K181 (1976).

5.2 THERMAL PROPERTIES

5.2.1 Melting Point and Its Related Parameters

Table 5.2.1 *Melting point T_m for ZnO.*

Parameter	Value
Melting point T_m (K)	1975 [2.1]

[2.1] See, J. A. Van Vechten, *Phys Rev. B* **7**,1479 (1973).

5.2.2 Specific Heat

Table 5.2.2 *Experimental specific heat C_p (at constant pressure) for ZnO [2.2].*

Temperature (K)	C_p (J/g K)	Temperature (K)	C_p (J/g K)
20	0.0087	350	0.530
30	0.031	400	0.550
50	0.102	500	0.576
100	0.218	600	0.597
150	0.320	700	0.607
200	0.370	800	0.623
250	0.453	900	0.633
300	0.497		

[2.2] Gmelin, *Handbuch d. Anorganischen Chemie* (Zink Verlag Chemie, Weinheim, 1956), No. 32, p. 803.

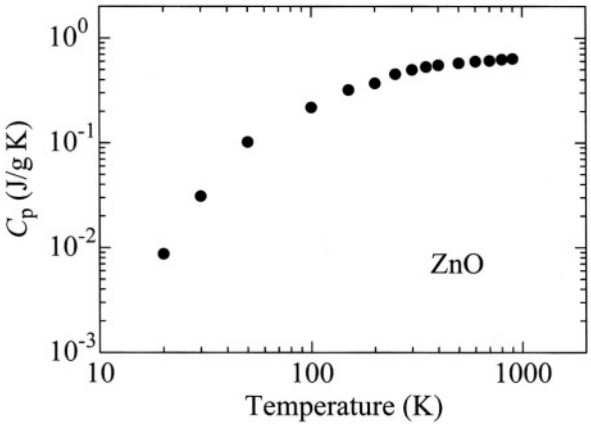

Fig. 5.2.1 Specific heat C_p (at constant pressure) versus temperature for ZnO. The solid circles are obtained from Gmelin [*Handbuch d. Anorganischen Chemie* (Zink Verlag Chemie, Weinheim, 1956), No. 32, p. 803].

5.2.3 Debye Temperature

Table 5.2.3 *Debye temperature θ_D for ZnO.*

θ_D (K)	Technique
416	Room-temperature mean sound velocity [2.3]
370	X-ray diffraction at T=298 K [2.4]

[2.3] R. A. Robie and J. L. Edwards, *J. Appl. Phys.* **37**, 2659 (1966).
[2.4] S. C. Abrahams and J. L. Bernstein, *Acta Crystallogr. B* **25,** 1233 (1969).

5.2.4 Thermal Expansion Coefficient

Table 5.2.4 *Thermal expansion coefficient α_{th} for ZnO [2.5]. Note that the expansion coefficient shows a minimum at T~60 K.*

Temperature (K)	α_{th} (10^{-6} K^{-1})		Temperature (K)	α_{th} (10^{-6} K^{-1})	
	α_a	α_c		α_a	α_c
9	–0.009	–0.018	150	1.69	0.50
13	–0.026	–0.059	200	2.88	1.51
17	–0.06	–0.122	250	3.90	2.25

Table 5.2.4 *Continued.*

Temperature (K)	α_{th} (10^{-6} K^{-1})		Temperature (K)	α_{th} (10^{-6} K^{-1})	
	α_a	α_c		α_a	α_c
22.5	–0.145	–0.25	300	4.75	2.92
30	–0.27	–0.48	400	6.07	3.82
40	–0.41	–0.72	500	7.15	4.38
60	–0.515	–0.885	600	7.85	4.70
80	–0.38	–0.865	700	8.13	4.90
100	0.04	–0.62	800	8.30	4.98
120	0.64	–0.16			

[2.5] H. Ibach, *Phys. Status Solidi* **33**, 257 (1969).

Table 5.2.5 *Thermal expansion coefficien α_{th} for ZnO [2.6].*

α_{th} (10^{-6} K^{-1})		Comment
α_a	α_c	
4.31	2.49	T=300 K
6.70	3.98	T=300–900 K (averaged)

[2.6] H. Iwanaga, A. Kunishige, and S. Takeuchi, *J. Mater. Sci.* **35**, 2451 (2000).

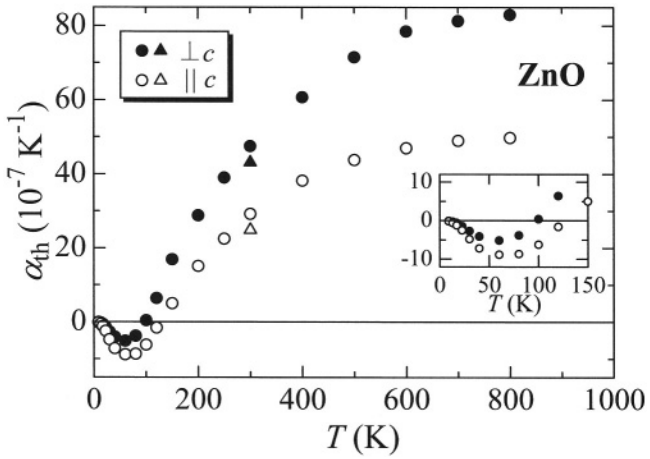

Fig. 5.2.2 Thermal expansion coefficient α_{th} versus temperature T for ZnO. The experimental data are taken from H. Ibach [*Phys. Status Solidi* **33**, 257 (1969); solid and open circles] and from H. Iwanaga, A. Kunishige, and S. Takeuchi [*J. Mater. Sci.* **35**, 2451 (2000); solid and open triangles].

5.2.5 Thermal Conductivity and Diffusivity

- **Room-temperature value**

Table 5.2.6 *Thermal conductivity K for ZnO at 300 K. Thermal diffusivity can be calculated from a relation $D=K/(C_p \cdot g)$, where C_p is the specific heat at constant pressure and g is the crystal density.*

K (W/cm K)	Comment
0.54	Heat flow || c [2.7]

[2.7] G. A. Slack, *Phys. Rev. B* **6**, 3791 (1972).

• **Temperature dependence**

Table 5.2.7 *Thermal conductivity K in the direction perpendicular to the c-axis for ZnO [2.8].*

Temperature (K)	K (W/cm K)	Temperature (K)	K (W/cm K)
3.5	1.15	28	7.3
3.9	1.50	35	5.5
4.8	1.85	42	4.8
5.5	2.5	48	4.1
6.7	3.1	55	3.4
8.4	3.7	65	2.8
8.6	4.7	84	2.2
9.4	5.3	108	1.75
10.5	6.2	138	1.40
11.8	7.2	158	1.13
13.8	8.4	182	0.94
18	8.5	210	0.82
22	8.3	240	0.70

[2.8] M. W. Wolf and J. J. Martin, *Phys. Status Solidi A* **17**, 215 (1973).

Table 5.2.8 *Thermal conductivity K in the direction along the c-axis for ZnO [2.9].*

Temperature (K)	K (W/cm K)	Temperature (K)	K (W/cm K)
2.65	0.76	16.8	11.7
2.90	0.87	21.5	11.0
3.15	1.1	29.0	9.6
3.35	1.3	37.5	7.5
3.6	1.6	42	6.7
4.0	1.8	51	5.3
4.3	2.2	70	4.1
4.7	2.7	79	3.7
5.2	3.4	102	2.8
6.0	4.3	130	2.2
7.3	6.3	150	1.9
8.3	7.9	165	1.6
9.7	9.6	190	1.4
12.6	10.6		

[2.9] M. W. Wolf and J. J. Martin, *Phys. Status Solidi A* **17**, 215 (1973).

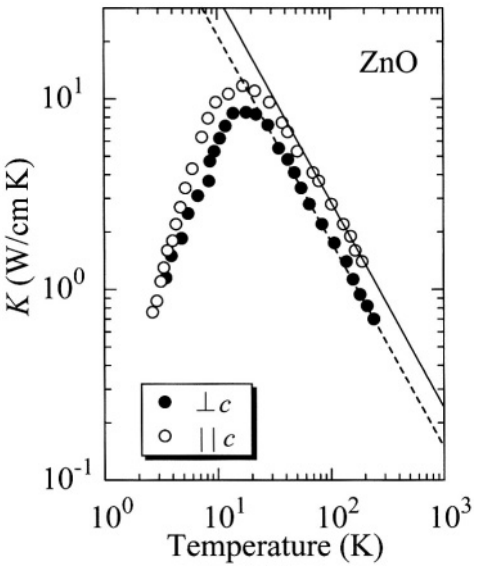

Fig. 5.2.3 Thermal conductivity K for ZnO. The experimental data are taken from M. W. Wolf and J. J. Martin [*Phys. Status Solidi A* **17**, 215 (1973)]. The solid (dashed) line is calculated from $K=AT^n$ with A=420 (260) W/cm K$^{-0.08}$ and n= –1.08 (–1.08).

5.3 ELASTIC PROPERTIES

5.3.1 Elastic Constant

- **Room-temperature value**

Table 5.3.1 *Room-temperature elastic stiffness* (C_{ij}) *and compliance constants* (S_{ij}) *for ZnO [3.1].*

C_{ij} (10^{11} dyn/cm^2)					
C_{11}	C_{12}	C_{13}	C_{33}	C_{44}	C_{66}*
20.9	12.0	10.4	21.8	4.41	4.45
S_{ij} (10^{-12} cm^2/dyn)					
S_{11}	S_{12}	S_{13}	S_{33}	S_{44}	S_{66}*
0.782	–0.345	–0.210	0.664	2.24	2.254

[3.1] *Numerical Data and Functional Relationships in Science and Technology,* edited by K.-H. Hellwege and A. M. Hellwege, Landolt–Börnstein, New Series, Group III, Vol. 11 (Springer, Berlin, 1979).

* C_{66}=½(C_{11}–C_{12}); S_{66}=2(S_{11}–S_{12}).

- **Temperature and/or pressure dependence**

Table 5.3.2 *Temperature derivative of the elastic stiffness constant,* dC_{ij}/dT, *for ZnO [3.2].*

dC_{ij}/dT (10^7 dyn/cm^2 K)				
C_{11}	C_{12}	C_{13}	C_{33}	C_{44}
			–26	–3.1

[3.2] *Numerical Data and Functional Relationships in Science and Technology,* edited by K.-H. Hellwege and A. M. Hellwege, Landolt–Börnstein, New Series, Group III, Vol. 11 (Springer, Berlin, 1979); I. B. Kobiakov, *Solid State Commun.* **35,** 305 (1980).

Table 5.3.3 *Pressure derivative of the elastic stiffness constant, dC_{ij}/dp, for ZnO [3.3].*

dC_{ij}/dT				
C_{11}	C_{12}	C_{13}	C_{33}	C_{44}
3.8	5.2	4.7	3.7	–0.53

[3.3] *Numerical Data and Functional Relationships in Science and Technology,* edited by K.-H. Hellwege and A. M. Hellwege, Landolt–Börnstein, New Series, Group III, Vol. 11 (Springer, Berlin, 1979).

5.3.2 Third-Order Elastic Constant

No detailed data are available for ZnO.

5.3.3 Young's Modulus, Poisson's Ratio, and Similar

- **Young's modulus**

Table 5.3.4 *Young's modulus Y for ZnO at 300 K.**

Direction	Y (10^{12} dyn/cm^2)
$c \perp l$	1.28
$c \parallel l$	1.51

*Calculated using $S_{11}=7.82\times10^{-13}$ and $S_{33}=6.64\times10^{-13}$ cm^2/dyn.
l: directional vector.

- **Poisson's ratio**

Table 5.3.5 *Poisson's ratio P for ZnO at 300 K.**

Direction	P
$c \perp l$	0.35
$c \parallel l$	–1.25

*Obtained from a definition $B_u=Y/[3(1-2P)]$, where B_u and Y are bulk and Young's moduli, respectively.
l: directional vector.

- **Bulk modulus, shear modulus, etc.**

Table 5.3.6 *Bulk modulus, B_u, pressure derivative of B_u, dB_u/dp, and linear compressibility, C_o, for ZnO at 300 K.*

Parameter	Value
B_u (10^{12} dyn/cm^2)	1.44 [3.4]
dB_u/dp	3.6, 4.4 (Theor., see [3.5])
	3.6 [3.5]
	9.4±1.5 [3.6]
	4 [3.7]
C_o (10^{-13} cm^2/dyn)	
$c \perp l$	2.27 [3.4]
$c \parallel l$	2.44 [3.4]

[3.4] Calculated using $C_{11}=2.09\times10^{12}$ dyn/cm^2, $C_{12}=1.20\times10^{12}$ dyn/cm^2, $C_{13}=1.04\times10^{12}$ dyn/cm^2, $C_{33}=2.18\times10^{1}$ dyn/cm^2, $S_{11}=7.82\times10^{-13}$ cm^2/dyn, $S_{12}=-3.45\times10^{-13}$ cm^2/dyn, $S_{13}=-2.10\times10^{-13}$ cm^2/dyn, and $S_{33}=6.64\times10^{-13}$ cm^2/dyn.
[3.5] Exper. [S. Desgreniers, *Phys. Rev. B* **58**, 14102 (1998)].

[3.6] Exper. [L. Gerward and J. S. Olsen, *J. Synchrotron Radiat* **2**, 233 (1995)].
[3.7] Exper. [H. Karzel, W. Potzel, M. Köfferlein, W. Schiessl, M. Steiner, U. Hiller, G. M. Kalvius, D. W. Mitchell, T. P. Das, P. Blaha, K. Schwarz, and M. P. Pasternak, *Phys. Rev. B* **53**,11425 (1996)].
l: directional vector.

5.3.4 Microhardness

Table 5.3.7 *Microhardness H for ZnO [3.8].*

H (GPa)
4.0

[3.8] See, L. Garbato and A. Rucci, *Phil. Mag.* **35**, 1681 (1977).

5.3.5 Sound Velocity

Table 5.3.8 *Sound velocity propagating in ZnO at 300 K.* LA=longitudinal acoustic; TA1, TA2=transverse acoustic.*

Propagation direction $\boldsymbol{a}$	Direction of polarization π	Mode	Sound velocity (10^5 cm/s)
$\boldsymbol{a} \parallel c$	$\pi \parallel c$	LA	6.20
$\boldsymbol{a} \parallel c$	$\pi \perp c$	TA1, TA2	2.79
$\boldsymbol{a} \perp c$	$\pi \perp c$	LA	6.07
$\boldsymbol{a} \perp c$	$\pi \perp c$	TA1	2.80
$\boldsymbol{a} \perp c$	$\pi \parallel c$	TA2	2.79

*Calculated using $C_{11}=2.09\times10^{12}$ dyn/cm^2, $C_{12}=1.20\times10^{12}$ dyn/cm^2, $C_{33}=2.18\times10^{12}$ dyn/cm^2, $C_{44}=4.41\times10^{11}$ dyn/cm^2, and $g=5.6768$ g/cm^3.

5.4 PHONONS AND LATTICE VIBRONIC PROPERTIES

5.4.1 Phonon Dispersion Relation

- **Dispersion curve**

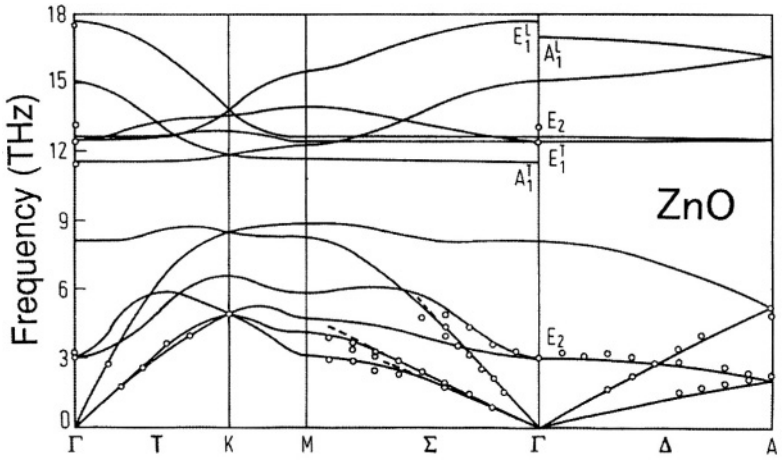

Fig. 5.4.1 Phonon dispersion curves for ZnO at 300 K predicted by a shell model based on experimental elastic constants and Raman spectrum. [From A. W. Hewat, *Solid State Commun.* **8**, 187 (1970).]

5.4.2 Phonon Frequency

- **Room-temperature value**

Table 5.4.1 *Long-wavelength ($q \to 0$) phonon frequencies for ZnO.*

Phonon frequency (cm^{-1})						Ref.
E_2 low	A_1 (TO)	E_1 (TO)	E_2 high	A_1 (LO)	E_1 (LO)	
101	380	407	437	574	583	[4.1]
	377	406		575	589	[4.2]
101	380	413	444	579	591	[4.3]
		413			585	[4.4]
	381	407	441		583	[4.5]
101	380	408	437		584	[4.6]
98	378	409.5	437.5	576	588	[4.7]
99	382	414	439	574	580	[4.8]
102	379	410	437		591	[4.9]
		408.2		577.1	592.1	[4.10]
100	380	410	439	576	587	Mean value

[4.1] T. C. Damen, S. P. S. Porto, and B. Tell, *Phys. Rev.* **142,** 570 (1966).
[4.2] E. C. Heltemes and H. L. Swinney, *J. Appl. Phys.* **38**, 2387 (1967).
[4.3] C. A. Arguello, D. L. Rousseau, and S. P. S. Porto, *Phys. Rev.* **181,** 1351 (1969).
[4.4] J. B. Bates and M. H. Brooker, *J. Phys. Chem. Solids* **32**, 2403 (1971).
[4.5] R. H. Callender, S. S. Sussman, M. Selders, and R. K. Chang, *Phys. Rev. B* **7**, 3788 (1973).
[4.6] J. M. Calleja and M. Cardona, *Phys. Rev. B* **16**, 3753 (1977).
[4.7] B. H. Bairamov, A. Heinrich, G. Irmer, V. V. Toporov, and E. Ziegler, *Phys. Status Solidi B* **119,** 227 (1983).
[4.8] F. Decremps, J. Jellicer-Porres, A. M. Saitta, J.-C. Chervin, and A. Polian, *Phys. Rev. B* **65**, 92101 (2002).
[4.9] Raman scattering [N. Ashkenov, B. N. Mbenkum, C. Bundesmann, V. Riede, M. Lorenz, D. Spemann, E. M. Kaidashev, A. Kasic, M. Schubert, M. Grundmann, G. Wagner, and H. Neumann, *J. Appl. Phys.* **93**, 126 (2003)].
[4.10] Infrared spectroscopic ellipsometry [N. Ashkenov, B. N. Mbenkum, C. Bundesmann, V. Riede, M. Lorenz, D. Spemann, E. M. Kaidashev, A. Kasic, M. Schubert, M. Grundmann, G. Wagner, and H. Neumann, *J. Appl. Phys.* **93**, 126 (2003)].

5.4.3 Mode Grüneisen Parameter

Table 5.4.2 *Mode Grüneisen parameter for the long-wavelength ($q \to 0$) phonons in ZnO [4.11].*

Phonon	Mode Grüneisen parameter
E_2 low	−1.6
A_1 (TO)	2.1
E_1 (TO)	1.8
E_2 high	2.0
A_1 (LO)	
E_1 (LO)	1.4

[4.11] F. Decremps, J. Jellicer-Porres, A. M. Saitta, J.-C. Chervin, and A. Polian, *Phys. Rev. B* **65**, 92101 (2002).

5.4.4 Phonon Deformation Potential

No detailed data are available for ZnO.

5.5 COLLECTIVE EFFECTS AND RELATED PROPERTIES

5.5.1 Piezoelectric Constant

Table 5.5.1 *Experimentally determined piezoelectric stress* (e_{ij}) *and strain constants* (d_{ij}) *for ZnO.*

e_{ij} (C/m^2)			d_{ij} (10^{-12} m/V)			Ref.
e_{15}	e_{31}	e_{33}	d_{15}	d_{31}	d_{33}	
			–13	–4.7	12.0	[5.1]
–0.31	–0.16	1.1				[5.2]
–0.59	–0.61	1.14	–13.9	–5.2	10.6	[5.3]
–0.36	–0.36	1.57	–8.3	–5.0	12.4	[5.4]
–0.37	–0.62	0.96	–8.3	–5.12	12.3	[5.5]
			–11.34	–5.43	11.67	[5.6]

[5.1] A. R. Hutson, *Phys. Rev. Lett.* **4**, 505 (1960).
[5.2] A. R. Hutson, *J. Appl. Phys.* **32**, 2287 (1961).
[5.3] H. Jaffe and D. A. Berlincourt, *Proc. IEEE* **53**, 1372 (1965).
[5.4] D. F. Crisler, J. J. Cupal, and A. R. Moore, *Proc. IEEE* **56**, 225 (1968).
[5.5] E. F. Tokarev, I. B. Kobyakov, I. P. Kuz'mina, A. N. Lobachev, and G. S. Pado, *Sov. Phys. Solid State* **17**, 629 (1975).
[5.6] B. A. Auld, *J. Acoust. Soc. Am.* **70**, 1577 (1981).

5.5.2 Fröhlich Coupling Constant

Table 5.5.2 *Fröhlich coupling constant* α_F *of ZnO.*

α_F	Ref.
0.849	[5.7]
1.19	[5.8]

[5.7] E. Kartheuser, in *Polarons in Ionic Crystals and Polar Semiconductors,* edited by J. T. Devreese (North-Holland, Amsterdam, 1972), p. 717.
[5.8] Y. Imanaka, M. Oshikiri, K. Takehana, T. Takamasu, and G. Kido, *Physica B* **298**, 211 (2001).

5.6 ENERGY-BAND STRUCTURE: ENERGY-BAND GAPS

5.6.1 Basic Properties

- **Electronic energy-band structure**

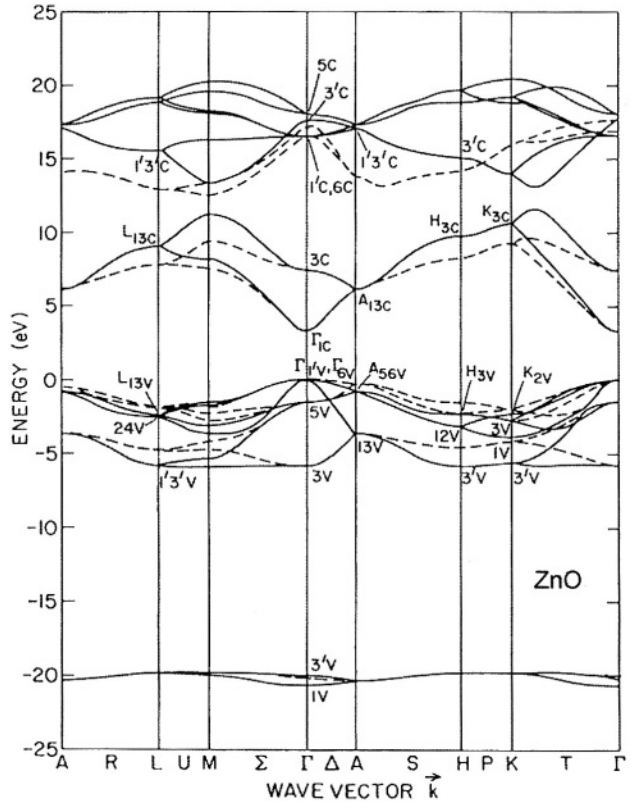

Fig. 5.6.1 Electronic energy-band structure of ZnO as calculated with the semiempirical tight-binding scheme. The dashed lines also show the results derived from the pseudopotential method by J. R. Chelikowsky [*Solid State Commun.* **22**, 351 (1977)]. [From A. Kobayashi, O. F. Sankey, S. M. Volz, and J. D. Dow, *Phys. Rev. B* **28**, 935 (1983).]

- **Electronic density of states**

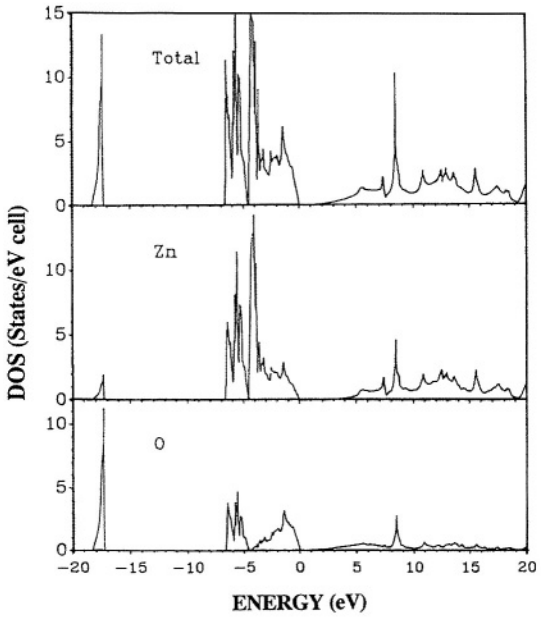

Fig. 5.6.2 Calculated density of states (DOS) and partial DOS for ZnO using the first-principles orthogonalized linear-combination-of-atomic-orbitals method. [From Y.-N. Xu and W. Y. Ching, *Phys. Rev. B* **48**, 4335 (1993).]

• **Energy eigenvalue**

Table 5.6.1 *Energy eigenvalues at the critical points for the valence and first few conduction bands of ZnO [6.1].*

Critical point	Level	Value (eV)
Γ	Γ_1^v	−20.68
	Γ_3^v	−5.85
	Γ_5^v	−1.52
	$\Gamma_6^v, \Gamma_1,^v$	0.00
	Γ_1^c	3.30
	Γ_3^c	7.39
	$\Gamma_6^c, \Gamma_1,^c$	16.51
K	$K_3,^v$	−5.63
	K_1^v	−3.90
	K_3^v	−2.63
	K_2^v	−2.30
L	$L_{1',3},^v$	−5.78
	$L_{2,4}^v$	−2.44
	$L_{1,3}^v$	−2.34
	$L_{1,3}^c$	9.05
	$L_{1',3},^c$	15.53
H	$H_3,^v$	−5.82
	$H_{1,2}^v$	−3.13
	H_3^v	−2.30
	H_3^c	9.74
A	$A_{1,3}^v$	−3.63
	$A_{5,6}^v$	−0.79
	$A_{1,3}^c$	6.11

[6.1] A. Kobayashi, O. F. Sankey, S. M. Volz, and J. D. Dow, *Phys. Rev. B* **28**, 935 (1983).

5.6.2 E_0-Gap Region

• **Room-temperature value**

Table 5.6.2 *$E_{0\alpha}$-gap energy (α=A, B, or C) for ZnO at room temperature.*

$E_{0\alpha}$ (eV)			Ref.
A	*B*	*C*	
3.36			[6.2] *
3.372±0.004	3.405±0.004		[6.3]
3.40	3.45	3.55	[6.4]

[6.2] V. Srikant and D. R. Clarke, *J. Appl. Phys.* **83**, 5447 (1998).
[6.3] G. E. Jellison, Jr. and L. A. Boatner, *Phys. Rev. B* **58**, 3586 (1998).
[6.4] J. F. Muth, R. M. Kolbas, A. K. Sharma, S. Oktabrsky, and J. Narayan, *J. Appl. Phys.* **85**, 7884 (1999).
* Estimated from excitonic gap by adding an exciton binding energy of G=60 meV.

• **Temperature dependence**

Table 5.6.3 *Empirical equation for the $E_{0\alpha}$-gap (α=A, B, or C) energy variation with temperature T for ZnO. 3D-CP=three-dimensional critical point.*

$$E_{0\alpha}(T) = E_{0\alpha}(0) - \frac{\alpha T^2}{T+\beta}$$

Parameter			Comment
$E_{0\alpha}(0)$ (eV)	α (10^{-4} eV/K)	β (K)	
3.3772	7.2	1077	n=1 exciton (A), T=10–300 K [6.5]
3.441	6.5	660	3D-CP (A), T=15–300 K, bulk ZnO [6.6]
3.455	6.5	660	3D-CP (B), T=15–300 K, bulk ZnO [6.6]
3.499	6.5	660	3D-CP (C), T=15–300 K, bulk ZnO [6.6]
3.373	6.5	660	n=1 exciton (A), T=15–300 K, bulk ZnO [6.6]
3.390	6.5	660	n=1 exciton (B), T=15–300 K, bulk ZnO [6.6]
3.436	6.5	660	n=1 exciton (C), T=15–300 K, bulk ZnO [6.6]

[6.5] H. J. Ko, Y. F. Chen, Z. Zhu, T. Yao, I. Kobayashi, and H. Uchiki, *Appl. Phys. Lett.* **76**, 1905 (2000).
[6.6] T. Mishima, S. Ozaki, and S. Adachi (unpublished).

Table 5.6.4 *Empirical equation for the $E_{0\alpha}$-gap (α=A, B, or C) energy variation with temperature T for ZnO. 3D-CP=three-dimensional critical point.*

$$E_{0\alpha}(T) = E_{0\alpha}(0) - \frac{\alpha\Theta_p}{2}\left[\sqrt[p]{1+\left(\frac{2T}{\Theta_p}\right)^p} - 1\right]$$

$E_{0\alpha}(0)$ (eV)	p	α (meV/K)	Θ_p (K)	Comment
3.441	2.8	0.30	215	3D-CP (A), T=15–300 K, bulk ZnO [6.7]
3.455	2.8	0.30	215	3D-CP (B), T=15–300 K, bulk ZnO [6.7]
3.499	2.8	0.30	215	3D-CP (C), T=15–300 K, bulk ZnO [6.7]
3.373	2.8	0.30	215	n=1 exciton (A), T=15–300 K, bulk ZnO [6.7]
3.390	2.8	0.30	215	n=1 exciton (B), T=15–300 K, bulk ZnO [6.7]
3.436	2.8	0.30	215	n=1 exciton (C), T=15–300 K, bulk ZnO [6.7]

[6.7] T. Mishima, S. Ozaki, and S. Adachi (unpublished).

• **Pressure dependence**

Table 5.6.5 *Empirical equation for the $E_{0\alpha}$-gap (α=A, B, or C) energy variation with pressure p for ZnO.*

$$E_{0\alpha}(p) = E_{0\alpha}(0)+ap+bp^2$$

Band gap	Parameter			Comment
	$E_{0\alpha}(0)$ (eV)	a (10^{-2} eV/GPa)	b (10^{-4} eV/GPa^2)	
A ($\Gamma_7^c - \Gamma_7^v$)	3.4410±0.0001	2.47±0.01	−2.8±0.1	T=6 K [6.8]
B ($\Gamma_7^c - \Gamma_9^v$)	3.4434±0.0001	2.53±0.01	−2.8±0.1	T=6 K [6.8]
C ($\Gamma_7^c - \Gamma_7^v$)	3.4817±0.0002	2.68±0.02	−2.8±0.1	T=6 K [6.8]

[6.8] A. Mang, K. Reimann, and St. Rübenacke, *Solid State Commun.* **94**, 251 (1995).

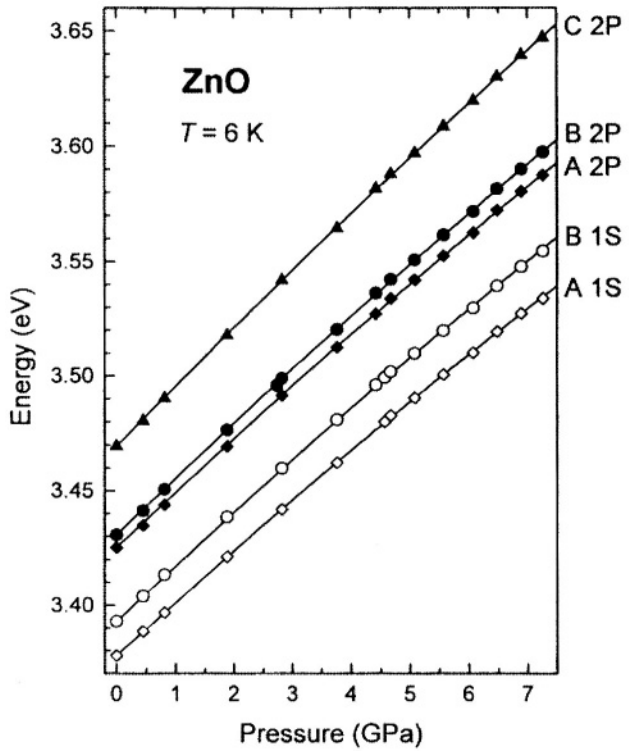

Fig. 5.6.3 Exciton energies in ZnO as a function of pressure at T=6 K. [From A. Mang, K. Reimann, and St. Rübenacke, *Solid State Commun.* **94**, 251 (1995).]

• **Temperature and/or pressure coefficient**

Table 5.6.6 *Linear temperature and pressure coefficients of the excitonic energy gap $E_{0\alpha}$ (α=A, B, or C) for ZnO.*

Coefficient	Value	Comment
$dE_{0\alpha}/dT$ (10^{-4} eV/K)	−8 (A)	T=97–670 K [6.9]
	−9.5 (A)	[6.10]
	−3.65 (A)	T>180 K [6.11]
	−2.90±0.05 (A, B)	T=80–293 K [6.12]
	−3.4 (A, B, C)	T=15–300 K [6.13]
	−2.9 (A, B, C)	T=15–300 K [6.13]

Table 5.6.6 *Continued.*

Coefficient	Value	Comment
$dE_{0\alpha}/dp$ (10^{-2} eV/GPa)	0.6–2.78 (*A*)	[6.12]
	2.7 (*A*)	[6.14]
	2.33 (*A*)	[6.15]
	2.7 (*A*)	[6.16]

[6.9] H. Watanabe, M. Wada, and T. Takahashi, *Jpn. J. Appll Phys.* **3**, 617 (1964).
[6.10] See, B. Ray, *II–VI Compounds* (Pergamon, Oxford, 1969).
[6.11] G. Hv Edstrup Jensen, *Phys. Status Solidi B* **64**, K51 (1974).
[6.12] V. V. Sobolev, V. I. Donetskikh, and E. F. Zagaĭnov, *Sov. Phys. Semicond* **12**, 646 (1978).
[6.13] T. Mishima, S. Ozaki, and S. Adachi (unpublished).
[6.14] R. L. Knell and D. W. Langer, *Phys. Lett.* **21**, 370 (1966).
[6.15] D. R. Huffman, L. A. Schwalbe, and D. Schiferl, *Solid State Commun.* **44**, 521 (1982).
[6.16] M. J. Peanasky and H. G. Drickamer, *J. Appl. Phys.* **56**, 3471 (1984).]

- **Doping dependence**

The excitonic energy-gap shift in In-doped ZnO films with carrier concentration has been studied using spectroscopic ellipsometry by K. J. Kim and Y. R. Park [*Appl. Phys. Lett.* **78**, 475 (2001)]. The fundamental absorption edge is found to show a blueshift below the carrier concentration $n=5\times10^{19}$ cm^{-3}, which can be explained in terms of the Burstein–Moss effect.

- **Crystal-field and spin–orbit–splitoff energies**

Table 5.6.7 *Theoretical crystal-field and spin-orbit–splitoff energies Δ_1, Δ_2, and Δ_3 for ZnO (in meV). Note that in the quasi-cubic approximation, $\Delta_{cr}=\Delta_1$ and $\Delta_{so}=3\Delta_2=3\Delta_3$.*

Δ_1 (Δ_{cr})	Δ_2	Δ_3	Δ_{so}	Comment
40	0	0		Calc. [6.17]

[6.17] See, T. Dietl, H. Ohno, and F. Matsukura, *Phys. Rev. B* **63**, 195205 (2001).

Table 5.6.8 *Experimental crystal-field and spin-orbit–splitoff energies Δ_1, Δ_2, and Δ_3 for ZnO (in meV). Note that in the quasi-cubic approximation, $\Delta_{cr}=\Delta_1$ and $\Delta_{so}=3\Delta_2=3\Delta_3$.*

Δ_1 (Δ_{cr})	Δ_2	Δ_3	Δ_{so}	Ref.
40.8±0.7			–4.7±0.7	[6.18]
36.3	1.9	7.4		[6.19]
43			19	[6.19]
39.4±0.2			–3.5±0.2	[6.20]
43			16	[6.21]*
30.5	4.2	11.5		[6.22]*
49			–19	[6.23]
45			27	[6.24]

[6.18] W. Y. Liang and A. D. Yoffe, *Phys. Rev. Lett.* **20**, 59 (1968).
[6.19] D. W. Langer, R. N. Euwema, K. Era, and T. Koda, *Phys. Rev. B* **2**, 4005 (1970).
[6.20] A. Mang, K. Reimann, and St. Rübenacke, *Solid State Commun.* **94**, 251 (1995).
[6.21] D. C. Reynolds, D. C. Look, B. Jogai, C. W. Litton, G. Catwell, and W. C. Harsch, *Phys. Rev. B* **60**, 2340 (1999).
[6.22] B. Gil, *Phys. Rev. B* **64**, 201310 (2001); B. Gil, A. Lusson, V. Sallet, S.-A. Said-Hassani, R. Triboulet, and P. Bigenwald, *Jpn. J. Appl. Phys.* **40**, L1089 (2001).
[6.23] Obtained assuming the valence-band ordering of Γ_7^v–Γ_9^v–Γ_7^v [T. Mishima, S. Ozaki, and S.

Adachi (unpublished)].
[6.24] Obtained assuming the valence-band ordering of Γ_9^v–Γ_7^v–Γ_7^v [T. Mishima, S. Ozaki, and S. Adachi (unpublished)].
*This study suggests the valence-band ordering of Γ_9^v–Γ_7^v–Γ_7^v, which is the same as that for *w*-CdS.

5.6.3 Higher-Lying Direct Gap

- **Room-temperature value**

Table 5.6.9 *Higher-lying direct-gap energies for ZnO measured at room temperature [6.25].*

Peak (eV)		Polarization
Reflectivity	ε_2	
7.00	7.10	$\boldsymbol{E}\perp c$
7.05	7.15	$\boldsymbol{E}\parallel c$
9.2	9.3	$\boldsymbol{E}\perp c$
8.95	9.0	$\boldsymbol{E}\parallel c$
12.6	12.5	$\boldsymbol{E}\perp c$
14.0	13.7	$\boldsymbol{E}\perp c$
13.8	13.4	$\boldsymbol{E}\parallel c$
14.7		$\boldsymbol{E}\parallel c$
15.2	14.8	$\boldsymbol{E}\perp c$
15.6		$\boldsymbol{E}\parallel c$
17.1		$\boldsymbol{E}\perp c$
18.9		$\boldsymbol{E}\parallel c$
19.3		$\boldsymbol{E}\perp c$
20.8		$\boldsymbol{E}\perp c$

[6.25] R. Klucker, H. Nelkowski, Y. S. Park, M. Skibowski, and T. S. Wagner, *Phys. Status Solidi B* **45**, 265 (1971).

5.6.4 Lowest Indirect Gap

- **Theoretical value**

Table 5.6.10 *Theoretically obtained lowest indirect-gap energy for ZnO.*

Band gap	Value (eV)		
	a	b	c
E_g^K ($\Gamma\rightarrow$K)	9.29	10.55	
E_g^M ($\Gamma\rightarrow$M)			
E_g^L ($\Gamma\rightarrow$L)	7.78	9.05	8.78
E_g^H ($\Gamma\rightarrow$H)	8.30	9.74	10.38
E_g^A ($\Gamma\rightarrow$A)	6.15	6.11	5.89

[a] J. R. Chelikowsky, *Solid State Commun.* **22**, 351 (1977).
[b] A. Kobayashi, O. F. Sankey, S. M. Volz, and J. D. Dow, *Phys. Rev. B* **28**, 935 (1983).
[c] M.-Z. Huang and W. Y. Ching, *J. Phys. Chem. Solids* **46**, 977 (1985).

5.6.5 Conduction-Valley Energy Separation

Table 5.6.11 *Theoretically obtained conduction-valley energy separation ΔE_g for ZnO.*

ΔE_g	Value (eV)		
	a	b	c
K–Γ	5.99	7.25	
M–Γ			
L–Γ	4.48	5.75	5.47
H–Γ	5.00	6.44	7.07
A–Γ	2.85	2.81	2.58

[a] J. R. Chelikowsky, *Solid State Commun.* **22,** 351 (1977).
[b] A. Kobayashi, O. F. Sankey, S. M. Volz, and J. D. Dow, *Phys. Rev. B* **28,** 935 (1983).
[c] M.-Z. Huang and W. Y. Ching, *J. Phys. Chem. Solids* **46**, 977 (1985).

5.6.6 Direct–Indirect-Gap Transition Pressure

No detailed data are available for ZnO.

5.7 ENERGY-BAND STRUCTURE: ELECTRON AND HOLE EFFECTIVE MASSES

5.7.1 Electron Effective Mass: Γ Valley

- **Theoretical value**

Table 5.7.1 *Theoretical electron effective masses $m_e^{\perp}$, $m_e^{/\!/}$, and m_e^{Γ} at the Γ valley for ZnO. $m_e^{\Gamma}=(m_e^{\perp 2}\, m_e^{/\!/})^{1/3}$: density-of-states effective mass.*

$m_e^{\perp}/m_0$	$m_e^{\parallel}/m_0$	m_e^{Γ}/m_0	Technique
0.329	0.307	0.322	Linear combination of atomic orbital method [7.1]
0.20	0.16	0.19	Monte Carlo calculation [7.2]
0.24	0.21	0.23	GW approximation [7.3]

[7.1] M.-Z. Huang and W. Y. Ching, *J. Phys. Chem. Solids* **46**, 977 (1985).
[7.2] J. D. Albrecht, P. P. Ruden, S. Limpijumnong, and W. R. L. Lambrecht, *J. Appl. Phys.* **86**, 6864 (1999).
[7.3] M. Oshikiri, Y. Imanaka, F. Aryasetiawan, and G. Kido, *Physica B* **298,** 472 (2001).

- **Experimental value**

Table 5.7.2 *Experimental electron effective masses $m_e^{\perp}$, $m_e^{/\!/}$, and m_e^{Γ} at the Γ valley for ZnO. $m_e^{\Gamma}=(m_e^{\perp 2}\, m_e^{/\!/})^{1/3}$: density-of-states effective mass. α_F=Fröhlich coupling constant.*

$m_e^{\perp}/m_0$	$m_e^{\parallel}/m_0$	m_e^{Γ}/m_0	Comment
		0.265±0.015	Free-carrier absorption, T=300 K [7.4]
0.24*[1]			Faraday rotation, α_F=1.0 [7.5]
0.29±0.02*[2]			Faraday rotation [7.5]

Table 5.7.2 *Continued.*

$m_e^{\perp}/m_0$	$m_e^{\parallel}/m_0$	m_e^{Γ}/m_0	Comment
		0.28	Zeeman splitting [7.6]
0.28	0.28	0.28	Zeeman splitting [7.7]
0.26	0.22		Infrared reflectivity, T=293 K [7.8]
0.234*[1]			Cyclotron resonance, T=4.2 K, α_F=1.19 [7.9]
0.292*[2]			Cyclotron resonance, T=4.2 K [7.9]

[7.4] R. L. Weiher, *Phys. Rev.* **152,** 736 (1966).
[7.5] W. S. Baer, *Phys. Rev.* **154,** 785 (1967).
[7.6] K. J. Button, D. R. Cohn, M. von Ortenbert, B. Lax, E. Mollwo, and R. Helbig, *Phys. Rev. Lett.* **28,** 1637 (1972).
[7.7] K. Hümmer, R. Helbig, and M. Baumgärtner, *Phys. Status Solidi B* **86**, 527 (1978) [see, G. Blattner, G. Kurtze, G. Schmieder, and C. Klingshirn, *Phys. Rev. B* **25,** 7413 (1982)].
[7.8] E. F. Venger, A. V. Melnichuk, L. Yu. Melnichuk, and Yu. A. Pasechnik, *Phys. Status Solidi B* **188**, 823 (1995).
[7.9] Y. Imanaka, M. Oshikiri, K. Takehana, T. Takamasu, and G. Kido, *Physica B* **298,** 211 (2001).
*[1]Bare mass.
*[2]Polaron mass.

• Temperature dependence

The cyclotron masses observed in *n*–ZnO at T=4.2 and 60 K by Y. Imanaka, M. Oshikiri, K. Takehana, T. Takamasu, and G. Kido [*Physica B* **298**, 211 (2001)] are m_{ep}*=0.292m_0 and 0.290m_0, respectively.

5.7.2 Electron Effective Mass: Satellite Valley

No detailed data are available for ZnO.

5.7.3 Hole Effective Mass

• Luttinger's valence-band parameter

Table 5.7.3 *Theoretical Luttinger's valence-band parameter A_i for ZnO. A_i (i=1–6) are in units of $\hbar^2/2m_0$ and A_7 is in units of eV/Å.*

A_1	A_2	A_3	A_4	A_5	A_6	$\lvert A_7\rvert$	Ref.
–2.41	–0.44	2.11	–1.06	–1.06	–1.51		[7.10]
–3.78	–0.44	3.45	–1.63	1.68	–2.23	0.025	[7.11]

[7.10] See, T. Dietl, H. Ohno, and F. Matsukura, *Phys. Rev. B* **63**, 195205 (2001).
[7.11] W. R. L. Lambrecht, A. V. Rodina, S. Limpijumnong, B. Segall, and B. K. Meyer, *Phys. Rev. B* **65**, 75207 (2002).

• Density-of-states mass

Table 5.7.4 *Density-of-states masses in ZnO (in m_0). $m_{H\alpha}$* (α=A, B, or C) represents the hole effective mass of the top three valence bands.*

$\perp c$			$\parallel c$		Comment
m_{HA}*	m_{HB}*	m_{HC}*	m_{HH}*	m_{LH}*	
5.417	3.427	0.389	4.520	0.325	Calc. [7.12]

[7.12] M.-Z. Huang and W. Y. Ching, *J. Phys. Chem. Solids* **46**, 977 (1985).

5.8 ELECTRONIC DEFORMATION POTENTIAL

5.8.1 Intravalley Deformation Potential: Γ Point

• Conduction band

Table 5.8.1 *Γ-conduction-band acoustic deformation potential E_1 for ZnO used in the transport data analysis.*

E_1 (eV)	Ref.
3.8	[8.1]

[8.1] D. L. Rode, in *Semiconductors and Semimetals,* edited by R. K. Willardson and A. C. Beer (Academic, New York, 1975), Vol. 10, p. 1.

• Valence band

Table 5.8.2 *Experimentally determined Γ-valence-band deformation potentials C_i's for ZnO.*

Deformation potential (eV)						Ref.
D_1–C_1	D_2–C_2	C_3	C_4	C_5	C_6	
–3.9	–4.0	1.2	–0.94	0.62		[8.2]
–3.8	–3.8	0.8	–1.4	–1.2	2.0	[8.3]
–3.90±0.03	–4.13±0.03	1.15±0.04	–1.22±0.04	–1.53±0.01	2.88±0.04	[8.4]

[8.2] J. E. Rowe, M. Cardona, and F. H. Pollak, *Solid State Commun.* **6**, 239 (1968) [see also, A. Gavini and M. Cardona, *Phys. Rev. B* **1**, 672 (1970)].
[8.3] D. W. Langer, R. N. Euwema, K. Era, and T. Koda, *Phys. Rev. B* **2**, 4005 (1970).
[8.4] J. Wrzesinski and D. Fröhlich, *Phys. Rev. B* **56**, 13087 (1997).

• E_0 gap

Table 5.8.3 *Hydrostatic deformation potential a_0^Γ for the E_0 gap of ZnO.*

a_0^Γ (eV)			Comment
A (Γ_7^c –Γ_7^v)	B (Γ_7^c –Γ_9^v)	C (Γ_7^c –Γ_7^v)	
–3.51±0.02	–3.59±0.02	–3.81±0.02	Exper. [8.5]
–3.9			Exper. *
–3.51	–3.59	–3.81	Recommended

[8.5] A. Mang, K. Reimann, and St. Rübenacke, *Solid State Commun.* **94**, 251 (1995).
*Estimated from dE_0/dp value.

5.8.2 Intravalley Deformation Potential: High-Symmetry Points

No detailed data are available for ZnO.

5.8.3 Intervalley Deformation Potential

No detailed data are available for ZnO.

5.9 ELECTRON AFFINITY AND SCHOTTKY BARRIER HEIGHT

5.9.1 Electron Affinity

Table 5.9.1 *Electron affinity χ_s for ZnO.*

χ_s (eV)	Comment
4.19	$(000\bar{1})$O face [9.1]
3.7	(0001)Zn face [9.2]
4.5	$(000\bar{1})$O face [9.2]
4.60	$(10\bar{1}0)$ face [9.2]

[9.1] H. Moormann, D. Kohl, and G. Heiland, *Surf. Sci.* **100,** 302 (1980).
[9.2] K. Jacobi, G. Zwicker, and A. Gutmann, *Surf. Sci.* **141,** 109 (1984).

5.9.2 Schottky Barrier Height

Table 5.9.2 *Summary of the Schottky barrier height ϕ_n for metal/n-ZnO contacts at 300 K.**

Metal	ϕ_n (eV)	Metal	ϕ_n (eV)
Ag	0.69–0.92	Pd	0.58–0.68
Al	0.68	Pt	0.7
Au	0.64–0.90	Ta	0.3
Cu	0.45	Ti	0-0.3
In	0–0.3		

*The data are gathered from various sources.

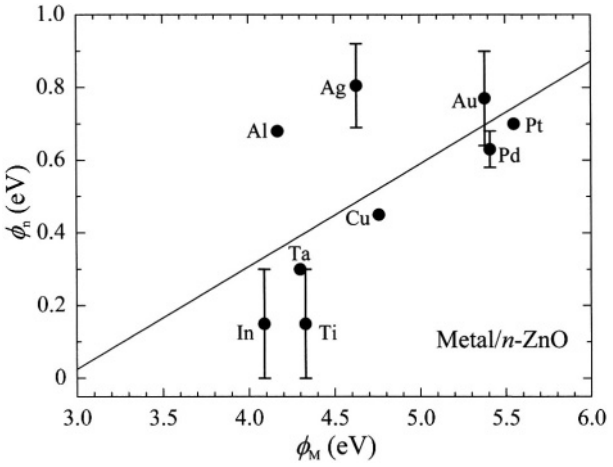

Fig. 5.9.1 Schottky barrier height ϕ_n versus metal work function ϕ_M observed for metal/*n*-ZnO contacts. Values of the metal work function were taken from H. P. R. Frederikse [in *CRC Handbook of Chemistry and Physics,* 78th Edition, edited by D. R. Lide (CRC Press, Boca Raton, 1997), p. 12-115]. The solid line represents the least-squares-fit result with $\phi_n=0.28\phi_M-0.82$ (ϕ_M and ϕ_n in eV).

- **Temperature and/or pressure coefficient**

Table 5.9.3 *Pressure coefficient of the Schottky barrier height ϕ_n for metal/n-ZnO contacts.*

Coefficient	Value	Comment
$d\phi_n/dp$ (meV/kbar)	11.6	Au, Pd/*n*-ZnO [9.3]

[9.3] M. J. Peanasky and H. G. Drickamer, *J. Appl. Phys.* **56,** 3471 (1984).

5.10 OPTICAL PROPERTIES

5.10.1 Summary of Optical Dispersion Relations

• $\varepsilon(E)$ and $n^*(E)$ spectra

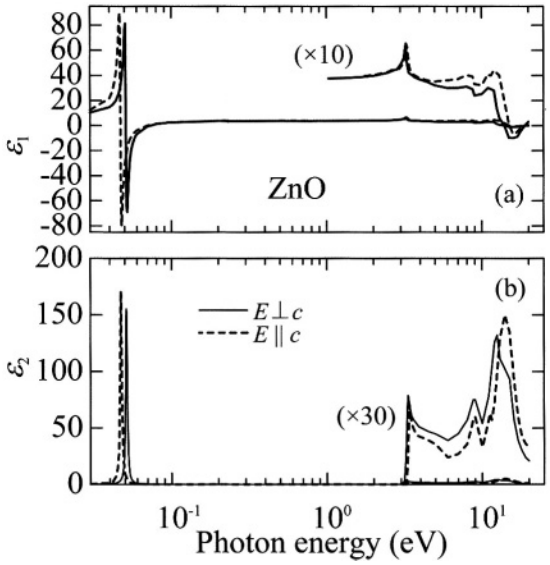

Fig. 5.10.1 Complex dielectric-constant spectra [$\varepsilon(E)=\varepsilon_1(E)+i\varepsilon_2(E)$] for ZnO at 300 K. The numerical data are taken from tabulation by S. Adachi [*Optical Constants of Crystalline and Amorphous Semiconductors: Numerical Data and Graphical Information* (Kluwer Academic, Boston, 1999)].

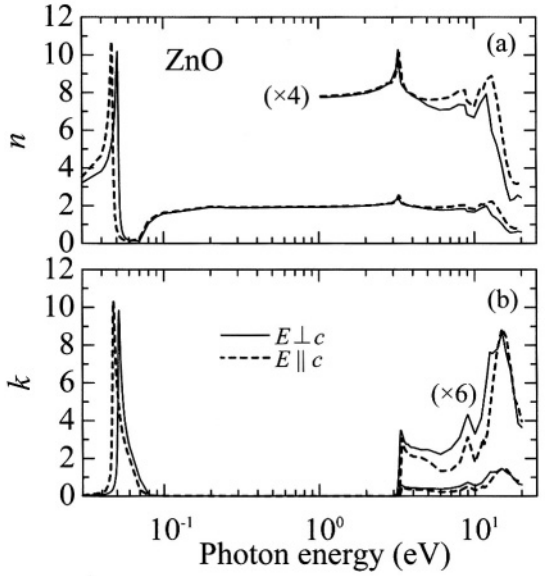

Fig. 5.10.2 Complex refractive-index spectra [$n^*(E)=n(E)+ik(E)$] for ZnO at 300 K. The numerical data are taken from tabulation by S. Adachi [*Optical Constants of Crystalline and Amorphous Semiconductors: Numerical Data and Graphical Information* (Kluwer Academic, Boston, 1999)].

• **$\alpha(E)$ and $R(E)$ spectra**

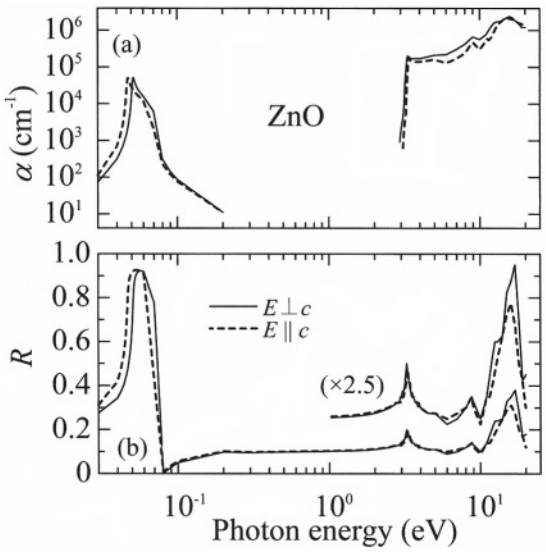

Fig. 5.10.3 (a) Absorption [$\alpha(E)$] and (b) normal-incidence reflectivity spectra [$R(E)$] for ZnO at 300 K. The numerical data are taken from tabulation by S. Adachi [*Optical Constants of Crystalline and Amorphous Semiconductors: Numerical Data and Graphical Information* (Kluwer Academic, Boston, 1999)].

5.10.2 The Reststrahlen Region

• **Static and high-frequency dielectric constants**

Table 5.10.1 *Static and high-frequency dielectric constants ε_s and ε_∞ for ZnO.*

$E \perp c$		$E \parallel c$		Comment
ε_s	ε_∞	ε_s	ε_∞	
9.26*[1]		11.0*[1]		[10.1]
8.33*[2]		8.84*[2]		
7.8±0.3	3.70	8.75±0.4	3.75	T=300 K [10.2]
8.67*[1]		11.26*[1]		T=300 K [10.3]
8.33*[2]		8.81*[2]		
6.1	5.1	6.1	5.1	T=300 K [10.4]
8.1	3.95	9.0	4.05	T=293 K [10.5]
7.77	3.70	8.91	3.78	T=300 K [10.6]
7.8	3.7	8.75	3.75	Recommended (T=300 K)

[10.1] H. Jaffe and D. A. Berlincourt, *Proc. IEEE* **53,** 1372 (1965).
[10.2] E. C. Heltemes and H. L. Swinney, *J. Appl. Phys.* **38**, 2387 (1967).
[10.3] I. B. Kobiakov, *Solid State Commun.* **35,** 305 (1980).
[10.4] A. N. Pikhtin and A. D. Yas'kov, *Sov. Phys. Semicond.* **15,** 8 (1981).
[10.5] A. V. Mel'nichuk, L. Yu. Mel'nichuk, and Yu. A. Pasechnik, *Phys. Solid State* **36**, 1430 (1994).
[10.6] N. Ashkenov, B. N. Mbenkum, C. Bundesmann, V. Riede, M. Lorenz, D. Spemann, E. M. Kaidashev, A. Kasic, M. Schubert, M. Grundmann, G. Wagner, and H. Neumann, *J. Appl. Phys.* **93**, 126 (2003).
*[1]Constant stress value.
*[2]Constant strain value.

Table 5.10.2 *Linear temperature andpressure coefficients ofthe static (ε_s) and high-frequency dielectric constants (ε_∞) for ZnO near 300 K and normal pressure.*

Coefficient	Value	Comment
$d\varepsilon_s/dT$ (10^{-4} K^{-1})	4.3	$\boldsymbol{E}\perp c$ [10.7]*
	4.4	$\boldsymbol{E} \parallel c$ [10.7]*
$d\varepsilon_\infty/dT$ (10^{-4} K^{-1})		
$d\varepsilon_s/dp$ (GPa^{-1})		
$d\varepsilon_\infty/dp$ (GPa^{-1})		

[10.7] I. B. Kobiakov, *Solid State Commun.* **35**, 305 (1980).
*Constant stress value.

- **Reststrahlen parameter**

Table 5.10.3 *A set of the reststrahlen parameters for ZnO.*

$$\varepsilon(\omega) = \varepsilon_\infty\left(1+\frac{\omega_{LO}^2-\omega_{TO}^2}{\omega_{TO}^2-\omega^2-i\omega\gamma}\right)$$

$\boldsymbol{E}\perp c$				$\boldsymbol{E} \parallel c$				Comment
ε_∞	ω_{LO} (cm^{-1})	ω_{TO} (cm^{-1})	γ (cm^{-1})	ε_∞	ω_{LO} (cm^{-1})	ω_{TO} (cm^{-1})	γ (cm^{-1})	
3.70	589	406	7.5	3.75	575	377	12.0	T=300 K [10.8]
3.95	591	412	11–40*	4.05	570	380	11–40*	T=293 K [10.9]

[10.8] E. C. Heltemes and H. L. Swinney, *J. Appl. Phys.* **38**, 2387 (1967).
[10.9] A. V. Mel'nichuk, L. Yu. Mel'nichuk, and Yu. A. Pasechnik, *Phys. Solid State* **36**, 1430 (1994).
*Depending on electron concentration.

- **Multiphonon optical absorption spectra**

The optical absorption spectra in the multiphonon region of ZnO have been measured by H. Lüth [*Solid State Commun.* **7**, 585 (1969)].

5.10.3 At or Near the Fundamental Absorption Edge

- **Free-exciton binding energy and related parameters**

Table 5.10.4 *Free-exciton binding (Rydberg) energy G for ZnO.*

G (meV)			Comment
A (Γ_7^v)	B (Γ_9^v)	C (Γ_7^v)	
42 (Γ_9^v)			T=1.2, 4.2 K [10.10]*
66.8±0.5	62.5	61.0±0.5	T=4.2 K [10.11]
61.2	58.9	58.8	T=1.6 K [10.12]
63.1±0.1	50.4±0.1	48.9±0.4	T=6 K [10.13]
59.7 (Γ_9^v)	57.3 (Γ_7^v)		T=2 K [10.14]*
68	65	63	T=15 K [10.15]
61	56	53	Recommended

[10.10] Y. S. Park, C. W. Litton, T. C. Collins, and D. C. Reynolds, *Phys. Rev.* **143**, 512 (1966).

[10.11] W. Y. Liang and A. D. Yoffe, *Phys. Rev. Lett.* **20**, 59 (1968).
[10.12] Estimated from data by K. Hümmer [*Phys. Status Solidi B* **56**, 249 (1973)].
[10.13] A. Mang, K. Reimann, and St. Rübenacke, *Solid State Commun.* **94**, 251 (1995).
[10.14] D. C. Reynolds, D. C. Look, B. Jogai, C. W. Litton, G. Catwell, and W. C. Harsch, *Phys. Rev. B* **60**, 2340(1999).
[10.15] T. Mishima, S. Ozaki, and S. Adachi (unpublished).
*This study suggests the valence-band ordering of Γ_9^v–Γ_7^v–Γ_7^v, which is the same as that for *w*-CdS.

Table 5.10.5 *Free-exciton parameters (G=binding energy; a_B=1st-orbital Bohr radius; μ=reduced mass) at the fundamental absorption edge of ZnO.*

Exciton	G (meV)	a_B (Å)*	μ (m_0)*
A	61	32	0.062
B	56	35	0.057
C	53	37	0.054

*Calculated using $\varepsilon_\infty=(\varepsilon_{\infty\perp}^2\varepsilon_{\infty\parallel})^{1/3}$ value.

Table 5.10.6 *Spin-exchange interaction constant j for ZnO.*

j (meV)	Ref.
5.6	[10.16]
4.73	[10.17]

[10.16] See, M. Julier, J. Campo, B. Gil, J. P. Lascaray, and S. Nakamura, *Phys. Rev. B* **57**, R6791 (1998); D. W. Langer, R. N. Euwema, K. Era, and T. Koda, *Phys. Rev. B* **2**, 4005 (1970).
[10.17] B. Gil, *Phys. Rev. B* **64**, 201310 (2001); B. Gil, A. Lusson, V. Sallet, S.-A. Said-Hassani, R. Triboulet, and P. Bigenwald, *Jpn. J. Appl. Phys.* **40**, L1089 (2001).

Table 5.10.7 *Pressure coefficient of the free-exciton binding (Rydberg) energy for ZnO [10.18].*

Exciton	$\frac{dG}{dp}$ (meV/GPa)
A (Γ_7^v)	1.11±0.02
B (Γ_9^v)	0.84±0.07
C (Γ_7^v)	1.0±0.5

[10.18] A. Mang, K. Reimann, and St. Rübenacke, *Solid State Commun.* **94,** 251 (1995).

- **Refractive index**

Table 5.10.8 *Refractive index n near the fundamental absorption edge of ZnO for $\boldsymbol{E}\perp c$ at 300 K [10.19].*

E (eV)	λ (μm)	n	E (eV)	λ (μm)	n
0.1	12.40	1.577	1.03	1.203	1.935
0.2	6.198	1.913	1.24	1.000	1.944
0.31	3.998	1.889	1.38	0.898	1.949
0.33	3.756	1.896	1.55	0.800	1.960
0.34	3.646	1.899	1.77	0.700	1.974
0.36	3.443	1.902	2.07	0.599	1.999
0.39	3.178	1.905	2.48	0.500	2.051
0.41	3.023	1.908	2.75	0.451	2.09
0.44	2.817	1.910	2.85	0.435	2.12
0.48	2.582	1.913	2.9	0.427	2.14
0.52	2.384	1.915	2.95	0.420	2.17

Table 5.10.8 *Continued.*

E (eV)	λ (μm)	n	E (eV)	λ (μm)	n
0.56	2.213	1.917	3	0.413	2.20
0.62	1.999	1.920	3.05	0.406	2.24
0.69	1.796	1.923	3.1	0.400	2.28
0.77	1.610	1.926	3.15	0.393	2.35
0.89	1.393	1.930	3.2	0.387	2.44

[10.19] See, S. Adachi, *Optical Constants of Crystalline and Amorphous Semiconductors: Numerical Data and Graphical Information* (Kluwer Academic, Boston, 1999).

Table 5.10.9 *Refractive index n near the fundamental absorption edge of ZnO for* $\boldsymbol{E} \parallel \boldsymbol{c}$ *at 300 K[10.20].*

E (eV)	λ (μm)	n	E (eV)	λ (μm)	n
0.1	12.40	1.625	0.89	1.393	1.943
0.2	6.198	1.939	1.03	1.203	1.950
0.31	3.998	1.907	1.24	1.000	1.959
0.33	3.756	1.910	1.38	0.898	1.965
0.34	3.646	1.913	1.55	0.800	1.975
0.36	3.443	1.916	1.77	0.700	1.990
0.39	3.178	1.919	2.07	0.599	2.015
0.41	3.023	1.921	2.48	0.500	2.06
0.44	2.817	1.925	2.75	0.451	2.09
0.48	2.582	1.927	2.95	0.420	2.13
0.52	2.384	1.930	3	0.413	2.15
0.56	2.213	1.931	3.05	0.406	2.18
0.62	1.999	1.933	3.1	0.400	2.21
0.69	1.796	1.937	3.15	0.393	2.26
0.77	1.610	1.940	3.2	0.387	2.32

[10.20] See, S. Adachi, *Optical Constants of Crystalline and Amorphous Semiconductors: Numerical Data and Graphical Information* (Kluwer Academic, Boston, 1999).

- **Refractive index: Temperature dependence**

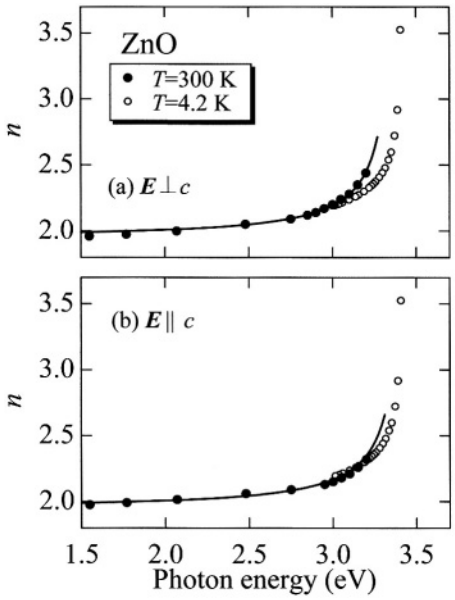

Fig. 5.10.4 Refractive index n in ZnO at T=300 and 4.2 K. The 4.2-K data are taken from Y. S. Park and J. R. Schneider [*J. Appl. Phys.* **39,** 3049 (1968)], while the 300-K data are taken from S. Adachi [*Optical Constants of Crystalline and Amorphous Semiconductors: Numerical Data and Graphical Information* (Kluwer Academic, Boston, 1999)]. The solid lines represent the calculated results using $n^2=3.65+[0.25\lambda^2/(\lambda^2-0.134)]$ for $\boldsymbol{E} \perp \boldsymbol{c}$ and $n^2=3.65+[0.25\lambda^2/(\lambda^2-0.130)]$ for $\boldsymbol{E} \parallel \boldsymbol{c}$ at 300 K with λ in μm.

- **Refractive index: Pressure dependence**

Table 5.10.10 *Pressure coefficient of the refractive index* $n^{-1}(dn/dp)$ *at* $\lambda=0.5893\ \mu m$ *for ZnO at 295 K [10.21].*

$\frac{1}{n}\frac{dn}{dp}$ (10^{-2} GPa^{-1})	
$E\perp c$	$E\parallel c$
–0.17	–0.17

[10.21] K. Vedam and T. A. Davis, *Phys. Rev.* **181**, 1196 (1969).

- **Fundamental absorption edge**

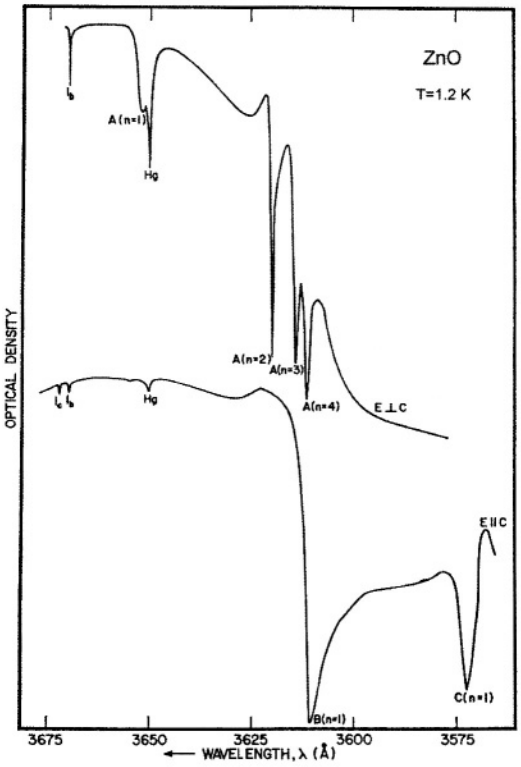

Fig. 5.10.5 Optical absorption spectra of a vapor-grown ZnO platelet at T=1.2 K in polarized light. The absorption lines were observed as the self-absorption of a continuum emission from the crystals when excited by the ultraviolet light from a high-pressure mercury lamp. Hg refers to the mercury emission lines. This study suggests the valence-band ordering of Γ_9^v–Γ_7^v–Γ_7^v, which is the same as that for *w*-CdS. [From Y. S. Park, C. W. Litton, T. C. Collins, and D. C. Reynolds, *Phys. Rev.* **143,** 512 (1966).]

5.10.4 The Interband Transition Region

- **Fundamental optical spectra**

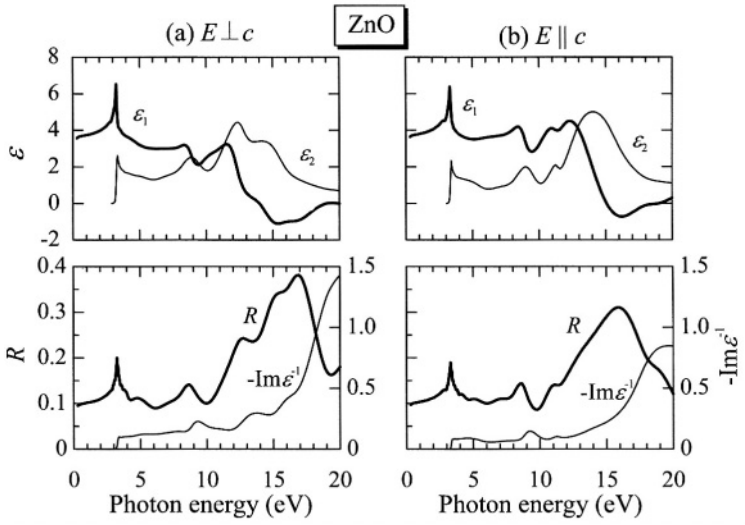

Fig. 5.10.6 Complex dielectric function, $\varepsilon(E)=\varepsilon_2(E)+i\varepsilon_2(E)$, fundamental reflectivity, $R(E)$, and energy-loss function, $-\mathrm{Im}\varepsilon^{-1}(E)$, for ZnO at 300 K. The experimental data are taken from tabulation by S. Adachi [*Optical Constants of Crystalline and Amorphous Semiconductors: Numerical Data and Graphical Information* (Kluwer Academic, Boston, 1999)].

• **$\varepsilon(E)$ spectrum: External perturbation and/or doping effects**

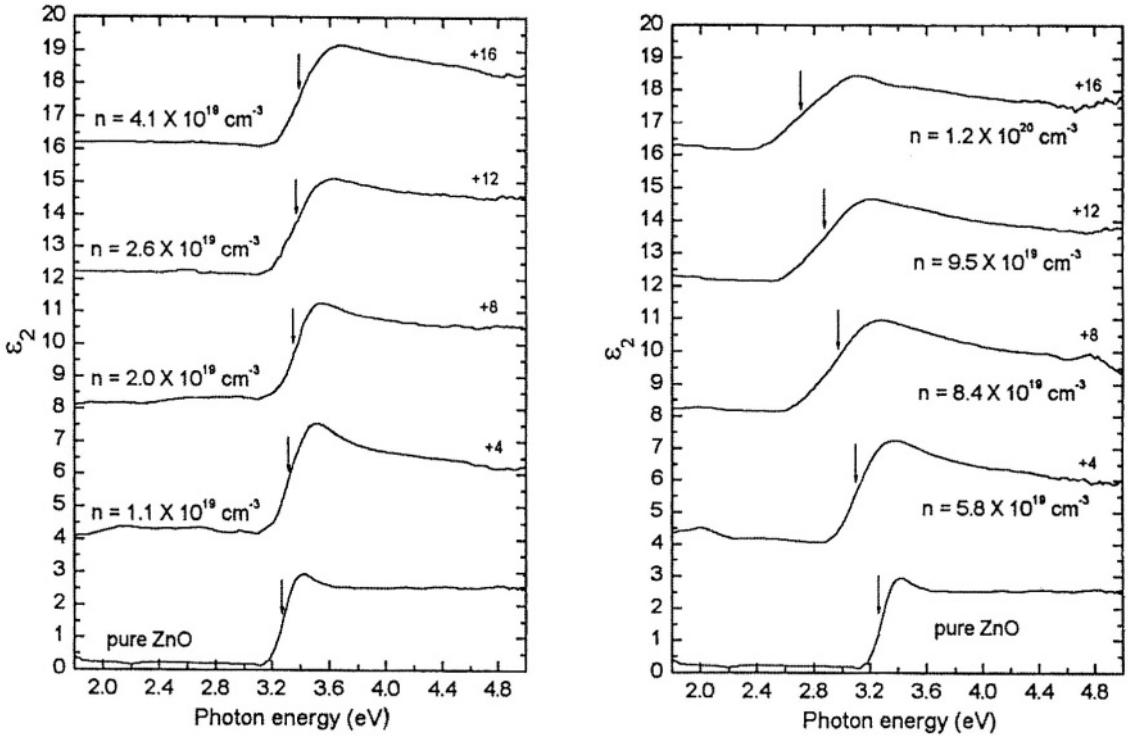

Fig. 5.10.7 Imaginary part ε_2 of the pseudodielectric function of pure and In-doped ZnO with carrier concentrations from n=1.1×10^{19} to 1.2×10^{20} cm^{-3}. Energy positions of the excitonic energy gap (E_0) are indicated by the vertical arrows. [From K. J. Kim and Y. R. Park, *Appl. Phys. Lett.* **78**, 475 (2001).]

5.10.5 Free-Carrier Absorption and Related Phenomena

No detailed data are available for ZnO.

5.11 ELASTOOPTIC, ELECTROOPTIC, AND NONLINEAR OPTICAL PROPERTIES

5.11.1 Elastooptic Effect

• **Photoelastic constant**

Table 5.11.1 *Photoelastic constant p_{ij} at λ=632.8 nm for ZnO [11.1].*

p_{11}	p_{12}	p_{13}	p_{31}	p_{33}	p_{44}	p_{66}
|0.222|	|0.099|	–0.111	|0.088|	–0.235	–0.0585	

[11.1] *Numerical Data and Functional Relationships in Science and Technology,* edited by K.-H. Hellwege and A. M. Hellwege, Landolt–Börnstein, New Series, Group III, Vol. 11 (Springer, Berlin, 1979).

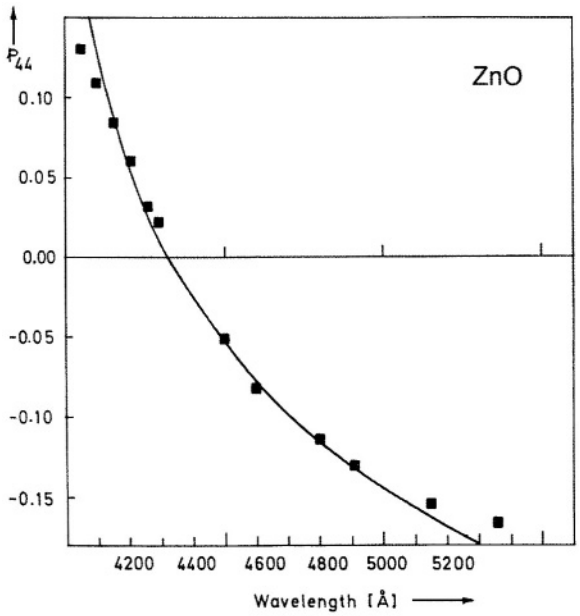

Fig. 5.11.1 Dispersion of the photoelastic constant p_{44} in ZnO at 300 K. The solid line represents the theoretical dispersion based on the piezobirefringence theory. [From R. Berkowicz and T. Skettrup, *Phys. Rev. B* **11**, 2316 (1975).]

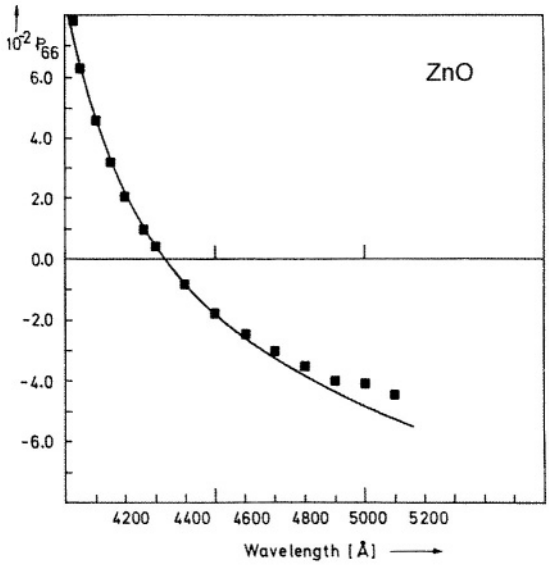

Fig. 5.11.2 Dispersion of the photoelastic constant p_{66} in ZnO at 300 K. The solid line represents the theoretical dispersion based on the piezobirefringence theory. [From R. Berkowicz and T. Skettrup, *Phys. Rev. B* **11**, 2316 (1975).]

5.11.2 Linear Electrooptic Constant

Table 5.11.2 *Linear electrooptic constant r_{ij} for ZnO.*

Wavelength (μm)	r_{ij} (pm/V)			Comment
	r_{13}	r_{33}	r_{42}	
0.396			−3.1	Free value (T) [11.2]
0.633	−1.4	+2.6		Clamped value (S) [11.3]
3.39	+0.96	+1.9		Clamped value (S) [11.3]

[11.2] O. W. Madelung and E. Mollwo, *Z. Phys.* **249**, 12 (1971).
[11.3] See, I. P. Kaminow and E. H. Turner, in *Handbook of Lasers,* edited by R. J. Pressley (Chemical Rubber, Cleveland, 1971), Chap. 15.

5.11.3 Quadratic Electrooptic Constant

No detailed data are available for ZnO.

5.11.4 Franz–Keldysh Effect

No detailed data are available for ZnO.

5.11.5 Nonlinear Optical Constant

• Second-order nonlinear optical susceptibility

Table 5.11.3 *Experimental second-order nonlinear optical susceptibility d_{ij} for ZnO.*

d_{ij} (pm/V)			Comment
d_{15}	d_{31}	d_{33}	
3.0	+2.7	–9.0	λ=1.06 μm [11.4]
	+0.68	–7.16	λ=1.064 μm [11.5]

[11.4] *Numerical Data and Functional Relationships in Science and Technology,* edited by K.-H. Hellwege and A. M. Hellwege, Landolt–Börnstein, New Series, Group III, Vol. 11 (Springer, Berlin, 1979).
[11.5] G. Wang, G. K. L. Wong, and J. B. Ketterson, *Appl. Opt.* **40**, 5436 (2001).

• Third-order nonlinear optical susceptibility

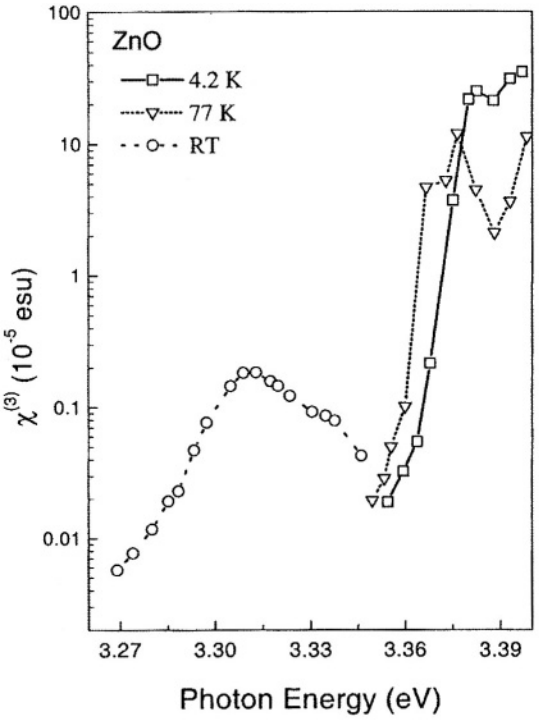

Fig. 5.11.3 Experimental third-order optical nonlinearity $\chi^{(3)}$ versus excitation energy for a ZnO microcrystalline thin film at three different temperatures. [From W. Zhang, H. Wang, K. S. Wong, Z. K. Tang, G. K. L. Wong, and R. Jain, *Appl. Phys. Lett.* **75**, 3321 (1999).]

• Two-photon optical absorption

Table 5.11.4 *Two-photon absorption coefficient β for ZnO.*

Wavelength (μm)	β (cm/GW)	Comment.
0.532	4.2	$\boldsymbol{E}\perp c$, T=300 K [11.6]
0.6943	16	$\boldsymbol{E}\perp c$, T=300 K [11.7]
	34	$\boldsymbol{E}\parallel c$, T=300 K [11.7]

[11.6] X. J. Zhang, W. Ji, and S. H. Tang, *J. Opt. Soc. Am. B* **14**, 1951 (1997).
[11.7] G. Kobbe and C. Klingshirn, *Z. Phys. B* **37**, 9 (1980).

5.12 CARRIER TRANSPORT PROPERTIES

5.12.1 Low-Field Mobility: Electrons

Table 5.12.1 *300-K (μ_{300K}) and peak Hall mobilities (μ_{peak}) for electrons in ZnO.*

Mobility	Value ($cm^2/V\,s$)	Comment
μ_{300K}	226	$\boldsymbol{j} \perp c$ [12.1]
	200	$\boldsymbol{j} \parallel c$, $\boldsymbol{B} \perp c$ [12.2]
μ_{peak}	2400	T=40 K, ($\boldsymbol{j} \perp c$, $\boldsymbol{B} \perp c$ and $\boldsymbol{B} \parallel c$) [12.2]
	1350	T=60 K, ($\boldsymbol{j} \parallel c$, $\boldsymbol{B} \perp c$) [12.2]

[12.1] W. S. Baer, *Phys. Rev.* **154**, 785 (1967).
[12.2] P. Wagner and R. Helbig, *J. Phys. Chem. Solids* **35**, 327 (1974).

- **Temperature dependence**

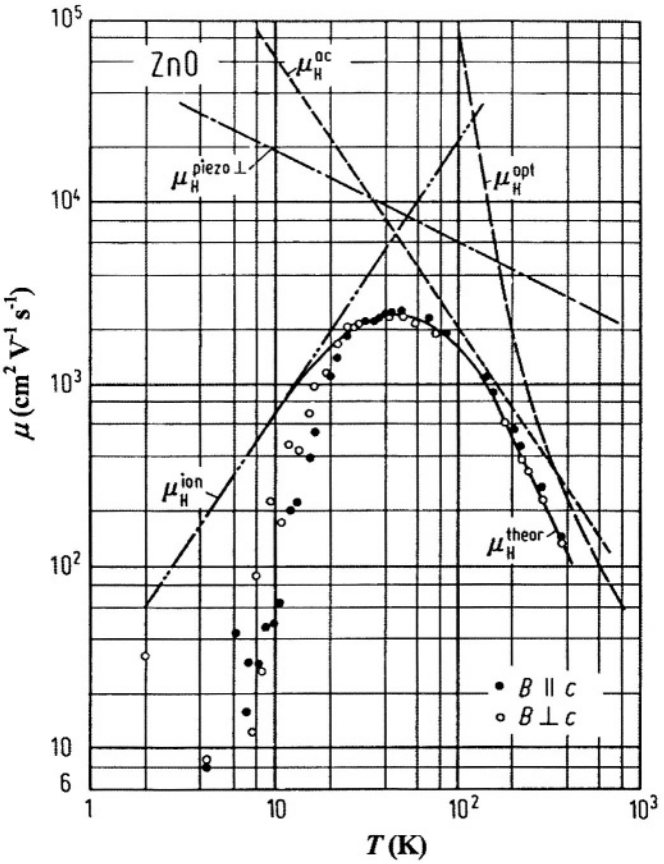

Fig. 5.12.1 Temperature dependence of the electron Hall mobility μ in ZnO ($\boldsymbol{j} \perp c$). The curves show the calculated mobilities limited for ionized-impurity scattering (ion), intravalley acoustic scattering (ac), polar optical scattering (opt), and piezoelectric scattering (piezo⊥). The solid line marked by "theor" takes into account all these scattering processes. [From P. Wagner and R. Helbig, *J. Phys. Chem. Solids* **35,** 327 (1974).]

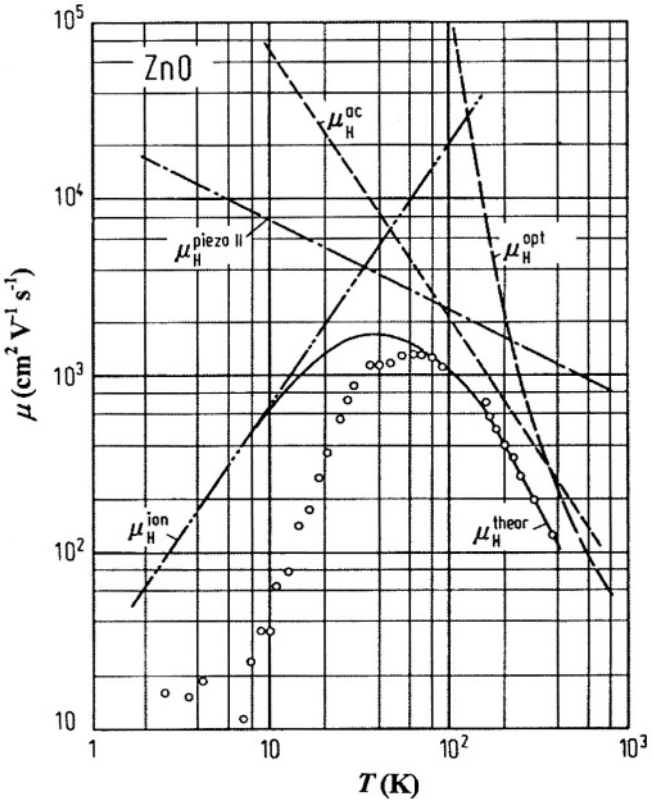

Fig. 5.12.2 Temperature dependence of the electron Hall mobility μ in ZnO ($\boldsymbol{j} \| c$, $\boldsymbol{B} \perp c$). The curves show the calculated mobilities limited for ionized-impurity scattering (ion), intravalley acoustic scattering (ac), polar optical scattering (opt), and piezoelectric scattering (piezo ||). The solid line marked by "theor" takes into account all these scattering processes. [From P. Wagner and R. Helbig, *J. Phys. Chem. Solids* **35**, 327 (1974).]

- **Donor concentration (free-carrier) dependence**

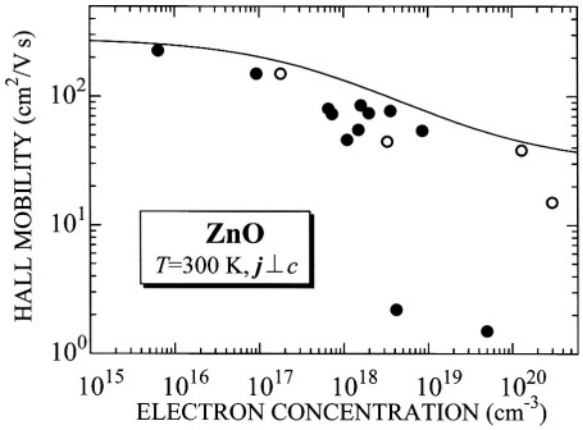

Fig. 5.12.3 Electron Hall mobility μ versus electron concentration n in n-type ZnO at 300 K for $\boldsymbol{j} \perp c$ (●). The experimental data are gathered from various sources, some of which (○) did not mention whether $\boldsymbol{j} \perp c$ or $\boldsymbol{j} \| c$. The solid line represents the calculated result with $\mu = 30 + 250/[1 + (n/5\times10^{17})^{0.50}]$, where n is in cm^{-3} and μ is in $\mathrm{cm}^2/\mathrm{V\,s}$.

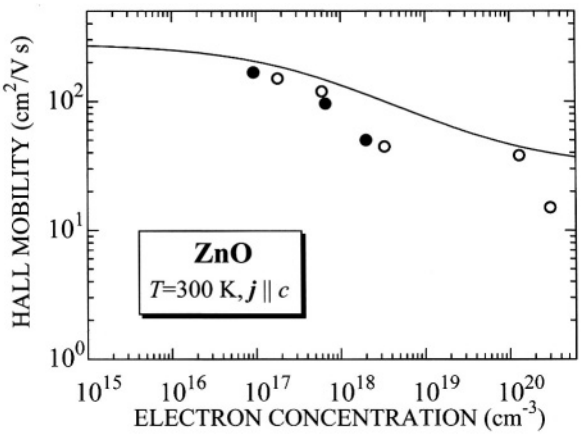

Fig. 5.12.4 Electron Hall mobility μ versus electron concentration n in n-type ZnO at 300 K for $\boldsymbol{j} \| c$ (●). The experimental data are gathered from various sources, some of which (○) did not mention whether $\boldsymbol{j} \| c$ or $\boldsymbol{j} \perp c$. The solid line represents the calculated result with $\mu = 30 + 250/[1 + (n/5\times10^{17})^{0.50}]$, where n is in cm^{-3} and μ is in $\mathrm{cm}^2/\mathrm{V\,s}$.

- **Hall factor**

The Hall factor as a function of electron concentration for *n*-ZnO has been discussed theoretically by D. L. Rode [in *Semiconductors and Semimetals,* edited by R. K. Willardson and A. C. Beer (Academic, New York, 1975), Vol. 10, p. 1].

5.12.2 Low-Field Mobility: Holes

No detailed data are available for ZnO.

5.12.3 High-Field Transport: Electrons

- **Electron drift velocity–field characteristic**

The electron drift velocity versus electric field characteristics for ZnO has been studied theoretically using a Monte Carlo technique by J. D. Albrecht, P. P. Ruden, S. Limpijumnong, W. R. L. Lambrecht, and K. F. Brennan [*J. Appl. Phys.* **86**, 6864 (1999)].

5.12.4 High-Field Transport: Holes

No detailed data are available for ZnO.

5.12.5 Minority-Carrier Transport: Electrons in *p*-Type Materials

No detailed data are available for ZnO.

5.12.6 Minority-Carrier Transport: Holes in *n*-Type Materials

No detailed data are available for ZnO.

5.12.7 Impact Ionization Coefficient

No detailed data are available for ZnO.

Chapter 6

Wurtzite Zinc Sulphide (α-ZnS)

6.1 STRUCTURAL PROPERTIES

6.1.1 Ionicity

Table 6.1.1 *Phillips's ionicity f_i for α-ZnS [1.1].*

f_i
0.623

[1.1] J. C. Phillips, *Bonds and Bands in Semiconductors* (Academic, New York, 1973).

6.1.2 Elemental Isotopic Abundance and Molecular Weight

- **Isotopic abundance**

Table 6.1.2 *Isotopic abundance in percent for zinc and sulfur [1.2].*

Isotope	% nat. abundance	Isotope	% nat. abundance
^{64}Zn	48.6	^{32}S	95.02
^{66}Zn	27.9	^{33}S	0.75
^{67}Zn	4.1	^{34}S	4.21
^{68}Zn	18.8	^{36}S	0.02
^{70}Zn	0.6		

[1.2] D. R. Lide, *CRC Handbook of Chemistry and Physics,* 78th Edition (CRC Press, Boca Raton, 1997).

• **Molecular weight**

Table 6.1.3 *Molecular (average atomic) weight M for* α*-ZnS.*

M (amu)
97.46

6.1.3 Crystal Structure and Space Group

Table 6.1.4 *Crystal structure and its space and pint groups for* α*-ZnS.*

Crystal structure	Space group	Point group
Wurtzite (Hexagonal)	$P6_3mc$	C_{6v}^4

6.1.4 Lattice Constant and Its Related Parameters

• **Lattice constant and molecular density**

Table 6.1.5 *Lattice constant (a, c) and molecular density* (d_M) *for* α*-ZnS at 300 K.*

Parameter	Value
Lattice constant a (Å)	3.8226 [1.3]
c (Å)	6.2605 [1.3]
Molecular density d_M (10^{22} cm^{-3})	2.5245*

[1.3] R. R. Reeber and G. W. Powell, *J. Appl. Phys.* **38,** 1531 (1967).
*Calculated.

• **Crystal density**

Table 6.1.6 *Crystal density g for* α*-ZnS at 300 K.**

g (g/cm^3)
4.0855

*Calculated using a=3.8226 Å and c=6.2605 Å.

6.1.5 Structural Phase Transition

Table 6.1.7 *Structural phase transition in* α*-ZnS at high pressures.*

Structure	Transition pressure (GPa)
Wurtzite ($P6_3mc$)	Normal pressure
Zincblende ($F\bar{4}3m$)	10.7–11.4 [1.4]
Rocksalt (NaCl)	12.4–13.5 [1.4]

[1.4] S. Desgreniers, L. Beaulieu, and I. Lepage, *Phys. Rev. B* **61**, 8726 (2000).

6.1.6 Cleavage Plane

Table 6.1.8 *Crystallographic plane most readily cleaved for* α*-ZnS.*

Cleavage plane
$(11\bar{2}0)$, $(10\bar{1}0)$

• **Surface energy**

Table 6.1.9 *Surface energy for α-ZnS (in J/m²).*

Plane		Comment
(0001)	$(000\bar{1})$	
1.30	0.96	Calc. [1.5]

[1.5] B. N. Oshcherin, *Phys. Status Solidi A* **34**, K181 (1976).

6.2 THERMAL PROPERTIES

6.2.1 Melting Point and Its Related Parameters

Table 6.2.1 *Melting point T_m and its related parameter for ZnS.*

Parameter	Value
Melting point T_m (K)	2196 [2.1]
Entropy of fusion ΔS_m (cal/mol K)	16.29 [2.2]

[2.1] See, J. A. Van Vechten, *Phys Rev. B* **7**, 1479 (1973).
[2.2] See, B. R. Nag, *J. Electron. Mater.* **26**, 70 (1997).

6.2.2 Specific Heat

No detailed data are available for α-ZnS.

6.2.3 Debye Temperature

Table 6.2.2 *Debye temperature θ_D for α-ZnS.*

θ_D (K)	Comment
351	Ultrasound pulse (T=300 K) [2.3]

[2.3] C. F. Cline, H. L. Dunegan, and G. W. Henderson, *J. Appl. Phys.* **38,** 1944 (1967).

6.2.4 Thermal Expansion Coefficient

Table 6.2.3 *Thermal expansion coefficient α_{th} for α-ZnS.*

α_{th} (10^{-6} K^{-1})		Comment
α_a	α_c	
6.54	4.59	T=298 K [2.4]

[2.4] R. R. Reeber and G. W. Powell, *J. Appl. Phys.* **38**, 1531 (1967).

6.2.5 Thermal Conductivity and Diffusivity

Table 6.2.4 *Thermal conductivity K for α-ZnS [2.5].* Thermal diffusivity can be calculated from a relation $D=K/(C_p g)$, where C_p is the specific heat at constant pressure and g is the crystal density.*

Temperature (K)	K (W/cm K)	Temperature (K)	K (W/cm K)
2.2	0.013	26	0.56
3.2	0.028	34	0.64
4.5	0.058	48	0.68
6.8	0.12	65	0.64
8.8	0.18	93	0.53
12	0.28	155	0.33
18	0.45	300	0.17

[2.5] G. A. Slack, *Phys. Rev. B* **6**, 3791 (1972).
*The heat flow is along the *c*-axis (|| *c*). Note that the α-ZnS crystal used in the experiment may be faulted; therefore, the values of this crystal are much smaller than those of β-ZnS [see, G. A. Slack, *Phys. Rev. B* **6**, 3791 (1972)].

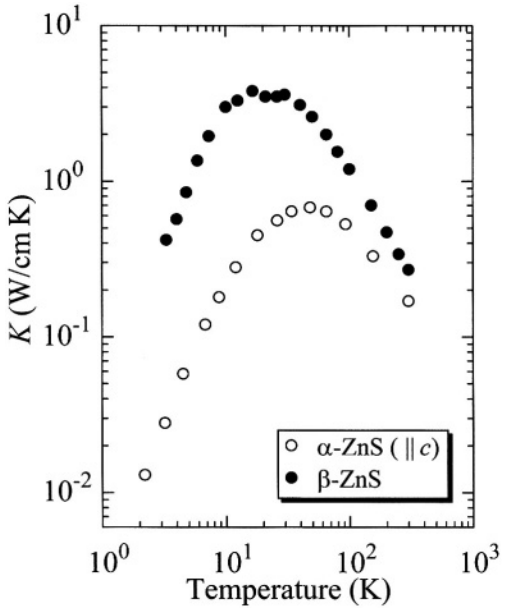

Fig. 6.2.1 Thermal conductivity K in the direction along the *c*-axis for α-ZnS (open circles), together with that for β-ZnS (solid circles). The experimental data are taken from G. A. Slack [*Phys. Rev. B* **6**, 3791 (1972)]. Note that the α-ZnS crystal used in the experiment may be faulted; therefore, the values of this crystal are much smaller than those of β-ZnS.

6.3 ELASTIC PROPERTIES

6.3.1 Elastic Constant

- **Room-temperature value**

Table 6.3.1 *Room-temperature elastic stiffness (C_{ij}) and compliance constants (S_{ij}) for α-ZnS [3.1].*

C_{ij} (10^{11} dyn/cm^2)					
C_{11}	C_{12}	C_{13}	C_{33}	C_{44}	C_{66}*
12.2	5.8	4.2	13.8	2.87	3.2

Table 6.3.1 *Continued.*

S_{ij} (10^{-12} cm^2/dyn)					
S_{11}	S_{12}	S_{13}	S_{33}	S_{44}	S_{66}*
1.10	–0.45	–0.20	0.86	3.48	3.10

[3.1] *Numerical Data and Functional Relationships in Science and Technology,* edited by K.-H. Hellwege and A. M. Hellwege, Landolt–Börnstein, New Series, Group III, Vol. 11 (Springer, Berlin, 1979).

* $C_{66}=\frac{1}{2}(C_{11}-C_{12})$; $S_{66}=2(S_{11}-S_{12})$.

• Temperature and/or pressure dependence

Table 6.3.2 *Temperature derivative of the elastic stiffness constant dC_{ij}/dT, for α-ZnS [3.2].*

dC_{ij}/dT (10^7 dyn/cm^2 K)				
C_{11}	C_{12}	C_{13}	C_{33}	C_{44}
–13.9	–7.7	–6.2	–15	–2.8

[3.2] *Numerical Data and Functional Relationships in Science and Technology,* edited by K.-H. Hellwege and A. M. Hellwege, Landolt–Börnstein, New Series, Group III, Vol. 11 (Springer, Berlin, 1979).

Table 6.3.3 *Pressure derivative of the elastic stiffness constant, dC_{ij}/dp, for α-ZnS [3.3].*

dC_{ij}/dT				
C_{11}	C_{12}	C_{13}	C_{33}	C_{44}
4.2	4.5	3.8	5.1	–0.083

[3.3] *Numerical Data and Functional Relationships in Science and Technology,* edited by K.-H. Hellwege and A. M. Hellwege, Landolt–Börnstein, New Series, Group III, Vol. 11 (Springer, Berlin, 1979).

6.3.2 Third-Order Elastic Constant

No detailed data are available for α-ZnS.

6.3.3 Young's Modulus, Poisson's Ratio, and Similar

• Young's modulus

Table 6.3.4 *Young's modulus Y for α-ZnS at 300 K.**

Direction	Y (10^{12} dyn/cm^2)
$c \perp l$	0.91
$c \parallel l$	1.16

*Calculated using $S_{11}=1.10\times10^{-12}$ and $S_{33}=8.6\times10^{-13}$ cm^2/dyn.
l: directional vector.

• Poisson's ratio

Table 6.3.5 *Poisson's ratio P for α-ZnS at 300 K.**

Direction	P
$c \perp l$	0.30
$c \parallel l$	0.24

*Obtained from a definition $B_u=Y/[3(1-2P)]$, where B_u and Y are bulk and Young's moduli, respectively.
l: directional vector.

- **Bulk modulus, shear modulus, etc.**

Table 6.3.6 *Bulk modulus, B_u, pressure derivative of B_u, dB_u/dp, and linear compressibility, C_o, for α-ZnS at 300 K.*

Parameter	Value
B_u (10^{11} dyn/cm^2)	7.40 [3.4]
dB_u/dp	4.41 [3.5]
	4 [3.6], [3.7]
C_o (10^{-13} cm^2/dyn)	
$c \perp l$	4.50 [3.4]
$c \parallel l$	4.60 [3.4]

[3.4] Calculated using C_{11}=1.22×10^{12} dyn/cm^2, C_{12}=5.8×10^{11} dyn/cm^2, C_{13}=4.2×10^{11} dyn/cm^2, C_{33}=1.38×10^{12} dyn/cm^2, S_{11}=1.10×10^{-12} cm^2/dyn, S_{12}=−4.5×10^{-13} cm^2/dyn, S_{13}= −2.0×10^{-13} cm^2/dyn, and S_{33}=8.6×10^{-13} cm^2/dyn.
[3.5] Exper. [E. Chang and G. R. Barsch, *J. Phys. Chem. Solids* **34**, 1543 (1973)].
[3.6] Exper. [H. Karzel, W. Potzel, M. Köfferlein, W. Schiessl, M. Steiner, U. Hiller, G. M. Kalvius, D. W. Mitchell, T. P. Das, P. Blaha, K. Schwarz, and M. P. Pasternak, *Phys. Rev. B* **53**, 11425 (1996)].
[3.7] Exper. [S. Desgreniers, L. Beaulieu, and I. Lepage, *Phys. Rev. B* **61**, 8726 (2000)].
l: directional vector.

6.3.4 Microhardness

Table 6.3.7 *Microhardness H for ZnS [3.8]. **

H (GPa)
1.78

[3.8] See, L. Garbato and A. Rucci, *Phil. Mag.* **35**, 1681 (1977).
*Type of crystal structure (α- or β-ZnS) was not described.

6.3.5 Sound Velocity

Table 6.3.8 *Sound velocity propagating in α-ZnS at 300 K.* LA=longitudinal acoustic; TA1, TA2=transverse acoustic.*

Propagation direction a	Direction of polarization π	Mode	Sound velocity (10^5 cm/s)
$a \parallel c$	$\pi \parallel c$	LA	5.81
$a \parallel c$	$\pi \perp c$	TA1, TA2	2.65
$a \perp c$	$\pi \perp c$	LA	5.47
$a \perp c$	$\pi \perp c$	TA1	2.80
$a \perp c$	$\pi \parallel c$	TA2	2.65

*Calculated using C_{11}=1.22×10^{12} dyn/cm^2, C_{12}=5.8×10^{11} dyn/cm^2, C_{33}=1.38×10^{12} dyn/cm^2, C_{44}=2.87×10^{11} dyn/cm^2, and g=4.0855 g/cm^3.

6.4 PHONONS AND LATTICE VIBRONIC PROPERTIES

6.4.1 Phonon Dispersion Relation

There have been reported neither theoretical nor experimental data on the phonon dispersion curves/phonon density of states for α-ZnS up to now.

6.4.2 Phonon Frequency

Table 6.4.1 *Long-wavelength ($q \to 0$) phonon frequencies for α-ZnS.*

Phonon frequency (cm^{-1})						Comment
E_2 low	A_1 (TO)	E_1 (TO)	E_2 high	A_1 (LO)	E_1 (LO)	
	280	280	280	356	356	T=25 K [4.1]
69.4	272	276	286		350.5	T=140 K [4.2]
55	274	274	274	352	352	T=298 K [4.1]
69.2	267	273	283		347.8	T=300 K [4.2]
	264	270		346	347	T=300 K [4.3]
72	273	273	286	351	351	T=300 K [4.4]
65	270	273	281	350	350	Mean value (T~300 K)

[4.1] C. A. Arguello, D. L. Rousseau, and S. P. S. Porto, *Phys. Rev.* **181**, 1351 (1969).
[4.2] J. Schneider and R. D. Kirby, *Phys. Rev. B* **6**,1290 (1972).
[4.3] G. Lucovsky, E. Lind, and E. A. Davis, in *II–VI Semiconducting Compounds,* edited by D. G. Thomas (Benjamin, New York, 1967), p. 1150.
[4.4] O. Brafman and S. S. Mitra, *Phys. Rev.* **171,** 931 (1968).

- **Temperature dependence**

Each long-wavelength phonon mode shows a decrease in its frequency with increasing temperature [see, C. A. Arguello, D. L. Rousseau, and S. P. S. Porto, *Phys. Rev.* **181,** 1351 (1969); J. Schneider and R. D. Kirby, *Phys. Rev. B* **6**, 1290 (1972)].

6.4.3 Mode Grüneisen Parameter

No detailed data are available for α-ZnS.

6.4.4 Phonon Deformation Potential

No detailed data are available for α-ZnS.

6.5 COLLECTIVE EFFECTS AND RELATED PROPERTIES

6.5.1 Piezoelectric Constant

Table 6.5.1 *Experimentally determined piezoelectric stress (e_{ij}) and strain constants (d_{ij}) for α-ZnS.*

e_{ij} (C/m^2)			d_{ij} (10^{-12} m/V)			Ref.
e_{15}	e_{31}	e_{33}	d_{15}	d_{31}	d_{33}	
			−2.8	−1.13	3.23	[5.1]
			2.6	0.95	3.3	[5.2]
−0.08	−0.097	0.347				[5.3]
0.093		0.43	3.27	−1.17	3.67	[5.4]
			−2.8	−1.13	3.23	[5.5]
−0.118	−0.238	0.265	−4.37	−2.14	3.66	[5.6]

[5.1] I. B. Kobyakov, *Sov. Phys.–Crystallogr.* **11,** 369 (1966).
[5.2] I. B. Kobyakov and G. S. Pado, *Sov. Phys.– Solid State* **9**, 1707 (1968).
[5.3] V. A. Zhdanov and L. A. Brysneva, *Sov. Phys. Crystallogr.* **19,** 223 (1974).
[5.4] M. M. Firsova, *Sov. Phys. Solid State* **16,** 350 (1974).
[5.5] B. A. Auld, *J. Acoust. Soc. Am.* **70**, 1577 (1981).
[5.6] I. A. Dan'kov, I. B. Kobyakov, and S. Yu. Dabydov, *Sov. Phys. Solid State* **24,** 2058 (1982).

6.5.2 Fröhlich Coupling Constant

No detailed data are available for α-ZnS.

6.6 ENERGY-BAND STRUCTURE: ENERGY-BAND GAPS

6.6.1 Basic Properties

- **Electronic energy-band structure**

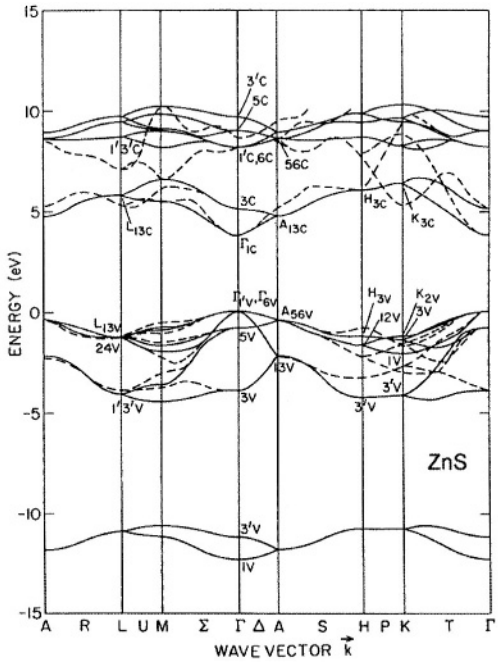

Fig. 6.6.1 Electronic energy-band structure of α-ZnS as calculated with the semiempirical tight-binding scheme. The dashed lines also show the results derived from the semiempirical pseudopotential method by T. K. Bergstresser and M. L. Cohen [*Phys. Rev.* **164,** 1069 (1967)]. [From A. Kobayashi, O. F. Sankey, S. M. Volz, and J. D. Dow, *Phys. Rev. B* **28**, 935 (1983).]

• **Electronic density of states**

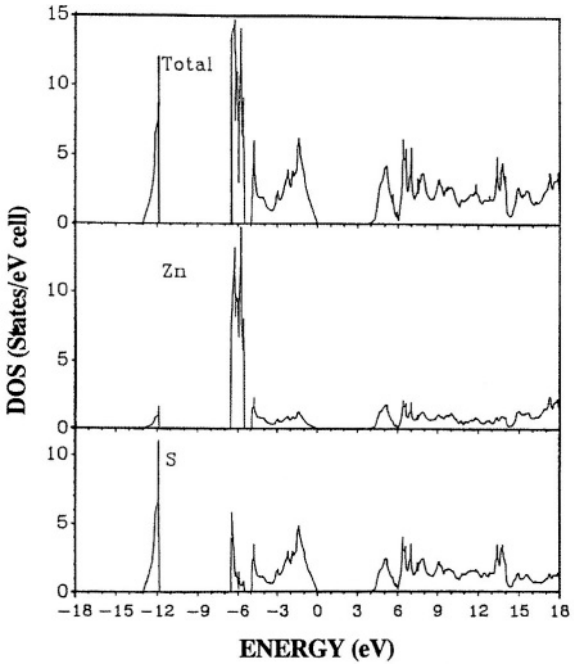

Fig. 6.6.2 Calculated density of states (DOS) and partial DOS for α-ZnS using the first-principles orthogonalized linear-combination-of-atomic-orbitals method. [From Y.-N. Xu and W. Y. Ching, *Phys. Rev. B* **48**, 4335 (1993).]

• **Energy eigenvalue**

Table 6.6.1 *Energy eigenvalues at the critical points for the valence and first few conduction bands of* α-ZnS *[6.1].*

Critical point	Level	Value (eV)	Critical point	Level	Value (eV)
Γ	Γ_1^v	−12.3	H	H_3^v	−4.25
	Γ_3^v	−3.9		$H_{1,2}^v$	−1.67
	Γ_5^v	−0.8		H_3^v	−1.22
	Γ_6^v, Γ_1^v	0.0		H_3^c	6.04
	Γ_1^c	3.8			
	Γ_3^c	5.1			
	Γ_6^c, Γ_1^c	8.2			
K	K_3^v	−4.15	A	$A_{1,3}^v$	−2.18
	K_1^v	−2.09		$A_{5,6}^v$	−0.42
	K_3^v	−1.40		$A_{1,3}^c$	4.75
	K_2^v	−1.22			
L	$L_{1',3}^v$	−4.09			
	$L_{2,4}^v$	−1.31			
	$L_{1,3}^v$	−1.24			
	$L_{1,3}^c$	5.80			
	$L_{1',3}^c$	8.71			

6.6.2 E_0-Gap Region

• Room-temperature value

Table 6.6.2 *$E_{0\alpha}$-gap energy (α=A, B, or C) for α-ZnS at room temperature.*

$E_{0\alpha}$ (eV)			Comment
A	*B*	*C*	
3.75 (3.71)*	3.78 (3.74)*	3.87 (3.83)*	Estimated

*Excitonic gap obtained by extracting an exciton binding energy (G^{α}=40 meV).

• Temperature dependence

Table 6.6.3 *Excitonic energy gap $E_{0\alpha}$ (α=A, B, or C) for α-ZnS determined at various temperatures.*

$E_{0\alpha}$ (eV)			Comment
A	*B*	*C*	
3.8715 (n=1)	3.8998 (n=1)		T=1.8 K [6.2]
3.9016 (n=2)	3.9304 (n=2)		
3.8726 (n=1)	3.9003 (n=1)	3.9907 (n=1)	T=4.2 K [6.3]
3.9027 (n=2)	3.9298 (n=2)		
3.8643 (n=1)	3.8932 (n=1)	3.9808 (n=1)	T=77 K [6.4]

[6.2] J. C. Miklosz and R. G. Wheeler, *Phys. Rev.* **153,** 913 (1967).
[6.3] E. F. Gross, L. G. Suslina, and E. B. Shadrin, *Sov. Phys.–Solid State* **10,** 818 (1968).
[6.4] I. B. Kobyakov, L. G. Suslina, and D. L. Fedorov, *Sov. Phys. Solid State* **16,** 374 (1974).

Table 6.6.4 *Empirical equation for the excitonic $E_{0\alpha}$-gap (α=A, B, or C) energy variation with temperature T for α-ZnS.*

$$E_{0\alpha}(T) = E_{0\alpha}(0) - \frac{\alpha T^2}{T+\beta}$$

Parameter			Comment
$E_{0\alpha}(0)$ (eV)	α (10^{-4} eV/K)	β (K)	
3.8652 (*A*)	10	600	T=4.2–300 K [6.5]
3.8927 (*B*)	10	600	

[6.5] K. A. Dmitrenko, L. V. Taranenko, S. G. Shevel', and A. V. Marinchenko, *Sov. Phys. Semicond.* **19,** 487 (1985).

Table 6.6.5 *Empirical equation for the $E_{0\alpha}$-gap (α=A, B, or C) energy variation with temperature T for α-ZnS [6.6].*

$$E_{0\alpha}(T) = E_{0\alpha}(0) - S\langle\hbar\Omega\rangle\left[\coth\left(\frac{\langle\hbar\Omega\rangle}{2kT}\right)-1\right]$$

$E_{0\alpha}(0)$ (eV)	S	$\langle\hbar\Omega\rangle$ (meV)
3.929 (*A*)	4.3	17.1

[6.6] K. P. O'Donnell and P. G. Middleton, in *Properties of Wide Bandgap II–VI Semiconductors,* EMIS Datareviews Series No. 17, edited by R. Bhargava (INSPEC, London, 1997), p. 33.

• **Temperature and/or pressure coefficient**

Table 6.6.6 *Linear temperature and pressure coefficients of the excitonic energy gap* $E_{0\alpha}$ *(*α*=A, B, or C) for* α*-ZnS.*

Coefficient	Value	Comment
$dE_{0\alpha}/dT$ (10^{-4} eV/K)	–(5–10)	[6.7]
	–7.4	$T \geq 300$ K [6.8]
$dE_{0\alpha}/dp$ (10^{-2} eV/GPa)	9	[6.9]
	6.3	[6.10]

[6.7] W. W. Piper, *Phys. Rev.* **92**, 23 (1953).
[6.8] K. P. O'Donnell and P. G. Middleton, in *Properties of Wide Bandgap II–VI Semiconductors,* EMIS Datareviews Series No. 17, edited by R. Bhargava (INSPEC, London, 1997), p. 33.
[6.9] W. W. Piper, D. T. F. Marple, and P. D. Johnson, *Phys. Rev.* **110**, 323 (1958).
[6.10] R. L. Knell and D. W. Langer, *Phys. Lett.* **21**, 370 (1966).

• **Crystal-field and spin–orbit–splitoff energies**

Table 6.6.7 *Theoretical crystal-field and spin-orbit–splitoff energies* Δ_1, Δ_2, *and* Δ_3 *for* α*-ZnS (in meV). Note that in the quasi-cubic approximation,* $\Delta_{cr}=\Delta_1$ *and* $\Delta_{so}=3\Delta_2=3\Delta_3$.

Δ_1 (Δ_{cr})	Δ_2	Δ_3	Δ_{so}	Ref.
57			89	[6.11]

[6.11] J.-B. Jeon, Yu. M. Sirenko, K. W. Kim, M. A. Littlejohn, and M. A. Stroscio, *Solid State Commun.* **99**, 423 (1996).

Table 6.6.8 *Experimental crystal-field and spin-orbit–splitoff energies* Δ_1, Δ_2, *and* Δ_3, *for* α*-ZnS (in meV). Note that in the quasi-cubic approximation,* $\Delta_{cr}=\Delta_1$ *and* $\Delta_{so}=3\Delta_2=3\Delta_3$.

Δ_1 (Δ_{cr})	Δ_2	Δ_3	Δ_{so}	Technique
52			83	Reflectivity [6.12]
55			92	[6.13]
58			86	Reflectivity (T=77 K) [6.14]

[6.12] See, J. O. Dimmock, in *II–VI Semiconducting Compounds,* edited by D. G. Thomas (Benjamin, New York, 1967), p. 277.
[6.13] J. O. Dimmock, in *II–VI Semiconducting Compounds,* edited by D. G. Thomas (Benjamin, New York, 1967), p. 277.
[6.14] I. B. Kobyakov, L. G. Suslina, and D. L. Fedorov, *Sov. Phys. Solid State* **16**, 374 (1974).

6.6.3 Higher-Lying Direct Gap

• **Room-temperature value**

Table 6.6.9 *Higher-lying direct-gap energies for* α*-ZnS measured at room temperature [6.15].*

Band gap	Value (eV)	
	$E \perp c$	$E \parallel c$
E_1	5.5	5.6
E_0'	5.74–5.80	5.76–5.86
E_2	7.00–7.52	6.98–7.56
E_1'	9.43–9.61	9.56–9.73
d_1	10.8	10.8
d_2	13.8	13.8

[6.15] M. Cardona and G. Harbeke, *Phys. Rev.* **137**, A1467 (1965).

6.6.4 Lowest Indirect Gap

- **Theoretical value**

Table 6.6.10 *Theoretically obtained lowest indirect-gap energy for α-ZnS.*

Band gap	Value (eV)			
	a	b	c	d
E_g^K (Γ→K)				
E_g^M (Γ→M)				5.55
E_g^L (Γ→L)	5.3	5.80	5.99	
E_g^H (Γ→H)	6.6	6.04	7.06	
E_g^A (Γ→A)	5.3	4.75	5.49	

[a] T. K. Bergstresser and M. L. Cohen, *Phys. Rev.* **164,** 1069 (1967).
[b] A. Kobayashi, O. F. Sankey, S. M. Volz, and J. D. Dow, *Phys. Rev. B* **28**, 935 (1983).
[c] M.-Z. Huang and W. Y. Ching, *J. Phys. Chem. Solids* **46,** 977 (1985).
[d] O. Zakharov, A. Rubio, X. Blasé, M. L. Cohen, and S. G. Louie, *Phys. Rev. B* **50**,10780 (1994).

6.6.5 Conduction-Valley Energy Separation

Table 6.6.11 *Theoretically obtained conduction-valley energy separation ΔE_g for α-ZnS.*

ΔE_g	Value (eV)			
	a	b	c	d
K–Γ				
M–Γ				1.47
L–Γ	1.5	2.00	2.07	
H–Γ	2.8	2.24	3.14	
A–Γ	1.5	0.95	1.57	

[a] T. K. Bergstresser and M. L. Cohen, *Phys. Rev.* **164,** 1069 (1967).
[b] A. Kobayashi, O. F. Sankey, S. M. Volz, and J. D. Dow, *Phys. Rev. B* **28**, 935 (1983).
[c] M.-Z. Huang and W. Y. Ching, J. *Phys. Chem. Solids* **46,** 977 (1985).
[d] O. Zakharov, A. Rubio, X. Blasé, M. L. Cohen, and S. G. Louie, *Phys. Rev. B* **50**, 10780 (1994).

6.6.6 Direct–Indirect-Gap Transition Pressure

No detailed data are available for α-ZnS.

6.7 ENERGY-BAND STRUCTURE: ELECTRON AND HOLE EFFECTIVE MASSES

6.7.1 Electron Effective Mass: Γ Valley

- **Theoretical value**

Table 6.7.1 *Theoretical electron effective masses $m_e^{\perp}$, $m_e^{//}$, and m_e^{Γ} at the Γ valley for α-ZnS. $m_e^{\Gamma}=(m_e^{\perp 2}\, m_e^{//})^{1/3}$: density-of-states effective mass.*

$m_e^{\perp}/m_0$	$m_e^{\parallel}/m_0$	m_e^{Γ}/m_0	Technique
0.275	0.234	0.261	Linear combination of atomic orbital method [7.1]

[7.1] M.-Z. Huang and W. Y. Ching, *J. Phys. Chem. Solids* **46,** 977 (1985).

• **Experimental value**

Table 6.7.2 *Experimental electron effective masses $m_e^{\perp}$, $m_e^{//}$, and m_e^{Γ} at the Γ valley for α-ZnS. $m_e^{\Gamma}=(m_e^{\perp 2}\, m_e^{//})^{1/3}$: density-of-states effective mass.*

$m_e^{\perp}/m_0$	$m_e^{\parallel}/m_0$	m_e^{Γ}/m_0	Comment
0.28±0.03*	0.28±0.03*	0.28±0.03	Magnetoabsorption, T=1.8 K [7.2]

[7.2] J. C. Miklosz and R. G. Wheeler, *Phys. Rev.* **153,** 913 (1967).
* Showing isotropy within the experimental error.

6.7.2 Electron Effective Mass: Satellite Valley

No detailed data are available for α-ZnS.

6.7.3 Hole Effective Mass

• **Luttinger's valence-band parameter**

Table 6.7.3 *Theoretical Luttinger's valence-band parameter A_i for α-ZnS. A_i (i=1–6) are in units of $\hbar^2/2m_0$ and A_7 is in units of eV/Å.*

A_1	A_2	A_3	A_4	A_5	A_6	$\lvert A_7\rvert$	Ref.
–4.58	–0.53	4.14	–2.34	–2.34	–3.69		[7.3]

[7.3] J.-B. Jeon, Yu. M. Sirenko, K. W. Kim, M. A. Littlejohn, and M. A. Stroscio, *Solid State Commun.* **99**, 423(1996).

• **Density-of-states mass**

Table 6.7.4 *Density-of-states masses in α-ZnS (in m_0). $m_{H\alpha}$* (α=A, B, or C) represents the hole effective mass of the top three valence bands.*

$\perp c$			$\parallel c$		Comment
m_{HA}*	m_{HB}*	m_{HC}*	m_{HH}*	m_{LH}*	
2.472	0.373	0.425	2.340	0.215	Calc. [7.4]
	0.49±0.06		1.4		Magnetoabsorption [7.5]

[7.4] M.-Z. Huang and W. Y. Ching, *J. Phys. Chem. Solids* **46**, 977 (1985).
[7.5] J. C. Miklosz and R. G. Wheeler, *Phys. Rev.* **153**, 913 (1967).

6.8 ELECTRONIC DEFORMATION POTENTIAL

6.8.1 Intravalley Deformation Potential: Γ Point

• **Conduction band**

Table 6.8.1 *Γ-conduction-band acoustic deformation potential E_1 for α-ZnS used in the transport data analysis.*

E_1 (eV)	Ref.
4.9	[8.1]

[8.1] See, B. R. Nag, *Electron Transport in Compound Semiconductors* (Springer, Berlin, 1980).

• **E_0 gap**

Table 6.8.2 *Hydrostatic deformation potential a_0^{Γ} for the E_0 gap of α-ZnS.**

a_0^{Γ} (eV)
–4.7

*Estimated from dE_0/dp value.

6.8.2 Intravalley Deformation Potential: High-Symmetry Points

No detailed data are available for α-ZnS.

6.8.3 Intervalley Deformation Potential

No detailed data are available for α-ZnS.

6.9 ELECTRON AFFINITY AND SCHOTTKY BARRIER HEIGHT

6.9.1 Electron Affinity

Table 6.9.1 *Electron affinity χ_s for α-ZnS.*

χ_s (eV)	Ref.
3.9	[9.1]

[9.1] A. G. Milnes and D. L. Feucht, *Heterojunctions and Metal-Semiconductor Junctions* (Academic, New York, 1972).

6.9.2 Schottky Barrier Height

Table 6.9.2 *Summary of the Schottky barrier height ϕ_n for metal/n-type α-ZnS contacts at 300 K.**

Metal	ϕ_n (eV)	Metal	ϕ_n (eV)
Ag	1.65–1.81	Mg	0.82
Al	0.8	Pd	1.87
Au	2.0–2.19	Pt	1.84
Cu	1.75	Ta	1.10
In	1.5	Ti	1.15

*The data are gathered from various sources. Type of crystal structure (α- or β-ZnS) was ignored in this tabulation work.

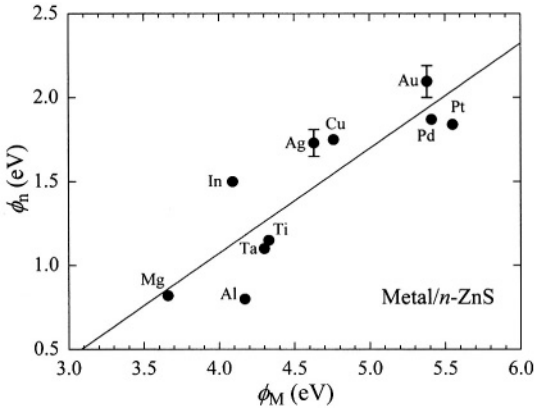

Fig. 6.9.1 Schottky barrier height ϕ_n versus metal/*n*-ZnS contacts. Values of the metal metal work function ϕ_M observed for work function were taken from H. P. R. Frederikse [in *CRC Handbook of Chemistry and Physics,* 78th Edition, edited by D. R. Lide (CRC Press, Boca Raton, 1997), p. 12-115]. The solid line represents the least-squares-fit result with $\phi_n = 0.62\phi_M - 1.43$ (ϕ_M and ϕ_n in eV).

6.10 OPTICAL PROPERTIES

6.10.1 Summary of Optical Dispersion Relations

• $\varepsilon(E)$ and $n^*(E)$ spectra

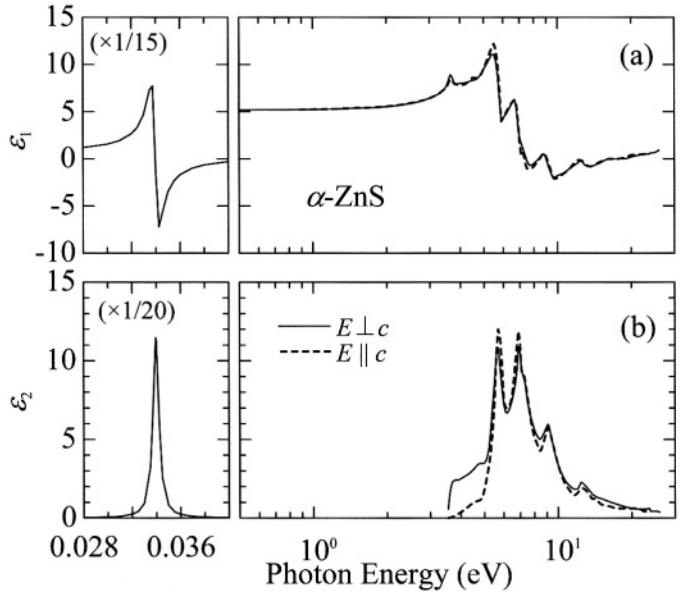

Fig. 6.10.1 Complex dielectric-constant spectra [$\varepsilon(E)=\varepsilon_1(E)+i\varepsilon_2(E)$] for α-ZnS at 300 K. The numerical data are taken from tabulation by S. Adachi [*Optical Constants of Crystalline and Amorphous Semiconductors: Numerical Data and Graphical Information* (Kluwer Academic, Boston, 1999)].

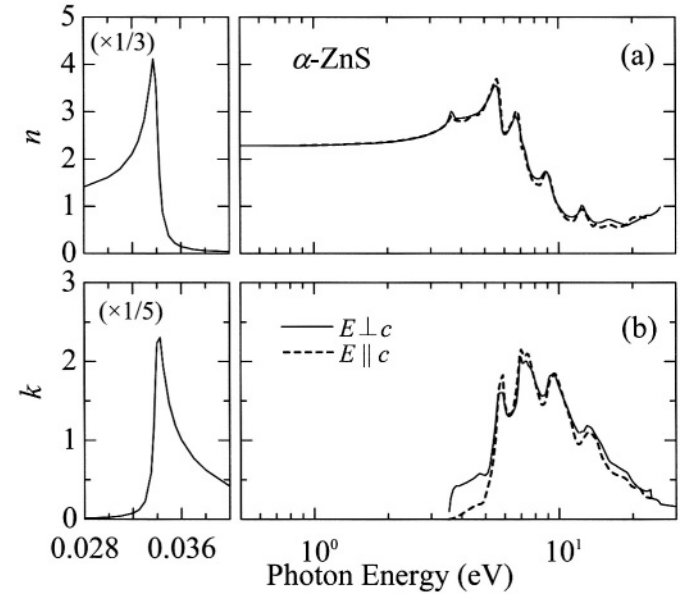

Fig. 6.10.2 Complex refractive-index spectra [$n^*(E)=n(E)+ik(E)$] for α-ZnS at 300 K. The numerical data are taken from tabulation by S. Adachi [*Optical Constants of Crystalline and Amorphous Semiconductors: Numerical Data and Graphical Information* (Kluwer Academic, Boston, 1999)].

• **$\alpha(E)$ and $R(E)$ spectra**

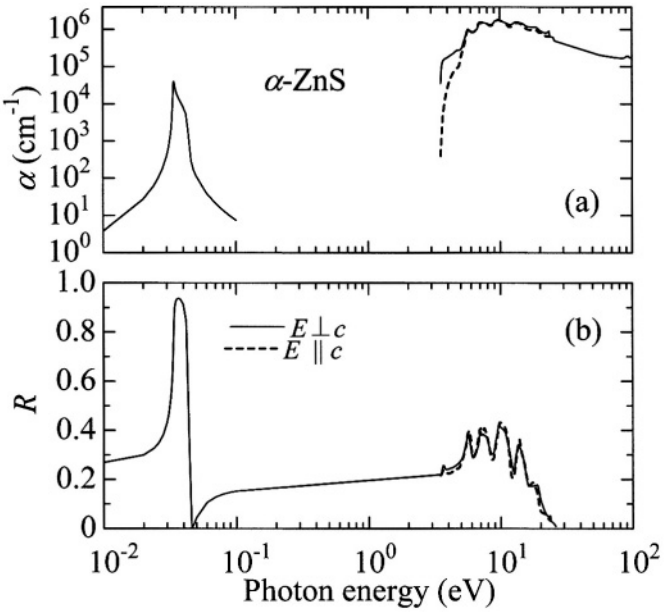

Fig. 6.10.3 (a) Absorption [$\alpha(E)$] and (b) normal-incidence reflectivity spectra [$R(E)$] for α-ZnS at 300 K. The numerical data are taken from tabulation by S. Adachi [*Optical Constants of Crystalline and Amorphous Semiconductors: Numerical Data and Graphical Information* (Kluwer Academic, Boston, 1999)].

6.10.2 The Reststrahlen Region

• **Static and high-frequency dielectric constants**

Table 6.10.1 *Static and high-frequency dielectric constants ε_s and ε_∞ for α-ZnS.*

$E\perp c$		$E \parallel c$		Comment
ε_s	ε_∞	ε_s	ε_∞	
8.7		8.7		T=300 K [10.1]
9.6	5.7	9.6	5.7	T=300 K [10.2]
6.1	5.1	6.1	5.1	T=300 K [10.3]
8.1	5.4	8.1	5.4	Mean value

[10.1] I. B. Kobyakov, *Sov. Phys. –Crystallogr.* **11**, 369 (1966).
[10.2] A. Manabe, A. Mitsuishi, and H. Yoshinaga, *Jpn. J. Appl. Phys.* **6**, 593 (1967).
[10.3] A. N. Pikhtin and A. D. Yas'kov, *Sov. Phys. Semicond.* **15**, 8 (1981).

• **Reststrahlen parameter**

Table 6.10.2 *A set of the reststrahlen parameters for α-ZnS.*

$$\varepsilon(\omega) = \varepsilon_\infty \left(1 + \frac{\omega_{LO}^2 - \omega_{TO}^2}{\omega_{TO}^2 - \omega^2 - i\omega\gamma} \right)$$

$E\perp c$				$E \parallel c$				Comment
ε_∞	ω_{LO} (cm^{-1})	ω_{TO} (cm^{-1})	γ (cm^{-1})	ε_∞	ω_{LO} (cm^{-1})	ω_{TO} (cm^{-1})	γ (cm^{-1})	
5.7	356	274	4.7	5.7	356	274	4.7	T=300 K [10.4]*

[10.4] A. Manabe, A. Mitsuishi, and H. Yoshinaga, *Jpn. J. Appl. Phys.* **6**, 593 (1967).
* Showing no strong polarization dependence.

6.10.3 At or Near the Fundamental Absorption Edge

- **Free-exciton binding energy and related parameters**

Table 6.10.3 *Free-exciton binding (Rydberg) energy G for α-ZnS.*

G (meV)			Comment
A	*B*	*C*	
40	41		Estimated from data in [10.5]
40	39		Estimated from data in [10.6]
40	40		Mean value

[6.5] J. C. Miklosz and R. G. Wheeler, *Phys. Rev.* **153**, 913 (1967).
[6.6] E. F. Gross, L. G. Suslina, and E. B. Shadrin, *Sov. Phys.–Solid State* **10**, 818 (1968).

Table 6.10.4 *Free-exciton parameters (G=binding energy; a_B=1st-orbital Bohr radius; μ=reduced mass) at the fundamental absorption edge of α-ZnS.*

Exciton	G (meV)	a_B (Å)*	μ (m_0)*
A, B (*C*)	40	27	0.128

*Calculated using $\varepsilon=(\varepsilon_0\varepsilon_\infty)^{1/2}=6.6$.

- **Refractive index**

Table 6.10.5 *Refractive index n near the fundamental absorption edge of α-ZnS for $\boldsymbol{E}\perp c$ at 300 K [10.7].*

E (eV)	λ (μm)	*n*	*E* (eV)	λ (μm)	*n*
0.1	12.40	2.278	2.53	0.490	2.428
0.885	1.401	2.285	2.582	0.480	2.438
1.033	1.200	2.290	2.609	0.475	2.445
1.24	1.000	2.301	2.637	0.470	2.448
1.377	0.900	2.310	2.695	0.460	2.459
1.549	0.800	2.324	2.754	0.450	2.473
1.771	0.700	2.332	2.817	0.440	2.486
1.836	0.675	2.339	2.883	0.430	2.502
1.907	0.650	2.346	2.916	0.425	2.511
1.983	0.625	2.354	2.951	0.420	2.522
2.066	0.600	2.363	3.023	0.410	2.539
2.156	0.575	2.375	3.099	0.400	2.560
2.254	0.550	2.386	3.305	0.375	2.637
2.361	0.525	2.402	3.443	0.360	2.705
2.479	0.500	2.421	3.5	0.354	2.757

[10.7] See, S. Adachi, *Optical Constants of Crystalline and Amorphous Semiconductors: Numerical Data and Graphical Information* (Kluwer Academic, Boston, 1999).

Table 6.10.6 *Refractive index n near the fundamental absorption edge of α-ZnS for $\boldsymbol{E}\parallel c$ at 300 K [10.8].*

E (eV)	λ (μm)	*n*	*E* (eV)	λ (μm)	*n*
0.885	1.401	2.288	2.582	0.480	2.443
1.033	1.200	2.294	2.609	0.475	2.449
1.24	1.000	2.303	2.637	0.470	2.453
1.377	0.900	2.315	2.695	0.460	2.463

Table 6.10.6 *Continued.*

E (eV)	λ (μm)	n	E (eV)	λ (μm)	n
1.549	0.800	2.328	2.754	0.450	2.477
1.771	0.700	2.337	2.817	0.440	2.488
1.836	0.675	2.343	2.883	0.430	2.505
1.907	0.650	2.350	2.916	0.425	2.514
1.983	0.625	2.358	2.951	0.420	2.525
2.066	0.600	2.368	3.023	0.410	2.544
2.156	0.575	2.378	3.099	0.400	2.564
2.254	0.550	2.392	3.305	0.375	2.640
2.361	0.525	2.407	3.443	0.360	2.709
2.479	0.500	2.425	3.5	0.354	2.739
2.53	0.490	2.433			

[10.8] See, S. Adachi, *Optical Constants of Crystalline and Amorphous Semiconductors: Numerical Data and Graphical Information* (Kluwer Academic, Boston, 1999).

• Refractive index: Pressure dependence

Table 6.10.7 *Pressure coefficient of the refractive index* n^{-1} *(dn/dp) at* λ*=0.5893 μm for* α*-ZnS at 295 K [10.9].*

$\frac{1}{n}\frac{dn}{dp}$ (10^{-2} GPa^{-1})	
$E \perp c$	$E \parallel c$
–0.12	–0.13

[10.9] K. Vedam and T. A. Davis, *Phys. Rev.* **181**, 1196 (1969).

• Fundamental absorption edge

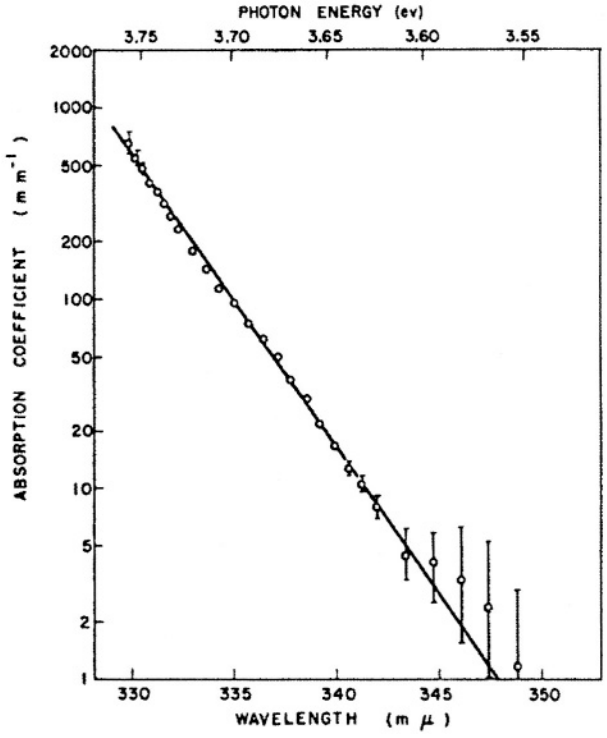

Fig. 6.10.4 Absorption coefficient for a hexagonal ZnS laminar measured at room temperature. [From W. W. Piper, *Phys. Rev.* **92**, 23 (1953).]

• **Fundamental absorption edge: Urbach tail**

The Urbach tail in α-ZnS has been studied by Y. Brada, B. G. Yacobi, and A. Peled [*Solid State Commun.* **17**, 1975 (1975)].

• **Fundamental absorption edge: Pressure dependence**

The optical absorption at the fundamental absorption edge of α-ZnS under pressures up to p~0.2 GPa has been studied by W. W. Piper, D. T. F. Marple, and P. D. Johnson [*Phys. Rev.* **110**, 323 (1958)].

6.10.4 The Interband Transition Region

• **Fundamental optical spectra**

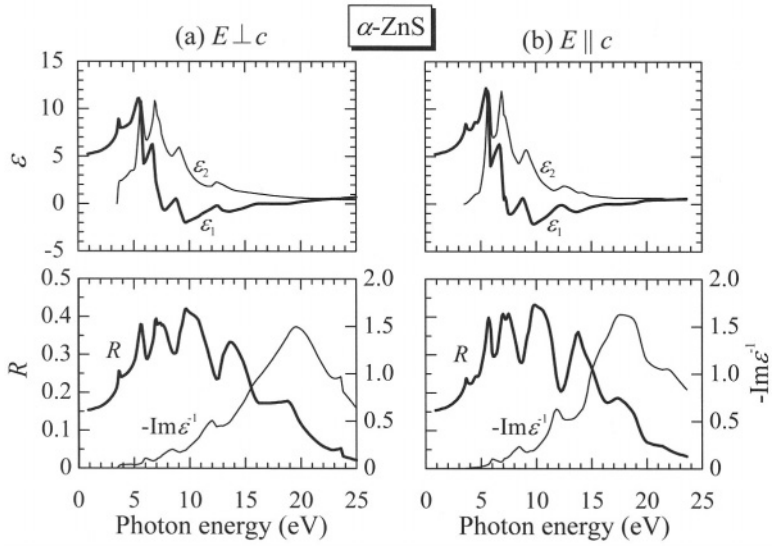

Fig. 6.10.5 Complex dielectric function, $\varepsilon(E)=\varepsilon_2(E)+i\varepsilon_2(E)$, fundamental reflectivity, $R(E)$, and energy-loss function, $-\mathrm{Im}\varepsilon^{-1}(E)$, for α-ZnS at 300 K. The experimental data are taken from tabulation by S. Adachi [*Optical Constants of Crystalline and Amorphous Semiconductors: Numerical Data and Graphical Information* (Kluwer Academic, Boston, 1999)].

6.10.5 Free-Carrier Absorption and Related Phenomena

No detailed data are available for α-ZnS.

6.11 ELASTOOPTIC, ELECTROOPTIC, AND NONLINEAR OPTICAL PROPERTIES

6.11.1 Elastooptic Effect

• **Photoelastic constant**

Table 6.11.1 *Photoelastic constant p_{ij} at λ=632.8 nm for α-ZnS [11.1].*

p_{11}	p_{12}	p_{13}	p_{31}	p_{33}	p_{44}	p_{66}
–0.115	0.017	0.025	0.0271	–0.13	–0.0627	–0.066

[11.1] *Numerical Data and Functional Relationships in Science and Technology,* edited by K.-H. Hellwege and A. M. Hellwege, Landolt–Börnstein, New Series, Group III, Vol. 11 (Springer, Berlin, 1979).

6.11.2 Linear Electrooptic Constant

Table 6.11.2 *Linear electrooptic constant r_{ij} for α-ZnS.*

Wavelength (μm)	r_{ij} (pm/V)			Comment
	r_{13}	r_{33}	r_{42}	
0.633	0.92	1.85		Clamped value (S) [11.2]
3.39		1.7		Clamped value (S) [11.3]

[11.2] I. P. Kaminow and E. H. Turner, *Proc. IEEE* **54**, 1374 (1966).
[11.3] See, I. P. Kaminow and E. H. Turner, in *Handbook of Lasers,* edited by R. J. Pressley (Chemical Rubber, Cleveland, 1971), Chap. 15.

6.11.3 Quadratic Electrooptic Constant

No detailed data are available for α-ZnS.

6.11.4 Franz–Keldysh Effect

No detailed data are available for α-ZnS.

6.11.5 Nonlinear Optical Constant

- **Second-order nonlinear optical susceptibility**

Table 6.11.3 *Experimental second-order nonlinear optical susceptibility d_{ij} for α-ZnS.*

d_{ij} (pm/V)			Comment
d_{15}	d_{31}	d_{33}	
8.0	8.1	17.0	$\lvert d_{ij}\rvert$, λ=0.852 μm [11.4]
5.8	6.2	12.5	$\lvert d_{ij}\rvert$, λ=1.064 μm [11.4]
		+44	λ=1.064 μm [11.5]
4.3	4.8	9.0	$\lvert d_{ij}\rvert$, λ=1.548 μm [11.4]
21	–19	+37	λ=10.6 μm [11.5]

[11.4] I. Shoji, T. Kondo, A. Kitamoto, M. Shirane, and R. Ito, *J. Opt. Soc. Am. B* **14**, 2268 (1997).
[11.5] *Numerical Data and Functional Relationships in Science and Technology,* edited by K.-H. Hellwege and A. M. Hellwege, Landolt–Börnstein, New Series, Group III, Vol. 11 (Springer, Berlin, 1979); C. K. N. Patel, *Phys. Rev. Lett.* **16**, 613 (1966).

- **Two-photon optical absorption**

Table 6.11.4 *Two-photon absorption coefficient β for α-ZnS.*

Wavelength (μm)	β (cm/GW)	Comment
0.6943	0	$\boldsymbol{E}\perp c$, T=300 K [11.6]
	20	$\boldsymbol{E}\parallel c$, T=300 K [11.6]

[11.6] G. Kobbe and C. Klingshirn, *Z. Phys. B* **37**, 9 (1980).

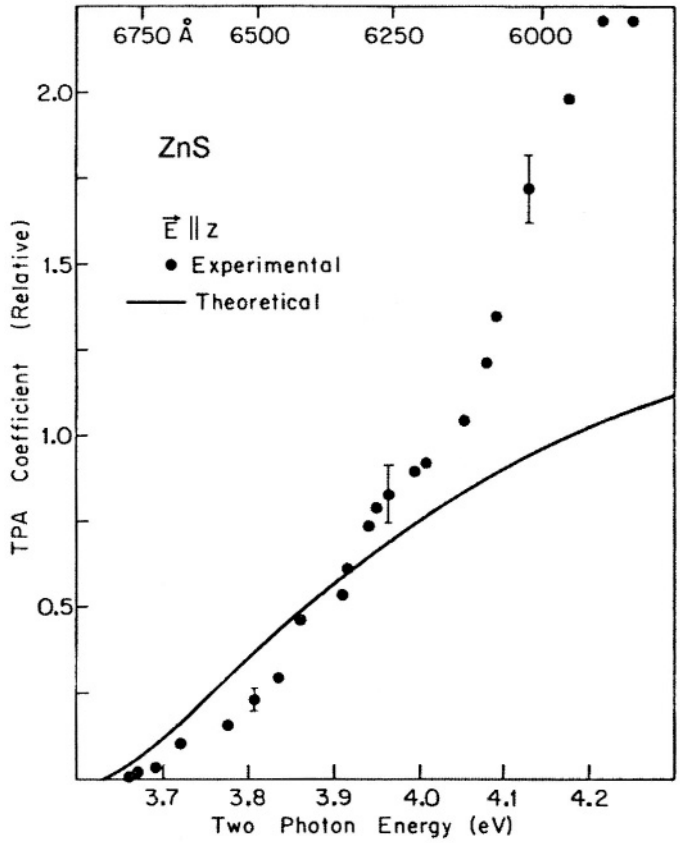

Fig. 6.11.1 Relative two-photon absorption (TPA) coefficient versus two-photon energy for $\boldsymbol{E} \| c$ (z) polarization in α-ZnS. The top horizontal scale represents the incident laser wavelength. [From Y. Bae, J. J. Song, and Y. B. Kim, *J. Appl. Phys.* **53**, 615 (1982).]

6.12 CARRIER TRANSPORT PROPERTIES

6.12.1 Low-Field Mobility: Electrons

Table 6.12.1 *300-K (μ_{300K}) and peak Hall mobilities (μ_{peak}) for electrons in α-ZnS.*

Mobility	Value ($cm^2/V\,s$)	Comment
μ_{300K}	140	n=1.6×10^{16} cm^{-3} [12.1]
	600	Photo-Hall effect, n~3×10^{12} cm^{-3} [12.2]*
	789	In-doped evaporated film (ρ=7.10 Ω·cm) [12.3]*
μ_{peak}	300	T=185 K [12.1]

[12.1] M. Aven and C. A. Mead, *Appl. Phys. Lett.* **7**, 8 (1965).
[12.2] S. Narita and K. Nagasaka, *J. Phys. Soc. Jpn* **20,** 1728 (1965).
[12.3] L. C. Olsen, R. C. Bohara, and D. L. Barton, *Appl. Phys. Lett.* **34,** 528 (1979).
*It was not mentioned or confirmed whether the ZnS sample used was hexagonal or cubic.

• **Temperature dependence**

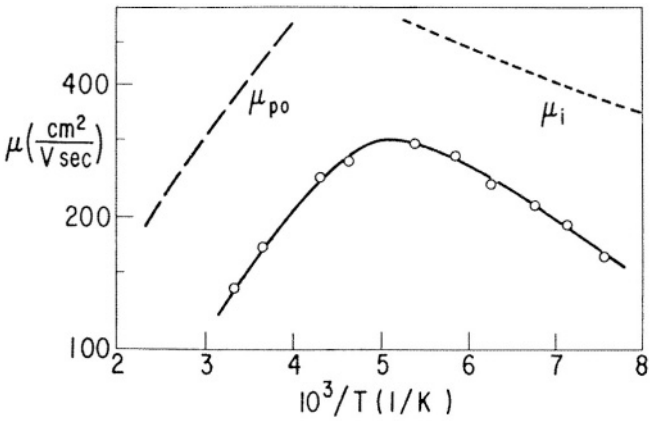

Fig. 6.12.1 Temperature variation of electron Hall mobility μ for Al-doped *n*-type α-ZnS. The dashed and dotted lines are obtained by assuming polar optical scattering (μ_{po}) and charged-impurity scattering (μ_i) as the predominant scattering mechanism, respectively. [From M. Aven and C. A. Mead, *Appl. Phys. Lett.* **7**, 8 (1965).]

• **Donor concentration (free-carrier) dependence**

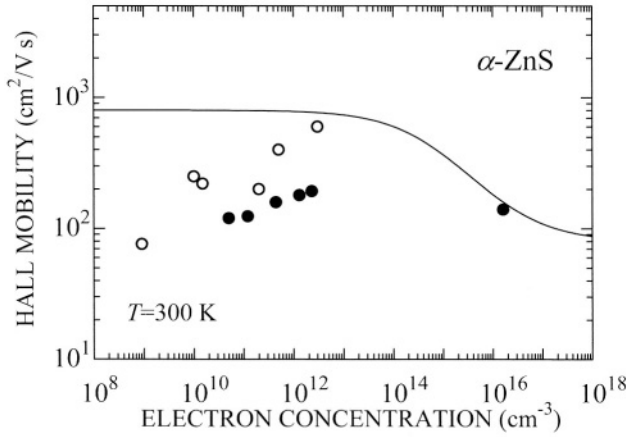

Fig. 6.12.2 Electron Hall mobility μ versus electron concentration n in *n*-type α-ZnS at 300 K. The experimental data are gathered from various sources, some of which (○) did not mention whether the sample used was hexagonal or cubic. The solid line represents the calculated result with $\mu = 80 + 720/[1 + (n/5\times10^{14})^{0.60}]$, where n is in cm^{-3} and μ is in cm^2/V s.

6.12.2 Low-Field Mobility: Holes

No detailed data are available for α-ZnS.

6.12.3 High-Field Transport: Electrons

• **Electron scattering rate**

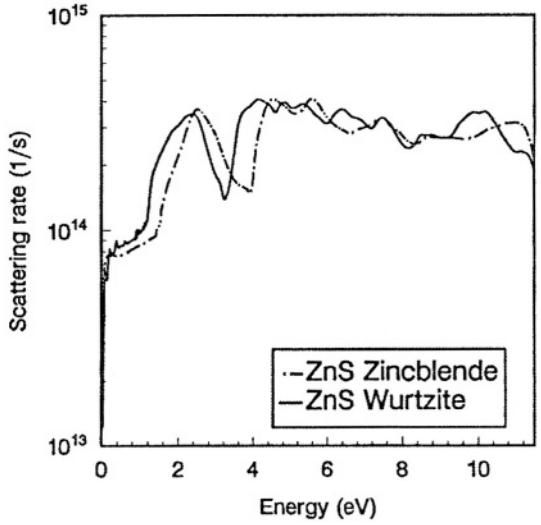

Fig. 6.12.3 Total electron–phonon scattering rate in α- (wurtzite) and β- (zincblende) ZnS as a function of electron energy. [From E. Bellotti, K. F. Brennan, R. Wang, and P. P. Ruden, *J. Appl. Phys.* **83**, 4765 (1998).]

• **Electron drift velocity–field characteristic**

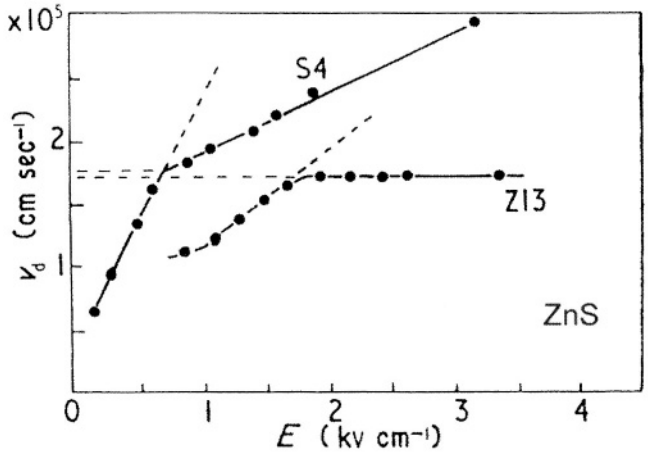

Fig. 6.12.4 Experimental electron drift velocity v_d (v_e) as a function of applied electric filed E for α-ZnS (Z13), together with that for w-CdS (S4). [From P. G. Le Comber, W. E. Spear, and A. Weinmann, *Brit. J. Appl. Phys.* **17**, 467 (1966).]

6.12.4 High-Field Transport: Holes

No detailed data are available for α-ZnS.

6.12.5 Minority-Carrier Transport: Electrons in p-Type Materials

No detailed data are available for α-ZnS.

6.12.6 Minority-Carrier Transport: Holes in n-Type Materials

No detailed data are available for α-ZnS.

6.12.7 Impact Ionization Coefficient

• **Electric-field dependence**

The impact ionization phenomenon in α-ZnS has been studied theoretically by E. Bellotti, K. F. Brennan, R. Wang, and P. P. Ruden [*J. Appl. Phys.* **83**, 4765 (1998)].

Chapter 7

Cubic Zinc Sulphide (β-ZnS)

7.1 STRUCTURAL PROPERTIES

7.1.1 Ionicity

Table 7.1.1 *Phillips's ionicity f_i for β-ZnS [1.1].*

f_i
0.623

[1.1] J. C. Phillips, *Bonds and Bands in Semiconductors* (Academic, New York, 1973).

7.1.2 Elemental Isotopic Abundance and Molecular Weight

- **Isotopic abundance**

Table 7.1.2 *Isotopic abundance in percent for zinc and sulfur [1.2].*

Isotope	% nat. abundance	Isotope	% nat. abundance
^{64}Zn	48.6	^{32}S	95.02
^{66}Zn	27.9	^{33}S	0.75
^{67}Zn	4.1	^{34}S	4.21
^{68}Zn	18.8	^{36}S	0.02
^{70}Zn	0.6		

[1.2] D. R. Lide, *CRC Handbook of Chemistry and Physics,* 78th Edition (CRC Press, Boca Raton, 1997).

• **Molecular weight**

Table 7.1.3 *Molecular (average atomic) weight M for β-ZnS.*

M (amu)
97.46

7.1.3 Crystal Structure and Space Group

Table 7.1.4 *Crystal structure and its space and pint groups for β-ZnS.*

Crystal structure	Space group	Point group
Zincblende (Cubic)	$F\bar{4}3m$	T_d

7.1.4 Lattice Constant and Its Related Parameters

• **Lattice constant, near-neighbor distance, etc.**

Table 7.1.5 *Lattice constant (a), near-neighbor distance (d), unit cube volume (a^3), and molecular density (d_M) for β-ZnS at 300 K.*

Parameter	Value
Lattice constant a (Å)	5.4102 [1.3]
d (Cation–Anion) (Å)	2.3427*
d (Cation–Cation) (Å)	3.8256*
Unit cube volume a^3 (10^{-22} cm^3)	1.5836*
Molecular density d_M (10^{22} cm^{-3})	2.5259*

[1.3] J. C. Jamieson and H. H. Demarest, Jr., *J. Phys. Chem. Solids* **41**, 963 (1980).
*Calculated.

• **Crystal density**

Table 7.1.6 *Crystal density g for β-ZnS at 300 K.**

g (g/cm^3)
4.0879

*Calculated using a=5.4102 Å.

7.1.5 Structural Phase Transition

Table 7.1.7 *Structural phase transition in β-ZnS at high pressures.*

Structure	Transition pressure (GPa)
Zincblende ($F\bar{4}3m$)	Normal pressure
Rocksalt (NaCl)	15.0±0.5 [1.4]
	15.5±0.7 [1.5]
	17.4±1.2 [1.6]
	14.7±1.0 [1.7]
	15.0±0.5 [1.8]
	15 [1.9]
	15.5 [1.10]
Orthorhombic (*Cmcm*)	~65 [1.11]

[1.4] S. C. Yu, I. L. Spain, and E. F. Skelton, *Solid State Commun.* **25**, 49 (1978).
[1.5] A. Onodera and A.Ohtani, *J. Appl. Phys.* **51**, 2581 (1980).
[1.6] W. H. Gust, *J. Appl. Phys.* **53**, 4843 (1982).
[1.7] S. Ves, U. Schwarz, N. E. Christensen, K. Syassen, and M. Cardona, *Phys. Rev. B* **42**, 9113 (1990).
[1.8] A. Béliveau and C. Carlone, *Phys. Rev. B* **44**, 3650 (1991).
[1.9] Y. Zhou, A. J. Campbell, and D. L. Heinz, *J. Phys. Chem. Solids* **52**, 821 (1991).
[1.10] M. Uchino, T. Mashimo, M. Kodama, T. Kobayashi, E. Takasawa, T. Sekine, Y. Noguchi, H. Hikosaka, K. Fukuoka, Y. Syono, T. Kondo, and T. Yagi, *J. Phys. Chem. Solids* **60**, 827 (1999).
[1.11] S. Desgreniers, L. Beaulieu, and I. Lepage, *Phys. Rev. B* **61**, 8726 (2000).

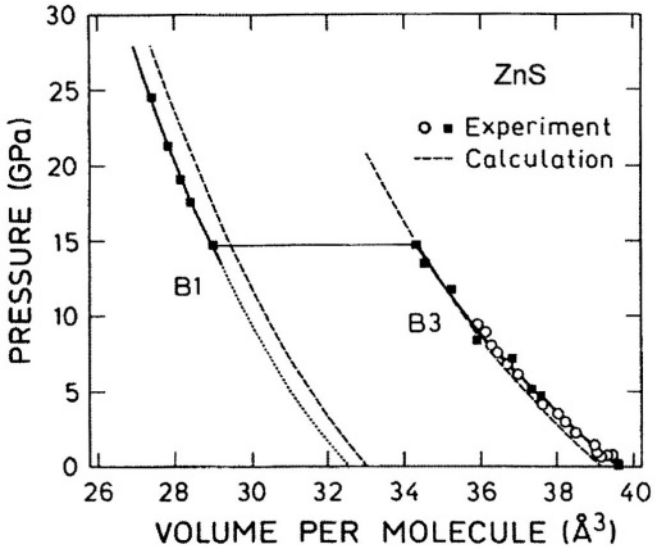

Fig. 7.1.1 Pressure–volume relation for ZnS in the zinc-blende (B3) and NaCl (B1) phases. The open circles refer to the experimental data taken by J. C. Jamieson and H. H. Demarest, Jr. [*J. Phys. Chem. Solids* **41**, 963 (1980)]. [From S. Ves, U. Schwarz, N. E. Christensen, K. Syassen, and M. Cardona, *Phys. Rev. B* **42**, 9113 (1990).]

7.1.6 Cleavage Plane

Table 7.1.8 *Crystallographic plane most readily cleaved for β-ZnS.*

Cleavage plane
(110)

• Surface energy

Table 7.1.9 *Surface energy for β-ZnS (in J/m^2).*

Plane			Comment
(110)	(111)	$(\bar{1}\,\bar{1}\,\bar{1})$	
1.225	1.150	0.850	Calc. [1.12]

[1.12] B. N. Oshcherin, *Phys. Status Solidi A* **34**, K181 (1976).

7.2 THERMAL PROPERTIES

7.2.1 Melting Point and Its Related Parameters

Table 7.2.1 *Melting point T_m and its related parameter for ZnS.*

Parameter	Value
Melting point T_m (K)	2196 [2.1]
Entropy of fusion ΔS_m (cal/mol K)	16.29 [2.2]

[2.1] See, J. A. Van Vechten, *Phys Rev. B* **7**, 1479 (1973).
[2.2] See, B. R. Nag, *J. Electron. Mater.* **26**, 70 (1997).

7.2.2 Specific Heat

Table 7.2.2 *Experimental specific heat C_p (at constant pressure) for β-ZnS.**

Temperature (K)	C_p (J/g K)	Temperature (K)	C_p (J/g K)
2.452	0.0150	40.9	0.0883
2.837	0.0236	55.0	0.134
3.836	0.0572	62.9	0.158
4.310	0.0813	71.5	0.180
5.139	0.139	77.2	0.197
5.687	0.189	85.8	0.218
6.001	0.223	93.1	0.234
6.533	0.297	99.8	0.252
7.148	0.384	109.4	0.274
7.586	0.481	117.9	0.293
8.047	0.586	126.4	0.310
9.041	0.859	135.1	0.330
9.22	0.919	142.7	0.345
9.42	1.035	150.3	0.351
9.86	1.231	158.4	0.367
10.36	1.43	167.9	0.378
11.44	2.09	177.9	0.388
18.65	0.0144	187.0	0.397
20.95	0.0185	196.3	0.403
23.75	0.0278	298.0	0.486
34.20	0.0630		

*The experimental data are taken for $T \leq 11.44$ K from J. A. Birch [*J. Phys. C: Solid State Phys.* **8**, 2043 (1975) (Irtran 2)] and for $T \geq 18.65$ K from K. Clusius and P. Harteck [*Z. Phys. Chem.* **134**, 243 (1928)].

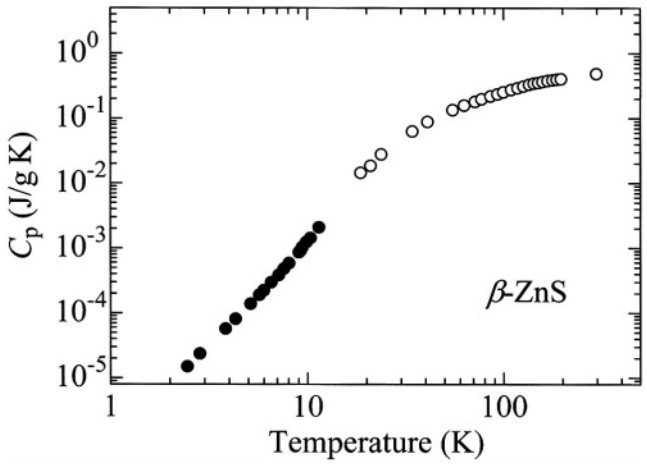

Fig. 7.2.1 Specific heat C_p (at constant pressure) versus temperature for β-ZnS. The experimental data are taken for $T \leq 11.44$ K from J. A. Birch [*J. Phys. C: Solid State Phys.* **8**, 2043 (1975); solid circles (Irtran 2)] and for $T \geq 18.65$ K from K. Clusius and P. Harteck [*Z. Phys. Chem.* **134**, 243 (1928); open circles].

7.2.3 Debye Temperature

Table 7.2.3 *Debye temperature θ_D for β-ZnS.*

θ_D (K)	Comment
340	T=0 K*[1]
440	T=300 K*[2]

*[1] In the low-temperature (0 K) limit [see, H. Siethoff and K. Ahlborn, *Phys. Status Solidi B* **190**, 179 (1995)].

*[2] Estimated from data by D. N. Talwar, M. Vandevyver, K. Kunc, and M. Zigone [*Phys. Rev. B* **24**, 741 (1981)].

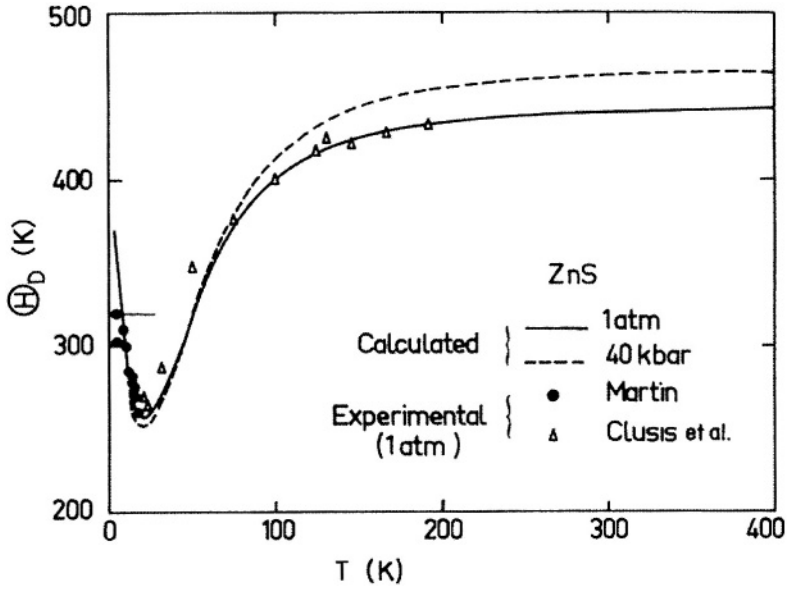

Fig. 7.2.2 Theoretical and experimental Debye temperature θ_D versus temperature T for β-ZnS. The experimental data are taken from D. L. Martin [*Philos. Mag.* **46**, 751 (1955)] and from K. Clusius and P. Harteck [*Z. Phys. Chem.* **134**, 243 (1928)]. [From D. N. Talwar, M. Vandevyver, K. Kunc, and M. Zigone, *Phys. Rev. B* **24**, 741 (1981).]

7.2.4 Thermal Expansion Coefficient

Table 7.2.4 *Thermal expansion coefficient α_{th} for β-ZnS.**

T (K)	α_{th} (10^{-6} K^{-1})	T (K)	α_{th} (10^{-6} K^{-1})	T (K)	α_{th} (10^{-6} K^{-1})
3	–0.0002	30	–0.316	250	6.10
4	–0.0002	90	1.14	260	6.24
5	–0.0004	100	1.63	270	6.41
6	–0.0008	110	2.15	280	6.48
7	–0.0014	120	2.61	290	6.58
8	–0.0023	130	3.07	300	6.71
9	–0.0037	140	3.44	313	6.7
10	–0.0058	150	3.81	333	6.7
12	–0.0141	160	4.18	353	6.7
14	–0.0304	170	4.50	373	6.8
16	–0.0544	180	4.74	393	7.1
18	–0.0855	190	5.02	413	7.3
20	–0.124	200	5.24	433	7.5
22	–0.163	210	5.43	453	7.9
24	–0.204	220	5.64	473	8.2
26	–0.244	230	5.81	493	8.5
28	–0.289	240	5.94	513	8.7

*The experimental data are taken for $T \leq 30$ K from F. W. Sheard, T. F. Smith, G. K. White, and J. A. Birch [*J. Phys. C: Solid State Phys.* **10**, 645 (1977) (Irtran 2)], for $90 \leq T \leq 300$ K from R. R. Reeber [*Phys. Status Solidi A* **32,** 321 (1975)], and for $T \geq 313$ K from S. S. Ballard, S. E. Brown, and J. S. Browder [*Appl. Opt.* **17**, 1152 (1978)].

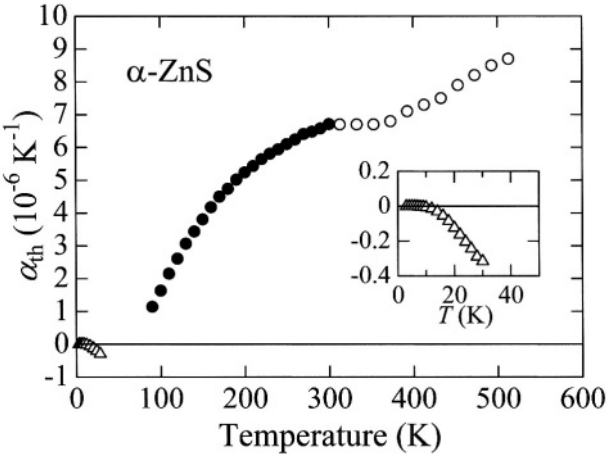

Fig. 7.2.3 Thermal expansion coefficient α_{th} versus temperature T for β-ZnS. The experimental data are taken for $T \leq 30$ K from F. W. Sheard, T. F. Smith, G. K. White, and J. A. Birch [*J. Phys. C: Solid State Phys.* **10**, 645 (1977); open triangles], for $90 \leq T \leq 300$ K from R. R. Reeber [*Phys. Status Solidi A* **32**, 321 (1975); solid circles], and for $T \geq 313$ K from S. S. Ballard, S. E. Brown, and J. S. Browder [*Appl. Opt.* **17**, 1152 (1978); open circles].

7.2.5 Thermal Conductivity and Diffusivity

Table 7.2.5 *Thermal conductivity K for β-ZnS [2.3]. Thermal diffusivity can be calculated from a relation $D=K/(C_p \cdot g)$, where C_p is the specific heat at constant pressure and g is the crystal density.*

Temperature (K)	*K* (W/cm K)	Temperature (K)	*K* (W/cm K)
3.3	0.42	30	3.6
4	0.57	40	3.1
4.8	0.85	50	2.6
5.9	1.36	65	2.0
7.3	1.95	80	1.55
10	3.0	100	1.20
12.5	3.3	150	0.70
16.5	3.8	200	0.47
21	3.5	250	0.34
26	3.5	300	0.27

[2.3] G. A. Slack, *Phys. Rev. B* **6**, 3791 (1972).

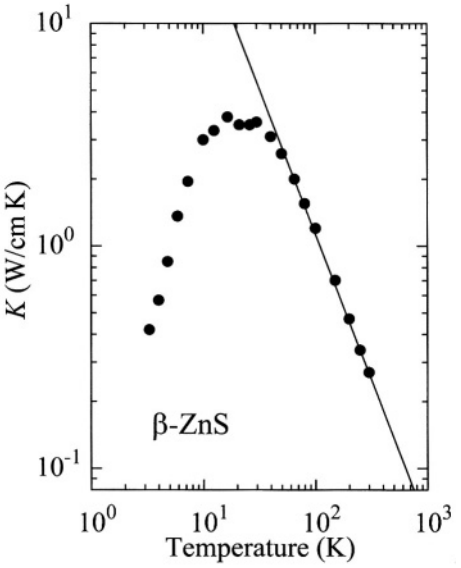

Fig. 7.2.4 Thermal conductivity *K* for β-ZnS. The experimental data are taken from G. A. Slack [*Phys. Rev. B* **6**, 3791 (1972)]. The solid line is calculated from $K=AT^n$ with $A=470$ W/cm K$^{-0.31}$ and $n=-1.31$.

7.3 ELASTIC PROPERTIES

7.3.1 Elastic Constant

- **Room-temperature value and its temperature and pressure derivatives**

Table 7.3.1 *Elastic constant and its temperature and pressure derivatives for β-ZnS at 300 K.*

Parameter	Value
Stiffness (10^{11} dyn/cm^2) [3.1]	
C_{11}	10.2
C_{12}	6.46
C_{44}	4.46

Table 7.3.1 *Continued.*

Parameter	Value
Compliance (10^{-12} cm^2/dyn) [3.1]	
S_{11}	1.95
S_{12}	–0.76
S_{44}	2.25
dC_{ij}/dT (10^7 dyn/cm^2 K) [3.2]	
C_{11}	–11.2
C_{12}	–7.8
C_{44}	–3.6
dC_{ij}/dp	
C_{11}	
C_{12}	
C_{44}	

[3.1] *Numerical Data and Functional Relationships in Science and Technology,* edited by K.-H. Hellwege and A. M. Hellwege, Landolt–Börnstein, New Series, Group III, Vol. 18 (Springer, Berlin, 1984).

[3.2] *Numerical Data and Functional Relationships in Science and Technology,* edited by K.-H. Hellwege and A. M. Hellwege, Landolt–Börnstein, New Series, Group III, Vol. 11 (Springer, Berlin, 1979).

7.3.2 Third-Order Elastic Constant

No detailed data are available for β-ZnS.

7.3.3 Young's Modulus, Poisson's Ratio, and Similar

- **Young's modulus**

Table 7.3.2 *Young's modulus Y for β-ZnS at 300 K.**

Crystallographic plane	Y (10^{12} dyn/cm^2)
(100) plane	
[001] direction	0.513
[011] direction	0.864
(110) plane	
[001] direction	0.513
[111] direction	1.12
(111) plane	0.864

*Calculated using S_{11}=1.95, S_{12}=–0.76, and S_{44}=2.25 (all in 10^{-12} cm^2/dyn).

- **Poisson's ratio**

Table 7.3.3 *Poisson's ratio P for β-ZnS at 300 K.**

Crystallographic plane	P
(100) plane	
m=[010], n=[001]	0.390
m=[011], n=[0$\bar{1}$1]	–0.028

Table 7.3.3 *Continued.*

Crystallographic plane	P
(110) plane	
m=[001], n=[1$\bar{1}$0]	0.390
m=[1$\bar{1}$1], n=[1$\bar{1}\bar{2}$]	0.259
(111) plane	0.428

*Calculated using S_{11}=1.95, S_{12}= –0.76, and S_{44}=2.25 (all in 10^{-12} cm^2/dyn).

- **Bulk modulus, shear modulus, etc.**

Table 7.3.4 *Bulk modulus, B_u, pressure derivative of B_u, dB_u/dp, shear modulus, C_s, isotropy factor, A, linear compressibility, C_o, Caucy ratio, C_a, and Born ratio, B_o, for β-ZnS at 300 K.*

Parameter	Value
B_u (10^{11} dyn/cm^2)	7.71 [3.3]
dB_u/dp	3.92–4.7 [3.4]
	4.91±1.2 [3.5]
	3.8±0.1 [3.6]
	4 [3.7]
C_s (10^{11} dyn/cm^2)	1.87 [3.3]
A	0.419 [3.3]
C_o (10^{-13} cm^2/dyn)	4.33 [3.3]
C_a	1.45 [3.3]
B_o	1.19 [3.3]

[3.3] Calculated using C_{11}=10.2, C_{12}=6.46, and C_{44}=4.46 (all in 10^{11} dyn/cm^2).
[3.4] Theor. [A. Nazzal and A. Qteish, *Phys. Rev. B* **53**, 8262 (1996)].
[3.5] Exper. [J. C. Jamieson and H. H. Demarest, Jr., *J. Phys. Chem. Solids* **41**, 963 (1980)].
[3.6] Exper. [M. Uchino, T. Mashimo, M. Kodama, T. Kobayashi, E. Takasawa, T. Sekine, Y. Noguchi, H. Hikosaka, K. Fukuoka, Y. Syono, T. Kondo, and T. Yagi, *J. Phys. Chem. Solids* **60**, 827 (1999)].
[3.7] Exper. [S. Desgreniers, L. Beaulieu, and I. Lepage, *Phys. Rev. B* **61**, 8726 (2000)].

7.3.4 Microhardness

Table 7.3.5 *Microhardness H for ZnS [3.8].**

H (GPa)
1.78

[3.8] See, L. Garbato and A. Rucci, *Phil. Mag.* **35**, 1681 (1977).
*Type of crystal (α- or β-ZnS) was not described.

7.3.5 Sound Velocity

Table 7.3.6 *Sound velocity propagating in β-ZnS at 300 K.* LA=longitudinal acoustic; TA1, TA2=transverse acoustic.*

Propagation direction	Mode	Sound velocity (10^5 cm/s)
[100]	LA	5.00
[100]	TA1, TA2	3.30
[110]	LA	5.59

Table 7.3.6 *Continued.*

Propagation direction	Mode	Sound velocity (10^5 cm/s)
[110]	TA1	2.14
[110]	TA2	3.30
[111]	LA	5.78
[111]	TA1, TA2	2.59

*Calculated using $C_{11}=1.02\times10^{12}$ dyn/cm^2, $C_{12}=6.46\times10^{11}$ dyn/cm^2, $C_{44}=4.46\times10^{11}$ dyn/cm^2, and $g=4.0879$ g/cm^3.

7.4 PHONONS AND LATTICE VIBRONIC PROPERTIES

7.4.1 Phonon Dispersion Relation

- **Dispersion curve**

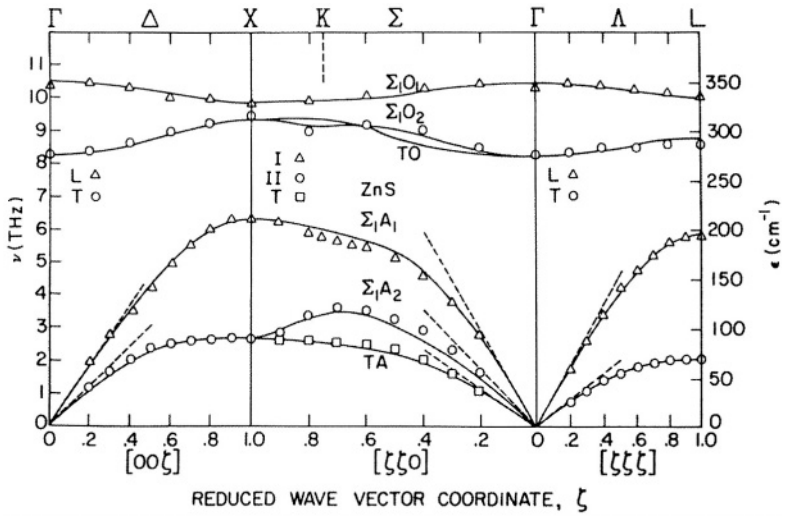

Fig. 7.4.1 Theoretical phonon dispersion curves for β-ZnS, together with the neutron scattering data at 300 K. [From N. Vagelatos, D. Wehe, and J. S. King, *J. Chem. Phys.* **60**, 3613 (1974).]

- **Phonon density of states**

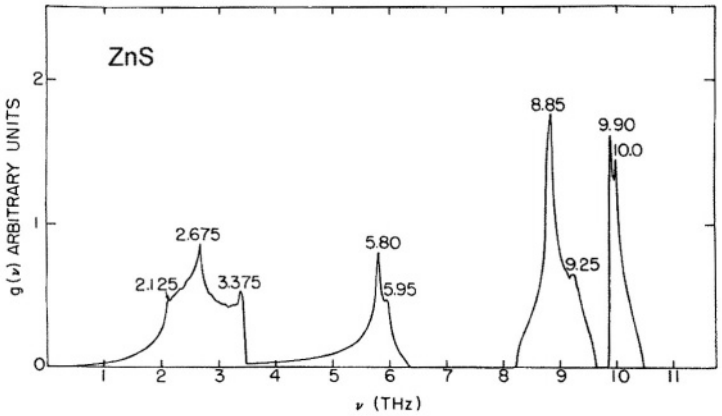

Fig. 7.4.2 Phonon density of states $g(\nu)$ for β-ZnS. [From N. Vagelatos, D. Wehe, and J. S. King, *J. Chem. Phys.* **60**, 3613 (1974).]

7.4.2 Phonon Frequency

- **Room-temperature value**

Table 7.4.1 *Long-wavelength ($q \to 0$) and zone-boundary phonon frequencies for β-ZnS [4.1].*

Critical point	Phonon	Phonon frequency (cm^{-1})
Γ	TO	277
		271–286 [4.2]
		273 [4.3]
		272.0±0.1 [4.4]
	LO	348
		350–352 [4.2]
		350 [4.3]
		350.5±0.1 [4.4]
X	TA	90
	LA	211
	TO	316
	LO	330
L	TA	70
	LA	195
	TO	289
	LO	337

[4.1] N. Vagelatos, D. Wehe, and J. S. King, *J. Chem. Phys.* **60**, 3613 (1974).
[4.2] *Numerical Data and Functional Relationships in Science and Technology,* edited by O. Madelung, M. Schulz, and H. Weiss, Landolt–Börnstein, New Series, Group III, Vol. 17, Pt. b (Springer, Berlin, 1982).
[4.3] A. Memon and D. B. Tanner, *Phys. Status Solidi B* **127,** 49 (1985).
[4.4] M. Siakavellas, A. G. Kontos, and E. Anastassakis, *J. Appl. Phys.* **84**, 517 (1998).

- **Temperature dependence**

It has been reported that the TO phonon frequency in β-ZnS shows a decrease of about 3 cm^{-1} in going from 2 to 300 K [T. Hattori, Y. Homma, A. Mitsuishi, and M. Tacke, *Opt. Commun.* **7**, 229 (1973)].

- **Pressure dependence**

Table 7.4.2 *Pressure variation of the long-wavelength ($q \to 0$) phonon frequency in β-ZnS [4.5].*

$$\omega_q(p) = \omega_q(0) + ap$$

ω_q	$\omega_q(0)$ (cm^{-1})	a (cm^{-1}/GPa)
ω_{TO}	271	6.6
ω_{LO}	352	3.3

[4.5] M. Cardona, *J. Phys. (Paris)* **45**, C8-29 (1984).

7.4.3 Mode Grüneisen Parameter

Table 7.4.3 *Mode Grüneisen parameter for phonons at a number of critical points in β-ZnS [4.6].*

Critical point	Phonon	Mode Grüneisen parameter
Γ	TO	1.85±0.2
		1.84±0.20 [4.7]
	LO	0.95±0.1
		1.02±0.14 [4.7]
X	TA	−1.2±0.2
	LA	
	TO	1.0±0.2
	LO	1.1±0.2
L	TA	−1.5±0.2
	LA	
	TO	1.0±0.1
	LO	1.1±0.2

[4.6] See, D. N. Talwar, M. Vandevyver, K. Kunc, and M. Zigone, *Phys. Rev. B* **24**, 741 (1981).
[4.7] M. Siakavellas, A. G. Kontos, and E. Anastassakis, *J. Appl. Phys.* **84**, 517 (1998).

7.4.4 Phonon Deformation Potential

Table 7.4.4 *Long-wavelength phonon deformation potential (PDP) for β-ZnS [4.8].*

PDP	TO	LO
K_{11}	−2.81±0.48	−1.23±0.28
K_{12}	−4.11±0.48	−2.45±0.28
K_{44}	−0.61±0.16	−0.30±0.10
$K_{11}-K_{12}$	1.30	1.22

[4.8] M. Siakavellas, A. G. Kontos, and E. Anastassakis, *J. Appl. Phys.* **84**, 517 (1998).

7.5 COLLECTIVE EFFECTS AND RELATED PROPERTIES

7.5.1 Piezoelectric Constant

Table 7.5.1 *Piezoelectric stress (e_{14}), strain (d_{14}), and electromechanical coupling constants ($K_{[110]}^2$) for β-ZnS [5.1].*

Parameter	Value
e_{14} (C/m^2)	0.147
d_{14} (10^{-12} m/V)	3.18
$K_{[110]}^2$	6.6×10^{-4} *

[5.1] D. Berlincourt, H. Jaffe, and L. R. Shiozawa, *Phys. Rev.* **129,** 1009 (1963).
*Calculated.

7.5.2 Fröhlich Coupling Constant

Table 7.5.2 *Fröhlich coupling constant α_F of β-ZnS.*

α_F	Ref.
0.649	[5.2]
0.63	[5.3]

[5.2] E. Kartheuser, in *Polarons in Ionic Crystals and Polar Semiconductors,* edited by J. T. Devreese (North-Holland, Amsterdam, 1972), p. 717.
[5.3] Y. Imanaka and N. Miura, *Phys. Rev. B* **50**, 14065 (1994).

7.6 ENERGY-BAND STRUCTURE: ENERGY-BAND GAPS

7.6.1 Basic Properties

• Electronic energy-band structure

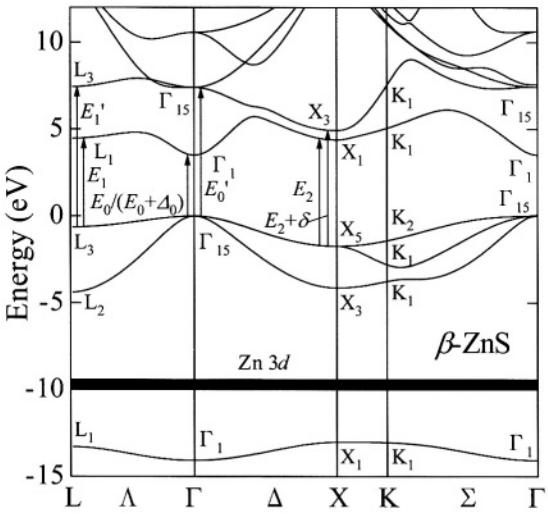

Fig. 7.6.1 Electronic energy-band structure of β-ZnS as calculated by an empirical pseudopotential method. The locations of several interband transitions are included by the vertical arrows. [From T. Tsuchiya, S. Ozaki, and S. Adachi, *J. Phys: Condens. Matter* 15, 3717 (2003).]

• Electronic density of states

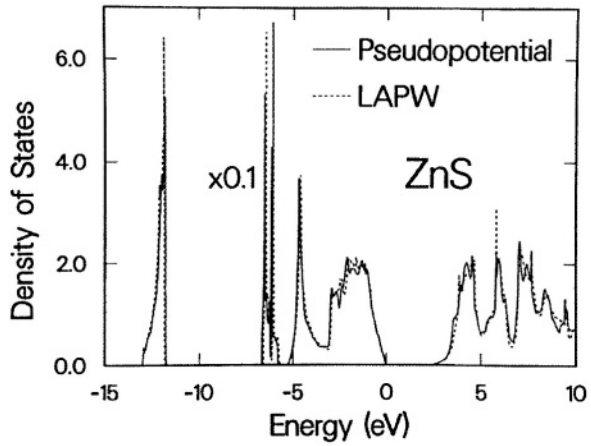

Fig. 7.6.2 Calculated electronic density of states for β-ZnS with the pseudopotential (solid line) and all-electron linearized-augmented-plane-wave (LAPW; dashed line) method. [From J. L. Martins, N. Troullier, and S.-H. Wei, *Phys. Rev. B* **43**, 2213 (1991).]

• **Energy eigenvalue**

Table 7.6.1 *Energy eigenvalues at the Γ, X, and L points for the valence and first few conduction bands of β-ZnS [6.1].*

Critical point	Level	Value (eV)	
		Calc.	Exper.*
Γ	Γ_6^v (Γ_1^v)	−13.42	−13.5
	Γ_7^v (Γ_{15}^v)	0.00	−0.070
	Γ_8^v		0.00
	Γ_6^c (Γ_1^c)	3.98	3.797–3.841
	Γ_7^c (Γ_{15}^c)	8.74	8.35
	Γ_8^c		
X	X_6^v (X_1^v)	−11.71	−12.0
	X_6^v (X_3^v)	−4.89	−5.5
	X_6^v (X_5^v)	−2.06	−2.5
	X_7^v		−1.4
	X_6^c (X_1^c)	5.14	4.9
	X_7^c (X_3^c)	6.03	
L	L_6^v (L_1^v)	−12.15	−12.4
	L_6^v (L_1^v)	−5.20	−5.5
	L_6^v (L_3^v)	−0.78	−1.4
	$L_{4,5}^v$		
	L_6^c (L_1^c)	5.28	
	L_6^c (L_3^c)	9.17	
	$L_{4,5}^c$		

[6.1] O. Zakharov, A. Rubio, X. Blase, M. L. Cohen, and S. G. Louie, *Phys. Rev. B* **50**, 10780 (1994).
*The data are gathered from various sources.

7.6.2 E_0-Gap Region

• **Room-temperature value**

Table 7.6.2 *E_0-, $E_0+\Delta_0$-, and Δ_0-gap energies for β-ZnS at room temperature.*

E_0 (eV)	$E_0+\Delta_0$ (eV)	Δ_0 (eV)	Comment
3.715			Epilayer on (100)GaAs [6.2]
3.723±0.001			Epilayer on GaAs [6.3]
3.741±0.004			Epilayer on (100)GaAs [6.4]
3.726	3.796*	(0.070)	Mean value

[6.2] O. Kanehisa, M. Shiiki, M. Migita, and H. Yamamoto, *J. Cryst. Growth* **86**, 367 (1988).
[6.3] T. K. Tran, W. Park, W. Tong, M. M. Kyi, B. K. Wagner, and C. J. Summers, *J. Appl. Phys.* **81**, 2803 (1997).
[6.4] R. Pässler, E. Griebl, H. Riepl, G. Lautner, S. Bauer, H. Preis, W. Gebhardt, B. Buda, D. J. As, D. Schikora, K. Lischka, K. Papagelis, and S. Ves, *J. Appl. Phys.* **86**, 4403 (1999).
*Obtained by adding a value of Δ_0=0.424 eV.

- **Temperature dependence**

Table 7.6.3 *Empirical equation for the E_0-gap energy variation with temperature T for β-ZnS.*

$$E_0(T) = E_0(0) - \frac{\alpha T^2}{T + \beta}$$

Parameter			Comment
$E_0(0)$ (eV)	α (10^{-4} eV/K)	β (K)	
3.8053	17	1050	n=1 exciton, T=4.2–300 K, bulk ZnS [6.5]
3.810	6.32	254	n=1 exciton, T=1.7–550 K, epilayer [6.6]

[6.5] K. A. Dmitrenko, L. V. Taranenko, S. G. Shevel', and A. V. Marinchenko, *Sov. Phys. Semicond.* **19**, 487 (1985).
[6.6] R. Pässler, E. Griebl, H. Riepl, G. Lautner, S. Bauer, H. Preis, W. Gebhardt, B. Buda, D. J. As, D. Schikora, K. Lischka, K. Papagelis, and S. Ves, *J. Appl. Phys.* **86**, 4403 (1999).

Table 7.6.4 *Empirical equation for the E_0- and $E_0+\Delta_0$-gap energy variations with temperature T for β-ZnS.*

$$E_g(T) = E_g(0) - \frac{\alpha_m T^4}{(T_m + \beta)^3}$$

Band gap	Parameter			Comment
	$E_g(0)$ (eV)	α_m (10^{-4} eV/K)	β_m (K)	
E_0	3.8022	6.86	76	n=1 exciton (heavy hole), T=10–300 K, epilayer on (100)GaAs [6.7]
	3.7970	6.7	75	n=1 exciton (light hole), T=10–300 K, epilayer on (100)GaAs [6.7]
$E_0+\Delta_0$	3.8684	7.0	77	n=1 exciton, T=10–300 K, epilayer on (100)GaAs [6.7]

[6.7] M. Fernández, P. Prete, N. Lovergine, A. M. Mancini, R. Cingolani, L. Vasanelli, and M. R. Perrone, *Phys. Rev. B* **55,** 7660 (1997).

Table 7.6.5 *Empirical equation for the E_0-gap energy variation with temperature T for β-ZnS [6.8].*

$$E_0(T) = E_0(0) - S\langle\hbar\Omega\rangle\left[\coth\left(\frac{\langle\hbar\Omega\rangle}{2kT}\right) - 1\right]$$

$E_0(0)$ (eV)	S	$\langle\hbar\Omega\rangle$ (meV)
3.836	2.82	16.1

[6.8] K. P. O'Donnell and P. G. Middleton, in *Properties of Wide Bandgap II–VI Semiconductors,* EMIS Datareviews Series No. 17, edited by R. Bhargava (INSPEC, London, 1997), p. 33.

Table 7.6.6 *Empirical equation for the E_0-gap energy variation with temperature T for β-ZnS.*

$$E_0(T) = E_0(0) - \frac{\alpha\Theta_p}{2}\left[\sqrt[p]{1+\left(\frac{2T}{\Theta_p}\right)^p} - 1\right]$$

$E_0(0)$ (eV)	p	α (meV/K)	Θ_p (K)	Comment
3.841	2.76	0.532	240	T=2–541 K [6.9]

[6.9] R. Pässler, *Phys. Status Solidi B* **216,** 975 (1999).

Table 7.6.7 *Empirical equation for the E_0-gap energy variation with temperature T for β-ZnS.*

$$E_0(T) = E_0(0) - \alpha\sum_{i=1,2}\frac{W_i\Theta_i}{\exp(\Theta_i/T)-1}$$

$E_0(0)$ (eV)	α (10^{-4} eV/K)	Θ_1 (K)	Θ_2 (K)	W_1	W_2	Comment
3.841	5.49	100	341	0.24	0.76	T=2–541 K [6.10]

[6.10] R. Pässler, *J. Appl. Phys.* **89**, 6235 (2001).

Table 7.6.8 *Spin–orbit–splitoff energy Δ_0 for β-ZnS.**

Δ_0 (eV)	Comment
0.071±0.04	T=77 K [6.11]
0.066	T=10 K [6.12]
0.070	Mean value

[6.11] E. Matatagui, A. G. Thompson, and M. Cardona, *Phys. Rev.* **176,** 950 (1968).
[6.12] M. Fernández, P. Prete, N. Lovergine, A. M. Mancini, R. Cingolani, L. Vasanelli, and M. R. Perrone, *Phys. Rev. B* **55**, 7660 (1997).
*Note that Δ_0 may not vary with temperature if one supposes the valence-band rigidity of the II–VI compounds.

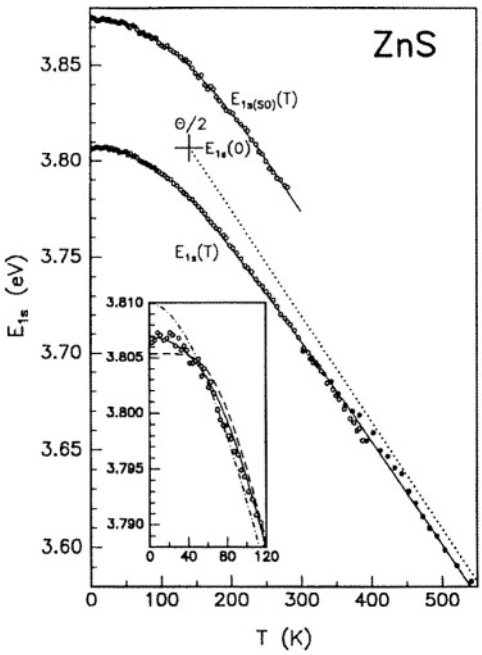

Fig. 7.6.3 Energy position of the n=1 exciton state E_{1S} in β-ZnS epilayer grown on (100)GaAs substrate determined at lower temperatures by absorption measurements (open circles) and at higher temperatures by reflectance measurements (solid circles). The curves represent the numerical fits using various models. [From R. Pässler, E. Griebl, H. Riepl, G. Lautner, S. Bauer, H. Preis, W. Gebhardt, B. Buda, D. J. As, D. Schikora, K. Lischka, K. Papagelis, and S. Ves, *J. Appl. Phys.* **86**, 4403 (1999).]

- **Pressure dependence**

Table 7.6.9 *Empirical equation for the E_0-gap energy variation with pressure p for β-ZnS.*

$$E_0(p) = E_0(0)+ap+bp^2$$

Parameter			Comment
$E_0(0)$ (eV)	a (10^{-2} eV/GPa)	b (10^{-4} eV/GPa^2)	
3.666±0.010	6.35±0.07	−13.1±0.5	T=300 K [6.13]
3.8375±0.0001	6.38±0.05	−15±1	T=7 K [6.14]

[6.13] S. Ves, U. Schwarz, N. E. Christensen, K. Syassen, and M. Cardona, *Phys. Rev. B* **42**, 9113 (1990).
[6.14] A. Mang, K. Reimann, St. Rübenacke, and M. Steube, *Phys. Rev. B* **53**, 16283 (1996).

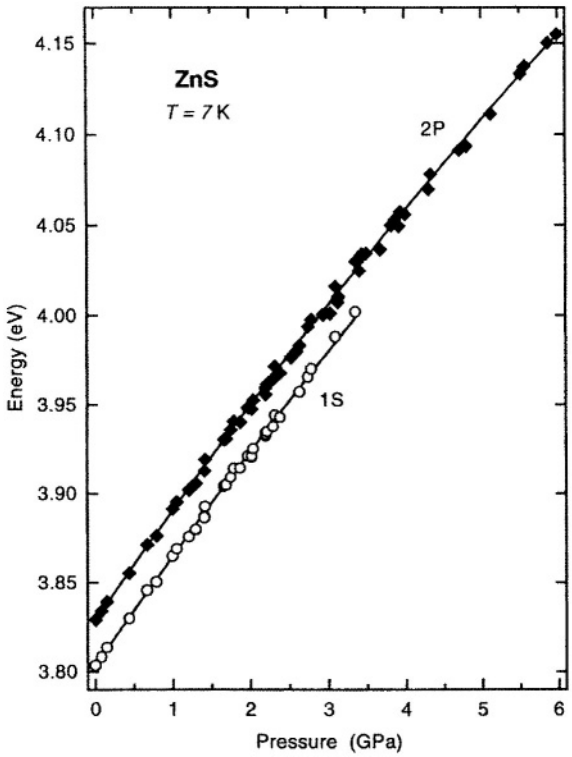

Fig. 7.6.4 Energy of the longitudinal 1*s* (1S) and 2*p* (2P) excitons in β-ZnS versus pressure at T=7 K. The solid lines show the quadratic fits. [From A. Mang, K. Reimann, St. Rübenacke, and M. Steube, *Phys. Rev. B* **53**, 16283 (1996).]

- **Temperature and/or pressure coefficient**

Table 7.6.10 *Linear temperature and pressure coefficients of the E_0- and $E_0+\Delta_0$-gap energies for β-ZnS.*

Band gap	Coefficient	Value	Comment
E_0	dE_g/dT (10^{-4} eV/K)	−4.7±0.5	T=300 K [6.15]
		−4.45±0.05	n=1 exciton, T=80–293 K [6.16]
		−4.7	T>80 K [6.17]
		−4.5±0.1	n=1exciton (heavy hole), T>76 K [6.18]
		−4.4±0.1	n=1exciton (light hole), T>75 K [6.18]
		−5.05±0.05	T=300 K [6.19]
	dE_g/dp (10^{-2} eV/GPa)	6.5±1.0	[6.20]

Table 7.6.10 *Continued.*

Band gap	Coefficient	Value	Comment
$E_0+\Delta_0$	dE_g/dT (10^{-4} eV/K)	–4.60±0.25	n=1 exciton, T=80–293 K [6.16]
		–4.7	T>80 K [6.17]
		–4.6±0.1	n=1exciton, T>77 K [6.18]
	dE_g/dp (10^{-2} eV/GPa)		

[6.15] J. Camassel and D. Auvergne, *Phys. Rev. B* **12**, 3258 (1975).
[6.16] V. V. Sobolev, V. I. Donetskikh, and E. F. Zagaĭnov, *Sov. Phys. Semicond.* **12**, 646 (1978).
[6.17] A. Abounadi, M. Di Blasio, D. Bouchara, J. Calas, M. Averous, O. Briot, N. Briot, T. Cloitre, R. L. Aulombard, and B. Gil, *Phys. Rev. B* **50**, 11677 (1994).
[6.18] M. Fernández, P. Prete, N. Lovergine, A. M. Mancini, R. Cingolani, L. Vasanelli, and M. R. Perrone, *Phys. Rev. B* **55**, 7660 (1997).
[6.19] R. Pässler, E. Griebl, H. Riepl, G. Lautner, S. Bauer, H. Preis, W. Gebhardt, B. Buda, D. J. As, D. Schikora, K. Lischka, K. Papagelis, and S. Ves, *J. Appl. Phys.* **86**, 4403 (1999).
[6.20] D. L. Camphausen, G. A. N. Connell, and W. Paul, *Phys. Rev. Lett.* **26**, 184 (1971).

7.6.3 Higher-Lying Direct Gap

• Room-temperature value

Table 7.6.11 *Higher-lying direct-gap energies for β-ZnS measured at room temperature [6.21].*

Band gap	Value (eV)
E_1	5.8
Δ_1	0.05*
E_2	7.0
E_1'	9.2
d	13

[6.21] See, S. Adachi, *Optical Constants of Crystalline and Amorphous Semiconductors: Numerical Data and Graphical Information* (Kluwer Academic, Boston, 1999).
*Theoretical value [see, S. N. Ekpenuma and C. W. Myles, *J. Phys. Chem. Solids* **51**, 93 (1990)].

• Temperature and/or pressure coefficient

Table 7.6.12 *Linear temperature and pressure coefficients of the higher-lying band-gap energy for β-ZnS.*

Band gap	Coefficient	Value	Comment
E_1	dE_g/dT (10^{-4} eV/K)	–5.1	T=100–300 K [6.22]
	dE_g/dp (10^{-2} eV/GPa)	3.5	Calc. [6.23]
		0.86	Calc. [6.24]
E_2	dE_g/dT (10^{-4} eV/K)	–3.0	T=100–300 K [6.22]
	dE_g/dp (10^{-2} eV/GPa)	3.0	Calc. [6.23]

[6.22] D. Theis, *J. Phys. Chem. Solids* **38**, 1125 (1977).
[6.23] D. L. Camphausen, G. A. N. Connell, and W. Paul, *Phys. Rev. Lett.* **26**, 184 (1971).
[6.24] Y. F. Tsay, S. S. Mitra, and B. Bendow, *Phys. Rev. B* **10**, 1476 (1974).

7.6.4 Lowest Indirect Gap

• Theoretical value

Table 7.6.13 *Theoretically obtained lowest indirect-gap energy for β-ZnS (in eV).*

E_g^{L} *1	E_g^{X} *2	Ref.
5.64	5.76	[6.25]
4.82	4.81	[6.26]
5.28	5.14	[6.27]

[6.25] M.-Z. Huang and W. Y. Ching, *J. Phys. Chem. Solids* **46**, 977 (1985).
[6.26] Y. Li and P. J. Lin-Chung, *Phys. Status Solidi B* **153**, 215 (1989).
[6.27] O. Zakharov, A. Rubio, X. Blase, M. L. Cohen, and S. L. Louie, *Phys. Rev. B* **50**, 10780 (1994).
*1 Γ_8^v (Γ_{15}^v)→L_6^c(L_1^c).
*2 Γ_8^v (Γ_{15}^v)→X_6^c(X_1^c).

• Temperature and/or pressure coefficient

Table 7.6.14 *Linear pressure coefficient of the lowest indirect-gap energy for β-ZnS.*

Coefficient	Value	Comment
dE_g^{L}/dp (10^{-2} eV/GPa)	1.7	Calc. [6.28]
	–0.1	Calc. [6.29]
	4.0	Calc. [6.30]
dE_g^{X}/dp (10^{-2} eV/GPa)	–1.7	Calc. [6.28]
	–5.2	Calc. [6.29]
	–1.4	Calc. [6.30]

[6.28] D. L. Camphausen, G. A. N. Connell, and W. Paul, *Phys. Rev. Lett.* **26,** 184 (1971).
[6.29] Y. F. Tsay, S. S. Mitra, and B. Bendow, *Phys. Rev. B* **10**, 1476 (1974).
[6.30] S.-H. Wei and A. Zunger, *Phys. Rev. B* **60**, 5404 (1999).

7.6.5 Conduction-Valley Energy Separation

No detailed data are available for β-ZnS.

7.6.6 Direct–Indirect-Gap Transition Pressure

No direct–indirect-gap crossing may occur in β-ZnS for pressures up to the first structural phase transition (p~15 GPa) [see, S. Ves, U. Schwarz, N. E. Christensen, K. Syassen, and M. Cardona, *Phys. Rev. B* **42**, 9113 (1990)].

7.7 ENERGY-BAND STRUCTURE: ELECTRON AND HOLE EFFECTIVE MASSES

7.7.1 Electron Effective Mass: Γ Valley

• Theoretical value

Table 7.7.1 *Theoretically obtained electron effective mass m_e^Γ at the Γ valley in β-ZnS.*

m_e^Γ/m_0	Ref.
0.39	[7.1]
0.23	[7.2]
0.28	[7.3]
0.184	[7.4]
0.262	[7.5]

[7.1] M. Cardona, *J. Phys. Chem. Solids* **24**, 1543 (1963).
[7.2] R. L. Bowers and G. D. Mahan, *Phys. Rev.* **185**, 1073 (1969).
[7.3] P. Lawaetz, *Phys. Rev. B* **4**, 3460 (1971).
[7.4] C. S. Wang and B. M. Klein, *Phys. Rev. B* **24**, 3393 (1981).
[7.5] M.-Z. Huang and W. Y. Ching, *J. Phys. Chem. Solids* **46**, 977 (1985).

• Experimental value

Table 7.7.2 *Experimentally determined effective polaron (m_{ep}*) and band masses (m_e^Γ) for electrons at the Γ-conduction band in β-ZnS. α_F=Fröhlich coupling constant.*

m_{ep}^*/m_0	m_e^Γ/m_0	Comment
	0.34±0.02	Infrared absorption [7.6]
0.22	0.20±0.01	Cyclotron resonance, T=300 K, α_F=0.63 [7.7]

[7.6] H. Kukimoto, S. Shionoya, T. Koda, and R. Hioki, *J. Phys. Chem. Solids* **29**, 935 (1968).
[7.7] Y. Imanaka and N. Miura, *Phys. Rev. B* **50**, 14065 (1994).

7.7.2 Electron Effective Mass: Satellite Valley

No detailed data are available for β-ZnS.

7.7.3 Hole Effective Mass

• Luttinger's valence-band parameter

Table 7.7.3 *Luttinger's valence-band parameter γ_i for β-ZnS (in $\hbar^2/2m_0$).*

γ_1	γ_2	γ_3	Technique
2.54	0.75	1.09	Five-level $\boldsymbol{k}\cdot\boldsymbol{p}$ calculation [7.8]
1.77	0.30	0.62	$\boldsymbol{k}\cdot\boldsymbol{p}$ calculation [7.9]

[7.8] P. Lawaetz, *Phys. Rev. B* **4**, 3460 (1971).
[7.9] See, T. Dietl, H. Ohno, and F. Matsukura, *Phys. Rev. B* **63**, 195205 (2001).

• **Band mass, cyclotron mass, etc.**

Table 7.7.4 *Band (m_{HH}, m_{LH}), density-of-states heavy-hole (m_{HH}*), averaged light-hole (m_{LH}*), and spherically-averaged heavy-hole (m_{HH}^s) and light-hole masses (m_{LH}^s) in β-ZnS.**

Mass	Value (m_0)	
	a	b
m_{HH} ([001] direction)	0.96	0.85
m_{LH} ([001] direction)	0.25	0.42
m_{HH} ([111] direction)	2.8	1.9
m_{LH} ([111] direction)	0.21	0.33
m_{HH}*	1.78	1.42
m_{LH}*	0.23	0.36
m_{HH}^s	1.6	1.3
m_{LH}^s	0.22	0.36

[a]P. Lawaetz, *Phys. Rev. B* **4**, 3460 (1971).
[b]See, T. Dietl, H. Ohno, and F. Matsukura, *Phys. Rev. B* **63**, 195205 (2001).
*Calculated using a set of the Luttinger's parameters.

• **Spin–orbit–splitoff hole effective mass**

Table 7.7.5 *Spin–orbit–splitoff hole effective mass m_{SO} for β-ZnS.*

m_{SO}/m_0	Technique
0.56	$\boldsymbol{k}\cdot\boldsymbol{p}$ method [7.10]
0.40	$\boldsymbol{k}\cdot\boldsymbol{p}$ method [7.11]
0.56	*

[7.10] M. Cardona, *J. Phys. Chem. Solids* **24**, 1543 (1963).
[7.11] P. Lawaetz, *Phys. Rev. B* **4**, 3460 (1971).
*Obtained from the Luttinger's parameter [see, T. Dietl, H. Ohno, and F. Matsukura, *Phys. Rev. B* **63**, 195205 (2001)] ($m_{SO}=1/\gamma_1$).

7.8 ELECTRONIC DEFORMATION POTENTIAL

7.8.1 Intravalley Deformation Potential: Γ Point

• **Conduction band**

Table 7.8.1 *Γ-conduction-band intravalley deformation potential a_c^Γ ($=E_1^\Gamma$) for β-ZnS.*

a_c^Γ (eV)	Comment
−8.23	Calc. [8.1]
−13.1	Calc. [8.2]
−4.09	Calc. [8.3]
−4.49	Calc. [8.4]

[8.1] J. H. Lee and G. Myers, *Phys. Status Solidi B* **77,** K81 (1976).
[8.2] A. Blacha, H. Presting, and M. Cardona, *Phys. Status Solidi B* **126**, 11 (1984).
[8.3] C. G. Van de Walle, *Phys. Rev. B* **39**, 1871 (1989).
[8.4] D. Bertho, D. Boiron, A. Simon, C. Jouanin, and C. Priester, *Phys. Rev. B* **44**, 6118 (1991).

Table 7.8.2 *Γ-conduction-band acoustic deformation potential E_1 for β-ZnS used in the transport data analysis.*

E_1 (eV)	Ref.
14.5	[8.5]
4.9	[8.6]

[8.5] D. L. Rode, *Phys. Rev. B* **2**, 4036 (1970).
[8.6] D. L. Rode, in *Semiconductors and Semimetals,* edited by R. K. Willardson and A. C. Beer (Academic, New York, 1975), Vol. 10, p. 1.

- **Valence band**

Table 7.8.3 *Γ-valence-band deformation potentials a, b, and d for β-ZnS.*

Deformation potential (eV)			Comment
a	*b*	*d*	
–9.2	1.1	–6.4	Calc. [8.7]
2.31	–1.25		Calc. [8.8]
1.47	–3.66		Calc. [8.9]
1.83	–1.39		Calc. [8.10]
	–0.8		Calc. [8.11]
	–1.25		Calc. [8.12]
	–1.18		Calc. [8.13]
	–1.29	–3.20	Calc. [8.14]
	–0.53	–3.7	Exper. [8.15]
	–0.7		Exper. [8.16]
	–1.7		Exper. [8.17]
	–1.5		Exper. [8.18]
		–5.0±0.7	Exper. [8.19]
	–1.0		Exper. [8.20]
(1.9)	–1.1	–4.4	Mean value (Exper.)

[8.7] A. Blacha, H. Presting, and M. Cardona, *Phys. Status Solidi B* **126**, 11 (1984).
[8.8] C. G. Van de Walle, *Phys. Rev. B* **39**, 1871 (1989).
[8.9] D. Bertho, D. Boiron, A. Simon, C. Jouanin, and C. Priester, *Phys. Rev. B* **44**, 6118 (1991).
[8.10] A. Qteish and R. J. Needs, *Phys. Rev. B* **45**, 1317 (1992).
[8.11] M. Silver, W. Batty, A. Ghiti, and E. P. O'Reilly, *Phys. Rev. B* **46**, 6781 (1992).
[8.12] T. Nakayama, *Solid-State Electron.* **37**, 1077 (1994).
[8.13] R. Said, A. Qteish, and N. Meskini, *J. Phys.: Condens. Matter* **10,** 8703 (1998).
[8.14] R. A. Casali and N. E. Christensen, *Solid State Commun.* **108,** 793 (1998).
[8.15] A. Gavini and M. Cardona, *Phys. Rev. B* **1**, 672 (1970).
[8.16]. D. W. Langer, R. N. Euwema, K. Era, and T. Koda, *Phys. Rev. B* **2**, 4005 (1970).
[8.17] G. L. Bir, G. E. Pikus, L. G. Suslina, and D. L. Fedorov, *Sov. Phys.–Solid State* **12**, 926 (1970).
[8.18] K. B. Ozanyan, L. May, J. E. Nicholls, J. H. C. Hogg, W. E. Hagston, B. Lunn, and D. E. Ashenford, *Solid State Commun.* **97**, 345 (1996).
[8.19] A. G. Areshkin, L. I. Vasiljeva, D. L. Fedorov, and L. S. Markov, *J. Opt. Soc. Am. B* **15**, 41 (1998).
[8.20] K. Ichino, K. Ueyama, H. Kariya, N. Suzuki, M. Kitagawa, and H. Kobayashi, *Appl. Phys. Lett.* **74**, 3486 (1999).

• E_0 gap

Table 7.8.4 *Hydrostatic deformation potential* a_0^{Γ} *for the* E_0 *gap of* β*-ZnS.*

a_0^{Γ} (eV)	Comment
–3.9	Calc. [8.21]
–4.0	Calc. [8.22]
–6.40	Calc. [8.23]
–5.96	Calc. [8.24]
–6.95	Calc. [8.25]
–5.16	Calc. [8.26]
–4.24	Calc. [8.27]
–4.0	Exper. [8.28]
–5.0±0.2	Exper. [8.29]
–4.64±0.03	Exper. [8.30]
–6.0	Exper. [8.31]
–6.4	Exper. [8.32]
–5.2	Mean value (Exper.)

[8.21] A. Blacha, H. Presting, and M. Cardona, *Phys. Status Solidi B* **126**, 11 (1984).
[8.22] J. E. Bernard and A. Zunger, *Phys. Rev. B* **36**, 3199 (1987).
[8.23] C. G. Van de Walle, *Phys. Rev. B* **39**, 1871 (1989).
[8.24] D. Bertho, D. Boiron, A. Simon, C. Jouanin, and C. Priester, *Phys. Rev. B* **44**, 6118 (1991).
[8.25] T. Nakayama, *Solid-State Electron.* **37**, 1077 (1994).
[8.26] S.-H. Wei and A. Zunger, *Phys. Rev. B* **60**, 5404 (1999).
[8.27] R. Said, A. Qteish, and N. Meskini, *J. Phys.: Condens. Matter* **10,** 8703 (1998).
[8.28]. D. W. Langer, R. N. Euwema, K. Era, and T. Koda, *Phys. Rev. B* **2,** 4005 (1970).
[8.29] S. Ves, U. Schwarz, N. E. Christensen, K. Syassen, and M. Cardona, *Phys. Rev. B* **42**, 9113 (1990).
[8.30] See, A. Mang, K. Reimann, St. Rübenacke, and M. Steube, *Phys. Rev. B* **53**, 16283 (1996).
[8.31] K. B. Ozanyan, L. May, J. E. Nicholls, J. H. C. Hogg, W. E. Hagston, B. Lunn, and D. E. Ashenford, *Solid State Commun.* **97**, 345 (1996).
[8.32] K. Ichino, K. Ueyama, H. Kariya, N. Suzuki, M. Kitagawa, and H. Kobayashi, *Appl. Phys. Lett.* **74**, 3486 (1999).

• **Optical-phonon deformation potential**

Table 7.8.5 *Optical-phonon deformation potential* d_0 *at the* Γ*-valence band of* β*-ZnS.*

d_0 (eV)	Comment
24.4	Calc. [8.33]
23.5	Calc. [8.34]
6.24	Calc. [8.35]
8.5	Calc. [8.36]
25	Exper. [8.37]
4	Exper. [8.38]
35	Exper. (see [8.38])
21	Mean value (Exper.)

[8.33] A. Blacha, H. Presting, and M. Cardona, *Phys. Status Solidi B* **126**, 11 (1984).
[8.34] L. Brey, N. E. Christensen, and M. Cardona, *Phys. Rev. B* **36**, 2638 (1987).
[8.35] R. A. Casali and N. E. Christensen, *Solid State Commun.* **108,** 793 (1998).
[8.36] R.-Z. Wang, S.-H. Ke, and M.-C. Huang, *J. Phys.: Condens. Matter* **4**, 6735 (1992).
[8.37] R. L. Schmidt and M. Cardona, in *Int. Conf. Phys. Semicond.,* edited by F. G. Fumi (Tipografia Marves, Rome, 1976), p. 239.

[8.38] J. M. Calleja, H. Vogt, and M. Cardona, *Phil. Mag.* **35**, 239 (1982).

7.8.2 Intravalley Deformation Potential: High-Symmetry Points

• Optical-phonon deformation potential: L point

Table 7.8.6 *Optical-phonon deformation potentials $d_{1o}(c)$, $d_{1o}(v)$, and d_{3o} at the L point of β-ZnS.*

Deformation potential	Value (eV)	Comment
$d_{1o}(c)$	–22.4	Calc. [8.39]
$d_{1o}(v)$	1.4	Calc. [8.39]
d_{3o}	22.1	Calc. [8.39]

[8.39] R.-Z. Wang, S.-H. Ke, and M.-C. Huang, *J. Phys.: Condens. Matter* **4**, 6735 (1992).

7.8.3 Intervalley Deformation Potential

• Absolute value

Table 7.8.7 *Intervalley deformation potential D_{ij} for electrons in β-ZnS [8.40].*

D_{ij}	Phonon	Value (eV/Å)
$D_{\Gamma L}$	LA	2.18
	LO	4.13
$D_{\Gamma X(1)}$	LA	1.10
	LO	0
$D_{\Gamma X(3)}$	LA	0
	LO	1.89

[8.40] Calculated [D. Olguín, M. Cardona, and A. Cantarero, *Solid State Commun.* **122,** 575 (2002)].

Table 7.8.8 *Intervalley deformation potential D_{ij} for electrons in β-ZnS [8.41].**

Scattering type	D_{ij} (eV/Å)	Phonon energy (meV)
$\Gamma - \Gamma$	0	0
$\Gamma - L$	10	26.7
$\Gamma - X$	10	27.9
$L - L$	10	26.7
$L - X$	9	27.3
$X - X$	9	27.9

[8.41] K. Brennan, *J. Appl. Phys.* **64**, 4024 (1988).

*Since the intervalley deformation potentials and related phonon energies are generally unknown even in the most-studied semiconductors, it has been chosen a set of similar values to those for GaAs and InP [K. Brennan and K. Hess, *Solid-State Electron.* **27**, 347 (1984)].

7.9 ELECTRON AFFINITY AND SCHOTTKY BARRIER HEIGHT

7.9.1 Electron Affinity

No detailed data are available for β-ZnS.

7.9.2 Schottky Barrier Height

Table 7.9.1 *Summary of the Schottky barrier height ϕ_n for metal/n-ZnS contacts at 300 K.**

Metal	ϕ_n (eV)	Metal	ϕ_n (eV)
Ag	1.65–1.81	Mg	0.82
Al	0.8	Pd	1.87
Au	2.0–2.19	Pt	1.84
Cu	1.75	Ta	1.10
In	1.5	Ti	1.15

*The data are gathered from various sources. Type of crystal (α- or β-ZnS) was ignored in this tabulation work.

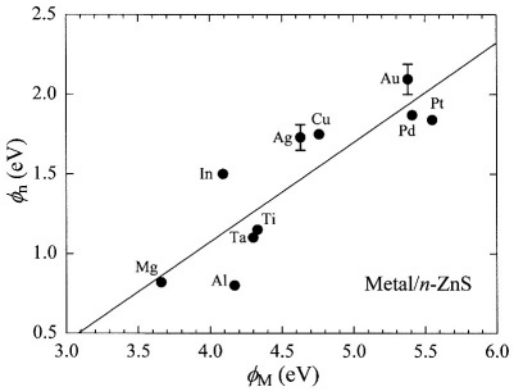

Fig. 7.9.1 Schottky barrier height ϕ_n versus metal work function ϕ_M observed for metal/*n*-ZnS contacts. Values of the metal work function were taken from H. P. R. Frederikse [in *CRC Handbook of Chemistry and Physics,* 78th Edition, edited by D. R. Lide (CRC Press, Boca Raton, 1997), p. 12-115].

7.10 OPTICAL PROPERTIES

7.10.1 Summary of Optical Dispersion Relations

- **$\varepsilon(E)$ and $n^*(E)$ spectra**

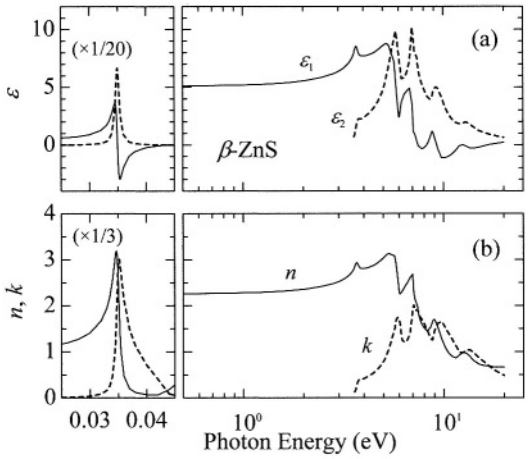

Fig. 7.10.1 (a) Complex dielectric-constant $[\varepsilon(E)=\varepsilon_1(E)+i\varepsilon_2(E)]$ and (b) complex refractive-index spectra $[n^*(E)=n(E)+ik(E)]$ for β-ZnS at 300 K. The numerical data are taken from tabulation by S. Adachi [*Optical Constants of Crystalline and Amorphous Semiconductors: Numerical Data and Graphical Information* (Kluwer Academic, Boston, 1999)].

• **$\alpha(E)$ and $R(E)$ spectra**

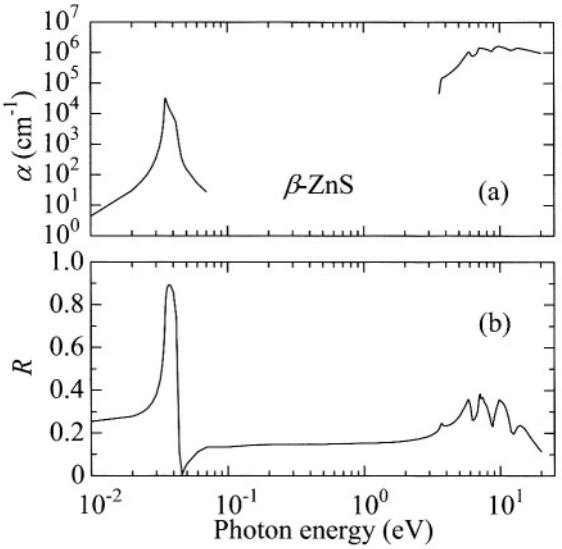

Fig. 7.10.2 (a) Absorption [$\alpha(E)$] and (b) normal-incidence reflectivity spectra [$R(E)$] for β-ZnS at 300 K. The numerical data are taken from tabulation by S. Adachi [*Optical Constants of Crystalline and Amorphous Semiconductors: Numerical Data and Graphical Information* (Kluwer Academic, Boston, 1999)].

7.10.2 The Reststrahlen Region

• **Static and high-frequency dielectric constants**

Table 7.10.1 *Static and high-frequency dielectric constants ε_s and ε_∞ for β-ZnS.*

ε_s	ε_∞	Comment
8.14		T=77 K [10.1]
8.37		T=298 K [10.1]
8.9	5.7	T=300 K [10.2]
8.04	4.9	T=2 K [10.3]
8.10	4.8	T=80 K [10.3]
8.34	4.7	T=300 K [10.3]
8.1		T=75.6 K [10.4]
8.3	5.20	T=300 K [10.4]
8.3	5.1	Recommended (T=300 K)

[10.1] D. Berlincourt, H. Jaffe, and L. R. Shiozawa, *Phys. Rev.* **129,** 1009 (1963).
[10.2] A. Manabe, A. Mitsuishi, and H. Yoshinaga, *Jpn. J. Appl. Phys.* **6**, 593 (1967).
[10.3] T. Hattori, Y. Homma, A. Mitsuishi, and M. Tacke, *Opt. Commun.* **7**, 229 (1973).
[10.4] G. A. Samara, *Phys. Rev. B* **27**, 3494 (1983).

Table 7.10.2 *Linear temperature and pressure coefficients of the static (ε_s) and high-frequency dielectric constants (ε_∞) for β-ZnS near 300 K and normal pressure [10.5].*

Coefficient	Value
$d\varepsilon_s/dT$ (10^{-4} K^{-1})	9.1
$d\varepsilon_\infty/dT$ (10^{-4} K^{-1})	3.4

Table 7.10.2 *Continued.*

Coefficient	Value
$d\varepsilon_s/dp$ (10^{-2} GPa^{-1})	–9.0
$d\varepsilon_\infty/dp$ (10^{-2} GPa^{-1})	–1.4

[10.5] G. A. Samara, *Phys. Rev. B* **27**, 3494 (1983).

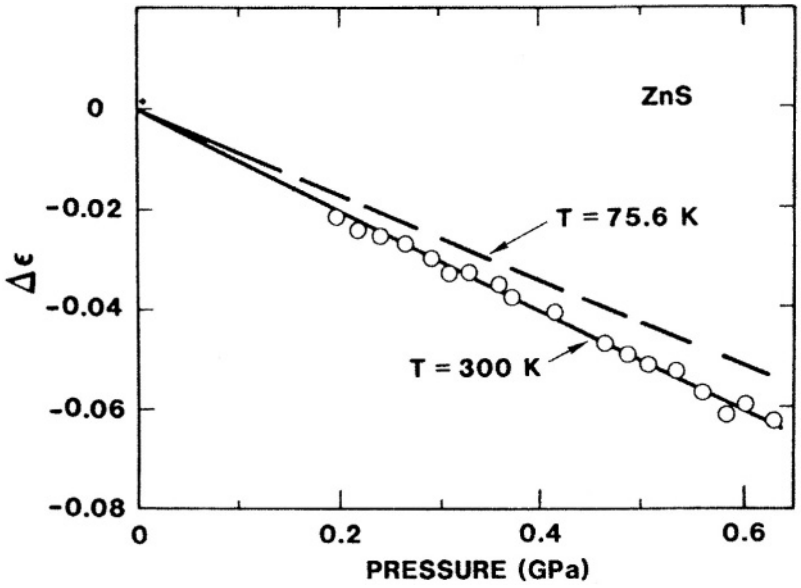

Fig. 7.10.3 Hydrostatic-pressure dependence of the static dielectric constant ε_s for β-ZnS at T=75.6 and 300 K. At atmospheric pressure, ε_s=8.3 at 300 K and 8.1 at 75.6 K. [From G. A. Samara, *Phys. Rev. B* **27**, 3494 (1983).]

• Reststrahlen parameter

Table 7.10.3 *A set of the reststrahlen parameters for* β*-ZnS.*

$$\varepsilon(\omega) = \varepsilon_\infty \left(1 + \frac{\omega_{LO}^2 - \omega_{TO}^2}{\omega_{TO}^2 - \omega^2 - i\omega\gamma} \right)$$

ε_∞	ω_{LO} (cm^{-1})	ω_{TO} (cm^{-1})	γ (cm^{-1})	Comment
5.7	352	282	6.8	T=300 K [10.6]

[10.6] A. Manabe, A. Mitsuishi, and H. Yoshinaga, *Jpn. J. Appl. Phys.* **6**, 593 (1967).

• **Multiphonon optical absorption spectra**

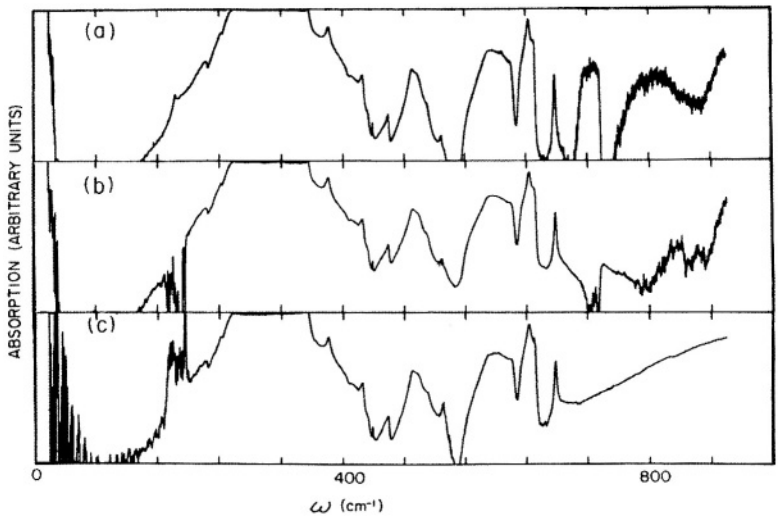

Fig. 7.10.4 Experimental absorption spectra of β-ZnS at T=15 K. These spectra were obtained by taking the ratio of the transmission spectrum with no sample present (background spectrum) to that of a spectrum with a sample in place with the following beamsplitter–filter combinations: (a) 3.5 μm mylar beamsplitter with black polyethylene filters at room temperature and at 1.4 K; (b) 3.5 μm mylar beamsplitter with a 12 μm mylar filter at room temperature and an InSb filter at 1.4 K; (c) 3 μm Teflon beamsplitter with a polyvinylidene chloride (saran wrap) filter at room temperature and an InSb filter at 1.4 K. [From E. A. Kwasniewski, E. S. Koteles, and W. R. Datars, *Can. J. Phys.* **54,** 1053 (1976).]

7.10.3 At or Near the Fundamental Absorption Edge

• **Free-exciton binding energy and related parameters**

Table 7.10.4 *Free-exciton binding (Rydberg) energy G for β-ZnS.*

G (meV)	Comment
39	T=4.2 K [10.7]
34.2±0.1	T=7 K [10.8]
38±1	Heavy-hole exciton, T=10 K [10.9]
34±2	T=1.7 K [10.10]

[10.7] T. Taguchi, T. Yokogawa, and H. Yamashita, *Solid State Commun.* **49,** 55 (1984).
[10.8] A. Mang, K. Reimann, St. Rübenacke, and M. Steube, *Phys. Rev. B* **53**, 16283 (1996).
[10.9] M. Fernández, P. Prete, N. Lovergine, A. M. Mancini, R. Cingolani, L. Vasanelli, and M. R. Perrone, *Phys. Rev. B* **55**, 7660 (1997).
[10.10] R. Pässler, E. Griebl, H. Riepl, G. Lautner, S. Bauer, H. Preis, W. Gebhardt, B. Buda, D. J. As, D. Schikora, K. Lischka, K. Papagelis, and S. Ves, *J. Appl. Phys.* **86**, 4403 (1999).

Table 7.10.5 *Free-exciton parameters (G=binding energy; a_B=1st-orbital Bohr radius; μ=reduced mass) at the fundamental absorption edge of β-ZnS.**

G (meV)	a_B (Å)	μ (m_0)	Comment
34	33	0.106	Direct exciton

*Calculated using $\varepsilon=(\varepsilon_0\varepsilon_\infty)^{1/2}$=6.5.

Table 7.10.6 *Spin-exchange interaction constant j for β-ZnS [10.11].*

j (meV)
4.0

[10.11] See, M. Julier, J. Campo, B. Gil, J. P. Lascaray, and S. Nakamura, *Phys. Rev. B* **57**, R6791 (1998); D. W. Langer, R. N. Euwema, K. Era, and T. Koda, *Phys. Rev. B* **2**, 4005 (1970).

Table 7.10.7 *Pressure coefficient of the free-exciton binding (Rydberg) energy for β-ZnS [10.12].*

$\frac{dG}{dp}$ (meV/GPa)
0.8±0.1

[10.12] A. Mang, K. Reimann, St. Rübenacke, and M. Steube, *Phys. Rev. B* **53,** 16283 (1996).

- **Refractive index**

Table 7.10.8 *Refractive index n near the fundamental absorption edge of β-ZnS at 300 K [10.13].*

E (eV)	λ (μm)	n	E (eV)	λ (μm)	n
0.05	24.79	1.627	2.92	0.424	2.503
0.06	20.66	2.014	2.94	0.422	2.509
0.07	17.71	2.153	2.96	0.419	2.514
0.103	12.03	2.169	2.98	0.416	2.519
0.113	10.97	2.185	3	0.413	2.524
0.124	9.996	2.199	3.02	0.410	2.529
0.138	8.982	2.211	3.04	0.408	2.534
0.155	7.997	2.221	3.06	0.405	2.540
0.177	7.003	2.230	3.08	0.402	2.547
0.207	5.988	2.238	3.1	0.400	2.553
0.248	4.998	2.245	3.12	0.397	2.559
0.31	3.998	2.250	3.14	0.395	2.565
0.413	3.001	2.256	3.16	0.392	2.571
0.516	2.402	2.260	3.18	0.390	2.578
0.563	2.202	2.264	3.2	0.387	2.585
0.62	1.999	2.265	3.22	0.385	2.593
0.689	1.799	2.268	3.24	0.383	2.600
0.775	1.599	2.272	3.26	0.380	2.608
0.885	1.401	2.276	3.28	0.378	2.616
1.033	1.200	2.282	3.3	0.376	2.626
1.24	1.000	2.293	3.32	0.373	2.631
1.377	0.900	2.303	3.34	0.371	2.644
1.549	0.800	2.315	3.36	0.369	2.653
1.771	0.700	2.333	3.38	0.367	2.662
2.066	0.600	2.364	3.4	0.365	2.673
2.479	0.500	2.421	3.42	0.362	2.684
2.754	0.450	2.471	3.44	0.360	2.698
2.78	0.446	2.472	3.46	0.358	2.712

Table 7.10.8 *Continued.*

E (eV)	λ (μm)	n	E (eV)	λ (μm)	n
2.8	0.443	2.476	3.48	0.356	2.720
2.82	0.440	2.481	3.5	0.354	2.741
2.84	0.436	2.485	3.52	0.352	2.751
2.86	0.433	2.489	3.54	0.350	2.773
2.88	0.430	2.493	3.56	0.348	2.794
2.9	0.427	2.498			

[10.13] See, S. Adachi, *Optical Constants of Crystalline and Amorphous Semiconductors: Numerical Data and Graphical Information* (Kluwer Academic, Boston, 1999).

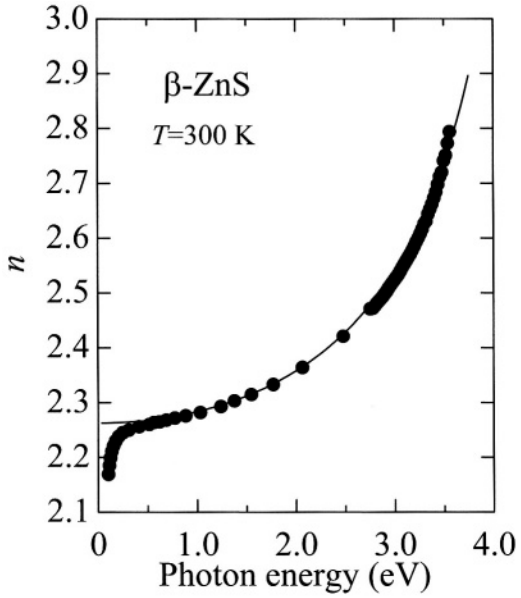

Fig. 7.10.5 Refractive index n for β-ZnS. The experimental data are taken from S. Adachi [*Optical Constants of Crystalline and Amorphous Semiconductors: Numerical Data and Graphical Information* (Kluwer Academic, Boston, 1999)]. The solid line represents the calculated result using $n^2=3.02+[2.10\lambda^2/(\lambda^2-0.0665)]$ with λ in μm.

• Refractive index: Temperature dependence

Table 7.10.9 *Temperature coefficient of the refractive index* $n^{-1}(dn/dT)$ *in the long-wavelength limit for β-ZnS [10.14].*

$\frac{1}{n}\frac{dn}{dT}$ $(10^{-5}\,K^{-1})$
1.9

[10.14] See, S. Adachi, *Optical Properties of Crystalline and Amorphous Semiconductors: Materials and Fundamental Properties* (Kluwer Academic, Boston, 1999).

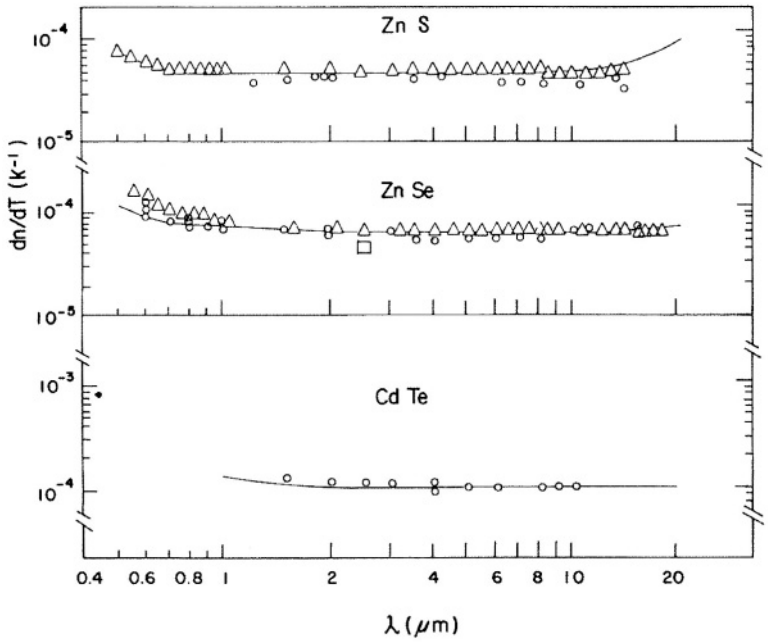

Fig. 7.10.6 Temperature coefficient of the refractive index *dn/dT* for β-ZnS, together with those for ZnSe and CdTe. [From M. Bertolotti, V. Bogdanov, A. Ferrari, A. Jascow, N. Nazorova, A. Pikhtin, and L. Schirone, *J. Opt. Soc. Am. B* **7**, 918 (1990).]

• Fundamental absorption edge: Temperature dependence

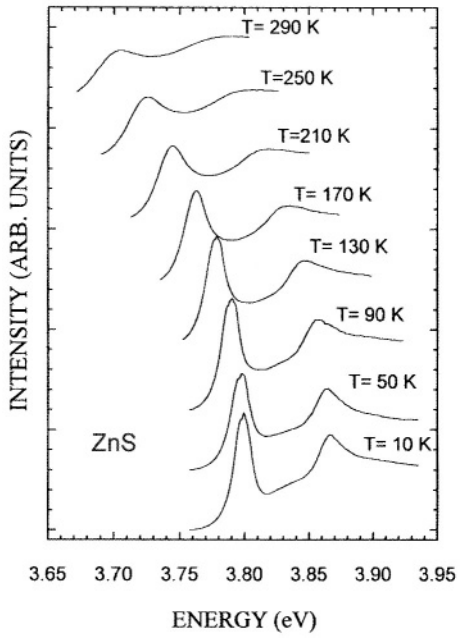

Fig. 7.10.7 Absorption spectra for β-ZnS epilayer on (100)GaAs substrate measured at various temperatures. [From M. Fernández, P. Prete, N. Lovergine, A. M. Mancini, R. Cingolani, L. Vasanelli, and M. R. Perrone, *Phys. Rev. B* **55**, 7660 (1997).]

• Fundamental absorption edge: Urbach tail

The Urbach tail in β-ZnS has been studied by Y. Brada, B. G. Yacobi, and A. Peled [*Solid State Commun.* **17**, 1975 (1975)].

• **Fundamental absorption edge: Pressure dependence**

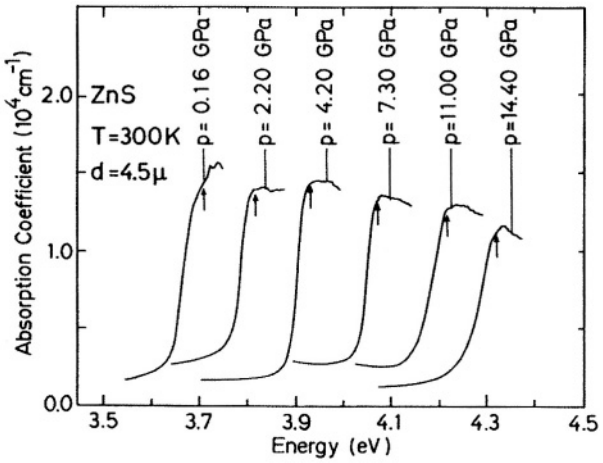

Fig. 7.10.8 Absorption coefficient α at the E_0 edge of a 4.5-μm-thick β-ZnS at different hydrostatic pressures at T=300 K. Vertical arrows indicate the positions of the direct absorption edge E_0. [From S. Ves, U. Schwarz, N. E. Christensen, K. Syassen, and M. Cardona, *Phys. Rev. B* **42**, 9113 (1990).]

7.10.4 The Interband Transition Region

• **Fundamental optical spectra**

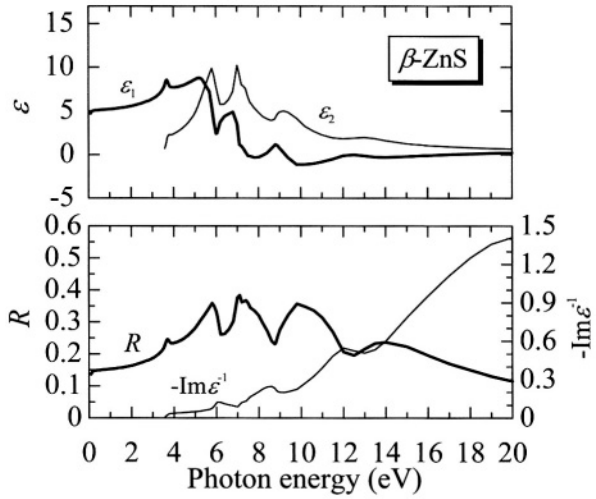

Fig. 7.10.9 Complex dielectric function, $\varepsilon(E)=\varepsilon_2(E)+i\varepsilon_2(E)$, fundamental reflectivity, $R(E)$, and energy-loss function, $-\mathrm{Im}\varepsilon^{-1}(E)$, for β-ZnS at 300 K. The experimental data are taken from tabulation by S. Adachi [*Optical Constants of Crystalline and Amorphous Semiconductors: Numerical Data and Graphical Information* (Kluwer Academic, Boston, 1999)].

7.10.5 Free-Carrier Absorption and Related Phenomena

No detailed data are available for β-ZnS.

7.11 ELASTOOPTIC, ELECTROOPTIC, AND NONLINEAR OPTICAL PROPERTIES

7.11.1 Elastooptic Effect

• **Photoelastic constant**

Table 7.11.1 *Photoelastic constant p_{ij} in the static limit ($E \to 0$ eV) for β-ZnS.*

$p_{11}-p_{12}$	p_{44}
−0.08	−0.08

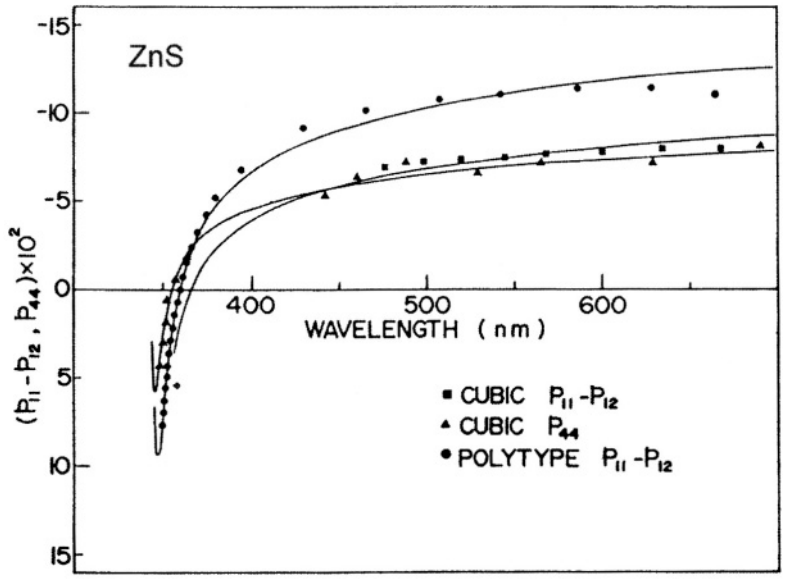

Fig. 7.11.1 Dispersion of the photoelastic constants, $p_{11}-p_{12}$ and p_{44}, for β-ZnS determined by piezobirefringence measurements at 300 K. The experimental data for polytype ZnS (hexagonal fraction of α=0.1) are also plotted by the solid circles. [From Y. Itoh, M. Fujii, C. Hamaguchi, and Y. Inuishi, *J. Phys. Soc. Jpn* **48,** 1972 (1980).]

7.11.2 Linear Electrooptic Constant

Table 7.11.2 *Free* (r_{41}^T) *and clamped values* (r_{41}^S) *of the linear electrooptic constant for* β-ZnS.

Wavelength (μm)	r_{41}^T (pm/V)	r_{41}^S (pm/V)	Ref.
0.4	−1.03	−1.03	[11.1]
0.404	1.2 ($\|r_{41}^T\|$)		[11.2]
0.436	1.6 ($\|r_{41}^T\|$)		[11.2]
0.504	1.9 ($\|r_{41}^T\|$)		[11.2]
0.529	−1.59	−1.59	[11.1]
0.546	2.1 ($\|r_{41}^T\|$)		[11.2]
0.589	2.2 ($\|r_{41}^T\|$)		[11.2]
0.633	−1.88	−1.88	[11.1]
		1.6 ($\|r_{41}^S\|$)	[11.3]
0.644	2.2 ($\|r_{41}^T\|$)		[11.2]
0.8	−2.07	−2.07	[11.1]
1.09	−2.11	−2.11	[11.1]
3.39		1.4 ($\|r_{41}^S\|$)	[11.3]

[11.1] L. Baldassarre, A. Gingolani, M. Ferrara, and M. Lugarà, *Solid State Commun.* **34,** 237 (1980).
[11.2] S. Namba, *J. Opt. Soc. Am.* **31**, 76 (1961).
[11.3] See, I. P. Kaminow and E. H. Turner, in *Handbook of Lasers,* edited by R. J. Pressley (Chemical Rubber, Cleveland, 1971), Chap. 15.

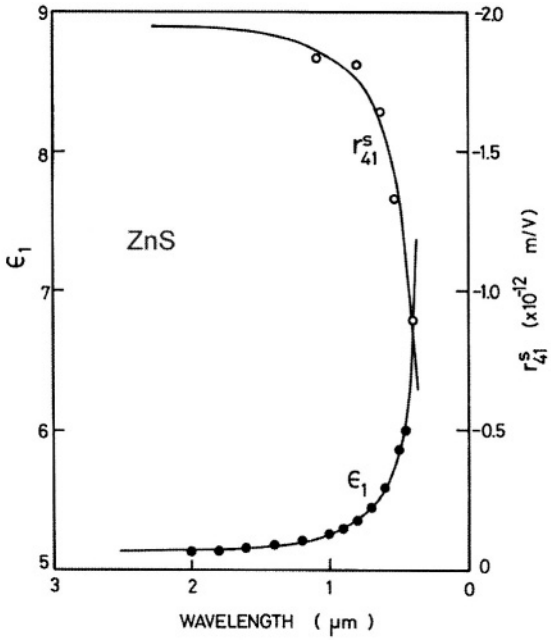

Fig. 7.11.2 Theoretical dispersion of ε_1 and $r_{41}{}^S$ in β-ZnS along with the experimental data. The solid lines represent the theoretical results. [From S. Adachi and K. Oe, *J. Appl. Phys.* **56,** 74 (1984).]

- **Temperature dependence**

Table 7.11.3 *Temperature coefficient of the linear electrooptic constant* $(1/r_{41})(dr_{41}/dT)$ *for* β*-ZnS.*

$\frac{1}{r_{41}}\frac{dr_{41}}{dT}$ (10^{-4} K^{-1})	Comment
9.1	λ=0.6328 μm [11.4]

[11.4] T. G. Okroashvili, *Opt. Spectrosc.* **47**, 442 (1979).

7.11.3 Quadratic Electrooptic Constant

No detailed data are available for β-ZnS.

7.11.4 Franz–Keldysh Effect

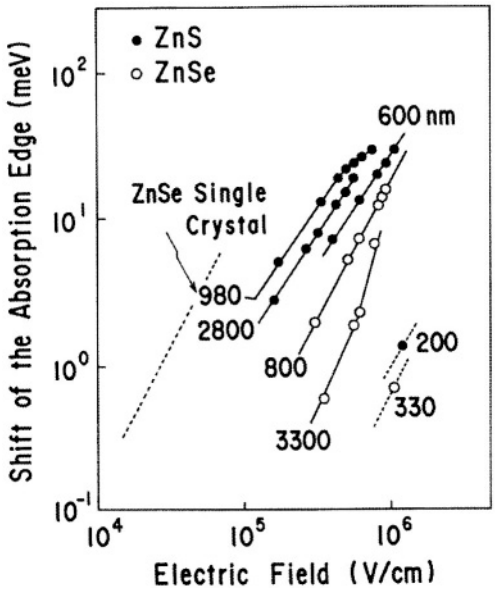

Fig. 7.11.3 Electric-field (E) dependence of the absorption-edge shift (ΔE_0) in polycrystalline ZnS and ZnSe films (200–3300 nm thick), together with that in single-crystalline ZnSe. The plots can be expressed by $\Delta E_0 = AE^n$ with n=1.6 (ZnS) and 1.9 (ZnSe), respectively. [From K. Hirabayashi and K. Ono, *Jpn. J. Appl. Phys.* **29**, L1672 (1990).]

7.11.5 Nonlinear Optical Constant

• Second-order nonlinear optical susceptibility

Table 7.11.4 *Experimental second-order nonlinear optical susceptibility d_{14} for β-ZnS.*

Wavelength, in μm (Energy, in eV)	d_{14} *	Ref.
1.047 (1.184)	12 (pm/V)	[11.5]
1.321 (0.938)	8 (pm/V)	[11.5]
10.6 (0.117)	7.3 (10^{-8} esu)	[11.6]

[11.5] H. P. Wagner, M. Kühnelt, W. Langbein, and J. M. Hvam, *Phys. Rev. B* **58**, 10494 (1998).
[11.61 C. K. N. Patel, *Phys. Rev. Lett.* **16**, 613 (1966).
*1 m/V=$3\times10^4/4\pi$ esu.

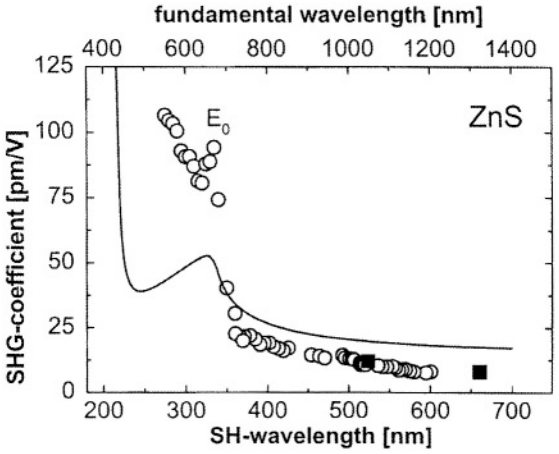

Fig. 7.11.4 Experimental dispersion of the second-harmonic-generation (SHG) coefficient $|d_{14}|$ in β-ZnS as a function of fundamental wavelength. The solid line gives the theoretical dispersion curve. [From H. P. Wagner, M. Kühnelt, W. Langbein, and J. M. Hvam, *Phys. Rev. B* **58**, 10494 (1998).]

• Third-order nonlinear optical susceptibility

Table 7.11.5 *Theoretical third-order nonlinear optical susceptibility $\chi^{(3)}_{ijkl}(-3\omega;\omega,\omega,\omega)$ in the static limit ($\hbar\omega\to0$ eV) for β-ZnS.*

$\chi^{(3)}_{ijkl}$ (10^{-11} esu)*		Ref.
$\chi^{(3)}_{1111}$	$\chi^{(3)}_{1212}$	
0.20	0.15	[11.7]

[11.7] W. Y. Ching and M.-Z. Huang, *Phys. Rev. B* **47**, 9479 (1993).
*1 $m^2/V^2=9\times10^8/4\pi$ esu.

• Two-photon optical absorption

Table 7.11.6 *Two-photon absorption coefficient β for β-ZnS.*

Wavelength (μm)	β (cm/GW)	Ref.
0.532	3.5	[11.8]
0.61	1.0	[11.9]
0.78	<0.02*	[11.9]
1.27	<0.003*	[11.9]

[11.8] E. W. Van Stryland, H. Vanherzeele, M. A. Woodall, M. J. Soileau, A. L. Smirl, S. Guha, and T. F. Boggess, *Opt. Eng.* **24**, 613 (1985).
[11.9] T. D. Krauss and F. W. Wise, *Appl. Phys. Lett.* **65**, 1739 (1994).
*Indicating that the signal was below the sensitivity of the experiment.

7.12 CARRIER TRANSPORT PROPERTIES

7.12.1 Low-Field Mobility: Electrons

Table 7.12.1 *300-K (μ_{300K}) and peak Hall mobilities (μ_{peak}) for electrons in β-ZnS.*

Mobility	Value ($cm^2/V\,s$)	Comment
μ_{300K}	107	$n=4.8\times10^{16}$ cm^{-3} [12.1]
	600	Photo-Hall effect, $n\sim3\times10^{12}$ cm^{-3} [12.2]*[1]
	789	In-doped evaporated film (ρ=7.10 Ω·cm) [12.3]*[1]
μ_{peak}		*[2]

[12.1] S. Fujita, H. Mimoto and H. Takebe, and T. Noguchi, *J. Cryst. Growth* **47**, 326 (1979).
[12.2] S. Narita and K. Nagasaka, *J. Phys. Soc. Jpn* **20**, 1728 (1965).
[12.3] L. C. Olsen, R. C. Bohara, and D. L. Barton, *Appl. Phys. Lett.* **34**, 528 (1979).
*[1] It was not mentioned or confirmed whether the ZnS sample used was cubic or hexagonal.
*[2] No Hall-effect data are available for *n*-type β-ZnS at temperatures below 300 K. This may be mainly due to Ohmic-contact problem.

• Temperature dependence

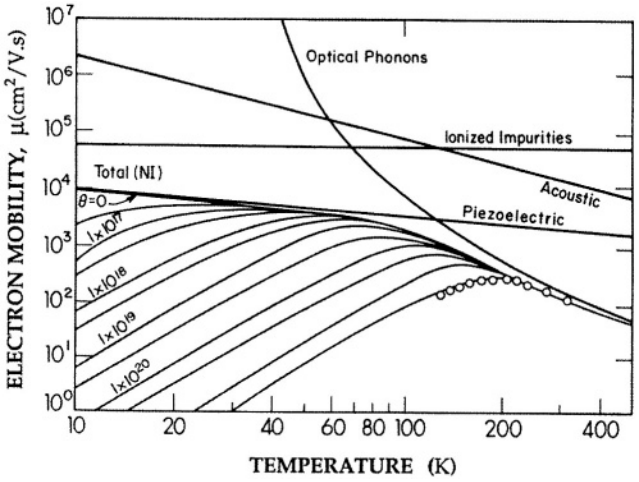

Fig. 7.12.1 Total and individual electron mobilities calculated at different ionized-impurity concentrations (N_I) versus temperature, together with a compensation-ratio limit curve (θ=0), in β-ZnS. The open circles represent the experimental data taken for α-ZnS (not β-ZnS) by M. Aven and C. A. Mead [*Appl. Phys. Lett.* **7**, 8 (1965)]. [From H. E. Ruda and B. Lai, *J. Appl. Phys.* **68**, 1714 (1990).]

• Donor concentration (free-carrier) dependence

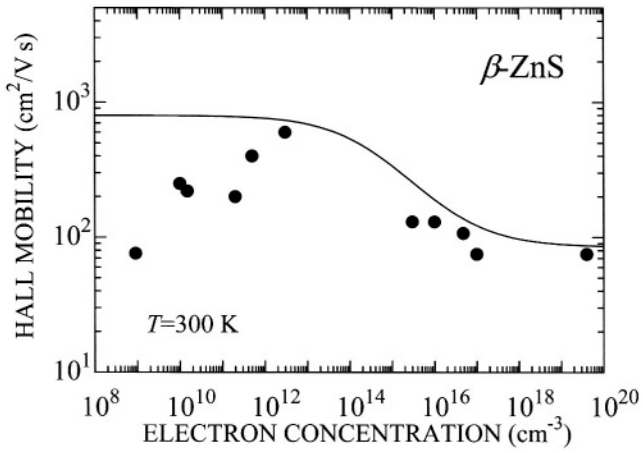

Fig. 7.12.2 Electron Hall mobility μ versus electron concentration n in n-type β-ZnS at 300 K. The experimental data, some of which were probably obtained from hexagonal ZnS, are gathered from various sources. The solid line represents the calculated result with $\mu = 85 + 715/[1+(n/3\times10^{14})^{0.50}]$, where n is in cm^{-3} and μ is in $cm^2/V\,s$.

• **Hall factor**

The Hall factor for β-ZnS has been obtained theoretically by D. L. Rode [*Phys. Status Solidi B* **55**, 687 (1973)], and its value is reported to be $\gamma \sim 1.22$ at T=300 K.

7.12.2 Low-Field Mobility: Holes

Table 6.12.2 *300-K (μ_{300K}) and peak Hall mobilities (μ_{peak}) for holes in β-ZnS.*

Mobility	Value (cm^2/V s)	Comment
μ_{300K}	72	$p=1.4\times10^{17}$ cm^{-3} [12.4]
μ_{peak}		*

[12.4] S. Kishimoto, T. Hasegawa, H. Kinto, O. Matsumoto, and S. Iida, *J. Cryst. Growth* **214/215,** 556 (2000).

*No Hall-effect data are available for p-type β-ZnS at temperatures below 300 K. This may be mainly due to Ohmic-contact problem.

• **Acceptor concentration (free-carrier) dependence**

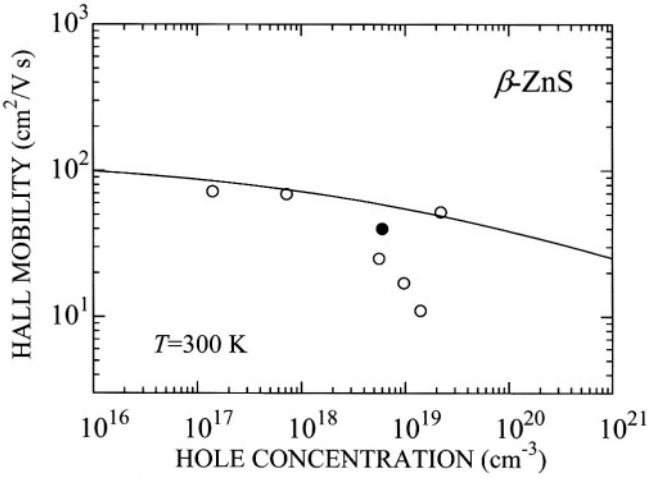

Fig. 7.12.3 Hole Hall mobility μ versus hole concentration p in p-type β-ZnS at 300 K. The experimental data are gathered from (●) S. Iida, T. Yatabe, and H. Kinto [*Jpn. J. Appl. Phys.* **28**, L535 (1989)] and from (○) S. Kishimoto, T. Hasegawa, H. Kinto, O. Matsumoto, and S. Iida [*J. Cryst. Growth* **214/215**, 556 (2000)]. The solid line represents the calculated result with $\mu = 120/[1+(p/5\times10^{18})^{0.25}]$, where p is in cm^{-3} and μ is in cm^2/V s.

7.12.3 High-Field Transport: Electrons

• **Electron scattering rate**

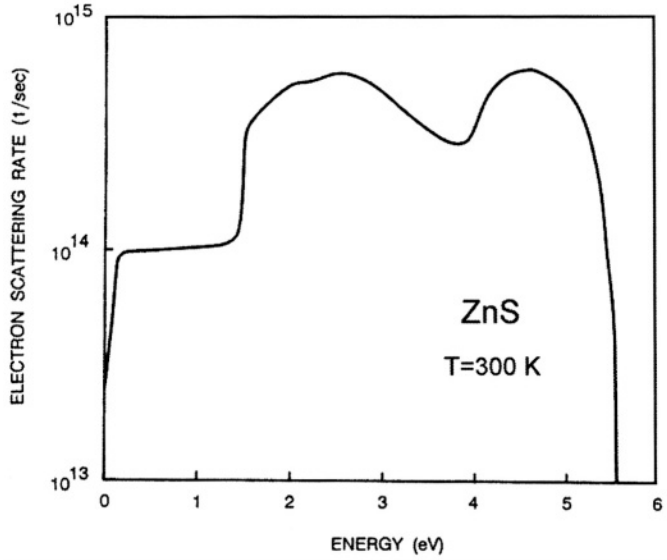

Fig. 7.12.4 Total electron–phonon scattering rate in β-ZnS as a function of electron energy at 300 K. Impact ionization is not included in the calculation. [From K. Brennan, *J. Appl. Phys.* **64**, 4024 (1988).]

• **Electron drift velocity–field characteristic**

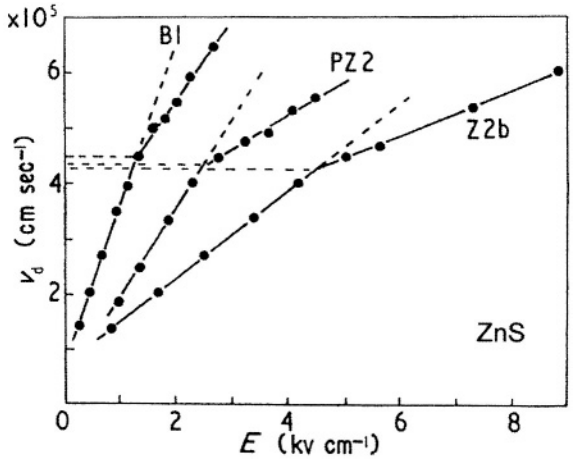

Fig. 7.12.5 Experimental electron drift velocity v_d (v_e) as a function of applied electric filed E for β-ZnS (Z2b, PZ2), together with that for w-CdS (B1). [From P. G. Le Comber, W. E. Spear, and A. Weinmann, *Brit. J. Appl. Phys.* **17**, 467 (1966).]

• **LO-phonon-scattering-limited electron saturation drift velocity**

Table 7.12.3 *Calculated LO-phonon-scattering-limited electron saturation drift velocity $v_{e,sat}$ in the lowest-conduction-band valley α for β-ZnS at 300 K.**

$$v_{e,sat}^{\alpha} = \left(\frac{8\hbar\omega_{LO}}{3\pi m_c^{\alpha}} \right)^{1/2}$$

Valley	$v_{e,sat}$ (10^7 cm/s)
Γ	1.8

*Calculated with $m_c^{\Gamma} = 0.20 m_0$ and $\omega_{LO} = 350.5$ cm^{-1}.

7.12.4 High-Field Transport: Holes

No detailed data are available for β-ZnS.

7.12.5 Minority-Carrier Transport: Electrons in p-Type Materials

No detailed data are available for β-ZnS.

7.12.6 Minority-Carrier Transport: Holes in n-Type Materials

No detailed data are available for β-ZnS.

7.12.7 Impact Ionization Coefficient

• **Electric-field dependence**

The impact ionization phenomenon in β-ZnS has been studied experimentally by T. D. Thompson and J. W. Allen [*J. Phys. C: Solid State Phys.* **20**, L449 (1987)] and theoretically by E. Bellotti, K. F. Brennan, R. Wang, and P. P. Ruden [*J. Appl. Phys.* **83**, 4765 (1998)].

Chapter 8

Zinc Selenide (ZnSe)

8.1 STRUCTURAL PROPERTIES

8.1.1 Ionicity

Table 8.1.1 *Phillips's ionicity f_i for Zn Se[1.1].*

f_i
0.630

[1.1] J. C. Phillips, *Bonds and Bands in Semiconductors* (Academic, New York, 1973).

8.1.2 Elemental Isotopic Abundance and Molecular Weight

- **Isotopic abundance**

Table 8.1.2 *Isotopic abundance in percent for zinc and selenium [1.2].*

Isotope	% nat. abundance	Isotope	% nat. abundance
^{64}Zn	48.6	^{74}Se	0.89
^{66}Zn	27.9	^{76}Se	9.36
^{67}Zn	4.1	^{77}Se	7.63
^{68}Zn	18.8	^{78}Se	23.78
^{70}Zn	0.6	^{80}Se	49.61
		^{82}Se	8.73

[1.2] D. R. Lide, *CRC Handbook of Chemistry and Physics*, 78th Edition (CRC Press, Boca Raton, 1997).

• **Molecular weight**

Table 8.1.3 *Molecular (average atomic) weight M for ZnSe.*

M (amu)
144.35

8.1.3 Crystal Structure and Space Group

Table 8.1.4 *Crystal structure and its space and pint groups for ZnSe.*

Crystal structure	Space group	Point group
Zincblende (Cubic)	$F\bar{4}3m$	T_d

8.1.4 Lattice Constant and Its Related Parameters

• **Lattice constant, near-neighbor distance, etc.**

Table 8.1.5 *Lattice constant (a), near-neighbor distance (d), unit cube volume (a^3), and molecular density (d_M) for ZnSe at 300 K.*

Parameter	Value
Lattice constant a (Å)	5.6692 [1.3]
d (Cation–Anion) (Å)	2.4548*
d (Cation–Cation) (Å)	4.0087*
Unit cube volume a^3 (10^{-22} cm^3)	1.8221*
Molecular density d_M (10^{22} cm^{-3})	2.1953*

[1.3] H. P. Singh and B. Dayal, *Phys. Status Solidi* **23**, K93 (1967).
*Calculated.

• **Crystal density**

Table 8.1.6 *Crystal density g for ZnSe at 300 K.**

g (g/cm^3)
5.2621

*Calculated using a=5.6692 Å.

8.1.5 Structural Phase Transition

Table 8.1.7 *Structural phase transition in ZnSe at high pressures.*

Structure	Transition pressure (GPa)
Zincblende ($F\bar{4}3m$)	Normal pressure
Rocksalt (NaCl)	13.7±0.3 [1.4]
	14.6±1.0 [1.5]
	13.5±0.2 [1.6]
	13.0±0.4 [1.7]
	13.5 [1.8]
	11.8±0.5 [1.9]
	13.0±0.5 [1.10]
Simple hexagonal	55±8 [1.9]

[1.4] G. J. Piermarini and S. Block, *Rev. Sci. Instrum.* **46,** 973 (1975).
[1.5] W. H. Gust, *J.Appl. Phys.* **53**, 4843 (1982).
[1.6] S. Ves, K. Strössner, N. E. Christensen, C. K. Kim, and M. Cardona, *Solid State Commun.* **56**, 479 (1985).
[1.7] S. R. Tiong, M. Hiramatsu, Y. Matsushima, and E. Ito, *Jpn. J. Appl. Phys.* **28**, 291 (1989).
[1.8] G. Itkin, G. R. Hearne, E. Sterer, M. P. Pasternak, and W. Potzel, *Phys. Rev. B* **51**, 3195 (1995).
[1.9] R. G. Greene, H. Luo, and A. L. Ruoff, *J. Phys. Chem. Solids* **56**, 521 (1995).
[1.10] H. Karzel, W. Potzel, M. Köfferlein, W. Schiessl, M. Steiner, U. Hiller, G. M. Kalvius, D. W. Mitchell, T. P. Das, P. Blaha, K. Schwarz, and M. P. Pasternak, *Phys. Rev. B* **53**, 11425 (1996).

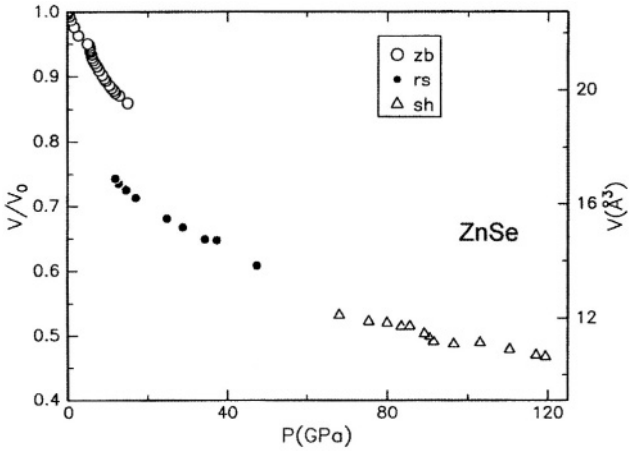

Fig. 8.1.1 Measured equation of state for ZnSe in the zinc-blende (zb), rocksalt (rs), and simple hexagonal phases (sh). [From R. G.Greene, H. Luo, and A. L. Ruoff, *J. Phys. Chem. Solids* **56**, 521 (1995).]

8.1.6 Cleavage Plane

Table 8.1.8 *Crystallographic plane most readily cleaved for ZnSe.*

Cleavage plane
(110)

- **Surface energy**

Table 8.1.9 *Surface energy for ZnSe (in* J/m^2*).*

Plane			Comment
(110)	(111)	$(\bar{1}\,\bar{1}\,\bar{1})$	
0.980	0.885	0.750	Calc. [1.11]

[1.11] B. N. Oshcherin, *Phys. Status Solidi A* **34**, K181 (1976).

8.2 THERMAL PROPERTIES

8.2.1 Melting Point and Its Related Parameters

Table 8.2.1 *Melting point* T_m *and its related parameter for ZnSe.*

Parameter	Value
Melting point T_m (K)	1793 [2.1]
Entropy of fusion ΔS_m (cal/mol K)	16.29 [2.2]

[2.1] See, M. R. Lorenz, in *Physics and Chemistry of II–VI Compounds,* edited by M. Aven and J. S. Prener (North-Holland, Amsterdam, 1967), p. 73.
[2.2] See, B. R. Nag, *J. Electron. Mater.* **26**, 70 (1997).

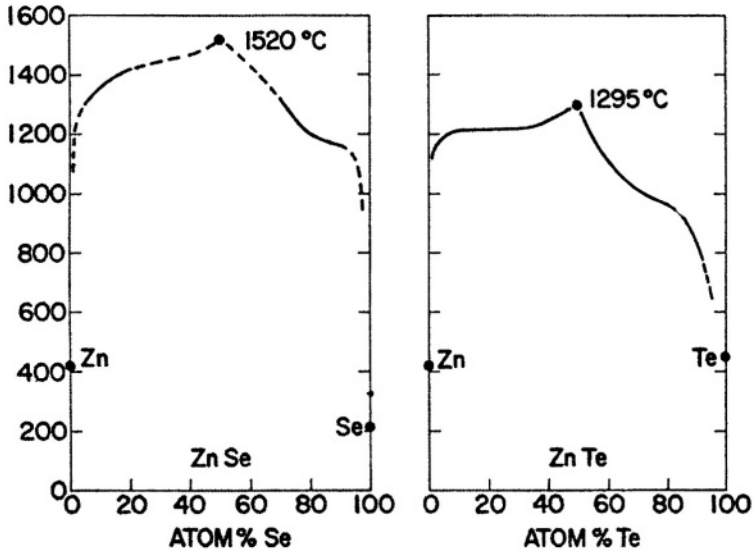

Fig. 8.2.1 *T–x* projects of the II–VI binary systems Zn–Se and Zn–Te. [From M. R. Lorenz, in *Physics and Chemistry of II–VI Compounds,* edited by M. Aven and J. S. Prener (North-Holland, Amsterdam, 1967), p. 73.]

8.2.2 Specific Heat

Table 8.2.2 *Experimental specific heat C_p (at constant pressure) for ZnSe [2.3].*

Temperature (K)	C_p (mJ/g K)	Temperature (K)	C_p (mJ/g K)
2.782	0.030	10.04	2.18
2.997	0.038	12.44	5.02
3.605	0.067	14.95	9.84
3.790	0.079	18.26	18.3
4.218	0.108	20.00	23.3
5.479	0.243	21.73	28.3
5.985	0.325	23.15	32.9
6.493	0.426	24.49	37.5
8.748	1.29		

[2.3] J. A. Birch, *J. Phys. C: Solid State Phys.* **8**, 2043 (1975).

Table 8.2.3 *Experimental specific heat C_p (at constant pressure) for ZnSe [2.4].*

Temperature (K)	C_p (mJ/g K)	Temperature (K)	C_p (mJ/g K)
20	29.3	70	169
25	46.1	80	189
30	63.2	90	208
35	79.2	100	225
40	93.7	110	241
45	104	120	254
50	117	130	267
55	131	140	280
60	144		

[2.4] J. C. Irwin and J. LaCombe, *J. Appl. Phys.* **45,** 567 (1974).

• **Functional expression**

Table 8.2.4 *Specific heat C_p (at constant pressure) as a function of temperature T for ZnSe.*

C_p (J/g K)
$0.348+4.00\times10^{-5}T$ [2.5]*

[2.5] P. Goldfinger and M. Jeunehomme, *Trans. Faraday Soc.* **59**, 2851 (1963).
*This expression gives a value of C_p~0.360 J/g K at T=300 K.

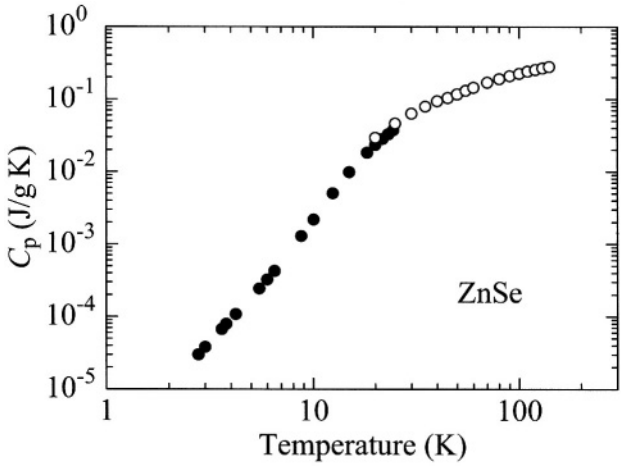

Fig. 8.2.2 Specific heat C_p (at constant pressure) versus temperature for ZnSe. The experimental data are taken from J. A. Birch [*J. Phys. C: Solid State Phys.* **8**, 2043 (1975); solid circles] and from J. C. Irwin and J. LaCombe [*J. Appl. Phys.* **45**, 567 (1974); open circles].

8.2.3 Debye Temperature

Table 8.2.5 *Debye temperature θ_D for ZnSe.*

θ_D (K)	Comment
275	T=0 K*[1]
340	T=300 K*[2]

*[1] In the low-temperature (0 K) limit [see, H. Siethoff and K. Ahlborn, *Phys. Status Solidi B* **190**, 179 (1995)].
*[2] Estimated from data by D. N. Talwar, M. Vandevyver, K. Kunc, and M. Zigone [*Phys. Rev. B* **24**, 741 (1981)].

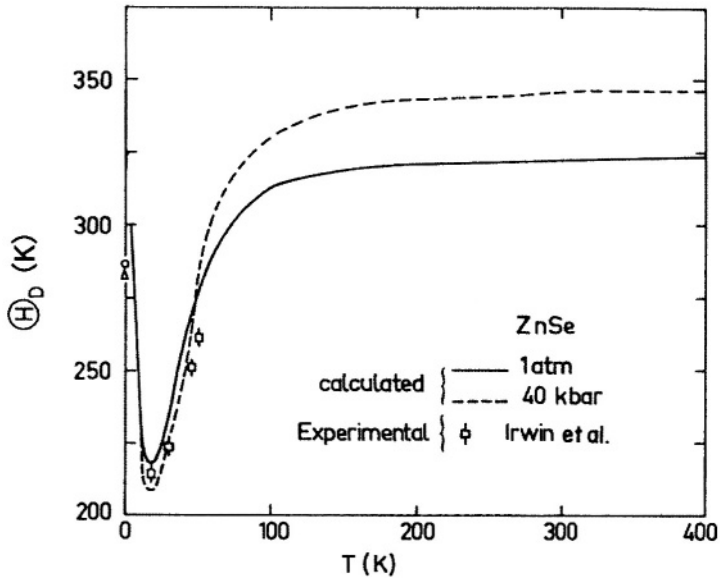

Fig. 8.2.3 Theoretical and experimental Debye temperature θ_D versus temperature T for ZnSe. The experimental data are taken from J. C. Irwin and J. LaCombe [*J. Appl. Phys.* **45**, 567 (1974)]. [From D. N. Talwar, M. Vandevyver, K. Kunc, and M. Zigone, *Phys. Rev. B* **24**, 741 (1981).]

8.2.4 Thermal Expansion Coefficient

Table 8.2.6 *Thermal expansion coefficient α_{th} for ZnSe [2.6].*

Temperature (K)	α_{th} (10^{-6} K^{-1})	Temperature (K)	α_{th} (10^{-6} K^{-1})
5	–0.0007	20	–0.341
6	–0.0016	22	–0.424
7	–0.0036	24	–0.501
8	–0.0070	25	–0.538
9	–0.0132	26	–0.572
10	–0.0237	28	–0.629
11	–0.0371	30	–0.668
12	–0.0564	32	–0.687
13	–0.0820	57.5	0.26
14	–0.1110	65	0.74
15	–0.1435	75	1.51
16	–0.1795	85	2.22
17	–0.219	283	6.84
18	–0.259	300	7.10*
19	–0.300		

[2.6] T. F. Smith and G. K. White, *J. Phys. C: Solid State Phys.* **8**, 2031 (1975).
*Estimated.

Table 8.2.7 *Thermal expansion coefficient α_{th} for ZnSe.**

Temperature (K)	α_{th} (10^{-6} K^{-1})	Temperature (K)	α_{th} (10^{-6} K^{-1})
60	0.57	333	7.5
70	1.3	353	7.7
80	1.9	373	8.0
90	2.6	393	8.2
100	3.1	413	8.4
110	3.6	433	8.5
120	4.1	453	8.6
130	4.5	473	8.7
140	4.8	493	8.8
300	7.8	513	9.0
313	7.1		

*The experimental data are taken for $T \leq 300$ K from J. S. Browder and S. S. Ballard [*Appl. Opt.* **16**, 3214 (1977)] and for $T \geq 313$ K from S. S. Ballard, S. E. Brown, and J. S. Browder [*Appl. Opt.* **17**, 1152 (1978)].

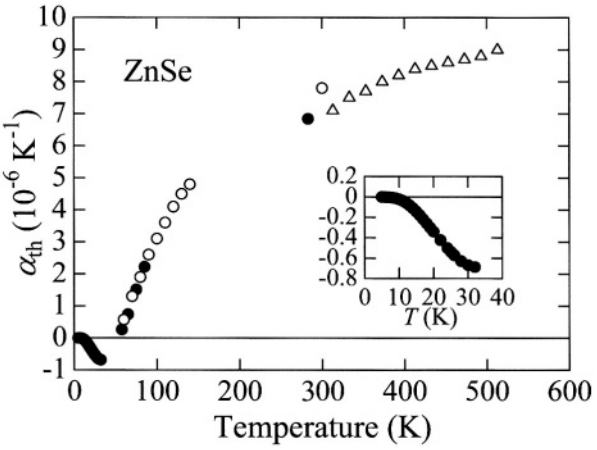

Fig. 8.2.4 Thermal expansion coefficient α_{th} versus temperature T for ZnSe. The experimental data are taken from T. F. Smith and G. K. White [*J. Phys. C: Solid State Phys.* **8**, 2031 (1975); solid circles], from J. S. Browder and S. S. Ballard [*Appl. Opt.* **16,** 3214 (1977); open circles], and from S. S. Ballard, S. E. Brown, and J. S. Browder [*Appl. Opt.* **17**, 1152 (1978); open triangles].

8.2.5 Thermal Conductivity and Diffusivity

Table 8.2.8 *Thermal conductivity K for ZnSe.* Thermal diffusivity can be calculated from a relation* $D=K/(C_p \cdot g)$, *where* C_p *is the specific heat at constant pressure and g is the crystal density.*

Temperature (K)	*K* (W/cm K)	Temperature (K)	*K* (W/cm K)
2.7	0.74	65	1.5
3.3	1.34	80	1.03
4.2	2.00	100	0.76
4.8	2.75	150	0.44
5.8	3.7	200	0.30
7.5	5.0	250	0.23
10	6.3	300	0.19
12	6.1	350	0.124
13	6.7	375	0.115
14	6.6	400	0.108
16.5	6.5	425	0.102
19.5	5.7	450	0.096
21	5.4	475	0.090
23	4.9	500	0.083
26	4.5	525	0.079
30	3.7	550	0.073
40	2.9	575	0.068
50	2.2		

*The experimental data are taken for $T \leq 300$ K from G. A. Slack [*Phys. Rev. B* **6**, 3791 (1972)] and for $T \geq 350$ K from A. A. Men', A. Z. Chechel'nitskii, V. A. Sokolov, and L. A. Kholodova [*Inorg. Mater.* **10**, 468(1974)].

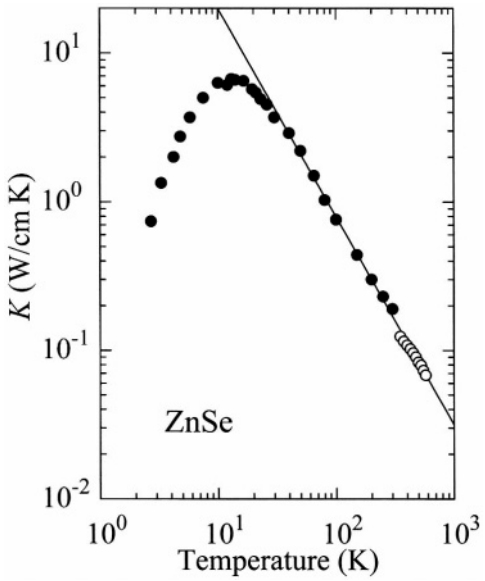

Fig. 8.2.5 Thermal conductivity K for ZnSe. The experimental data are taken from G. A. Slack [*Phys. Rev. B* **6**, 3791 (1972); solid circles] and from A. A. Men', A. Z. Chechel'nitskii, V. A. Sokolov, and L. A. Kholodova [*Inorg. Mater.* **10,** 468 (1974); open circles]. The solid line is calculated from $K=AT^n$ with A=500 W/cm K$^{-0.4}$ and n= –1.40.

8.3 ELASTIC PROPERTIES

8.3.1 Elastic Constant

• Room-temperature value and its temperature and pressure derivatives

Table 8.3.1 *Elastic constant and its temperature and pressure derivatives for ZnSe at 300 K.*

Parameter	Value
Stiffness (10^{11} dyn/cm^2) [3.1]	
C_{11}	8.57
C_{12}	5.07
C_{44}	4.05
Compliance (10^{-12} cm^2/dyn) [3.1]	
S_{11}	2.09
S_{12}	–0.78
S_{44}	2.47
dC_{ij}/dT (10^7 dyn/cm^2 K) [3.2]	
C_{11}	–14.2
C_{12}	–9.58
C_{44}	–4.33
dC_{ij}/dp [3.2]	
C_{11}	4.5
C_{12}	4.9
C_{44}	0.45

[3.1] *Numerical Data and Functional Relationships in Science and Technology,* edited by K.-H. Hellwege and A. M. Hellwege, Landolt–Börnstein, New Series, Group III, Vol. 18 (Springer, Berlin, 1984).

[3.2] *Numerical Data and Functional Relationships in Science and Technology,* edited by K.-H. Hellwege and A. M. Hellwege, Landolt–Börnstein, New Series, Group III, Vol. 11 (Springer, Berlin, 1979).

8.3.2 Third-Order Elastic Constant

Table 8.3.2 *Third-order elastic constant of ZnSe [3.3].*

Modulus	Value (10^{12} dyn/cm^2)
C_{111}	−8.27
C_{112}	−1.36
C_{123}	−5.11
C_{144}	+2.22
C_{166}	−2.65
C_{456}	−2.78

[3.3] *Numerical Data and Functional Relationships in Science and Technology,* edited by K.-H. Hellwege and A. M. Hellwege, Landolt–Börnstein, New Series, Group III, Vol. 18 (Springer, Berlin, 1984).

8.3.3 Young's Modulus, Poisson's Ratio, and Similar

- **Young's modulus**

Table 8.3.3 *Young's modulus Y for ZnSe at 300 K.**

Crystallographic plane	Y (10^{12} dyn/cm^2)
(100) plane	
[001] direction	0.478
[011] direction	0.786
(110) plane	
[001] direction	0.478
[111] direction	1.00
(111) plane	0.786

*Calculated using S_{11}=2.09, S_{12}= −0.78, and S_{44}=2.47 (all in 10^{-12} cm^2/dyn).

- **Poisson's ratio**

Table 8.3.4 *Poisson's ratio P for ZnSe at 300 K.**

Crystallographic plane	P
(100) plane	
m=[010], n=[001]	0.373
m=[011], n=[$0\bar{1}1$]	−0.030
(110) plane	
m=[001], n=[$\bar{1}10$]	0.373
m=[$\bar{1}11$], n=[$\bar{1}\bar{1}2$]	0.235
(111) plane	0.399

*Calculated using S_{11}=2.09, S_{12}= −0.78, and S_{44}=2.47 (all in 10^{-12} cm^2/dyn).

● **Bulk modulus, shear modulus, etc.**

Table 8.3.5 *Bulk modulus, B_u, pressure derivative of B_u, dB_u/dp, shear modulus. C_s, isotropy factor, A, linear compressibility, C_o, Caucy ratio, C_a, and Born ratio, B_o, for ZnSe at 300 K.*

Parameter	Value
B_u (10^{11} dyn/cm^2)	6.24 [3.4]
dB_u/dp	3.81–4.05 [3.5]
	4.36 [3.6]
	4.77±0.18 [3.7]
	4 [3.8]
C_s (10^{11} dyn/cm^2)	1.75 [3.4]
A	0.432 [3.4]
C_o (10^{-13} cm^2/dyn)	5.34 [3.4]
C_a	1.25 [3.4]
B_o	1.20 [3.4]

[3.4] Calculated using C_{11}=8.57, C_{12}=5.07, and C_{44}=4.05 (all in 10^{11} dyn/cm^2).
[3.5] Theor. [V. I. Smelyansky and J. S. Tse, *Phys. Rev. B* **52**, 4658 (1995)].
[3.6] Theor. [A. Qteish and A. Muñoz, *J. Phys.: Condens. Matter* **12**, 1705 (2000)].
[3.7] Exper. [B. H. Lee, *J. Appl. Phys.* **41**, 2988 (1970)].
[3.8] Exper. [H. Karzel, W. Potzel, M. Köfferlein, W. Schiessl, M. Steiner, U. Hiller, G. M. Kalvius, D. W. Mitchell, T. P. Das, P. Blaha, K. Schwarz, and M. P. Pasternak, *Phys. Rev. B* **53**, 11425 (1996)].

8.3.4 Microhardness

Table 8.3.6 *Microhardness H for ZnSe.*

H (GPa)	Ref.
1.37–1.83	[3.9]
1.1±0.1	[3.10]

[3.9] See, L. Garbato and A. Rucci, *Phil. Mag.* **35**, 1681 (1977).
[3.10] Vickers's microhardness [K. Maruyama, K. Suto, and J. Nishizawa, *Jpn. J. Appl. Phys.* **39**, 5180 (2000)].

8.3.5 Sound Velocity

Table 8.3.7 *Sound velocity propagating in ZnSe at 300 K.* LA=longitudinal acoustic; TA1, TA2=transverse acoustic.*

Propagation direction	Mode	Sound velocity (10^5 cm/s)
[100]	LA	4.04
[100]	TA1, TA2	2.77
[110]	LA	4.55
[110]	TA1	1.82
[110]	TA2	2.77
[111]	LA	4.70
[111]	TA1, TA2	2.19

*Calculated using C_{11}=8.57×10^{11} dyn/cm^2, C_{12}=5.07×10^{11} dyn/cm^2, C_{44}=4.05×10^{11} dyn/cm^2, and g=5.2621 g/cm^3.

8.4 PHONONS AND LATTICE VIBRONIC PROPERTIES

8.4.1 Phonon Dispersion Relation

- **Dispersion curve**

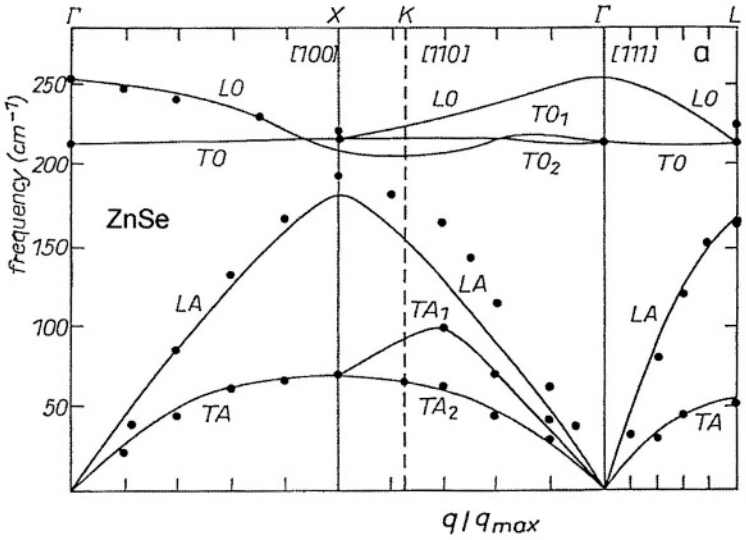

Fig. 8.4.1 Theoretical phonon dispersion curves for ZnSe. The solid circles represent the neutron scattering data measured at 300 K by B. Hennion, F. Moussa, G. Pepy, and K. Kunc [*Phys. Lett.* **36A**, 376 (1971)]. [From R. K. Ram, S. S. Kushwaha, and A. Shukla, *Phys. Status Solidi B* **154**, 553 (1989).]

- **Phonon density of states**

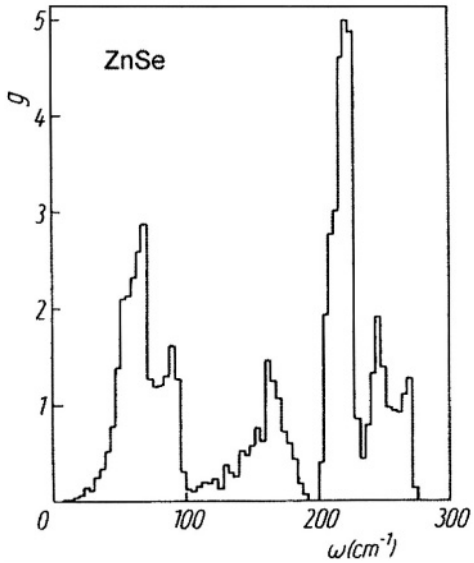

Fig. 8.4.2 Phonon density of states g versus ω for ZnSe as calculated in the deformation-bond approximation. [From K. Kunc, M. Balkanski, and M. A. Nusimovici, *Phys. Status Solidi B* **72**, 229 (1975).]

8.4.2 Phonon Frequency

• Room-temperature value

Table 8.4.1 *Long-wavelength (q→0) and zone-boundary phonon frequencies for ZnSe [4.1].*

Critical point	Phonon	Phonon frequency (cm^{-1})
Γ	TO	213
		203–213 [4.2]
		205 [4.3], [4.4], [4.5]
		204.2 [4.6]
	LO	252
		242–255 [4.2]
		250 [4.3]
		252 [4.4], [4.5]
		251.9 [4.6]
X	TA	71
	LA	193
	TO	220
	LO	213
L	TA	57
	LA	170
	TO	217
	LO	222

[4.1] K. Kunc, M. Balkanski, and M. A. Nusimovici, *Phys. Status Solidi B* **72**, 229 (1975).
[4.2] *Numerical Data and Functional Relationships in Science and Technology,* edited by O. Madelung, M. Schulz, and H. Weiss, Landolt–Börnstein, New Series, Group III, Vol. 17, Pt. b (Springer, Berlin, 1982).
[4.3] M. Cardona, *J. Phys. (Paris)* **45**, C8-29 (1984).
[4.4] D. Huang, C. Jin, D. Wang, X. Liu, J. Wang, and X. Wang, *Appl. Phys. Lett.* **67**, 3611 (1995).
[4.5] M. Kozielski, M. Szybowicz, F. Rirszt, S. Legowski, H. Meczynska, J. Szatkowski,and W. Paszkowicz, *Cryst. Res. Technol.* **34**, 699 (1999).
[4.6] C.-M. Lin, D.-S. Chuu, T.-J. Yang, W.-C. Chou, J. Xu, and E. Huang, *Phys. Rev. B* **55**, 13641 (1997).

• Temperature dependence

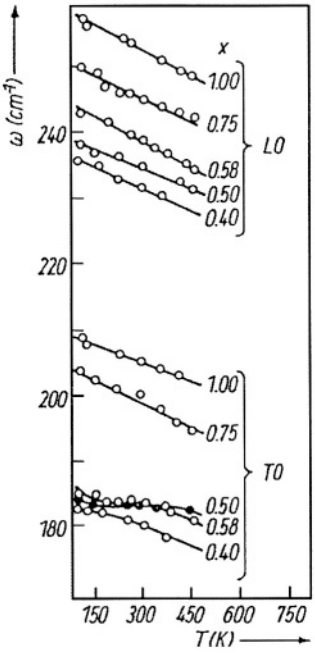

Fig. 8.4.3 Temperature dependence of the long-wavelength ($q \rightarrow 0$) phonon frequencies ω_{TO} and ω_{LO} in ZnSe (x=1.0), together with those in $Zn_xCd_{1-x}Se$ alloy (x=0.40–0.75). [From M. Ya. Valakh, M. P. Lisitsa, G. S. Pekar, G. N. Polysskii, V. I. Sidorenko, and A. M. Yaremko, *Phys. Status Solidi B* **113**, 635 (1982).]

• **Pressure dependence**

Table 8.4.2 *Pressure variation of the long-wavelength ($q \to 0$) phonon frequency in ZnSe.*

$$\omega_q(p) = \omega_q(0) + ap + bp^2$$

ω_q	$\omega_q(0)$ (cm^{-1})	a (cm^{-1}/GPa)	b (cm^{-1}/GPa^2)	Ref.
ω_{TO}	205	4.8		[4.7]
		4.82		[4.8]
		5.40	–0.0947	[4.8]
	204.2	4.98	–0.07	[4.9]
ω_{LO}	250	3.8		[4.7]
		3.66		[4.8]
		4.79	–0.137	[4.8]
	251.9	3.44	–0.02	[4.9]

[4.7] M. Cardona, *J. Phys. (Paris)* **45**, C8-29 (1984).
[4.8] R. G. Greene, H. Luo, A. L. Ruoff, *J. Phys. Chem. Solids* **56**, 521 (1995).
[4.9] C.-M. Lin, D.-S. Chuu, T.-J. Yang, W.-C. Chou, J. Xu, and E. Huang, *Phys. Rev. B* **55**, 13641 (1997).

8.4.3 Mode Grüneisen Parameter

Table 8.4.3 *Mode Grüneisen parameter for phonons at a number of critical points in ZnSe [4.10].*

Critical point	Phonon	Mode Grüneisen parameter
Γ	TO	1.4±0.1
		1.52 [4.11]
	LO	0.9±0.1
		0.85 [4.11]
X	TA	–1.3±0.2
	LA	1.1±0.2
	TO	1.6±0.2
	LO	0.9±0.2
L	TA	–1.5±0.2
	LA	1.1±0.2
	TO	1.6±0.3
	LO	0.9±0.2

[4.10] See, D. N. Talwar, M. Vandevyver, K. Kunc, and M. Zigone, *Phys. Rev. B* **24**, 741 (1981).
[4.11] C.-M. Lin, D.-S. Chuu, T.-J. Yang, W.-C. Chou, J. Xu, and E. Huang, *Phys. Rev. B* **55**, 13641 (1997).

8.4.4 Phonon Deformation Potential

Table 8.4.4 *Long-wavelength phonon deformation potential (PDP) for ZnSe [4.12].*

PDP	TO	LO
K_{11}	−1.97	−0.97
K_{12}	−3.21	−2.21
K_{44}	−0.43	−0.43
$K_{11}-K_{12}$	1.24	1.24

[4.12] F. Cerdeira, C. J. Buchenauer, F. H. Pollak, and M. Cardona, *Phys. Rev. B* **5**, 580 (1972).

8.5 COLLECTIVE EFFECTS AND RELATED PROPERTIES

8.5.1 Piezoelectric Constant

Table 8.5.1 *Piezoelectric stress (e_{14}), strain (d_{14}), and electromechanical coupling constants ($K_{[110]}^2$) for ZnSe [5.1].*

Parameter	Value
e_{14} (C/m^2)	0.049
d_{14} (10^{-12} m/V)	1.10
$K_{[110]}^2$	7.6×10^{-5} *

[5.1] D. Berlincourt, H. Jaffe, and L. R. Shiozawa, *Phys. Rev.* **129**, 1009 (1963).
*Calculated.

8.5.2 Fröhlich Coupling Constant

Table 8.5.2 *Fröhlich coupling constant α_F of ZnSe [5.2].*

α_F
0.432

[5.2] E. Kartheuser, in *Polarons in Ionic Crystals and Polar Semiconductors,* edited by J. T. Devreese (North-Holland, Amsterdam, 1972), p. 717.

8.6 ENERGY-BAND STRUCTURE: ENERGY-BAND GAPS

8.6.1 Basic Properties

• Electronic energy-band structure

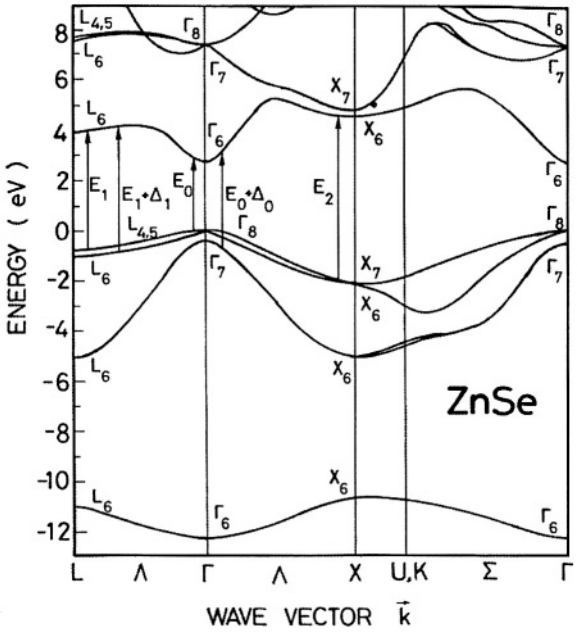

Fig. 8.6.1 Electronic energy-band structure of ZnSe as calculated by an empirical nonlocal pseudopotential method. The electronic states are labeled using the notation for the representations of the double group of the zinc-blende structure. [From J. R. Chelikowsky and M. L. Cohen, *Phys. Rev. B* **14**, 556 (1976).] The main interband transitions are indicated by the vertical arrows.

• Electronic density of states

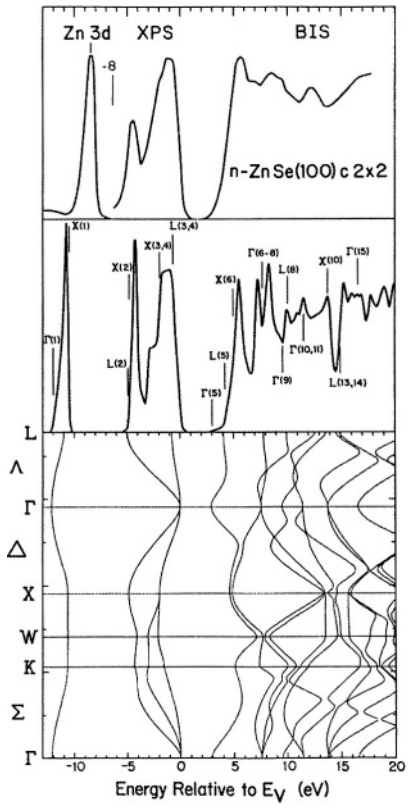

Fig. 8.6.2 Calculated energy bands and Gaussian-broadened density of states for ZnSe compared to experimental XPS (X-ray photoelectron spectroscopy) and BIS (bremsstrahlung isochromat spectroscopy) results taken with E=1486.6 eV. The XPS and BIS results are normalized for visual clarity. [From J. R. Chelikowsky, T. J. Wagener, J. H. Weaver, and A. Jin, *Phys. Rev. B* **40**, 9644 (1989).]

• **Energy eigenvalue**

Table 8.6.1 *Energy eigenvalues at the Γ, X, and L points for the valence and first few conduction bands of ZnSe [6.1].*

Critical point	Level	Value (eV)	
		Calc.	Exper.*
Γ	Γ_6^v (Γ_1^v)	−12.25	−14.5, −15.2
	Γ_7^v (Γ_{15}^v)	−0.45	−(0.42–0.43)
	Γ_8^v	0.00	0.00
	Γ_6^c (Γ_1^c)	2.76	2.80–2.825
	Γ_7^c (Γ_{15}^c)	7.33	7.15–7.80
	Γ_8^c	7.42	7.38
X	X_6^v (X_1^v)	−10.72	−12.5
	X_6^v (X_3^v)	−4.96	−4.8, −5.3, −5.6
	X_6^v (X_5^v)	−2.17	−2.4, −2.5
	X_7^v	−1.96	−2.1, −2.3
	X_6^c (X_1^c)	4.54	
	X_7^c (X_3^c)	5.17	
L	L_6^v (L_1^v)	−11.08	−13.1
	L_6^v (L_1^v)	−5.08	−5.6
	L_6^v (L_3^v)	−1.04	
	$L_{4,5}^v$	−0.76	−0.7, −1.3
	L_6^c (L_1^c)	3.96	4.22
	L_6^c (L_3^c)	7.68	
	$L_{4,5}^c$	7.72	

[6.1] J. R. Chelikowsky and M. L. Cohen, *Phys. Rev. B* **14**, 556 (1976).
*The data are gathered from various sources.

8.6.2 E_0-Gap Region

• **Room-temperature value**

Table 8.6.2 *E_0-, $E_0+\Delta_0$-, and Δ_0-gap energies for ZnSe at room temperature.*

E_0 (eV)	$E_0+\Delta_0$ (eV)	Δ_0 (eV)	Ref.
2.720±0.002			[6.2]
2.722±0.003			[6.3]
2.721	3.145 *	(0.424)	Mean value

[6.2] E. Tournié, C. Morhain, G. Neu, M. Laügt, C. Ongaretto, J.-P. Faurie, R. Triboulet, and J. O. Ndap, *J. Appl. Phys.* **80,** 2983 (1996).
[6.3] R. Pässler, E. Griebl, H. Riepl, G. Lautner, S. Bauer, H. Preis, W. Gebhardt, B. Buda, D. J. As, D. Schikora, K. Lischka, K. Papagelis, and S. Ves, *J. Appl. Phys.* **86,** 4403 (1999).
*Obtained by adding a value of Δ_0=0.424 eV.

● **Temperature dependence**

Table 8.6.3 *Empirical equation for the E_0- and $E_0+\Delta_0$-gap energy variations with temperature T for ZnSe.*

$$E_g(T) = E_g(0) - \frac{\alpha T^2}{T+\beta}$$

Band gap	Parameter			Comment
	$E_g(0)$ (eV)	α (10^{-4} eV/K)	β (K)	
E_0	2.804	8.59	405	n=1 exciton, T=4.2–220 K, bulk ZnSe [6.4]
	2.7944	11.5	700	n=1 exciton, T=4.2–300 K, bulk ZnSe [6.5]
		8	370	n=1 exciton (heavy & light holes), epilayer [6.6]
		5.9	197	n=1 exciton (heavy hole), T=8–250 K, epilayer [6.7]
		5.6	196	n=1 exciton (light hole), T=8–250 K, epilayer [6.7]
	2.800	7.3	295	n=1 exciton, T=27–370 K, epilayers [6.8]
	2.804	6.02	203	n=1 exciton, T=10–250 K, bulk ZnSe [6.9]
		5.78	175	n=1 exciton (heavy hole), T=15–200 K, epilayer [6.10]
		8.40	405	n=1 exciton (light hole), T=15–200 K, epilayer [6.10]
	2.8071	5.58	187	n=1 exciton, T=2–300 K, epilayer [6.11]
$E_0+\Delta_0$	3.2235	8	370	Epilayer [6.6]

[6.4] Y. Shirakawa and H. Kukimoto, *J. Appl. Phys.* **51**, 2014 (1980).
[6.5] K. A. Dmitrenko, L. V. Taranenko, S. G. Shevel', and A. V. Marinchenko, *Sov. Phys. Semicond.* **19**, 487 (1985).
[6.6] D. Coquillat, F. Hamdani, J. P. Lascaray, O. Briot, N. Briot, and R. L. Aulombard, *Phys. Rev. B* **47**, 10489 (1993).
[6.7] R. J. Thomas, B. Rockwell, H. R. Chandrasekhar, M. Chandrasekhar, A. K. Ramdas, M. Kobayashi, and R. L. Gunshor, *J. Appl. Phys.* **78**, 6569 (1995).
[6.8] W. Krystek, L. Malikova, F. H. Pollak, M. C. Tamargo, N. Dai, L. Zeng, and A. Cavus, *Acta Phys. Polon. A* **88**, 10113 (1995).
[6.9] E. Tournié, C. Morhain, G. Neu, M. Laügt, C. Ongaretto, J.-P. Faurie, R. Triboulet, and J. O. Ndap, *J. Appl. Phys.* **80**, 2983 (1996).
[6.10] R. C. Tu, Y. K. Su, C. F. Li, Y. S. Huang, S. T. Chou, W. H. Lan, S. L. Tu, and H. Chang, *J. Appl. Phys.* **83**, 1664 (1998).
[6.11] R. Pässler, E. Griebl, H. Riepl, G. Lautner, S. Bauer, H. Preis, W. Gebhardt, B. Buda, D. J. As, D. Schikora, K. Lischka, K. Papagelis, and S. Ves, *J. Appl. Phys.* **86**, 4403 (1999).

Table 8.6.4 *Empirical equation for the E_0- and $E_0+\Delta_0$-gap energy variation with temperature T for ZnSe.*

$$E_g(T) = E_B - 2a_B\left(\frac{1}{2} + \frac{1}{e^{\Theta/T}-1}\right)$$

Band gap	Parameter			Comment
	E_B (eV)	a_B (meV)	Θ (K)	
E_0	2.887	70	248	T=20–380 K [6.12]
$E_0+\Delta_0$	3.283	47	171	Excitonic transition, T=20–380 K [6.12]

[6.12] R. Granger, J. T. Benhlal, O. Ndap, and R. Triboulet, *Eur. Phys. J. B* **13**, 429 (2000).

Table 8.6.5 *Empirical equation for the E_0-gap energy variation with temperature T for ZnSe [6.13].*

$$E_0(T) = E_0(0) - S < \hbar\Omega > \left[\coth\left(\frac{< \hbar\Omega >}{2kT} \right) - 1 \right]$$

$E_0(0)$ (eV)	S	$<\hbar\Omega>$ (meV)
2.818	3.12	15.1

[6.13] K. P. O'Donnell and P. G. Middleton, in *Properties of Wide Bandgap II–VI Semiconductors,* EMIS Datareviews Series No. 17, edited by R. Bhargava (INSPEC, London, 1997), p. 33.

Table 8.6.6 *Empirical equation for the E_0-gap energy variation with temperature T for ZnSe.*

$$E_0(T) = E_0(0) - \frac{\alpha \Theta_p}{2} \left[\sqrt[p]{1 + \left(\frac{2T}{\Theta_p} \right)^p} - 1 \right]$$

$E_0(0)$ (eV)	p	α (meV/K)	Θ_p (K)	Comment
2.825	2.67	0.490	190	T=4–500 K [6.14]

[6.14] R. Pässler, *Phys. Status Solidi B* **216**, 975 (1999).

Table 8.6.7 *Empirical equation for the E_0-gap energy variation with temperature T for ZnSe.*

$$E_0(T) = E_0(0) - \alpha \sum_{i=1,2} \frac{W_i \Theta_i}{\exp(\Theta_i / T) - 1}$$

$E_0(0)$ (eV)	α (10^{-4} eV/K)	Θ_1 (K)	Θ_2 (K)	W_1	W_2	Comment
2.825	5.00	85	259	0.24	0.76	T=4–500 K [6.15]

[6.15] R. Pässler, *J. Appl. Phys.* **89**, 6235 (2001).

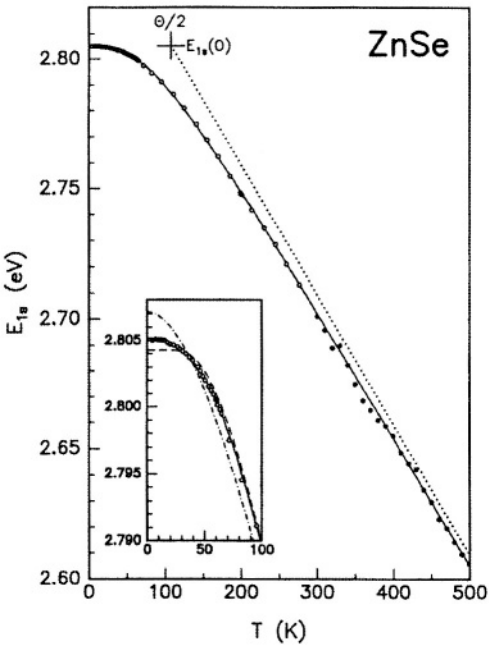

Fig. 8.6.3 Energy position of the n=1 exciton state E_{1S} in ZnSe epilayer grown on (100)GaAs substrate determined at lower temperatures by absorption measurements (open circles) and at higher temperatures by reflectance measurements (solid circles). The curves represent the numerical fits using various models. [From R. Pässler, E. Griebl, H. Riepl, G. Lautner, S. Bauer, H. Preis, W. Gebhardt, B. Buda, D. J. As, D. Schikora, K. Lischka, K. Papagelis, and S. Ves, *J. Appl. Phys.* **86**, 4403 (1999).]

● **Pressure dependence**

Table 8.6.8 *Empirical equation for the E_0-gap energy variation with pressure p for ZnSe.*

$$E_0(p) = E_0(0)+ap+bp^2$$

Parameter			Comment
$E_0(0)$ (eV)	a (10^{-2} eV/GPa)	b (10^{-4} eV/GPa^2)	
2.688±0.004	7.2±0.2	−15±1	T=300 K [6.16]
	6.48±0.20	−7±1	Heavy hole, T=80 K [6.17]
	6.33±0.20	−12±1	Light hole, T=80 K [6.17]
2.7971±0.0024	6.47±0.19	−7.7±3.0	T=80 K [6.18]
	6.7±0.2	−14±3	T=9 K [6.19]
2.8222±0.0001	7.02±0.02	−14.4±0.2	T=6 K [6.20]

[6.16] S. Ves, K. Strössner, N. E. Christensen, C. K. Kim, and M. Cardona, *Solid State Commun.* **56**, 479 (1985).
[6.17] B. Rockwell, H. R. Chandrasekhar, M. Chandrasekhar, A. K. Ramdas, M. Kobayashi, and R. L. Gunshor, *Phys. Rev. B* **44**, 11307 (1991).
[6.18] R. J. Thomas, H. R. Chandrasekhar, M. Chandrasekhar, N. Samarth, H. Luo, and J. Furdyna, *Phys. Rev. B* **45**, 9505 (1992).
[6.19] J. A. Tuchman, S. Kim, Z. Sui, and I. P. Herman, *Phys. Rev. B* **46**, 13371 (1992).
[6.20] See, A. Mang, K. Reimann, St. Rübenacke, and M. Steube, *Phys. Rev. B* **53**, 16283 (1996).

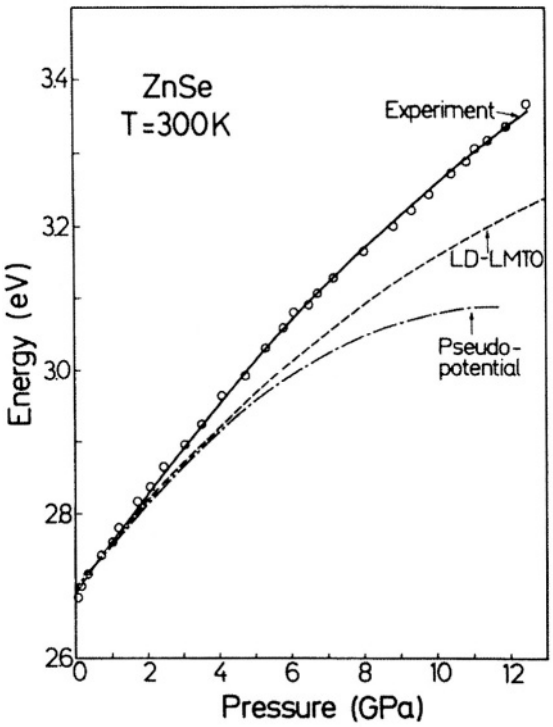

Fig. 8.6.4 Variation of the E_0-gap energy with hydrostatic pressure for ZnSe at room temperature as obtained from absorption measurements. The dash-dotted and dashed lines show the theoretical results with the pseudopotential and LD-LMTO (local-density linear muffin-tin orbital) methods, respectively. [From S. Ves, K. Strössner, N. E. Christensen, C. K. Kim, and M. Cardona, *Solid State Commun.* **56**, 479 (1985).]

• **Temperature and/or pressure coefficient**

Table 8.6.9 *Linear temperature and pressure coefficients of the E_0- and $E_0+\Delta_0$-gap energies for ZnSe.*

Band gap	Coefficient	Value	Comment
E_0	dE_g/dT (10^{-4} eV/K)	–4.5±0.5	[6.21]
		–4.30±0.01	n=1 exciton, T=80–293 K [6.22]
		–4.3	T≥80 K [6.23]
		–4.76±0.03	T=300 K [6.24]
		–4.7	T=100–300 K [6.25]
	dE_g/dp (10^{-2} eV/GPa)	7	[6.26]
		7.4±0.5	T=85 K [6.27]
		7.5±0.3	T=300 K [6.27]
		7.51±0.06	T=4.2 K [6.28]
$E_0+\Delta_0$	dE_g/dT (10^{-4} eV/K)	–4.4±0.2	n=1 exciton, T=80–293 K [6.22]
		–5	T=100–300 K [6.25]
	dE_g/dp (10^{-2} eV/GPa)		

[6.21] J. Camassel and D. Auvergne, *Phys. Rev. B* **12**, 3258 (1975).
[6.22] V. V. Sobolev, V. I. Donetskikh, and E. F. Zagaĭnov, *Sov. Phys. Semicond.* **12**, 646 (1978).
[6.23] E. Tournié, C. Morhain, G. Neu, M. Laügt, C. Ongaretto, J.-P. Faurie, R. Triboulet, and J. O. Ndap, *J. Appl. Phys.* **80,** 2983 (1996).
[6.24] R. Pässler, E. Griebl, H. Riepl, G. Lautner, S. Bauer, H. Preis, W. Gebhardt, B. Buda, D. J. As, D. Schikora, K. Lischka, K. Papagelis, and S. Ves, *J. Appl. Phys.* **86**, 4403 (1999).
[6.25] R. Granger, J. T. Benhlal, O. Ndap, and R. Triboulet, *Eur. Phys. J. B* **13**, 429 (2000).
[6.26] D. L. Camphausen, G. A. N. Connell, and W. Paul, *Phys. Rev. Lett.* **26**, 184 (1971).
[6.27] P. Jaszczyn-Kopec, B. Canny, G. Syfosse, and G. Hamel, *Solid State Commun.* **49**, 795 (1984).
[6.28] K. Reimann and M. Steube, in *Proc. 25th Int. Conf. Phys. Semicond.,* edited by N. Miura and T. Ando (Springer, Berlin, 2001), p.1533.

8.6.3 Higher-Lying Direct Gap

• **Room-temperature value**

Table 8.6.10 *Higher-lying direct-gap energies for ZnSe measured at room temperature.**

Band gap	Value (eV)	Mean value (eV)
E_1	4.7–4.853	4.79
$E_1+\Delta_1$	5.03–5.2	5.08
Δ_1	0.26–0.35	0.29
E_0'	7.25–8.5	8.1
E_2	6.25–7.15	6.6
$E_2+\delta$	6.62–7.2	6.9
E_1'	8.27–9.25	8.9
$E_1'+\Delta_1'$	8.97–9.6	9.4
d_1	10.6	10.6
d_2	13.4–13.8	13.6

*The data are taken from various sources [see, e.g., S. Adachi and T. Taguchi, *Phys. Rev. B* **43**, 9569 (1991)].

● **Temperature dependence**

Table 8.6.11 *Empirical equation for the higher-lying direct-gap energy variation with temperature T for ZnSe. 2D-CP=two-dimensional critical point.*

$$E_g(T) = E_B - 2a_B\left(\frac{1}{2} + \frac{1}{e^{\Theta/T} - 1}\right)$$

Band gap	Parameter			Comment
	E_B (eV)	a_B (meV)	Θ (K)	
E_1	5.082	116	267	2D-CP, T=20–380 K [6.29]
	5.038	67	195	Excitonic transition, T=20–380 K [6.29]
$E_1+\Delta_1$	5.285	67	280	2D-CP, T=20–380 K [6.29]
	5.290	67	280	Excitonic transition, T=20–380 K [6.29]

[6.29] R. Granger, J. T. Benhlal, O. Ndap, and R. Triboulet, *Eur. Phys. J. B* **13**, 429 (2000).

● **Pressure dependence**

Table 8.6.12 *Empirical equation for the higher-lying band-gap energy variation with pressure p for ZnSe.*

$$E_g(p) = E_g(0) + ap + bp^2$$

Band gap	Parameter			Comment
	$E_g(0)$ (eV)	a (10^{-2} eV/GPa)	b (10^{-4} eV/GPa^2)	
E_1	4.67	4.7	–20.5	Calc. [6.30]

[6.30] S. Ves, K. Strössner, N. E. Christensen, C. K. Kim, and M. Cardona, *Solid State Commun.* **56,** 479 (1985).

● **Temperature and/or pressure coefficient**

Table 8.6.13 *Linear temperature and pressure coefficients of the higher-lying band-gap energy for ZnSe. 2D-CP=two-dimensional critical point.*

Band gap	Coefficient	Value	Comment
E_1	dE_g/dT (10^{-4} eV/K)	–5.2±0.3	T<295 K [6.31]
		–5.6	T=100–300 K [6.32]
		–6.6	2D-CP, T=100-300 K [6.33]
		–6.2	Excitonic transition, T=100-300 K [6.33]
	dE_g/dp (10^{-2} eV/GPa)	4.0	Calc. [6.34]
		2.5	Calc. [6.35]
		4.88	Calc. [6.36]
$E_1+\Delta_1$	dE_g/dT (10^{-4} eV/K)	–4.1±0.5	T<295 K [6.31]
		–8.0	T=100–300 K [6.32]
		–3.7	2D-CP, T=100-300 K [6.33]
		–7.9	Excitonic transition, T=100-300 K [6.33]
	dE_g/dp (10^{-2} eV/GPa)		

Table 8.6.13 *Continued.*

Band gap	Coefficient	Value	Comment
E_2	dE_g/dT (10^{-4} eV/K)	–4.7	T=100–300 K [6.32]
	dE_g/dp (10^{-2} eV/GPa)	3.3	Calc. [6.34]
		–0.3	Calc. [6.35]
		1.33	Calc. [6.36]

[6.31] M. Cardona and G. Harbeke, *J. Appl. Phys.* **34**, 813 (1963).
[6.32] D. Theis, *J. Phys. Chem. Solids* **38,** 1125 (1977).
[6.33] R. Granger, J. T. Benhlal, O. Ndap, and R. Triboulet, *Eur. Phys. J. B* **13**, 429 (2000).
[6.34] D. L. Camphausen, G. A. N. Connell, and W. Paul, *Phys. Rev. Lett.* **26**, 184 (1971).
[6.35] Y. F. Tsay, S. S. Mitra, and B. Bendow, *Phys. Rev. B* **10**, 1476 (1974).
[6.36] D. Bertho, J.-M. Jancu, and C. Jouanin, *Phys. Rev. B* **48**, 2452 (1993).

8.6.4 Lowest Indirect Gap

• Theoretical value

Table 8.6.14 *Theoretically obtained lowest indirect-gap energy for ZnSe (in eV).*

E_g^{L} *1	E_g^{X} *2	Ref.
3.96	4.54	[6.37]
4.23	4.42	[6.38]
4.289	4.371	[6.39]
4.08	4.60	[6.40]
4.43	4.13	[6.41]
4.70	4.59	[6.42]
4.14	4.41	[6.43]
3.122	3.399	[6.44]

[6.37] J. R. Chelikowsky and J. L. Cohen, *Phys. Rev. B* **14**, 556 (1976).
[6.38] M.-Z. Huang and W. Y. Ching, *J. Phys. Chem. Solids* **46**, 977 (1985).
[6.39] S. Ves, K. Strössner, N. E. Christensen, C. K. Kim, and M. Cardona, *Solid State Commun.* **56,** 479 (1985).
[6.40] J. R. Chelikowsky, T. J. Wagener, J. H. Weaver, and A. Jin, *Phys. Rev. B* **40**, 9644 (1989).
[6.41] Y. Li and P. J. Lin-Chung, *Phys. Status Solidi B* **153**, 215 (1989).
[6.42] S. J. Jenkins, G. P. Srivastava, and J. C. Inkson, *Phys. Rev. B* **48**, 4388 (1993).
[6.43] O. Zakharov, A. Rubio, X. Blase, M. L. Cohen, and S. L. Louie, *Phys. Rev. B* **50**, 10780 (1994).
[6.44] F. Benkabou, H. Aourag, M. Certier, and T. Kobayashi, *Superlatt. Microstruct.* **30**, 9 (2001).
*1 Γ_8^v (Γ_{15}^v)→L_6^c(L_1^c).
*2 Γ_8^v (Γ_{15}^v)→X_6^c(X_1^c).

• Experimental value

Table 8.6.15 *Experimentally obtained lowest indirect-gap energy for ZnSe (in eV).*

E_g^{L}	E_g^{X}	Ref.
4.22		*
3.8	3.4	[6.45]

[6.45] See, F. Benkabou, H. Aourag, M. Certier, and T. Kobayashi, *Superlatt. Microstruct.* **30**, 9 (2001).
* See Sec. 8.6.1.

• **Pressure dependence**

Table 8.6.16 *Empirical equation for the lowest indirect-gap energy variation with pressure p for ZnSe.*

$$E_g^{L,X}(p) = E_g^{L,X}(0) + ap + bp^2$$

Band gap	Parameter			Comment
	$E_g^{L,X}(0)$ (eV)	a (10^{-2} eV/GPa)	b (10^{-4} eV/GPa^2)	
E_g^L	4.289	2.2	−15.3	Calc. [6.46]
E_g^X	4.371	−1.4	−9.2	Calc. [6.46]

[6.46] S. Ves, K. Strössner, N. E. Christensen, C. K. Kim, and M. Cardona, *Solid State Commun.* **56**, 479 (1985).

• **Temperature and/or pressure coefficient**

Table 8.6.17 *Linear pressure coefficient of the lowest indirect-gap energy for ZnSe.*

Coefficient	Value	Comment
dE_g^L/dp (10^{-2} eV/GPa)	2.0	Calc. [6.47]
	1.4	Calc. [6.48]
	4.7	Calc. [6.49]
dE_g^X/dp (10^{-2} eV/GPa)	−1.8	Calc. [6.47]
	−3.7	Calc. [6.48]
	−2.2	Calc. [6.49]
	−2.6	Calc. [6.50]
	−2	Exper. [6.51]

[6.47] D. L. Camphausen, G. A. N. Connell, and W. Paul, *Phys. Rev. Lett.* **26**, 184 (1971).
[6.48] Y. F. Tsay, S. S. Mitra, and B. Bendow, *Phys. Rev. B***10**,1476 (1974).
[6.49] S.-H. Wei and A. Zunger, *Phys. Rev. B* **60**, 5404 (1999).
[6.50] V. I. Smelyansky and J. S. Tse, *Phys. Rev. B* **52**, 4658 (1995).
[6.51] See, Y. F. Tsay, S. S. Mitra, and B. Bendow, *Phys. Rev. B* **10**, 1476 (1974).

8.6.5 Conduction-Valley Energy Separation

Table 8.6.18 *Conduction-valley energy separation ΔE_g for ZnSe.*

ΔE_g	Value (eV)	Comment
$L_6^c - \Gamma_6^c$	1.4	T=77 K [6.52]
	1.30	Ultrafast carrier dynamics, T=300 K [6.53]
	~1.1	*
$X_6^c - \Gamma_6^c$	~0.7	*

[6.52] R. Markowski, M. Piacentini, D. Debowska, M. Zimnal-Starnawska, F. Lama, N. Zema, and A. Kisiel, *J. Phys.: Condens. Matter* **6**, 3207 (1994).
[6.53] D. J. Dougherty, S. B. Fleischer, E. L. Warlick, J. L. House, G. S. Petrich, L. A. Kolodziejski, and E. P. Ippen, *Appl. Phys. Lett.* **71**, 3144 (1997).
*Estimated from E_0, E_g^X, and E_g^L.

8.6.6 Direct–Indirect-Gap Transition Pressure

No direct–indirect-gap crossing occurs in ZnSe for pressures up to the first structural phase transition (p~13 GPa) [see, S. Ves, K. Strössner, N. E. Christensen, C. K. Kim, and M. Cardona, *Solid State Commun.* **56,** 479 (1985)].

8.7 ENERGY-BAND STRUCTURE: ELECTRON AND HOLE EFFECTIVE MASSES

8.7.1 Electron Effective Mass: Γ Valley

Table 8.7.1 *Effective polaron (m_{ep}*) and band masses (m_e^Γ) for electrons at the Γ-conduction band in ZnSe. α_F=Fröhlich coupling constant.*

m_{ep}*/m_0	m_e^Γ/m_0	Comment
0.17±0.025		Infrared reflectance & Faraday rotation [7.1]
0.16±0.01		Zeeman splitting, T=1.6 K [7.2]
0.160±0.002		Phtoluminescence, T=4.2 K [7.3]
0.147±0.001		Two-photon magnetoabsorption, T=2.2 K [7.4]
0.145±0.002	0.135	Cyclotron resonance, T=4.2 K, α_F=0.432 [7.5]
0.145	0.137	Cyclotron resonance, T=7 K, α_F=0.42 [7.6]
0.15	0.123	Magnetoabsorption, T=1.7 K [7.7]
0.145	0.137	Cyclotron resonance, T=6 K, α_F=0.42 [7.8]
0.154±0.001		Two-photon magnetoabsorption, T=4.2 K [7.9]

[7.1] D. T. F. Marple, *J. Appl. Phys.* **35**, 1879 (1964).
[7.2] J. L. Merz, H. Kukimoto, K. Nassau, and J. W. Shiever, *Phys. Rev. B* **6**, 545 (1972).
[7.3] P. J. Dean, D. C. Herbert, C. J. Werkhoven, B. J. Fitzpatrick, and R. N. Bhargava, *Phys. Rev. B* **23**, 4888 (1981).
[7.4] H. W. Hölscher and A. Nöthe, *Physica* **117B&118B,** 395 (1983).
[7.5] T. Ohyama, E. Otsuka, T. Yoshida, M. Isshiki, and K. Igaki, *Jpn. J. Appl. Phys.* **23**, L382 (1984).
[7.6] Y. Imanaka, N. Miura, and H. Kukimoto, *Phys. Rev. B* **49**, 16965 (1994).
[7.7] G. N. Aliev, R. M. Datsiev, S. V. Ivanov, P. S. Kop'ev, R. P. Seisyan, and S. V. Sorokin, *J. Cryst. Growth* **159,** 523 (1996).
[7.8] M. Drechsler, B. K. Meyer, D. M. Hofmann, P. Ruppert, and D. Hommel, *Appl. Phys. Lett.* **71,** 1116 (1997).
[7.9] K. Reimann and M. Steube, in *Proc. 25th Int. Conf. Phys. Semicond.,* edited by N. Miura and T. Ando (Springer, Berlin, 2001), p.1533.

- **Temperature and/or pressure dependence**

Table 8.7.2 *Hydrostatic-pressure coefficient $(m_e^\Gamma)^{-1}(dm_e^\Gamma/dp)$ for ZnSe.*

$\frac{1}{m_e^\Gamma}\frac{dm_e^\Gamma}{dp}$ (%/kbar)	Comment
0.00±0.04	T=4.2 K [7.10]

[7.10] K. Reimann and M. Steube, in *Proc. 25th Int. Conf. Phys. Semicond.*, edited by N. Miura and T. Ando (Springer, Berlin, 2001), p. 1533.

8.7.2 Electron Effective Mass: Satellite Valley

No detailed data are available for ZnSe.

8.7.3 Hole Effective Mass

• Luttinger's valence-band parameter

Table 8.7.3 *Luttinger's valence-band parameter γ_i for ZnSe (in $\hbar^2/2m_0$).*

γ_1	γ_2	γ_3	Technique
3.77	1.24	1.67	Five-level $\boldsymbol{k\cdot p}$ calculation [7.11]
4.32±0.20	0.662±0.013	1.13±0.02	Magnetoreflectance [7.12]
4.8±0.67	0.67±0.08	1.53±0.35	Magnetoreflectance [7.13]
(4.3±0.5)	(0.59±0.07)	(1.34±0.30)	(Polaron parameters [7.13])
4.30	1.14	1.84	Resonant Brillouin scattering [7.14]
2.45±0.05	0.61±0.12	1.11±0.10	Two-photon magnetoabsorption [7.15]
2.75±0.2	0.5±0.1	1.11±0.11	Standing polariton-wave method [7.16]
6.44	2.58	2.74	Infrared absorption [7.17]
2.65±0.05	0.633±0.004	1.04±0.01	Two-photon magnetoabsorption [7.18]
3.94	1.00	1.52	Mean value

[7.11] P. Lawaetz, *Phys. Rev. B* **4**, 3460 (1971).
[7.12] S. Feierabend and H. G. Weber, *Solid State Commun.* **26**, 191 (1978).
[7.13] H. Venghaus, *Phys. Rev. B* **19**, 3071 (1979).
[7.14] B. Sermage and G. Fishman, *Phys. Rev. B* **23**, 5107 (1981).
[7.15] H. W. Hölscher, A. Nöthe, and Ch. Uihlein, *Phys. Rev. B* **31**, 2379 (1985).
[7.16] S. Lankes, M. Meier, T. Reisinger, and W. Gebhardt, *J. Appl. Phys.* **80**, 4049 (1996).
[7.17] H. Nakata, K. Yamada, and T. Ohyama, *Phys. Rev. B* **60**, 13269 (1999).
[7.18] K. Reimann and M. Steube, in *Proc. 25th Int. Conf. Phys. Semicond.,* edited by N. Miura and T. Ando (Springer, Berlin, 2001), p. 1533.

• Band mass, cyclotron mass, etc.

Table 8.7.4 *Band (m_{HH}, m_{LH}), density-of-states heavy-hole (m_{HH}*), averaged light-hole (m_{LH}*), and spherically-averaged heavy-hole (m_{HH}^s) and light-hole masses (m_{LH}^s) in ZnSe.**

Mass	Value (m_0)
m_{HH} ([001] direction)	0.52
m_{LH} ([001] direction)	0.168
m_{HH} ([111] direction)	1.11
m_{LH} ([111] direction)	0.143
m_{HH}*	0.82
	0.75 [7.19]
m_{LH}*	0.154
m_{HH}^s	0.76
m_{LH}^s	0.152

[7.19] G. E. Hite, D. T. F. Marple, M. Aven, and B. Segall, *Phys. Rev.* **156,** 850 (1967).
*Calculated using a set of the Luttinger's parameters, γ_1=3.94, γ_2=1.00, and γ_3=1.52.

• Spin–orbit–splitoff hole effective mass

Table 8.7.5 *Spin–orbit–splitoff hole effective mass m_{SO} for ZnSe.*

m_{SO}/m_0	Technique
0.67	$\boldsymbol{k}\cdot\boldsymbol{p}$ method [7.20]
0.30	$\boldsymbol{k}\cdot\boldsymbol{p}$ method [7.21]
0.28	Linear-muffin-tin-orbitals calculation [7.22]
0.239	$\boldsymbol{k}\cdot\boldsymbol{p}$ method [7.23]
0.24	*

[7.20] M. Cardona, *J. Phys. Chem. Solids* **24**, 1543 (1963).
[7.21] P. Lawaetz, *Phys. Rev. B* **4**, 3460 (1971).
[7.22] M. Cardona, N. E. Christensen, and G. Fasol, *Phys. Rev. B* **38**, 1806 (1988).
[7.23] N. P. Belov, V. T. Prokopenko, and A. D. Yas'kov, *Sov. Phys. Semicond.* **23**, 1296 (1989).
*Obtained from the Luttinger's parameter ($m_{SO}=1/\gamma_1$).

• Temperature and/or pressure dependence

Table 8.7.6 *Hydrostatic-pressure coefficient of the hole effective mass in ZnSe [7.24]. HH=heavy hole; LH-light hole.*

Effective mass	Value (%/kbar)	Comment
$\frac{1}{m_{HH}}\frac{dm_{HH}}{dp}$	–3.0±0.3	$\boldsymbol{k}\|\|[100]$
	21±5	$\boldsymbol{k}\|\|[111]$
	0.2±0.8	Average
$\frac{1}{m_{LH}}\frac{dm_{LH}}{dp}$	0.47±0.3	$\boldsymbol{k}\|\|[100]$
	–0.21±0.05	$\boldsymbol{k}\|\|[111]$
	–0.01±0.03	Average

[7.24] Two-photon magnetoabsorption at T=4.2 K [K. Reimann and M. Steube, in *Proc. 25th Int. Conf. Phys. Semicond.*, edited by N. Miura and T. Ando (Springer, Berlin, 2001), p. 1533].

8.8 ELECTRONIC DEFORMATION POTENTIAL

8.8.1 Intravalley Deformation Potential: Γ Point

• Conduction band

Table 8.8.1 *Γ-conduction-band intravalley deformation potential a_c^{Γ} ($=E_1^{\Gamma}$) for ZnSe.*

a_c^{Γ} (eV)	Comment
–7.51	Calc. [8.1]
–14.8	Calc. [8.2]
–7.4	Calc. [8.3]
–4.17	Calc. [8.4]
–4.26	Calc. [8.5]

[8.1] J. H. Lee and G. Myers, *Phys. Status Solidi B* **77**, K81 (1976).
[8.2] A. Blacha, H. Presting, and M. Cardona, *Phys. Status Solidi B* **126**, 11 (1984).
[8.3] M. Cardona and N. E. Christensen, *Phys. Rev. B* **35**, 6182 (1987); erratum, *ibid.* **36**, 2906 (1987).
[8.4] C. G. Van de Walle, *Phys. Rev. B* **39**, 1871 (1989).
[8.5] D. Bertho, D. Boiron, A. Simon, C. Jouanin, and C. Priester, *Phys. Rev. B* **44**, 6118 (1991).

Table 8.8.2 *Γ-conduction-band acoustic deformation potential E_1 for ZnSe obtained from transport data analysis.*

E_1 (eV)	Ref.
11.5	[8.6]
4.2	[8.7]

[8.6] D. L. Rode, *Phys. Rev. B* **2**, 4036 (1970).
[8.7] D. L. Rode, in *Semiconductors and Semimetals,* edited by R. K. Willardson and A. C. Beer (Academic, New York, 1975), Vol. 10, p. 1.

- **Valence band**

Table 8.8.3 *Γ-valence-band deformation potentials a, b, and d for ZnSe.*

Deformation potential (eV)			Comment
a	*b*	*d*	
−8.6	1.2	−5.9	Calc. [8.8]
−0.7			Calc. [8.9]
1.65	−1.20		Calc. [8.10]
1.45	−3.18		Calc. [8.11]
1.27	−1.36		Calc. [8.12]
	−1.2		Calc. [8.13]
	−1.23		Calc. [8.14]
	0.8		Calc. [8.15]
	−1.32		Calc. [8.16]
	−1.27	−3.40	Calc. [8.17]
	−1.2	−3.8	Exper. [8.18]
	−2.65	−6.8	Exper. [8.19]
	−1.05		Exper. [8.20]
	−1.27		Exper. [8.21]
	−1.17±0.03		Exper. [8.22]
	−1.02		Exper. [8.23]
	−0.74		Exper. [8.24]
	−1.24±0.07	−4.25±0.05	Exper. [8.25]
	−3.9		Exper. (ZnSe/GaAs [8.26])
	−4.1		Exper. (bulk ZnSe [8.26])
	−1.8	−5.0	Mean value (Exper.)

[8.8] A. Blacha, H. Presting, and M. Cardona, *Phys. Status Solidi B* **126**, 11 (1984).
[8.9] M. Cardona and N. E. Christensen, *Phys. Rev. B* **35**, 6182 (1987); erratum, *ibid.* **36**, 2906 (1987).
[8.10] C. G. Van de Walle, *Phys. Rev. B* **39**, 1871 (1989).
[8.11] D. Bertho, D. Boiron, A. Simon, C. Jouanin, and C. Priester, *Phys. Rev. B* **44**, 6118 (1991).
[8.12] A. Qteish and R. J. Needs, *Phys. Rev. B* **45**, 1317 (1992).
[8.13] M. Silver, W. Batty, A. Ghiti, and E. P. O'Reilly, *Phys. Rev. B* **46**, 6781 (1992).
[8.14] T. Nakayama, *Solid-State Electron.* **37**, 1077 (1994).
[8.15] B. Koopmans, P. V Santos, and M. Cardona, *Phys. Status Solidi B* **205**, 419 (1998).
[8.16] R. Said, A. Qteish, and N. Meskini, *J. Phys.: Condens. Matter* **10,** 8703 (1998).

[8.17] R. A. Casali and N. E. Christensen, *Solid State Commun.* **108**, 793 (1998).
[8.18]. D. W. Langer, R. N. Euwema, K. Era, and T. Koda, *Phys. Rev. B* **2**, 4005 (1970).
[8.19] K. Tada, K. Kikuchi, and K. Sato, *Jpn. J. Appl. Phys.* **16**, 757 (1977).
[8.20] R. L. Gunshor, L. A. Kolodziejski, M. R. Melloch, M. Vaziri, C. Choi, and N. Otsuka, *Appl. Phys. Lett.* **50**, 200 (1987).
[8.21] Y. R. Lee, A. K. Ramdas, L. A. Kolodziejski, and R. L. Gunshor, *Phys. Rev.B* **38**, 13143 (1988).
[8.22] B. Rockwell, H. R. Chandrasekhar, M. Chandrasekhar, A. K. Ramdas, M. Kobayashi, and R. L. Gunshor, *Phys. Rev. B* **44**, 11307 (1991).
[8.23] J. A. Tuchman, S. Kim, Z. Sui, and I. P. Herman, *Phys. Rev. B* **46**, 13371(1992).
[8.24] H. L. Cotal, J. B. Maxson, S. W. S. McKeever, and E. Cantwell, *Appl. Phys. Lett.* **64**, 1532 (1994).
[8.25] D. Fröhlich, W. Nieswand, U. W. Pohl, and J. Wrzesinski, *Phys. Rev. B* **52**, 14652 (1995).
[8.26] F. Kubacki, J. Gutowski, D. Hommel, M. Heuken, and U. W. Pohl, *Phys. Rev. B* **54**, 2028 (1996).

• **E_0 gap**

Table 8.8.4 *Hydrostatic deformation potential a_0^{Γ} for the E_0 gap of ZnSe.*

a_0^{Γ} (eV)	Comment
–6.2	Calc. [8.27]
–4.2	Calc. [8.28]
–5.82	Calc. [8.29]
–5.71	Calc. [8.30]
–4.73	Calc. [8.31]
–4.08	Calc. [8.32]
–4.99	Calc. [8.33]
–5.4	Exper. [8.34]
–6.8	Exper. [8.35]
–4.87	Exper. [8.36]
–5.26	Exper. [8.37]
–4.37	Exper. [8.38]
–5.1	Exper. [8.39]
–4.8	Exper. [8.40]
–4.7±0.2	Exper. [8.41]
–4.54±0.02	Exper. [8.42]
–5.1	Exper. (ZnSe/GaAs [8.43])
–4.9	Exper. (bulk ZnSe [8.43])
–5.1	Mean value (Exper.)

[8.27] A. Blacha, H. Presting, and M. Cardona, *Phys. Status Solidi B* **126**, 11 (1984).
[8.28] J. E. Bernard and A. Zunger, *Phys. Rev. B* **36**, 3199 (1987).
[8.29] C. G. Van de Walle, *Phys. Rev. B* **39**, 1871 (1989).
[8.30] D. Bertho, D. Boiron, A. Simon, C. Jouanin, and C. Priester, *Phys. Rev. B* **44**, 6118 (1991).
[8.31] T. Nakayama, *Solid-State Electron.* **37**, 1077 (1994).
[8.32] R. Said, A. Qteish, and N. Meskini, *J. Phys.: Condens. Matter* **10**, 8703 (1998).
[8.33] S.-H. Wei and A. Zunger, *Phys. Rev. B* **60**, 5404 (1999).
[8.34]. D. W. Langer, R. N. Euwema, K. Era, and T. Koda, *Phys. Rev. B* **2**, 4005 (1970).
[8.35] K. Tada, K. Kikuchi, and K. Sato, *Jpn. J. Appl. Phys.* **16**, 757 (1977).
[8.36] R. L. Gunshor, L. A. Kolodziejski, M. R. Melloch, M. Vaziri, C. Choi, and N. Otsuka, *Appl. Phys.* Lett **50**, 200 (1987).
[8.37] Y. R. Lee, A. K. Ramdas, L. A. Kolodziejski, and R. L. Gunshor, *Phys. Rev. B* **38**, 13143 (1988).
[8.38] J. A. Tuchman, S. Kim, Z. Sui, and I. P. Herman, *Phys. Rev. B* **46**, 13371 (1992).
[8.39] H. L. Cotal, J. B. Maxson, S. W. S. McKeever, and E. Cantwell, *Appl. Phys. Lett.* **64**, 1532 (1994).
[8.40] S. Ves, K.Strössner, N. E. Christensen, C. K. Kim, and M. Cardona, *Solid State Commun.* **56**, 479 (1985).

[8.41] D. Fröhlich, W. Nieswand, U. W. Pohl, and J. Wrzesinski, *Phys. Rev. B* **52**, 14652 (1995).
[8.42] See, A. Mang, K. Reimann, St. Rübenacke, and M. Steube, *Phys. Rev. B* **53**, 16283 (1996).
[8.43] F. Kubacki, J. Gutowski, D. Hommel, M. Heuken, and U. W. Pohl, *Phys. Rev. B* **54**, 2028 (1996).

- **Optical-phonon deformation potential**

Table 8.8.5 *Optical-phonon deformation potential d_0 at the Γ-valence band of ZnSe.*

d_0 (eV)	Comment
21.6	Calc. [8.44]
25.2	Calc. [8.45]
19.2	Calc. [8.46]
11.7	Calc. [8.47]
8.17	Calc. [8.48]
27	Exper. (see [8.44])
12	Exper. [8.49]
20	Mean value (Exper.)

[8.44] W. Pötz and P. Vogl, *Phys. Rev. B* **24**, 2025 (1981).
[8.45] A. Blacha, H. Presting, and M. Cardona, *Phys. Status Solidi B* **126**, 11 (1984).
[8.46] L. Brey, N. E. Christensen, and M. Cardona, *Phys. Rev. B* **36**, 2638 (1987).
[8.47] R.-Z. Wang, S.-H. Ke, and M.-C. Huang, *J. Phys.: Condens. Matter* **4**, 6735 (1992).
[8.48] R. A. Casali and N. E. Christensen, *Solid State Commun.* **108**, 793 (1998).
[8.49] J. M. Calleja, H. Vogt, and M. Cardona, *Phil. Mag.* **35**, 239 (1982).

8.8.2 Intravalley Deformation Potential: High-Symmetry Points

- **Optical-phonon deformation potential: L point**

Table 8.8.6 *Optical-phonon deformation potentials $d_{1o}(c)$, $d_{1o}(v)$, and d_{3o} at the L point of ZnSe.*

Deformation potential	Value (eV)	Comment
$d_{1o}(c)$	−8.9	Calc. [8.50]
	−23.8	Calc. [8.51]
$d_{1o}(v)$	−14.2	Calc. [8.50]
	−2.1	Calc. [8.51]
d_{3o}	28.9	Calc. [8.50]
	24.9	Calc. [8.51]

[8.50] W. Pötz and P. Vogl, *Phys. Rev. B* **24**, 2025 (1981).
[8.51] R.-Z. Wang, S.-H. Ke, and M.-C. Huang, *J. Phys.: Condens. Matter* **4**, 6735 (1992).

- **Valence-band deformation potential: L point**

Table 8.8.7 *Valence-band deformation potentials D_3^5 and D_3^3 at the L point of ZnSe.*

Deformation potential	Value (eV)	Comment
D_3^5	2.78	Calc. [8.52]
	−27±9	Exper. [8.53]
D_3^3	3.71	Calc. [8.52]
	−17±5	Exper. [8.53]

[8.52] D. Rönnow, N. E. Christensen, and M. Cardona, *Phys. Rev. B* **59**, 5575 (1999).
[8.53] D. Rönnow, M. Cardona, and L. F. Lastras-Martínez, *Phys. Rev. B* **59**, 5581 (1999).

• **Hydrostatic and interband deformation potentials: E_1 and $E_1+\Delta_1$ gaps**

Table 8.8.8 *Hydrostatic a_l^L $(=D_l^l/\sqrt{3})$ and interband deformation potentials D_l^5 for the E_l and $E_l+\Delta_l$ gaps of ZnSe.*

Deformation potential	Value (eV)	Comment
a_1^L	−3.33	Calc. [8.54]
D_1^5	6.39	Calc. [8.54]
	30±30	Exper. [8.55]

[8.54] D. Rönnow, N. E. Christensen, and M. Cardona, *Phys. Rev. B* **59**, 5575 (1999).
[8.55] D. Rönnow, M. Cardona, and L. F. Lastras-Martínez, *Phys. Rev. B* **59**, 5581 (1999).

8.8.3 Intervalley Deformation Potential

• **Absolute value**

Table 8.8.9 *Intervalley deformation potential D_{ij} for electrons in ZnSe [8.56].*

D_{ij}	Phonon	Value (eV/Å)
$D_{\Gamma L}$	LA	2.71
	LO	2.17
$D_{\Gamma X(1)}$	LA	0
	LO	0.72
$D_{\Gamma X(3)}$	LA	1.37
	LO	0

[8.56] Calculated [D. Olguín, M. Cardona, and A. Cantarero, *Solid State Commun.* **122,** 575 (2002)].

Table 8.8.10 *Intervalley deformation potential D_{ij} for electrons in ZnSe [8.57].**

Scattering type	D_{ij} (eV/Å)	Phonon energy (meV)
Γ – Γ	0	0
Γ – L	10	26.7
Γ – X	10	27.9
L – L	10	26.7
L – X	9	27.3
X – X	9	27.9

[8.57] K. Brennan, *J. Appl. Phys.* **64**, 4024 (1988).
* Since the intervalley deformation potentials and related phonon energies are generally unknown even in the most-studied semiconductors, it has been chosen a set of similar values to those for GaAs and InP [K. Brennan and K. Hess, *Solid-State Electron.* **27**, 347 (1984)].

8.9 ELECTRON AFFINITY AND SCHOTTKY BARRIER HEIGHT

8.9.1 Electron Affinity

Table 8.9.1 *Electron affinity χ_s for ZnSe.*

χ_s (eV)	Comment
4.09	[9.1]
3.51±0.10	Zn-rich *c*(2×2) ZnSe(100) [9.2]
4.06	Vacuum-cleaved ZnSe(110) [9.2]

[9.1] A. G. Milnes and D. L. Feucht, *Heterojunctions and Metal-Semiconductor Junctions* (Academic, New York, 1972).
[9.2] F. Xu, M. Vos, J. H. Weaver, and H. Cheng, *Phys. Rev. B* **38**, 13418 (1988).

8.9.2 Schottky Barrier Height

Table 8.9.2 *Summary of the Schottky barrier height ϕ_n for metal/n-ZnSe contacts at 300 K.**

Metal	ϕ_n (eV)	Metal	ϕ_n (eV)
Ag	1.21	Mg	0.70
Al	0.58–0.76	Pb	1.16
Au	1.36–1.55	Pd	1.48
Ce	0.50	Pt	1.40
Cu	1.10	Ti	0.75
In	0.91	Zn	0.82–0.89

*The data are gathered from various sources.

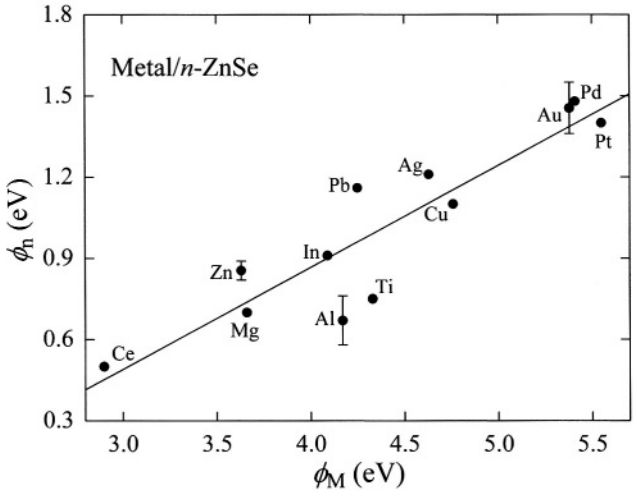

Fig. 8.9.1 Schottky barrier height ϕ_n versus metal work function ϕ_M observed for metal/*n*-ZnSe contacts. Values of the metal work function were taken from H. P. R. Frederikse [in *CRC Handbook of Chemistry and Physics,* 78th Edition, edited by D. R. Lide (CRC Press, Boca Raton, 1997), p. 12-115]. The solid line represents the least-squares-fit result with $\phi_n = 0.38\phi_M - 0.64$ (ϕ_M and ϕ_n in eV).

Table 8.9.3 *Summary of the Schottky barrier height ϕ_p for metal/p-ZnSe contacts at 300 K. I–V=current–voltage characteristics; C–V=capacitance voltage characteristics; XPS=X-ray photoelectron spectroscopy.*

Metal	ϕ_p (eV)	Measurement
Ag, Au, Cd, Cu, In, Nb, Ni, Pt, Se, Ti, W	1.2±0.1	*I–V* [9.3]
Zn	1.85	*I–V*, *C–V*, XPS [9.4]

[9.3] Y. Koide, T. Kawakami, N. Teraguchi, Y. Tomomura, A. Suzuki, and M. Murakami, *J. Appl. Phys.* **82**, 2393 (1997).
[9.4] S. Rubini, E. Pelucchi, M. Lazzarino, D. Kumer, A. Franciosi, C. Berthod, N. Binggeli, and A. Baldereschi, *Phys. Rev. B* **63**, 235307 (2001).

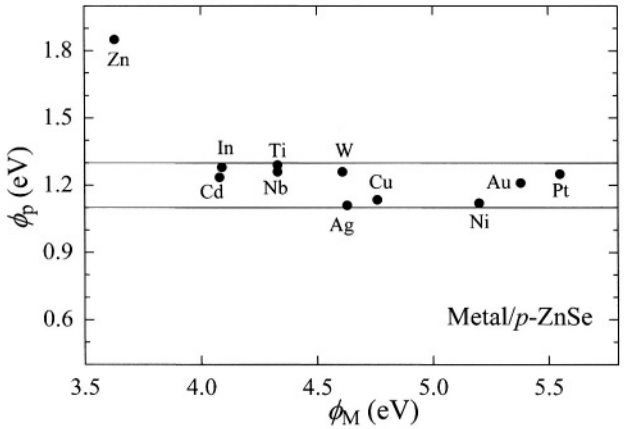

Fig. 8.9.2 Schottky barrier height for a variety of metal contacts to *p*-ZnSe at 300 K. The experimental data are taken from Y. Koide, T. Kawakami, N. Teraguchi, Y. Tomomura, A. Suzuki, and M. Murakami [*J. Appl. Phys.* **82**, 2393 (1997)] and from S. Rubini, E. Pelucchi, M. Lazzarino, D. Kumer, A. Franciosi, C. Berthod, N. Binggeli, and A. Baldereschi [*Phys. Rev. B* **63**, 235307 (2001)].The solid lines indicate the range of the barrier height ϕ_p=1.2±0.1 eV. The results suggest that the Fermi level is pinned at the metal/*p*-ZnSe interface.

8.10 OPTICAL PROPERTIES

8.10.1 Summary of Optical Dispersion Relations

- **$\varepsilon(E)$ and $n^*(E)$ spectra**

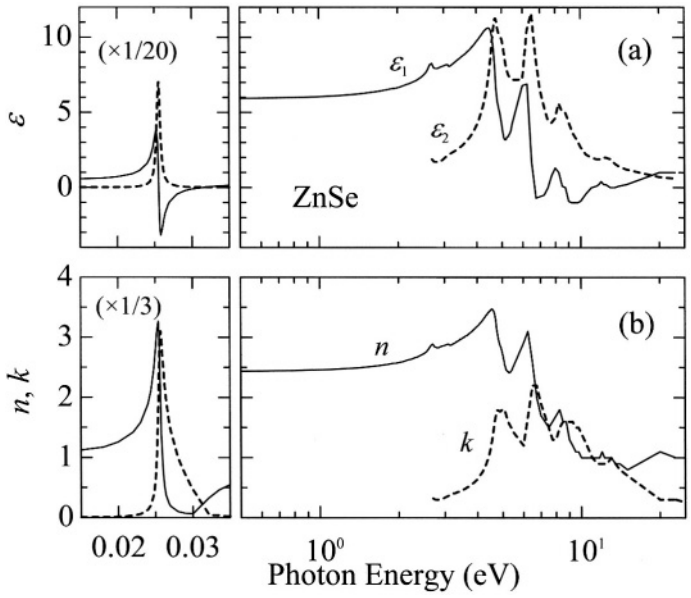

Fig. 8.10.1 (a) Complex dielectric-constant [$\varepsilon(E)=\varepsilon_1(E)+i\varepsilon_2(E)$] and (b) complex refractive-index spectra [$n^*(E)=n(E)+ik(E)$] for ZnSe at 300 K. The numerical data are taken from tabulation by S. Adachi [*Optical Constants of Crystalline and Amorphous Semiconductors: Numerical Data and Graphical Information* (Kluwer Academic, Boston, 1999)].

• **$\alpha(E)$ and $R(E)$ spectra**

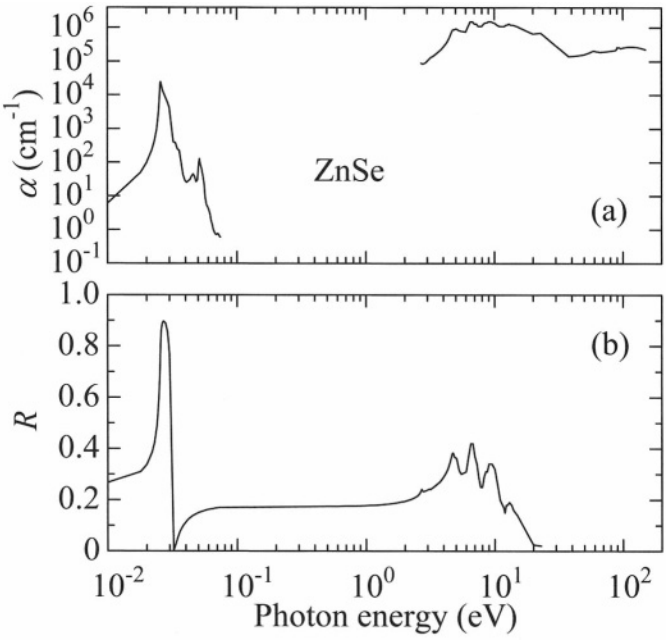

Fig. 8.10.2 (a) Absorption [$\alpha(E)$] and (b) normal-incidence reflectivity spectra [$R(E)$] for ZnSe at 300 K. The numerical data are taken from tabulation by S. Adachi [*Optical Constants of Crystalline and Amorphous Semiconductors: Numerical Data and Graphical Information* (Kluwer Academic, Boston, 1999)].

8.10.2 The Reststrahlen Region

• **Static and high-frequency dielectric constants**

Table 8.10.1 *Static and high-frequency dielectric constants ε_s and ε_∞ for ZnSe.*

ε_s	ε_∞	Comment
8.1±0.3	5.75±0.1	T=300 K [10.1]
9.12		T=298 K [10.2]
	5.90	T=300 K [10.3]
7.6	5.4	T=100, 300 K [10.4]
9.2	6.2	T=295[10.5]
9.53	6.3	T=80 K [10.6]
9.6	6.3	T=290 K [10.6]
8.68	5.6	T=2 K [10.7]
8.76	5.5	T=80 K [10.7]
8.99	5.3	T=300 K [10.7]
9.25		T=296 K [10.8]
8.6	5.9	T=300 K [10.9]
9.3	6.2	T=300 K [10.10]
8.6	5.7	T=300 K [10.11]
8.87±0.01		T=4.2 K [10.12]
8.9	5.9	Mean value at T~300 K

[10.1] M. Aven, D. T. F. Marple, and B. Segall, *J. Appl. Phys.* **32** (Suppl.), 2261 (1961).
[10.2] D. Berlincourt, H. Jaffe, and L. R. Shiozawa, *Phys. Rev.* **129**, 1009 (1963).
[10.3] D. T. F. Marple, *J. Appl. Phys.* **35**, 539 (1964).
[10.4] A. Manabe, A. Mitsuishi, and H. Yoshinaga, *Jpn. J. Appl. Phys.* **6**, 593 (1967).
[10.5] H. D. Riccius, *J. Appl. Phys.* **39**, 4381 (1968).

[10.6] A. Hadni, J. Claudel, and P. Strimer, *Phys. Status Solidi* **26,** 241 (1968).
[10.7] T. Hattori, Y. Homma, A. Mitsuishi, and M. Tacke, *Opt. Commun.* **7**, 229 (1973).
[10.8] I. Strzalkowski, S. Joshi, and C. R. Crowell, *Appl. Phys. Lett.* **28**, 350 (1976).
[10.9] A. N. Pikhtin and A. D. Yas'kov, *Sov. Phys. Semicond.* **12,** 622 (1978).
[10.10] A. Deneuville, D. Tanner, and P. H. Holloway, *Phys. Rev. B* **43**, 6544 (1991).
[10.11] S. Adachi and T. Taguchi, *Phys. Rev. B* **43**, 9569 (1991).
[10.12] K. Reimann and M. Steube, in *Proc. 25th Int. Conf. Phys. Semicond.,* edited by N. Miura and T. Ando (Springer, Berlin, 2001), p.1533.

Table 8.10.2 *Linear temperature and pressure coefficients of the static (ε_s) and high-frequency dielectric constants (ε_∞) for ZnSe.*

Coefficient	Value
$d\varepsilon_s/dT$ (10^{-3} K^{-1})	1.50±0.02 [10.13]
$d\varepsilon_\infty/dT$ (10^{-4} K^{-1})	
$d\varepsilon_s/dp$ (GPa^{-1})	
$d\varepsilon_\infty/dp$ (GPa^{-1})	–0.136±0.006 [10.14]

[10.13] I. Strzalkowski, S. Joshi, and C. R. Crowell, *Appl. Phys. Lett.* **28**, 350 (1976).
[10.14] K. Reimann and M. Steube, in *Proc. 25th Int. Conf. Phys. Semicond.,* edited by N. Miura and T. Ando (Springer, Berlin, 2001), p.1533.

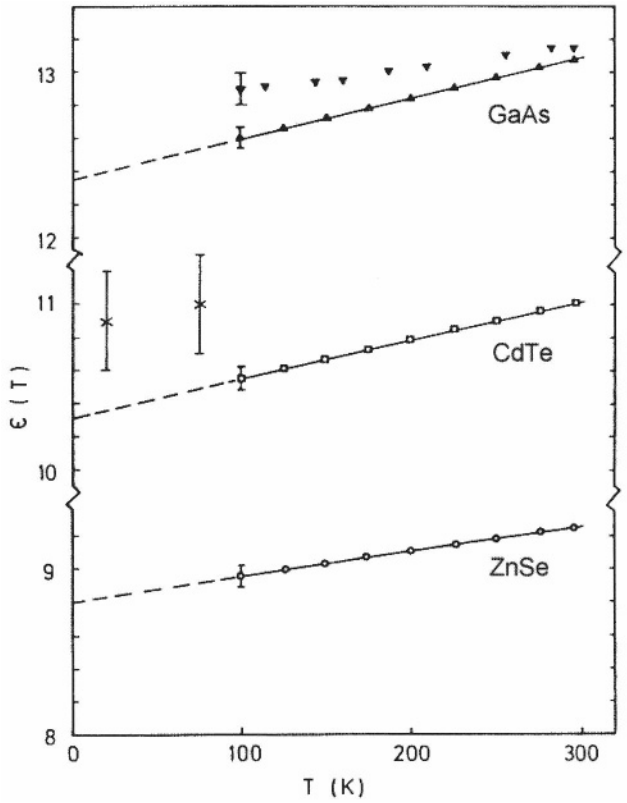

Fig. 8.10.3 Temperature dependence of the static dielectric constant ε_s (ε) for ZnSe (○), together with those for GaAs (△) and CdTe (□). The symbols are: (×) from D. de Nobel [*Philips Res. Rep.* **14**, 361 (1959)]; (▼) from K. S. Champlin and G. H. Glover [*Appl. Phys. Lett.* **12**, 23 (1968)]. [From I. Strzalkowski, S. Joshi, and C. R. Crowell, *Appl. Phys. Lett.* **28,** 350 (1976).]

- **Reststrahlen parameter**

Table 8.10.3 *A set of the reststrahlen parameters for ZnSe.*

$$\varepsilon(\omega) = \varepsilon_\infty \left(1 + \frac{\omega_{LO}^2 - \omega_{TO}^2}{\omega_{TO}^2 - \omega^2 - i\omega\gamma} \right)$$

ε_∞	ω_{LO} (cm^{-1})	ω_{TO} (cm^{-1})	γ (cm^{-1})	Comment
5.4	250	211	2.1	T=100 K [10.15]
5.4	246	207	3.7	T=300 K [10.15]
6.3	259.3	210.8	2.1	T=80 K [10.16]
6.3	252.1	204.2	4.5	T=290 K [10.16]

[10.15] A. Manabe, A. Mitsuishi, and H. Yoshinaga, *Jpn. J. Appl. Phys.* **6**, 593 (1967).
[10.16] A. Hadni, J. Claudel, and P. Strimer, *Phys. Status Solidi* **26**, 241 (1968).

- **Multiphonon optical absorption spectra**

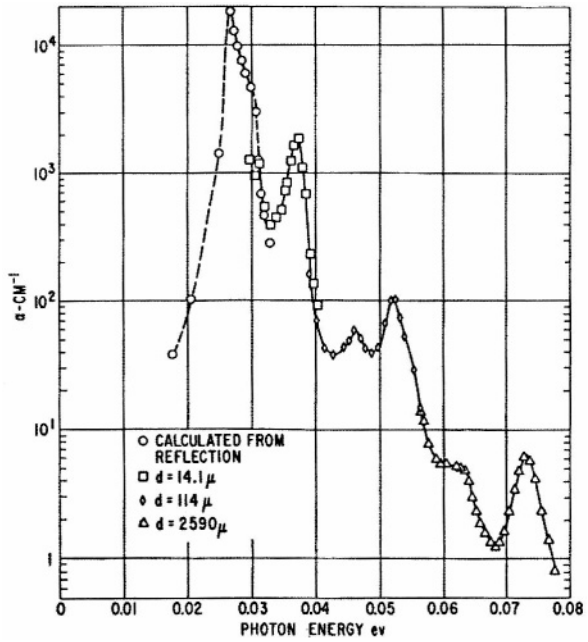

Fig. 8.10.4 Absorption coefficient α for ZnSe in the infrared region as a function of photon energy at room temperature. [From M. Aven, D. T. F. Marple, and B. Segall, *J. Appl. Phys.* **32** (Suppl.), 2261 (1961).]

8.10.3 At or Near the Fundamental Absorption Edge

- **Free-exciton binding energy and related parameters**

Table 8.10.4 *Free-exciton binding (Rydberg) energy G for ZnSe.*

G (meV)	Comment
20±4	T=23 K [10.17]
21	T=2 K [10.18]
19.9±0.7	T=1.6 K [10.19]
18	T=4.2 K [10.20]
17.4±0.4	T=4.2 K [10.21]

Table 8.10.4 *Continued.*

G (meV)	Comment
20.2	T=2 K [10.22]
18.7±0.1	T=6 K [10.23]
20.1	T=1.7 K [10.24]
20.0±0.3	T=2–280 K [10.25]
22.0±0.5	T=1.5 K [10.26]
18.86±0.02	T=4.2 K [10.27]

[10.17] M. Aven, D. T. F. Marple, and B. Segall, *J. Appl. Phys.* **32** (Suppl.), 2261 (1961).
[10.18] G. E. Hite, D. T. F. Marple, M. Aven, and B. Segall, *Phys. Rev.* **156**, 850 (1967).
[10.19] M. Sondergeld and R. G. Stafford, *Phys. Rev. Lett.* **35**, 1529 (1975).
[10.20] G. Röppischer, I. Jacobs, and B. V. Novikov, *Sov. Phys. Solid State* **17**, 1442 (1976).
[10.21] H. Venghaus, *Phys. Rev. B* **19**, 3071 (1979).
[10.22] G. N. Aliev, N. P. Gavaleshko, O. S. Koshchug, V. I. Pleshko, R. P. Seĭsyan, and K. D. Sushkevich, *Sov. Phys. Solid State* **34**,1286 (1992).
[10.23] See, A. Mang, K. Reimann, St. Rübenacke, and M. Steube, *Phys. Rev. B* **53**, 16283 (1996).
[10.24] G. N. Aliev, R. M. Datsiev, S. V. Ivanov, P. S. Kop'ev, R. P. Seisyan, and S. V. Sorokin, *J. Cryst. Growth* **159**, 523 (1996).
[10.25] R. Pässler, F. Blaschta, E. Griebl, K. Papagelis, B. Haserer, T. Reisinger, S. Ves, and W. Gebhardt, *Phys. Status Solidi B* **204**, 685 (1997).
[10.26] S. Lee, F. Michl, U. Rössler, M. Dobrowolska, and J. K. Furdyna, *Phys. Rev. B* **57**, 9695 (1998).
[10.27] K. Reimann and M. Steube, in *Proc. 25th Int. Conf. Phys. Semicond.,* edited by N. Miura and T. Ando (Springer, Berlin, 2001), p.1533.

Table 8.10.5 *Free-exciton parameters (G=binding energy; a_B=1st-orbital Bohr radius; μ=reduced mass) at the fundamental absorption edge of ZnSe [10.28].*

G (meV)	a_B (Å)	μ (m_0)	Comment
18.7	41	0.119	Direct exciton

[10.28] From tabulation by S. Adachi [*Optical Properties of Crystalline and Amorphous Semiconductors: Materials and Fundamental Properties* (Kluwer Academic, Boston, 1999)].

Table 8.10.6 *Spin-exchange interaction constant j for ZnSe [10.29].*

j (meV)
1.0

[10.29] See, M. Julier, J. Campo, B. Gil, J. P. Lascaray, and S. Nakamura, *Phys. Rev. B* **57**, R6791 (1998); D. W. Langer, R. N. Euwema, K. Era, and T. Koda, *Phys. Rev. B* **2**, 4005 (1970).

Table 8.10.7 *Pressure coefficient of the free-exciton binding (Rydberg) energy for ZnSe [10.30].*

$\frac{dG}{dp}$ (meV/GPa)
0.66±0.01

[10.30] K. Reimann and M. Steube, in *Proc. 25th Int. Conf. Phys. Semicond.,* edited by N. Miura and T. Ando (Springer, Berlin, 2001), p. 1533.

● **Refractive index**

Table 8.10.8 *Refractive index n near the fundamental absorption edge of ZnSe at 300 K [10.31].*

E (eV)	λ (μm)	n	E (eV)	λ (μm)	n
0.5	2.479	2.436	1.95	0.636	2.57
0.6	2.066	2.440	2	0.620	2.58
0.7	1.771	2.444	2.05	0.605	2.59
0.8	1.549	2.448	2.1	0.590	2.60
0.9	1.377	2.454	2.15	0.577	2.62
1	1.240	2.460	2.2	0.563	2.63
1.1	1.127	2.467	2.25	0.551	2.64
1.2	1.033	2.475	2.3	0.539	2.66
1.3	0.953	2.484	2.35	0.527	2.67
1.4	0.885	2.494	2.4	0.516	2.69
1.5	0.826	2.505	2.45	0.506	2.71
1.6	0.775	2.518	2.5	0.496	2.73
1.7	0.729	2.532	2.55	0.486	2.76
1.8	0.689	2.548	2.6	0.477	2.80
1.9	0.652	2.566	2.65	0.468	2.86

[10.31] See, S. Adachi, *Optical Constants of Crystalline and Amorphous Semiconductors: Numerical Data and Graphical Information* (Kluwer Academic, Boston, 1999).

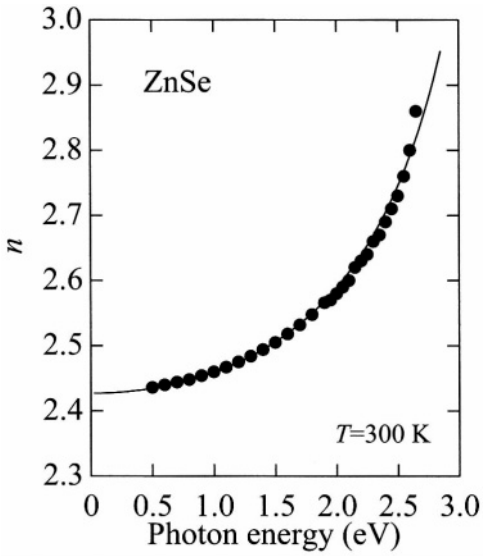

Fig. 8.10.5 Refractive index n for ZnSe. The experimental data are taken from S. Adachi [*Optical Constants of Crystalline and Amorphous Semiconductors: Numerical Data and Graphical Information* (Kluwer Academic, Boston, 1999)]. The solid line represents the calculated result using $n^2=3.86+[2.03\lambda^2/(\lambda^2-0.110)]$ with λ in μm.

● **Refractive index: Temperature dependence**

Table 8.10.9 *Temperature coefficient of the refractive index $n^{-1}(dn/dT)$ in the long-wavelength limit for ZnSe [10.32].*

$\frac{1}{n}\frac{dn}{dT}$ $(10^{-5}\ K^{-1})$
2.6

[10.32] See, S. Adachi, *Optical Properties of Crystalline and Amorphous Semiconductors: Materials and Fundamental Properties* (Kluwer Academic, Boston, 1999).

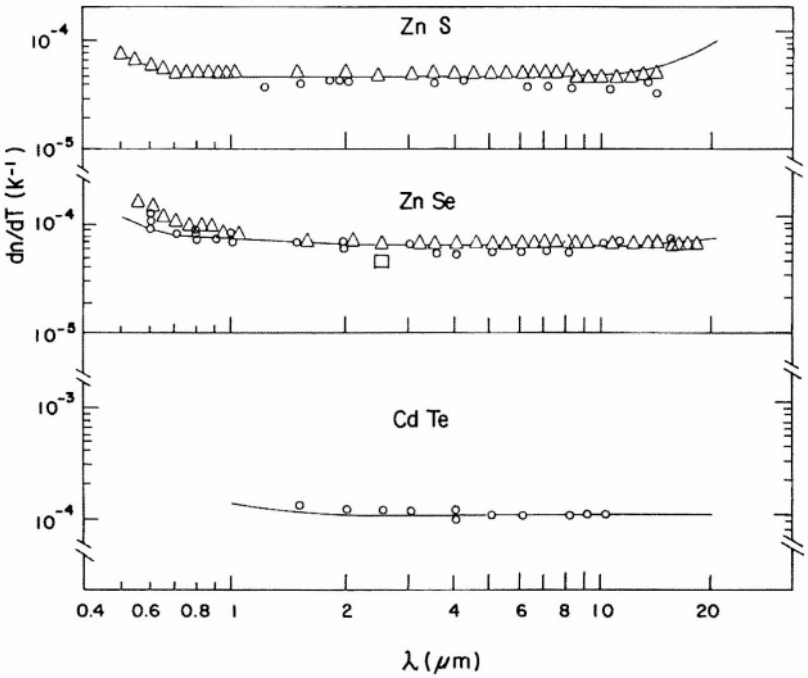

Fig. 8.10.6 Temperature coefficient of the refractive index *dn/dT* for ZnSe, together with those for β-ZnS and CdTe. [From M. Bertolotti, V. Bogdanov, A. Ferrari, A. Jascow, N. Nazorova, A. Pikhtin, and L. Schirone, *J. Opt. Soc. Am. B* **7**, 918 (1990).]

• Fundamental absorption edge: Temperature dependence

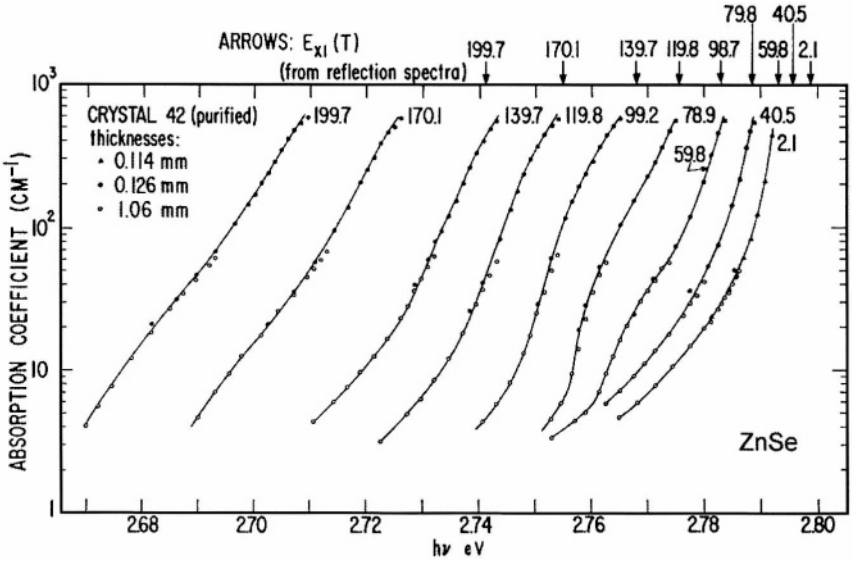

Fig. 8.10.7 Absorption coefficient measured for bulk ZnSe at various temperatures. The ZnSe single crystals used in this experiment were purified with liquid zinc. Energies for maximum absorption by n=1 excitons are indicated by vertical arrows for various temperatures. [From G. E. Hite, D. T. F. Marple, M. Aven, and B. Segall, *Phys. Rev.* **156,** 850 (1967).]

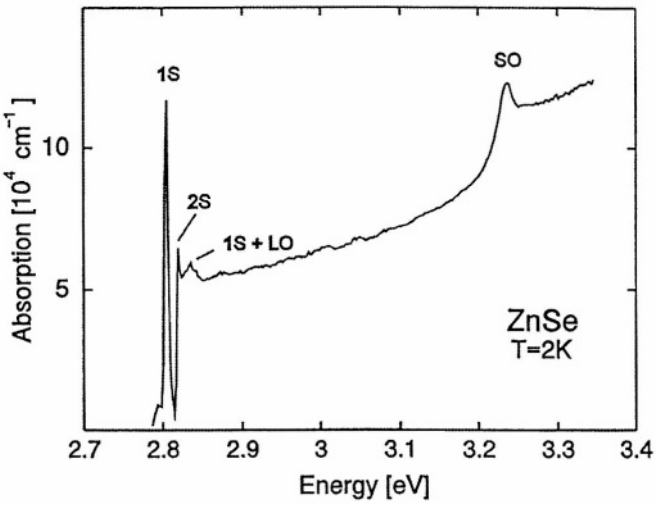

Fig. 8.10.8 Optical absorption of a free-standing MBE-grown ZnSe epilayer of thickness d=0.40 μm with peaks of Is and 2*s* excitons, the 1*s*+1LO-phonon and spin–orbit–splitoff (SO) excitons at $E_0+\Delta_0$. [From W. Gebhardt and G. Schötz, in *Properties of Wide Bandgap II–VI Semiconductors,* EMIS Datareviews Series No. 17, edited by R. Bhargava (INSPEC, London, 1997), p. 113.]

- **Fundamental absorption edge: Pressure dependence**

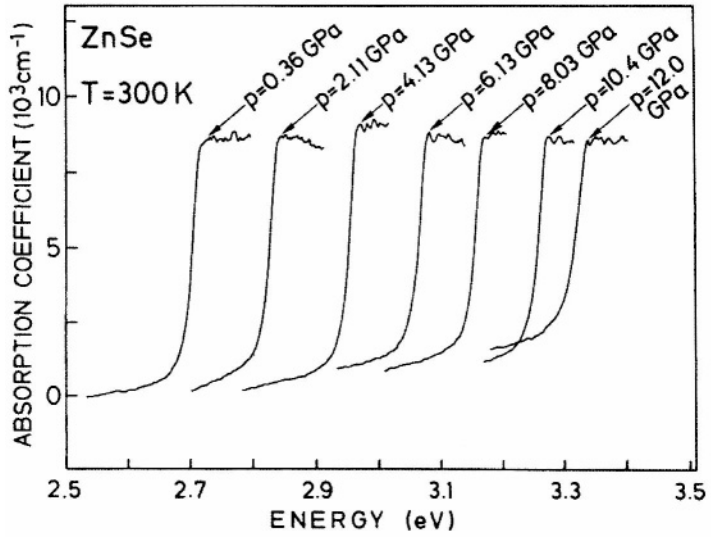

Fig. 8.10.9 Absorption coefficient α in ZnSe near the E_0 edge at different hydrostatic pressures. The arrows indicate the energy position taken to be the "exciton edge" at the given pressure. [From S. Ves, K. Strössner, N. E. Christensen, C. K. Kim, and M. Cardona, *Solid State Commun.* **56**, 479 (1985).]

8.10.4 The Interband Transition Region

- **Fundamental optical spectra**

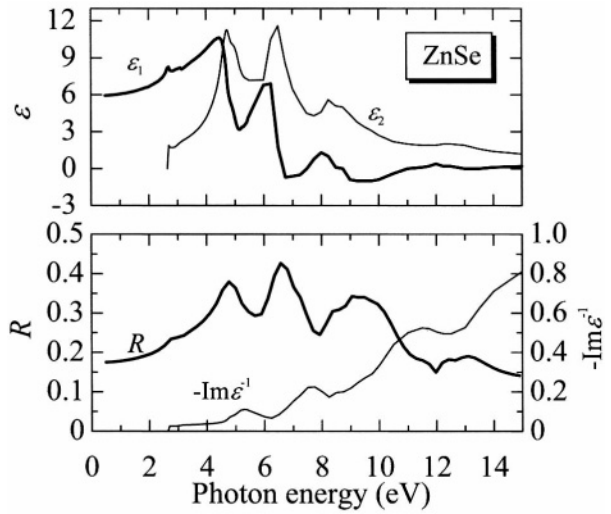

Fig. 8.10.10 Complex dielectric function, $\varepsilon(E)=\varepsilon_2(E)+i\varepsilon_2(E)$, fundamental reflectivity, $R(E)$, and energy-loss function, $-\mathrm{Im}\varepsilon^{-1}(E)$, for ZnSe at 300 K. The experimental data are taken from tabulation by S. Adachi [*Optical Constants of Crystalline and Amorphous Semiconductors: Numerical Data and Graphical Information* (Kluwer Academic, Boston, 1999)].

• **$\varepsilon(E)$ spectrum: External perturbation and/or doping effects**

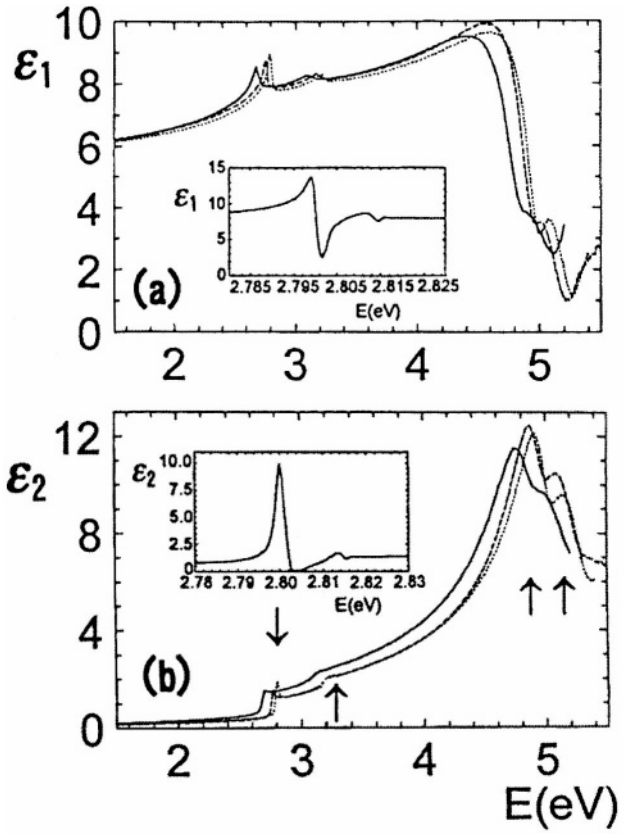

Fig. 8.10.11 (a) Real and (b) imaginary parts of the dielectric function $\varepsilon(E)$ of ZnSe measured at T=20 K. (·····), 145 K (- - -), and 292 K (—). The inset gives a blowup of ε_1 and ε_2 around the fundamental gap at 20 K. [From R. Granger, J. T. Benhlal, O. Ndap, and R. Triboulet, *Eur. Phys. J. B* **13**, 429 (2000).]

8.10.5 Free-Carrier Absorption and Related Phenomena

No detailed data are available for ZnSe.

8.11 ELASTOOPTIC, ELECTROOPTIC, AND NONLINEAR OPTICAL PROPERTIES

8.11.1 Elastooptic Effect

• **Photoelastic constant**

Table 8.11.1 *Photoelastic constant p_{ij} in the static limit ($E \to 0$ eV) for ZnSe.*

$p_{11}-p_{12}$	p_{44}
−0.08	−0.08

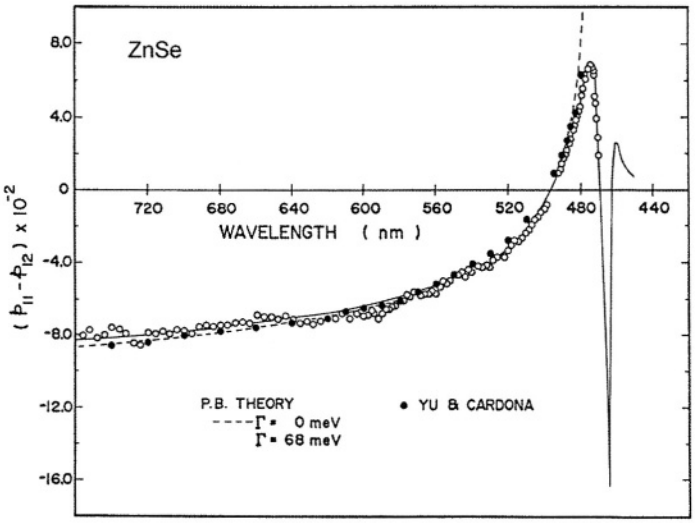

Fig. 8.11.1 Dispersion of the photoelastic constant $p_{11}-p_{12}$ in ZnSe determined by Brillouin scattering at 300 K. The dashed and solid lines are theoretically obtained without and with considering damping effect (Γ), respectively. The piezobirefringence data measured by P. Y. Yu and M. Cardona [*J. Phys. Chem. Solids* **34**, 29 (1973)] are also shown by the solid circles. [From S. Adachi and C. Hamaguchi, *Phys. Rev. B* **19**, 938 (1979).]

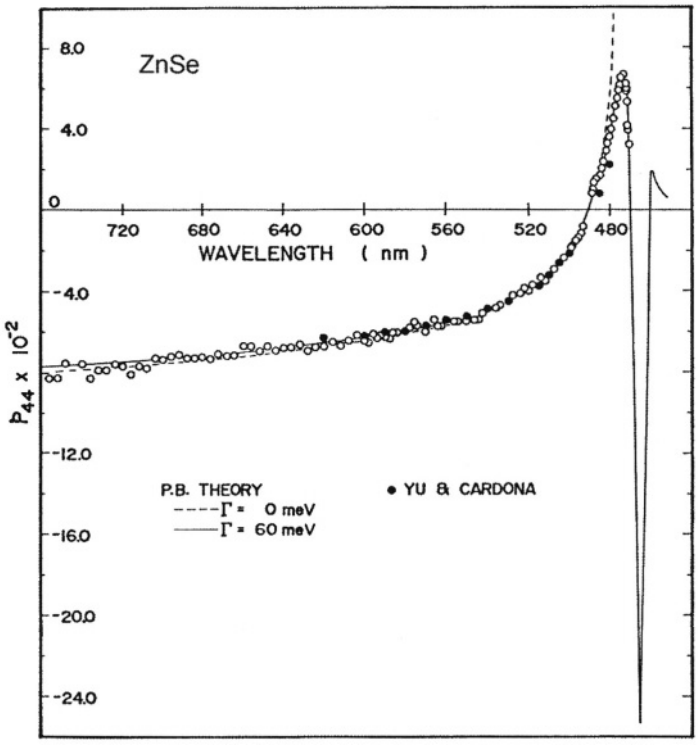

Fig. 8.11.2 Dispersion of the photoelastic constant p_{44} in ZnSe determined by Brillouin scattering at 300 K. The dashed and solid lines are theoretically obtained without and with considering damping effect (Γ), respectively. The piezobirefringence data measured by P. Y. Yu and M. Cardona [*J. Phys. Chem. Solids* **34**, 29 (1973)] are also shown by the solid circles. [From S. Adachi and C. Hamaguchi, *Phys. Rev. B* **19**, 938 (1979).]

8.11.2 Linear Electrooptic Constant

Table 8.11.2 *Free (r_{41}^T) and clamped values (r_{41}^S) of the linear electrooptic constant for ZnSe.*

Wavelength (μm)	r_{41}^T (pm/V)	r_{41}^S (pm/V)	Ref.
0.478	−1.5		[11.1]
0.488	−1.7		[11.1]
0.497	−1.8		[11.1]
0.502	−1.8		[11.1]
0.515	−1.9		[11.1]
0.546	2.0 ($\lvert r_{41}^T \rvert$)		[11.2]
0.633	−2.2		[11.1]
		2.0 ($\lvert r_{41}^S \rvert$)	[11.2]
10.6	2.2 ($\lvert r_{41}^T \rvert$)		[11.2]

[11.1] K. Kikuchi and K. Tada, *Jpn. J. Appl. Phys.* **17**, 825 (1978).
[11.2] See, I. P. Kaminow and E. H. Turner, in *Handbook of Lasers,* edited by R. J. Pressley (Chemical Rubber, Cleveland, 1971), Chap. 15.

- **Temperature dependence**

Table 8.11.3 *Temperature coefficient of the linear electrooptic constant $(1/r_{41})(dr_{41}/dT)$ for ZnSe.*

$\frac{1}{r_{41}}\frac{dr_{41}}{dT}$ (10^{-4} K^{-1})	Comment
15	λ=0.6328 μm [11.3]

[11.3] T. G. Okroashvili, *Opt. Spectrosc.* **47**, 442 (1979).

8.11.3 Quadratic Electrooptic Constant

No detailed data are available for ZnSe.

8.11.4 Franz–Keldysh Effect

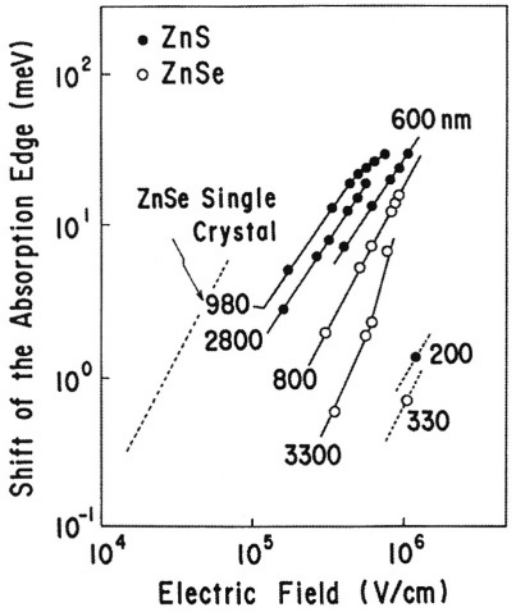

Fig. 8.11.3 Electric-field (E) dependence of the absorption-edge shift (ΔE_0) in polycrystalline ZnSe and ZnS films (200–3300 nm thick), together with that in single-crystalline ZnSe. The plots can be expressed by $\Delta E_0 = AE^n$ with n=1.9 (ZnSe) and 1.6 (ZnS), respectively. [From K. Hirabayashi and K. Ono, *Jpn. J. Appl. Phys.* **29**, L1672 (1990).]

8.11.5 Nonlinear Optical Constant

• Second-order nonlinear optical susceptibility

Table 8.11.4 *Experimental second-order nonlinear optical susceptibility d_{14} for ZnSe.*

Wavelength, in μm (Energy, in eV)	d_{14} *	Ref.
0.852 (1.455)	53.8 (pm/V)	[11.4]
1.047 (1.184)	43 (pm/V)	[11.5]
1.064 (1.165)	33 (pm/V)	[11.6]
1.321 (0.938)	30 (pm/V)	[11.5]
10.6 (0.117)	18.7 (10^{-8} esu)	[11.7]

[11.4] I. Shoji, T. Kondo, A. Kitamoto, M. Shirane, and R. Ito, *J. Opt. Soc. Am. B* **14**, 2268 (1997).
[11.5] H. P. Wagner, M. Kühnelt, W. Langbein, and J. M. Hvam, *Phys. Rev. B* **58**, 10494 (1998).
[11.6] Y. Hase, K. Kumata, S. S. Kano, M. Ohashi, T. Kondo, R. Ito, and Y. Shiraki, *Appl. Phys. Lett.* **61**, 145 (1992).
[11.7] C. K. N. Patel, *Phys. Rev. Lett.* **16**, 613 (1966).
*1 m/V=$3\times10^4/4\pi$ esu.

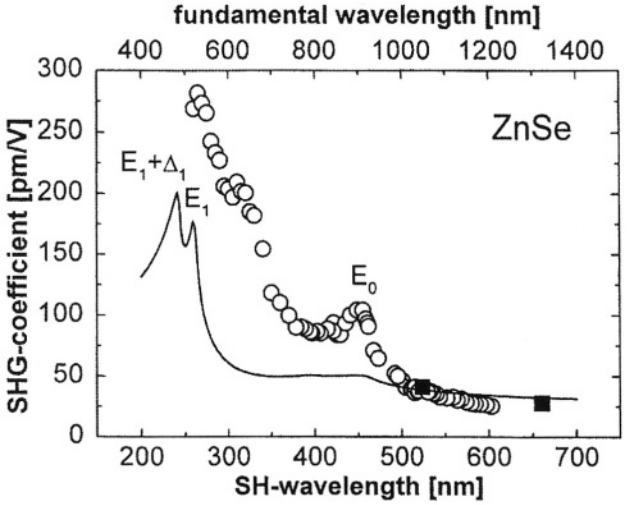

Fig. 8.11.4 Experimental dispersion of the second-harmonic-generation (SHG) coefficient $|d_{14}|$ in ZnSe as a function of fundamental wavelength. The solid line gives the theoretical dispersion curve. [From H. P. Wagner, M. Kühnelt, W. Langbein, and J. M. Hvam, *Phys. Rev. B* **58**, 10494 (1998).]

• Third-order nonlinear optical susceptibility

Table 8.11.5 *Experimental third-order nonlinear optical susceptibility $\chi^{(3)}(\omega)$ observed in ZnSe [11.8].*

Wavelength (μm)	$\lvert\chi^{(3)}(\omega)\rvert$ (10^{-11} esu)*
0.532	1.9±0.57
1.064	1.2±0.35

[11.8] E. J. Canto-Said, D. J. Hagan, J. Young, and E. W. Van Stryland, *IEEE Quantum Electron.* **27**, 2274 (1991).
*1 $m^2/V^2=9\times10^8/4\pi$ esu.

Table 8.11.6 *Theoretical third-order nonlinear optical susceptibility* $\chi^{(3)}_{ijkl}(-3\omega;\omega,\omega,\omega)$ *in the static limit* ($\hbar\omega \to 0$ *eV) for ZnSe.*

$\chi^{(3)}_{ijkl}$ (10^{-11} esu)*		Ref.
$\chi^{(3)}_{1111}$	$\chi^{(3)}_{1212}$	
0.02	0.11	[11.9]
0.55	0.33	[11.10]

[11.9] Ed Ghahramani, D. J. Moss, and J. E. Sipe, *Phys. Rev. B* **43**, 9700 (1991).
[1 1.10] W. Y. Ching and M.-Z. Huang, *Phys. Rev. B* **47**, 9479 (1993).
*1 $m^2/V^2 = 9\times10^8/4\pi$ esu.

• Two-photon optical absorption

Table 8.11.7 *Two-photon absorption coefficient* β *for ZnSe.*

Wavelength (μm)	β (cm/GW)	Ref.
0.532	5.5	[11.11]
	5.8	[11.12]
0.61	2.4	[11.13]
0.6943	45	[11.14]
	17000	[11.15]
	80	[11.16]
0.78	3.5	[11.13]
1.27	<0.005*	[11.13]

[11.11] E. W. Van Stryland, H. Vanherzeele, M. A. Woodall, M. J. Soileau, A. L. Smirl, S. Guha, and T. F. Boggess, *Opt. Eng.* **24**, 613 (1985).
[11.12] A. A. Said, M. Sheik-Bahae, D. J. Hagan, T. H. Wei, J. Wang, J. Young, and E. W. Van Stryland, *J. Opt. Soc. Am. B* **9**, 405 (1992).
[11.13] T. D. Krauss and F. W. Wise, *Appl. Phys. Lett.* **65**, 1739 (1994).
[11.14] M. S. Brodin and D. B. Goer, *Sov. Phys.–Semicond.* **5**, 219 (1971).
[11.15] G. Kobbe and C. Klingshirn, *Z. Phys. B* **37**, 9 (1980).
[11.16] I. M. Catalano and A. Cingolani, *Solid State Commun.* **43**, 213 (1982).
*Indicating that the signal was below the sensitivity of the experiment.

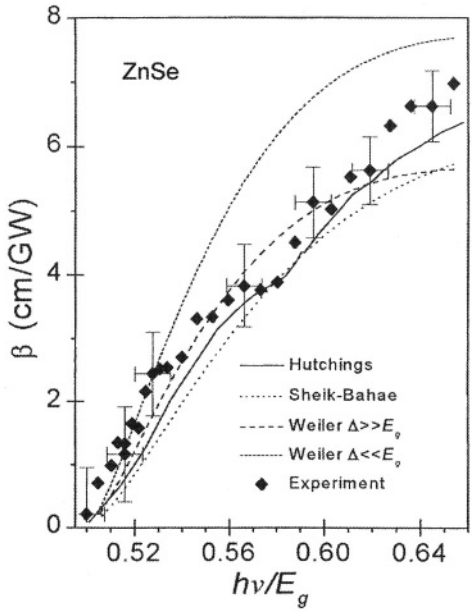

Fig. 8.11.5 Two-photon absorption coefficient β in ZnSe at room temperature. Symbols represent the measured values. Horizontal error bars account for the spread in the value of the ZnSe energy gap. Lines show the predictions of different theoretical models. [From M. Dabbicco and M. Brambilla, *Solid State Commun.* **114**, 515 (2000).]

8.12 CARRIER TRANSPORT PROPERTIES

8.12.1 Low-Field Mobility: Electrons

Table 8.12.1 *300-K (μ_{300K}) and peak Hall mobilities (μ_{peak}) for electrons in ZnSe.*

Mobility	Value ($cm^2/V\,s$)	Comment
μ_{300K}	1500	[12.1]
μ_{peak}	1.36×10^4 (1.2×10^4)	Dark (light), T=55.6 K [12.2]
	2.3×10^5	Cyclotron mobility, T=4.2 K [12.3]

[12.1] S. G. Parker, J. E. Pinnell, and L. N. Swink, *J. Phys. Chem. Solids* **32**,139 (1971).
[12.2] M. Aven, *J. Appl. Phys.* **42**, 1204 (1971).
[12.3] T. Ohyama, E. Otsuka, T. Yoshida, M. Isshiki, and K. Igaki, *Jpn. J. Appl. Phys.* **23**, L382 (1984).

- **Temperature dependence**

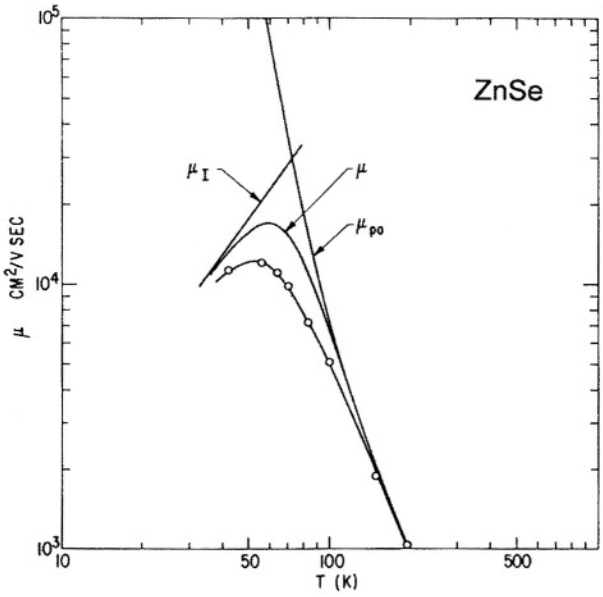

Fig. 8.12.1 Electron Hall mobility μ versus temperature T for n-type ZnSe as compared to the mobility as limited by charged impurity scattering (μ_I) and polar optical scattering (μ_{po}). The curve marked (μ) represents the resultant mobility using Matthiessen's rule. [From M. Aven, *J. Appl. Phys.* **42**, 1204 (1971).]

- **Donor concentration (free-carrier) dependence**

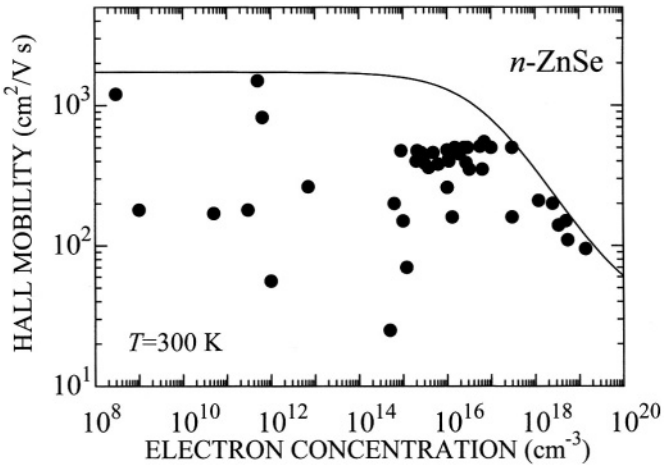

Fig. 8.12.2 Electron Hall mobility μ versus electron concentration n in n-ZnSe at 300 K. The experimental data are gathered from various sources. The solid line represents the calculated result with

$$\mu = 30 + 1700/[1 + (n/7\times10^{16})^{0.55}]\ ,$$

where n is in cm^{-3} and μ is in $cm^2/V\,s$.

• **Hall factor**

The Hall factor for ZnSe has been obtained theoretically by D. L. Rode [*Phys. Status Solidi B* **55**, 687 (1973)], and its value is reported to be $\gamma \sim 1.13$ at T=300 K.

8.12.2 Low-Field Mobility: Holes

Table 8.12.2 *300-K (μ_{300K}) and peak Hall mobilities (μ_{peak}) for holes in ZnSe.*

Mobility	Value ($cm^2/V\,s$)	Comment
μ_{300K}	355	[12.4]
μ_{peak}	596	T=77 K [12.5]

[12.4] H. Goto, T. Ido, and A. Takatsuka, *J. Cryst. Growth* **214/215**, 529 (2000).
[12.5] Y. Fan, J. Han, L. He, J. Saraie, R. L. Cunshor, M. Hagerott, and A. V. Nurmikko, *Appl. Phys. Lett.* **63**, 1812 (1993).

• **Temperature dependence**

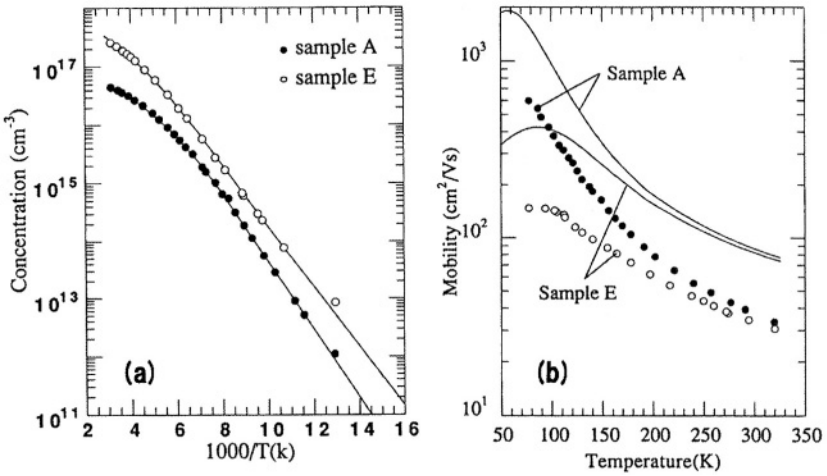

Fig. 8.12.3 Temperature variation of (a) hole carrier concentration p and (b) Hall mobility μ for two p-type ZnSe samples. The solid lines in (b) show the theoretical results. [From Y. Fan, J. Han, L. He, J. Saraie, R. L. Gunshor, M. M. Hagerott, and A. V. Nurmikko, *Appl. Phys. Lett.* **63**, 1812 (1993).]

• **Acceptor concentration (free-carrier) dependence**

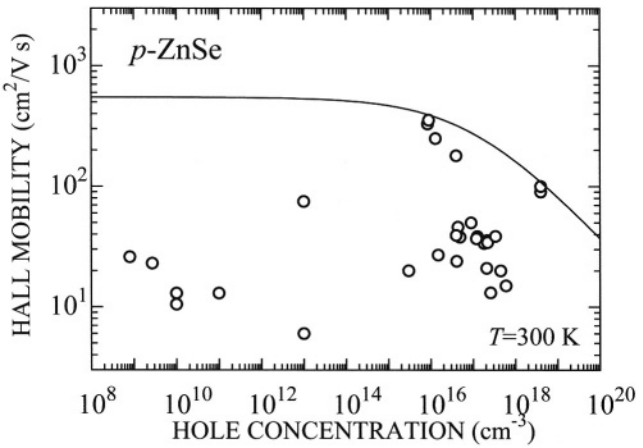

Fig. 8.12.4 Hole Hall mobility μ versus hole concentration p in p-ZnSe at 300 K. The experimental data are gathered from various sources. The solid line represents the calculated result with $\mu = 550/[1+(p/10^{17})^{0.38}]$, where p is in cm^{-3} and μ is in $cm^2/V\,s$.

8.12.3 High-Field Transport: Electrons

• Electron scattering rate

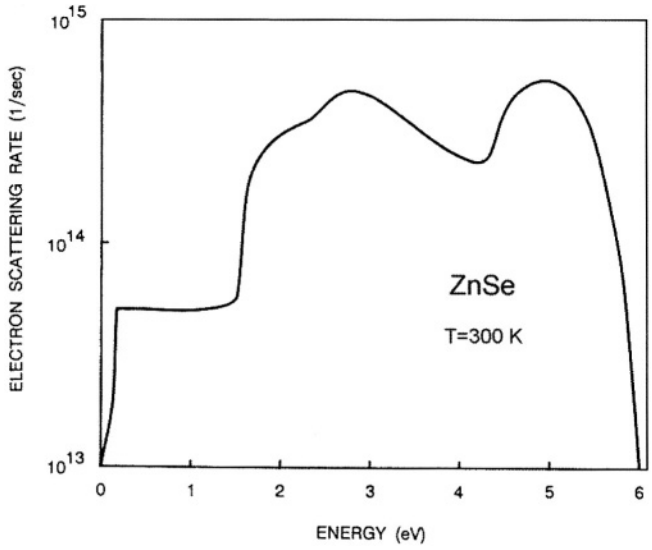

Fig. 8.12.5 Total electron–phonon scattering rate in ZnSe as a function of electron energy at 300 K. Impact ionization is not included in the calculation. [From K. Brennan, *J. Appl. Phys.* **64**, 4024 (1988).]

• Electron drift mobility and velocity–field characteristic

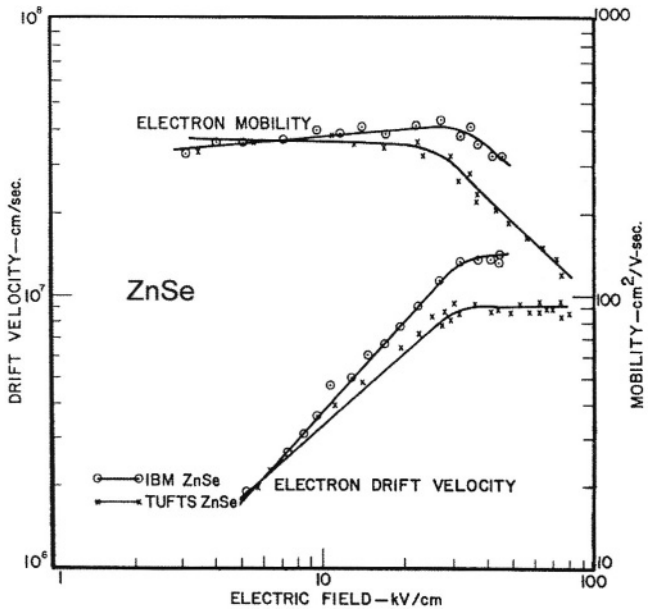

Fig. 8.12.6 Electron drift velocity and mobility versus electric field in IBM-(n~10^{13} cm^{-3}) and Tufts-grown ZnSe (n~10^{12} cm^{-3}). [From J. L. Heaton III, G. H. Hammond, and R. B. Goldner, *Appl. Phys. Lett.* **20**, 333 (1972).]

• LO-phonon-scattering-limited electron saturation drift velocity

Table 8.12.3 *Calculated LO-phonon-scattering-limited electron saturation drift velocity $v_{e,sat}$ in the lowest-conduction-band valley α for ZnSe at 300 K.**

$$v_{e,sat}^{\alpha} = \left(\frac{8\hbar\omega_{LO}}{3\pi m_c^{\alpha}}\right)^{1/2}$$

Valley	$v_{e,sat}$ (10^7 cm/s)
Γ	1.8

*Calculated with $m_c^{\Gamma}=0.137m_0$ and $\omega_{LO}=252$ cm^{-1}.

8.12.4 High-Field Transport: Holes

• Hole drift velocity–field characteristic

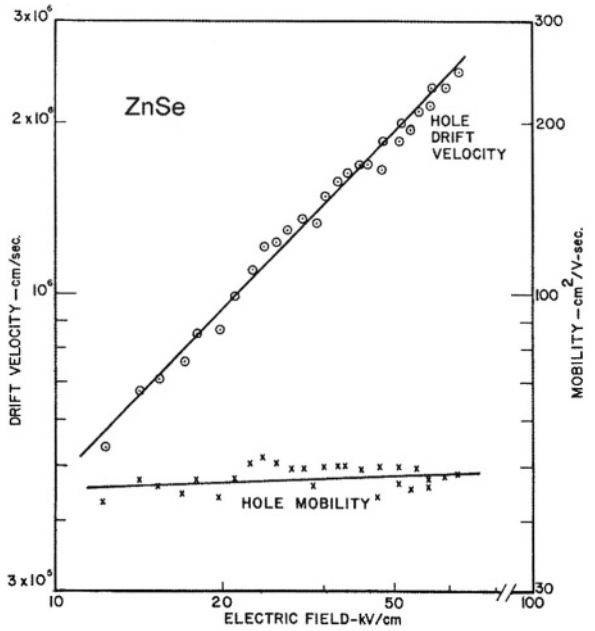

Fig. 8.12.7 Hole drift velocity and mobility versus electric field in Bell Telephone Laboratories vapor-"mineralization"-grown ZnSe (p~10^{11} cm^{-3}). [From J. L. Heaton III, G. H. Hammond, and R. B. Goldner, *Appl. Phys. Lett*. **20**, 333 (1972).]

8.12.5 Minority-Carrier Transport: Electrons in *p*-Type Materials

No detailed data are available for ZnSe.

8.12.6 Minority-Carrier Transport: Holes in *n*-Type Materials

• Minority-hole lifetime and diffusion length: Room-temperature values

Table 8.12.4 *Minority-hole lifetime τ and diffusion length L in n-ZnSe at room temperature.*

τ (s)	L (μm)	Comment
	0.5	n~10^{16} cm^{-3} [12.6]
2×10^{-9} *	0.45±0.07	σ=2 Ω^{-1}·cm^{-1} [12.7]
	0.025	n=7×10^{17} cm^{-3} [12.8]
	1.20	n=2×10^{15} cm^{-3} [12.9]
	0.15	n=2×10^{16} cm^{-3} [12.9]
	0.06	n=1×10^{17} cm^{-3} [12.9]
	0.025	n=6×10^{17} cm^{-3} [12.9]
	0.017	n=1×10^{18} cm^{-3} [12.9]
7×10^{-8}	0.80	N_D=1.04×10^{16} cm^{-3} [12.10]
	0.017	N_D=3.2×10^{17} cm^{-3} [12.11]
	0.011	N_D=3×10^{18} cm^{-3} [12.11]
5×10^{-11} *	0.08	N_D=3×10^{17} cm^{-3} [12.12]
	0.075	N_D=2.9×10^{17} cm^{-3} [12.13]
	0.1	n=1.6×10^{17} cm^{-3} [12.14]
	0.06	n=9.0×10^{17} cm^{-3} [12.14]

[12.6] R. Mach and W. Ludwig, *Phys. Status Solidi A* **23**, 507 (1974).
[12.7] S. Mora, N. Romeo, and L. Tarricone, *Solid State Commun.* **33**, 1147 (1980).

[12.8] A. Etchebery, M. Etman, B. Fotouhi, J. Gautron, J.-L. Sculfort, and P. Lemasson, *J. Appl. Phys.* **53**, 8867 (1982).
[12.9] J. Gautron and P. Lemasson, *J. Cryst. Growth* **59**, 332 (1982).
[12.10] H. Takenoshita and T. Nakau, *Jpn. J. Appl. Phys.* **22**, 1570 (1983).
[12.11] J. O. Williams, E. S. Crawford, B. Miller, A. M. Patterson, and M. D. Scott, *J. Phys. D: Appl. Phys.* **16**, 2297 (1983).
[12.12] A. P. Okonechnikov and N. N. Mel'nik, *Sov. Phys. Semicond.* **23**, 562 (1989).
[12.13] A. P. Okonechnikov, N. N. Mel'nik, and F. F. Gavrilov, *Sov. Phys. Semicod.* **24**, 470 (1990).
[12.14] J. Zheng and J. W. Allen, *J. Cryst. Growth* **138**, 477 (1994).
*Obtained assuming μ=50 cm^2/V s.

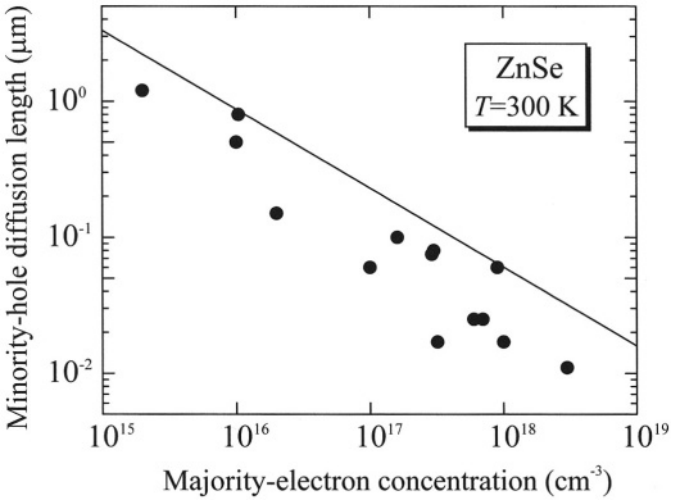

Fig. 8.12.8 Minority-hole diffusion length (L) versus majority-electron concentration (n) in n-type ZnSe. The experimental data are gathered from various sources. The solid line represents the calculated relation of $L=(n/10^{15.9})^{-0.58}$.

• Minority-hole diffusion length: External perturbation effect

Influence of temperature and ion irradiation on the minority-hole diffusion length in n-ZnSe has been studied by A. P. Okonechnikov and N. N. Mel'nik [*Sov. Phys. Semicond.* **23**, 562 (1989)] and by A. P. Okonechnikov, N. N. Mel'nik, and F. F. Gavrilov [*Sov. Phys. Semicod.* **24**, 470 (1990)], respectively.

8.12.7 Impact Ionization Coefficient

• Electric-field dependence

Table 8.12.5 *Impact ionization parameter for electrons (α) and holes (β) in ZnSe.*

$$\alpha(E) \text{ or } \beta(E) = A\exp-\left(\frac{B}{E}\right)$$

Parameter		Comment
A (10^7 cm^{-1})	B (10^6 V/cm)	
4.2	4.23	Electrons, $5.5\times10^5<E<7\times10^5$ V/cm [12.5]

[12.5] R. Mach and W. Ludwig, *Phys. Status Solidi A* **23**, 507 (1974).

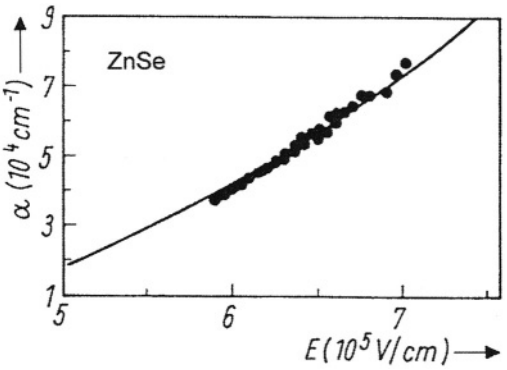

Fig. 8.12.9 Electric-filed dependence of the impact ionization coefficient (α) for electrons in ZnSe. The solid circles show the experimental points, while the solid line represents the theoretical curve obtained with threshold energy and mean free path for electron–phonon scattering as fitting parameters. [From R. Mach and W. Ludwig, *Phys. Status Solidi A* **23**, 507 (1974).]

Chapter 9

Zinc Telluride (ZnTe)

9.1 STRUCTURAL PROPERTIES

9.1.1 Ionicity

Table 9.1.1 *Phillips's ionicity f_i for ZnTe [1.1].*

f_i
0.609

[1.1] J. C. Phillips, *Bonds and Bands in Semiconductors* (Academic, New York, 1973).

9.1.2 Elemental Isotopic Abundance and Molecular Weight

- **Isotopic abundance**

Table 9.1.2 *Isotopic abundance in percent for zinc and tellurium [1.2].*

Isotope	% nat. abundance	Isotope	% nat. abundance	Isotope	% nat. abundance
^{64}Zn	48.6	^{120}Te	0.096	^{126}Te	18.95
^{66}Zn	27.9	^{122}Te	2.603	^{128}Te	31.69
^{67}Zn	4.1	^{123}Te	0.908	^{130}Te	33.80
^{68}Zn	18.8	^{124}Te	4.816		
^{70}Zn	0.6	^{125}Te	7.139		

[1.2] D. R. Lide, *CRC Handbook of Chemistry and Physics,* 78th Edition (CRC Press, Boca Raton, 1997).

• **Molecular weight**

Table 9.1.3 *Molecular (average atomic) weight M for ZnTe.*

M (amu)
192.99

9.1.3 Crystal Structure and Space Group

Table 9.1.4 *Crystal structure and its space and pint groups for ZnTe.*

Crystal structure	Space group	Point group
Zincblende (Cubic)	$F\bar{4}3m$	T_d

9.1.4 Lattice Constant and Its Related Parameters

• **Lattice constant, near-neighbor distance, etc.**

Table 9.1.5 *Lattice constant (a), near-neighbor distance (d), unit cube volume* (a^3)*, and molecular density* (d_M) *for ZnTe at 300 K.*

Parameter	Value
Lattice constant a (Å)	6.009 [1.3]
d (Cation–Anion) (Å)	2.602*
d (Cation–Cation) (Å)	4.249*
Unit cube volume a^3 (10^{-22} cm^3)	2.170*
Molecular density d_M (10^{22} cm^{-3})	1.844*

[1.3] T. Yao, in *The Technology and Physics of Molecular Beam Epitaxy,* edited by E. H. C. Parker (Plenum, New York, 1985), p. 313.
*Calculated.

• **Crystal density**

Table 9.1.6 *Crystal density g for ZnTe at 300 K.**

g (g/cm^3)
5.908

*Calculated using a=6.009 Å.

9.1.5 Structural Phase Transition

Table 9.1.7 *Structural phase transition in ZnTe at high pressures.*

Structure	Transition pressure (GPa)
Zincblende ($F\bar{4}3m$)	Normal pressure
Cinnabar *[1]	7 [1.4]
	9.4±0.3 [1.5]
	8.5 [1.6]
	9.5±0.5 [1.7]
	8.9 [1.8]

Table 9.1.7 *Continued.*

Structure	Transition pressure (GPa)
Orthorhombic (*Cmcm*)*[2]	12 [1.4]
	11.9±0.3 [1.5]
	13 [1.6]
	12.0±0.5 [1.7]
	11.5 [1.8]
	12.9±0.6 [1.9]

[1.4] S. Endo, A. Yoneda, M. Ichikawa, S. Tanaka, and S. Kawabe, *J. Phys. Soc. Jpn.* **51**, 138 (1982).
[1.5] K. Strössner, S. Ves, C. K. Kim, and M. Cardona, *Solid State Commun.* **61**, 275 (1987).
[1.6] A. Ohtani, M. Motobayashi, and A. Onodera, *Phys. Lett.* **75A**, 435 (1980).
[1.7] A. San-Miguel, A. Polian, M. Gauthier, and J. P. Itié, *Phys. Rev. B* **48**, 8683 (1993).
[1.8] R. J. Nelmes, M. I. McMahon, N. G. Wright, and D. R. Allan, *Phys. Rev. Lett.* **73**,1805 (1994).
[1.9] A. Onodera and A. Ohtani, *J. Appl. Phys.* **51**, 2581 (1980).
*[1]R. N. Nelmes, M. I. McMahon, N. G. Wright, and D. R. Allan, *J. Phys. Chem. Solids* **56**, 545 (1995) [see also M. I. McMahon and R. J. Nelmes, *J. Phys. Chem. Solids* **56**, 485 (1995)].
*[2] R. J. Nelmes, M. I. McMahon, N. G. Wright, and D. R. Allan, *Phys. Rev. Lett.* **73**, 1805 (1994) [see also M. I. McMahon and R. J. Nelmes, *J. Phys. Chem. Solids* **56**, 485 (1995)].

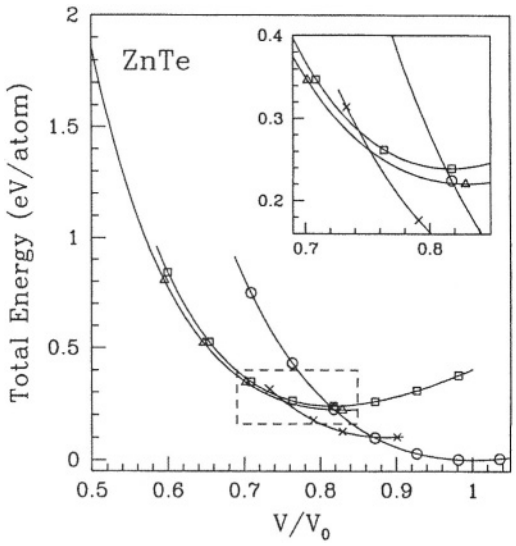

Fig. 9.1.1 Theoretical total energy versus volume for ZnTe in the zinc-blende (circles), cinnabar (crosses), rocksalt (squares), and orthorhombic phases (triangles), V_0 is the calculated zero-pressure volume for the zinc-blende phase. The energy of the zinc-blende phase is arbitrary chosen to be zero at zero pressure. [From M. Côté, O. Zakharov, A. Rubio, and M. L. Cohen, *Phys. Rev. B* **55**, 13025 (1997).]

9.1.6 Cleavage Plane

Table 9.1.8 *Crystallographic plane most readily cleaved for ZnTe.*

Cleavage plane
(110)

• Surface energy

Table 9.1.9 *Surface energy for ZnTe (in J/m^2).*

Plane			Comment
(110)	(111)	$(\bar{1}\,\bar{1}\,\bar{1})$	
0.960	0.808	0.840	Calc. [1.10]

[1.10] B. N. Oshcherin, *Phys. Status Solidi A* **34**, K181 (1976).

9.2 THERMAL PROPERTIES

9.2.1 Melting Point and Its Related Parameters

Table 9.2.1 *Melting point T_m and its related parameter for ZnTe.*

Parameter	Value
Melting point T_m (K)	1568 [2.1]
Entropy of fusion ΔS_m (cal/mol K)	16.34 [2.2]

[2.1] J. Carides and A. G. Fischer, *Solid State Commun.* **2**, 217 (1964).
[2.2] See, B. R. Nag, *J. Electron. Mater.* **26**, 70 (1997).

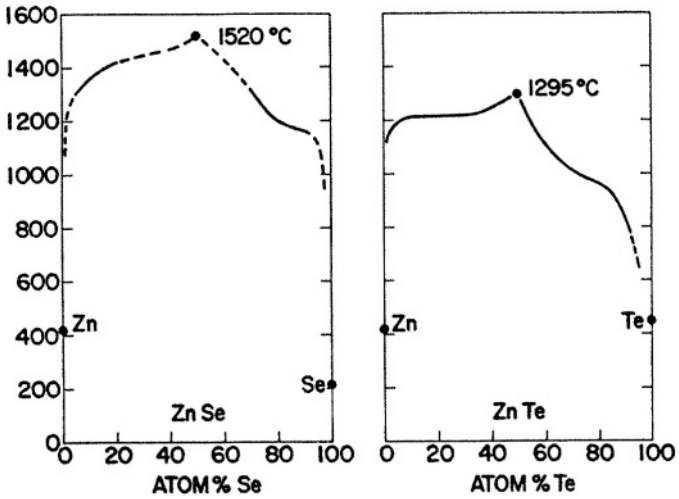

Fig. 9.2.1 *T–x* projects of the II–VI binary systems Zn–Se and Zn–Te. [From M. R. Lorenz, in *Physics and Chemistry of II–VI Compounds,* edited by M. Aven and J. S. Prener (North-Holland, Amsterdam, 1967), p. 73.]

9.2.2 Specific Heat

Table 9.2.2 *Experimental specific heat C_p (at constant pressure) for ZnTe [2.3].*

Temperature (K)	C_p (J/g K)	Temperature (K)	C_p (J/g K)
15	0.016	60	0.131
20	0.031	70	0.152
25	0.049	80	0.167
30	0.063	90	0.179
35	0.073	100	0.191
40	0.086	110	0.202
45	0.096	120	0.211
50	0.109	130	0.217
55	0.120	140	0.223

[2.3] J. C. Irwin and J. LaCombe, *J. Appl. Phys.* **45**, 567 (1974).

Table 9.2.3 *Experimental specific heat C_p (at constant pressure) for ZnTe [2.4].*

Temperature (K)	C_p (J/g K)	Temperature (K)	C_p (J/g K)
100	0.192	700	0.278
200	0.242	900	0.284
298.15	0.257	1100	0.289
400	0.264	1300	0.294
500	0.269	1500	0.299

[2.4] K. S. Gavrichev, G. A. Sharpataya, V. N. Guskov, J. H. Greenberg, T. Feltgen, M. Fiederle, and K. W. Benz, *Phys. Status Solidi B* **229**, 133 (2002).

- **Functional expression**

Table 9.2.4 *Specific heat C_p (at constant pressure) as a function of temperature T for ZnTe.*

C_p (J/g K)	Comment
$0.258+3.75\times10^{-5}T$	[2.5]
$0.2285+9.71\times10^{-5}T$ *	T=298–1300 K [2.6]
$0.23296+6.9489\times10^{-5}T$	T=360–640 K [2.7]

[2.5] P. Goldfinger and M. Jeunehomme, *Trans. Faraday Soc.* **59**, 2851 (1963).
[2.6] K. C. Mills, *Themodynamic Date for Inorganic Sulphides, Selenides and Tellurides* (Butterworths, London, 1974).
[2.7] H. Maleki and L. R. Holland, in *Properties of Narrow Gap Cadmium-based Compounds,* EMIS Datareviews Series No. 10, edited by P. Capper (INSPEC, London, 1994), p. 408.
*This expression gives a value of C_p~0.258 J/g K at T=300 K.

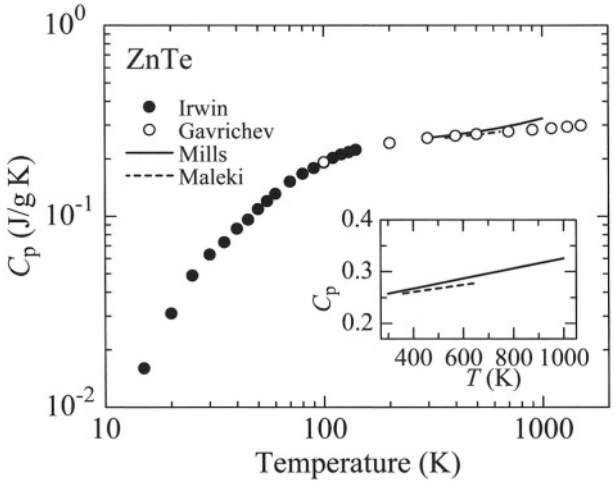

Fig. 9.2.2 Specific heat C_p (at constant pressure) versus temperature for ZnTe. The experimental data are taken from J. C. Irwin and J. LaCombe [*J. Appl. Phys.* **45**, 567 (1974); solid circles], from K. S. Gavrichev, G. A. Sharpataya, V. N. Guskov, J. H. Greenberg, T. Feltgen, M. Fiederle, and K. W. Benz [*Phys. Status Solidi B* **229**, 133 (2002); open circles], from K. C. Mills [*Themodynamic Date for Inorganic Sulphides, Selenides and Tellurides* (Butterworths, London, 1974); solid line], and from H. Maleki and L. R. Holland [in *Properties of Narrow Gap Cadmium-based Compounds,* EMIS Datareviews Series No. 10, edited by P. Capper (INSPEC, London, 1994), p. 408; dashed line].

9.2.3 Debye Temperature

Table 9.2.5 *Debye temperature θ_D for ZnTe.*

θ_D (K)	Comment
228	T=0 K*[1]
190±20	T=0 K*[2]
260	T=300 K*[3]

*[1] In the low-temperature (0 K) limit [see, H. Siethoff and K. Ahlborn, *Phys. Status Solidi B* **190**, 179 (1995)].
*[2] In the low-temperature (0 K) limit [K. S. Gavrichev, G. A. Sharpataya, V. N. Guskov, J. H. Greenberg, T. Feltgen, M. Fiederle, and K. W. Benz, *Phys. Status Solidi B* **229**, 133 (2002)].
*[3] Estimated from data by D. N. Talwar, M. Vandevyver, K. Kunc, and M. Zigone [*Phys. Rev. B* **24**, 741 (1981)].

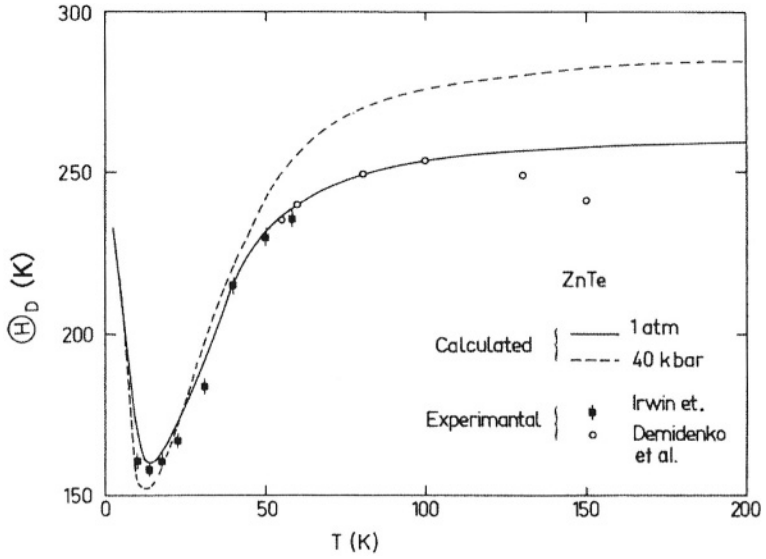

Fig. 9.2.3 Theoretical and experimental Debye temperature θ_D versus temperature T for ZnTe. The experimental data are taken from J. C. Irwin and J. LaCombe [*J. Appl. Phys.* **45**, 567 (1974)] and from A. F. Demidenko and A. K. Maltsen [*Inrog. Mater.* **5**, 158 (1969)]. [From D. N. Talwar, M. Vandevyver, K. Kunc, and M. Zigone, *Phys. Rev. B* **24**, 741 (1981).]

9.2.4 Thermal Expansion Coefficient

Table 9.2.6 *Thermal expansion coefficient α_{th} for ZnTe [2.8]. Note that the expansion coefficient shows a minimum at T~28 K.*

Temperature (K)	α_{th} (10^{-6} K^{-1})	Temperature (K)	α_{th} (10^{-6} K^{-1})
3	0.0002	22	–0.587
4	0.0004	24	–0.645
5	0.0004	26	–0.67
6	–0.0014	28	–0.68
7	–0.0066	30	–0.66
8	–0.0170	32	–0.615
10	–0.061	57.5	1.19
12	–0.130	65	2.00

Table 9.2.6 *Continued.*

Temperature (K)	α_{th} (10^{-6} K^{-1})	Temperature (K)	α_{th} (10^{-6} K^{-1})
14	–0.228	75	2.94
16	–0.328	85	3.73
18	–0.429	283	8.19
20	–0.516		

[2.8] J. G. Collins, G. K. White, J. A. Birch, and T. F. Smith, *J. Phys. C: Solid State Phys.* **13**, 1649 (1980).

Table 9.2.7 *Thermal expansion coefficient α_{th} for ZnTe [2.9].*

Temperature (K)	α_{th} (10^{-6} K^{-1})	Temperature (K)	α_{th} (10^{-6} K^{-1})
60	1.22	210	7.71
70	2.26	220	7.86
80	2.99	230	7.98
90	3.77	240	8.06
100	4.30	250	8.10
110	4.82	260	8.16
120	5.27	270	8.24
130	5.66	280	8.26
140	6.05	290	8.28
150	6.45	300	8.33
160	6.74	310	8.37
170	7.08	320	8.41
180	7.27	330	8.45
190	7.43	340	8.49
200	7.65		

[2.9] S. N. Novikova and N. Kh. Abrikosov, *Sov. Phys.–Solid State* **5**, 1558 (1964).

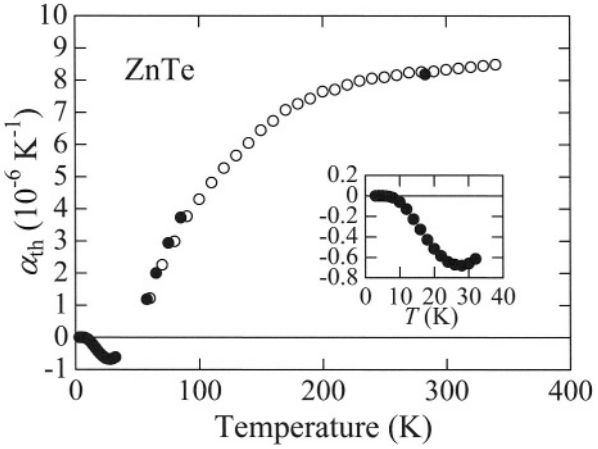

Fig. 9.2.4 Thermal expansion coefficient α_{th} versus temperature for ZnTe. The experimental data are taken from J. G. Collins, G. K. White, J. A. Birch, and T. F. Smith [*J. Phys. C: Solid State Phys.* **13**, 1649 (1980); solid circles] and from S. N. Novikova and N. Kh. Abrikosov [*Sov. Phys.–Solid State* **5**, 1558 (1964); open circles].

9.2.5 Thermal Conductivity and Diffusivity

Table 9.2.8 *Thermal conductivity K for ZnTe [2.10]. Thermal diffusivity can be calculated from a relation $D=K/(C_p \cdot g)$, where C_p is the specific heat at constant pressure and g is the crystal density.*

Temperature (K)	K (W/cm K)	Temperature (K)	K (W/cm K)
3.2	0.38	30	3.0
3.8	0.55	40	2.4
4.2	0.95	50	1.9
5	1.44	65	1.40
5.5	1.68	80	1.08
8.4	2.35	100	0.80
10.3	3.0	150	0.46
13	3.4	200	0.31
15	3.6	250	0.23
22	3.6	300	0.18

[2.10] G. A. Slack, *Phys. Rev. B* **6**, 3791 (1972).

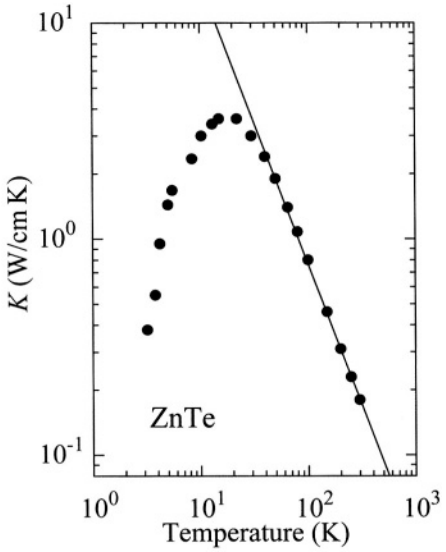

Fig. 9.2.5 Thermal conductivity K for ZnTe. The experimental data are taken from G. A. Slack [*Phys. Rev. B* **6**, 3791 (1972)]. The solid line is calculated from $K=AT^n$ with $A=320$ W/cm K$^{-0.31}$ and $n=-1.31$.

9.3 ELASTIC PROPERTIES

9.3.1 Elastic Constant

- **Room-temperature value and its temperature and pressure derivatives**

Table 9.3.1 *Elastic constant and its temperature and pressure derivatives for ZnTe at 300 K [3.1].*

Parameter	Value
Stiffness (10^{11} dyn/cm^2)	
C_{11}	7.15
C_{12}	4.08
C_{44}	3.11

Table 9.3.1 *Continued.*

Parameter	Value
Compliance (10^{-12} cm^2/dyn)	
S_{11}	2.39
S_{12}	–0.85
S_{44}	3.25
dC_{ij}/dT (10^7 dyn/cm^2 K)	
C_{11}	–13.4
C_{12}	–8.28
C_{44}	–4.39
dC_{ij}/dp	
C_{11}	4.9
C_{12}	5.1
C_{44}	0.44

[3.1] *Numerical Data and Functional Relationships in Science and Technology,* edited by K.-H. Hellwege and A. M. Hellwege, Landolt–Börnstein, New Series, Group III, Vol. 11 (Springer, Berlin, 1979).

9.3.2 Third-Order Elastic Constant

Table 9.3.2 *Third-order elastic constant of ZnTe [3.2].*

Modulus	Value (10^{12} dyn/cm^2)
C_{111}	–7.07
C_{112}	–1.21
C_{123}	–4.12
C_{144}	+1.83
C_{166}	–2.17
C_{456}	–2.29

[3.2] *Numerical Data and Functional Relationships in Science and Technology,* edited by K.-H. Hellwege and A. M. Hellwege, Landolt–Börnstein, New Series, Group III, Vol. 18 (Springer, Berlin, 1984).

9.3.3 Young's Modulus, Poisson's Ratio, and Similar

- **Young's modulus**

Table 9.3.3 *Young's modulus Y for ZnTe at 300 K.**

Crystallographic plane	Y (10^{11} dyn/cm^2)
(100) plane	
[001] direction	4.18
[011] direction	6.32
(110) plane	
[001] direction	4.18
[111] direction	7.61
(111) plane	6.32

*Calculated using S_{11}=2.39, S_{12}=–0.85, and S_{44}=3.25 (all in 10^{-12} cm^2/dyn).

● **Poisson's ratio**

Table 9.3.4 *Poisson's ratio P for ZnTe at 300 K.**

Crystallographic plane	*P*
(100) plane	
m=[010], *n*=[001]	0.356
m=[011], *n*=[0$\bar{1}$1]	0.027
(110) plane	
m=[001], *n*=[1$\bar{1}$0]	0.356
m=[1$\bar{1}$1], *n*=[1$\bar{1}\bar{2}$]	0.237
(111) plane	0.367

*Calculated using S_{11}=2.39, S_{12}= −0.85, and S_{44}=3.25 (all in 10^{-12} cm^2/dyn).

● **Bulk modulus, shear modulus, etc.**

Table 9.3.5 *Bulk modulus, B_u, pressure derivative of B_u, dB_u/dp, shear modulus, C_s, isotropy factor, A, linear compressibility, C_o, Caucy ratio, C_a, and Born ratio, B_o, for ZnTe at 300 K.*

Parameter	Value
B_u (10^{11} dyn/cm^2)	5.10 [3.3]
dB_u/dp	5.04±0.18 [3.4]
	4.7 [3.5]
C_s (10^{11} dyn/cm^2)	1.54 [3.3]
A	0.494 [3.3]
C_o (10^{-13} cm^2/dyn)	6.53 [3.3]
C_a	1.31 [3.3]
B_o	1.09 [3.3]

[3.3] Calculated using C_{11}=7.15, C_{12}=4.08, and C_{44}=3.11 (all in 10^{11} dyn/cm^2).
[3.4] Exper. [B. H. Lee, *J. Appl. Phys.* **41**, 2988 (1970)].
[3.5] Exper. [K. Strössner, S. Ves, C. K. Kim, and M. Cardona, *Solid State Commun.* **61**, 275 (1987)].

9.3.4 Microhardness

Table 9.3.6 *Microhardness H for ZnTe.*

H (GPa)	Ref.
0.82–0.9	[3.6]
0.6–0.9	[3.7]

[3.6] See, L. Garbato and A. Rucci, *Phil. Mag.* **35**, 1681 (1977).
[3.7] A. M. Andrukhiv, V. I. Ivanov–Omskiĭ, and P. G. Sidorchuk, *Sov. Phys. Solid State* **34**, 1934 (1992).

9.3.5 Sound Velocity

Table 9.3.7 *Sound velocity propagating in ZnTe at 300 K.* LA=longitudinal acoustic; TA1, TA2=transverse acoustic.*

Propagation direction	Mode	Sound velocity (10^5 cm/s)
[100]	LA	3.48
[100]	TA1, TA2	2.29
[110]	LA	3.84
[110]	TA1	1.61
[110]	TA2	2.29
[111]	LA	3.96
[111]	TA1, TA2	1.87

*Calculated using $C_{11}=7.15\times10^{11}$ dyn/cm^2, $C_{12}=4.08\times10^{11}$ dyn/cm^2, $C_{44}=3.11\times10^{11}$ dyn/cm^2, and $g=5.908$ g/cm^3.

9.4 PHONONS AND LATTICE VIBRONIC PROPERTIES

9.4.1 Phonon Dispersion Relation

- **Dispersion curve**

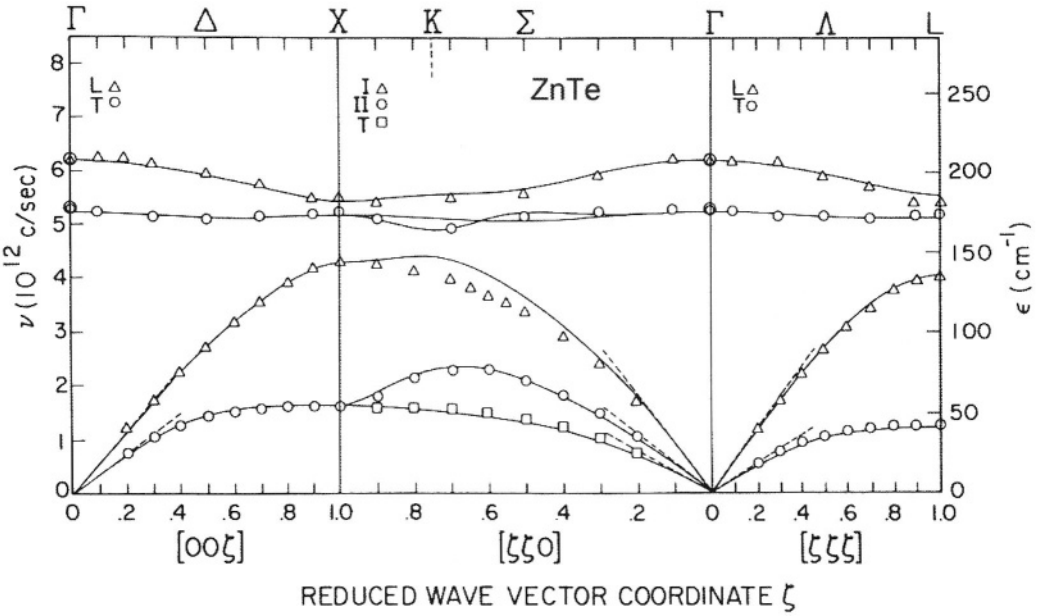

Fig. 9.4.1 Theoretical phonon dispersion curves for ZnTe, together with the neutron scattering data at 300 K. The two enlarged points at Γ are optical data. [From N. Vagelatos, D. Wehe, and J. S. King, *J. Chem. Phys.* **60**, 3613 (1974).]

• **Phonon density of states**

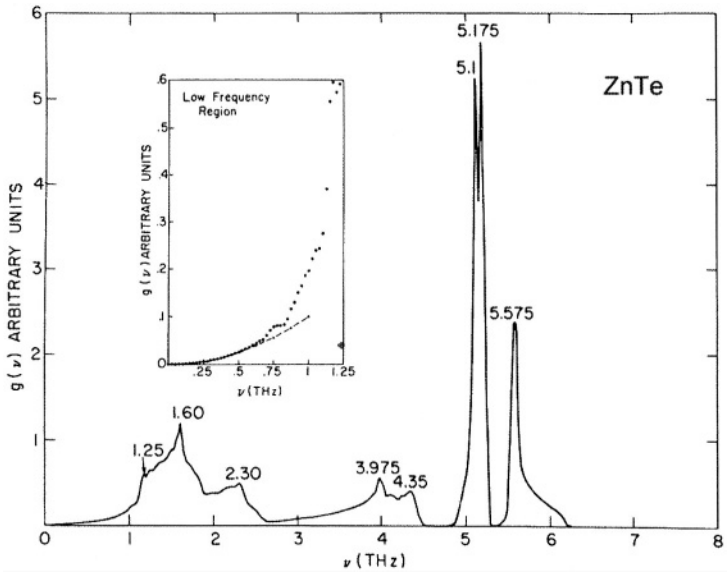

Fig. 9.4.2 Phonon density of states $g(\nu)$ for ZnTe. [From N. Vagelatos, D. Wehe, and J. S. King, *J. Chem. Phys.* **60**, 3613 (1974).]

9.4.2 Phonon Frequency

• **Room-temperature value**

Table 9.4.1 *Long-wavelength* $(q \to 0)$ *and zone-boundary phonon frequencies for ZnTe [4.1].*

Critical point	Phonon	Phonon frequency (cm^{-1})
Γ	TO	177
		177 [4.2]
		181 [4.3]
		176.9 [4.4]
	LO	207
		205 [4.2]
		210 [4.3]
		206.1 [4.4]
X	TA	54
		55.0 [4.4]
	LA	143
	TO	174
	LO	184
		186.2 [4.4]
L	TA	42
		43.1 [4.4]
	LA	135
	TO	173
	LO	180
		185.4 [4.4]

[4.1] N. Vagelatos, D. Wehe, and J. S. King, *J. Chem. Phys.* **60**, 3613 (1974).
[4.2] M. Cardona, *J. Phys. (Paris)* **45**, C8-29 (1984).
[4.3] D. L. Peterson, A. Petrou, W. Giriat, A. K. Ramdas, and S. Rodriguez, *Phys. Rev. B* **33**, 1160 (1986).
[4.4] J. Camacho, I. Loa, A. Cantarero, and K. Syassen, *J. Phys.: Condens. Matter* **14**, 739 (2002).

• **Temperature dependence**

It has been reported that the TO (LO) phonon frequency in ZnTe shows a decrease of about 3 (4) cm^{-1} in going from 100 to 300 K [A. Manabe, A. Mitsuishi, and H. Yoshinaga, *Jpn. J. Appl. Phys.* **6**, 593 (1967)]. A decrease in ω_{TO} of about 12 cm^{-1} in going from 2 to 300 K has also been observed by T. Hattori, Y. Homma, A. Mitsuishi, and M. Tacke [*Opt. Commun.* **7**, 229 (1973)].

Table 9.4.2 *Temperature dependence of the TO phonon frequency ω_{TO} for ZnTe.*

$$\omega_{TO}(T) = A + B\left(\frac{T}{\theta}\right) + C\left(\frac{T}{\theta}\right)^2$$

Parameter				Comment
A (THz)	B (THz)	C (THz)	θ(K)	
5.409	–0.0457	–0.0341	255	T=10–300 K [4.5]

[4.5] M. Schall, M. Walther, and P. U. Jepsen, *Phys. Rev. B* **64**, 94301 (2001).

• **Pressure dependence**

Table 9.4.3 *Pressure variation of the long-wavelength ($q \to 0$) phonon frequency in ZnTe.*

$$\omega_q(p) = \omega_q(0) + ap + bp^2$$

ω_q	$\omega_q(0)$ (cm^{-1})	a (cm^{-1}/GPa)	b (cm^{-1}/GPa^2)	Ref.
ω_{TO}	177	5.1		[4.6]
	176.9	5.82	–0.13	[4.7]
ω_{LO}	205	4.8		[4.6]
	206.1	4.74	–0.12	[4.7]

[4.6] M. Cardona, *J. Phys. (Paris)* **45**, C8-29 (1984).
[4.7] J. Camacho, I. Loa, A. Cantarero, and K. Syassen, *J. Phys.: Condens. Matter* **14**, 739 (2002).

9.4.3 Mode Grüneisen Parameter

Table 9.4.4 *Mode Grüneisen parameter for phonons at a number of critical points in ZnTe.*

Critical point	Phonon	Mode Grüneisen parameter
Γ	TO	1.7±0.1 [4.8]
		1.58±0.05 [4.9]
	LO	1.2±0.1 [4.8]
		1.10±0.03 [4.9]
		0.99±0.04 [4.10]
X	TA	–1.55±0.2 [4.8]
		–1.47±0.05 [4.9]
	TO	1.8±0.4 [4.8]
	LO	1.7±0.3 [4.8]
		1.63±0.08 [4.9]

Table 9.4.4 *Continued.*

Critical point	Phonon	Mode Grüneisen parameter
L	TA	−1.0±0.2 [4.8]
		−1.85±0.06 [4.9]
	LO	1.8±0.3 [4.8]
		1.63±0.11 [4.9]

[4.8] See, D. N. Talwar, M. Vandevyver, K. Kunc, and M. Zigone, *Phys. Rev. B* **24**, 741 (1981).
[4.9] J. Camacho, I. Loa, A. Cantarero, and K. Syassen, *J. Phys.: Condens. Matter* **14**, 739 (2002).
[4.10] R. J. Thomas, M. S. Boley, H. R Chandrasekhar, M. Chandrasekhar, C. Parks, A. K. Adams, J. Han, M. Kobayashi, and R. L. Gunshor, *Phys. Rev. B* **49**, 2181 (1994).

9.4.4 Phonon Deformation Potential

Table 9.4.5 *Long-wavelength phonon deformation potential (PDP) for ZnTe.*

PDP	TO	LO	Ref.
K_{11}		−2.3±0.3	[4.11]
	−3.0	−1.8	[4.12]
K_{12}		−1.7±0.3	[4.11]
	−3.6	−2.7	[4.12]
K_{44}	−0.5	−0.2	[4.12]
$K_{11}-K_{12}$		0.6	[4.11]
	0.6	0.9	[4.12]

[4.11] R. J. Thomas, M. S. Boley, H. R Chandrasekhar, M. Chandrasekhar, C. Parks, A. K. Adams, J. Han, M. Kobayashi, and R. L. Gunshor, *Phys. Rev. B* **49**, 2181 (1994).
[4.12] Calculated from $K_{11}+2K_{12}=-10.2$ (−7.2) and $K_{11}-K_{12}=0.6$ (0.9) for the TO (LO) phonons, where values of $K_{11}+2K_{12}$ are taken from B. Jusserand and M. Cardona [in *Light Scattering in Solids V,* edited by M. Cardona and G. Güntherodt (Springer, Berlin, 1989), p. 49] and $K_{11}-K_{12}$ (and K_{44}) correspond to those for InSb. [It should be noted that the TO (LO) phonon frequency in ZnTe is almost the same as that in InSb.]

9.5 COLLECTIVE EFFECTS AND RELATED PROPERTIES

9.5.1 Piezoelectric Constant

Table 9.5.1 *Piezoelectric stress (e_{14}), strain (d_{14}), and electromechanical coupling constants ($K_{[110]}^2$) for ZnTe [5.1].*

Parameter	Value
e_{14} (C/m^2)	0.0284
d_{14} (10^{-12} m/V)	0.91
$K_{[110]}^2$	3.1×10^{-5} *

[5.1] D. Berlincourt, H. Jaffe, and L. R. Shiozawa, *Phys. Rev.* **129**, 1009 (1963).
*Calculated.

9.5.2 Frohlich Coupling Constant

Table 9.5.2 *Fröhlich coupling constant α_F of ZnTe [5.2].*

α_F
0.332

[5.2] E. Kartheuser, in *Polarons in Ionic Crystals and Polar Semiconductors,* edited by J. T. Devreese (North-Holland, Amsterdam, 1972), p. 717.

9.6 ENERGY-BAND STRUCTURE: ENERGY-BAND GAPS

9.6.1 Basic Properties

- **Electronic energy-band structure**

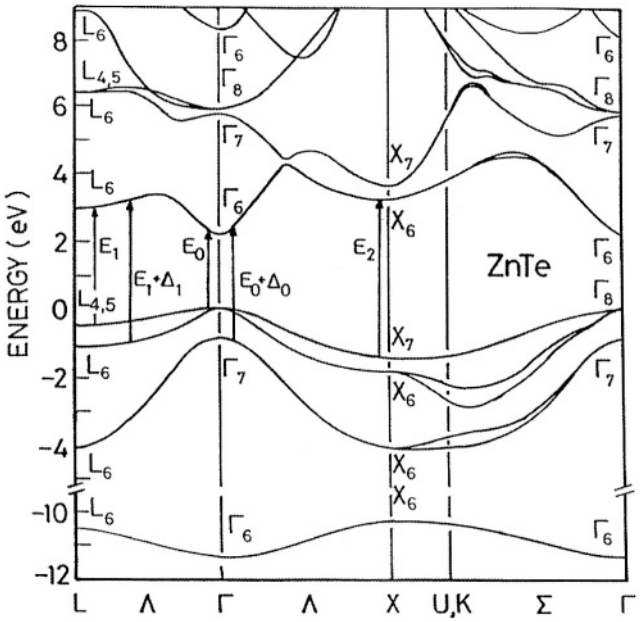

Fig. 9.6.1 Electronic energy-band structure of ZnTe as calculated with the empirical pseudopotential method. The electronic states are labeled using the notation for the representations of the double group of the zinc-blende structure. [From J. P. Walter, M. L. Cohen, Y. Petroff, and M. Balkanski, *Phys. Rev. B* **1**, 2661 (1970).] The locations of several interband transitions are included by the vertical arrows.

- **Electronic density of states**

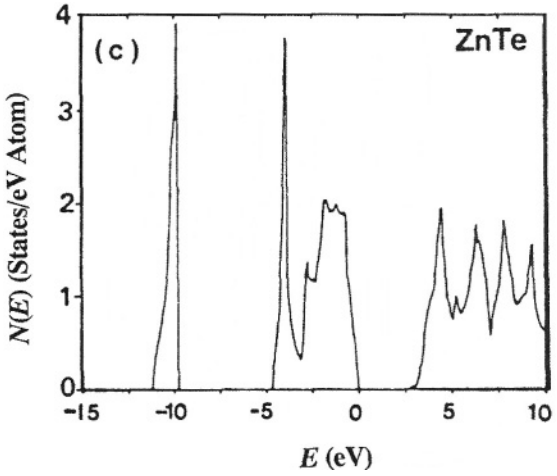

Fig. 9.6.2 Calculated electronic density of states $N(E)$ for ZnTe with an orthogonalized linear combination of atomic orbital method. [From M.-Z. Huang and W. Y. Ching, *J. Phys. Chem. Solids* **46**, 977 (1985).]

• **Energy eigenvalue**

Table 9.6.1 *Energy eigenvalues at the Γ, X, and L points for the valence and first few conduction bands of ZnTe [6.1].*

Critical point	Level	Value (eV)	
		Calc.	Exper.*
Γ	Γ_6^v (Γ_1^v)	−12.07	−13.0
	Γ_7^v (Γ_{15}^v)	0.00	−(0.92–0.976)
	Γ_8^v		0.00
	Γ_6^c (Γ_1^c)	2.57	2.38–2.394
	Γ_7^c (Γ_{15}^c)	5.91	4.82–5.40
	Γ_8^c		
X	X_6^v (X_1^v)	−10.52	−11.6
	X_6^v (X_3^v)	−5.27	−5.2, −5.5
	X_6^v (X_5^v)	−2.16	−2.4, −2.5
	X_7^v		−2.2
	X_6^c (X_1^c)	3.47	3.05
	X_7^c (X_3^c)	3.53	
L	L_6^v (L_1^v)	−10.95	−12.0
	L_6^v (L_1^v)	−5.31	−5.0, −5.5
	L_6^v (L_3^v)	−0.88	−1.1, −1.5
	$L_{4,5}^v$		−0.9
	L_6^c (L_1^c)	3.07	
	L_6^c (L_3^c)	6.52	
	$L_{4,5}^c$		

[6.1] O. Zakharov, A. Rubio, X. Blase, M. L. Cohen, and S. G. Louie, *Phys. Rev. B* **50**, 10780 (1994).
*The data are gathered from various sources.

9.6.2 E_0-Gap Region

• **Room-temperature value**

Table 9.6.2 *E_0-, $E_0+\Delta_0$-, and Δ_0-gap energies for ZnTe at room temperature.*

E_0 (eV)	$E_0+\Delta_0$ (eV)	Δ_0 (eV)	Ref.
2.255±0.005			[6.2]
2.26±0.02			[6.3]
2.27±0.008			[6.4]
2.27±0.01			[6.5]
2.229±0.001	3.205±0.01	0.976	[6.6]
2.290±0.002			[6.7]
2.273	3.193	0.920	[6.8]
2.278			[6.9]
2.27	(3.22)	0.95	Mean value

[6.2] B. A. Weinstein, R. Zallen, M. L. Slade, and A. deLozanne, *Phys. Rev. B* **24**, 4652 (1981).
[6.3] R. Brun de Re, T. Donofro, J. Avon, J. Magid, and J. C. Woolley, *Nuovo Cimento* **2D**, 1911 (1983).
[6.4] S. Ves, K. Strössner, W. Gebhardt, and M. Cardona, *Phys. Rev. B* **33**, 4077 (1986).
[6.5] K. Strössner, S. Ves, C. K. Kim, and M. Cardona, *Solid State Commun.* **61,** 275 (1987).

[6.6] Y. D. Kim, S. G. Choi, M. V. Klein, S. D. Yoo, D. E. Aspnes, S. H. Xin, and J. K. Furdyna, *Appl. Phys. Lett.* **70**, 610 (1997).
[6.7] R. Pässler, E. Griebl, H. Riepl, G. Lautner, S. Bauer, H. Preis, W. Gebhardt, B. Buda, D. J. As, D. Schikora, K. Lischka, K. Papagelis, and S. Ves, *J. Appl. Phys.* **86**, 4403 (1999).
[6.8] O. Casting, J. T Benhlal, and R. Granger, *Eur. Phys. J. B* **7**, 563 (1999).
[6.9] Y.-M. Yu, S. Nam, K.-S. Lee, Y. D. Choi, and B. O, *J. Appl. Phys.* **90,** 807 (2001).

- **Temperature dependence**

Table 9.6.3 *Empirical equation for the E_0-gap energy variation with temperature T for ZnTe.*

$$E_0(T) = E_0(0) - \frac{\alpha T^2}{T + \beta}$$

Parameter			Comment
$E_0(0)$ (eV)	α (10^{-4} eV/K)	β (K)	
2.3815	13	500	n=1 exciton, T=4.2–300 K, bulk ZnTe [6.10]
2.3815	5.2	165	n=1 exciton, T=15–300 K, epilayer [6.11]
2.380	4.8	71	T=6–315 K, bulk ZnTe [6.12]
2.3832	5.49	159	n=1 exciton, T=2–300 K, epilayer [6.13]
2.3872	5.4	150	T=10–200 K, epilayer [6.14]

[6.10] K. A. Dmitrenko, L. V. Taranenko, S. G. Shevel', and A. V. Marinchenko, *Sov. Phys. Semicond.* **19**, 487 (1985).
[6.11] B. Langen, H. Leiderer, W. Limmer, W. Gebhardt, M. Ruff, and U. Rössler, *J. Cryst. Growth* **101**, 718 (1990).
[6.12] H.-C. Mertins, H.-E. Gumlich, and Ch. Jung, *Semicond. Sci. Technol.* **8**, 1634 (1993).
[6.13] R. Pässler, E. Griebl, H. Riepl, G. Lautner, S. Bauer, H. Preis, W. Gebhardt, B. Buda, D. J. As, D. Schikora, K. Lischka, K. Papagelis, and S. Ves, *J. Appl. Phys.* **86**, 4403 (1999).
[6.14] Y.-M. Yu, S. Nam, K.-S. Lee, Y. D. Choi, and B. O, *J. Appl. Phys.* **90**, 807 (2001).

Table 9.6.4 *Empirical equation for the E_0-gap energy variation with temperature T for ZnTe [6.15].*

$$E_0(T) = E_0(0) - S\langle\hbar\Omega\rangle\left[\coth\left(\frac{\langle\hbar\Omega\rangle}{2kT}\right) - 1\right]$$

$E_0(0)$ (eV)	S	$\langle\hbar\Omega\rangle$ (meV)
2.390	2.29	10.8

[6.15] K. P. O'Donnell and P. G. Middleton, in *Properties of Wide Bandgap II–VI Semiconductors,* EMIS Datareviews Series No. 17, edited by R. Bhargava (INSPEC, London, 1997), p. 33.

Table 9.6.5 *Empirical equation for the E_0-gap energy variation with temperature T for ZnTe.*

$$E_0(T) = E_0(0) - \frac{\alpha\Theta_p}{2}\left[\sqrt[p]{1 + \left(\frac{2T}{\Theta_p}\right)^p} - 1\right]$$

$E_0(0)$ (eV)	p	α (meV/K)	Θ_p (K)	Comment
2.394	2.71	0.454	145	T=2–291 K [6.16]

[6.16] R. Pässler, *Phys. Status Solidi B* **216**, 975 (1999).

Table 9.6.6 *Empirical equation for the E_0-gap energy variation with temperature T for ZnTe.*

$$E_0(T) = E_0(0) - \alpha \sum_{i=1,2} \frac{W_i \Theta_i}{\exp(\Theta_i / T) - 1}$$

$E_0(0)$ (eV)	α (10^{-4} eV/K)	Θ_1 (K)	Θ_2 (K)	W_1	W_2	Comment
2.394	4.68	60	202	0.23	0.77	T=2–291 K [6.17]

[6.17] R. Pässler, *J. Appl. Phys.* **89**, 6235 (2001).

Table 9.6.7 *Spin–orbit–splitoff energy Δ_0 for ZnTe.**

Δ_0 (eV)	Comment
0.925	T=300 K [6.18]
0.976	T=300 K [6.19]
0.970	[6.20]
0.920	T=300 K [6.21]
0.95	Mean value

[6.18] M. Cardona, K. L. Shaklee, and F. H. Pollak, *Phys. Rev.* **154**, 696 (1967).
[6.19] Y. D. Kim, S. G. Choi, M. V. Klein, S. D. Yoo, D. E. Aspnes, S. H. Xin, and J. K. Furdyna, *Appl. Phys. Lett.* **70**, 610 (1997).
[6.20] See, S. Lee, F. Michl, U. Rössler, M. Dobrowolska, and J. K. Furdyna, *Phys. Rev. B* **57**, 9695 (1998).
[6.21] O. Casting, J. T Benhlal, and R. Granger, *Eur. Phys. J. B* **7**, 563 (1999).
*Note that Δ_0 may not vary with temperature if one supposes the valence-band rigidity of the II–VI compounds.

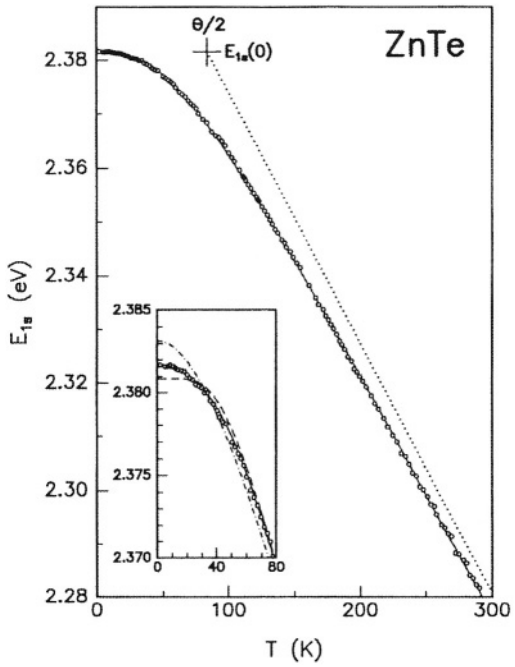

Fig. 9.6.3 Energy position of the n=1 exciton state E_{1S} in ZnTe epilayer grown on (100)GaAs substrate determined at lower temperatures by absorption measurements (open circles) and at higher temperatures by reflectance measurements (solid circles). The curves represent the numerical fits using various models. [From R. Pässler, E. Griebl, H. Riepl, G. Lautner, S. Bauer, H. Preis, W. Gebhardt, B. Buda, D. J. As, D. Schikora, K. Lischka, K. Papagelis, and S. Ves, *J. Appl. Phys.* **86**, 4403 (1999).]

● **Pressure dependence**

Table 9.6.8 *Empirical equation for the E_0-gap energy variation with pressure p for ZnTe.*

$$E_0(p) = E_0(0)+ap+bp^2$$

Parameter			Comment
$E_0(0)$ (eV)	a (10^{-2} eV/GPa)	b (10^{-4} eV/GPa^2)	
2.255±0.005	11.5±0.5	–50±3	T=300 K [6.22]
	9.3±0.6	–22±6	[6.23]
2.27±0.01	10.4±0.5	–28±5	T=300 K [6.24]
2.38±0.01	10.5±0.5	–32±5	T=7.7 K [6.25]
2.36±0.01	11.5±0.5	–31±5	T=115 K [6.25]
2.29±0.01	10.3±0.5	–24±5	T=300 K [6.25]
2.3944±0.0001	9.95±0.03	–20.0±0.7	T=7 K [6.26]

[6.22] B. A. Weinstein, R. Zallen, M. L. Slade, and A. deLozanne, *Phys. Rev. B* **24**, 4652 (1981).
[6.23] Y. Ohno *et al.* [see, S. Ves, K. Strössner, W. Gebhardt, and M. Cardona, *Phys. Rev. B* **33**, 4077 (1986)].
[6.24] K. Strössner, S. Ves, C. K. Kim, and M. Cardona, *Solid State Commun.* **61**, 275 (1987).
[6.25] M. Lindner, G. F. Schötz, P. Link, H. P. Wagner, W. Kuhn, and W. Gebhardt, *J. Phys.: Condens. Matter* **4**, 6401 (1992).
[6.26] See, K. Reimann, M. Haselhoff, St. Rübenacke, and M. Steube, *Phys. Status Solidi B* **198**, 71 (1996).

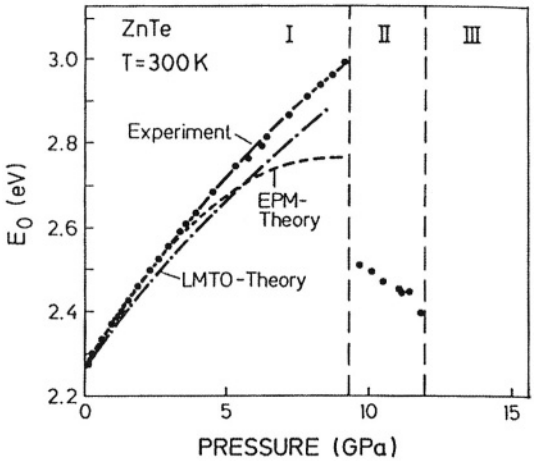

Fig. 9.6.4 Variation of the E_0-gap energy with hydrostatic pressure for ZnTe at room temperature. The two vertical dashed lines represent the phase transitions between the phases I (zincblende)–II and II–III (monoclinic). [From K. Strössner, S. Ves, C. K. Kim, and M. Cardona, *Solid State Commun.* **61**, 275 (1987).]

● **Temperature and/or pressure coefficient**

Table 9.6.9 *Linear temperature and pressure coefficients of the E_0- and $E_0+\Delta_0$-gap energies for ZnTe.*

Band gap	Coefficient	Value	Comment
E_0	dE_g/dT (10^{-4} eV/K)	–4.1±0.5	[6.27]
		–5.6	T=150–400 K [6.28]
		–2.8	T=90–293 K [6.29]
		–4.53±0.03	T=300 K [6.30]
	dE_g/dp (10^{-2} eV/GPa)	7	[6.31]
		10.5±0.4	T=2 K [6.32]
		10.2±0.3	T=300 K [6.33]

Table 9.6.9 *Continued.*

Band gap	Coefficient	Value	Comment
$E_0+\Delta_0$	dE_g/dT (10^{-4} eV/K)		
	dE_g/dp (10^{-2} eV/GPa)		

[6.27] J. Camassel and D. Auvergne, *Phys. Rev. B* **12**, 3258 (1975).
[6.28] Y. Furumura, A. Ebina, and T. Takahashi, *Phys. Rev. B* **19**, 1031 (1979).
[6.29] V. V. Sobolev, O. G. Maksimova, and S. G. Kroitoru, *Phys. Status Solidi B* **103**, 499 (1981).
[6.30] R. Pässler, E. Griebl, H. Riepl, G. Lautner, S. Bauer, H. Preis, W. Gebhardt, B. Buda, D. J. As, D. Schikora, K. Lischka, K. Papagelis, and S. Ves, *J. Appl. Phys.* **86**, 4403 (1999).
[6.31] D. L. Camphausen, G. A. N. Connell, and W. Paul, *Phys. Rev. Lett.* **26**, 184 (1971).
[6.32] H. Leiderer, G. Jahn, M. Silberbauer, W. Kuhn, H. P. Wagner, W. Limmer, and W. Gebhardt, *J. Appl. Phys.* **70**, 398 (1991).
[6.33] M. D. Frogley, D. J. Dunstan, and W. Palosz, *Solid State Commun.* **107**, 537 (1998).

9.6.3 Higher-Lying Direct Gap

- **Room-temperature value**

Table 9.6.10 *Higher-lying direct-gap energiesfor ZnTe at room temperature.*

Band gap	Value (eV)
E_1	3.59 *[1]
$E_1+\Delta_1$	4.17 *[1]
Δ_1	0.58 *[2]
E_0'	4.92 [6.34]
E_2	5.30 [6.34]
E_1'	~6.8 [6.34]
$E_1'+\Delta_1'$	~7.5 [6.34]

[6.34] See, S. Adachi, *Optical Constants of Crystalline and Amorphous Semiconductors: Numerical Data and Graphical Information* (Kluwer Academic, Boston, 1999).
*[1] Mean value obtained from various sources.
*[2] Note that Δ_1 may not vary with temperature if one supposes the valence-band rigidity of the II–VI compounds.

- **Temperature dependence**

Table 9.6.11 *E_1-, $E_1+\Delta_1$-, and Δ_1-gap energies for ZnTe determined at various temperatures [6.35].*

Temperature (K)	E_1 (eV)	$E_1+\Delta_1$ (eV)	Δ_1 (eV)
20	3.66	4.19	0.53
77	3.71	4.28	0.57
	3.7	4.27	0.57
78	3.64	4.18	0.54
90	3.75	4.32	0.57
	3.68	4.25	0.57
100	3.745	4.32	0.575
110	3.74	4.32	0.58
120	3.735	4.31	0.575
130	3.73	4.305	0.575
140	3.725	4.3	0.575

Table 9.6.11 *Continued.*

Temperature (K)	E_1 (eV)	$E_1+\Delta_1$ (eV)	Δ_1 (eV)
150	3.72	4.29	0.57
180	3.7	4.285	0.585
200	3.57	4.14	0.57
210	3.685	4.27	0.585
240	3.66	4.25	0.59
270	3.64	4.22	0.58
293	3.6	4.17	0.57
	3.629	4.221	0.592
295	3.58	4.14	0.56
	3.52	4.1	0.58
297	3.52	4.1	0.58
	3.64	4.23	0.59
	3.57	4.13	0.56
300	3.58	4.16	0.58
	3.62	4.2	0.58
	3.623	4.219	0.596
	3.58	4.18	0.6
	3.58	4.16	0.58
	3.6	4.15	0.55

[6.35] See, A. Kaneta and S. Adachi, *J. Phys. D: Appl. Phys.* **33**, 901 (2000).

Table 9.6.12 *Empirical equation for the higher-lying direct-gap energy variation with temperature T for ZnTe.*

$$E_g(T) = E_g(0) - \frac{\alpha T^2}{T+\beta}$$

Band gap	Parameter			Ref.
	$E_g(0)$ (eV)	α (10^{-4} eV/K)	β (K)	
E_1	3.772	9.50	260	[6.36]
$E_1+\Delta_1$	4.345	8.80	260	[6.36]

[6.36] A. Kaneta and S. Adachi, *J. Phys. D: Appl. Phys.* **33**, 901 (2000).

Table 9.6.13 *Empirical equation for the higher-lying direct-gap energy variation with temperature T for ZnTe.*

$$E_g(T) = E_B - 2a_B\left(\frac{1}{2} + \frac{1}{e^{\Theta/T}-1}\right)$$

Band gap	Parameter			Ref.
	E_B (eV)	a_B (meV)	Θ (K)	
E_1	3.859	97.7	260	[6.37]
$E_1+\Delta_1$	4.427	91.0	260	[6.37]

[6.37] A. Kaneta and S. Adachi, *J. Phys. D: Appl. Phys.* **33**, 901 (2000).

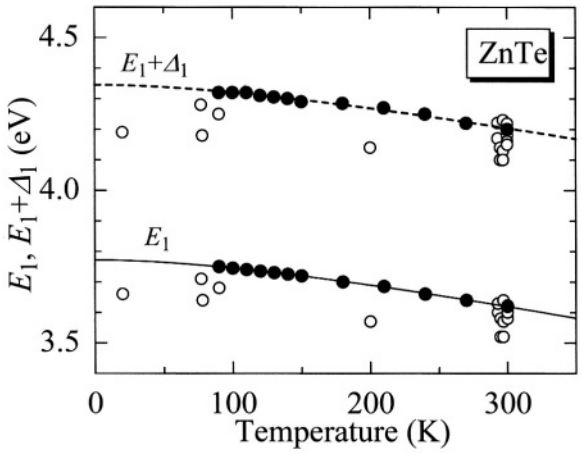

Fig. 9.6.5 E_1- and $E_1+\Delta_1$-gap energies versus temperature for ZnTe. The experimental data are gathered from various sources [see, A. Kaneta and S. Adachi, *J. Phys. D: Appl. Phys.* **33**, 901 (2000)]. The solid (dashed) line shows the calculated result of $E_g(T)=E_g(0)-[\alpha T^2/(T+\beta)]$ with $E_g(0)$=3.772 eV (4.345 eV), α=9.50×10^{-4} eV/K (8.80×10^{-4} eV/K), and β=260 K (260 K).

- **Temperature and/or pressure coefficient**

Table 9.6.14 *Linear temperature and pressure coefficients of the higher-lying band-gap energy for ZnTe.*

Band gap	Coefficient	Value	Ref.
E_1	dE_g/dT (10^{-4} eV/K)	–5.0	[6.38]
		–5.2	[6.39]
		–6.0	[6.40]
		–5.9	[6.41]
		–6.5	[6.42]
		–2.5	[6.43]
		–4.2	[6.44]
		–7.06	[6.45]
		–7.45	[6.45]
	dE_g/dp (10^{-2} eV/GPa)	8.3	[6.46]
$E_1+\Delta_1$	dE_g/dT (10^{-4} eV/K)	–4.1	[6.39]
		–6.4	[6.40]
		–5.9	[6.41]
		–1.4	[6.43]
		–3.8	[6.44]
		–6.58	[6.45]
		–6.90	[6.45]
	dE_g/dp (10^{-2} eV/GPa)	8.3	[6.46]
E_2	dE_g/dT (10^{-4} eV/K)	–6.0	[6.40]
		–6.1	[6.44]
	dE_g/dp (10^{-2} eV/GPa)	3.3*	[6.46]
		1.3*	[6.47]

[6.38] M. Cardona, *J. Appl. Phys.* **32**, 2151 (1961).
[6.39] M. Cardona and G. Harbeke, *J. Appl. Phys.* **34**, 813 (1963).
[6.40] M. Cardona and D. L. Greenaway, *Phys. Rev.* **131**, 98 (1963).
[6.41] A. Kisiel, *Acta Phys. Polonica A* **38**, 691 (1970).
[6.42] Y. Furumura, A. Ebina, and T. Takahashi, *Phys. Rev. B* **19**, 1031 (1979).
[6.43] A. D. Brothers and J. B. Brungardt, *Phys. Status Solidi B* **99**, 291 (1980).

[6.44] V. V. Sobolev, O. G. Maksimova, and S. G. Kroitoru, *Phys. Status Solidi B* **103**, 499 (1981).
[6.45] A. Kaneta and S. Adachi, *J. Phys. D: Appl. Phys.* **33**, 901 (2000).
[6.46] D. L. Camphausen, G. A. N. Connell, and W. Paul, *Phys. Rev. Lett.* **26**, 184 (1971).
[6.47] Y. F. Tsay, S. S. Mitra, and B. Bendow, *Phys. Rev. B* **10**, 1476 (1974).
* Calculated.

9.6.4 Lowest Indirect Gap

• Theoretical value

Table 9.6.15 *Theoretically obtained lowest indirect-gap energy for ZnTe (in eV).*

E_g^{L} *1	E_g^{X} *2	Ref.
3.39	3.01	[6.48]
2.50	2.60	[6.49]
3.07	3.47	[6.50]
2.12	2.35	[6.51]

[6.48] M.-Z. Huang and W. Y. Ching, *J. Phys. Chem. Solids* **46,** 977 (1985).
[6.49] Y. Li and P. J. Lin-Chung, *Phys. Status Solidi B* **153**, 215 (1989).
[6.50] O. Zakharov, A. Rubio, X. Blase, M. L. Cohen, and S. L. Louie, *Phys. Rev. B* **50**, 10780 (1994).
[6.51] G-D. Lee, M. H. Lee, and J.Ihm, *Phys. Rev. B* **52**, 1459 (1995).
*1 $\Gamma_8^v(\Gamma_{15}^v) \rightarrow L_6^c(L_1^c)$.
*2 $\Gamma_8^v(\Gamma_{15}^v) \rightarrow X_6^c(X_1^c)$.

• Experimental value

Table 9.6.16 *Experimentally obtained lowest indirect-gap energy for ZnTe (in eV).**

E_g^{L}	E_g^{X}
	3.05

*See Sec. 9.6.1.

• Temperature and/or pressure coefficient

Table 9.6.17 *Linear pressure coefficient of the lowest indirect-gap energy for ZnTe.*

Coefficient	Value	Comment
dE_g^{L}/dp (10^{-2} eV/GPa)	1.7	Calc. [6.52]
	3.0	Calc. [6.53]
	4.7	Calc. [6.54]
dE_g^{X}/dp (10^{-2} eV/GPa)	–1.7	Calc. [6.52]
	–1.6	Calc. [6.53]
	–3.4	Calc. [6.54]

[6.52] D. L. Camphausen, G. A. N. Connell, and W. Paul, *Phys. Rev. Lett.* **26**, 184 (1971).
[6.53] Y. F. Tsay, S. S. Mitra, and B. Bendow, *Phys. Rev. B* **10**, 1476 (1974).
[6.54] S.-H. Wei and A. Zunger, *Phys. Rev. B* **60**, 5404 (1999).

9.6.5 Conduction-Valley Energy Separation

Table 9.6.18 *Conduction-valley energy separation ΔE_g for ZnTe.**

ΔE_g	Value (eV)
$L_6^c - \Gamma_6^c$	
$X_6^c - \Gamma_6^c$	~0.7

*Estimated from E_0 and E_g^{X}.

9.6.6 Direct–Indirect-Gap Transition Pressure

Table 9.6.19 *Direct–indirect-gap (E_0–E_g^X) transition pressure for ZnTe.*

Transition pressure (GPa)	Comment
~6.5	T= 300 K [6.55]*

[6.55] B. A. Weinstein, R. Zallen, M. L. Slade, and A. deLozanne, *Phys. Rev. B* **27**, 4652 (1981).

*Note, however, that the indirect-gap transitions could be excluded in the zinc-blende phase by using estimates of the $E_0 \rightarrow E_g^X$ and $E_0 \rightarrow E_g^L$ pressure shifts [see, M. Lindner, G. F. Schötz, P. Link, H. P. Wagner, W. Kuhn, and W. Gebhardt, *J. Phys.: Condens. Matter* **4**, 6401 (1992)].

9.7 ENERGY-BAND STRUCTURE: ELECTRON AND HOLE EFFECTIVE MASSES

9.7.1 Electron Effective Mass: Γ Valley

Table 9.7.1 *Effective polaron mass m_{ep}* for electrons at the Γ-conduction band in ZnTe.*

m_{ep}*/m_0	Temperature (K)	Technique
0.122±0.002	3.5	Cyclotron resonance [7.1]
0.116±0.003	4.2	Two-photon magnetoabsorption [7.2]
0.117±0.002	2	Magnetophotoluminescence [7.3]
0.124±0.002	1.5	Cyclotron resonance [7.4]
0.124±0.002	6	Cyclotron resonance [7.5]

[7.1] B. Clerjaud, A.Gélineau, D. Galland, and K. Saminadayar, *Phys. Rev. B* **19**, 2056 (1979).
[7.2] Ch. Neumann, A. Nöthe, and N. O. Lipari, *Phys. Rev. B* **37**, 922 (1988).
[7.3] H. P. Wagner, S. Lankes, K. Wolf, W. Kuhn, P. Link, and W. Gebhardt, *J. Cryst. Growth* **117**, 303 (1992).
[7.4] P. Emanuelsson, M. Drechsler, D. M. Hofmann, Al. L. Efros, B. K. Meyer, and B. Clerjaud, *Solid State Commun.* **90,** 635 (1994).
[7.5] M. Drechsler, P. Emanuelsson, B. K. Meyer, H. Mayer, U. Rössler, and B. Clerjaud, *Phys. Rev. B* **50**, 2649 (1994).

Table 9.7.2 *Effective band mass m_e^Γ for electrons at the Γ-conduction band in ZnTe.*

m_e^Γ/m_0
0.117

*Estimated from a polaron mass m_{ep}=0.124m_0 with Fröhlich coupling constant of α_F=0.332.

9.7.2 Electron Effective Mass: Satellite Valley

No detailed data are available for ZnTe.

9.7.3 Hole Effective Mass

• Luttinger's valence-band parameter

Table 9.7.3 *Luttinger's valence-band parameter γ_i for ZnTe (in $\hbar^2/2m_0$).*

γ_1	γ_2	γ_3	Technique
4.0	1.15	1.29	Cyclotron resonance [7.6]
3.74	1.07	1.64	Five-level $\boldsymbol{k\cdot p}$ calculation [7.7]
3.8	0.83	1.28	Photoluminescence [7.888
$4.20^{+0}_{-0.2}$	$0.91^{+0.1}_{-0.4}$	1.54±0.1	Electronic Raman scattering [7.9]
4.4±0.7	0.95±0.09	1.48±0.14	Magnetoreflectance [7.10]
(3.9±0.7)	(0.83±0.08)	(1.30±0.12)	(Polaron parameters [7.10])
4.00	0.83	1.30	Spin-flip Raman scattering [7.11]
3.9±0.5	0.6±0.3	0.9±0.4	Reflectivity & two-photon Raman
3.9	0.8±0.2	1.7±0.2	Two-photon absorption [7.13]
4.07±0.10	0.78±0.14	1.59±0.11	Two-photon magnetoabsorption [7.14]
3.80	0.86	1.32	Excited acceptor-state analysis [7.15]
3.8	0.72	1.3	Magnetophotoluminescence [7.16]
3.96	0.86	1.39	Mean value

[7.6] R. A. Stradling, *Solid State Commun.* **6**, 665 (1968).
[7.7] P. Lawaetz, *Phys. Rev. B* **4**, 3460 (1971).
[7.8] D. C. Herbert, P. J. Dean, H. Venghaus, and J. C. Pfister, *J. Phys. C: Solid State Phys.* **11**, 3641 (1978).
[7.9] S. Nakashima, T. Hattori, P. E. Simmonds, and E. Amzallag, *Phys. Rev. B* **19**, 3045 (1979).
[7.10] H. Venghaus and B. Jusserand, *Phys. Rev. B* **22**, 932 (1980).
[7.11] Y. Oka and M. Cardona, *Phys. Rev. B* **23**, 4129 (1981).
[7.12] W. Maier, G. Schmieder, and C. Klingshirn, *Z. Phys. B* **50**, 193 (1983).
[7.13] D. Fröhlich, A. Nöthe, and K. Reimann, *Phys. Status Solidi B* **125**, 653 (1984).
[7.14] Ch. Neumann, A. Nöthe, and N. O. Lipari, *Phys. Rev. B* **37**, 922 (1988).
[7.15] M. Said and M.A. Kanehisa, *Phys. Status Solidi B* **157**, 311 (1990).
[7.16] H. P. Wagner, S. Lankes, K. Wolf, W. Kuhn, P. Link, and W. Gebhardt, *J. Cryst. Growth* **117**, 303 (1992).

• Band mass, cyclotron mass, etc.

Table 9.7.4 *Band (m_{HH}, m_{LH}), density-of-states heavy-hole (m_{HH}*), averaged light-hole (m_{LH}*), and spherically-averaged heavy-hole (m_{HH}^s) and light-hole masses (m_{LH}^s) in ZnTe.**

Mass	Value (m_0)
m_{HH} ([001] direction)	0.45
m_{LH} ([001] direction)	0.176
m_{HH} ([111] direction)	0.85
m_{LH} ([111] direction)	0.148
m_{HH}*	0.67
m_{LH}*	0.159
m_{HH}^s	0.62
m_{LH}^s	0.158

*Calculated using a set of the Luttinger's parameters, γ_1=3.96, γ_2=0.86, and γ_3=1.39.

- **Spin–orbit–splitoff hole effective mass**

Table 9.7.5 *Spin–orbit–splitoff hole effective mass m_{SO} for ZnTe.*

m_{SO}/m_0	Technique
0.42	$\boldsymbol{k}\cdot\boldsymbol{p}$ method [7.17]
0.33	$\boldsymbol{k}\cdot\boldsymbol{p}$ method [7.18]
0.25	*

[7.17] M. Cardona, *J. Phys. Chem. Solids* **24**, 1543 (1963).
[7.18] P. Lawaetz, *Phys. Rev. B* **4**, 3460 (1971).
*Obtained from the Luttinger's parameter ($m_{SO}=1/\gamma_1$).

9.8 ELECTRONIC DEFORMATION POTENTIAL

9.8.1 Intravalley Deformation Potential: Γ Point

- **Conduction band**

Table 9.8.1 *Γ-conduction-band intravalley deformation potential a_c^{Γ} ($=E_1^{\Gamma}$) for ZnTe.*

a_c^{Γ} (eV)	Comment
−6.64	Calc. [8.1]
−12.6	Calc. [8.2]
−7.3	Calc. [8.3]
−5.83	Calc. [8.4]
−5.19	Calc. [8.5]

[8.1] J. H. Lee and G. Myers, *Phys. Status Solidi B* **77**, K81 (1976).
[8.2] A. Blacha, H. Presting, and M. Cardona, *Phys. Status Solidi B* **126**, 11 (1984).
[8.3] M. Cardona and N. E. Christensen, *Phys. Rev. B* **35**, 6182 (1987); erratum, *ibid.* **36**, 2906 (1987).
[8.4] C. G. Van de Walle, *Phys. Rev. B* **39**, 1871 (1989).
[8.5] D. Bertho, D. Boiron, A. Simon, C. Jouanin, and C. Priester, *Phys. Rev. B* **44**, 6118 (1991).

Table 9.8.2 *Γ-conduction-band acoustic deformation potential E_1 for ZnTe obtained from transport data analysis.*

E_1 (eV)	Ref.
9.5	[8.6]
3.5	[8.7]

[8.6] D. L. Rode, *Phys. Rev. B* **2**, 4036 (1970).
[8.7] D. L. Rode, in *Semiconductors and Semimetals,* edited by R. K. Willardson and A. C. Beer (Academic, New York, 1975), Vol. 10, p. 1.

• **Valence band**

Table 9.8.3 *Γ-valence-band deformation potentials a, b, and d for ZnTe.*

Deformation potential (eV)			Comment
a	*b*	*d*	
−3.0	−1.0	−6.0	Calc. [8.8]
−2.0			Calc. [8.9]
0.79	−1.26		Calc. [8.10]
0.34	−2.21		Calc. [8.11]
−0.07	−1.44		Calc. [8.12]
	−1.0		Calc. [8.13]
	−1.31		Calc. [8.14]
	−1.33		Calc. [8.15]
	−1.78	−4.61	Exper. [8.16]
	−1.30	−4.3	Exper. [8.17]
	−1.4±0.1		Exper. [8.18]
	−1.27±0.01		Exper. [8.19]
	−1.26±0.03	−4.19±0.08	Exper. [8.20]
	−1.4	−4.4	Mean value (Exper.)

[8.8] A. Blacha, H. Presting, and M. Cardona, *Phys. Status Solidi B* **126**, 11 (1984).
[8.9] M. Cardona and N. E. Christensen, *Phys. Rev. B* **35**, 6182 (1987); erratum, *ibid.* **36**, 2906 (1987).
[8.10] C. G. Van de Walle, *Phys. Rev. B* **39**, 1871 (1989).
[8.11] D. Bertho, D. Boiron, A. Simon, C. Jouanin, and C. Priester, *Phys. Rev. B* **44**, 6118 (1991).
[8.12] A. Qteish and R. J. Needs, *Phys. Rev. B* **45**, 1317 (1992).
[8.13] M. Silver, W. Batty, A. Ghiti, and E. P. O'Reilly, *Phys. Rev. B* **46**, 6781 (1992).
[8.14] T. Nakayama, *Solid-State Electron.* **37**, 1077 (1994).
[8.15] R. Said, A. Qteish, and N. Meskini, *J. Phys.: Condens. Matter* **10,** 8703 (1998).
[8.16] A. A. Kaplyanskii and L. G. Suslina, *Sov. Phys.–Solid State* **7**, 1881 (1966).
[8.17] W. Wardzyński, W. Giriat, H. Szymczak, and R. Kowalczyk, *Phys. Status Solidi B* **49**, 71 (1972).
[8.18] H. Leiderer, G. Jahn, M. Silberbauer, W. Kuhn, H. P. Wagner, W. Limmer, and W. Gebhardt, *J. Appl. Phys.* **70**, 398 (1991).
[8.19] D. Fröhlich, F. Kubacki, M. Schlierkamp, and R. Triboulet, *Europhys. Lett.* **17,** 237 (1992).
[8.20] D. Fröhlich, F. Kubacki, M. Schlierkamp, H. Mayer, and U. Rössler, *Phys. Status Solidi B* **177,** 379 (1993).

• E_0 **gap**

Table 9.8.4 *Hydrostatic deformation potential* a_0^Γ *for the* E_0 *gap of ZnTe.*

a_0^Γ (eV)	Comment
−9.6	Calc. [8.21]
−5.8	Calc. [8.22]
−6.62	Calc. [8.23]
−5.53	Calc. [8.24]
−5.91	Calc. [8.25]
−4.64	Calc. [8.26]
−5.60	Calc. [8.27]
−5.48	Exper. [8.28]
−5.5±0.2	Exper. [8.29]

Table 9.8.4 *Continued.*

a_0^{Γ} (eV)	Comment
−5.38±0.05	Exper. [8.30]
−5.47±0.15	Exper. [8.31]
−5.0±0.2	Exper. [8.32]
−5.25±0.02	Exper. [8.33]
−5.3	Mean value (Exper.)

[8.21] A. Blacha, H. Presting, and M. Cardona, *Phys. Status Solidi B* **126**, 11 (1984).
[8.221] J. E. Bernard and A. Zunger, *Phys. Rev. B* **36**, 3199 (1987).
[8.23] C. G. Van de Walle, *Phys. Rev. B* **39**, 1871 (1989).
[8.24] D. Bertho, D. Boiron, A. Simon, C. Jouanin, and C. Priester, *Phys. Rev. B* **44**, 6118 (1991).
[8.25] T. Nakayama, *Solid-State Electron.* **37**, 1077 (1994).
[8.261] R. Said, A. Qteish, and N. Meskini, *J. Phys.: Condens. Matter* **10**, 8703 (1998).
[8.27] S.-H. Wei and A. Zunger, *Phys. Rev. B* **60**, 5404 (1999).
[8.28] W. Wardzyński, W. Giriat, H. Szymczak, and R. Kowalczyk, *Phys. Status Solidi B* **49**, 71 (1972).
[8.29] H. Leiderer, G. Jahn, M. Silberbauer, W. Kuhn, H. P. Wagner, W. Limmer, and W. Gebhardt, *J. Appl. Phys.* **70**, 398 (1991).
[8.30] D. Fröhlich, F. Kubacki, M. Schlierkamp, and R. Triboulet, *Europhys. Lett.* **17**, 237 (1992).
[8.31] D. Fröhlich, F. Kubacki, M. Schlierkamp, H. Mayer, and U. Rössler, *Phys. Status Solidi B* **177**, 379(1993).
[8.32] R. J. Thomas, M. S. Boley, H. R Chandrasekhar, M. Chandrasekhar, C. Parks, A. K. Adams, J. Han, M. Kobayashi, and R. L. Gunshor, *Phys. Rev. B* **49**, 2181 (1994).
[8.33] See, K. Reimann, M. Haselhoff, St. Rübenacke, and M. Steube, *Phys. Status Solidi B* **198**, 71 (1996).

• Optical-phonon deformation potential

Table 9.8.5 *Optical-phonon deformation potential d_0 at the Γ-valence band of ZnTe.*

d_0 (eV)	Comment
26.3	Calc. [8.34]
13.8	Calc. [8.35]
16.4	Calc. [8.36]
28	Exper. [8.37]
37	Exper. [8.38]
23	Exper. (see [8.38])
29	Mean value (Exper.)

[8.34] A. Blacha, H. Presting, and M. Cardona, *Phys. Status Solidi B* **126**, 11 (1984).
[8.35] L. Brey, N. E. Christensen, and M. Cardona, *Phys. Rev. B* **36**, 2638 (1987).
[8.36] R.-Z. Wang, S.-H. Ke, and M.-C. Huang, *J. Phys.: Condens. Matter* **4**, 6735 (1992).
[8.37] R. L. Schmidt, B. D. McCombe, and M. Cardona, *Phys. Rev. B* **11**, 746 (1975).
[8.38] J. M. Calleja, H. Vogt, and M. Cardona, *Phil. Mag.* **35**, 239 (1982).

9.8.2 Intravalley Deformation Potential: High-Symmetry Points

• Optical-phonon deformation potential: L point

Table 9.8.6 *Optical-phonon deformation potentials $d_{1o}(c)$, $d_{1o}(v)$, and d_{3o} at the L point of ZnTe.*

Deformation potential	Value (eV)	Comment
$d_{1o}(c)$	−21.5	Calc. [8.39]
$d_{1o}(v)$	−5.1	Calc. [8.39]
d_{3o}	27.9	Calc. [8.39]

[8.39] R.-Z. Wang, S.-H. Ke, and M.-C. Huang, *J. Phys.: Condens. Matter* **4**, 6735 (1992).

• **Valence-band deformation potential: L point**

Table 9.8.7 *Valence-band deformation potentials* D_3^5 *and* D_3^3 *at the L point of ZnTe.*

Deformation potential	Value (eV)	Comment
D_3^5	3.99	Calc. [8.40]
	−15±5	Exper. [8.41]
D_3^3	4.27	Calc. [8.40]
	−29±8	Exper. [8.41]
	2.45	Exper. [8.42]

[8.40] D. Rönnow, N. E. Christensen, and M. Cardona, *Phys. Rev. B* **59**, 5575 (1999).
[8.41] D. Rönnow, M. Cardona, and L. F. Lastras-Martínez, *Phys. Rev. B* **59**, 5581 (1999).
[8.42] J. H. Bahng, M. S. Jang, M. Lee, J. C. Choi, H. L. Park, K. J. Kim, and C. Lee, *Solid State Commun.* **120**, 343 (2001).

• **Hydrostatic and interband deformation potentials:** E_1 **and** $E_1+\Delta_1$ **gaps**

Table 9.8.8 *Hydrostatic* a_l^L $(= D_l^l/\sqrt{3})$ *and interband deformation potentials* D_l^5 *for the* E_l *and* $E_l+\Delta_l$ *gaps of ZnTe.*

Deformation potential	Value (eV)	Comment
a_1^L	−2.95	Calc. [8.43]
	−3.16	Exper. [8.44]
D_1^5	7.31	Calc. [8.43]
	40±20	Exper. [8.45]

[8.43] D. Rönnow, N. E. Christensen, and M. Cardona, *Phys. Rev. B* **59**, 5575 (1999).
[8.44] J. H. Bahng, M. S. Jang, M. Lee, J. C. Choi, H. L. Park, K. J. Kim, and C. Lee, *Solid State Commun.* **120**, 343 (2001).
[8.45] D. Rönnow, M. Cardona, and L. F. Lastras-Martínez, *Phys. Rev. B* **59**, 5581 (1999).

9.8.3 Intervalley Deformation Potential

• **Absolute value**

Table 9.8.9 *Intervalley deformation potential* D_{ij} *for electrons in ZnTe [8.46].*

D_{ij}	Phonon	Value (eV/Å)
$D_{\Gamma L}$	LA	3.31
	LO	3.19
$D_{\Gamma X(1)}$	LA	0
	LO	1.43
$D_{\Gamma X(3)}$	LA	1.17
	LO	0

[8.46] Calculated [D. Olguín, M. Cardona, and A. Cantarero, *Solid State Commun.* **122,** 575 (2002)].

9.9 ELECTRON AFFINITY AND SCHOTTKY BARRIER HEIGHT

9.9.1 Electron Affinity

Table 9.9.1 *Electron affinity χ_s for ZnTe.*

χ_s (eV)	Comment
3.5	[9.1]
3.68	Chemically prepared sample [9.2]

[9.1] A. G. Milnes and D. L. Feucht, *Heterojunctions and Metal-Semiconductor Junctions* (Academic, New York, 1972).
[9.2] F. El Akkad, A. Felimban, and F. Sallam, *J. Vac. Sci. Technol. A* **5**, 111 (1987).

9.9.2 Schottky Barrier Height

Table 9.9.2 *Summary of the Schottky barrier height ϕ_p for metal/p-ZnTe contacts at 300 K.**

Metal	ϕ_p (eV)	Metal	ϕ_p (eV)
Ag	0.94–1.06	In	0.99–1.13
Al	0.90–12.0	Ni	0.65
Au	0.51–0.64	Ta	1.50
Cu	0.80–0.84		

*The data are gathered from various sources.

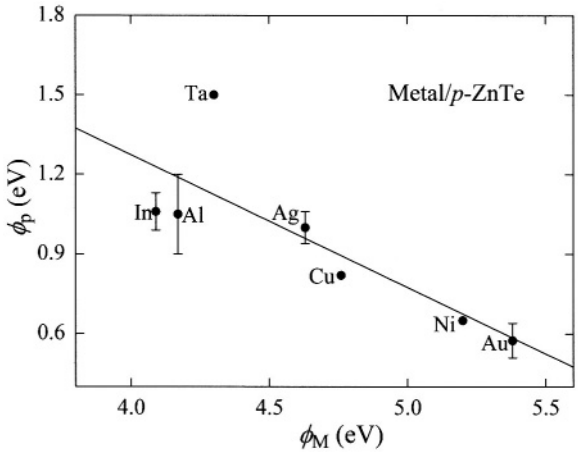

Fig. 9.9.1 Schottky barrier height ϕ_p versus metal work function ϕ_M observed for metal/*p*-ZnTe contacts. Values of the metal work function were taken from H. P. R. Frederikse [in *CRC Handbook of Chemistry and Physics,* 78th Edition, edited by D. R. Lide (CRC Press, Boca Raton, 1997), p. 12-115]. The solid line represents the least-squares-fit result with ϕ_p=3.27–0.50ϕ_M (ϕ_M and ϕ_p in eV).

9.10 OPTICAL PROPERTIES

9.10.1 Summary of Optical Dispersion Relations

• **$\varepsilon(E)$ and $n^*(E)$ spectra**

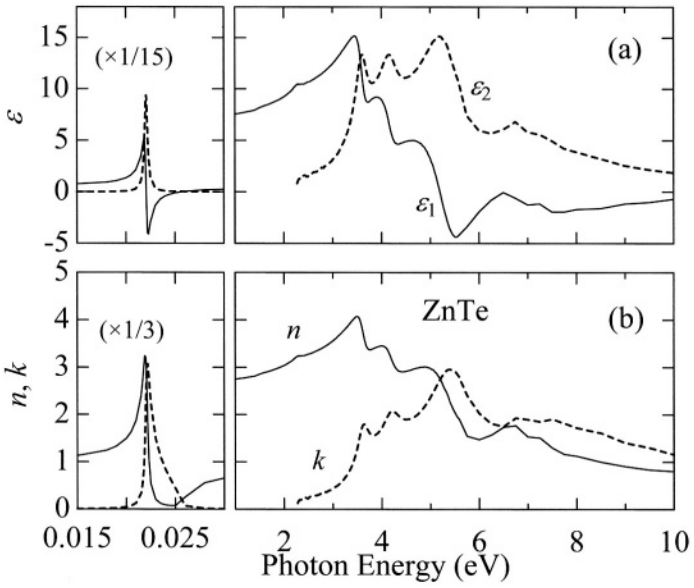

Fig. 9.10.1 (a) Complex dielectric-constant [$\varepsilon(E)=\varepsilon_1(E)+i\varepsilon_2(E)$] and (b) complex refractive-index spectra [$n^*(E)=n(E)+ik(E)$] for ZnTe at 300 K. The numerical data are taken from tabulation by S. Adachi [*Optical Constants of Crystalline and Amorphous Semiconductors: Numerical Data and Graphical Information* (Kluwer Academic, Boston, 1999)].

• **$\alpha(E)$ and $R(E)$ spectra**

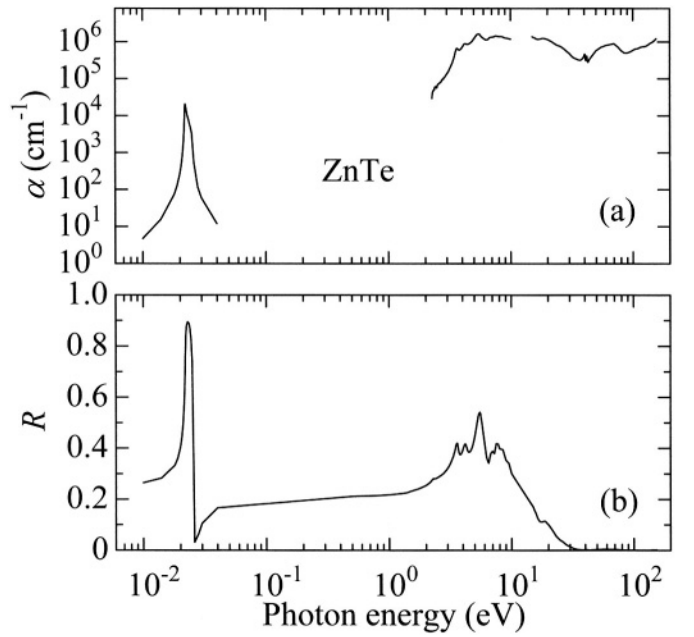

Fig. 9.10.2 (a) Absorption [$\alpha(E)$] and (b) normal-incidence reflectivity spectra [$R(E)$] for ZnTe at 300 K. The numerical data are taken from tabulation by S. Adachi [*Optical Constants of Crystalline and Amorphous Semiconductors: Numerical Data and Graphical Information* (Kluwer Academic, Boston, 1999)].

9.10.2 The Reststrahlen Region

• Static and high-frequency dielectric constants

Table 9.10.1 *Static and high-frequency dielectric constants ε_s and ε_∞ for ZnTe.*

ε_s	ε_∞	Comment
10.10		T=298 K [10.1]
	7.28	T=300 K [10.2]
9.1	6.7	T=100, 300 K [10.3]
10.3	7.62	T=295 K [10.4]
8.3	6.1	T=80 K [10.5]
8.3	6.2	T=290 K [10.5]
9.63	6.3	T=2 K [10.6]
9.65	6.2	T=80 K [10.6]
9.92	6.0	T=300 K [10.6]
8.7	7.2	T=300 K [10.7]
9.3	6.9	T=4.2 K [10.8]
	7.3±0.15	T=300 K [10.9]
10.07	7.29	T=80 K [10.10]
9.4±0.1		T=2 K [10.11]
	7.26	T=300 K [10.12]
9.4	6.9	Mean value at T~300 K

[10.1] D. Berlincourt, H. Jaffe, and L. R. Shiozawa, *Phys. Rev.* **129**, 1009 (1963).
[10.2] D. T. F. Marple, *J. Appl. Phys.* **35**, 539 (1964).
[10.3] A. Manabe, A. Mitsuishi, and H. Yoshinaga, *Jpn. J. Appl. Phys.* **6**, 593 (1967).
[10.4] H. D. Riccius, *J. Appl. Phys.* **39**, 4381 (1968).
[10.5] A. Hadni, J. Claudel, and P. Strimer, *Phys. Status Solidi* **26**, 241 (1968).
[10.6] T. Hattori, Y. Homma, A. Mitsuishi, and M. Tacke, *Opt. Commun.* **7**, 229 (1973).
[10.7] A. N. Pikhtin and A. D. Yas'kov, *Sav. Phys. Semicond.* **12**, 622 (1978).
[10.8] H. Venghaus and B. Jusserand, *Phys. Rev. B* **22**, 932 (1980).
[10.9] B. Oles and H. G. von Schnering, *J. Phys. C: Solid State Phys.* **18**, 6289 (1985).
[10.10] G. Le Bastard, R. Granger, S. Rolland, Y. Marqueton, and R. Triboulet, *J. Phys. (France)* **50,** 3223 (1989).
[10.11] H. P. Wagner, S. Lankes, K. Wolf, W. Kuhn, P. Link, and W. Gebhardt, *J. Cryst. Growth* **117**, 303 (1992).
[10.12] S. Adachi and T. Kimura, *Jpn. J. Appl. Phys.* **32**, 3866 (1993).

Table 9.10.2 *Temperature dependence of the static dielectric constant ε_s for ZnTe.*

$$\varepsilon_s(T) = A + B\left(\frac{T}{\theta}\right) + C\left(\frac{T}{\theta}\right)^2$$

Parameter				Comment
A	B	C	θ(K)	
9.624	0.1583	0.1318	255	T=10–300 K [10.13]

[10.13] M. Schall, M. Walther, and P. U. Jepsen, *Phys. Rev. B* **64**, 94301 (2001).

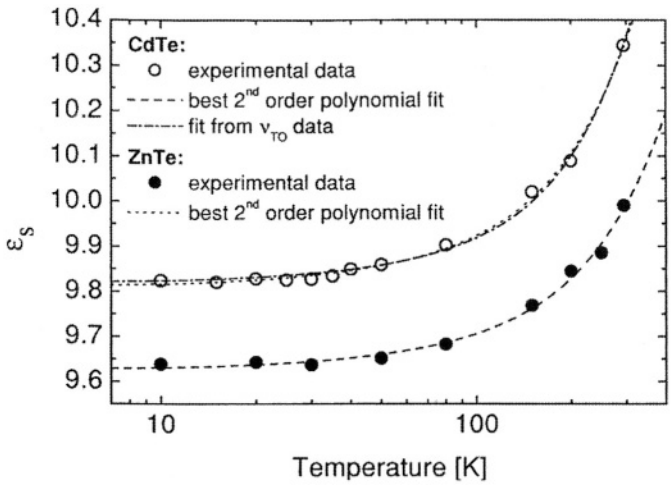

Fig. 9.10.3 Temperature dependence of the static dielectric constant ε_s for ZnTe, together with that for CdTe. [From M. Schall, M. Walther, and P. U. Jepsen, *Phys. Rev. B* **64**, 94301 (2001).]

- **Reststrahlen parameter**

Table 9.10.3 *A set of the reststrahlen parameters for ZnTe.*

$$\varepsilon(\omega) = \varepsilon_\infty \left(1 + \frac{\omega_{LO}^2 - \omega_{TO}^2}{\omega_{TO}^2 - \omega^2 - i\omega\gamma} \right)$$

ε_∞	ω_{LO} (cm^{-1})	ω_{TO} (cm^{-1})	γ (cm^{-1})	Comment
6.7	210	180	2.3	T=100 K [10.14]
6.7	206	177	3.0	T=300 K [10.14]
6.1	210.8	180.7	11.4	T=80 K [10.15]
6.2	205	177	13.3	T=290 K [10.15]

[10.14] A. Manabe, A. Mitsuishi, and H. Yoshinaga, *Jpn. J. Appl. Phys.* **6**, 593 (1967).
[10.15] A. Hadni, J. Claudel, and P. Strimer, *Phys. Status Solidi* **26**, 241 (1968).

9.10.3 At or Near the Fundamental Absorption Edge

- **Free-exciton binding energy and related parameters**

Table 9.10.4 *Free-exciton binding (Rydberg) energy G for ZnTe.*

G (meV)	Comment
8	T=80 K [10.16]
13.2±0.3	T=1.6 K [10.17]
12.8	T=2 K [10.18]
12.7 (Heavy hole) 11.5 (Light hole)	T=2 K [10.19]
13.6	T=10 K [10.20]
12.9±0.1	T=2 K [10.21]
12.1±0.1	T=7 K [10.22]
12.4±0.5	T=4.2 K [10.23]
12.8±0.2	T=300 K [10.24]
12.7	[10.25]

[10.16] K. Kase, *Jpn. J. Appl. Phys.* **12**, 1098 (1973).

[10.17] H. Venghaus and P. J. Dean, *Solid State Commun.* **31**, 897 (1979).
[10.18] W. Maier, G. Schmieder, and C. Klingshirn, *Z. Phys. B* **50**, 193 (1983).
[10.19] H. Leiderer, G. Jahn, M. Silberbauer, W. Kuhn, H. P. Wagner, W. Limmer, and W. Gebhardt, *J. Appl. Phys.* **70**, 398 (1991).
[10.20] G. N. Aliev, N. P. Gavaleshko, O. S. Koshchug, V. I. Pleshko, R. P. Seĭsyan, and K. D. Sushkevich, *Sov. Phys. Solid State* **34**, 1286 (1992).
[10.21] H. P. Wagner, S. Lankes, K. Wolf, W. Kuhn, P. Link, and W. Gebhardt, *J. Cryst. Growth* **117**, 303 (1992).
[10.22] See, K. Reimann, M. Haselhoff, St. Rübenacke, and M. Steube, *Phys. Status Solidi B* **198**, 71 (1996).
[10.23] S. Lee, F. Michl, U. Rössler, M. Dobrowolska, and J. K. Furdyna, *Phys. Rev. B* **57**, 9695 (1998).
[10.24] R. Pässler, E. Griebl, H. Riepl, G. Lautner, S. Bauer, H. Preis, W. Gebhardt, B. Buda, D. J. As, D. Schikora, K. Lischka, K. Papagelis, and S. Ves, *J. Appl. Phys.* **86**, 4403 (1999).
[10.25] Y.-M. Yu, S. Nam, K.-S. Lee, Y. D. Choi, and B. O, *J. Appl. Phys.* **90**, 807 (2001).

Table 9.10.5 *Free-exciton parameters (G=binding energy; a_B=1st-orbital Bohr radius; μ=reduced mass) at the fundamental absorption edge of ZnTe [10.26].*

G (meV)	a_B (Å)	μ (m_0)	Comment
12.8	62	0.078	Direct exciton

[10.26] From tabulation by S. Adachi [*Optical Properties of Crystalline and Amorphous Semiconductors: Materials and Fundamental Properties* (Kluwer Academic, Boston, 1999)].

Table 9.10.6 *Spin-exchange interaction constant j for ZnTe.*

j (meV)	Ref.
0.7±0.1	[10.27]
0.21	[10.28]

[10.27] See, K. Reimann, M. Haselhoff, St. Rübenacke, and M. Steube, *Phys. Status Solidi B* **198**, 71 (1996).
[10.28] See, M. Julier, J. Campo, B. Gil, J. P. Lascaray, and S. Nakamura, *Phys. Rev. B* **57**, R6791 (1998); D. W. Langer, R. N. Euwema, K. Era, and T. Koda, *Phys. Rev. B* **2**, 4005 (1970).

Table 9.10.7 *Pressure coefficient of the free-exciton binding (Rydberg) energy for ZnTe [10.29].*

$\frac{dG}{dp}$ (meV/GPa)
0.61±0.02

[10.29] See, K. Reimann, M. Haselhoff, St. Rübenacke, and M. Steube, *Phys. Status Solidi B* **198**, 71 (1996).

- **Refractive index**

Table 9.10.8 *Refractive index n near the fundamental absorption edge of ZnTe at 300 K [10.30].*

E (eV)	λ (μm)	n	E (eV)	λ (μm)	n
0.5	2.479	2.706	2.07	0.599	3.079
0.6	2.066	2.712	2.091	0.593	3.093
0.7	1.771	2.720	2.112	0.587	3.106
0.8	1.549	2.728	2.131	0.582	3.117
0.9	1.377	2.739	2.153	0.576	3.135
1	1.240	2.750	2.172	0.571	3.150

Table 9.10.8 *Continued.*

E (eV)	λ (μm)	n	E (eV)	λ (μm)	n
1.1	1.127	2.764	2.187	0.567	3.158
1.2	1.033	2.779	2.195	0.565	3.170
1.3	0.953	2.796	2.202	0.563	3.181
1.4	0.885	2.820	2.21	0.561	3.184
1.505	0.824	2.847	2.218	0.559	3.192
1.606	0.772	2.880	2.226	0.557	3.194
1.708	0.726	2.912	2.234	0.555	3.204
1.808	0.686	2.958	2.242	0.553	3.214
1.908	0.650	2.997	2.25	0.551	3.219
2.01	0.617	3.043	2.259	0.549	3.222
2.029	0.611	3.054	2.267	0.547	3.228
2.05	0.605	3.068			

[10.30] See, S. Adachi, *Optical Constants of Crystalline and Amorphous Semiconductors: Numerical Data and Graphical Information* (Kluwer Academic, Boston, 1999).

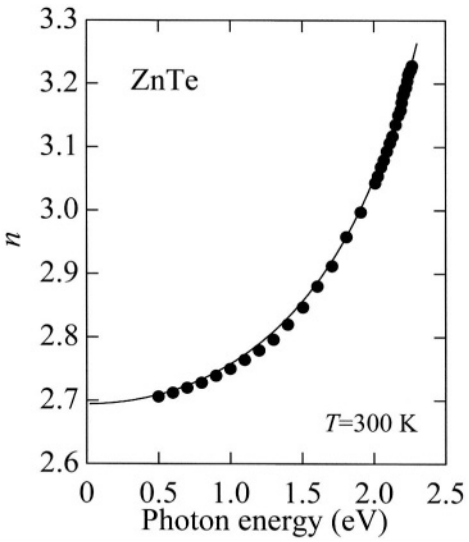

Fig. 9.10.4 Refractive index n for ZnTe. The experimental data are taken from S. Adachi [*Optical Constants of Crystalline and Amorphous Semiconductors: Numerical Data and Graphical Information* (Kluwer Academic, Boston, 1999)]. The solid line represents the calculated result using $n^2=4.04+[3.22\lambda^2/(\lambda^2-0.149)]$ with λ in μm.

- **Refractive index: Temperature dependence**

Table 9.10.9 *Temperature coefficient of the refractive index $n^{-1}(dn/dT)$ in the long-wavelength limit for ZnTe [10.31].*

$\frac{1}{n}\frac{dn}{dT}$ $(10^{-5}\ K^{-1})$
6

[10.31] See, S. Adachi, *Optical Properties of Crystalline and Amorphous Semiconductors: Materials and Fundamental Properties* (Kluwer Academic, Boston, 1999).

- **Refractive index: Pressure dependence**

The pressure dependence of the refractive index n for a thin ZnTe eplilayer grown on (100)GaAs substrate has been measured in the spectral range from the discrete-exciton peak to 900 nm by M. Lindner, G. F. Schötz, P. Link, H. P. Wagner, W. Kuhn, and W. Gebhardt [*J. Phys.: Condens. Matter* **4**, 6401 (1992)].

• **Fundamental absorption edge: Temperature dependence**

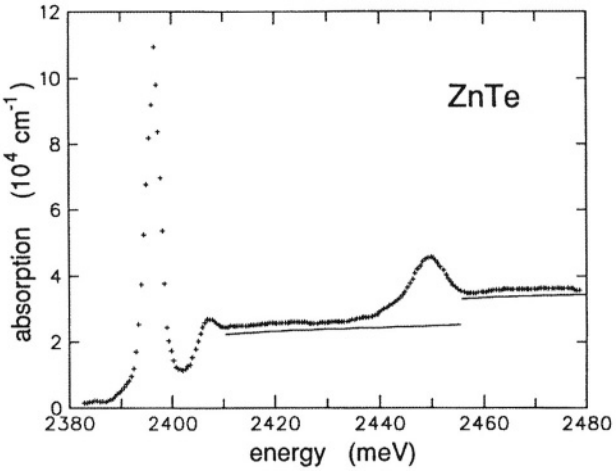

Fig. 9.10.5 Theoretical and experimental excitonic absorption in ZnTe. The experimental spectrum was taken at T=2 K from a thin biaxially-strained ZnTe epilayer glued on glass [H. Leiderer, A. Supritz, M. Silberbauer, M. Lindner, W. Kuhn, H. P. Wagner, and W. Gebhardt, *Semicond. Sci. Technol.* **6**, A101 (1991)]. The biaxial strain is estimated from an energy splitting between the heavy- and light-hole exciton states to be 0.85%. [From H. Mayer, U. Rössler, and M. Ruff, *Phys. Rev. B* **47**, 12929 (1993).]

• **Fundamental absorption edge: Pressure dependence**

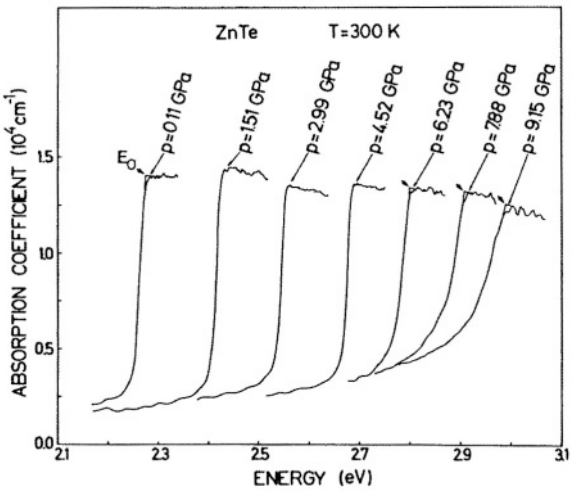

Fig. 9.10.6 Absorption coefficient α in pure ZnTe near the E_0 edge at different hydrostatic pressures. A phase transition occurs at 9.5 GPa. [From S. Ves, K. Strössner, W. Gebhardt, and M. Cardona, *Phys. Rev. B* **33**, 4077 (1986).]

9.10.4 The Interband Transition Region

• **Fundamental optical spectra**

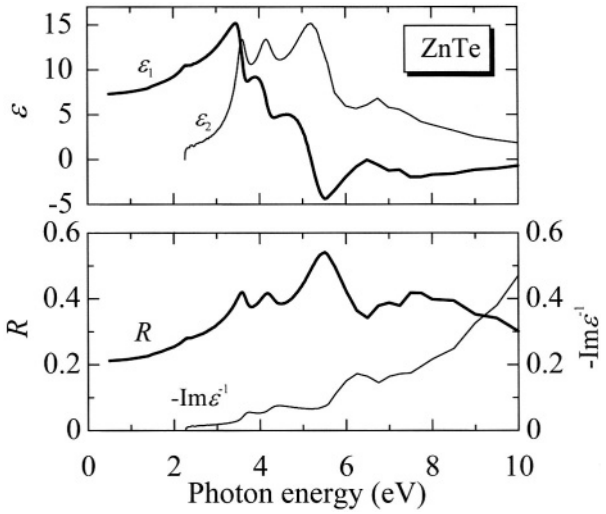

Fig. 9.10.7 Complex dielectric function, $\varepsilon(E)=\varepsilon_2(E)+i\varepsilon_2(E)$, fundamental reflectivity, $R(E)$, and energy-loss function, $-\mathrm{Im}\varepsilon^{-1}(E)$, for ZnTe at 300 K. The experimental data are taken from tabulation by S. Adachi [*Optical Constants of Crystalline and Amorphous Semiconductors: Numerical Data and Graphical Information* (Kluwer Academic, Boston, 1999)].

• **$\varepsilon(E)$ spectrum: External perturbation and/or doping effects**

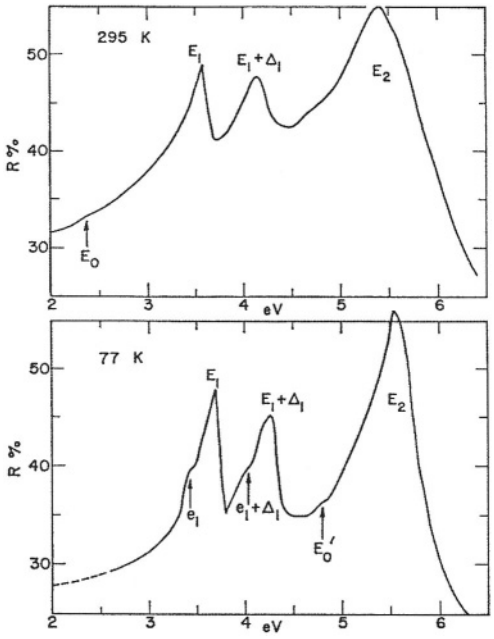

Fig. 9.10.8 Fundamental reflectivity R of ZnTe measured at 295 and 77 K. [From M. Cardona and D. L. Greenaway, *Phys. Rev.* **131**, 98 (1963).]

9.10.5 Free-Carrier Absorption and Related Phenomena

No detailed data are available for ZnTe.

9.11 ELASTOOPTIC, ELECTROOPTIC, AND NONLINEAR OPTICAL PROPERTIES

9.11.1 Elastooptic Effect

• **Photoelastic constant**

Table 9.11.1 *Photoelastic constant p_{ij} in the static limit $(E \to 0\ eV)$ for ZnTe.*

$p_{11}-p_{12}$	p_{44}
–0.04	–0.03

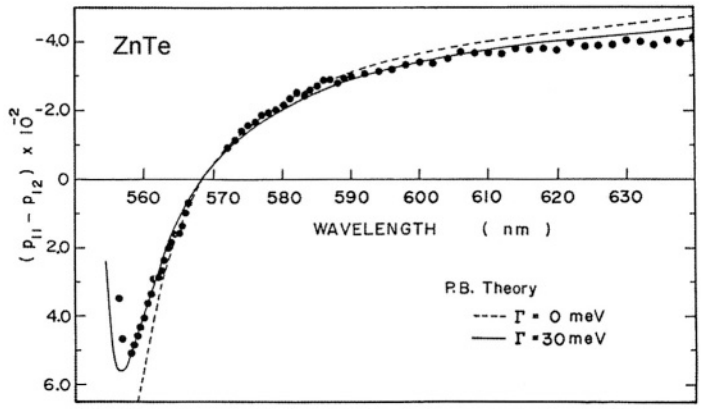

Fig. 9.11.1 Dispersion of the photoelastic constant $p_{11}-p_{12}$ in ZnTe determined by Brillouin scattering at 300 K. The dashed and solid lines are theoretically obtained without and with considering damping effect (Γ), respectively. [From S. Adachi and C. Hamaguchi, *J. Phys. Soc. Jpn* **43**, 1637 (1977).]

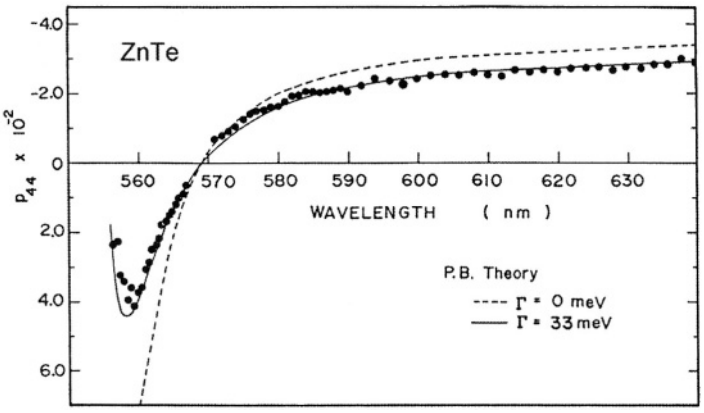

Fig. 9.11.2 Dispersion of the photoelastic constant p_{44} in ZnTe determined by Brillouin scattering at 300 K. The dashed and solid lines are theoretically obtained without and with considering damping effect (Γ), respectively. [From S. Adachi and C. Hamaguchi, *J. Phys. Soc. Jpn* **43**, 1637 (1977).]

9.11.2 Linear Electrooptic Constant

Table 9.11.2 *Free (r_{41}^T) and clamped values (r_{41}^S) of the linear electrooptic constant for ZnTe.*

Wavelength (μm)	$\lvert r_{41}^T \rvert$ (pm/V)	$\lvert r_{41}^S \rvert$ (pm/V)	Ref.
0.59	4.51		[11.1]
0.61	4.38		[11.1]
0.615	4.27		[11.1]
0.625	4.19		[11.1]
0.633		4.3	[11.2]
0.65	4.06		[11.1]
0.675	3.97		[11.1]
0.69	3.98		[11.1]
3.39		3.2	[11.2]
3.41	4.2		[11.3]
10.6	3.9		[11.3]

[11.1] T. R. Sliker and J. M. Jost, *J. Opt. Soc. Am.* **56**, 130 (1966).
[11.2] See, I. P. Kaminow and E. H. Turner, in *Handbook of Lasers,* edited by R. J. Pressley (Chemical Rubber, Cleveland, 1971), Chap. 15.
[11.3] K. Tada and M. Aoki, *Jpn. J. Appl. Phys.* **10**, 998 (1971).

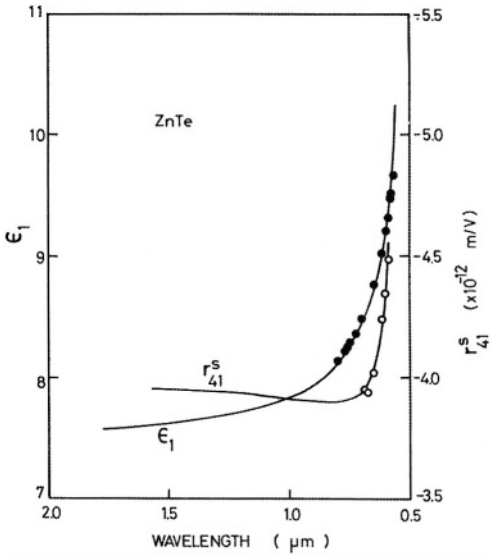

Fig. 9.11.3 Theoretical dispersion of ε_1 and r_{41}^S in ZnTe along with the experimental data. The solid lines represent the theoretical results. [From S. Adachi and K. Oe, *J. Appl. Phys.* **56**, 74 (1984).]

9.11.3 Quadratic Electrooptic Constant

No detailed data are available for ZnTe.

9.11.4 Franz–Keldysh Effect

No detailed data are available for ZnTe.

9.11.5 Nonlinear Optical Constant

• Second-order nonlinear optical susceptibility

Table 9.11.3 *Experimental second-order nonlinear optical susceptibility d_{14} for ZnTe.*

Wavelength, in μm (Energy, in eV)	d_{14} *	Ref.
1.047 (1.184)	119 (pm/V)	[11.4]
1.321 (0.938)	52 (pm/V)	[11.4]
1.5 (0.83)	58 (pm/V)	[11.5]
1.9 (0.65)	48 (pm/V)	[11.5]
10.6 (0.117)	22 (10^{-8} esu)	[11.6]

[11.4] H. P. Wagner, M. Kühnelt, W. Langbein, and J. M. Hvam, *Phys. Rev. B* **58**, 10494 (1998).
[11.5] A. Zappettini, S. M. Pietralunga, A. Milani, D. Piccinin, M. Feré, and M. Martinelli, *J. Electron. Mater.* **30**, 738 (2001).
[11.6] C. K. N. Patel, *Phys. Rev. Lett.* **16**, 613 (1966).
*1 m/V=$3\times10^4/4\pi$ esu.

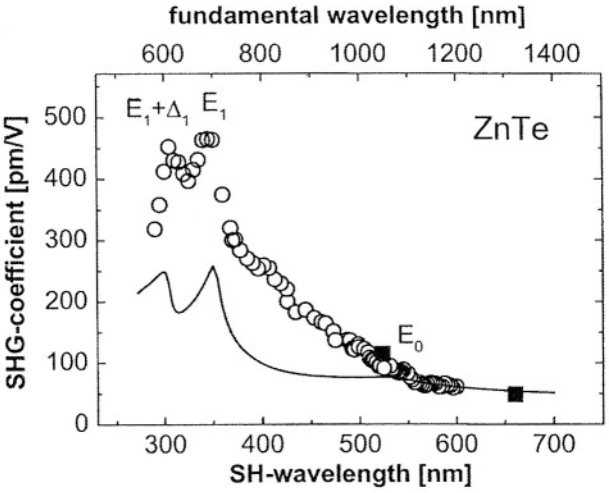

Fig. 9.11.4 Experimental dispersion of the second-harmonic-generation (SHG) coefficient $|d_{14}|$ in ZnTe as a function of fundamental wavelength. The solid line gives the theoretical dispersion curve. [From H. P. Wagner, M. Kühnelt, W. Langbein, and J. M. Hvam, *Phys. Rev. B* **58**, 10494 (1998).]

• Third-order nonlinear optical susceptibility

Table 9.11.4 *Theoretical third-order nonlinear optical susceptibility $\chi^{(3)}_{ijkl}(-3\omega;\omega,\omega,\omega)$ in the static limit ($\hbar\omega\to0$ eV) for ZnTe.*

$\chi^{(3)}_{ijkl}$ (10^{-11} esu)*		Ref.
$\chi^{(3)}_{1111}$	$\chi^{(3)}_{1212}$	
0.06	0.22	[11.7]
2.87	1.53	[11.8]

[11.7] Ed Ghahramani, D. J. Moss, and J. E. Sipe, *Phys. Rev. B* **43**, 9700 (1991).
[11.8] W. Y. Ching and M.-Z. Huang, *Phys. Rev. B* **47**, 9479 (1993).
*1 $m^2/V^2=9\times10^8/4\pi$ esu.

• **Two-photon optical absorption**

Table 9.11.5 *Two-photon absorption coefficient β for ZnTe.*

Wavelength (μm)	β (cm/GW)	Ref.
0.6943	500	(T=77 K) [11.9]
	8000	[11.10]
1.064	4.5	[11.11]
	4.2	[11.12]

[11.9] G. N. Yablonskii, *Sov. Phys. Semicond.* **8**, 881 (1975).
[11.10] G. Kobbe and C. Klingshirn, *Z. Phys. B* **37**, 9 (1980).
[11.11] E. W. Van Stryland, H. Vanherzeele, M. A. Woodall, M. J. Soileau, A. L. Smirl, S. Guha, and T. F. Boggess, *Opt. Eng.* **24**, 613 (1985).
[11.12] A. A. Said, M. Sheik-Bahae, D. J. Hagan, T. H. Wei, J. Wang, J. Young, and E. W. Van Stryland, *J. Opt. Soc. Am. B* **9**, 405 (1992).

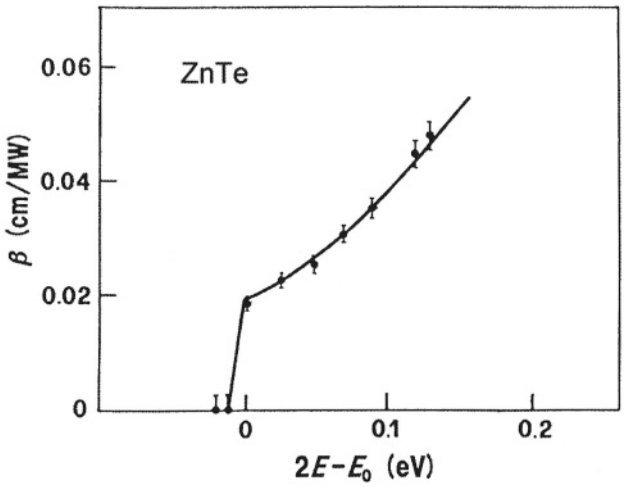

Fig. 9.11.5 Two-photon absorption coefficient β versus $2E-E_0$ (E: incident photon energy) for ZnTe. [From I. M. Catalano and A. Cingolani, *Phys. Rev. B* **19**, 1049 (1979).]

9.12 CARRIER TRANSPORT PROPERTIES

9.12.1 Low-Field Mobility: Electrons

Table 9.12.1 *300-K (μ_{300K}) and peak Hall mobilities (μ_{peak}) for electrons in ZnTe.*

Mobility	Value (cm^2/V s)	Comment
μ_{300K}	600	[12.1]
μ_{peak}		*

[12.1] J. H. Chang, T. Takai, B. H. Koo, J. S. Song, T. Handa, and T. Yao, *Appl. Phys. Lett.* **79**, 785 (2001).

*No Hall-effect data are available for *n*-ZnTe at temperatures below 300 K. This may be mainly due to Ohmic-contact problem.

• **Temperature dependence**

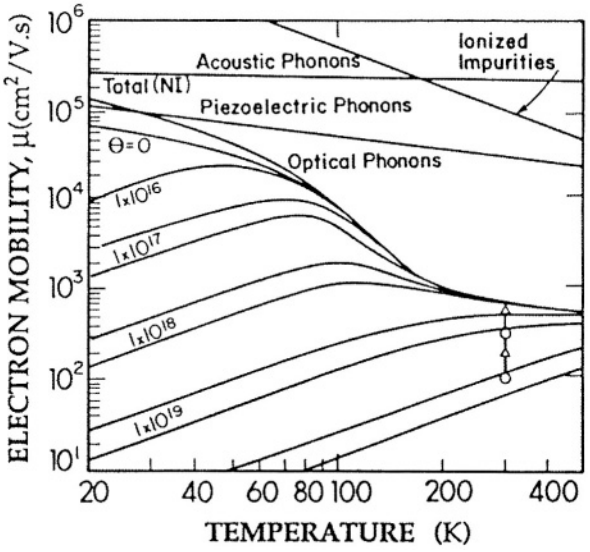

Fig. 9.12.1 Total and individual electron mobilities calculated at different ionized-impurity concentrations (N_I) versus temperature, together with a compensation-ratio limit curve (θ=0), in *n*-ZnTe. The open circles and triangles represent the experimental data. [From H. E. Ruda, *J. Phys. D: Appl. Phys.* **24**, 1158 (1991).]

• **Donor concentration (free-carrier) dependence**

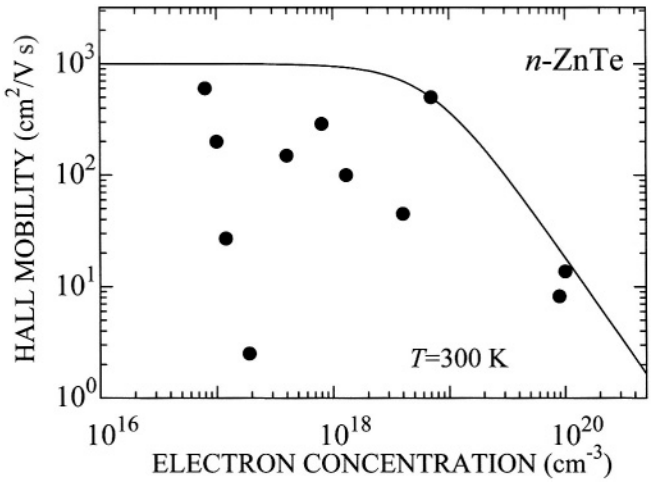

Fig. 9.12.2 Electron Hall mobility μ versus electron concentration n in *n*-ZnTe at 300 K. The experimental data are gathered from various sources. The solid line represents the calculated result with $\mu = 1000/[1+(n/7\times10^{18})^{1.5}]$, where n is in cm^{-3} and μ is in $cm^2/V\,s$.

• **Hall factor**

The Hall factor for ZnTe has been obtained theoretically by D. L. Rode [*Phys. Status Solidi B* **55**, 687 (1973)], and its value is reported to be $\gamma \sim 1.07$ at T=300 K.

9.12.2 Low-Field Mobility: Holes

Table 9.12.2 *300-K (μ_{300K}) and peak Hall mobilities (μ_{peak}) for electrons in ZnTe.*

Mobility	Value ($cm^2/V\,s$)	Comment
μ_{300K}	100	[12.2]
μ_{peak}	6.5×10^3	T=35 K [12.2]
	8.5×10^5	Cyclotron mobility, T=3.5 K [12.3]

[12.2] M. Aven, *J. Appl. Phys.* **38**, 4421 (1967).
[12.3] B. Clerjaud, A. Gélineau, D. Galland, and K. Saminadayar, *Phys. Rev. B* **19**, 2056 (1979).

• **Temperature dependence**

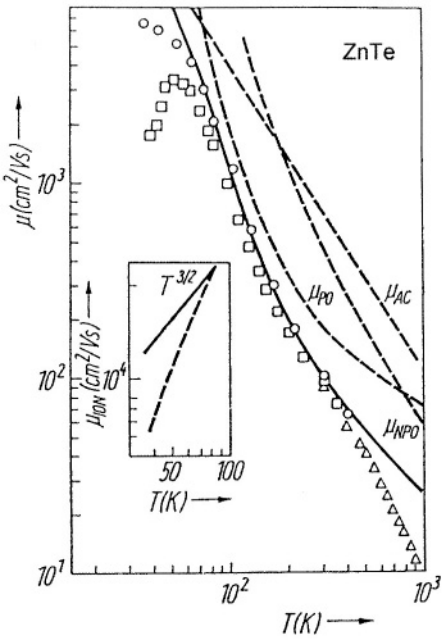

Fig. 9.12.3 Temperature variation of the hole Hall mobility μ for *p*-ZnTe. The experimental data are taken from M. Aven [open circles, *J. Appl. Phys.* **38**, 4421 (1967)], from T. L. Larsen and D. A. Stevenson [open squares, *J. Appl. Phys.* **43**, 172 (1972)], and from F. T. J. Smith [open triangles, *Solid State Commun.* **9**, 957 (1971)]. The dashed lines represent the mobilities limited by polar optical phonon scattering (μ_{PO}), by nonpolar optical phonon scattering (μ_{NPO}), and by nonpolar acoustic phonon scattering (μ_{AC}). The solid line represents the resultant mobility using Matthiessen's rule. The inset gives the temperature dependence of the mobility due to ionized-impurity scattering. [From D. Kranzer, *Phys. Status Solidi A* **26**, 11 (1974).]

• **Acceptor concentration (free-carrier) dependence**

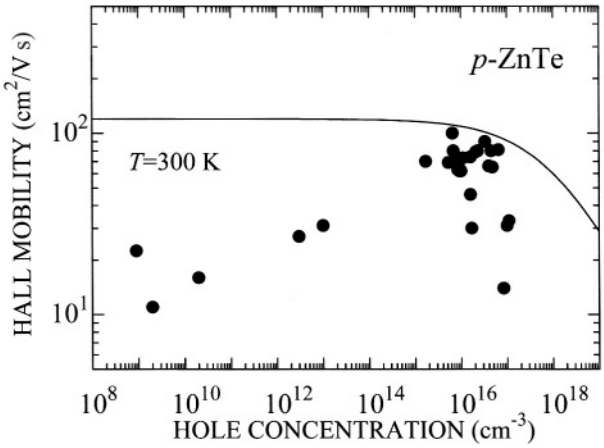

Fig. 9.12.4 Hole Hall mobility μ versus hole concentration p in *p*-ZnTe at 300 K. The experimental data are gathered from various sources. The solid line represents the calculated result with $\mu = 120/[1 + (p/10^{18})^{0.50}]$, where p is in cm^{-3} and μ is in cm^2/V s.

9.12.3 High-Field Transport: Electrons

• **LO-phonon-scattering-limited electron saturation drift velocity**

Table 9.12.3 *Calculated LO-phonon-scattering-limited electron saturation drift velocity $v_{e,sat}$ in the lowest-conduction-band valley α for ZnTe at 300 K.**

$$v_{e,sat}^{\alpha} = \left(\frac{8\hbar\omega_{LO}}{3\pi m_c^{\alpha}}\right)^{1/2}$$

Valley	$v_{e,sat}$ (10^7 cm/s)
Γ	1.8

*Calculated with $m_c^{\Gamma}=0.117m_0$ and $\omega_{LO}=210$ cm^{-1}.

9.12.4 High-Field Transport: Holes

No detailed data are available for ZnTe.

9.12.5 Minority-Carrier Transport: Electrons in *p*-Type Materials

- **Minority-electron lifetime**

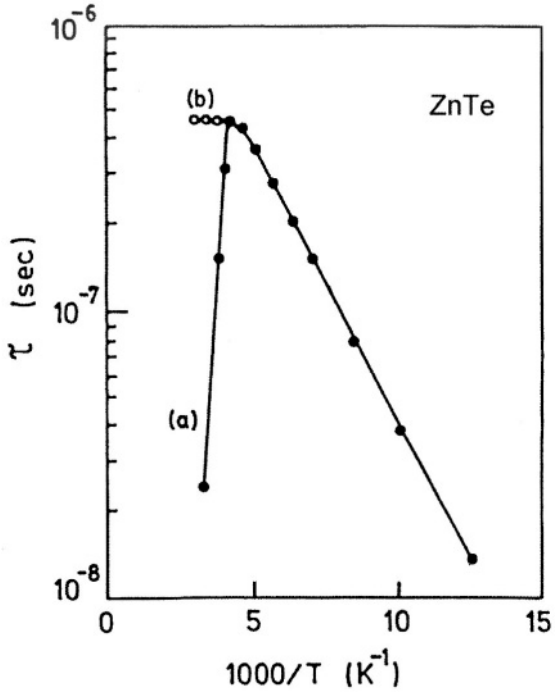

Fig. 9.12.5 Minority-electron lifetime versus reciprocal temperature for *p*-type ZnTe before (curve a) and after 60 min of hydrogen passivation (curve b). [From S. Bhunia, D. Pal, and D. N. Bose, *Semicond. Sci. Technol.* **13**, 1434 (1998).]

- **Minority-electron diffusion length**

Table 9.12.4 *Minority-electron diffusion length L in p-ZnTe at 300 K.*

L (μm)	Comment
0.3	$p=5\times10^{16}$ cm^{-3} [12.4]
12	$N_A=4.80\times10^{15}$ cm^{-3} [12.5]
5.8	$N_A=1.35\times10^{16}$ cm^{-3} [12.5]
7.0	$N_A=1.98\times10^{16}$ cm^{-3} [12.5]
9.8	$N_A=3.10\times10^{16}$ cm^{-3} [12.5]
13	$N_A=3.50\times10^{17}$ cm^{-3} [12.5]

[12.4] J. Gautron and P. Lemasson, *J. Cryst. Growth* **59**, 332 (1982).
[12.5] F. El Akkad, A. Al-Shahrany, *Phys. Status Solidi A* **118**, K79 (1990).

9.12.6 Minority-Carrier Transport: Holes in *n*-Type Materials

No detailed data are available for ZnTe.

9.12.7 Impact Ionization Coefficient

No detailed data are available for ZnTe.

Chapter 10

Cubic Cadmium Sulphide (*c*-CdS)

10.1 STRUCTURAL PROPERTIES

10.1.1 Ionicity

Table 10.1.1 *Phillips's ionicity f_i for c-CdS [1.1].*

f_i
0.685

[1.1] J. C. Phillips, *Bonds and Bands in Semiconductors* (Academic, New York, 1973).

10.1.2 Elemental Isotopic Abundance and Molecular Weight

- **Isotopic abundance**

Table 10.1.2 *Isotopic abundance in percent for cadmium and sulfur [1.2].*

Isotope	% nat. abundance	Isotope	% nat. abundance	Isotope	% nat. abundance
^{106}Cd	1.25	^{112}Cd	24.13	^{32}S	95.02
^{108}Cd	0.89	^{113}Cd	12.22	^{33}S	0.75
^{110}Cd	12.49	^{114}Cd	28.73	^{34}S	4.21
^{111}Cd	12.80	^{116}Cd	7.49	^{36}S	0.02

[1.2] D. R. Lide, *CRC Handbook of Chemistry and Physics,* 78th Edition (CRC Press, Boca Raton, 1997).

- **Molecular weight**

Table 10.1.3 *Molecular (average atomic) weight M for c-CdS.*

M (amu)
144.477

10.1.3 Crystal Structure and Space Group

Table 10.1.4 *Crystal structure and its space and pint groups for c-CdS.*

Crystal structure	Space group	Point group
Zincblende (Cubic)	$F\bar{4}3m$	T_d

10.1.4 Lattice Constant and Its Related Parameters

- **Lattice constant, near-neighbor distance, etc.**

Table 10.1.5 *Lattice constant (a), near-neighbor distance (d), unit cube volume (a^3), and molecular density (d_M) for c-CdS at 300 K.*

Parameter	Value
Lattice constant a (Å)	5.825 [1.3]
d (Cation–Anion) (Å)	2.522*
d (Cation–Cation) (Å)	4.119*
Unit cube volume a^3 (10^{-22} cm^3)	1.976*
Molecular density d_M (10^{22} cm^{-3})	2.024*

[1.3] W. R. Cook, Jr., *J. Am. Ceram. Soc.* **51**, 518 (1968).
*Calculated.

- **Crystal density**

Table 10.1.6 *Crystal density g for c-CdS at 300 K.**

g (g/cm^3)
4.855

*Calculated using a=5.825 Å.

10.1.5 Structural Phase Transition

Table 10.1.7 *Structural phase transition in c-CdS at high temperatures.*

Structure	Transition temperature (°C)
Zincblende ($F\bar{4}3m$)	Room temperature
Wurtzite ($P6_3mc$)	300 [1.4]

[1.4] O. Zelaya-Angel and R. Lozada-Morales, *Phys. Rev. B* **62**, 13064 (2000).

10.1.6 Cleavage Plane

Table 10.1.8 *Crystallographic plane most readily cleaved for c-CdS.**

Cleavage plane
(110)

*Expected.

- **Surface energy**

Table 10.1.9 *Surface energy for c-CdS (in J/m^2).*

Plane			Comment
(110)	(111)	$(\bar{1}\,\bar{1}\,\bar{1})$	
1.06	1.07	0.69	Calc. [1.5]

[1.5] B. N. Oshcherin, *Phys. Status Solidi A* **34**, K181 (1976).

10.2 THERMAL PROPERTIES

10.2.1 Melting Point and Its Related Parameters

Table 10.2.1 *Melting point T_m and its related parameter for CdS.*

Parameter	Value
Melting point T_m (K)	1748 [2.1]
Entropy of fusion ΔS_m (cal/mol K)	16.21 [2.2]

[2.1] H. H. Woodbury, *J. Phys. Chem. Solids* **24**, 881 (1963).
[2.2] See, B. R. Nag, *J. Electron. Mater.* **26**, 70 (1997).

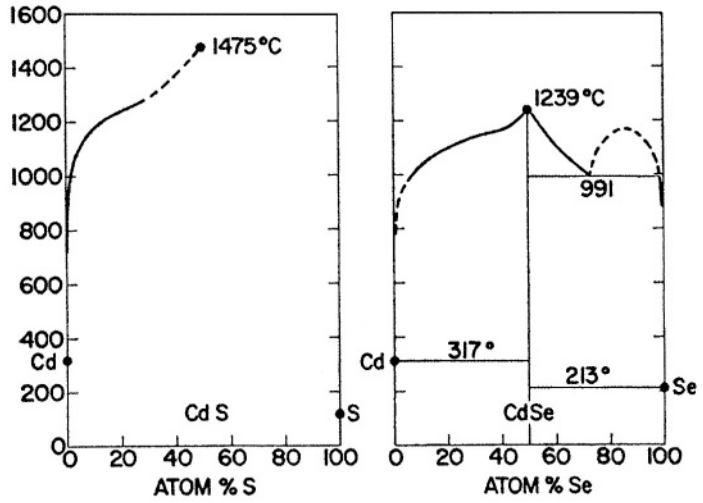

Fig. 10.2.1 *T–x* projects of the II–VI binary systems Cd–S and Cd–Se. [From M. R. Lorenz, in *Physics and Chemistry of II–VI Compounds,* edited by M. Aven and J. S. Prener (North-Holland, Amsterdam, 1967), p. 73.]

10.2.2 Specific Heat

No detailed data are available for *c*-CdS.

10.2.3 Debye Temperature

No detailed data are available for *c*-CdS.

10.2.4 Thermal Expansion Coefficient

No detailed data are available for *c*-CdS.

10.2.5 Thermal Conductivity and Diffusivity

No detailed data are available for *c*-CdS.

10.3 ELASTIC PROPERTIES

10.3.1 Elastic Constant

- **Room-temperature value**

Table 10.3.1 *Elastic stiffness and compliance constants for c-CdS at 300 K.*

Parameter	Value
Stiffness (10^{11} dyn/cm^2) [3.1]	
C_{11}	7.70
C_{12}	5.39
C_{44}	2.36
Compliance (10^{-12} cm^2/dyn) [3.2]	
S_{11}	3.07
S_{12}	−1.26
S_{44}	4.24

[3.1] Average values [see, *Data and Functional Relationships in Science and Technology,* edited by K.-H. Hellwege and A. M. Hellwege, Landolt–Börnstein, New Series, Group III, Vol. 11 (Springer, Berlin, 1979)].
[3.2] Calculated from C_{ij} values.

10.3.2 Third-Order Elastic Constant

Table 10.3.2 *Third-order elastic constant of c-CdS [3.3].*

Modulus	Value (10^{12} dyn/cm^2)
C_{111}	−2.5
C_{112}	−2.8
C_{123}	−1.9
C_{144}	+0.3
C_{166}	−0.6
C_{456}	+0.4

[3.3] *Numerical Data and Functional Relationships in Science and Technology,* edited by K.-H. Hellwege and A. M. Hellwege, Landolt–Börnstein, New Series, Group III, Vol. 11 (Springer, Berlin, 1979).

10.3.3 Young's Modulus, Poisson's Ratio, and Similar

- **Young's modulus**

Table 10.3.3 *Young's modulus Y for c-CdS at 300 K.**

Crystallographic plane	Y (10^{11} dyn/cm^2)
(100) plane	
[001] direction	3.26
[011] direction	5.09
(110) plane	
[001] direction	3.26
[111] direction	6.26
(111) plane	5.09

*Calculated using S_{11}=3.07, S_{12}=−1.26, and S_{44}=4.24 (all in 10^{-12} cm^2/dyn).

- **Poisson's ratio**

Table 10.3.4 *Poisson's ratio P for c-CdS at 300 K.**

Crystallographic plane	P
(100) plane	
m=[010], n=[001]	0.410
m=[011], n=[0$\bar{1}$1]	0.079
(110) plane	
m=[001], n=[1$\bar{1}$0]	0.410
m=[$\bar{1}$11], n=[1$\bar{1}\bar{2}$]	0.328
(111) plane	0.454

*Calculated using S_{11}=3.07, S_{12}= −1.26, and S_{44}=4.24 (all in 10^{-12} cm^2/dyn).

- **Bulk modulus, shear modulus, etc.**

Table 10.3.5 *Bulk modulus, B_u, pressure derivative of B_u, dB_u/dp, shear modulus, C_s, isotropy factor, A, linear compressibility, C_o, Caucy ratio, C_a, and Born ratio, B_o, for c-CdS at 300 K.*

Parameter	Value
B_u (10^{11} dyn/cm^2)	6.16 [3.4]
dB_u/dp	4.8 [3.5]
C_s (10^{11} dyn/cm^2)	1.16 [3.4]
A	0.489 [3.4]
C_o (10^{-13} cm^2/dyn)	5.41 [3.4]
C_a	2.28 [3.4]
B_o	1.04 [3.4]

[3.4] Calculated using C_{11}=7.70, C_{12}=5.39, and C_{44}=2.36 (all in 10^{11} dyn/cm^2).
[3.5] Theor. [S.-H. Wei and A. Zunger, *Phys. Rev. B* **60**, 5404 (1999)].

10.3.4 Microhardness

No detailed data are available for *c*-CdS.

10.3.5 Sound Velocity

Table 10.3.6 *Sound velocity propagating in c-CdS at 300 K.* LA=longitudinal acoustic; TA1, TA2=transverse acoustic.*

Propagation direction	Mode	Sound velocity (10^5 cm/s)
[100]	LA	3.98
[100]	TA1, TA2	2.20
[110]	LA	4.28
[110]	TA1	1.54
[110]	TA2	2.20
[111]	LA	4.38
[111]	TA1, TA2	1.79

*Calculated using $C_{11}=7.70\times10^{11}$ dyn/cm^2, $C_{12}=5.39\times10^{11}$ dyn/cm^2, $C_{44}=2.36\times10^{11}$ dyn/cm^2, and $g=4.855$ g/cm^3.

10.4 PHONONS AND LATTICE VIBRONIC PROPERTIES

10.4.1 Phonon Dispersion Relation

Lattice dynamics and phonon dispersion curves for *c*-CdS has been discussed theoretically by M. A. Nusimovici and J. L. Birman [*Phys. Rev.* **156**, 925 (1967)].

10.4.2 Phonon Frequency

- **Room-temperature value**

Table 10.4.1 *Long-wavelength ($q\rightarrow0$) and zone-boundary phonon frequencies for c-CdS.**

Critical point	Phonon	Phonon frequency (cm^{-1})
Γ	TO	237
	LO	303
X	TA	
	LA	
	TO	
	LO	
L	TA	41
	LA	
	TO	255
	LO	

*Estimated from *w*-CdS data.

10.4.3 Mode Grüneisen Parameter

No detailed data are available for *c*-CdS.

10.4.4 Phonon Deformation Potential

No detailed data are available for *c*-CdS.

10.5 COLLECTIVE EFFECTS AND RELATED PROPERTIES

10.5.1 Piezoelectric Constant

No detailed data are available for *c*-CdS.

10.5.2 Fröhlich Coupling Constant

No detailed data are available for *c*-CdS.

10.6 ENERGY-BAND STRUCTURE: ENERGY-BAND GAPS

10.6.1 Basic Properties

- **Electronic energy-band structure**

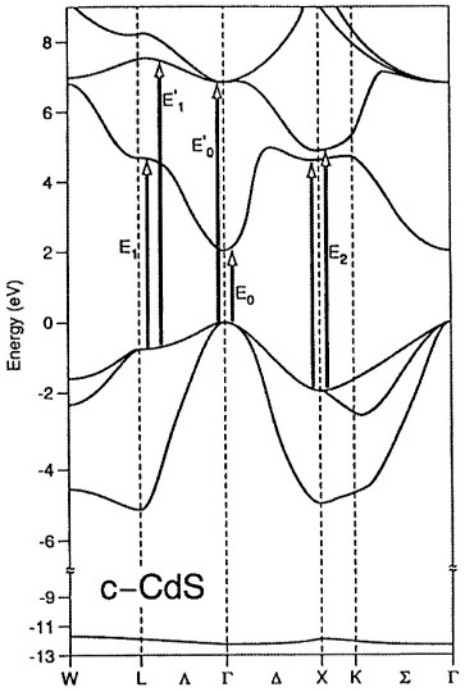

Fig. 10.6.1 Electronic energy-band structure of *c*-CdS as calculated within the local-density-functional formalism. [From A. Zunger and A. J. Freeman, *Phys. Rev. B* **17**, 4850 (1978).] The locations of several interband transitions are included by the vertical arrows.

• **Electronic density of states**

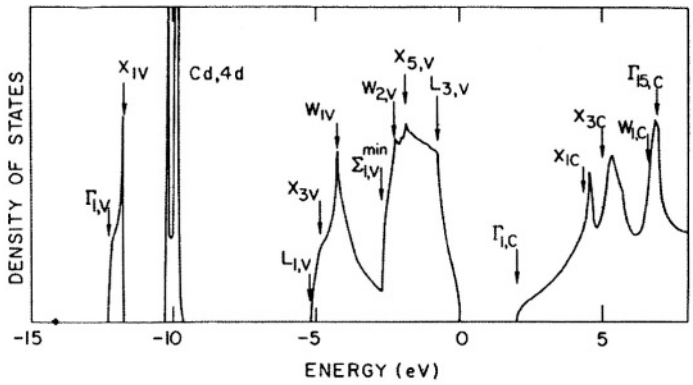

Fig. 10.6.2 Electronic density of states for *c*-CdS as calculated within the local-density-functional formalism. [From A. Zunger and A. J. Freeman, *Phys. Rev. B* **17**, 4850 (1978).]

• **Energy eigenvalue**

Table 10.6.1 *Energy eigenvalues at the Γ, X, and L points for the valence and first few conduction bands of c-CdS [6.1].*

Critical point	Level	Value (eV)	
		Calc.	Exper.*
Γ	Γ_6^v (Γ_1^v)	−11.46	
	Γ_7^v (Γ_{15}^v)	0.00	−0.07
	Γ_8^v		0.00
	Γ_6^c (Γ_1^c)	2.62	2.40–2.55
	Γ_7^c (Γ_{15}^c)	7.61	7.4
	Γ_8^c		
X	X_6^v (X_1^v)	−11.42	−13.85
	X_6^v (X_3^v)	−2.64	−3.7, −4.8
	X_6^v (X_5^v)	−1.06	−1.54, −1.9
	X_7^v		
	X_6^c (X_1^c)	5.24	
	X_7^c (X_3^c)	5.45	
L	L_6^v (L_1^v)	−11.43	
	L_6^v (L_1^v)	−2.75	−4.18, −4.8
	L_6^v (L_3^v)	−0.41	−0.62, −0.8
	$L_{4,5}^v$		
	L_6^c (L_1^c)	4.04	
	L_6^c (L_3^c)	8.36	
	$L_{4,5}^c$		

[6.1] A. Zunger and A. J. Feeman, *Phys. Rev. B* **17**, 4850 (1978).
*The data are gathered from various sources.

10.6.2 E_0-Gap Region

- **Temperature dependence**

Table 10.6.2 *E_0- and $E_0+\Delta_0$-gap energies for c-CdS determined at various temperatures.*

Temperature (K)	E_0 (eV)	$E_0+\Delta_0$ (eV)	Comment
4.2	2.48		Epilayer on (110)InP [6.2]
300	2.50 *[1]		Epilayer on (111)GaAs [6.3]
	2.55 *[2]		
	2.41		Epilayer on (110)InP [6.4]
	2.40±0.01		Polycrystalline film [6.5]
	2.45		Polycrystalline film [6.6]
	2.42		Polycrystalline film [6.7]
	2.46	(2.53)	Mean value (T=300 K)

[6.2] D. R. T. Zahn, G. Kudlek, U. Rossow, A. Hoffmann, I. Broser, and W. Richter, *Adv. Mater. Opt. Electron.* **3**, 11 (1994).
[6.3] M. Cardona, M. Weinstein, and G. A. Wolff, *Phys. Rev.* **140,** A633 (1965).
[6.4] U. Rossow, T. Werninghaus, D. R. T. Zahn, W. Richter, and K. Horn, *Thin Solid Films* **233,** 176 (1993).
[6.5] O. Zelaya-Angel, J. J. Alvarado-Gil, R. Lozada-Morales, H. Vargas, and A. F. da Silva, *Appl. Phys. Lett.* **64**, 291 (1994).
[6.6] O. Zelaya-Angel and R. Lozada-Morales, *Phys. Rev. B* **62**, 13064 (2000).
[6.7] O. Vigil, O. Zelaya-Angel, and Y. Rodrìguez, *Semicond. Sci. Technol.* **15**, 259 (2000).
*[1] Peak in R.
*[2] Peak in ε_2.

Table 10.6.3 *Empirical equation for the heavy-hole (HH) and light-hole (LH) band-gap energy variation with temperature T for c-CdS.*

$$E_0(T) = E_0(0) - \frac{\alpha T^2}{T+\beta}$$

Parameter			Comment
E_0 (0) (eV)	α (10^{-4} eV/K)	β (K)	
2.445 (HH)	3.451	208	n=1 exciton, epilayer on (100)GaAs, T=13–200 K [6.8]
2.455 (LH)	3.966	222	

[6.8] T. Nagai, Y. Kanemitsu, M. Ando, T. Kushida, S. Nakamura, Y. Yamada, and T. Taguchi, *Phys. Status Solidi B* **229**, 611 (2002).

Table 10.6.4 *Empirical equation for the heavy-hole (HH) and light-hole (LH) band-gap energy variation with temperature T for c-CdS.*

$$E_0(T) = E_B - a_B\left(1 + \frac{2}{e^{\Theta/T}-1}\right)$$

Parameter			Comment
E_B (eV)	a_B (mV)	Θ (K)	
2.464 (HH)	20.5	165	n=1 exciton, epilayer on (100)GaAs, T=13–200 K [6.9]
2.479 (LH)	25.4	177	

[6.9] T. Nagai, Y. Kanemitsu, M. Ando, T. Kushida, S. Nakamura, Y. Yamada, and T. Taguchi, *Phys. Status Solidi B* **229**, 611 (2002).

Table 10.6.5 *Spin–orbit–splitoff energy Δ_0 for c-CdS.**

Δ_0 (eV)	Comment
0.079	Calc. [6.10]
~0.07	T=1.7 K [6.11]

[6.10] M. Willatzen, M. Cardona, and N. E. Christensen, *Phys. Rev. B* **51**, 17992 (1995).
[6.11] See, D. W. Niles and H. Höchst, *Phys. Rev. B* **44**, 10965 (1991).
*Note that Δ_0 may not vary with temperature if one supposes the valence-band rigidity of the III–V compounds.

- **Temperature and/or pressure coefficient**

Table 10.6.6 *Linear temperature and pressure coefficients of the E_0- and $E_0+\Delta_0$-gap energies for c-CdS.*

Band gap	Coefficient	Value	Comment
E_0	dE_g/dT (10^{-4} eV/K)		
	dE_g/dp (10^{-2} eV/GPa)	5.5	Calc. [6.12]
		4.7	Calc. [6.13]
		–0.7	p>6 GPa [6.14]
$E_0+\Delta_0$	dE_g/dT (10^{-4} eV/K)		
	dE_g/dp (10^{-2} eV/GPa)		

[6.12] K. J. Chang, S. Froyen, and M. L. Cohen, *Solid State Commun.* **50**, 105 (1984).
[6.13] S.-H. Wei and A. Zunger, *Phys. Rev. B* **60**, 5404 (1999).
[6.14] See, B. Ray, *II–VI Compounds* (Pergamon, Oxford, 1969).

10.6.3 Higher-Lying Direct Gap

- **Temperature dependence**

Table 10.6.7 *Higher-lying direct-gap energies for c-CdS at several temperatures.*

Band gap	Value (eV)	
	T=90 K [6.15]	T=300 K [6.16]
E_1	5.0	5.1
E_2	6.4, 6.9	
E_0'	7.4	
E_1'	8.3	

[6.15] Ph. Hofmann, K. Horn, A. M. Bradshaw, R. L. Johnson, D.Fuchs, and M. Cardona, *Phys. Rev.* **47**, 1639 (1993).
[6.16] U. Rossow, T. Werninghaus, D. R. T. Zahn, W. Richter, and K. Horn, *Thin Solid Films* **233**, 176 (1993).

10.6.4 Lowest Indirect Gap

- **Theoretical value**

Table 10.6.8 *Theoretically obtained lowest indirect-gap energy for c-CdS (in eV).*

E_g^{L} *1	E_g^{X} *2	Ref.
4.04	5.24	[6.17]
4.30	4.72	[6.18]

Table 10.6.8 *Continued.*

E_g^{L} *1	E_g^{X} *2	Ref.
4.13	4.05	[6.19]
4.82	5.08	[6.20]

[6.17] A. Zunger and A. J. Feeman, *Phys. Rev. B***17**, 4850 (1978).
[6.18] M.-Z. Huang and W. Y. Ching, *J. Phys. Chem. Solids* **46**, 977 (1985).
[6.19] Y. Li and P. J. Lin-Chung, *Phys. Status Solidi B* **153**, 215 (1989).
[6.20] O. Zakharov, A. Rubio, X. Blase, M. L. Cohen, and S. L. Louie, *Phys. Rev. B* **50**, 10780 (1994).
*1 $\Gamma_8^v(\Gamma_{15}^v) \rightarrow L_6^c(L_1^c)$.
*2 $\Gamma_8^v(\Gamma_{15}^v) \rightarrow X_6^c(X_1^c)$.

- **Temperature and/or pressure coefficient**

Table 10.6.9 *Linear pressure coefficient of the lowest indirect-gap energy for c-CdS.*

Coefficient	Value	Comment
dE_g^{L}/dp (10^{-2} eV/GPa)	4.2	Calc. [6.21]
	3.6	Calc. [6.22]
dE_g^{X}/dp (10^{-2} eV/GPa)	−1.0	Calc. [6.21]
	−1.4	Calc. [6.22]

[6.21] K. J. Chang, S. Froyen, and M. L. Cohen, *Solid State Commun.* **50,** 105 (1984).
[6.22] S.-H. Wei and A. Zunger, *Phys. Rev. B* **60**, 5404 (1999).

10.6.5 Conduction-Valley Energy Separation

No detailed data are available for *c*-CdS.

10.6.6 Direct–Indirect-Gap Transition Pressure

No detailed data are available for *c*-CdS.

10.7 ENERGY-BAND STRUCTURE: ELECTRON AND HOLE EFFECTIVE MASSES

10.7.1 Electron Effective Mass: Γ Valley

- **Theoretical value**

Table 10.7.1 *Theoretically obtained electron effective mass m_e^{Γ} at the Γ valley for c-CdS.*

m_e^{Γ}/m_0	Technique
0.14	*f*-sum rule [7.1]
0.209	Linear combination of atomic orbital method [7.2]

[7.1] R. Dalven, *Phys. Status Solidi B* **48**, K23 (1971).
[7.2] M.-Z. Huang and W. Y. Ching, *J. Phys. Chem. Solids* **46**, 977 (1985).

10.7.2 Electron Effective Mass: Satellite Valley

No detailed data are available for *c*-CdS.

10.7.3 Hole Effective Mass

• Luttinger's valence-band parameter

Table 10.7.2 *Luttinger's valence-band parameter γ_i for c-CdS (in $\hbar^2/2m_0$).*

γ_1	γ_2	γ_3
4.11	0.77	1.53

*Estimated from a plot of E_0 versus γ_i for some cubic group-IV, III–V, and II–VI semiconductors (see figure, below).

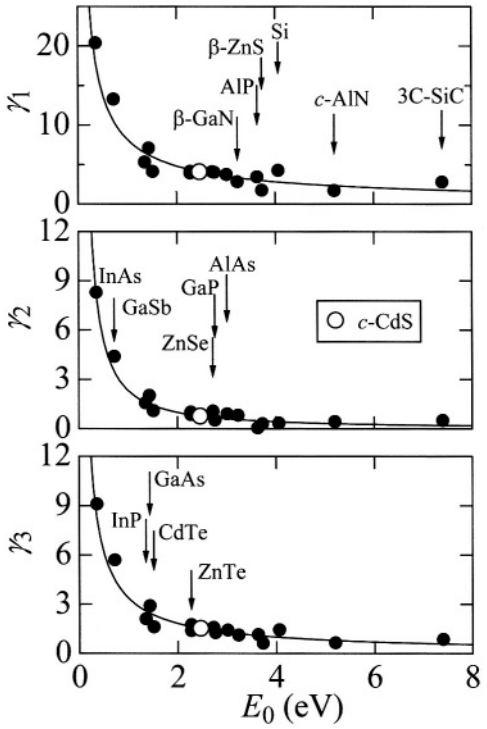

Fig. 10.7.1 Luttinger's valence-band parameter γ_i versus E_0 for a number of the group-IV, III–V, and II–VI semiconductors in the cubic structure. From this plot, we can estimate γ_i values for *c*-CdS to be γ_1=4.11, γ_2=0.77, and γ_3=1.53 (in $\hbar^2/2m_0$).

• Band mass, cyclotron mass, etc.

Table 10.7.3 *Band (m_{HH}, m_{LH}), density-of-states heavy-hole (m_{HH}*), averaged light-hole (m_{LH}*), and spherically-averaged heavy-hole (m_{HH}^s) and light-hole masses (m_{LH}^s) in c-CdS.**

Mass	Value (m_0)
m_{HH} ([001] direction)	0.39
m_{LH} ([001] direction)	0.18
m_{HH} ([111] direction)	0.95
m_{LH} ([111] direction)	0.14
m_{HH}*	0.68
m_{LH}*	0.15
m_{HH}^s	0.60
m_{LH}^s	0.15

*Calculated using a set of the Luttinger's parameters, γ_1=4.11, γ_2=0.77, and γ_3=1.53.

• **Spin–orbit–splitoff hole effective mass**

Table 10.7.4 *Spin–orbit–splitoff hole effective mass* m_{SO} *for c-CdS.*

m_{SO}/m_0
0.24

*Obtained from the Luttinger's parameter ($m_{SO}=1/\gamma_1$).

10.8 ELECTRONIC DEFORMATION POTENTIAL

10.8.1 Intravalley Deformation Potential: Γ Point

• **Conduction band**

Table 10.8.1 *Γ-conduction-band intravalley deformation potential* a_c^{Γ} $(=E_1^{\Gamma})$ *for c-CdS.*

a_c^{Γ} (eV)	Comment
−27.1	Calc. [8.1]

[8.1] A. Blacha, H. Presting, and M. Cardona, *Phys. Status Solidi B* **126**,11 (1984).

• **Valence band**

Table 10.8.2 *Γ-valence-band deformation potentials a, b, and d for c-CdS.*

Deformation potential (eV)			Comment
a	*b*	*d*	
−17.5	1.6		Calc. [8.2]
0.92	−1.18		Calc. [8.3]
	−1.07		Calc. [8.4]
	−1.05		Calc. [8.5]
	−4.7		Exper. [8.6]

[8.2] A. Blacha, H. Presting, and M. Cardona, *Phys. Status Solidi B* **126**, 11 (1984).
[8.3] A. Qteish and R. J. Needs, *Phys. Rev. B* **45,** 1317 (1992).
[8.4] T. Nakayama, *Solid-State Electron.* **37**, 1077 (1994).
[8.5] R. Said, A. Qteish, and N. Meskini, *J. Phys.: Condens. Matter* **10,** 8703 (1998).
[8.6] D. W. Niles and H. Höchst, *Phys. Rev. B* **44**, 10965 (1991).

• **E_0 gap**

Table 10.83 *Hydrostatic deformation potential* a_0^{Γ} *for the* E_0 *gap of c-CdS.*

a_0^{Γ} (eV)	Comment
−9.6	Calc. [8.7]
−3.77	Calc. [8.8]
−2.27	Calc. [8.9]
−2.94	Calc. [8.10]
+0.43	Exper. *

[8.7] A. Blacha, H. Presting, and M. Cardona, *Phys. Status Solidi B* **126**, 11 (1984).
[8.8] T. Nakayama, *Solid-State Electron.* **37**, 1077 (1994).
[8.9] R. Said, A. Qteish, and N. Meskini, *J. Phys.: Condens. Matter* **10,** 8703 (1998).
[8.10] S.-H. Wei and A. Zunger, *Phys. Rev. B* **60**, 5404 (1999).
*Estimated from dE_0/dp value.

• **Optical-phonon deformation potential**

Table 10.8.4 *Optical-phonon deformation potential d_0 at the Γ-valence band of c-CdS.*

d_0 (eV)	Comment
6.9	Calc. [8.11]

[8.11] A. Blacha, H. Presting, and M. Cardona, *Phys. Status Solidi B* **126,** 11 (1984).

10.8.2 Intravalley Deformation Potential: High-Symmetry Points

No detailed data are available for *c*-CdS.

10.8.3 Intervalley Deformation Potential

No detailed data are available for *c*-CdS.

10.9 ELECTRON AFFINITY AND SCHOTTKY BARRIER HEIGHT

10.9.1 Electron Affinity

No detailed data are available for *c*-CdS.

10.9.2 Schottky Barrier Height

No detailed data are available for *c*-CdS.

10.10 OPTICAL PROPERTIES

10.10.1 Summary of Optical Dispersion Relations

• **$\varepsilon(E)$ and $n^*(E)$ spectra**

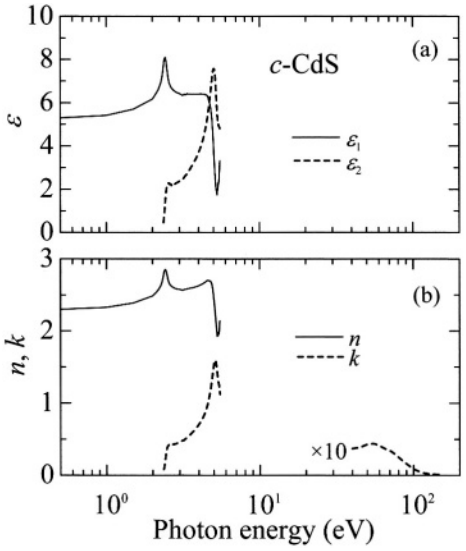

Fig. 10.10.1 (a) Complex dielectric-constant $[\varepsilon(E)=\varepsilon_1(E)+i\varepsilon_2(E)]$ and (b) complex refractive-index spectra $[n^*(E)=n(E)+ik(E)]$ for *c*-CdS at 300 K. The numerical data are taken from tabulation by S. Adachi [*Optical Constants of Crystalline and Amorphous Semiconductors: Numerical Data and Graphical Information* (Kluwer Academic, Boston, 1999)].

• **$\alpha(E)$ and $R(E)$ spectra**

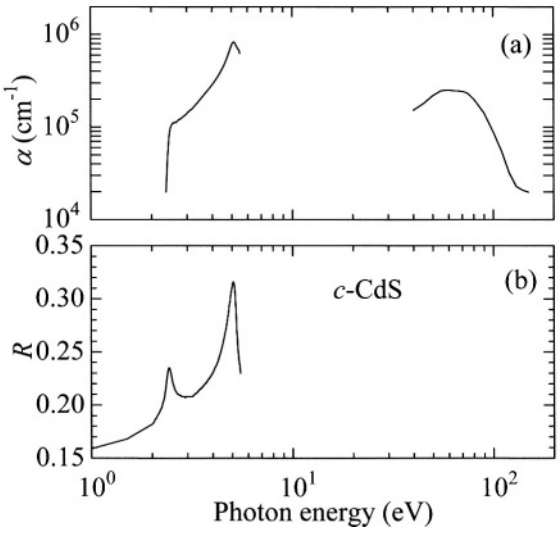

Fig. 10.10.2 (a) Absorption [$\alpha(E)$] and (b) normal-incidence reflectivity spectra [$R(E)$] for *c*-CdS at 300 K. The numerical data are taken from tabulation by S. Adachi [*Optical Constants of Crystalline and Amorphous Semiconductors: Numerical Data and Graphical Information* (Kluwer Academic, Boston, 1999)].

10.10.2 The Reststrahlen Region

• **Static and high-frequency dielectric constants**

Table 10.10.1 *Static and high-frequency dielectric constants ε_s and ε_∞ for c-CdS.*

ε_s	ε_∞	Comment
9.8	5.4	T=300 K

* Estimated from *w*-CdS data [$\varepsilon_s=(\varepsilon_{s\perp}^2\varepsilon_{s\parallel})^{1/3}$, $\varepsilon_\infty=(\varepsilon_{\infty\perp}^2\varepsilon_{\infty\parallel})^{1/3}$].

10.10.3 At or Near the Fundamental Absorption Edge

• **Refractive index**

Table 10.10.2 *Refractive index n near the fundamental absorption edge of c-CdS at 300 K [10.1].*

E (eV)	λ (μm)	n	E (eV)	λ (μm)	n
0.5	2.479	2.30	2.16	0.574	2.563
1	1.240	2.33	2.18	0.569	2.575
1.5	0.826	2.37	2.2	0.563	2.586
2	0.620	2.486	2.22	0.558	2.599
2.02	0.614	2.494	2.24	0.553	2.614
2.04	0.608	2.503	2.26	0.548	2.630
2.06	0.602	2.513	2.28	0.544	2.650
2.08	0.596	2.523	2.3	0.539	2.673
2.1	0.590	2.532	2.32	0.534	2.703
2.12	0.585	2.542	2.34	0.530	2.739
2.14	0.579	2.551			

[10.1] See, S. Adachi, *Optical Constants of Crystalline and Amorphous Semiconductors: Numerical Data and Graphical Information* (Kluwer Academic, Boston, 1999).

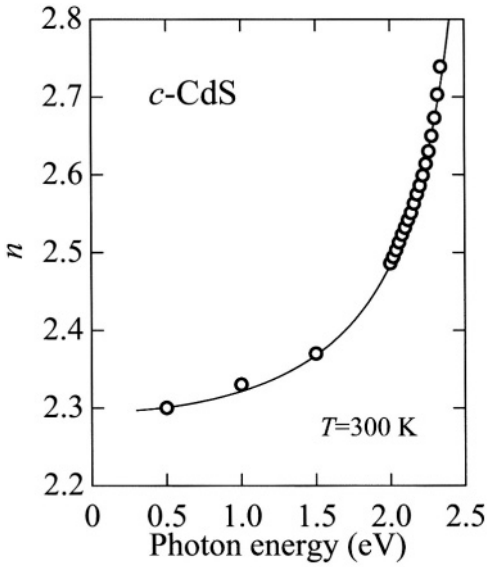

Fig. 10.10.3 Refractive index n for c-CdS at T=300 K. The experimental data are taken from S. Adachi [*Optical Constants of Crystalline and Amorphous Semiconductors: Numerical Data and Graphical Information* (Kluwer Academic, Boston, 1999)]. The solid line represents the calculated result using $n^2=4.46+[0.806\lambda^2/(\lambda^2-0.203)]$ with λ in μm.

- **Fundamental absorption edge**

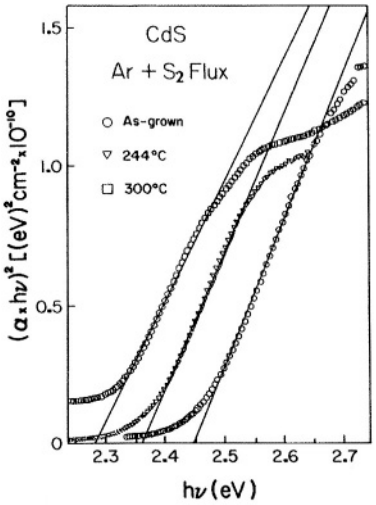

Fig. 10.10.4 $(\alpha h\nu)^2$ versus photon energy $h\nu$ plots for as-grown and two annealed samples. Polycrystalline thin films in the c–CdS phase were grown on glass substrates at 80±1°C by chemical bath deposition. Solid–solid phase transformation from the cubic, zinc-blende or sphalerite metastable modification of CdS (c-CdS) to the hexagonal, wurtzite stable phase (w-CdS) gradually occurred by annealing in $Ar+S_2$ in the temperature range 100–550°C. The extrapolation of the straight line to the $h\nu$ axis gives E_0. [From O. Zelaya-Angel and R. Lozada-Morales, *Phys. Rev. B* **62**, 13064 (2000).]

10.10.4 The Interband Transition Region

- **Fundamental optical spectra**

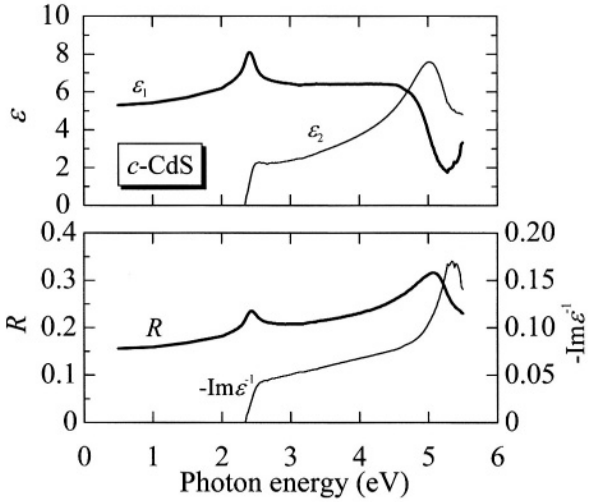

Fig. 10.10.5 Complex dielectric function, $\varepsilon(E)=\varepsilon_2(E)+i\varepsilon_2(E)$, fundamental reflectivity, $R(E)$, and energy-loss function, $-\mathrm{Im}\varepsilon^{-1}(E)$, for c-CdS at 300 K. The experimental data are taken from tabulation by S. Adachi [*Optical Constants of Crystalline and Amorphous Semiconductors: Numerical Data and Graphical Information* (Kluwer Academic, Boston, 1999)].

10.10.5 Free-Carrier Absorption and Related Phenomena

No detailed data are available for *c*-CdS.

10.11 ELASTOOPTIC, ELECTROOPTIC, AND NONLINEAR OPTICAL PROPERTIES

10.11.1 Elastooptic Effect

No detailed data are available for *c*-CdS.

10.11.2 Linear Electrooptic Constant

No detailed data are available for *c*-CdS.

10.11.3 Quadratic Electrooptic Constant

No detailed data are available for *c*-CdS.

10.11.4 Franz–Keldysh Effect

No detailed data are available for *c*-CdS.

10.11.5 Nonlinear Optical Constant

• Second-order nonlinear optical susceptibility

Table 10.11.1 *Theoretical second-order nonlinear optical susceptibility* $\chi^{(2)}_{123}(-2\omega;\omega;\omega)$ *in the static limit* $(\hbar\omega \to 0\ eV)$ *for c-CdS.*

$\chi^{(2)}_{123}$ (10^{-8} esu)*	Ref.
7.4	[11.1]

[11.1] M.-Z. Huang and W. Y. Ching, *Phys. Rev. B* **47**, 9464 (1993).
*1 m/V=$3\times10^4/4\pi$ esu.

• Third-order nonlinear optical susceptibility

Table 10.11.2 *Theoretical third-order nonlinear optical susceptibility* $\chi^{(3)}_{ijkl}(-3\omega;\omega,\omega,\omega)$ *in the static limit* $(\hbar\omega \to 0\ eV)$ *for c-CdS.*

$\chi^{(3)}_{ijkl}$ (10^{-11} esu)*		Ref.
$\chi^{(3)}_{1111}$	$\chi^{(3)}_{1212}$	
1.00	0.57	[11.2]

[11.2] W. Y. Ching and M.-Z. Huang, *Phys. Rev. B* **47**, 9479 (1993).
*1 $m^2/V^2=9\times10^8/4\pi$ esu.

10.12 CARRIER TRANSPORT PROPERTIES

10.12.1 Low-Field Mobility: Electrons

Table 10.12.1 *300-K (μ_{300K}) and peak Hall mobilities (μ_{peak}) for electrons in c-CdS.*

Mobility	Value ($cm^2/V\,s$)	Comment
μ_{300K}	70–85	MOCVD-grown layer on GaAs(100) n=5.0×10^{18}–6.5×10^{19} cm^{-3} [12.1]
μ_{peak}		

[12.1] K. Yasuda, H. B. Samion, M. Miyata, N. Araki, Y. Masuda, and Y. Tomita, *J. Cryst. Growth* **222**, 477(2001).

10.12.2 Low-Field Mobility: Holes

No detailed data are available for *c*-CdS.

10.12.3 High-Field Transport: Electrons

- **LO-phonon-scattering-limited electron saturation drift velocity**

Table 10.12.2 *Calculated LO-phonon-scattering-limited electron saturation drift velocity $v_{e,sat}$ in the lowest-conduction-band valley α for c-CdS at 300 K.**

$$v_{e,sat}^{\alpha} = \left(\frac{8\hbar\omega_{LO}}{3\pi m_c^{\alpha}} \right)^{1/2}$$

Valley	$v_{e,sat}$ (10^7 cm/s)
Γ	2.0

*Calculated with $m_c^{\Gamma} = 0.14 m_0$ and $\omega_{LO} = 303$ cm^{-1}.

10.12.4 High-Field Transport: Holes

No detailed data are available for *c*-CdS.

10.12.5 Minority-Carrier Transport: Electrons in *p*-Type Materials

No detailed data are available for *c*-CdS.

10.12.6 Minority-Carrier Transport: Holes in *n*-Type Materials

No detailed data are available for *c*-CdS.

10.12.7 Impact Ionization Coefficient

No detailed data are available for *c*-CdS.

Chapter 11

Wurtzite Cadmium Sulphide (*w*-CdS)

11.1 STRUCTURAL PROPERTIES

11.1.1 Ionicity

Table 11.1.1 *Phillips's ionicity f_i for w-CdS [1.1].*

f_i
0.685

[1.1] J. C. Phillips, *Bonds and Bands in Semiconductors* (Academic, New York, 1973).

11.1.2 Elemental Isotopic Abundance and Molecular Weight

- **Isotopic abundance**

Table 11.1.2 *Isotopic abundance in percent for cadmium and sulfur [1.2].*

Isotope	% nat. abundance	Isotope	% nat. abundance	Isotope	% nat. abundance
^{106}Cd	1.25	^{112}Cd	24.13	^{32}S	95.02
^{108}Cd	0.89	^{113}Cd	12.22	^{33}S	0.75
^{110}Cd	12.49	^{114}Cd	28.73	^{34}S	4.21
^{111}Cd	12.80	^{116}Cd	7.49	^{36}S	0.02

[1.2] D. R. Lide, *CRC Handbook of Chemistry and Physics,* 78th Edition (CRC Press, Boca Raton, 1997).

• **Molecular weight**

Table 11.1.3 *Molecular (average atomic) weight M for w-CdS.*

M (amu)
144.477

11.1.3 Crystal Structure and Space Group

Table 11.1.4 *Crystal structure and its space and pint groups for w-CdS.*

Crystal structure	Space group	Point group
Wurtzite (Hexagonal)	$P6_3mc$	C_{6v}^4

11.1.4 Lattice Constant and Its Related Parameters

• **Lattice constant and molecular density**

Table 11.1.5 *Lattice constant (a, c) and molecular density (d_M) for w-CdS at 300 K.*

Parameter	Value
Lattice constant a (Å)	4.1367 [1.3]
c (Å)	6.7161 [1.3]
Molecular density d_M (10^{22} cm^{-3})	2.0094*

[1.3] W. R. Cook, Jr., *J. Am. Ceram. Soc.* **51**, 518 (1968).
*Calculated.

• **Crystal density**

Table 11.1.6 *Crystal density g for w-CdS at 300 K.**

g (g/cm^3)
4.8208

*Calculated using a=4.1367 Å and c=6.7161 Å.

11.1.5 Structural Phase Transition

Table 11.1.7 *Structural phase transition in w-CdS at high pressures.**

Structure	Transition pressure (GPa)
Wurtzite ($P6_3mc$)	Normal pressure
Rocksalt (NaCl)	2 [1.4]
	2.8 [1.5]
	2.3±0.1 [1.6]
	1.75 [1.7]
	3 [1.8]
	~2.8 [1.9]
	2.5±0.2 [1.10]
	2.92±1.0 [1.11]
Orthorhombic ($Pmmn$)	56 [1.8]

[1.4] A. Jayaraman, W. Klement, Jr., and G. C. Kennedy, *Phys. Rev.* **130**, 2277 (1963).

[1.5] J. A. Kafalas and A. N. Mariano, *Science* **143**, 952 (1964)].
[1.6] G. A. Samara and A. A. Giardini, *Phys. Rev.* **140**, A388 (1965).
[1.7] C. F. Cline and D. R. Stephens, *J. Appl. Phys.* **36**, 2869 (1965).
[1.8] T. Suzuki, T. Yagi, S. Akimoto, T. Kawamura, S. Toyoda, and S. Endo, *J. Appl. Phys.* **54**, 748 (1983).
[1.9] B. Batlogg, A. Jayaraman, J. E. Van Cleve, and R. G. Maines, *Phys. Rev. B* **27**, 3920 (1983).
[1.10] A. Béliveau and C. Carlone, *Phys. Rev. B* **44**, 3650 (1991).
[1.11] S. M. Sharma and Y. M. Gupta, *Phys. Rev. B* **58**, 5964 (1998).
*Upon the release of the pressure, the rocksalt phase transformed mostly into the zinc-blende structure rather than reverting completely to the wurtzite form [see, e.g., G. A. Samara and A. A. Giardini, *Phys. Rev.* **140**, A388 (1965)].

11.1.6 Cleavage Plane

Table 11.1.8 *Crystallographic plane most readily cleaved for w-CdS.*

Cleavage plane
$(11\bar{2}0)$, $(10\bar{1}0)$

11.2 THERMAL PROPERTIES

11.2.1 Melting Point and Its Related Parameters

Table 11.2.1 *Melting point T_m and its related parameter for CdS.*

Parameter	Value
Melting point T_m (K)	1748 [2.1]
Entropy of fusion ΔS_m (cal/mol K)	16.21 [2.2]

[2.1] H. H. Woodbury, *J. Phys. Chem. Solids* **24**, 881 (1963).
[2.2] See, B. R. Nag, *J. Electron. Mater.* **26**, 70 (1997).

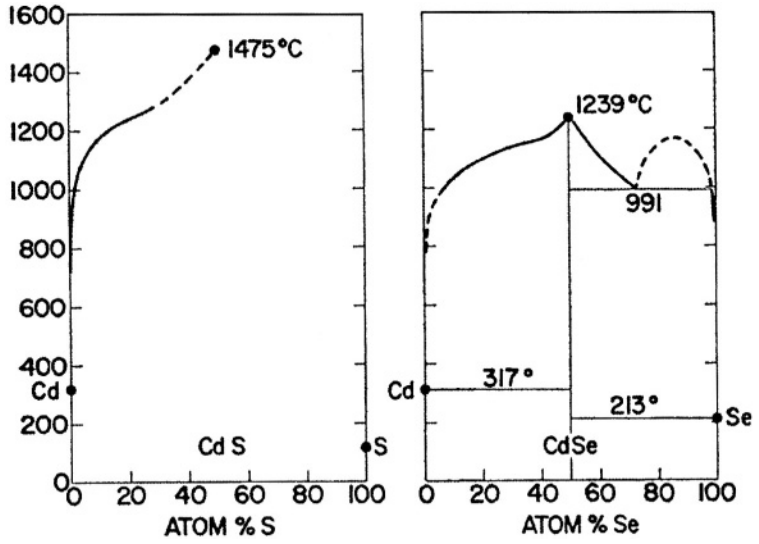

Fig. 11.2.1 *T–x* projects of the II–VI binary systems Cd–S and Cd–Se. [From M. R. Lorenz, in *Physics and Chemistry of II–VI Compounds,* edited by M. Aven and J. S. Prener (North-Holland, Amsterdam, 1967), p. 73.]

11.2.2 Specific Heat

Table 11.2.2 *Experimental specific heats C_p (at constant pressure) and C_v (at constant volume) for w-CdS (in J/gK) [2.3].*

Temperature (K)	C_p	C_v	Temperature (K)	C_p	C_v
55	0.1295	0.1295	190	0.2922	0.2919
60	0.1387	0.1387	200	0.2968	0.2965
70	0.1562	0.1562	210	0.3013	0.3009
80	0.1746	0.1746	220	0.3060	0.3056
90	0.1913	0.1913	230	0.3100	0.3096
100	0.2067	0.2066	240	0.3137	0.3133
110	0.2211	0.2210	250	0.3169	0.3164
120	0.2336	0.2335	260	0.3192	0.3188
130	0.2450	0.2449	270	0.3217	0.3211
140	0.2556	0.2554	273.16	0.3224	0.3218
150	0.2648	0.2646	280	0.3241	0.3236
160	0.2731	0.2729	290	0.3264	0.3258
170	0.2803	0.2801	300	0.3280	0.3275
180	0.2865	0.2862			

[2.3] A. F. Demidenko, *Inorg. Mater.* **5**, 210 (1969).

Table 11.2.3 *Specific heat C_p (at constant pressure) as a function of temperature T for w-CdS.*

C_p (J/g K)
$0.374+2.6\times10^{-5}T$ [2.4]

[2.4] P. Goldfinger and M. Jeunehomme, *Trans. Faraday Soc.* **59,** 2851 (1963).

11.2.3 Debye Temperature

Table 11.2.4 *Debye temperature θ_D for w-CdS [2.5].*

Temperature (K)	θ_D (K)	Temperature (K)	θ_D (K)
0*	265	180	355
55	272	190	354
60	284	200	354
70	305	210	354
80	319	220	349
90	330	230	345
100	340	240	337
110	345	250	333
120	350	260	332
130	354	270	327
140	356	273.16	326
150	356	280	319
160	357	290	313
170	358	300	310

[2.5] A. F. Demidenko, *Inorg. Mater.* **5**, 210 (1969).
*In the low-temperature (0 K) limit [see, M. A. Nusimovici and J. L. Birman, in *II–VI Semiconducting Compounds,* edited by D. G. Thomas (Benjamin, New York, 1967), p. 1204].

11.2.4 Thermal Expansion Coefficient

Table 11.2.5 *Thermal expansion coefficient α_{th} for w-CdS at 300 K.**

α_{th} (10^{-6} K^{-1})		Ref.
α_a	α_c	
5.0	3.5	[2.6]
5.0.	2.5	[2.7]
4.30	2.77	[2.8]

[2.6] A. B. Francis and A. L. Carlson, *J. Opt. Soc. Am.* **50**, 118 (1960).
[2.7] R. R. Reeber and B. A. Kulp, *Trans. Metal. Soc. AIME* **233**, 698 (1965).
[2.8] H. Iwanaga, A. Kunishige, and S. Takeuchi, *J. Mater. Sci.* **35**, 2451 (2000).
*Note that α_{th} value for *w*-CdS shows a negative value at *T* below about 150 K [see, R. R. Reeber and B. A. Kulp, *Trans. Metal. Soc. AIME* **233,** 698 (1965)].

11.2.5 Thermal Conductivity and Diffusivity

Table 11.2.6 *Thermal conductivity K for w-CdS.* Thermal diffusivity can be calculated from a relation $D=K/(C_p \cdot g)$, where C_p is the specific heat at constant pressure and g is the crystal density.*

Temperature (K)	*K* (W/cm K)	Temperature (K)	*K* (W/cm K)
1.4	0.40	10.0	5.8
1.6	0.48	11.5	5.3
1.7	0.50	13.0	5.1
1.9	0.80	15.0	4.4
2.1	0.99	17.2	3.9
2.3	1.25	20.5	3.4
2.5	1.40	24.5	2.9
2.7	1.75	29.5	2.45
3.0	2.1	36	2.05
3.4	2.6	43	1.85
3.7	3.1	53	1.42
4.2	3.7	66	1.20
4.5	4.0	80	0.98
5.0	4.5	87	0.90
5.6	5.0	110	0.68
6.3	5.5	150	0.43
6.9	5.8	160	0.39
7.4	5.9	225	0.26
8.0	6.0	262	0.22
8.5	5.9	283	0.20
9.1	5.9		

*The experimental data are taken for $T \leq 80$ K from G. E. Moore, Jr. and M. V. Klein [*Phys. Rev.* **179**, 722 (1969)] and for $T \geq 87$ K from M. G. Holland [*Phys. Rev.* **134**, A471 (1964)]. The heat flow is along the *c*-axis ($\parallel c$). Note that the data showed no strong dependence on the heat flow direction between $\parallel c$ and $\perp c$ [see, G. E. Moore, Jr. and M. V. Klein, *Phys. Rev.* **179**, 722 (1969)].

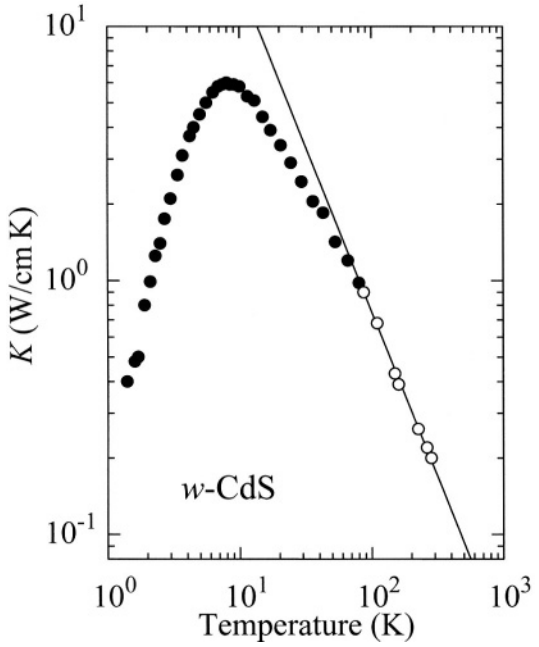

Fig. 11.2.2 Thermal conductivity K in the direction along the c-axis for w-CdS. The experimental data are taken from G. E. Moore, Jr. and M. V. Klein [*Phys. Rev.* **179,** 722 (1969); solid circles] and from M. G. Holland [*Phys. Rev.* **134,** A471 (1964); open circles]. The solid line is calculated from $K=AT^n$ with A=300 W/cm K$^{-0.3}$ and n= –1.30.

11.3 ELASTIC PROPERTIES

11.3.1 Elastic Constant

• Room-temperature value

Table 11.3.1 *Room-temperature elastic stiffness (C_{ij}) and compliance constants (S_{ij}) for w-CdS [3.1].*

C_{ij} (10^{11} dyn/cm^2)					
C_{11}	C_{12}	C_{13}	C_{33}	C_{44}	C_{66}*
8.65	5.40	4.73	9.44	1.50	1.63
S_{ij} (10^{-12} cm^2/dyn)					
S_{11}	S_{12}	S_{13}	S_{33}	S_{44}	S_{66}*
2.08	–1.00	–0.54	1.60	6.66	6.16

[3.1] *Numerical Data and Functional Relationships in Science and Technology,* edited by K.-H. Hellwege and A. M. Hellwege, Landolt–Börnstein, New Series, Group III, Vol. 18 (Springer, Berlin, 1984).

* C_{66}=½(C_{11}–C_{12}); S_{66}=2(S_{11}–S_{12}).

• Temperature and/or pressure dependence

Table 11.3.2 *Temperature derivative of the elastic stiffness constant, dC_{ij}/dT, for w-CdS [3.2].*

dC_{ij}/dT (10^7 dyn/cm^2 K)				
C_{11}	C_{12}	C_{13}	C_{33}	C_{44}
–15	–11	–9.9	–16	–0.9

[3.2] *Numerical Data and Functional Relationships in Science and Technology,* edited by K.-H. Hellwege and A. M. Hellwege, Landolt–Börnstein, New Series, Group III, Vol. 11 (Springer, Berlin, 1979).

Table 11.3.3 *Pressure derivative of the elastic stiffness constant dC_{ij}/dp, for w-CdS [3.3].*

dC_{ij}/dT				
C_{11}	C_{12}	C_{13}	C_{33}	C_{44}
3.08	5.24	4.73	3.25	–0.63

[3.3] *Numerical Data and Functional Relationships in Science and Technology,* edited by K.-H. Hellwege and A. M. Hellwege, Landolt–Börnstein, New Series, Group III, Vol. 11 (Springer, Berlin, 1979).

11.3.2 Third-Order Elastic Constant

Table 11.3.4 *Third-order elastic constant ofw-CdS [3.4].*

Modulus	Value (10^{12} dyn/cm^2)	Modulus	Value (10^{12} dyn/cm^2)
C_{111}	–4.59	C_{144}	–0.27
C_{112}	–2.07	C_{155}	+0.09
C_{113}	–1.82	C_{222}	–3.55
C_{123}	–2.35	C_{333}	–3.27
C_{133}	–3.06	C_{344}	–0.69

[3.4] *Numerical Data and Functional Relationships in Science and Technology,* edited by K.-H. Hellwege and A. M. Hellwege, Landolt–Börnstein, New Series, Group III, Vol. 11 (Springer, Berlin, 1979).

11.3.3 Young's Modulus, Poisson's Ratio, and Similar

- **Young's modulus**

Table 11.3.5 *Young's modulus Y for w-CdS at 300 K.**

Direction	Y (10^{11} dyn/cm^2)
$c \perp l$	4.81
$c \parallel l$	6.25

*Calculated using $S_{11}=2.08\times10^{-12}$ and $S_{33}=1.60\times10^{-12}$ cm^2/dyn.
l: directional vector.

- **Poisson's ratio**

Table 11.3.6 *Poisson's ratio P for w-CdS at 300 K.**

Direction	P
$c \perp l$	0.37
$c \parallel l$	0.33

*Obtained from a definition $B_u=Y/[3(1-2P)]$, where B_u and Y are bulk and Young's moduli, respectively.
l: directional vector.

- **Bulk modulus, shear modulus, etc.**

Table 11.3.7 *Bulk modulus, B_u, pressure derivative of B_u, dB_u/dp, and linear compressibility, C_o, for w-CdS at 300 K.*

Parameter	Value
B_u (10^{11} dyn/cm^2)	6.27 [3.5]
dB_u/dp	

Table 11.3.7 *Continued.*

Parameter	Value
C_o (10^{-13} cm^2/dyn)	
$c \perp l$	5.40 [3.5]
$c \parallel l$	5.20 [3.5]

[3.5] Calculated using C_{11}=8.65×10^{11} dyn/cm^2, C_{12}=5.40×10^{11} dyn/cm^2, C_{13}=4.73×10^{11} dyn/cm^2, C_{33}=9.44×10^{11} dyn/cm^2, S_{11}=2.08×10^{-12} cm^2/dyn, S_{12}= −1.00×10^{-12} cm^2/dyn, S_{13}= −5.4×10^{-13} cm^2/dyn, and S_{33}=1.60×10^{-12} cm^2/dyn.
l: directional vector.

11.3.4 Microhardness

Table 11.3.8 *Microhardness Hfor w-CdS.*

H (GPa)	Ref.
1.21	[3.6]
1.4–2.3*	[3.7]

[3.6] See, L. Garbato and A. Rucci, *Phil. Mag.* **35**, 1681 (1977).
[3.7] Vickers's microhardness [K. Balakrishnan, J. Kumar, P. Ramasamy, and G. Attolini, *J. Mater. Sci. Lett.***14**, 720 (1995)].
*Depending on applied load.

11.3.5 Sound Velocity

Table 11.3.9 *Sound velocity propagating in w-CdS at 300 K.* LA=longitudinal acoustic; TA1, TA2=transverse acoustic.*

Propagation direction ***a***	Direction of polarization π	Mode	Sound velocity (10^5 cm/s)
$a \parallel c$	$\pi \parallel c$	LA	4.43
$a \parallel c$	$\pi \perp c$	TA1, TA2	1.76
$a \perp c$	$\pi \perp c$	LA	4.24
$a \perp c$	$\pi \perp c$	TA1	1.84
$a \perp c$	$\pi \parallel c$	TA2	1.76

*Calculated using C_{11}=8.65×10^{11} dyn/cm^2, C_{12}=5.40×10^{11} dyn/cm^2, C_{33}=9.44×10^{11} dyn/cm^2, C_{44}=1.50×10^{11} dyn/cm^2, and g=4.8208 g/cm^3.

11.4 PHONONS AND LATTICE VIBRONIC PROPERTIES

11.4.1 Phonon Dispersion Relation

- **Dispersion curve**

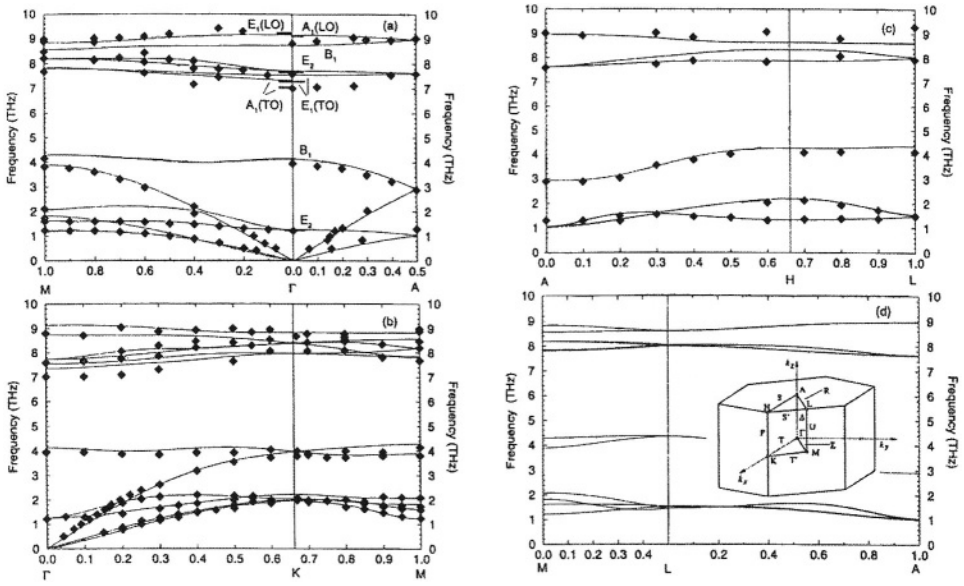

Fig. 11.4.1 Phonon dispersion curves along different high symmetry directions in the Brillouin zone for *w*-CdS. The symbols indicate the experimental data; the solid lines are from *ab-initio* calculation. The inset in (d) shows the Brillouin zone. [From A. Debernardi, N. M. Pyka, A. Göbel, T. Ruf, R. Lauck, S.Kramp, and M. Cardona, *Solid State Commun.* **103,** 297 (1997).]

11.4.2 Phonon Frequency

Table 11.4.1 *Long-wavelength ($q \to 0$) phonon frequencies for w-CdS.*

Phonon frequency (cm^{-1})						Comment
E_2 low	A_1 (TO)	E_1 (TO)	E_2 high	A_1 (LO)	E_1 (LO)	
	235	244				T=15 K [4.1]
43	234	243	256	305	307	T=25 K [4.2]
44*	228	235	252	305	305	T=77 K [4.3]
41.8	234.7	242.6	255.7	303.6	306.9	T=77 K [4.4]
	235	242	257.5			T=300 K [4.1]
	233	239.5		301	304.5	T=300 K [4.5]
41	233	239	255	301	304	Recommended value (T=300 K)

[4.1] H. W. Verleur and A. S. Barker, Jr., *Phys. Rev.* **155**, 750 (1967).
[4.2] C. A. Arguello, D. L. Rousseau, and S. P. S. Porto, *Phys. Rev.* **181**, 1351 (1969).
[4.3] B. Tell, T. C. Damen, and S. P. S. Porto, *Phys. Rev.* **144**, 771 (1966).
[4.4] R. J. Briggs and A. K. Ramdas, *Phys. Rev. B* **13**, 5518 (1976).
[4.5] R. Beserman and M. Balkanski, *Phys. Rev. B* **1**, 608 (1970).
*At T=300 K.

• **Pressure dependence**

Table 11.4.2 *Pressure variation of the long-wavelength ($q \to 0$) phonon frequency in w-CdS.*

$$\omega_q(p) = \omega_q(0) + ap$$

ω_q	$\omega_q(0)$ (cm^{-1})	a (cm^{-1}/GPa)	Comment
ω_{LO}	301.13±0.46	0.564±0.031	p<2.5 GPa, T=300 K [4.6]
	303.9±1.8	0.42±0.05	p>2.7 GPa, T=300 K [4.6]
	—	0.56±0.04	p<2.6 GPa, T=6 K [4.7]

[4.6] U. Venkateswaran, M. Chandrasekhar, and H. R. Chandrasekhar, *Phys. Rev. B* **30**, 3316 (1984).
[4.7] U. Venkateswaran and M. Chandrasekhar, *Phys. Rev.B* **31**, 1219 (1985).

11.4.3 Mode Grüneisen Parameter

Table 11.4.3 *Mode Grüneisen parameter for LO phonons in w-CdS [4.8].*

Phonon	γ
1 LO	0.87±0.06
2 LO	0.848±0.06

[4.8] U. Venkateswaran, M. Chandrasekhar, and H. R. Chandrasekhar, *Phys. Rev. B* **30**, 3316 (1984).

11.4.4 Phonon Deformation Potential

Table 11.4.4 *Long-wavelength phonon deformation potential (PDP) for w-CdS measured at 77 K [4.9].*

Definition: $\Delta\Omega = a(e_{xx}+e_{yy}) + be_{zz} \pm c[(e_{xx}-e_{yy})^2 + 4e_{xy}^2]^{1/2}$

Phonon	ω_q (cm^{-1})	PDP (cm^{-1})		
		a	b	c
E_2 low	41.8	~96	~104	16
A_1 (TO)	234.7	–526	–328	
E_1 (TO)	242.6	–235	–330	57
E_2 high	255.7	–404	–483	107
A_1 (LO)	303.6	–526	–328	
E_1 (LO)	306.9	–235	–330	57

[4.9] R. J. Briggs and A. K. Ramdas, *Phys. Rev. B* **13**, 5518 (1976).

11.5 COLLECTIVE EFFECTS AND RELATED PROPERTIES

11.5.1 Piezoelectric Constant

Table 11.5.1 *Experimentally determined piezoelectric stress (e_{ij}) and strain constants (d_{ij}) for w-CdS.*

e_{ij} (C/m^2)			d_{ij} (10^{-12} m/V)			Ref.
e_{15}	e_{31}	e_{33}	d_{15}	d_{31}	d_{33}	
			−14.3	−3.7	10.7	[5.1]
−0.21	−0.25	0.49				[5.2]
−0.210	−0.244	0.440	−13.98	−5.18	10.32	[5.3]
−0.183	−0.262	0.385	−11.91	−5.09	9.71	[5.4]
	−0.265	0.384				[5.5]
			−14	−5	10.3	[5.6]

[5.1] A. R. Hutson, *Phys. Rev. Lett.* **4**, 505 (1960).
[5.2] A. R. Hutson, *J. Appl. Phys.* **32**, 2287 (1961).
[5.3] D. Berlincourt, H. Jaffe, and L. R. Shiozawa, *Phys. Rev.* **129**, 1009 (1963).
[5.4] I. A. Dan'kov, G. S. Pado, I. B. Kobyakov, and V. V. Berdnik, *Sov. Phys. Solid State* **21**, 1481 (1979).
[5.5] N. D. Gavrilova, I. B. Kobyakov, V. K. Novik, and A. V. Solodukhin, *Sov. Phys. Tech. Phys.* **25**, 379 (1980).
[5.6] B.A. Auld, *J. Acoust. Soc. Am.* **70**,1577 (1981).

11.5.2 Fröhlich Coupling Constant

Table 11.5.2 *Fröhlich coupling constant α_F of w-CdS.*

α_F	Ref.
0.527	[5.7]
0.514	[5.8]

[5.7] E. Kartheuser, in *Polarons in Ionic Crystals and Polar Semiconductors,* edited by J. T. Devreese (North-Holland, Amsterdam, 1972), p. 717.
[5.8] Y. Imanaka, N. Miura, and H. Nojiri, *Physica B* **246-247**, 328 (1998).

11.6 ENERGY-BAND STRUCTURE: ENERGY-BAND GAPS

11.6.1 Basic Properties

• Electronic energy-band structure

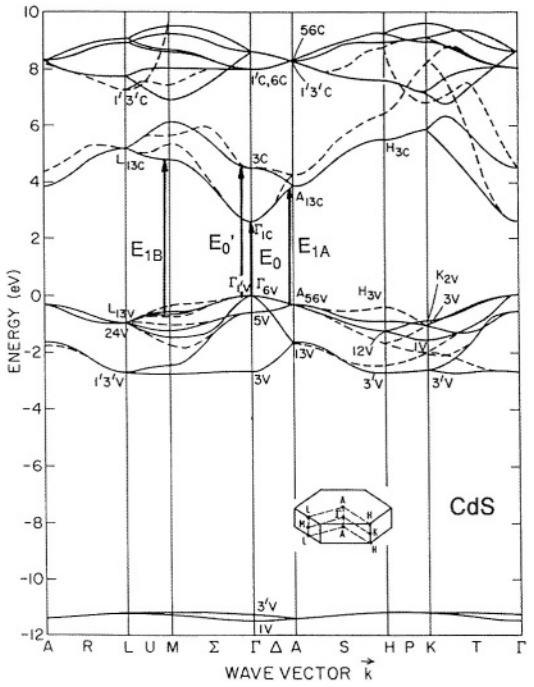

Fig. 11.6.1 Electronic energy-band structure of *w*-CdS as calculated with the semiempirical tight-binding scheme. The dashed lines also show the results derived from the semiempirical pseudopotential method by T. K. Bergstresser and M. L. Cohen [*Phys. Rev.* **164,** 1069 (1967)]. [From A. Kobayashi, O. F. Sankey, S. M. Volz, and J. D. Dow, *Phys. Rev. B* **28**, 935 (1983).] The main interband transitions are indicated by the vertical arrows.

• Electronic density of states

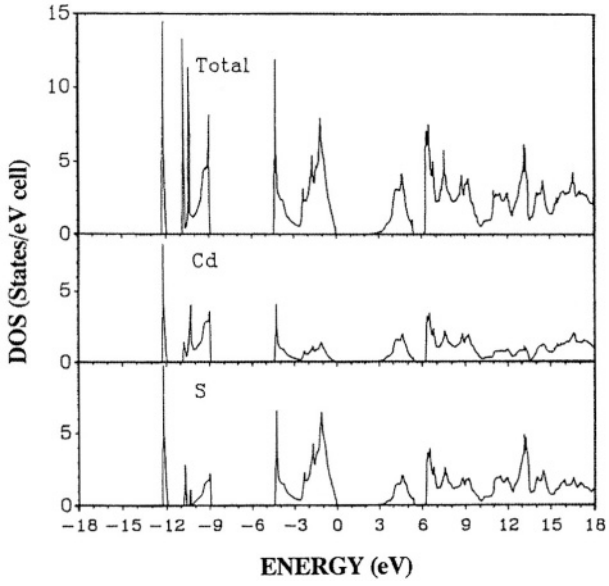

Fig. 11.6.2 Calculated density of states (DOS) and partial DOS for *w*-CdS using the first-principles orthogonalized linear-combination-of-atomic-orbitals method. [From Y.-N. Xu and W. Y. Ching, *Phys. Rev. B* **48**, 4335 (1993).]

• **Energy eigenvalue**

Table 11.6.1 *Energy eigenvalues at the critical points for the valence and first few conduction bands of w-CdS [6.1].*

Critical point	Level	Value (eV)	Critical point	Level	Value (eV)
Γ	Γ_1^v	−11.49	H	H_3^v	−2.74
	Γ_3^v	−2.7		$H_{1,2}^v$	−1.26
	Γ_5^v	−0.6		H_3^v	−0.92
	Γ_6^v, Γ_1^v	0.0		H_3^c	5.49
	Γ_1^c	2.6			
	Γ_3^c	4.5			
	Γ_6^c, Γ_1^c	8.0			
K	K_3^v	−2.66	A	$A_{1,3}^v$	−1.63
	K_1^v	−1.58		$A_{5,6}^v$	−0.31
	K_3^v	−1.05		$A_{1,3}^c$	3.86
	K_2^v	−0.92			
L	$L_{1',3}^v$	−2.70			
	$L_{2,4}^v$	−0.98			
	$L_{1,3}^v$	−0.93			
	$L_{1,3}^c$	5.19			
	$L_{1',3}^c$	7.75			

[6.1] A. Kobayashi, O. F. Sankey, S. M. Volz, and J. D. Dow, *Phys. Rev. B* **28**, 935 (1983).

11.6.2 E_0-Gap Region

• **Room-temperature value**

Table 11.6.2 $E_{0\alpha}$*-gap energy* (α=*A, B, or C*) *for w-CdS at room temperature.*

$E_{0\alpha}$ (eV)			Ref.
A	*B*	*C*	
2.501	2.516	2.579	[6.2]

[6.2] E. Gutsche and J. Voigt, in *II–VI Semiconducting Compounds,* edited by D. G. Thomas (Benjamin, New York, 1967), p. 337.

• **Temperature dependence**

Table 11.6.3 *Empirical equation for the* $E_{0\alpha}$*-gap* (α=*A, B, or C*) *energy variation with temperature T for w-CdS. 3D-CP=three-dimensional critical point.*

$$E_{0\alpha}(T) = E_{0\alpha}(0) - \frac{\alpha T^2}{T + \beta}$$

Parameter			Comment
$E_{0\alpha}(0)$ (eV)	α (10^{-4} eV/K)	β (K)	
2.5535	9.7	600	*n*=1 exciton (*A*), *T*=4.2–300 K, bulk CdS [6.3]
2.5675	9.6	700	*n*=1 exciton (*B*), *T*=4.2–300 K, bulk CdS [6.3]
2.579	4.7	230	3D-CP (*A*), *T*=13–300 K, bulk CdS [6.4]

Table 11.6.3 *Continued.*

Parameter			Comment
$E_{0\alpha}(0)$ (eV)	α (10^{-4} eV/K)	β (K)	
2.599	4.8	230	3D-CP (*B*), *T*=13–300 K, bulk CdS [6.4]
2.659	5.1	230	3D-CP (*C*), *T*=13–300 K, bulk CdS [6.4]
2.550	4.4	220	*n*=1 exciton (*A*), *T*=13–300 K, bulk CdS [6.4]
2.567	4.7	230	*n*=1 exciton (*B*), *T*=13–300 K, bulk CdS [6.4]
2.629	5.0	230	*n*=1 exciton (*C*), *T*=13–300 K, bulk CdS [6.4]

[6.3] K. A. Dmitrenko, L. V. Taranenko, S. G. Shevel', and A. V. Marinchenko, *Sov. Phys. Semicond.* **19**, 487 (1985).
[6.4] A. Imada, S. Ozaki, and S. Adachi, *J. Appl. Phys.* **92**, 1793 (2002).

Table 11.6.4 *Empirical equation for the $E_{0\alpha}$-gap (α=A, B, or C) energy variation with temperature T for w-CdS.*

$$E_{0\alpha}(T) = E_{\mathrm{B}} - 2a_{\mathrm{B}}\left(\frac{1}{2} + \frac{1}{e^{\Theta/T} - 1}\right)$$

Parameter			Comment
E_{B} (eV)	a_{B} (meV)	Θ (K)	
2.600	60	315	*n*=1 exciton (*A*), *T*=10–300 K [6.5]

[6.5] G. Perna, S. Pagliara, V. Capozzi, M. Ambrico, and M. Pallara, *Solid State Commun.* **114,** 161 (2000).

Table 11.6.5 *Empirical equation for the $E_{0\alpha}$-gap (α=A, B, or C) energy variation with temperature T for w-CdS [6.6].*

$$E_{0\alpha}(T) = E_{0\alpha}(0) - S\langle\hbar\Omega\rangle\left[\coth\left(\frac{\langle\hbar\Omega\rangle}{2kT}\right) - 1\right]$$

$E_{0\alpha}(0)$ (eV)	S	$\langle\hbar\Omega\rangle$ (meV)
2.568	1.54	13.9

[6.6] K. P. O'Donnell and P. G. Middleton, in *Properties of Wide Bandgap II–VI Semiconductors,* EMIS Datareviews Series No. 17, edited by R. Bhargava (INSPEC, London, 1997), p. 33.

Table 11.6.6 *Empirical equation for the $E_{0\alpha}$-gap (α=A, B, or C) energy variation with temperature T for w-CdS. 3D-CP=three-dimensional critical point.*

$$E_{0\alpha}(T) = E_{0\alpha}(0) - \frac{\alpha\Theta_{\mathrm{p}}}{2}\left[\sqrt[p]{1 + \left(\frac{2T}{\Theta_{\mathrm{p}}}\right)^{p}} - 1\right]$$

$E_{0\alpha}(0)$ (eV)	p	α (meV/K)	Θ_{p} (K)	Comment
2.583	2.47	0.402	147	*T*=2–289 K [6.7]
2.573	2.8	0.49	325	3D-CP (*A*), *T*=13–300 K, bulk CdS [6.8]

Table 11.6.6 *Continued.*

$E_{0\alpha}(0)$ (eV)	p	α (meV/K)	Θ_p (K)	Comment
2.595	2.8	0.49	300	3D-CP (*B*), *T*=13–300 K, bulk CdS [6.8]
2.656	2.8	0.49	270	3D-CP (*C*), *T*=13–300 K, bulk CdS [6.8]
2.546	2.8	0.49	325	*n*=1 exciton (*A*), *T*=13–300 K, bulk CdS [6.8]
2.563	2.8	0.48	325	*n*=1 exciton (*B*), *T*=13–300 K, bulk CdS [6.8]
2.625	2.8	0.49	283	*n*=1 exciton (*C*), *T*=13–300 K, bulk CdS [6.8]

[6.7] R. Pässler, *Phys. Status Solidi B* **216**, 975 (1999).
[6.8] A. Imada, S. Ozaki, and S. Adachi, *J. Appl. Phys.* **92**, 1793 (2002).

Table 11.6.7 *Empirical equation for the $E_{0\alpha}$-gap (α=A, B, or C) energy variation with temperature T for w-CdS.*

$$E_{0\alpha}(T) = E_{0\alpha}(0) - \alpha \sum_{i=1,2} \frac{W_i \Theta_i}{\exp(\Theta_i / T) - 1}$$

$E_{0\alpha}(0)$ (eV)	α (10^{-4} eV/K)	Θ_1 (K)	Θ_2 (K)	W_1	W_2	Comment
2.582	4.09	50	208	0.28	0.72	*T*=2–289 K [6.9]

[6.9] R. Pässler, *J. Appl. Phys.* **89**, 6235 (2001).

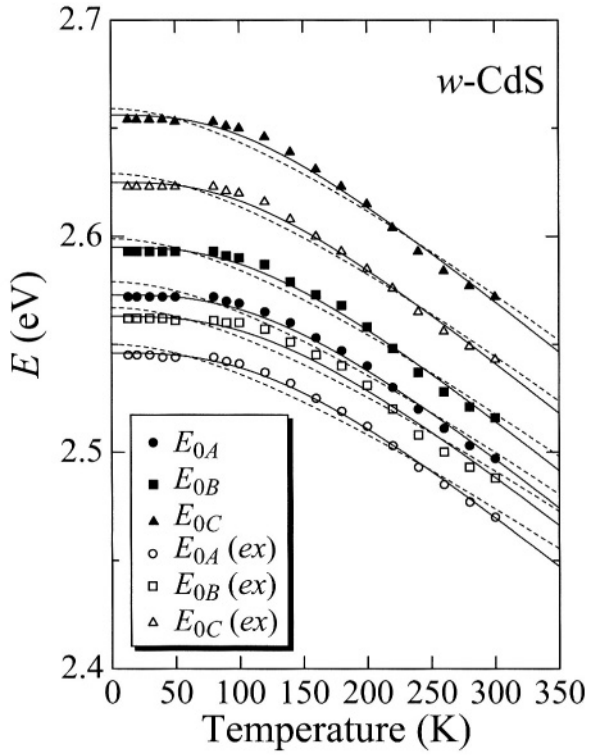

Fig. 11.6.3 Temperature dependence of the one-electron and excitonic $E_{0\alpha}$-gap energies for *w*-CdS determined by photoreflectance spectroscopy. The solid and dashed lines represent the theoretical curves. [From A. Imada, S. Ozaki, and S.Adachi, *J Appl. Phys.* **92**, 1793 (2002).]

• **Pressure dependence**

Table 11.6.8 *Empirical equation for the $E_{0\alpha}$-gap (α=A, B, or C) energy variation with pressure p for w-CdS.*

$$E_{0\alpha}(p) = E_{0\alpha}(0)+ap+bp^2$$

Parameter			Comment
$E_{0\alpha}(0)$ (eV)	a (10^{-2} eV/GPa)	b (10^{-4} eV/GPa^2)	
2.5753±0.0003	4.62±0.08	−18±1	n=2 exciton (A), T=7 K [6.10]
2.5909±0.0003	4.67±0.08	−18±1	n=2 exciton (B), T=7 K [6.10]

[6.10] A. Mang, K. Reimann, St. Rübenacke, and M. Steube, *Phys. Rev. B* **53**, 16283 (1996).

• **Temperature and/or pressure coefficient**

Table 11.6.9 *Linear temperature and pressure coefficients of the excitonic energy gap $E_{0\alpha}$ (α=A, B, or C) for w-CdS. 3D-CP=three-dimensional critical point.*

Coefficient	Value	Comment
$dE_{0\alpha}/dT$ (10^{-4} eV/K)	−5.2	[6.11]
	−3.66 (A, B)	[6.12]
	−2.58 (C)	
	−4.1±0.1 (A, B, C)	T=80–293 K [6.13]
	−4.45	[6.14]
	−(3.8–4.6) (A, B, C)	3D-CP, T=13–300 K [6.15]
	−(3.6–4.6) (A, B, C)	n=1 exciton, T=13–300 K [6.15]
$dE_{0\alpha}/dp$ (10^{-2} eV/GPa)	3.3	[6.16]
	4.5	[6.17]
	4.55±0.05	T=295 K [6.18]
	5.1	[6.19]
	4.47±0.22	T=300 K [6.20]
	4.36±0.13	T=6 K [6.21]
	4.50±0.05	T=77 K [6.22]
	4.2±0.3	T=300 K [6.23]
	4.3±0.3	T=78 K [6.24]
	4.7±0.3	T=300 K [6.24]
	4.4	(Mean value)

[6.11] See, B. Ray, *II–VI Compounds* (Pergamon, Oxford, 1969).
[6.12] E. Gutsche and J. Voigt, in *II–VI Semiconducting Compounds,* edited by D. G. Thomas (Benjamin, New York, 1967), p. 337.
[6.13] V. V. Sobolev, V. I. Donetskikh, and E. F. Zagaĭnov, *Sov. Phys. Semicond.* **12**, 646 (1978).
[6.14] A. E. Rakhshani, *J. Phys.: Condens. Matter* **12**, 4391 (2000).
[6.15] A. Imada, S.Ozaki, and S. Adachi, *J. Appl. Phys.* **92**,1793 (2002).
[6.16] A. L. Edwards and H. G. Drickamer, *Phys. Rev.* **122**, 1149 (1961).
[6.17] R. L. Knell and D. W. Langer, *Phys. Lett.* **21**, 370 (1966).
[6.18]B. Batlogg, A.Jayaraman, J. E. Van Cleve, and R. G. Maines, *Phys. Rev. B* **27**, 3920 (1983).
[6.19] D. A. Gulino, L. R. Faulkner, and H. G. Drickamer, *J. Appl. Phys.* **54**, 2483 (1983).
[6.20] U. Venkateswaran, M. Chandrasekhar, and H. R. Chandrasekhar, *Phys. Rev. B* **30**, 3316 (1984).
[6.21] U. Venkateswaran and M. Chandrasekhar, *Phys. Rev. B* **31**, 1219 (1985).
[6.22] X.-S. Zhao, J. Schroeder, T. G. Bilodeau, and L. G. Hwa, *Phys. Rev. B* **40**, 1257 (1989).

[6.23] A. Béliveau and C. Carlone, *Semicond. Sci. Technol.* **4**, 277 (1989).
[6.24] M. Lindner, S. H. L. Zott, G. F. Schötz, W. Gebhardt, P. Perlin, and P. Wisniewski, *High Pres. Res.* **10**, 408 (1992).

• Crystal-field and spin–orbit–splitoff energies

Table 11.6.10 *Theoretical crystal-field and spin-orbit–splitoff energies Δ_1, Δ_2, and Δ_3 for w-CdS (in meV). Note that in the quasi-cubic approximation, $\Delta_{cr}=\Delta_1$ and $\Delta_{so}=3\Delta_2=3\Delta_3$.*

Δ_1 (Δ_{cr})	Δ_2	Δ_3	Δ_{so}	Ref.
27			65	[6.25]
30	22	22		[6.26]

[6.25] J.-B. Jeon, Yu. M. Sirenko, K. W. Kim, M. A. Littlejohn, and M. A. Stroscio, *Solid State Commun.* **99**,423 (1996).
[6.26] See, T. Dietl, H. Ohno, and F. Matsukura, *Phys. Rev. B* **63**, 195205 (2001).

Table 11.6.11 *Experimental crystal-field and spin-orbit–splitoff energies Δ_1, Δ_2, and Δ_3, for w-CdS (in meV). Note that in the quasi-cubic approximation, $\Delta_{cr}=\Delta_1$ and $\Delta_{so}=3\Delta_2=3\Delta_3$.*

Δ_1 (Δ_{cr})	Δ_2	Δ_3	Δ_{so}	Ref.
28			68	[6.27]
27			65	[6.28]
28.4	20.9	20.7		[6.29]
28.8			64.3	[6.29]
26.5			63.5	[6.30]
28			62	[6.31]
28			65	Mean value

[6.27] D. G. Thomas and J. J. Hopfield, *Phys. Rev.* **116**, 573 (1959).
[6.28] See, J. O. Dimmock, in *II–VI Semiconducting Compounds,* edited by D. G. Thomas (Benjamin, New York, 1967), p. 277.
[6.29] D. W. Langer, R. N. Euwema, K. Era, and T. Koda, *Phys. Rev. B* **2**, 4005 (1970).
[6.30] A. Morawski, R. Banisch, and J. Lagowski, *Surf. Sci.* **69**, 444 (1977).
[6.31] O. Goede, D. Hennig, and L. John, *Phys. Status Solidi B* **96**, 671 (1979).

11.6.3 Higher-Lying Direct Gap

• Room-temperature value

Table 11.6.12 *Higher-lying direct-gap energies for w-CdS measured at room temperature [6.32].*

Band gap	Value (eV)	
	$\boldsymbol{E}\perp c$	$\boldsymbol{E}\parallel c$
$E_1(A)$	4.98	
$E_1(B)$	5.50	5.48
E_0'	6.1	6.2
E_2	7.8	7.8

[6.32] M. Cardona and G. Harbeke, *Phys. Rev.* **137**, A1467 (1965).

• **Temperature and/or pressure coefficient**

Table 11.6.13 *Linear temperature and pressure coefficients of the higher-lying band-gap energy for w-CdS.*

Band gap	Coefficient	Value	Comment
E_1	dE_g/dT (10^{-4} eV/K)		
	dE_g/dp (10^{-2} eV/GPa)	3.0	Calc. [6.33]
E_2	dE_g/dT (10^{-4} eV/K)		
	dE_g/dp (10^{-2} eV/GPa)	1.8	Calc. [6.33]

[6.33] D. L. Camphausen, G. A. N. Connell, and W. Paul, *Phys. Rev. Lett.* **26**, 184 (1971).

11.6.4 Lowest Indirect Gap

• **Theoretical value**

Table 11.6.14 *Theoretically obtained lowest indirect-gap energy for w-CdS.*

Band gap	Value (eV)			
	a	b	c	d
E_g^K (Γ→K)				
E_g^M (Γ→M)				5.50
E_g^L (Γ→L)	5.2	5.19	4.72	
E_g^H (Γ→H)	6.4	5.49	5.59	
E_g^A (Γ→A)	4.3	3.86	4.11	

[a]T. K. Bergstresser and M. L. Cohen, *Phys. Rev.* **164**,1069 (1967).
[b]A. Kobayashi, O. F. Sankey, S. M. Volz, and J. D. Dow, *Phys. Rev. B* **28**, 935 (1983).
[c]M.-Z. Huang and W. Y. Ching, *J. Phys. Chem. Solids* **46**, 977 (1985).
[d]O. Zakharov, A. Rubio, X. Blasé, M. L. Cohen, and S. G. Louie, *Phys. Rev. B* **50**, 10780 (1994).

11.6.5 Conduction-Valley Energy Separation

Table 11.6.15 *Theoretically obtained conduction-valley energy separation ΔE_g for w-CdS.*

ΔE_g	Value (eV)			
	a	b	c	d
K–Γ				
M–Γ				2.71
L–Γ	2.6	2.59	2.16	
H–Γ	3.8	2.89	3.03	
A–Γ	1.7	1.26	1.55	

[a]T. K. Bergstresser and M. L. Cohen, *Phys. Rev.* **164**, 1069 (1967).
[b]A. Kobayashi, O. F. Sankey, S. M. Volz, and J. D. Dow, *Phys. Rev. B* **28**, 935 (1983).
[c]M.-Z. Huang and W. Y. Ching, *J. Phys. Chem. Solids* **46**, 977 (1985).
[d]O. Zakharov, A. Rubio, X. Blasé, M. L. Cohen, and S. G. Louie, *Phys. Rev. B* **50**, 10780 (1994).

11.6.6 Direct–Indirect-Gap Transition Pressure

No detailed data are available for *w*-CdS.

11.7 ENERGY-BAND STRUCTURE: ELECTRON AND HOLE EFFECTIVE MASSES

11.7.1 Electron Effective Mass: Γ Valley

• Theoretical value

Table 11.7.1 *Theoretical electron effective masses $m_e^{\perp}$, $m_e^{\parallel}$, and m_e^{Γ} at the Γ valley for w-CdS. $m_e^{\Gamma}=(m_e^{\perp 2} m_e^{\parallel})^{1/3}$: density-of-states effective mass.*

$m_e^{\perp}/m_0$	$m_e^{\parallel}/m_0$	m_e^{Γ}/m_0	Technique
0.230	0.198	0.219	Linear combination of atomic orbital method [7.1]

[7.1] M.-Z. Huang and W. Y. Ching, *J. Phys. Chem. Solids* **46**, 977 (1985).

• Experimental value

Table 11.7.2 *Experimental electron effective masses $m_e^{\perp}$, $m_e^{\parallel}$, and m_e^{Γ} at the Γ valley for w-CdS. $m_e^{\Gamma}=(m_e^{\perp 2} m_e^{\parallel})^{1/3}$: density-of-states effective mass. α_F=Fröhlich coupling constant.*

$m_e^{\perp}/m_0$	$m_e^{\parallel}/m_0$	m_e^{Γ}/m_0	Comment
0.204±0.010	0.204±0.010	0.204	Magnetooptical effect, T=1.6 K [7.2]
		0.20	Infrared reflectivity, T=4.2 K [7.3]
		0.17	Cyclotron resonance, T=100 K [7.4]
0.20	0.19	0.197	Cyclotron resonance, T=77 K [7.5]
		0.19	Transport analysis [7.6]
		0.135–0.200	Faraday rotation, T=77 K [7.7]
0.155±0.005			Cyclotron resonance, T=19 K [7.8]
0.210±0.003			Two-photon spectroscopy [7.9]
0.168 *[1]			Cyclotron resonance, T=300 K, α_F=0.514 [7.10]
0.188 *[2]			Cyclotron resonance, T=300 K [7.10]
0.150±0.003	0.152±0.005	0.151	Cyclotron resonance [7.11]

[7.2] J. J. Hopfield and D. G. Thomas, *Phys. Rev.* **122**, 35 (1961).
[7.3] T. J. McMahon and R. J. Bell, *Phys. Rev.* **182**, 526 (1969).
[7.4] K. J. Button, B. Lax, and D. R. Cohn, *Phys. Rev. Lett.* **24**, 375 (1970).
[7.5] K. Nagasaka, G. Kido, and S. Narita, *J. Phys. Soc. Jpn* **28**, 1376 (1970).
[7.6] M. A. Subhan, M. N. Islam, and J. Woods, *J. Phys. Chem. Solids* **33**, 229 (1972).
[7.7] G. P. Srivastava, P. C. Mathur, N. D. Kataria, and R. Shyam, *J. Phys. D: Appl. Phys.* **8**, 523 (1975).
[7.8] K. Nagasaka, *Phys. Rev. B* **15**, 2273 (1977).
[7.9] D. G. Seiler, D. Heiman, R. Feigenblatt, R. L. Aggarwal, and B. Lax, *Phys. Rev. B* **25**, 7666 (1982).
[7.10] Y. Imanaka, N. Miura, and H. Nojiri, *Physica B* **246-247**, 328 (1998).

[7.11] Y. H. Matsuda, N. Miura, S. Kuroda, M. Shibuya, K. Takita, and A. Twardowski, *Physica B* **294-295**, 467 (2001).
*[1]Bare mass.
*[2]Polaron mass.

- **Temperature dependence**

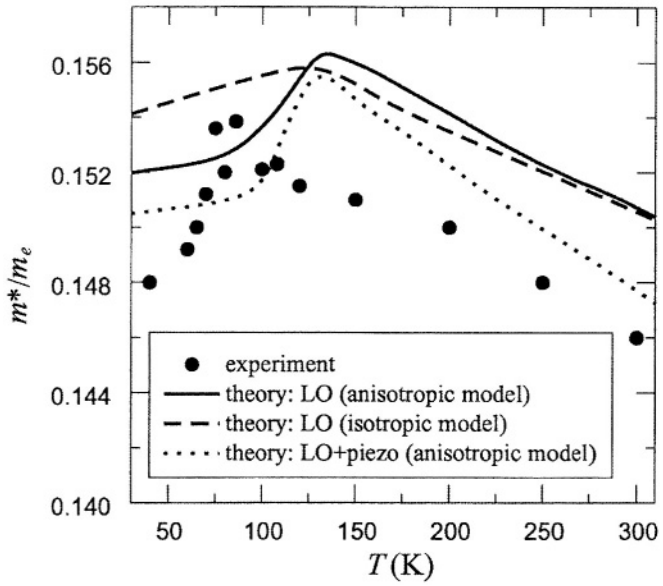

Fig. 11.7.1 Cyclotron mass, m^*/m_e (m_e=m_0: free electron mass), obtained from the magnetoabsorption spectra of polarons in *n*–type *w*-CdS, as a function of temperature T at λ=16.9 μm. The bare-mass value of m_e^{Γ}/m_e =0.168 is used in the theory. [From J. T. Devreese, V. M. Fomin, V. N. Gladilin, Y. Imanaka, and N. Miura, *Physica B* **298**, 207 (2001).]

11.7.2 Electron Effective Mass: Satellite Valley

No detailed data are available for *w*-CdS.

11.7.3 Hole Effective Mass

- **Luttinger's valence-band parameter**

Table 11.7.3 *Theoretical Luttinger's valence-band parameter A_i for w-CdS. A_i (i=1–6) are in units of $\hbar^2/2m_0$ and A_7 is in units of eV/Å.*

A_1	A_2	A_3	A_4	A_5	A_6	$\lvert A_7\rvert$	Ref.
–4.53	–0.39	4.0250	–1.92	–1.92	–2.59		[7.12]
–5.92	–0.70	5.37	–1.82	–1.82	–1.36		[7.13]

[7.12] J.-B. Jeon, Yu. M. Sirenko, K. W. Kim, M. A. Littlejohn, and M. A. Stroscio, *Solid State Commun.* **99**, 423 (1996).
[7.13] See, T. Dietl, H. Ohno, and F. Matsukura, *Phys. Rev. B* **63**, 195205 (2001).

- **Density-of-states mass**

Table 11.7.4 *Density-of-states masses in w-CdS (in m_0). $m_{H\alpha}$* (α=A, B, or C) represents the hole effective mass of the top three valence bands.*

$\perp c$			$\parallel c$		Comment
m_{HA}*	m_{HB}*	m_{HC}*	m_{HH}	m_{LH}	
2.263	0.244	0.394	2.153	0.177	Calc. [7.14]

[7.14] M.-Z. Huang and W. Y. Ching, *J. Phys. Chem. Solids* **46**, 977 (1985).

11.8 ELECTRONIC DEFORMATION POTENTIAL

11.8.1 Intravalley Deformation Potential: Γ Point

• Conduction band

Table 11.8.1 *Γ-conduction-band acoustic deformation potential E_1 for w-CdS used in the transport data analysis.*

E_1 (eV)	Ref.
16±2	[8.1]
14.5	[8.2]
3.3	[8.3]

[8.1] M. Saitoh, *J. Phys. Soc. Jpn* **21,** 2540 (1966).
[8.2] D. L. Rode, *Phys. Rev. B* **2**, 4036 (1970).
[8.3] D. L. Rode, in *Semiconductors and Semimetals,* edited by R. K. Willardson and A. C. Beer (Academic, New York, 1975), Vol. 10, p. 1.

• Valence band

Table 11.8.2 *Experimentally determined Γ-valence-band deformation potentials C_i's for w-CdS.*

Deformation potential (eV)						Ref.
D_1–C_1	D_2–C_2	C_3	C_4	C_5	C_6	
–2.8	–4.5	1.3	–2.9	–1.5	–2.4	[8.4]
–1.7	–3.7	2.7	–1.5	±0.58	±0.8	[8.5]
–1.36	–2.28	1.54	–2.34	–0.73		[8.6]
–1.36	–2.28	1.54	–2.34	–1.20		[8.7]

[8.4] D. W. Langer, R. N. Euwema, K. Era, and T. Koda, *Phys. Rev. B* **2**, 4005 (1970).
[8.5] J. E. Rowe, M. Cardona, and F. H. Pollak, in *II–VI Semiconducting Compounds,* edited by D. G. Thomas (Benjamin, New York, 1967), p. 112.
[8.6] O. Goede, M. Blaschke, and K. H. Klohs, *Phys. Status Solidi B* **76**, 267 (1976).
[8.7] O. Goede, H.-J. Krug, and A. Horst, *Phys. Status Solidi B* **85**, 239 (1978).

• E_0 gap

Table 11.8.3 *Hydrostatic deformation potential a_0^Γ for the E_0 gap of w-CdS.*

a_0^Γ (eV)	Comment
–2.91±0.05	n=2 exciton (A) [8.8]
–2.94±0.05	n=2 exciton (B) [8.8]
–2.8	*
–2.9	Recommended

[8.8] K. Reimann, M. Haselhoff, St. Rübenacke, and M. Steube, *Phys. Status Solidi B* **198**, 71 (1996).
*Estimated from dE_0/dp value.

11.8.2 Intravalley Deformation Potential: High-Symmetry Points

No detailed data are available for *w*-CdS.

11.8.3 Intervalley Deformation Potential

No detailed data are available for *w*-CdS.

11.9 ELECTRON AFFINITY AND SCHOTTKY BARRIER HEIGHT

11.9.1 Electron Affinity

Table 11.9.1 *Electron affinity χ_s for w-CdS.*

χ_s (eV)	Ref.
4.5	[9.1]

[9.1] A. G. Milnes and D. L. Feucht, *Heterojunctions and Metal-Semiconductor Junctions* (Academic, New York, 1972).

11.9.2 Schottky Barrier Height

Table 11.9.2 *Summary of the Schottky barrier height ϕ_n for metal/n-type w-CdS contacts at 300 K.**

Metal	ϕ_n (eV)	Metal	ϕ_n (eV)
Ag	0.35–0.62	Pb	0.59
Al	0–0.7	Pd	0.51–0.63
Au	0.68–0.84	Pt	0.85–1.2
Cu	0.35–0.50	Ti	0.84
Ni	0.45		

*The data are gathered from various sources.

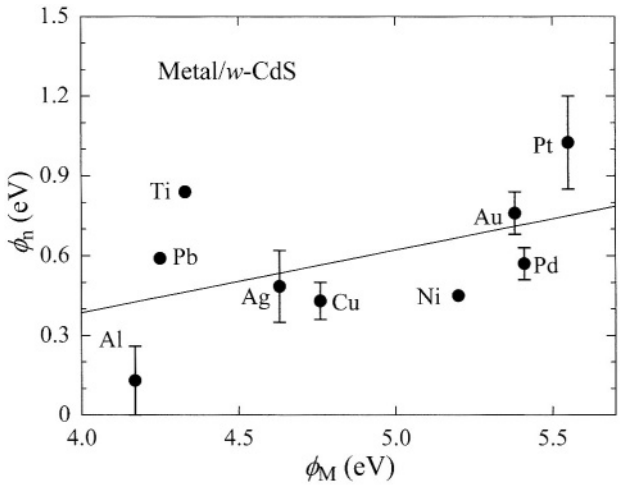

Fig. 11.9.1 Schottky barrier height ϕ_n versus metal work function ϕ_M observed for metal/*n*-type *w*-CdS contacts. Values of the metal work function were taken from H. P. R. Frederikse [in *CRC Handbook of Chemistry and Physics,* 78th Edition, edited by D. R. Lide (CRC Press, Boca Raton, 1997), p. 12-115]. The solid line represents the least-squares-fit result with ϕ_n=0.24ϕ_M–0.56 (ϕ_M and ϕ_n in eV).

● **Temperature and/or pressure coefficient**

Table 11.9.3 *Pressure coefficient of the Schottky barrier height ϕ_n for metal/n-type w-CdS contact.*

Coefficient	Value	Comment
$d\phi_n/dp$ (meV/kbar)	~10	Au/*w*-CdS (*n* type) [9.2]

[9.2] M. J. Peanasky and H. G. Drickamer, *J. Appl. Phys.* **56**, 3471 (1984).

11.10 OPTICAL PROPERTIES

11.10.1 Summary of Optical Dispersion Relations

● **$\varepsilon(E)$ and $n^*(E)$ spectra**

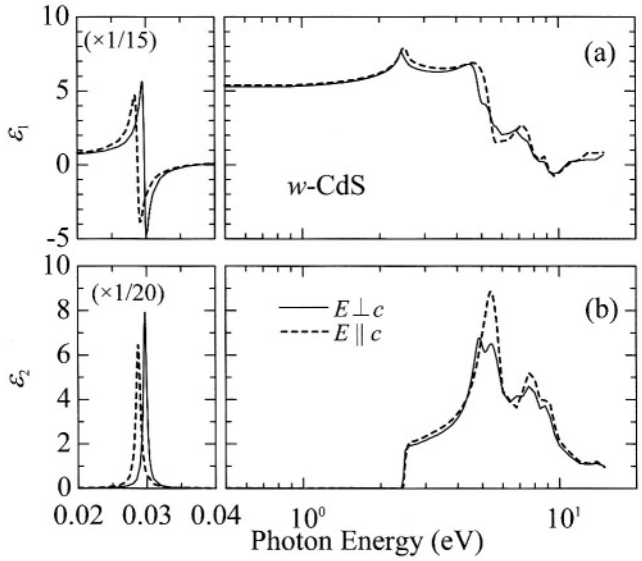

Fig. 11.10.1 Complex dielectric-constant spectra [$\varepsilon(E)=\varepsilon_1(E)+i\varepsilon_2(E)$] for *w*-CdS at 300 K. The numerical data are taken from tabulation by S. Adachi [*Optical Constants of Crystalline and Amorphous Semiconductors: Numerical Data and Graphical Information* (Kluwer Academic, Boston, 1999)].

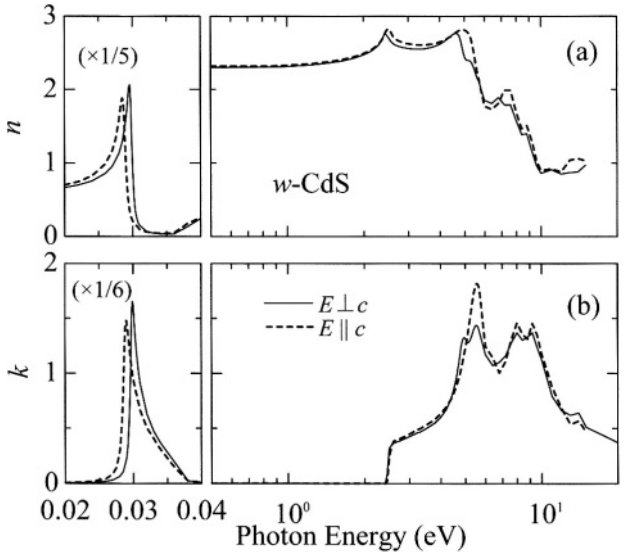

Fig. 11.10.2 Complex refractive-index spectra [$n^*(E)=n(E)+ik(E)$] for *w*-CdS at 300 K. The numerical data are taken from tabulation by S. Adachi [*Optical Constants of Crystalline and Amorphous Semiconductors: Numerical Data and Graphical Information* (Kluwer Academic, Boston, 1999)].

• **$\alpha(E)$ and $R(E)$ spectra**

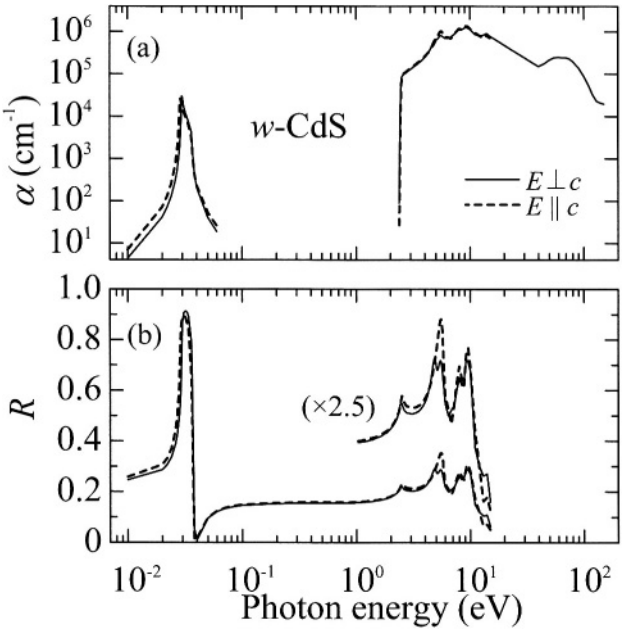

Fig. 11.10.3 (a) Absorption [$\alpha(E)$] and (b) normal-incidence reflectivity spectra [$R(E)$] for *w*-CdS at 300 K. The numerical data are taken from tabulation by S. Adachi [*Optical Constants of Crystalline and Amorphous Semiconductors: Numerical Data and Graphical Information* (Kluwer Academic, Boston, 1999)].

11.10.2 The Reststrahlen Region

• **Static and high-frequency dielectric constants**

Table 11.10.1 *Static and high-frequency dielectric constants ε_s and ε_∞ for w-CdS.*

$E\perp c$		$E \parallel c$		Comment
ε_s	ε_∞	ε_s	ε_∞	
9.35*[1]		10.3*[1]		*T*=300 K [10.1]
9.02*[2]		9.53*[2]		
	5.27		5.27	*T*=15 K [10.2]
8.5	5.3	8.9	5.4	*T*=300 K [10.3]
8.4	5.3	8.9	5.4	*T*=290 K [10.4]
9.67		10.69		*T*= 5K [10.5]
	5.25			*T*=300 K [10.6]
8.92*[1]		10.20*[1]		*T*=300 K [10.7]
8.67*[2]		9.53*[2]		
9.6±0.2				*T*=1.6 K [10.8]
8.1	5.1	8.5	5.2	*T*=100 K [10.9]
8.1	5.2	8.6	5.2	*T*=300 K [10.9]
10.21	5.38	8.99	5.31	*T*=300 K [10.10]
9.6±0.2				*T*=1.6 K [10.11]
10.2	5.4	9.0	5.3	Recommended (*T*=300 K)

[10.1] H. Jaffe and D. A. Berlincourt, *Proc. IEEE* **53**,1372 (1965).
[10.2] H. W. Verleur and A. S. Barker, Jr., *Phys. Rev.* **155,** 750 (1967).
[10.3] A. Manabe, A. Mitsuishi, and H. Yoshinaga, *Jpn. J. Appl. Phys.* **6**, 593 (1967).
[10.4] M. Balkanski, in *Optical Properties of Solids,* edited by F. Abelés (North-Holland, Amsterdam, 1972), p. 529.
[10.5] T. Hattori, Y. Homma, A. Mitsuishi, and M. Tacke, *Opt. Commun.* **7**, 229 (1973).
[10.6] M. Giehler and E. Jahne, *Phys. Status Solidi B* **73**, 503 (1976).

[10.7] I. B. Kobiakov, *Solid State Commun.* **35**, 305 (1980).
[10.8] I. V. Makarenko, I. N. Uraltsev, and V. A. Kiselev, *Phys. Status Solidi B* **98**, 773 (1980).
[10.9] A. N. Pikhtin and A. D. Yas'kov, *Sov. Phys. Semicond.* **15**, 8 (1981).
[10.10] G. A. Samara, *Phys. Rev. B* **27**, 3494 (1983).
[10.11] I. V. Makarenko, I. N. Uraltsev, and V. A. Kiselev, *Phys. Status Solidi B* **98**, 773 (1980).
*[1] Constant stress value.
*[2] Constant strain value.

Table 11.10.2 *Linear temperature and pressure coefficients of the static (ε_s) and high-frequency dielectric constants (ε_∞) for w-CdS near 300 K and normal pressure.*

Coefficient	Value		Ref.
	$\boldsymbol{E}\perp c$	$\boldsymbol{E}\parallel c$	
$d\varepsilon_s/dT$ (10^{-4} K^{-1})	1.92	2.12	[10.12]*
	22.5	16.8	[10.13]
$d\varepsilon_\infty/dT$ (10^{-4} K^{-1})	4.9	4.4	[10.13]
$d\varepsilon_s/dp$ (10^{-1} GPa^{-1})	+1.35	+0.35	[10.13]
$d\varepsilon_\infty/dp$ (10^{-2} GPa^{-1})	−5.9	−5.7	[10.13]

[10.12] I. B. Kobiakov, *Solid State Commun.* **35**, 305 (1980).
[10.13] G. A. Samara, *Phys. Rev. B* **27**, 3494 (1983).
* Constant stress value.

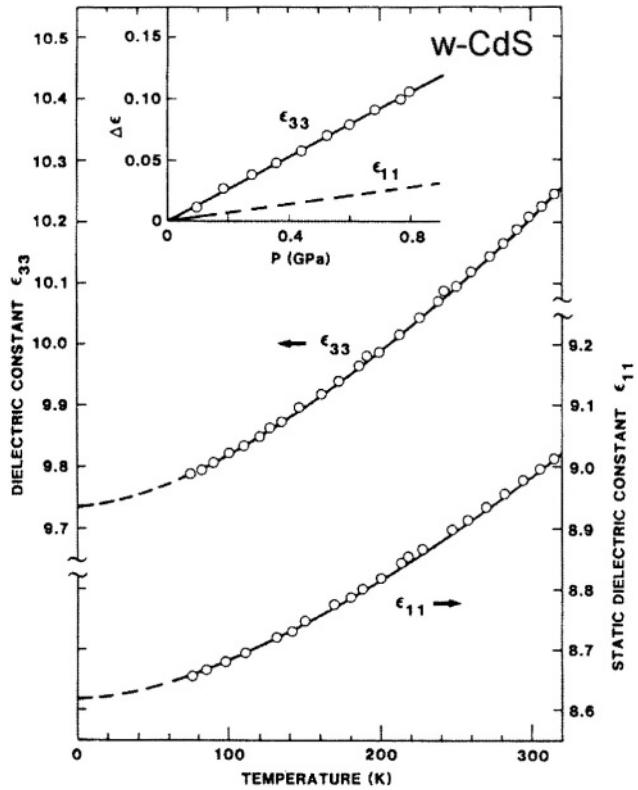

Fig. 11.10.4 Temperature dependence of the static dielectric constant ε_s in *w*-CdS for $\boldsymbol{E}\perp c$ (ε_{11}) and $\boldsymbol{E}\parallel c$ polarizations (ε_{33}) at atmospheric pressure. The data were taken at 100 kHz. Inset shows the anomalous hydrostatic pressure dependence of ε_{11} and ε_{33} at 300 K. Results have been corrected for dimensional changes due to the finite compressibility of *w*-CdS. [From G. A. Samara, *Phys. Rev. B* **27**, 3494 (1983).]

● **Reststrahlen parameter**

Table 11.10.3 *A set of the reststrahlen parameters for w-CdS.*

$$\varepsilon(\omega) = \varepsilon_\infty \left(1 + \frac{\omega_{LO}^2 - \omega_{TO}^2}{\omega_{TO}^2 - \omega^2 - i\omega\gamma} \right)$$

$E \perp c$				$E \parallel c$				Comment
ε_∞	ω_{LO} (cm^{-1})	ω_{TO} (cm^{-1})	γ (cm^{-1})	ε_∞	ω_{LO} (cm^{-1})	ω_{TO} (cm^{-1})	γ (cm^{-1})	
5.3	306	241	5.5	5.4	300	234	4.0	T=300 K [10.14]
5.3	302	240	4.7	5.4	298	232	6.3	T=290 K [10.15]
5.25	305.0	242.0	4.0					T=300 K [10.16]

[10.14] A. Manabe, A. Mitsuishi, and H. Yoshinaga, *Jpn. J. Appl. Phys.* **6**, 593 (1967).
[10.15] M. Balkanski, in *Optical Properties of Solids,* edited by F. Abelés (North-Holland, Amsterdam, 1972), p. 529.
[10.16] M. Giehler and E. Jahne, *Phys. Status Solidi B* **73**, 503 (1976).

● **Multiphonon optical absorption spectra**

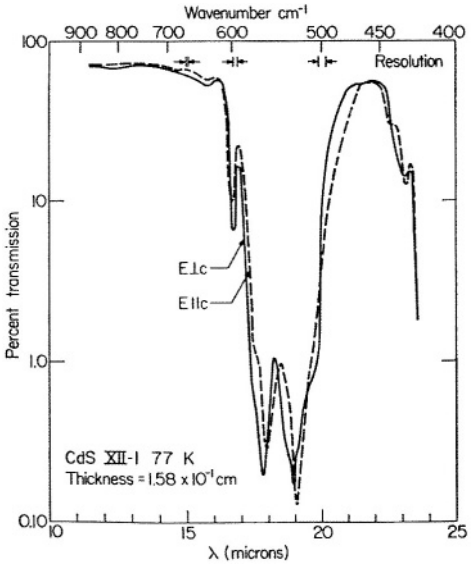

Fig. 11.10.5 Percent transmission in a *w*-CdS sample measured at T=77 K for $\boldsymbol{E} \perp c$ and $\boldsymbol{E} \parallel c$ polarizations. [From T. Deutsch, *J. Appl. Phys.* **33**, 751 (1962).]

11.10.3 At or Near the Fundamental Absorption Edge

● **Free-exciton binding energy and related parameters**

Table 11.10.4 *Free-exciton binding (Rydberg) energy G for w-CdS.*

G (meV)			Comment
A (Γ_9^V)	B (Γ_7^V)	C (Γ_7^V)	
28	28		T=4.2 K [10.17]
29.4±0.1	29.5±0.1		$T \leq$15 K [10.18]
30.2	30.8		T=1.8 K [10.19]
27.4±0.8	27.4±0.8		T=1.8 K [10.20]
27	31	30	T=13–300 K [10.21]
28	29	30	Mean value

[10.17] D. G. Thomas and J. J. Hopfield, *Phys. Rev.* **116**, 573 (1959).
[10.18] B. Segall and D. T. F. Marple, in *Physics and Chemistry of II–VI Compounds,* edited by M. Aven and J. S. Prener (North-Holland, Amsterdam, 1967), p. 317.
[10.19] J. Voigt, F. Spiegelberg, and M. Senoner, *Phys. Status Solidi* **91**, 189 (1979).
[10.20] D. G. Seiler, D. Heiman, and B. S. Wherrett, *Phys. Rev. B* **27**, 2355 (1983).
[10.21] A. Imada, S. Ozaki, and S. Adachi, *J. Appl. Phys.* **92**, 1793 (2002).

Table 11.10.5 *Free-exciton parameters (G=binding energy; a_B=1st-orbital Bohr radius; μ=reduced mass) at the fundamental absorption edge of w-CdS.*

Exciton	G (meV)	a_B (Å)*	μ (m_0)*
A	28	26	0.197
B	29	25	0.204
C	30	25	0.211

*Calculated using $\varepsilon_s=(\varepsilon_{s\perp}^2\varepsilon_{s\parallel})^{1/3}$ value.

Table 11.10.6 *Spin-exchange interaction constant j for w-CdS [10.22].*

j (meV)
2.5

[10.22] See, M. Julier, J. Campo, B. Gil, J. P. Lascaray, and S. Nakamura, *Phys. Rev. B* **57**, R6791 (1998); D. W. Langer, R. N. Euwema, K. Era, and T. Koda, *Phys. Rev. B* **2**, 4005 (1970).

- **Refractive index**

Table 11.10.7 *Refractive index n near the fundamental absorption edge of w-CdS for $\boldsymbol{E}\perp c$ at 300 K [10.23].*

E (eV)	λ (μm)	n	E (eV)	λ (μm)	n
0.1	12.395	2.236	2.066	0.6000	2.493
0.2	6.1975	2.287	2.156	0.5749	2.528
0.3	4.1317	2.295	2.254	0.5499	2.580
0.4	3.0988	2.298	2.264	0.5475	2.587
0.5	2.4790	2.300	2.274	0.5451	2.594
0.885	1.4006	2.304	2.285	0.5425	2.602
0.918	1.3502	2.306	2.295	0.5401	2.609
0.953	1.3006	2.309	2.306	0.5375	2.617
0.992	1.2495	2.312	2.317	0.5350	2.628
1.033	1.1999	2.316	2.328	0.5324	2.638
1.078	1.1498	2.320	2.339	0.5299	2.649
1.127	1.0998	2.324	2.35	0.5274	2.661
1.18	1.0504	2.328	2.361	0.5250	2.674
1.24	0.9996	2.334	2.365	0.5241	2.681
1.305	0.9498	2.341	2.37	0.5230	2.687
1.377	0.9001	2.350	2.375	0.5219	2.694
1.458	0.8501	2.361	2.379	0.5210	2.700
1.549	0.8002	2.374	2.384	0.5199	2.702
1.653	0.7498	2.390	2.388	0.5191	2.709
1.771	0.6999	2.414	2.393	0.5180	2.718
1.836	0.6751	2.427	2.397	0.5171	2.727
1.907	0.6500	2.446	2.402	0.5160	2.735
1.983	0.6251	2.467			

[10.23] See, S. Adachi, *Optical Constants of Crystalline and Amorphous Semiconductors: Numerical Data and Graphical Information* (Kluwer Academic, Boston, 1999).

Table 11.10.8 *Refractive index n near the fundamental absorption edge of w-CdS for* $\boldsymbol{E} \parallel c$ *at 300 K [10.24].*

E (eV)	λ (μm)	n	E (eV)	λ (μm)	n
0.1	12.395	2.255	2.254	0.5499	2.593
0.2	6.1975	2.308	2.264	0.5475	2.600
0.3	4.1317	2.317	2.274	0.5451	2.606
0.4	3.0988	2.320	2.285	0.5425	2.612
0.5	2.4790	2.321	2.295	0.5401	2.622
0.885	1.4006	2.321	2.306	0.5375	2.628
0.918	1.3502	2.323	2.317	0.5350	2.637
0.953	1.3006	2.326	2.328	0.5324	2.644
0.992	1.2495	2.329	2.339	0.5299	2.654
1.033	1.1999	2.332	2.35	0.5274	2.665
1.078	1.1498	2.336	2.361	0.5250	2.675
1.127	1.0998	2.340	2.365	0.5241	2.680
1.18	1.0504	2.346	2.37	0.5230	2.685
1.24	0.9996	2.352	2.375	0.5219	2.689
1.305	0.9498	2.359	2.379	0.5210	2.694
1.377	0.9001	2.368	2.384	0.5199	2.698
1.458	0.8501	2.378	2.388	0.5191	2.702
1.549	0.8002	2.392	2.393	0.5180	2.706
1.653	0.7498	2.409	2.397	0.5171	2.714
1.771	0.6999	2.432	2.402	0.5160	2.720
1.836	0.6751	2.446	2.407	0.5150	2.726
1.907	0.6500	2.463	2.411	0.5141	2.737
1.983	0.6251	2.484	2.416	0.5130	2.743
2.066	0.6000	2.511	2.421	0.5120	2.751
2.156	0.5749	2.545			

[10.24] See, S. Adachi, *Optical Constants of Crystalline and Amorphous Semiconductors: Numerical Data and Graphical Information* (Kluwer Academic, Boston, 1999).

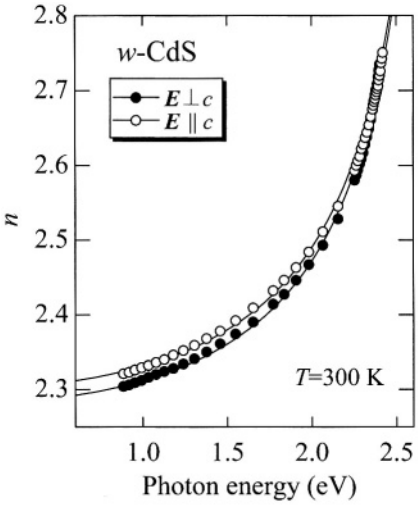

Fig. 11.10.6 Refractive index dispersion in *w*-CdS at T=300 K.. The experimental data are taken from S. Adachi [*Optical Constants of Crystalline and Amorphous Semiconductors: Numerical Data and Graphical Information* (Kluwer Academic, Boston, 1999)]. The solid lines represent the calculated results using $n^2=4.21+[1.00\lambda^2/(\lambda^2-0.182)]$ for $\boldsymbol{E} \perp c$ and $n^2=4.30+[1.00\lambda^2/(\lambda^2-0.182)]$ for $\boldsymbol{E} \parallel c$ with λ in μm.

• **Refractive index: Temperature dependence**

Table 11.10.9 *Temperature coefficient of the refractive index, $n^{-1}(dn/dT)$, in the long-wavelength limit for w-CdS [10.25].*

$\frac{1}{n}\frac{dn}{dT}$ (10^{-5} K^{-1})	Comment
4	$E \perp c$, $E \parallel c$

[10.25] See, S. Adachi, *Optical Properties of Crystalline and Amorphous Semiconductors: Materials and Fundamental Properties* (Kluwer Academic, Boston, 1999).

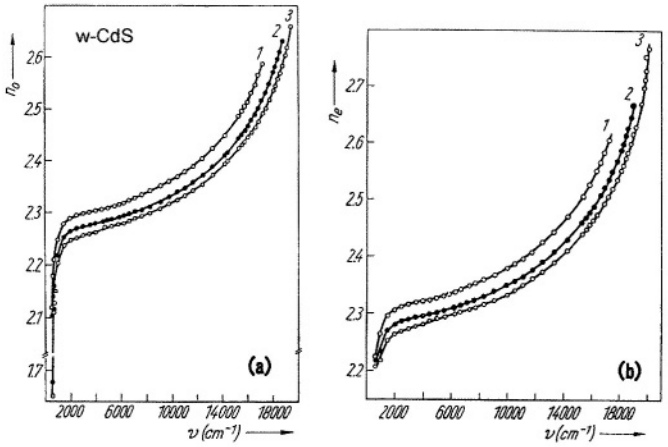

Fig. 11.10.7 Refractive index in *w*-CdS for (a) $E \perp c$ (n_o) and (b) $E \parallel c$ (n_e) measured at three different temperatures, T=600 (1), 300 (2), and 100 K (3). [From M. P. Lisitsa, L. F. Gudymenko, V. N. Malinko, and S. F. Terekhova, *Phys. Status Solidi* **31**, 389 (1969).]

• **Refractive index: Pressure dependence**

Table11.10.10 *Pressure coefficient of the refractive index n^{-1} (dn/dp) at λ=0.5893 μm for w-CdS at 295 K [10.26].*

$\frac{1}{n}\frac{dn}{dp}$ (10^{-2} GPa^{-1})	
$E \perp c$	$E \parallel c$
–0.55	–0.54

[10.26] K. Vedam and T. A. Davis, *Phys. Rev.* **181**, 1196 (1969).

• **Fundamental absorption edge: Temperature dependence**

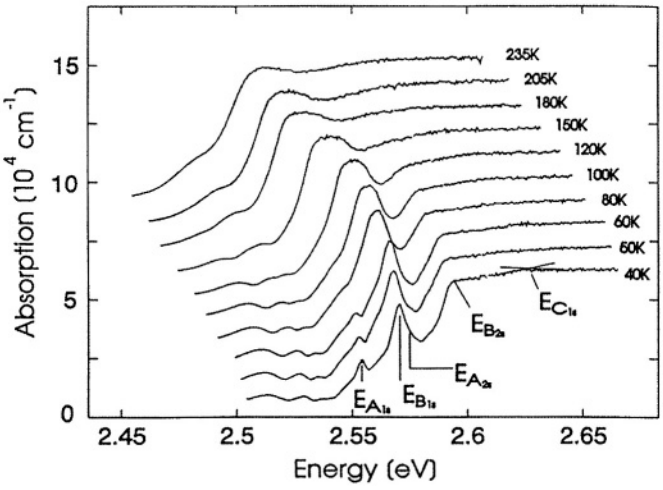

Fig. 11.10.8 Optical absorption in a thin *w*-CdS platelet at various temperatures. The excitonic transitions A_{1s}, B_{1s}, A_{2s}, B_{2s}, and C_{1s} are clearly visible at T=40 K. [From W. Gebhardt and G. Schötz, in *Properties of Wide Band-gap II–VI Semiconductors,* EMIS Datareviews Series No. 17, edited by R. Bhargava (INSPEC, London, 1997), p. 113.]

• **Fundamental absorption edge: Urbach tail**

The Urbach tail in *w*-CdS has been studied by A. E. Rakhshani [*J. Phys.: Condens. Matter* **12**, 4391 (2000)].

• **Fundamental absorption edge: Pressure dependence**

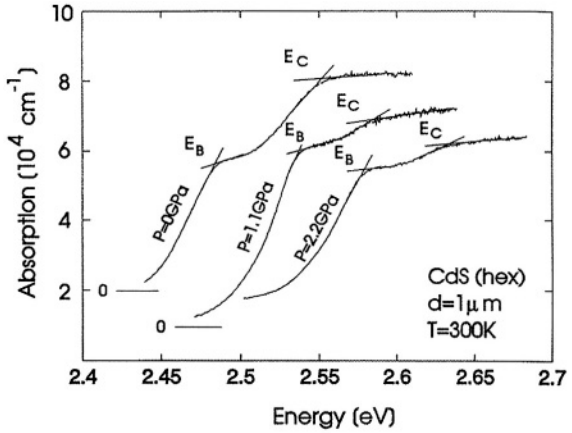

Fig. 11.10.9 Hydrostatic-pressure shift of the *B* and *C* excitonic absorptions in *w*-CdS at *T*=300 K. [From W. Gebhardt and G. Schötz, in *Properties of Wide Bandgap II–VI Semiconductors,* EMIS Datareviews Series No. 17, edited by R. Bhargava (INSPEC, London, 1997), p. 113.]

• **Fundamental absorption edge: Excitation-intensity dependence**

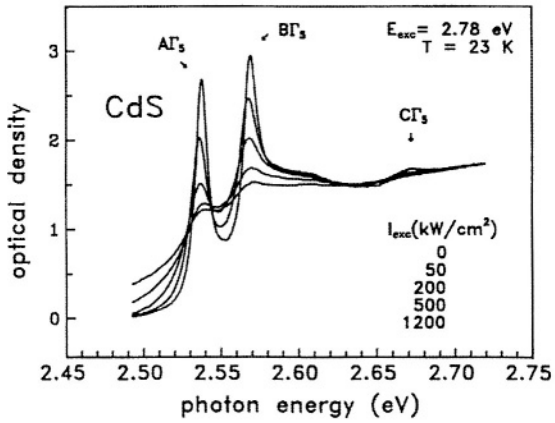

Fig. 11.10.10 Absorption spectra at different excitation intensities obtained from a 350-nm-thick *w*-CdS epilayer grown on BaF_2, illustrating the bleaching of the *A, B,* and *C* (*n*=1) excitons. [From M. Grün, U. Becker, H. Gieβen, Th. Gilsdorf, F. Zhou, J. Loidolt, M. Müller, H. Zangerle, M. Hetterich, and C. Klingshirn, *Opt. Mater.* **2**, 163 (1993).]

11.10.4 The Interband Transition Region

• **Fundamental optical spectra**

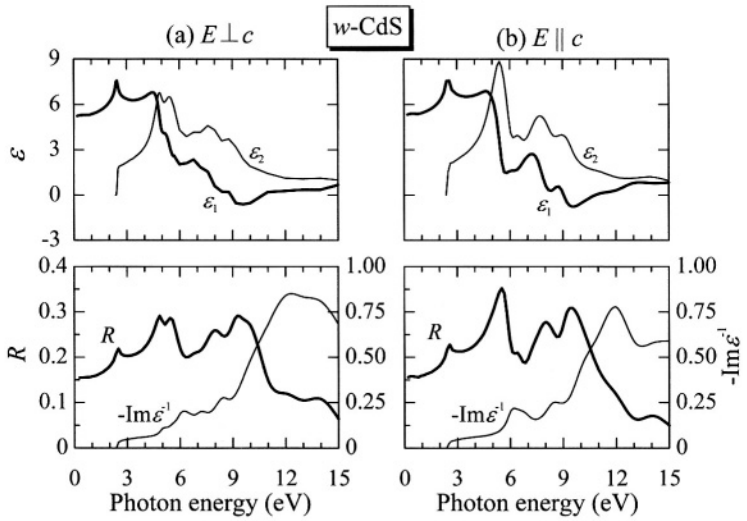

Fig. 11.10.11 Complex dielectric function, $\varepsilon(E)=\varepsilon_2(E)+i\varepsilon_2(E)$, fundamental reflectivity, $R(E)$, and energy-loss function, $-\mathrm{Im}\varepsilon^{-1}(E)$, for *w*-CdS at 300 K. The experimental data are taken from tabulation by S. Adachi [*Optical Constants of Crystalline and Amorphous Semiconductors: Numerical Data and Graphical Information* (Kluwer Academic, Boston, 1999)].

11.10.5 Free-Carrier Absorption and Related Phenomena

No detailed data are available for *w*-CdS.

11.11 ELASTOOPTIC, ELECTROOPTIC, AND NONLINEAR OPTICAL PROPERTIES

11.11.1 Elastooptic Effect

- **Photoelastic constant**

Table 11.11.1 *Photoelastic constant p_{ij} in the static limit ($E \to 0$ eV) for w-CdS.*

p_{11}	p_{12}	p_{13}	p_{31}	p_{33}	p_{44}	p_{66}
			– 0.03		–0.08	–0.04

Table 11.11.2 *Photoelastic constant p_{ij} at λ=632.8 nm for w-CdS [11.1].*

p_{11}	p_{12}	p_{13}	p_{31}	p_{33}	p_{44}	p_{66}
–0.142	–0.066	–0.057	–0.041	–0.20	|~0054|	–0.038

[11.1] *Numerical Data and Functional Relationships in Science and Technology,* edited by K.-H. Hellwege and A. M. Hellwege, Landolt–Börnstein, New Series, Group III, Vol. 11 (Springer, Berlin, 1979).

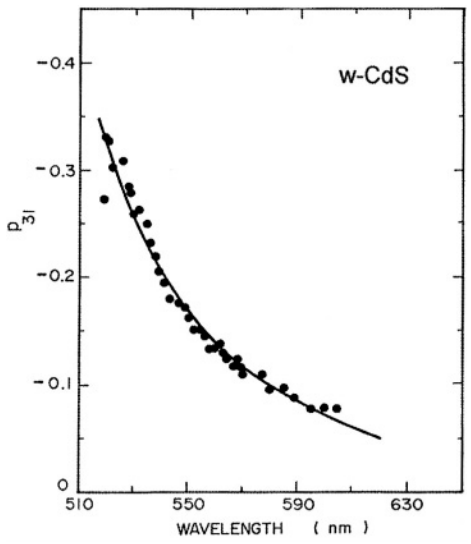

Fig. 11.11.1 Dispersion of the photoelastic constant p_{31} in *w*-CdS determined by Brillouin scattering at 300 K. The solid line represents the theoretical dispersion based on the piezobirefringence theory. [From Y. Itoh, K. Yamabe,S. Adachi, and C. Hamaguchi, *J. Phys. Soc. Jpn* **46**, 542 (1979).]

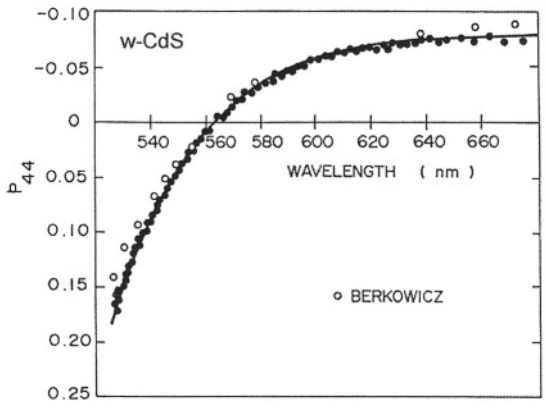

Fig. 11.11.2 Dispersion of the photoelastic constant p_{44} in *w*-CdS determined by Brillouin scattering at 300 K. The solid line represents the theoretical dispersion based on the piezobirefringence theory. The piezobirefringence data of R. Berkowicz and T. Skettrup [*Phys. Rev. B* **11**, 2316 (1975)] are also plotted by the open circles. [From S. Adachi and C. Hamaguchi (unpublished).]

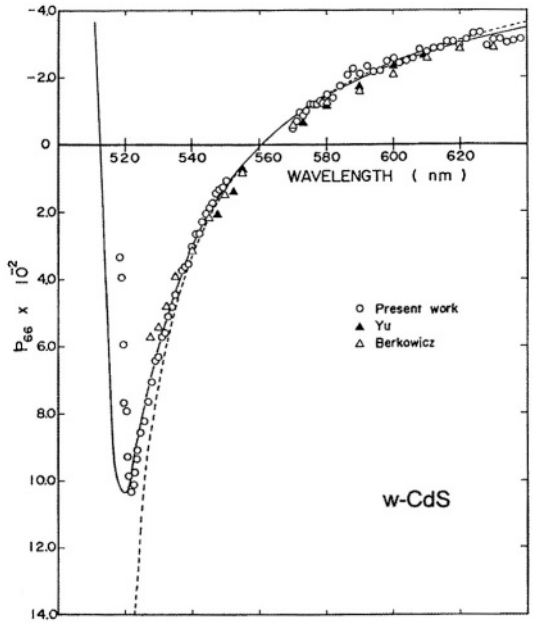

Fig. 11.11.3 Dispersion of the photoelastic constant p_{66} in *w*-CdS determined by Brillouin scattering at 300 K. The dashed and solid lines are theoretically obtained without and with considering damping effect (Γ), respectively. The piezobirefringence data of P. Y. Yu and M. Cardona [*J. Phys. Chem. Solids* **34**, 29 (1973)] and R. Berkowicz and T. Skettrup [*Phys. Rev. B* **11**, 2316 (1975)] are also shown by the solid and open triangles, respectively. [From S. Adachi and C. Hamaguchi, *J. Phys. Soc. Jpn* **45**, 505 (1978).]

11.11.2 Linear Electrooptic Constant

Table 11.11.3 *Linear electrooptic constant r_{ij} for w-CdS.*

Wavelength (μm)	r_{ij} (pm/V)			Comment
	r_{13}	r_{33}	r_{42}	
0.5105	1.0	0.7	0.5	From Raman scattering [11.2]
0.589			3.7	Free value (T) [11.3]
0.6328	1.1	2.4		Clamped value (S) [11.4]
			1.6	Free value (T) [11.5]
1.15	3.1	3.2		Free value (T) [11.5]
3.39	3.5	2.9		Free value (T) [11.5]
10.6	2.45	2.75		Free value (T) [11.5]

[11.2] V. S. Gorelik, O. G. Zolotukhin, and M. M. Sushchinskiĭ, *Sov. Phys. Semicond.* **17**, 730 (1983).
[11.3] D. J. A. Gainon, *J. Opt. Soc. Am.* **54**, 270 (1964).
[11.4] I. P. Kaminow and E. H. Turner, *Proc. IEEE* **54**, 1374 (1966).
[11.5] M. Sugie and K. Tada, *Jpn. J. Appl. Phys.* **15**, 421 (1976).

11.11.3 Quadratic Electrooptic Constant

No detailed data are available for *w*-CdS.

11.11.4 Franz–Keldysh Effect

No detailed data are available for *w*-CdS.

11.11.5 Nonlinear Optical Constant

- **Second-order nonlinear optical susceptibility**

Table 11.11.4 *Experimental second-order nonlinear optical susceptibility d_{ij} for w-CdS.*

d_{ij} (pm/V)			Comment
d_{15}	d_{31}	d_{33}	
10.7	10.1	19.1	$\|d_{ij}\|$, λ=1.064 μm [11.6]
		+100	λ=1.064 μm [11.7]
8.8	8.3	16.8	$\|d_{ij}\|$, λ=1.313 μm [11.6]
8.0	7.4	14.2	$\|d_{ij}\|$, λ=1.548 μm [11.6]
29	–26	+44	λ=10.6 μm [11.7]

[11.6] I. Shoji, T. Kondo, A. Kitamoto, M. Shirane, and R. Ito, *J. Opt. Soc. Am. B* **14**, 2268 (1997).
[11.7] *Numerical Data and Functional Relationships in Science and Technology,* edited by K.-H. Hellwege and A. M. Hellwege, Landolt–Börnstein, New Series, Group III, Vol. 11 (Springer, Berlin, 1979).

- **Two-photon optical absorption**

Table 11.11.5 *Two-photon absorption coefficient β for w-CdS.*

Wavelength (μm)	β (cm/GW)	Comment
0.61	3.2	[11.8]
0.6943	20	$\boldsymbol{E}\perp c$ [11.9]
	15	$\boldsymbol{E}\parallel c$ [11.9]
	56	$\boldsymbol{E}\perp c$ [11.10]
	120	$\boldsymbol{E}\parallel c$ [11.10]
	56–70	[11.11]
0.78	6.4	[11.8]
1.27	<0.01*	[11.8]

[11.8] T. D. Krauss and F. W. Wise, *Appl. Phys. Lett.* **65**, 1739 (1994).
[11.9] R. Baltrameyunas, V. Gavryushin, and Yu. Vaitkus, *Sov. Phys. Solid State* **18**, 660 (1976).
[11.10] G. Kobbe and C. Klingshirn, *Z. Phys. B* **37**, 9 (1980).
[11.11] I. M. Catalano and A. Cingolani, *Solid State Commun.* **34**, 761 (1980).
*Indicating that the signal was below the sensitivity of the experiment.

11.12 CARRIER TRANSPORT PROPERTIES

11.12.1 Low-Field Mobility: Electrons

Table 11.12.1 *300-K (μ_{300K}) and peak Hall mobilities (μ_{peak}) for electrons in w-CdS.*

Mobility	Value (cm^2/V s)	Comment
μ_{300K}	390	[12.1]
μ_{peak}	7.0×10^4	Photo-Hall effect, T=1.8 K, $\boldsymbol{j}\perp c$ [12.2]
	5.5×10^4	Photo-Hall effect, T=1.8 K, $\boldsymbol{j}\parallel c$ [12.2]

[12.1] J. D. Zook and R. N. Dexter, *Phys. Rev.* **129**, 1980 (1963).
[12.2] M. Onuki and K. Shiga, in *Proc. Int. Conf. Phys. Semicond.* Kyoto (1966), p. 427.

• **Temperature dependence**

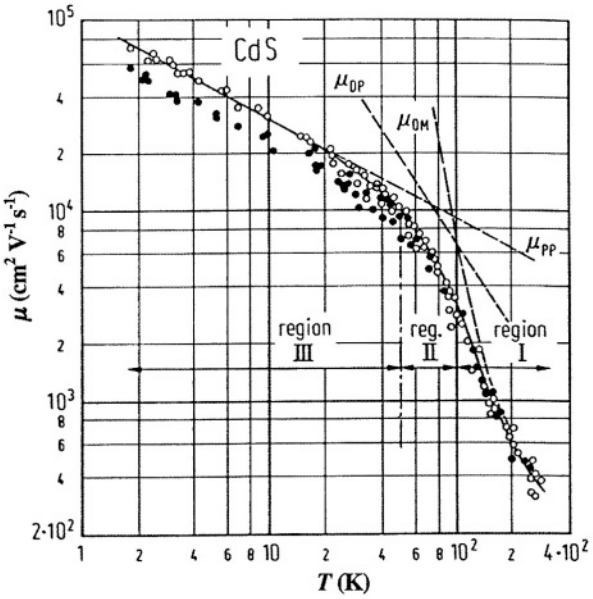

Fig. 11.12.1 Photo-Hall mobility μ versus temperature T for electrons in *w*-CdS. (●) $\boldsymbol{j} \perp c$; (○) $\boldsymbol{j} \| c$. Region I: optical phonon scattering; region II: deformation potential scattering; region III: piezoelectric scattering. [From M. Onuki and K. Shiga, *J. Phys. Soc. Jpn* **21** (Suppl.), 427 (1966).]

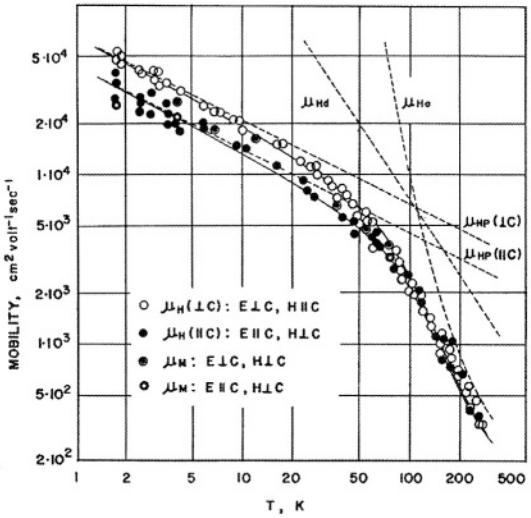

Fig. 11.12.2 Hall mobility μ_H and magnetoresistance mobility μ_M versus temperature T for electrons in *w*-CdS. The solid lines represent the theoretical mobilities by combining the optical phonon scattering (μ_{Ho}), deformation potential scattering (μ_{Hd}), and piezoelectric scattering (μ_{HP}). [From K. Kobayashi, in *II–VI Semiconducting Compounds,* edited by D. G. Thomas (Benjamin, New York, 1967), p. 755.]

• **Pressure dependence**

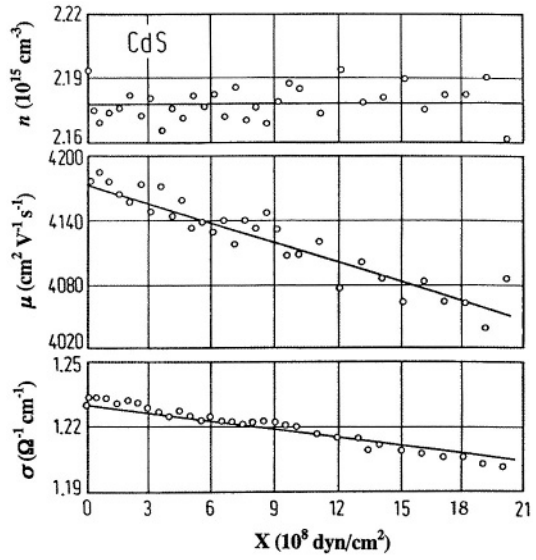

Fig. 11.12.3 Carrier concentration n, carrier mobility μ, and electrical conductivity σ versus uniaxial stress $X \| c$ in *w*-CdS at T=77 K. [From K. Matsuura and I. Tsurumi, *J. Phys. Soc. Jpn* **39**, 1543 (1975).]

• **Donor concentration (free-carrier) dependence**

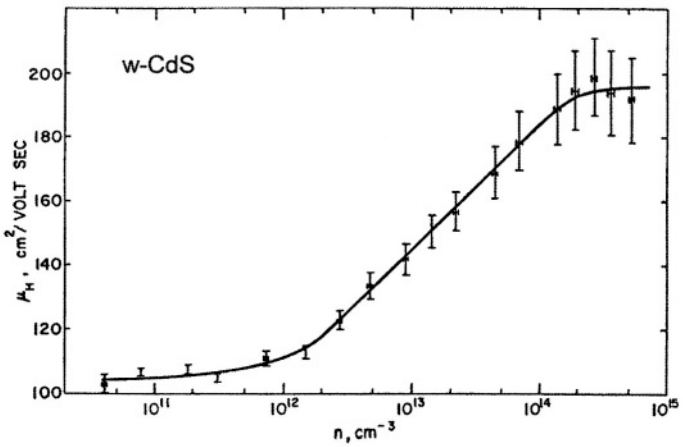

Fig. 11.12.4 Hall mobility μ_H as a function of electron density n, as varied by photoexcitation intensity in *w*-CdS. [From R. H. Bube, in *Physics and Chemistry of II–VI Compounds,* edited by M. Aven and J. S. Prener (North-Holland, Amsterdam, 1967), p. 657.]

• **Hall factor**

The Hall factor for *w*-CdS has been obtained theoretically by D. L. Rode [*Phys. Status Solidi B* **55**, 687 (1973)], and its value is reported to be $\gamma \sim 1.15$ at T=300 K.

11.12.2 Low-Field Mobility: Holes

Table 11.12.2 *300-K (μ_{300K}) and peak Hall mobilities (μ_{peak}) for holes in w-CdS.*

Mobility	Value ($cm^2/V\,s$)	Comment
μ_{300K}	48	Estimated from ambipolar photo-Hall data [12.3]
μ_{peak}		

[12.3] M. Onuki and N. Hase, *J. Phys. Soc. Jpn* **20**, 171 (1965).

• **Temperature dependence**

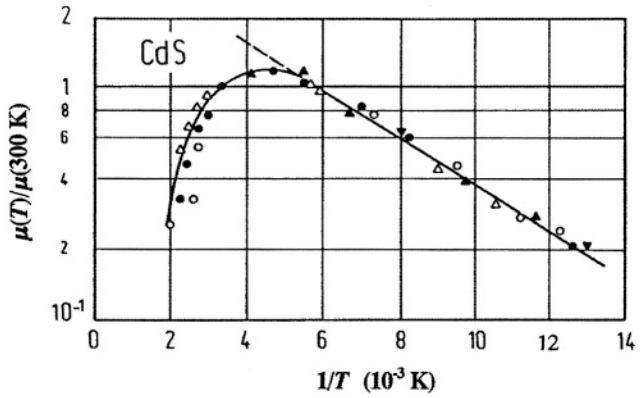

Fig. 11.12.5 Temperature dependence of the hole drift mobility $\mu(T)$, normalized to its room-temperature value $\mu(300\ K)$ in *w*-CdS. [From W. E. Spear and J. Mort, *Proc. Phys. Soc.* **81**, 130 (1963).]

11.12.3 High-Field Transport: Electrons

- **Electron scattering rate**

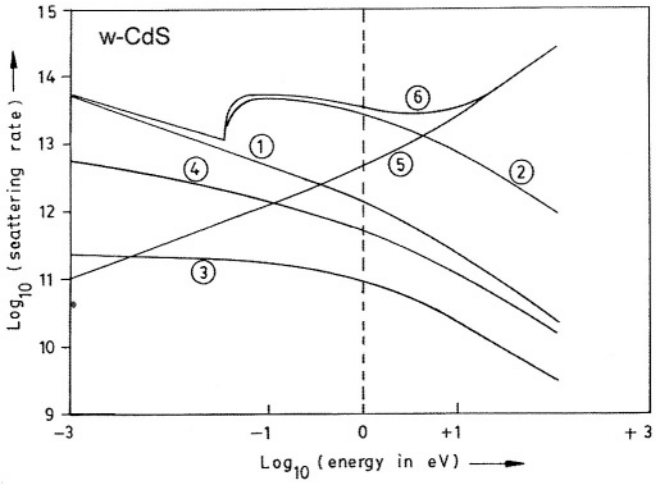

Fig. 11.12.6 Electron scattering rate for *w*-CdS at 77 K. ① Polar optical (absorption); ② polar optical (emission); ③ impurity (10^{15} cm^{-3}); ④ piezoelectric; ⑤ acoustic; ⑥ total. [From A. Dutta, P. S. Mallick, and D. Mukhopadhyay, *Int. J. Electron,* **84**, 203 (1998).]

- **Electron drift velocity–field characteristic**

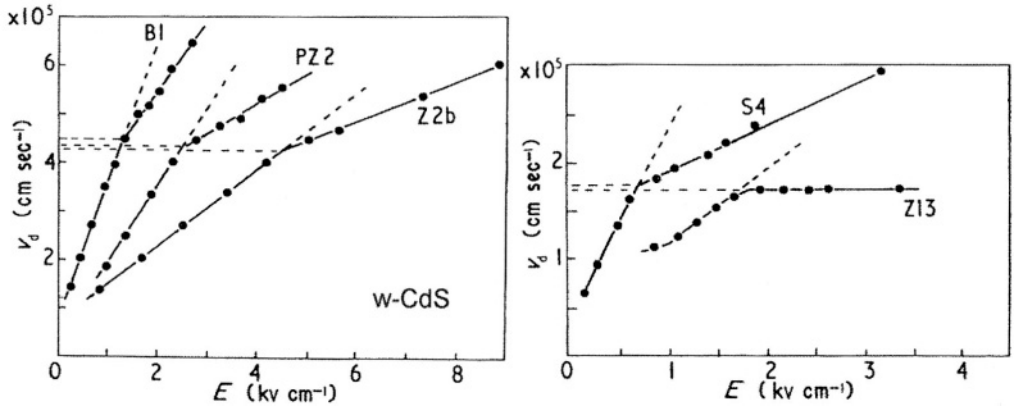

Fig. 11.12.7 Experimental electron drift velocity v_d (v_e) as a function of applied electric filed E for a number of *w*-CdS, α-ZnS, and β-ZnS specimens. B1: CdS, $\boldsymbol{j} \parallel c$; Z2b and PZ2: β-ZnS, $\boldsymbol{j} \parallel$ [111]; S4: *w*-CdS, $\boldsymbol{j} \perp c$; Z13: α-ZnS, $\boldsymbol{j} \perp c$. [From P. G. Le Comber, W. E. Spear, and A. Weinmann, *Brit. J. Appl. Phys.* **17**, 467 (1966).]

- **Electron saturation drift velocity**

Table 11.12.3 *Electron saturation drift velocity* $v_{e,sat}$ *for w-CdS.*

$v_{e,sat}$ (10^7 cm/s)	Comment
1.7	T=4.2 K [12.4]

[12.4] Y. Iye and K. Kajita, *Solid State Commun.* **17**, 957 (1975).

11.12.4 High-Field Transport: Holes

- **Hole drift velocity–field characteristic**

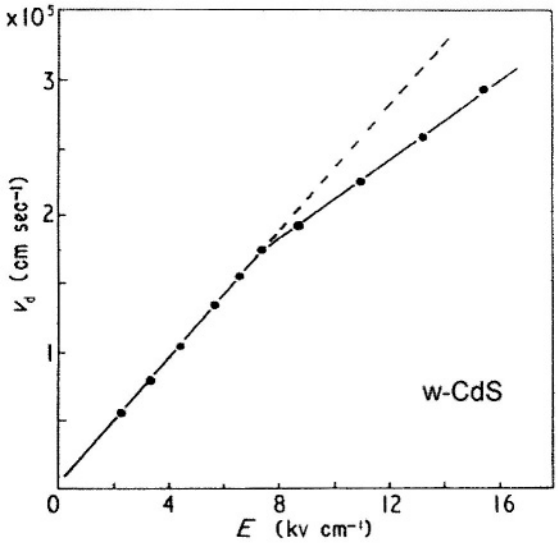

Fig. 11.12.8 Hole drift velocity v_d (v_h) as a function of applied electric filed E for w-CdS ($\boldsymbol{E}\perp\boldsymbol{c}$). [From P. G. Le Comber, W. E. Spear, and A. Weinmann, *Brit. J. Appl. Phys.* **17**, 467 (1966).]

11.12.5 Minority-Carrier Transport: Electrons in *p*-Type Materials

No detailed data are available for w-CdS.

11.12.6 Minority-Carrier Transport: Holes in *n*-Type Materials

- **Minority-hole lifetime and diffusion length**

Table 11.12.4 *Minority-hole lifetime τ and diffusion length L in n-type w-CdS at room temperature.*

τ(s)	L (μm)	Comment
	0.41–0.46	[12.5]
1.7×10^{-9}	0.25±0.05	ρ=0.1 Ω·cm, $n\sim10^{18}$ cm^{-3} [12.6]
	0.275	$R_{\square}$=(2–10)×10^3 Ω/□ [12.7]
4×10^{-9}	0.4	ρ=6 Ω·cm [12.8]

[12.5] L. D. Partain, G. A. Armantrout, and D. Okubo, *IEEE Trans. Electron. Dev.* **ED-27**, 2127 (1980).
[12.6] S. Mora, N. Romeo, and L. Tarricone, *Nuovo Cimento* **60B**, 97 (1980).
[12.7] S. Melinte, A. Jeflea, M. Moise, and N. Mateescu, *J. Less-Common Met.* **95**, 99 (1983).
[12.8] R. B. Stephens, *Phys. Rev. B* **29**, 3283 (1984).

11.12.7 Impact Ionization Coefficient

No detailed data are available for w-CdS.

Chapter 12

Cubic Cadmium Selenide (*c*-CdSe)

12.1 STRUCTURAL PROPERTIES

12.1.1 Ionicity

Table 12.1.1 *Phillips's ionicity f_i for c-CdSe [1.1].*

f_i
0.699

[1.1] J. C. Phillips, *Bonds and Bands in Semiconductors* (Academic, New York, 1973).

12.1.2 Elemental Isotopic Abundance and Molecular Weight

- **Isotopic abundance**

Table 12.1.2 *Isotopic abundance in percent for cadmium and selenium [1.2].*

Isotope	% nat. abundance	Isotope	% nat. abundance	Isotope	% nat. abundance
^{106}Cd	1.25	^{114}Cd	28.73	^{74}Se	0.89
^{108}Cd	0.89	^{116}Cd	7.49	^{76}Se	9.36
^{110}Cd	12.49			^{77}Se	7.63
^{111}Cd	12.80			^{78}Se	23.78
^{112}Cd	24.13			^{80}Se	49.61
^{113}Cd	12.22			^{82}Se	8.73

[1.2] D. R. Lide, *CRC Handbook of Chemistry and Physics,* 78th Edition (CRC Press, Boca Raton, 1997).

- **Molecular weight**

Table 12.1.3 *Molecular (average atomic) weight M for c-CdSe.*

M (amu)
191.37

12.1.3 Crystal Structure and Space Group

Table 12.1.4 *Crystal structure and its space and pint groups for c-CdSe.*

Crystal structure	Space group	Point group
Zincblende (Cubic)	$F\bar{4}3m$	T_d

12.1.4 Lattice Constant and Its Related Parameters

- **Lattice constant, near-neighbor distance, etc.**

Table 12.1.5 *Lattice constant (a), near-neighbor distance (d), unit cube volume* (a^3)*, and molecular density* (d_M) *for c-CdSe at 300 K.*

Parameter	Value
Lattice constant a (Å)	6.077 [1.3]
d (Cation–Anion) (Å)	2.631*
d (Cation–Cation) (Å)	4.297*
Unit cube volume a^3 (10^{-22} cm^3)	2.244*
Molecular density d_M (10^{22} cm^{-3})	1.782*

[1.3] See, N. Samarth, H. Luo, J. K. Furdyna, S. B. Qadri, Y. R. Lee, A. K. Ramdas, and N. Otsuka, *Appl. Phys. Lett.* **54**, 2680 (1989).
*Calculated.

- **Crystal density**

Table 12.1.6 *Crystal density g for c-CdSe at 300 K.**

g (g/cm^3)
5.664

*Calculated using a=6.077 Å.

12.1.5 Structural Phase Transition

Table 12.1.7 *Structural phase transition in c-CdSe at high temperatures.*

Structure	Transition temperature (°C)
Zincblende ($F\bar{4}3m$)	Room temperature
Wurtzite ($P6_3mc$)	95±5 [1.4]

[1.4] V. A. Fedorov, V. A. Ganshin, and Yu. N. Korkishko, *Phys. Status Solidi A* **126**, K5 (1991).

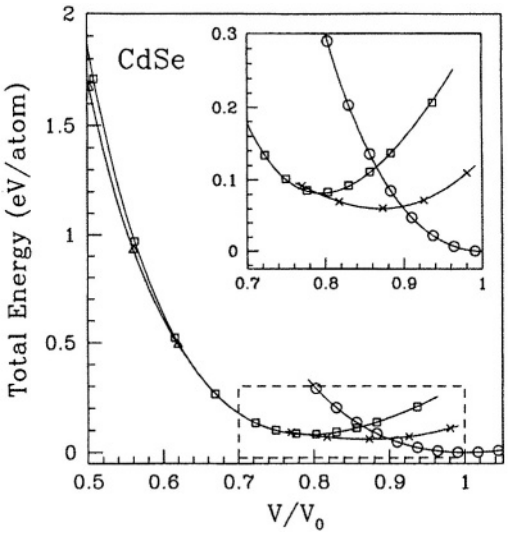

Fig. 12.1.1 Theoretical total energy versus volume for CdSe in the zinc-blende (circles), cinnabar (crosses), rocksalt (squares), and orthorhombic phases (triangles). V_0 is the calculated zero-pressure volume for the zinc-blende phase. The energy of the zinc-blende phase is arbitrary chosen to be zero at zero pressure. [From M. Côté, O. Zakharov, A. Rubio, and M. L. Cohen, *Phys. Rev. B* **55**, 13025 (1997).]

12.1.6 Cleavage Plane

Table 12.1.8 *Crystallographic plane most readily cleaved for c-CdSe.**

Cleavage plane
(110)

*Expected.

- **Surface energy**

Table 12.1.9 *Surface energy for c-CdSe (in J/m^2).*

Plane			Comment
(110)	(111)	$(\bar{1}\,\bar{1}\,\bar{1})$	
0.94	0.91	0.88	Calc. [1.5]

[1.5] B. N. Oshcherin, *Phys. Status Solidi A* **34**, K181 (1976).

12.2 THERMAL PROPERTIES

12.2.1 Melting Point and Its Related Parameters

Table 12.2.1 *Melting point T_m and its related parameter for CdSe.*

Parameter	Value
Melting point T_m (K)	1512 [2.1]
	1531±2 [2.2]
Entropy of fusion ΔS_m (cal/mol K)	16.07 [2.3]

[2.1] A. Reisman, M. Berkenblit, and M. Witzen, *J. Phys. Chem.* **66**, 2210 (1962).
[2.2] W. R. Cook, Jr., *J. Am. Ceram. Soc.* **51**, 518 (1968).
[2.3] See, B. R. Nag, *J. Electron. Mater.* **26**, 70 (1997).

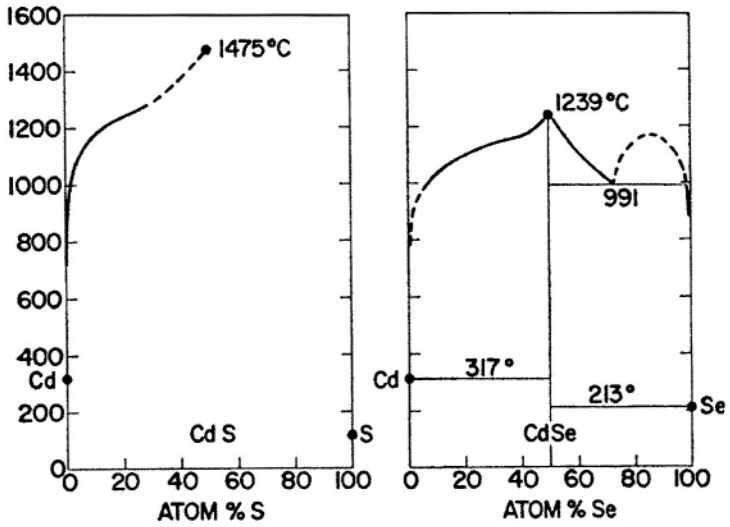

Fig. 12.2.1 *T–x* projects of the II–VI binary systems Cd–S and Cd–Se. [From M. R. Lorenz, in *Physics and Chemistry of II–VI Compounds,* edited by M. Aven and J. S. Prener (North-Holland, Amsterdam, 1967), p. 73.]

12.2.2 Specific Heat

No detailed data are available for *c*-CdSe.

12.2.3 Debye Temperature

No detailed data are available for *c*-CdSe.

12.2.4 Thermal Expansion Coefficient

No detailed data are available for *c*-CdSe.

12.2.5 Thermal Conductivity and Diffusivity

No detailed data are available for *c*-CdSe.

12.3 ELASTIC PROPERTIES

12.3.1 Elastic Constant

- **Room-temperature value**

Table 12.3.1 *Elastic stiffness and compliance constants for c-CdSe at 300 K.*

Parameter	Value
Stiffness (10^{11} dyn/cm^2) [3.1]	
C_{11}	6.67
C_{12}	4.63
C_{44}	2.23

Table 12.3.1 *Continued.*

Parameter	Value
Compliance (10^{-12} cm^2/dyn) [3.1]	
S_{11}	3.48
S_{12}	−1.42
S_{44}	4.48

[3.1] *Numerical Data and Functional Relationships in Science and Technology,* edited by K.-H. Hellwege and A. M. Hellwege, Landolt–Börnstein, New Series, Group III, Vol. 11 (Springer, Berlin, 1979).

12.3.2 Third-Order Elastic Constant

No detailed data are available for *c*-CdSe.

12.3.3 Young's Modulus, Poisson's Ratio, and Similar

- **Young's modulus**

Table 12.3.2 *Young's modulus Y for c-CdSe at 300K.**

Crystallographic plane	Y (10^{11} dyn/cm^2)
(100) plane	
[001] direction	2.87
[011] direction	4.65
(110) plane	
[001] direction	2.87
[111] direction	5.86
(111) plane	4.65

*Calculated using S_{11}=3.48, S_{12}=−1.42, and S_{44}=4.48 (all in 10^{-12} cm^2/dyn).

- **Poisson's ratio**

Table 12.3.3 *Poisson's ratio P for c-CdSe at 300 K. **

Crystallographic plane	P
(100) plane	
m=[010], n=[001]	0.408
m=[011], n=[0$\bar{1}$1]	0.042
(110) plane	
m=[001], n=[1$\bar{1}$0]	0.408
m=[1$\bar{1}$1], n=[1$\bar{1}\bar{2}$]	0.313
(111) plane	0.454

*Calculated using S_{11}=3.48, S_{12}=−1.42, and S_{44}=4.48 (all in 10^{-12} cm^2/dyn).

- **Bulk modulus, shear modulus, etc.**

Table 12.3.4 *Bulk modulus, B_u, pressure derivative of B_u, dB_u/dp, shear modulus, C_s, isotropy factor, A, linear compressibility, C_o, Caucy ratio, C_a, and Born ratio, B_o, for c-CdSe at 300 K.*

Parameter	Value
B_u (10^{11} dyn/cm^2)	5.31 [3.2]
dB_u/dp	4.8 [3.3]
C_s (10^{11} dyn/cm^2)	1.02 [3.2]
A	0.457 [3.2]
C_o (10^{-13} cm^2/dyn)	6.28 [3.2]
C_a	2.08 [3.2]
B_o	1.08 [3.2]

[3.2] Calculated using C_{11}=6.67, C_{12}=4.63, and C_{44}=2.23 (all in 10^{11} dyn/cm^2).
[3.3] Theor. [S.-H. Wei and A. Zunger, *Phys. Rev. B* **60**, 5404 (1999)].

12.3.4 Microhardness

No detailed data are available *c*-CdSe.

12.3.5 Sound Velocity

Table 12.3.5 *Sound velocity propagating in c-CdSe at 300 K.* LA=longitudinal acoustic; TA1, TA2=transverse acoustic.*

Propagation direction	Mode	Sound velocity (10^5 cm/s)
[100]	LA	3.43
[100]	TA1, TA2	1.98
[110]	LA	3.73
[110]	TA1	1.34
[110]	TA2	1.98
[111]	LA	3.82
[111]	TA1, TA2	1.59

*Calculated using C_{11}=6.67×10^{11} dyn/cm^2, C_{12}=4.63×10^{11} dyn/cm^2, C_{44}=2.23×10^{11} dyn/cm^2, and g=5.664 g/cm^3.

12.4 PHONONS AND LATTICE VIBRONIC PROPERTIES

12.4.1 Phonon Dispersion Relation

- **Dispersion curve**

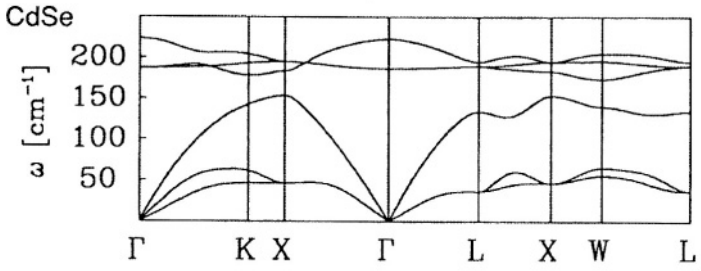

Fig. 12.4.1 Theoretical phonon dispersion curves for *c*-CdSe. [From A. Dal Corso, S. Baroni, R. Resta, S. de Gironcoli, *Phys. Rev. B* **47**, 3588 (1993).]

12.4.2 Phonon Frequency

- **Room-temperature value**

Table 12.4.1 *Long-wavelength ($q \to 0$) and zone-boundary phonon frequencies for c-CdSe.**

Critical point	Phonon	Phonon frequency (cm^{-1})
Γ	TO	169
	LO	211
X	TA	
	LA	
	TO	
	LO	
L	TA	34
	LA	
	TO	
	LO	

*Estimated from *w*-CdSe data.

12.4.3 Mode Grüneisen Parameter

No detailed data are available for *c*-CdSe.

12.4.4 Phonon Deformation Potential

No detailed data are available for *c*-CdSe.

12.5 COLLECTIVE EFFECTS AND RELATED PROPERTIES

12.5.1 Piezoelectric Constant

No detailed data are available for *c*-CdSe.

12.5.2 Fröhlich Coupling Constant

No detailed data are available for *c*-CdSe.

12.6 ENERGY-BAND STRUCTURE: ENERGY-BAND GAPS

12.6.1 Basic Properties

- **Electronic energy-band structure**

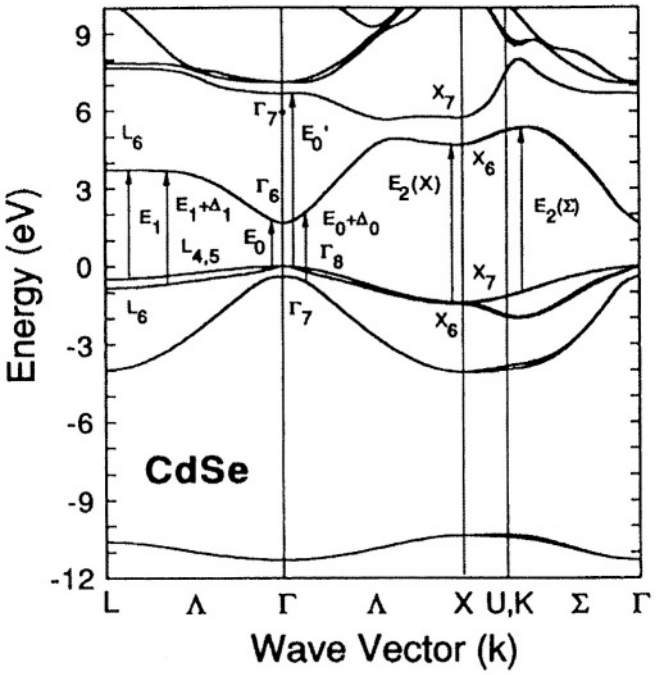

Fig. 12.6.1 Electronic energy-band structure of *c*-CdSe as calculated within the empirical nonlocal pseudopotential formalism. [From Y. D. Kim, M. V. Klein, S. F. Ren, Y. C. Chang, H. Luo, N. Samarthj, and J. K. Furdyna, *Phys. Rev. B* **49**, 7262 (1994).] The locations of several interband transitions are included by the vertical arrows.

- **Energy eigenvalue**

Table 12.6.1 *Energy eigenvalues at the Γ, X, and L points for the valence and first few conduction bands of c-CdSe [6.1].*

Critical point	Level	Value (eV)	
		Calc.	Exper.*
Γ	Γ_6^v (Γ_1^v)	−12.71	
	Γ_7^v (Γ_{15}^v)	0.00	−0.41, −0.42
	Γ_8^v		0.00
	Γ_6^c (Γ_1^c)	2.01	1.764–1.765
	Γ_7^c (Γ_{15}^c)	7.601	6.80
	Γ_8^c		
X	X_6^v (X_1^v)	−11.65	
	X_6^v (X_3^v)	−4.22	−4.0
	X_6^v (X_5^v)	−1.78	−1.85
	X_7^v		
	X_6^c (X_1^c)	4.37	
	X_7^c (X_3^c)	5.206	

Table 12.6.1 *Continued.*

Critical point	Level	Value (eV)	
		Calc.	Exper.*
L	L_6^v (L_1^v)	–11.91	
	L_6^v (L_1^v)	–4.42	
	L_6^v (L_3^v)	–0.71	
	$L_{4,5}^v$		
	L_6^c (L_1^c)	3.87	
	L_6^c (L_3^c)	8.04	
	$L_{4,5}^c$		

[6.1] O. Zakharov, A. Rubio, X. Blase, M. L. Cohen, and S. G. Louie, *Phys. Rev. B* **50**, 10780 (1994).
*The data are gathered from various sources.

12.6.2 E_0-Gap Region

- **Temperature dependence**

Table 12.6.2 *E_0- and $E_0+\Delta_0$-gap energies for c-CdSe determined at various temperatures.*

Temperature (K)	E_0 (eV)	$E_0+\Delta_0$ (eV)	Comment
4.5	1.764 *		Epilayer on (100)GaAs [6.2]
10	1.765 *		Epilayer on (100)GaAs [6.3]
80	1.755 *		Epilayer on (100)GaAs [6.3]
295	1.661 *		Epilayer on (100)GaAs [6.4]
300	1.685 *		Epilayer on (100)GaAs [6.3]
	~1.675 *	~2.065 *	Epilayer on (100)GaAs [6.5]
	1.74	2.15	Epilayer on (100)GaAs [6.6]
	1.675	2.07	Recommended (T=300 K)

[6.2] O. Z. Karimov, D. Wolverson, J. J. Davies, S. I. Stepanov, T. Ruf, S. V. Ivanov, S. V. Sorokin, C. B. O'Donnell, and K. A. Prior, *Phys. Rev. B* **62**, 16582 (2000).
[6.3] N. Samarth, H. Luo, J. K. Furdyna, S. B. Qadri, Y. R. Lee, A. K. Ramdas, and N. Otsuka, *Appl. Phys. Lett.* **54**, 2680 (1989).
[6.4] W. Shan, J. J. Song, H. Luo, and J. K. Furdyna, *Phys. Rev. B* **50**, 8012 (1994).
[6.5] Y. D. Kim, M. V. Klein, S. F. Ren, Y. C. Chang, H. Luo, N. Samarth, and J. K. Furdyna, *Phys. Rev. B* **49**, 7262 (1994).
[6.6] C. Janowitz, O. Günther, G. Jungk, R. L. Johnson, P. V. Santos, M. Cardona, W. Faschinger, and H. Sitter, *Phys. Rev. B* **50**, 2181 (1994).
* Obtained by adding the free-exciton binding energy of 15 meV (*w*-CdSe).

Table 12.6.3 *Spin–orbit–splitoff energy Δ_0 for c-CdSe.**

Δ_0 (eV)	Comment
0.47	Calc. [6.7]
~0.39	T=300 K [6.8]
0.41	T=300 K [6.9]
0.42	T=295 K [6.10]
0.41	Mean value (Exper.)

[6.7] M. Willatzen, M. Cardona, and N. E. Christensen, *Phys. Rev. B* **51**, 17992 (1995).
[6.8] Y. D. Kim, M. V. Klein, S. F. Ren, Y. C. Chang, H. Luo, N. Samarth, and J. K. Furdyna, *Phys. Rev. B* **49**, 7262 (1994).

[6.9] C. Janowitz, O. Günther, G. Jungk, R. L. Johnson, P. V. Santos, M. Cardona, W. Faschinger, and H. Sitter, *Phys. Rev. B* **50**, 2181 (1994).
[6.10] W. Shan, J. J. Song, H. Luo, and J. K. Furdyna, *Phys. Rev. B* **50**, 8012 (1994).

Table 12.6.4 *Empirical equation for the E_0-gap energy variation with temperature T for c-CdSe.*

$$E_0(T) = E_0(0) - \frac{\alpha T^2}{T+\beta}$$

Band gap	Parameter			Comment
	$E_g(0)$ (eV)	α (10^{-4} eV/K)	β (K)	
E_0	1.766	6.96	281	T=10–295 K [6.11]

[6.11] W. Shan, J. J. Song, H. Luo, and J. K. Furdyna, *Phys. Rev. B* **50**, 8012 (1994).

Table 12.6.5 *Empirical equation for the E_0-gap energy variation with temperature T for c-CdSe [6.12].*

$$E_0(T) = E_0(0) - S<\hbar\Omega>\left[\coth\left(\frac{<\hbar\Omega>}{2kT}\right)-1\right]$$

$E_0(0)$ (eV)	S	$<\hbar\Omega>$ (meV)
1.764	2.83	18.9

[6.12] K. P. O'Donnell and P. G. Middleton, in *Properties of Wide Bandgap II–VI Semiconductors,* EMIS Datareviews Series No. 17, edited by R. Bhargava (INSPEC, London, 1997), p. 33.

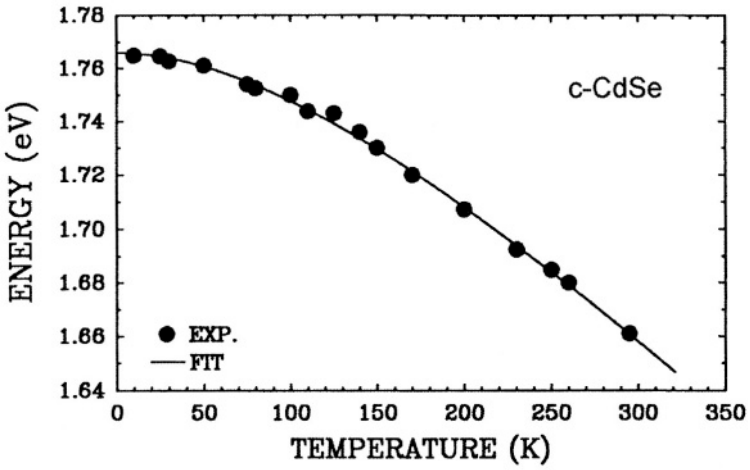

Fig. 12.6.2 E_0-gap energy versus temperature for *c*-CdSe. The excitonic binding energy is taken into account. The solid line represents the best fit to the Varshni equation, $E_0(T)=E_0(0)-\alpha T^2/(T+\beta)$. [From W. Shan, J. J. Song, H. Luo, and J. K. Furdyna, *Phys. Rev. B* **50**, 8012 (1994).]

• Temperature and/or pressure coefficient

Table 12.6.6 *Linear temperature and pressure coefficients of the E_0- and $E_0+\Delta_0$-gap energies for c-CdSe.*

Band gap	Coefficient	Value	Comment
E_0	dE_g/dT (10^{-4} eV/K)	–5.3	T~300 K [6.13]
	dE_g/dp (10^{-2} eV/GPa)	–1.5	p>3 GPa [6.14]

Table 12.6.6 *Continued.*

Band gap	Coefficient	Value	Comment
$E_0+\Delta_0$	dE_g/dT (10^{-4} eV/K)		
	dE_g/dp (10^{-2} eV/GPa)		

[6.13] Estimated from data by W. Shan, J. J. Song, H. Luo, and J. K. Furdyna [*Phys. Rev. B* **50**, 8012 (1994)].
[6.14] See, B. Ray, *II–VI Compounds* (Pergamon, Oxford, 1969).

12.6.3 Higher-Lying Direct Gap

- **Temperature dependence**

Table 12.6.7 *Higher-lying direct-gap energies for c-CdSe at several temperatures.*

Band gap	Value (eV)			
	T=80 K [6.15]	T=90 K [6.16]	T=300 K [6.15]	T=300 K [6.17]
E_1	4.43	4.29	4.30	4.314
$E_1+\Delta_1$	4.65	4.49	4.56	4.568
Δ_1	0.22	0.20	0.26	0.254
E_2	6.26, 6.42	6.09, 6.39	6.34	~6.0
E_0'		6.80		≥6.5
E_1'		7.40		
E_1'+Δ_1'		7.80		

[6.15] R. Ludeke and W. Paul, *Phys. Status Solidi* **23**, 413 (1967).
[6.16] Y. D. Kim, M. V. Klein, S. F. Ren, Y. C. Chang, H. Luo, N. Samarth, and J. K. Furdyna, *Phys. Rev. B* **49**, 7262 (1994).
[6.17] C. Janowitz, O. Günther, G. Jungk, R. L. Johnson, P. V. Santos, M. Cardona, W. Faschinger, and H. Sitter, *Phys. Rev. B* **50**, 2181 (1994).

- **Temperature and/or pressure coefficient**

Table 12.6.8 *Linear temperature and pressure coefficients of the higher-lying band-gap energy for c-CdSe.*

Band gap	Coefficient	Value	Comment
E_1	dE_g/dT (10^{-4} eV/K)	–5.9±0.5	T=80–300 K [6.18]
	dE_g/dp (10^{-2} eV/GPa)		
$E_1+\Delta_1$	dE_g/dT (10^{-4} eV/K)	–4.1±0.5	T=80–300 K [6.18]
	dE_g/dp (10^{-2} eV/GPa)		
E_2	dE_g/dT (10^{-4} eV/K)	–3.6±1.0	T=80–300 K [6.18]
	dE_g/dp (10^{-2} eV/GPa)		

[6.18] R. Ludeke and W. Paul, *Phys. Status Solidi* **23**, 413 (1967).

12.6.4 Lowest Indirect Gap

- **Theoretical value**

Table 12.6.9 *Theoretically obtained lowest indirect-gap energy for c-CdSe (in eV).*

E_g^{L} *1	E_g^{X} *2	Ref.
3.87	4.37	[6.19]
3.612	3.875	[6.20]

[6.19] O. Zakharov, A. Rubio, X. Blase, M. L. Cohen, and S. L. Louie, *Phys. Rev. B* **50**, 10780 (1994).

[6.20] L. W. Wang and A. Zunger, *Phys. Rev. B* **51**, 17398 (1995).
*1 Γ_8^v (Γ_{15}^v)→L_6^c(L_1^c).
*2 Γ_8^v (Γ_{15}^v)→X_6^c(X_1^c).

• **Temperature and/or pressure coefficient**

Table 12.6.10 *Linear pressure coefficient of the lowest indirect-gap energy for c-CdSe.*

Coefficient	Value	Comment
dE_g^L/dp (10^{-2} eV/GPa)	4.5	Calc. [6.21]
	4.1	Calc. [6.22]
dE_g^X/dp (10^{-2} eV/GPa)	−1.7	Calc. [6.21]
	−1.9	Calc. [6.22]

[6.21] K. J. Chang, S. Froyen, and M. L. Cohen, *Solid State Commun.* **50**, 105 (1984).
[6.22] S.-H. Wei and A. Zunger, *Phys. Rev. B* **60**, 5404 (1999).

12.6.5 Conduction-Valley Energy Separation

No detailed data are available for *c*-CdSe.

12.6.6 Direct–Indirect-Gap Transition Pressure

No detailed data are available for *c*-CdSe.

12.7 ENERGY-BAND STRUCTURE: ELECTRON AND HOLE EFFECTIVE MASSES

12.7.1 Electron Effective Mass: Γ Valley

• **Theoretical value**

Table 12.7.1 *Theoretically obtained electron effective mass m_e^Γ at the Γ valley for c-CdSe.*

m_e^Γ/m_0	Technique
0.11	*f*-sum rule [7.1]
0.12	Nonlocal empirical pseudopotential calculation [7.2]

[7.1] R. Dalven, *Phys. Status Solidi B* **48**, K23 (1971).
[7.2] Y. D. Kim, M. V. Klein, S. F .Ren, Y. C. Chang, H. Luo, N. Samarth, and J. K. Furdyna, *Phys. Rev. B* **49**, 7262 (1994).

• **Experimental value**

Table 12.7.2 *Experimentally determined electron effective mass m_e^Γ at the Γ valley for c-CdSe.*

m_e^Γ/m_0	Technique
0.119±0.002	Cyclotron resonance in CdSe/ZnTe single quantum well [7.3]

[7.3] H. K. Ng, Y. A. Leem, R. Knobel, I. P. Smorchkova, A. A. Sirenko, and N. Samarth, *Appl. Phys. Lett.* **75**, 7262 (1994).

12.7.2 Electron Effective Mass: Satellite Valley

No detailed data are available for *c*-CdSe.

12.7.3 Hole Effective Mass

- **Luttinger's valence-band parameter**

Table 12.7.3 *Luttinger's valence-band parameter γ_i for c-CdSe (in $\hbar^2/2m_0$).*

γ_1	γ_2	γ_3
5.51	1.24	2.14

*Estimated from a plot of E_0 versus γ_i for some cubic group-IV, III–V, and II–VI semiconductors (see figure, below).

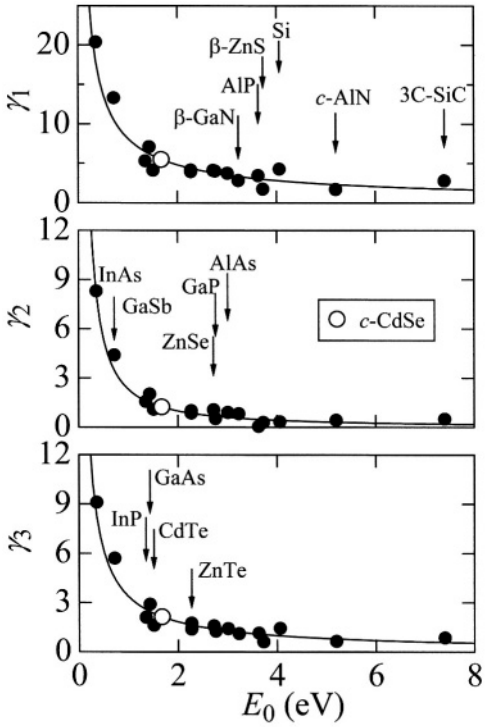

Fig. 12.7.1 Luttinger's valence-band parameter γ_i versus E_0 for a number of the group-IV, III–V, and II–VI semiconductors in the cubic structure. From this plot, we can estimate γ_i values for *c*-CdSe to be γ_1=5.51, γ_2=1.24, and γ_3=2.14 (in $\hbar^2/2m_0$).

- **Band mass, cyclotron mass, etc.**

Table 12.7.4 *Band (m_{HH}, m_{LH}), density-of-states heavy-hole (m_{HH}*), averaged light-hole (m_{LH}*), and spherically-averaged heavy-hole (m_{HH}^s) and light-hole masses (m_{LH}^s) in c-CdSe.**

Mass	Value (m_0)
m_{HH} ([001] direction)	0.33
m_{LH} ([001] direction)	0.13
m_{HH} ([111] direction)	0.81
m_{LH} ([111] direction)	0.10
m_{HH}*	0.57
m_{LH}*	0.11
m_{HH}^s	0.51
m_{LH}^s	0.11

*Calculated using a set of the Luttinger's parameters, γ_1=5.51, γ_2=1.24, and γ_3=2.14.

• **Spin–orbit–splitoff hole effective mass**

Table 12.7.5 *Spin–orbit–splitoff hole effective mass* m_{SO} *for c-CdSe.*

m_{SO}/m_0
0.18

*Obtained from the Luttinger's parameter ($m_{SO}=1/\gamma_1$).

12.8 ELECTRONIC DEFORMATION POTENTIAL

12.8.1 Intravalley Deformation Potential: Γ Point

• **Conduction band**

Table 12.8.1 *Γ-conduction-band intravalley deformation potential* a_c^{Γ} *(=*E_1^{Γ}*) for c-CdSe.*

a_c^{Γ} (eV)	Comment
−11.0	Calc. [8.1]

[8.1] A. Blacha, H. Presting, and M. Cardona, *Phys. Status Solidi B* **126**, 11 (1984).

• **Valence band**

Table 12.8.2 *Γ-valence-band deformation potentials a, b, and d for c-CdSe.*

Deformation potential (eV)			Comment
a	*b*	*d*	
−8.9	0.7		Calc. [8.2]
	−1.14		Calc. [8.3]
	−0.8		Exper. [8.4]

[8.2] A. Blacha, H. Presting, and M. Cardona, *Phys. Status Solidi B* **126**, 11 (1984).
[8.3] T. Nakayama, *Solid-State Electron.* **37**, 1077 (1994).
[8.4] H. J. Lozykowski and V. K. Shastri, *J. Appl. Phys.* **69,** 3235 (1991).

• E_0 **gap**

Table 12.8.3 *Hydrostatic deformation potential* a_0^{Γ} *for the* E_0 *gap of c-CdSe.*

a_0^{Γ} (eV)	Comment
−2.1	Calc. [8.5]
−3.664	Estimated [8.6]
−4.64	Calc. [8.7]
−2.90	Calc. [8.8]
+0.80	Exper.*

[8.5] A. Blacha, H. Presting, and M. Cardona, *Phys. Status Solidi B* **126**, 11 (1984).
[8.6] H. J. Lozykowski and V. K. Shastri, *J. Appl. Phys.* **69,** 3235 (1991).
[8.7] T. Nakayama, *Solid-State Electron.* **37**, 1077 (1994).
[8.8] S.-H. Wei and A. Zunger, *Phys. Rev. B* **60**, 5404 (1999).
*Estimated from dE_0/dp value.

• **Optical-phonon deformation potential**

Table 12.8.4 *Optical-phonon deformation potential d_0 at the Γ-valence band of c-CdSe.*

d_0 (eV)	Comment
8.9	Calc. [8.9]

[8.9] A. Blacha, H. Presting, and M. Cardona, *Phys. Status Solidi B* **126**, 11 (1984).

12.8.2 Intravalley Deformation Potential: High-Symmetry Points

No detailed data are available for *c*-CdSe.

12.8.3 Intervalley Deformation Potential

No detailed data are available for *c*-CdSe.

12.9 ELECTRON AFFINITY AND SCHOTTKY BARRIER HEIGHT

12.9.1 Electron Affinity

No detailed data are available for *c*-CdSe.

12.9.2 Schottky Barrier Height

No detailed data are available for *c*-CdSe.

12.10 OPTICAL PROPERTIES

12.10.1 Summary of Optical Dispersion Relations

• **$\varepsilon(E)$ and $n^*(E)$ spectra**

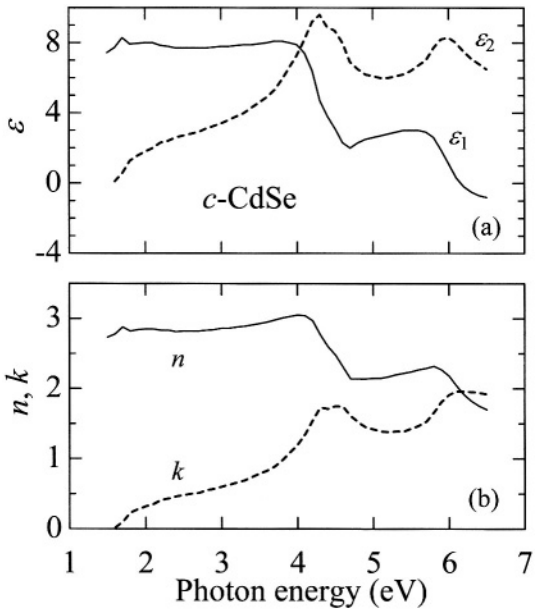

Fig. 12.10.1 (a) Complex dielectric-constant $[\varepsilon(E)=\varepsilon_1(E)+i\varepsilon_2(E)]$ and (b) complex refractive-index spectra $[n^*(E)=n(E)+ik(E)]$ for *c*-CdSe at 300 K. The numerical data are taken from tabulation by S. Adachi [*Optical Constants of Crystalline and Amorphous Semiconductors: Numerical Data and Graphical Information* (Kluwer Academic, Boston, 1999)].

• **$\alpha(E)$ and $R(E)$ spectra**

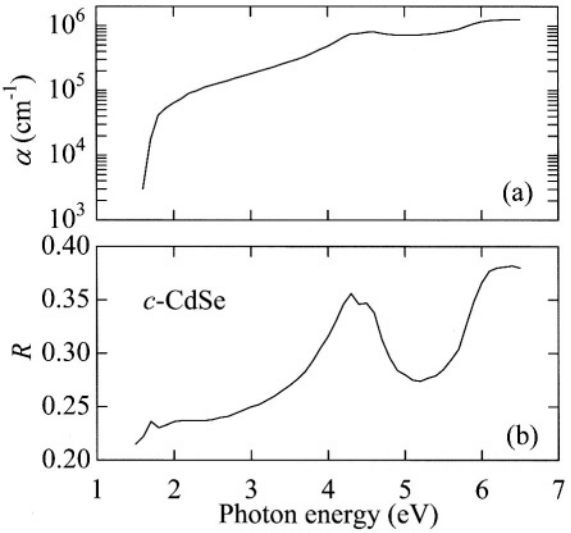

Fig. 12.10.2 (a) Absorption [$\alpha(E)$] and (b) normal-incidence reflectivity spectra [$R(E)$] for *c*-CdSe at 300 K. The numerical data are taken from tabulation by S. Adachi [*Optical Constants of Crystalline and Amorphous Semiconductors: Numerical Data and Graphical Information* (Kluwer Academic, Boston, 1999)].

12.10.2 The Reststrahlen Region

• **Static and high-frequency dielectric constants**

Table 12.10.1 *Static and high-frequency dielectric constants ε_s and ε_∞ for c-CdSe.*

ε_s	ε_∞	Comment
9.6	6.2	T=300 K

* Estimated from *w*-CdSe data [$\varepsilon_s=(\varepsilon_{s\perp}{}^2\varepsilon_{s\parallel})^{1/3}$, $\varepsilon_\infty=(\varepsilon_{\infty\perp}{}^2\varepsilon_{\infty\parallel})^{1/3}$].

12.10.3 At or Near the Fundamental Absorption Edge

• **Fundamental absorption edge: Pressure dependence**

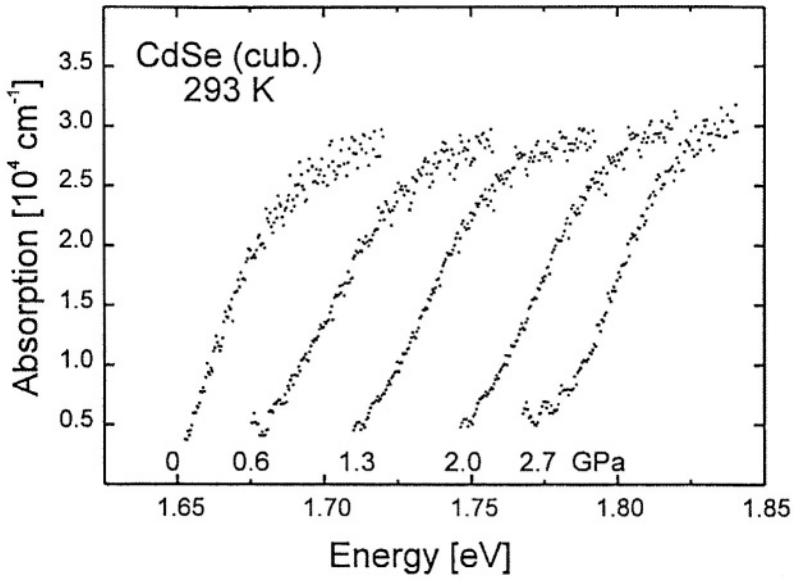

Fig. 12.10.3 Absorption coefficient α at the E_0 edge of a MBE-grown *c*-CdSe at various hydrostatic pressure. [From W. Gebhardt and G. Schötz, in *Properties of Wide Bandgap II–VI Semiconductors,* EMIS Datareviews Series No. 17, edited by R. Bhargava (INSPEC, London, 1997), p. 113.]

12.10.4 The Interband Transition Region

● **Fundamental optical spectra**

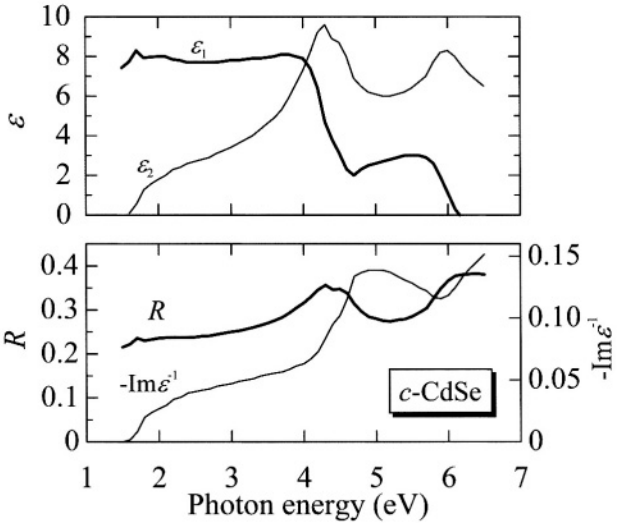

Fig. 12.10.4 Complex dielectric function, $\varepsilon(E)=\varepsilon_2(E)+i\varepsilon_2(E)$, fundamental reflectivity, $R(E)$, and energy-loss function, $-\mathrm{Im}\varepsilon^{-1}(E)$, for *c*-CdSe at 300 K. The experimental data are taken from tabulation by S. Adachi [*Optical Constants of Crystalline and Amorphous Semiconductors: Numerical Data and Graphical Information* (Kluwer Academic, Boston, 1999)].

12.10.5 Free-Carrier Absorption and Related Phenomena

No detailed data are available for *c*-CdSe.

12.11 ELASTOOPTIC, ELECTROOPTIC, AND NONLINEAR OPTICAL PROPERTIES

12.11.1 Elastooptic Effect

No detailed data are available for *c*-CdSe.

12.11.2 Linear Electrooptic Constant

No detailed data are available for *c*-CdSe.

12.11.3 Quadratic Electrooptic Constant

No detailed data are available for *c*-CdSe.

12.11.4 Franz–Keldysh Effect

No detailed data are available for *c*-CdSe.

12.11.5 Nonlinear Optical Constant

● **Second-order nonlinear optical susceptibility**

Table 12.11.1 *Theoretical second-order nonlinear optical susceptibility* $\chi^{(2)}_{123}(-2\omega;\omega;\omega)$ *in the static limit* $(\hbar\omega\to 0\ eV)$ *for c-CdSe.*

$\chi^{(2)}_{123}$ (10^{-8} esu)*	Ref.
23.7	[11.1]

[11.1] M.-Z. Huang and W. Y. Ching, *Phys. Rev. B* **47**, 9464 (1993).
*1 m/V=$3\times10^4/4\pi$ esu.

• **Third-order nonlinear optical susceptibility**

Table 12.11.2 *Theoretical third-order nonlinear optical susceptibility* $\chi^{(3)}_{ijkl}(-3\omega;\omega,\omega,\omega)$ *in the static limit* $(\hbar\omega \to 0\ eV)$ *for c-CdSe.*

$\chi^{(3)}_{ijkl}$ (10^{-11} esu)*		Ref.
$\chi^{(3)}_{1111}$	$\chi^{(3)}_{1212}$	
2.95	1.52	[11.2]

[11.2] W. Y. Ching and M.-Z. Huang, *Phys. Rev. B* **47**, 9479 (1993).
*1 $m^2/V^2 = 9\times10^8/4\pi$ esu.

12.12 CARRIER TRANSPORT PROPERTIES

12.12.1 Low-Field Mobility: Electrons

No detailed data are available for *c*-CdSe.

12.12.2 Low-Field Mobility: Holes

No detailed data are available for *c*-CdSe.

12.12.3 High-Field Transport: Electrons

• **LO-phonon-scattering-limited electron saturation drift velocity**

Table 12.12.1 *Calculated LO-phonon-scattering-limited electron saturation drift velocity* $v_{e,sat}$ *in the lowest-conduction-band valley* α *for c-CdSe at 300 K.**

$$v^{\alpha}_{e,sat} = \left(\frac{8\hbar\omega_{LO}}{3\pi m^{\alpha}_{c}}\right)^{1/2}$$

Valley	$v_{e,sat}$ (10^7 cm/s)
Γ	1.8

*Calculated with $m_c^{\Gamma} = 0.12m_0$ and $\omega_{LO} = 211$ cm^{-1}.

12.12.4 High-Field Transport: Holes

No detailed data are available for *c*-CdSe.

12.12.5 Minority-Carrier Transport: Electrons in *p*-Type Materials

No detailed data are available for *c*-CdSe.

12.12.6 Minority-Carrier Transport: Holes in *n*-Type Materials

No detailed data are available for *c*-CdSe.

12.12.7 Impact Ionization Coefficient

No detailed data are available for *c*-CdSe.

Chapter 13

Wurtzite Cadmium Selenide (*w*-CdSe)

13.1 STRUCTURAL PROPERTIES

13.1.1 Ionicity

Table 13.1.1 *Phillips's ionicity f_i for w-CdSe [1.1].*

f_i
0.699

[1.1] J. C. Phillips, *Bonds and Bands in Semiconductors* (Academic, New York, 1973).

13.1.2 Elemental Isotopic Abundance and Molecular Weight

- **Isotopic abundance**

Table 13.1.2 *Isotopic abundance in percent for cadmium and selenium [1.2].*

Isotope	% nat. abundance	Isotope	% nat. abundance	Isotope	% nat. abundance
^{106}Cd	1.25	^{114}Cd	28.73	^{74}Se	0.89
^{108}Cd	0.89	^{116}Cd	7.49	^{76}Se	9.36
^{110}Cd	12.49			^{77}Se	7.63
^{111}Cd	12.80			^{78}Se	23.78
^{112}Cd	24.13			^{80}Se	49.61
^{113}Cd	12.22			^{82}Se	8.73

[1.2] D. R. Lide, *CRC Handbook of Chemistry and Physics,* 78th Edition (CRC Press, Boca Raton, 1997).

• **Molecular weight**

Table 13.1.3 *Molecular (average atomic) weight M for w-CdSe.*

M (amu)
191.37

13.1.3 Crystal Structure and Space Group

Table 13.1.4 *Crystal structure and its space and pint groups for w-CdSe.*

Crystal structure	Space group	Point group
Wurtzite (Hexagonal)	$P6_3mc$	C_{6v}^4

13.1.4 Lattice Constant and Its Related Parameters

• **Lattice constant and molecular density**

Table 13.1.5 *Lattice constant (a, c) and molecular density (d_M) for w-CdSe at 300 K.*

Parameter	Value
Lattice constant *a* (Å)	4.2999 [1.3]
c (Å)	7.0109 [1.3]
Molecular density d_M (10^{22} cm^{-3})	1.7816*

[1.3] R. R. Reever, *J. Mater. Sci.* **11**, 590 (1976).
*Calculated.

• **Crystal density**

Table 13.1.6 *Crystal density g for w-CdSe at 300 K.**

g (g/cm^3)
5.6615

*Calculated using *a*=4.2999 Å and *c*=7.0109 Å.

13.1.5 Structural Phase Transition

Table 13.1.7 *Structural phase transition in w-CdSe at high pressures.**

Structure	Transition pressure (GPa)
Wurtzite ($P6_3mc$)	Normal pressure
Rocksalt (NaCl)	2.3 [1.4]
	2.13 [1.5]
	2.9 [1.6]

[1.4] A. Jayaraman, W. Klement, Jr., and G. C. Kennedy, *Phys. Rev.* **130**, 2277 (1963).
[1.5] C. F. Cline and D. R. Stephens, *J. Appl. Phys.* **36**, 2869 (1965).
[1.6] J. R. Mei and V. Lemos, *Solid State Commun.* **52**, 785 (1984).
*No serious attempt has been made to obtain information on the *w*-CdSe–*c*-CdSe transition pressure, due to the extreme sluggishness of the transition.

13.1.6 Cleavage Plane

Table 13.1.8 *Crystallographic plane most readily cleaved for w-CdSe.*

Cleavage plane
$(11\bar{2}0), (10\bar{1}0)$

13.2 THERMAL PROPERTIES

13.2.1 Melting Point and Its Related Parameters

Table 13.2.1 *Melting point T_m and its related parameter for CdSe.*

Parameter	Value
Melting point T_m (K)	1512 [2.1]
	1531±2 [2.2]
Entropy of fusion ΔS_m (cal/mol K)	16.07 [2.3]

[2.1] A. Reisman, M. Berkenblit, and M. Witzen, *J. Phys. Chem.* **66**, 2210 (1962).
[2.2] W. R. Cook, Jr., *J. Am. Ceram. Soc.* **51**, 518 (1968).
[2.3] See, B. R. Nag, *J. Electron. Mater.* **26**, 70 (1997).

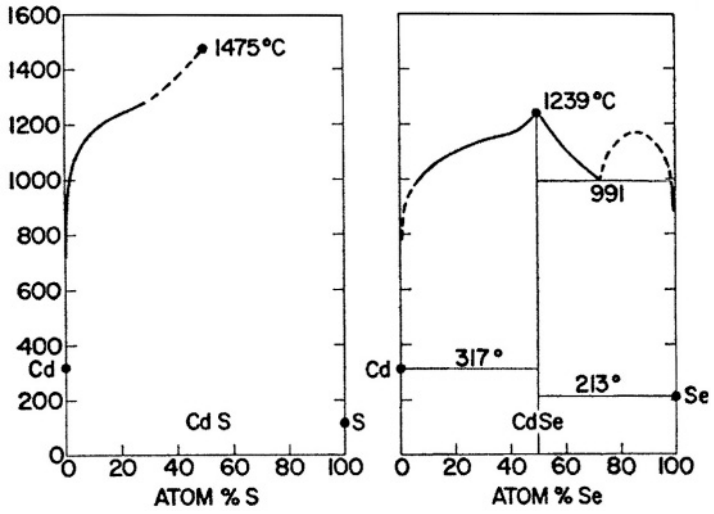

Fig. 13.2.1 *T–x* projects of the II–VI binary systems Cd–S and Cd–Se. [From M. R. Lorenz, in *Physics and Chemistry of II–VI Compounds,* edited by M. Aven and J. S. Prener (North-Holland, Amsterdam, 1967), p. 73.]

13.2.2 Specific Heat

Table 13.2.2 *Experimental specific heats C_p (at constant pressure) and C_v (at constant volume) for w-CdSe (in J/gK) [2.4].*

Temperature (K)	C_p	C_v	Temperature (K)	C_p	C_v
55	0.1243	0.1243	190	0.2425	0.2421
60	0.1338	0.1334	200	0.2447	0.2443
70	0.1525	0.1525	210	0.2468	0.2464
80	0.1687	0.1687	220	0.2485	0.2481

Table 13.2.2 *Continued.*

Temperature (K)	C_p	C_v	Temperature (K)	C_p	C_v
90	0.1830	0.1829	230	0.2500	0.2496
100	0.1942	0.1941	240	0.2515	0.2511
110	0.2032	0.2031	250	0.2527	0.2523
120	0.2112	0.2111	260	0.2537	0.2533
130	0.2183	0.2181	270	0.2549	0.2544
140	0.2239	0.2238	273.16	0.2553	0.2548
150	0.2294	0.2292	280	0.2561	0.2559
160	0.2334	0.2332	290	0.2573	0.2568
170	0.2372	0.2369	300	0.2586	0.2580
180	0.2398	0.2396			

[2.4] A. F. Demidenko, *Inorg. Mater.* **5**, 210 (1969).

- **Functional expression**

Table 13.2.3 *Specific heat C_p (at constant pressure) as a function of temperature T for w-CdSe.*

C_p (J/g K)	Comment
$0.261+3.3\times10^{-5}T$	[2.5]
$0.270+3.17\times10^{-5}T$	T=320–760 K [2.6]
$0.245+4.88\times10^{-5}T$	T=298–1500 K [2.7]

[2.5] P. Goldfinger and M. Jeunehomme, *Trans. Faraday Soc.* **59**, 2851 (1963).
[2.6] A. G. Sigai and H. Wiedemeier, *J. Electrochem. Soc.* **119**, 910 (1972).
[2.7] K. C. Mills, *Themodynamic Date for Inorganic Sulphides, Selenides and Tellurides* (Butterworths, London, 1974).
*These expressions give an average value of C_p~0.281 J/g K at T=300 K.

13.2.3 Debye Temperature

Table 13.2.4 *Debye temperature θ_D for w-CdSe [2.8].*

Temperature (K)	θ_D (K)	Temperature (K)	θ_D (K)
55	230	190	234
60	236	200	230
70	244	210	223
80	248	220	220
90	249	230	218
100	251	240	211
110	253	250	205
120	251	260	195
130	251	270	188
140	248	273.16	183
150	244	280	168
160	243	290	146
170	238	300	135
180	236		

[2.8] A. F. Demidenko, *Inorg. Mater.* **5**, 210 (1969).

13.2.4 Thermal Expansion Coefficient

Table 13.2.5 *Thermal expansion coefficient α_{th} for w-CdSe [2.9].*

α_{th} (10^{-6} K^{-1})		Comment
α_a	α_c	
4.13	2.76	T=300 K
5.47	3.26	T=300–900 K (averaged)

[2.9] H. Iwanaga, A. Kunishige, and S. Takeuchi, *J. Mater. Sci.* **35**, 2451 (2000).

13.2.5 Thermal Conductivity and Diffusivity

Table 13.2.6 *Thermal conductivity K for w-CdSe. Thermal diffusivity can be calculated from a relation $D=K/(C_p \cdot g)$, where C_p is the specific heat at constant pressure and g is the crystal density.*

K (W/cm K)	Comment
~0.09	T=300 K (see [2.10])
$0.136–0.268T+0.186T^2$ (T in kilokelvins)	Polycrystalline sample, T=300–700 K [2.11]

[2.10] See, G. A. Slack, *Phys. Rev. B* **6**, 3791 (1972).
[2.11] A. M. Abousehly, H. M. A. Basha, and A. A. El-Sharkawy, *High Temp.–High Press.* **21**, 187 (1990) [see also, H. Maleki and L. R. Holland, in *Properties of Narrow Gap Cadmium-based Compounds,* EMIS Datareviews Series No. 10, edited by P. Capper (INSPEC, London, 1994), p. 408].

13.3 ELASTIC PROPERTIES

13.3.1 Elastic Constant

- **Room-temperature value**

Table 13.3.1 *Room-temperature elastic stiffness (C_{ij}) and compliance constants (S_{ij}) for w-CdSe [3.1].*

C_{ij} (10^{11} dyn/cm^2)					
C_{11}	C_{12}	C_{13}	C_{33}	C_{44}	C_{66}*
7.41	4.52	3.89	8.43	1.34	1.45
S_{ij} (10^{-12} cm^2/dyn)					
S_{11}	S_{12}	S_{13}	S_{33}	S_{44}	S_{66}*
2.32	–1.12	–0.55	1.69	7.47	6.88

[3.1] *Numerical Data and Functional Relationships in Science and Technology,* edited by K.-H. Hellwege and A. M. Hellwege, Landolt–Börnstein, New Series, Group III, Vol. 18 (Springer, Berlin, 1984).
* $C_{66}=½(C_{11}-C_{12})$; $S_{66}=2(S_{11}-S_{12})$.

• **Temperature and/or pressure dependence**

Table 13.3.2 *Temperature derivative of the elastic stiffness constant, dC_{ij}/dT, for w-CdSe [3.2].*

dC_{ij}/dT (10^7 dyn/cm^2 K)					
C_{11}	C_{12}	C_{13}	C_{33}	C_{44}	C_{66}
−16.4	−12.6		−17.7	−1.5	−1.9

[3.2] B. Bonello and B. Fernandez, *J. Phys. Chem. Solids* **54**, 209 (1993).

13.3.2 Third-Order Elastic Constant

No detailed data are available for *w*-CdSe.

13.3.3 Young's Modulus, Poisson's Ratio, and Similar

• **Young's modulus**

Table 13.3.3 *Young's modulus Y for w-CdSe at 300 K.**

Direction	Y (10^{11} dyn/cm^2)
$c \perp l$	4.31
$c \parallel l$	5.92

*Calculated using S_{11}=2.32×10^{-12} and S_{33}=1.69×10^{-12} cm^2/dyn.
l: directional vector.

• **Poisson's ratio**

Table 13.3.4 *Poisson's ratio P for w-CdSe at 300 K.**

Direction	P
$c \perp l$	0.37
$c \parallel l$	0.31

*Obtained from a definition $B_u = Y/[3(1-2P)]$, where B_u and Y are bulk and Young's moduli, respectively.
l: directional vector.

• **Bulk modulus, shear modulus, etc.**

Table 13.3.5 *Bulk modulus, B_u, pressure derivative of B_u, dB_u/dp, and linear compressibility, C_o, for w-CdSe at 300 K.*

Parameter	Value
B_u (10^{11} dyn/cm^2)	5.31 [3.3]
dB_u/dp	
C_o (10^{-13} cm^2/dyn)	
$c \perp l$	6.50 [3.3]
$c \parallel l$	5.90 [3.3]

[3.3] Calculated using C_{11}=7.41×10^{11} dyn/cm^2, C_{12}=4.52×10^{11} dyn/cm^2, C_{13}=3.89×10^{11} dyn/cm^2, C_{33}=8.43×10^{11} dyn/cm^2, S_{11}=2.32×10^{-12} cm^2/dyn, S_{12}= −1.12×10^{-12} cm^2/dyn, S_{13}= −5.5×10^{-13} cm^2/dyn, and S_{33}=1.69×10^{-12} cm^2/dyn.
l: directional vector.

13.3.4 Microhardness

Table 13.3.6 *Microhardness H for w-CdSe [3.4].*

H (GPa)
0.90

[3.4] See, L. Garbato and A. Rucci, *Phil. Mag.* **35**, 1681 (1977).

13.3.5 Sound Velocity

Table 13.3.7 *Sound velocity propagating in w-CdSe at 300 K.* LA=longitudinal acoustic; TA1, TA2=transverse acoustic.*

Propagation direction $\boldsymbol{a}$	Direction of polarization π	Mode	Sound velocity (10^5 cm/s)
$\boldsymbol{a} \parallel c$	$\pi \parallel c$	LA	3.86
$\boldsymbol{a} \parallel c$	$\pi \perp c$	TA1, TA2	1.54
$\boldsymbol{a} \perp c$	$\pi \perp c$	LA	3.62
$\boldsymbol{a} \perp c$	$\pi \perp c$	TA1	1.60
$\boldsymbol{a} \perp c$	$\pi \parallel c$	TA2	1.54

*Calculated using $C_{11}=7.41\times10^{11}$ dyn/cm^2, $C_{12}=4.52\times10^{11}$ dyn/cm^2, $C_{33}=8.43\times10^{11}$ dyn/cm^2, $C_{44}=1.34\times10^{11}$ dyn/cm^2, and $g=5.6615$ g/cm^3.

13.4 PHONONS AND LATTICE VIBRONIC PROPERTIES

13.4.1 Phonon Dispersion Relation

There have been reported neither theoretical nor experimental data on the phonon dispersion curves/phonon density of states for *w*-CdSe up to now.

13.4.2 Phonon Frequency

Table 11.4.1 *Long-wavelength ($\boldsymbol{q}\rightarrow0$) phonon frequencies for w-CdSe.*

Phonon frequency (cm^{-1})						Comment
E_2 low	A_1 (TO)	E_1 (TO)	E_2 high	A_1 (LO)	E_1 (LO)	
	170	173.5				T=15 K [4.1]
	168	175		210	212	T=100 K [4.2]
	168	171				T=300 K [4.1]
	166	172		211	210	T=300 K [4.2]
	166.5	169		210	212	T=300 K [4.3]
	165			209		T=300 K [4.4]
34	166	169		209	211	T=300 K [4.5]
34	166	170		210	211	Mean value (T=300 K)

[4.1] R. Geick, C. H. Perry, and S. S. Mitra, *J. Appl. Phys.* **37**, 1994 (1966).

[4.2] H. W. Verleur and A. S. Barker, Jr., *Phys. Rev.* **155,** 750 (1967).
[4.3] R. Beserman and M. Balkanski, *Phys. Rev. B* **1**, 608 (1970).
[4.4] M. Górska and W. Nazarewicz, *Phys. Status Solidi B* **65**, 193 (1974).
[4.5] V. G. Plotnichenko, Yu. A. Mityagin, and L. K. Vodop'yanov, *Sov. Phys. Solid State* **19**, 1584 (1977).

• **Temperature dependence**

No detailed data are available for *w*-CdSe; however, it is generally accepted that the phonon frequency decreases with increasing temperature [see, e.g., M. Ya. Valakh, M. P. Lisitsa, G. S. Pekar, G. N. Polysskii, V. I. Sidorenko, and A. M. Yaremko, *Phys. Status Solidi B* **113**, 635 (1982)].

13.4.3 Mode Grüneisen Parameter

No detailed data are available for *w*-CdSe.

13.4.4 Phonon Deformation Potential

No detailed data are available for *w*-CdSe.

13.5 COLLECTIVE EFFECTS AND RELATED PROPERTIES

13.5.1 Piezoelectric Constant

Table 13.5.1 *Experimentally determined piezoelectric stress (e_{ij}) and strain constants (d_{ij}) for w-CdSe.*

e_{ij} (C/m^2)			d_{ij} (10^{-12} m/V)			Ref.
e_{15}	e_{31}	e_{33}	d_{15}	d_{31}	d_{33}	
–0.138	–0.160	0.347	–10.51	–3.92	7.84	[5.1]
			–10.1	–3.80	7.81	[5.2]

[5.1] D. Berlincourt, H. Jaffe, and L. R. Shiozawa, *Phys. Rev.* **129**, 1009 (1963).
[5.2] E. F. Tokarev, G. S. Pado, L. A. Chernozatonskii, and V. V. Drachev, *Sov. Phys. Solid State* **15**, 1064 (1973).

13.5.2 Fröhlich Coupling Constant

Table 13.5.2 *Fröhlich coupling constant α_F of w-CdSe [5.3].*

α_F
0.46

[5.3] E. Kartheuser, in *Polarons in Ionic Crystals and Polar Semiconductors,* edited by J. T. Devreese (North-Holland, Amsterdam, 1972), p. 717.

13.6 ENERGY-BAND STRUCTURE: ENERGY-BAND GAPS

13.6.1 Basic Properties

- **Electronic energy-band structure**

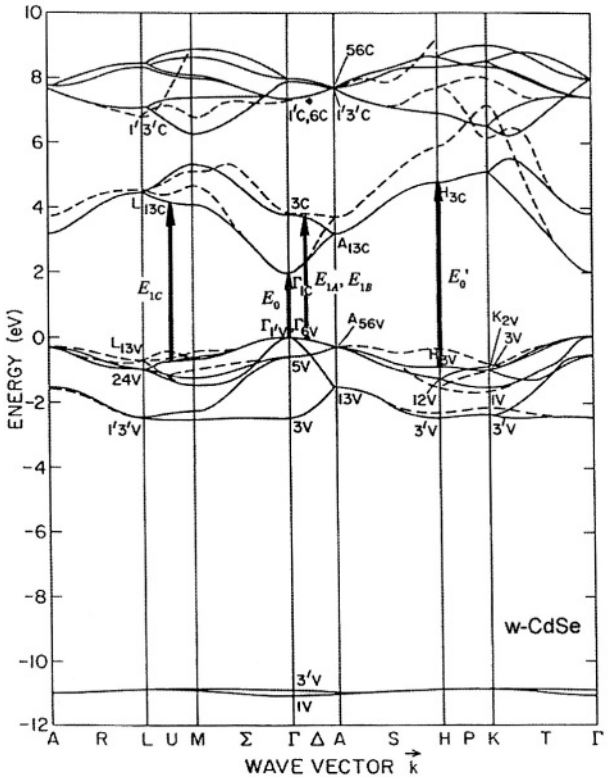

Fig. 13.6.1 Electronic energy-band structure of *w*-CdSe as calculated with the semiempirical tight-binding scheme. The dashed lines also show the results derived from the semiempirical pseudopotential method by T. K. Bergstresser and M. L. Cohen [*Phys. Rev.* **164**, 1069 (1967)]. [From A. Kobayashi, O. F. Sankey, S. M. Volz, and J. D. Dow, *Phys. Rev. B* **28**, 935 (1983).] The main interband transitions are indicated by the vertical arrows.

- **Electronic density of states**

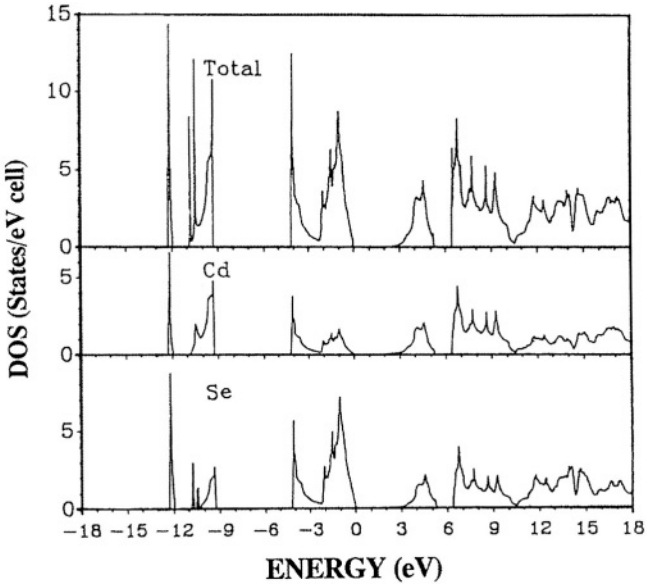

Fig. 13.6.2 Calculated density of states (DOS) and partial DOS for *w*-CdSe using the first-principles orthogonalized linear-combination-of-atomic-orbitals method. [From Y.-N. Xu and W. Y. Ching, *Phys. Rev. B* **48**, 4335 (1993).]

• **Energy eigenvalue**

Table 13.6.1 *Energy eigenvalues at the critical points for the valence and first few conduction bands of w-CdSe [6.1].*

Critical point	Level	Value (eV)	Critical point	Level	Value (eV)
Γ	Γ_1^v	–11.1	H	H_3^v	–2.50
	Γ_3^v	–2.5		$H_{1,2}^v$	–1.26
	Γ_5^v	–0.6		H_3^v	–0.92
	Γ_6^v, Γ_1^v	0.0		H_3^c	4.76
	Γ_1^c	2.0			
	Γ_3^c	3.8			
	Γ_6^c, Γ_1^c	7.4			
K	K_3^v	–2.42	A	$A_{1,3}^v$	–1.53
	K_1^v	–1.57		$A_{5,6}^v$	–0.31
	K_3^v	–1.05		$A_{1,3}^c$	3.20
	K_2^v	–0.92			
L	$L_{1',3}^v$	–2.48			
	$L_{2,4}^v$	–0.98			
	$L_{1,3}^v$	–0.93			
	$L_{1,3}^c$	4.48			
	$L_{1',3}^c$	7.10			

[6.1] A. Kobayashi, O. F. Sankey, S. M. Volz, and J. D. Dow, *Phys. Rev. B* **28**, 935 (1983).

13.6.2 E_0-Gap Region

• **Room-temperature value**

Table 13.6.2 *$E_{0\alpha}$-gap energy (α=A, B, or C) for w-CdSe at room temperature.*

$E_{0\alpha}$ (eV)			Ref.
A	*B*	*C*	
1.751	1.771	2.176	[6.2]

[6.2] V. V. Sobolev, V. I. Donetskikh, and E. F. Zagaĭnov, *Sov. Phys. Semicond.* **12**, 646 (1978).

• **Temperature dependence**

Table 13.6.3 *Empirical equation for the $E_{0\alpha}$-gap (α=A, B, or C) energy variation with temperature T for w-CdSe.*

$$E_{0\alpha}(T) = E_{0\alpha}(0) - \frac{\alpha T^2}{T + \beta}$$

Parameter			Comment
$E_{0\alpha}(0)$ (eV)	α (10^{-4} eV/K)	β (K)	
1.8265	17	1150	n=1 exciton (*A*), T=4.2–300 K, bulk CdSe [6.3]
1.8503	17	1050	n=1 exciton (*B*), T=4.2–300 K, bulk CdSe [6.3]

[6.3] K. A. Dmitrenko, L. V. Taranenko, S. G. Shevel', and A. V. Marinchenko, *Sov. Phys. Semicond.* **19**, 487 (1985).

Table 13.6.4 *Empirical equation for the $E_{0\alpha}$-gap (α=A, B, or C) energy variation with temperature T for w-CdSe.*

$$E_{0\alpha}(T) = E_{\mathrm{B}} - 2a_{\mathrm{B}}\left(\frac{1}{2} + \frac{1}{e^{\Theta/T} - 1}\right)$$

Parameter			Comment
E_{B} (eV)	a_{B} (meV)	Θ (K)	
1.852	32	176	n=1 exciton (A), T=10–300 K [6.4]

[6.4] G. Perna, S. Pagliara, V. Capozzi, M. Ambrico, and M. Pallara, *Solid State Commun.* **114**, 161 (2000).

Table 13.6.5 *Empirical equation for the $E_{0\alpha}$-gap (α=A, B, or C) energy variation with temperature T for w-CdSe [6.5].*

$$E_{0\alpha}(T) = E_{0\alpha}(0) - S < \hbar\Omega > \left[\coth\left(\frac{< \hbar\Omega >}{2kT}\right) - 1\right]$$

$E_{0\alpha}(0)$ (eV)	S	$<\hbar\Omega>$ (meV)
1.849	2.94	25.4

[6.5] K. P. O'Donnell and P. G. Middleton, in *Properties of Wide Bandgap II–VI Semiconductors,* EMIS Datareviews Series No. 17, edited by R. Bhargava (INSPEC, London, 1997), p. 33.

Table 13.6.6 *Empirical equation for the $E_{0\alpha}$-gap (α=A, B, or C) energy variation with temperature T for w-CdSe.*

$$E_{0\alpha}(T) = E_{0\alpha}(0) - \frac{\alpha\Theta_{\mathrm{p}}}{2}\left[\sqrt[p]{1 + \left(\frac{2T}{\Theta_{\mathrm{p}}}\right)^{p}} - 1\right]$$

$E_{0\alpha}(0)$ (eV)	p	α (meV/K)	Θ_{p} (K)	Comment
1.846	2.58	0.405	168	T=15–550 K [6.6]

[6.6] R. Pässler, *Phys. Status Solidi B* **216**, 975 (1999).

Table 13.6.7 *Empirical equation for the $E_{0\alpha}$-gap (α=A, B, or C) energy variation with temperature T for w-CdSe.*

$$E_{0\alpha}(T) = E_{0\alpha}(0) - \alpha \sum_{i=1,2} \frac{W_i \Theta_i}{\exp(\Theta_i / T) - 1}$$

$E_{0\alpha}(0)$ (eV)	α (10^{-4} eV/K)	Θ_1 (K)	Θ_2 (K)	W_1	W_2	Comment
1.846	4.09	50	203	0.10	0.90	T=15–550 K [6.7]

[6.7] R. Pässler, *J. Appl. Phys.* **89**, 6235 (2001).

• Pressure dependence

Table 13.6.8 *Empirical equation for the $E_{0\alpha}$-gap (α=A, B, or C) energy variation with pressure p for w-CdSe.*

$$E_{0\alpha}(p) = E_{0\alpha}(0)+ap+bp^2$$

Parameter			Comment
$E_{0\alpha}(0)$ (eV)	a (10^{-2} eV/GPa)	b (10^{-4} eV/GPa^2)	
1.751 (1.738 *)	5.8	–50	T=300 K [6.8]

[6.8] J. R. Mei and V. Lemos, *Solid State Commun.* **52**, 785 (1984).
* Photoluminescence peak energy.

• Temperature and/or pressure coefficient

Table 13.6.9 *Linear temperature and pressure coefficients of the excitonic energy gap $E_{0\alpha}$ (α=A, B, or C) for w-CdSe.*

Coefficient	Value	Comment
$dE_{0\alpha}/dT$ (10^{-4} eV/K)	–4.6 (*A*)	[6.9]
	–2.8 (*B*)	[6.10]
	–3.63±0.05 (*A*)	T=80–293 K [6.11]
	–3.53±0.05 (*B*)	
	–4.1±0.1 (*C*)	
$dE_{0\alpha}/dp$ (10^{-2} eV/GPa)	3.7 (*A*)	[6.9]
	6 (*A*)	[6.12]
	5.0 (*A*)	[6.13]

[6.9] See, B. Ray, *II-VI Compounds* (Pergamon, Oxford, 1969).
[6.10] J. Voigt, F. Spiegelberg, and M. Senoner, *Phys. Status Solidi* **91**, 189 (1979).
[6.11] V. V. Sobolev, V. I. Donetskikh, and E. F. Zagaĭnov, *Sov. Phys. Semicond.* **12**, 646 (1978).
[6.12] R. L. Knell and D. W. Langer, *Phys. Lett.* **21**, 370 (1966).
[6.13] M. J. Peanasky and H. G. Drickamer, *J. Appl. Phys.* **56**, 3471 (1984).]

• Crystal-field and spin–orbit–splitoff energies

Table 13.6.10 *Theoretical crystal-field and spin-orbit–splitoff energies Δ_1, Δ_2, and Δ_3 for w-CdSe (in meV). Note that in the quasi-cubic approximation, $\Delta_{cr}=\Delta_1$ and $\Delta_{so}=3\Delta_2=3\Delta_3$.*

Δ_1 (Δ_{cr})	Δ_2	Δ_3	Δ_{so}	Ref.
39			416	[6.14]
32			462	[6.15]
39	139	139		[6.16]

[6.14] J.-B. Jeon, Yu. M. Sirenko, K. W. Kim, M. A. Littlejohn, and M. A. Stroscio, *Solid State Commun.* **99**, 423 (1996).
[6.15] H. Fu, L.-W. Wang, and A. Zunger, *Phys. Rev. B* **59**, 5568 (1999).
[6.16] See, T. Dietl, H. Ohno, and F. Matsukura, *Phys. Rev. B* **63**, 195205 (2001).

Table 13.6.11 *Experimental crystal-field and spin-orbit–splitoff energies Δ_1, Δ_2, and Δ_3, for w-CdSe (in meV). Note that in the quasi-cubic approximation, $\Delta_{cr}=\Delta_1$ and $\Delta_{so}=3\Delta_2=3\Delta_3$.*

Δ_1 (Δ_{cr})	Δ_2	Δ_3	Δ_{so}	Ref.
41			420	[6.17]
39			418	[6.18]
40			420	[6.19]
38.8	138.0	150.7		[6.20]
39			443	[6.20]
37.9			423.6	[6.21]
39			416	[6.22]
40			420	Recommended

[6.17] R. G. Wheeler and J. O. Dimmock, *Phys. Rev.* **125,** 1805 (1962).
[6.18] F. L. Pedrotti and D. C. Reynolds, *Phys. Rev.* **127**, 1584 (1962).
[6.19] See, J. O. Dimmock, in *II–VI Semiconducting Compounds,* edited by D. G. Thomas (Benjamin, New York, 1967), p. 277.
[6.20] D. W. Langer, R. N. Euwema, K. Era, and T. Koda, *Phys. Rev. B* **2**, 4005 (1970).
[6.21] M. Iliev and M. Baleva, *Phys. Status Solidi B* **47**, K87 (1971).
[6.22] O. Goede, D. Hennig, and L. John, *Phys. Status Solidi B* **96**, 671 (1979).

13.6.3 Higher-Lying Direct Gap

• Room-temperature value

Table 13.6.12 *Higher-lying direct-gap energies for w-CdSe measured at room temperature [6.23].*

Band gap	Value (eV)	
	$\boldsymbol{E}\perp c$	$\boldsymbol{E}\parallel c$
E_{1A}	4.10	
E_{1B}	4.55	
E_{1C}	4.85	4.78
E_0'	5.6	6.0
E_2	7.6, 8.7 *	
E_1'	9.5 *	

[6.23] See, S. Adachi, *Optical Constants of Crystalline and Amorphous Semiconductors: Numerical Data and Graphical Information* (Kluwer Academic, Boston, 1999).
* For unpolarized light.

• Temperature dependence

Table 13.6.13 *Empirical equation for the higher-lying direct-gap energy variation with temperature T for w-CdSe [6.24].*

$$E_g(T) = E_g(0) - \frac{\alpha T^2}{T+\beta}$$

Band gap	Parameter			Comment
	$E_g(0)$ (eV)	α (10^{-4} eV/K)	β (K)	
E_{1A}	4.316	8.47	174	$\boldsymbol{E}\perp c$
E_{1B}	4.567	8.92	265	$\boldsymbol{E}\perp c$
E_{1C}	5.063	8.24	40	$\boldsymbol{E}\perp c$
	5.131	8.89	39	$\boldsymbol{E}\parallel c$

[6.24] S. Logothetidids, M. Cardona, P. Lautenschlager, and M. Garriga, *Phys. Rev. B* **34**, 2458 (1986).

Table 13.6.14 *Empirical equation for the higher-lying direct-gap energy variation with temperature T for w-CdSe [6.25].*

$$E_g(T) = E_B - 2a_B\left(\frac{1}{2} + \frac{1}{e^{\Theta/T} - 1}\right)$$

Band gap	Parameter			Comment
	E_B (eV)	a_B (meV)	Θ(K)	
E_{1A}	4.386	77	206	$\boldsymbol{E}\perp c$
E_{1B}	4.67	112	290	$\boldsymbol{E}\perp c$
E_{1C}	5.092	35	84	$\boldsymbol{E}\perp c$
	5.163	39	89	$\boldsymbol{E}\parallel c$

[6.25] S. Logothetidids, M. Cardona, P. Lautenschlager, and M. Garriga, *Phys. Rev. B* **34**, 2458 (1986).

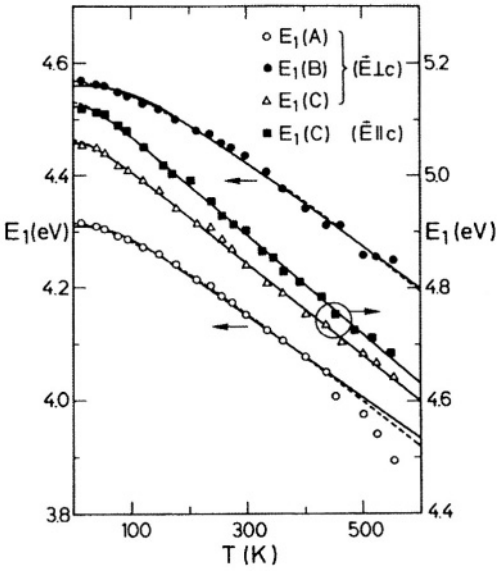

Fig. 13.6.3 Temperature dependence of the E_1 critical-point energies in *w*-CdSe for $\boldsymbol{E}\perp c$ and $\boldsymbol{E}\parallel c$. [From S. Logothetidids, M. Cardona, P. Lautenschlager, and M. Garriga, *Phys. Rev. B* **34**, 2458 (1986).]

• Temperature and/or pressure coefficient

Table 13.6.15 *Linear temperature and pressure coefficients of the higher-lying band-gap energy for w-CdSe.*

Band gap	Coefficient	Value	Comment
E_1	dE_g/dT (10^{-4} eV/K)	−7.2±0.5 (E_{1A})	T=80–300 K [6.26]
		−6.8±0.5 (E_{1B})	
		−1.8±0.5 (E_{1C})	
		−6.9 (E_{1A})	T=109–300 K [6.27]
		−6.4 (E_{1B})	
		−6.9 (E_{1C})	
	dE_g/dp (10^{-2} eV/GPa)	3.2	Calc. [6.28]
E_0'	dE_g/dT (10^{-4} eV/K)	−5.0±0.5	T=80–300 K [6.26]
		−5.9	T=109–300 K [6.27]

Table 13.6.15 *Continued.*

Band gap	Coefficient	Value	Comment
E_2	dE_g/dT (10^{-4} eV/K)	−3.6±1.0	T=80–300 K [6.26]
	dE_g/dp (10^{-2} eV/GPa)	2.7	Calc. [6.28]

[6.26] R. Ludeke and W. Paul, in *II–VI Semiconducting Compounds,* edited by D. G. Thomas (Benjamin, New York, 1967), p. 123.
[6.27] H. Lange and I. A. Iliev, *Phys. Status Solidi B* **84**, 569 (1977).
[6.28] D. L. Camphausen, G. A. N. Connell, and W. Paul, *Phys. Rev. Lett.* **26**, 184 (1971).

13.6.4 Lowest Indirect Gap

- **Theoretical value**

Table 13.6.16 *Theoretically obtained lowest indirect-gap energy for w-CdSe.*

Band gap	Value (eV)			
	a	b	c	d
E_g^K (Γ→K)				
E_g^M (Γ→M)				4.63
E_g^L (Γ→L)	4.6	4.48	3.70	
E_g^H (Γ→H)	5.7	4.76	4.41	
E_g^A (Γ→A)	3.7	3.20	3.27	

[a] T. K. Bergstresser and M. L. Cohen, *Phys. Rev.* **164**, 1069 (1967).
[b] A. Kobayashi, O. F. Sankey, S. M. Volz, and J. D. Dow, *Phys. Rev. B* **28**, 935 (1983).
[c] M.-Z. Huang and W. Y. Ching, *J. Phys. Chem. Solids* **46**, 977 (1985).
[d] O. Zakharov, A. Rubio, X. Blasé, M. L. Cohen, and S. G. Louie, *Phys. Rev. B* **50**, 10780 (1994).

13.6.5 Conduction-Valley Energy Separation

Table 13.6.17 *Theoretically obtained conduction-valley energy separation ΔE_g for w-CdSe.*

ΔE_g	Value (eV)			
	a	b	c	d
K–Γ				
M–Γ				2.72
L–Γ	2.6	2.48	1.84	
H–Γ	3.7	2.76	2.55	
A–Γ	1.7	1.20	1.41	

[a] T. K. Bergstresser and M. L. Cohen, *Phys. Rev.* **164**, 1069 (1967).
[b] A. Kobayashi, O. F. Sankey, S. M. Volz, and J. D. Dow, *Phys. Rev. B* **28**, 935 (1983).
[c] M.-Z. Huang and W. Y. Ching, *J. Phys. Chem. Solids* **46**, 977 (1985).
[d] O. Zakharov, A. Rubio, X. Blasé, M. L. Cohen, and S. G. Louie, *Phys. Rev. B* **50**, 10780 (1994).

13.6.6 Direct–Indirect-Gap Transition Pressure

No detailed data are available for *w*-CdSe.

13.7 ENERGY-BAND STRUCTURE: ELECTRON AND HOLE EFFECTIVE MASSES

13.7.1 Electron Effective Mass: Γ Valley

• Theoretical value

Table 13.7.1 *Theoretical electron effective masses $m_e^{\perp}$, $m_e^{//}$, and m_e^{Γ} at the Γ valley for w-CdSe. $m_e^{\Gamma}=(m_e^{\perp 2}\, m_e^{//})^{1/3}$: density-of-states effective mass.*

$m_e^{\perp}/m_0$	$m_e^{\parallel}/m_0$	m_e^{Γ}/m_0	Technique
0.161	0.137	0.153	Linear combination of atomic orbital method [7.1]

[7.1] M.-Z. Huang and W. Y. Ching, *J. Phys. Chem. Solids* **46**, 977 (1985).

• Experimental value

Table 13.7.2 *Experimental electron effective masses $m_e^{\perp}$, $m_e^{//}$, and m_e^{Γ} at the Γ valley for w-CdSe. $m_e^{\Gamma}=(m_e^{\perp 2}\, m_e^{//})^{1/3}$: density-of-states effective mass.*

$m_e^{\perp}/m_0$	$m_e^{\parallel}/m_0$	m_e^{Γ}/m_0	Comment
0.13±0.01	0.13±0.03	0.13	Zeeman splitting, T=1.8 K [7.2]
		0.15	Optical reflection & absorption [7.3]
		0.13±0.005	Zeeman splitting, T=1.6 K [7.4]
0.120 *[1]	0.115 *[1]	0.118 *[1]	Magnetophonon effect, T=80 K [7.5]
0.127 *[2]	0.122 *[2]	0.125 *[2]	Magnetophonon effect, T=80 K [7.5]
		0.116±0.005 *[1]	Magnetooptics, T=1.7 K [7.6]
		0.125±0.005 *[2]	Magnetooptics, T=1.7 K [7.6]

[7.2] R. G. Wheeler and J. O. Dimmock, *Phys. Rev.* **125**, 1805 (1962).
[7.3] S. Kubo and M. Onuki, *J. Phys. Soc. Jpn* **20**, 1280 (1965).
[7.4] C. H. Henry, K. Nassau, and J. W. Shiever, *Phys. Rev. B* **5**, 458 (1972).
[7.5] L. Eaves, R. A. Stradling, S. Askenazy, G. Carrère, J. Leotin, J.C. Portal, and J. P. Ulmet, *J. Phys. C: Solid State Phys.* **5**, L19 (1972).
[7.6] A. B. Kapustina, B. V. Petrov, A. V. Rodina, and R. P. Seisyan, *J. Cryst. Growth* **214/215,** 899 (2000).
*[1] Bare mass.
*[2] Polaron mass.

• Temperature dependence

Table 13.7.3 *Electron effective mass m_e^{Γ} at the Γ valley for w-CdSe determined by Faraday rotation at T=100 and 293 K [7.7].*

Temperature (K)	m_e^{Γ}/m_0	Comment
100	0.096±0.006	n=1.0×10^{16}–2.1×10^{17} cm^{-3}
293	0.126±0.006	n=2.1×10^{16}–3.5×10^{17} cm^{-3}

[7.7] V. V. Volkov, L. V. Vokkova, and P. S. Kireev, *Sov. Phys. Semicond.* **7**, 478 (1973).

• **Doping dependence and hot-carrier effect**

Table 13.7.4 *Electron-density-dependent electron effective mass m_e^Γ in w-CdSe at T=293 K [7.8].*

n (cm^{-3})	m_e^Γ/m_0
2.1×10^{16}	0.120
1.8×10^{17}	0.130
2.8×10^{17}	0.132
3.5×10^{17}	0.127

[7.8] V. V. Volkov, L. V. Vokkova, and P. S. Kireev, *Sov. Phys. Semicond.* **7**, 478 (1973).

13.7.2 Electron Effective Mass: Satellite Valley

No detailed data are available for *w*-CdSe.

13.7.3 Hole Effective Mass

• **Luttinger's valence-band parameter**

Table 13.7.5 *Theoretical Luttinger's valence-band parameter A_i for w-CdSe. A_i (i=1–6) are in units of $\hbar^2/2m_0$ and A_7 is in units of eV/Å.*

A_1	A_2	A_3	A_4	A_5	A_6	$\lvert A_7\rvert$	Ref.
–5.06	–0.43	4.50	–1.29	–1.29	–0.47		[7.9]
–10.2	–0.76	9.53	–3.2	–3.2	–2.31		[7.10]

[7.9] J.-B. Jeon, Yu. M. Sirenko, K. W. Kim, M. A. Littlejohn, and M. A. Stroscio, *Solid State Commun.* **99**, 423 (1996).
[7.10] See, T. Dietl, H. Ohno, and F. Matsukura, *Phys. Rev. B* **63**, 195205 (2001).

• **Density-of-states mass**

Table 13.7.6 *Density-of-states masses in w-CdSe (in m_0). $m_{H\alpha}$* (α=A, B, or C) represents the hole effective mass of the top three valence bands.*

$\perp c$			$\parallel c$		Comment
m_{HA}*	m_{HB}*	m_{HC}*	m_{HH}	m_{LH}	
1.815	0.158	0.236	1.720	0.119	Calc. [7.11]

[7.11] M.-Z. Huang and W. Y. Ching, *J. Phys. Chem. Solids* **46**, 977 (1985).

13.8 ELECTRONIC DEFORMATION POTENTIAL

13.8.1 Intravalley Deformation Potential: Γ Point

• **Conduction band**

Table 13.8.1 *Γ-conduction-band acoustic deformation potential E_1 for w-CdSe obtained from transport data analysis.*

E_1 (eV)	Ref.
11.5	[8.1]
3.7	[8.2]

[8.1] D. L. Rode, *Phys. Rev. B* **2**, 4036 (1970).

[8.2] D. L. Rode, in *Semiconductors and Semimetals,* edited by R. K. Willardson and A. C. Beer (Academic, New York, 1975), Vol. 10, p. 1.

• Valence band

Table 13.8.2 *Experimentally determined Γ-valence-band deformation potentials C_i's for w-CdSe.*

Deformation potential (eV)						Ref.
D_1–C_1	D_2–C_2	C_3	C_4	C_5	C_6	
2.8	1.3	8.4	3.9			[8.3]
3.4	1.5	9.9	4.6			[8.4]
–1.0	–4.1	4.2	–1.9	1.2		[8.5]
–0.76	–3.7	4.0	–2.2	1.2	3.0	[8.6]

[8.3] Absolute value taken at T=300 K [M. Grynberg, *Phys. Status Solidi* **27**, 255 (1968)].
[8.4] Absolute value taken at T=77 K [M. Grynberg, *Phys. Status Solidi* **27**, 255 (1968)].
[8.5] See, A. Gavini and M. Cardona, *Phys. Rev. B* **1**, 672 (1970).
[8.6] D. W. Langer, R. N. Euwema, K. Era, and T. Koda, *Phys. Rev. B* **2**, 4005 (1970).

• E_0 gap

Table 13.8.3 *Hydrostatic deformation potential a_0^Γ for the E_0 gap of w-CdSe.*

a_0^Γ (eV)	Comment
–2.7	Exper. *

*Estimated from dE_0/dp value.

• Optical-phonon deformation potential

Table 13.8.4 *Optical-phonon deformation potential d_0 at the Γ-valence band of w-CdSe.*

d_0 (eV)	Comment
32±4	Exper. [8.7]

[8.7] D. Braun, W. W. Rühle, C. Trallero-Giner, and J. Collet, *Phys. Rev. Lett.* **67**, 2335 (1991).

13.8.2 Intravalley Deformation Potential: High-Symmetry Points

No detailed data are available for *w*-CdSe.

13.8.3 Intervalley Deformation Potential

No detailed data are available for *w*-CdSe.

13.9 ELECTRON AFFINITY AND SCHOTTKY BARRIER HEIGHT

13.9.1 Electron Affinity

Table 13.9.1 *Electron affinity χ_s for w-CdSe.*

χ_s (eV)	Ref.
4.95	[9.1]

[9.1] A. G. Milnes and D. L. Feucht, *Heterojunctions and Metal-Semiconductor Junctions* (Academic, New York, 1972).

13.9.2 Schottky Barrier Height

Table 13.9.2 *Summary of the Schottky barrier height ϕ_n for metal/n-type w-CdSe contacts at 300 K.**

Metal	ϕ_n (eV)	Metal	ϕ_n (eV)
Ag	0.43–0.67	Cu	0.3–0.33
Al	<0.2	In	<0.2
Au	0.49–0.7	Pt	0.37–0.68

*The data are gathered from various sources.

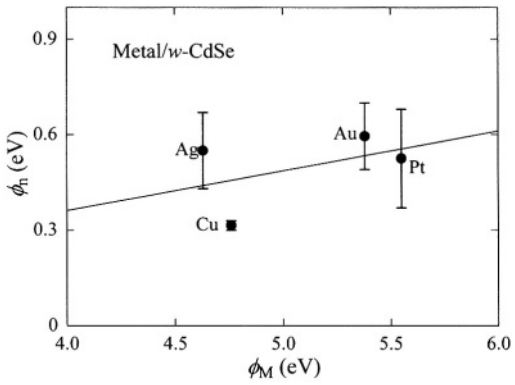

Fig. 13.9.1 Schottky barrier height ϕ_n versus metal work function ϕ_M observed for metal/*n*-type *w*-CdSe contacts. Values of the metal work function were taken from H. P. R. Frederikse [in *CRC Handbook of Chemistry and Physics,* 78th Edition, edited by D. R. Lide (CRC Press, Boca Raton, 1997), p. 12-115]. The solid line represents the least-squares-fit result with $\phi_n=0.12\phi_M-0.14$ (ϕ_M and ϕ_n in eV).

- **Temperature and/or pressure coefficient**

Table 13.9.3 *Pressure coefficient of the Schottky barrier height ϕ_n for metal/n-type w-CdSe contact.*

Coefficient	Value	Comment
$d\phi_n/dp$ (meV/kbar)	7.0	Au/*w*-CdSe (*n* type) [9.2]

[9.2] M. J. Peanasky and H. G. Drickamer, *J. Appl. Phys.* **56**, 3471 (1984).

13.10 OPTICAL PROPERTIES

13.10.1 Summary of Optical Dispersion Relations

- **$\varepsilon(E)$ and $n^*(E)$ spectra**

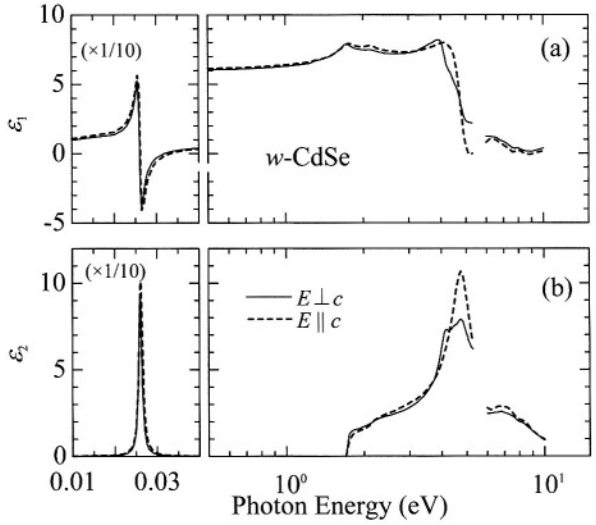

Fig. 13.10.1 Complex dielectric-constant spectra $[\varepsilon(E)=\varepsilon_1(E)+i\varepsilon_2(E)]$ for *w*-CdSe at 300 K. The numerical data are taken from tabulation by S. Adachi [*Optical Constants of Crystalline and Amorphous Semiconductors: Numerical Data and Graphical Information* (Kluwer Academic, Boston, 1999)].

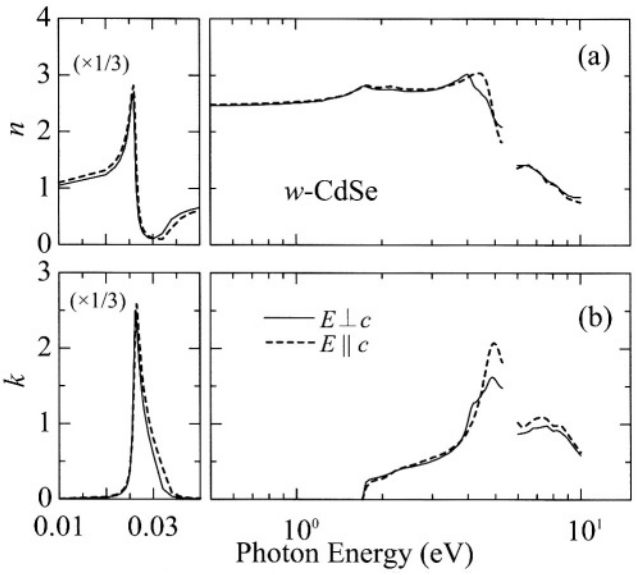

Fig. 13.10.2 Complex refractive-index spectra [$n^*(E)=n(E)+ik(E)$] for *w*-CdSe at 300 K. The numerical data are taken from tabulation by S. Adachi [*Optical Constants of Crystalline and Amorphous Semiconductors: Numerical Data and Graphical Information* (Kluwer Academic, Boston, 1999)].

- **$\alpha(E)$ and $R(E)$ spectra**

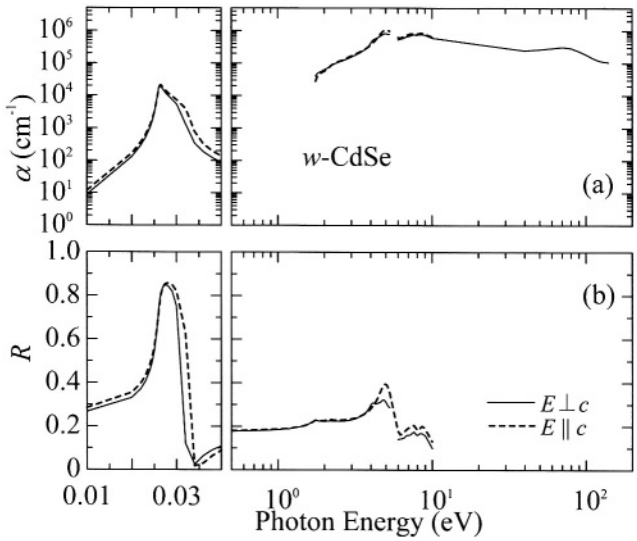

Fig. 13.10.3 (a) Absorption [$\alpha(E)$] and (b) normal-incidence reflectivity spectra [$R(E)$] for *w*-CdSe at 300 K. The numerical data are taken from tabulation by S. Adachi [*Optical Constants of Crystalline and Amorphous Semiconductors: Numerical Data and Graphical Information* (Kluwer Academic, Boston, 1999)].

13.10.2 The Reststrahlen Region

- **Static and high-frequency dielectric constants**

Table 13.10.1 *Static and high-frequency dielectric constants ε_s and ε_∞ for w-CdSe.*

$E \perp c$		$E \parallel c$		Comment
ε_s	ε_∞	ε_s	ε_∞	
9.70*[1]		10.6*[1]		*T*=300 K [10.1]
9.53*[2]		10.2*[2]		
9.15	6.20	9.91	6.30	*T*=100 K [10.2]
9.29	6.20	10.16	6.30	*T*=300 K [10.2]
	6.1		6.0	*T*=15 K [10.3]
	6.1		6.1	*T*=300 K [10.3]
9.4*[3]	5.8*[3]	9.4*[3]	5.8*[3]	*T*=300 K [10.4]

Table 13.10.1 *Continued.*

$E \perp c$		$E \parallel c$		Comment
ε_s	ε_∞	ε_s	ε_∞	
9.80*[1]		10.65*[1]		T=293 K [10.5]
8.1	5.9	8.3	6.0	T=100 K [10.6]
8.2	5.9	8.3	6.1	T=300 K [10.6]
9.29	6.20	10.16	6.30	Recommended (T=300 K)

[10.1] H. Jaffe and D. A. Berlincourt, *Proc. IEEE* **53**, 1372 (1965).
[10.2] R. Geick, C. H. Perry, and S. S. Mitra, *J. Appl. Phys.* **37**, 1994 (1966).
[10.3] H. W. Verleur and A. S. Barker, Jr., *Phys. Rev.* **155**, 750 (1967).
[10.4] A. Manabe, A. Mitsuishi, and H. Yoshinaga, *Jpn. J. Appl. Phys.* **6**, 593 (1967).
[10.5] E. F. Tokarev, G. S. Pado, L. A. Chernozakonskii, and V. V. Drachev, *Sov. Phys. Solid State* **15**, 1064 (1973).
[10.6] A. N. Pikhtin and A. D. Yas'kov, *Sov. Phys. Semicond.* **15**, 8 (1981).
*[1] Constant stress value.
*[2] Constant strain value.
*[3] For unpolarized light.

Table 13.10.2 *Linear temperature and pressure coefficients of the static (ε_s) and high-frequency dielectric constants (ε_∞) for w-CdSe.*

Coefficient	Value		comment
	$E \perp c$	$E \parallel c$	
$d\varepsilon_s/dT$ (10^{-2} K^{-1})	0.19 *	0.14 *	T=4–40 K [10.7]
	1.3 *	1.2 *	T~293 K [10.7]
$d\varepsilon_\infty/dT$ (10^{-4} K^{-1})			
$d\varepsilon_s/dp$ (10^{-1} GPa^{-1})			
$d\varepsilon_\infty/dp$ (10^{-2} GPa^{-1})			

[10.7] E. F. Tokarev, G. S. Pado, L. A. Chernozakonskii, and V. V. Drachev, *Sov. Phys. Solid State* **15**, 1064 (1973).

• Reststrahlen parameter

Table 13.10.3 *A set of the reststrahlen parameters for w-CdSe.*

$$\varepsilon(\omega) = \varepsilon_\infty \left(1 + \frac{\omega_{LO}^2 - \omega_{TO}^2}{\omega_{TO}^2 - \omega^2 - i\omega\gamma} \right)$$

$E \perp c$				$E \parallel c$				Comment
ε_∞	ω_{LO} (cm^{-1})	ω_{TO} (cm^{-1})	γ (cm^{-1})	ε_∞	ω_{LO} (cm^{-1})	ω_{TO} (cm^{-1})	γ (cm^{-1})	
6.20	212	175	5.0	6.30	210	168	6.0	T=100 K [10.8]
6.20	210	172	7.0	6.30	211	166	8.0	T=300 K
5.8	213	167	6.7	5.8	213	167	6.7	T=300 K [10.9] *

[10.8] R. Geick, C. H. Perry, and S. S. Mitra, *J. Appl. Phys.* **37**, 1994 (1966).
[10.9] A. Manabe, A. Mitsuishi, and H. Yoshinaga, *Jpn. J. Appl. Phys.* **6**, 593 (1967).
* For unpolarized light.

• Multiphonon optical absorption spectra

The extinction coefficient k in the multiphonon spectral region of *w*-CdSe has been measured by R. Geick, C. H. Perry, and S. S. Mitra [*J. Appl. Phys.* **37**, 1994 (1966)].

13.10.3 At or Near the Fundamental Absorption Edge

• Free-exciton binding energy and related parameters

Table 13.10.4 *Free-exciton binding (Rydberg) energy G for w-CdSe.*

G (meV)			Comment
A (Γ_9^v)	B (Γ_7^v)	C (Γ_7^v)	
15.7	16.7		T=1.8 K [10.10]
15	16		T=1.8 K [10.11]
15.7	16.7		Recommended

[10.10] B. Segall and D.T. F. Marple, in *Physics and Chemistry of II–VI Compounds,* edited by M. Aven and J. S. Prener (North-Holland, Amsterdam, 1967), p. 317.
[10.11] J. Voigt, F. Spiegelberg, and M. Senoner, *Phys. Status Solidi* **91**, 189 (1979).

Table 13.10.5 *Free-exciton parameters (G=binding energy; a_B=1st-orbital Bohr radius; μ=reduced mass) at the fundamental absorption edge of w-CdSe.*

Exciton	G (meV)	a_B (Å)*	μ (m_0)*
A	15.7	48	0.106
B	16.7	45	0.112
C			

*Calculated using $\varepsilon_s=(\varepsilon_{s\perp}^2\varepsilon_{s\parallel})^{1/3}$ value.

Table 13.10.6 *Spin-exchange interaction constant j for w-CdSe [10.12].*

j (meV)
0.4

[10.12] See, M. Julier, J. Campo, B. Gil, J. P. Lascaray, and S. Nakamura, *Phys. Rev. B* **57**, R6791 (1998); D. W. Langer, R. N. Euwema, K. Era, and T. Koda, *Phys. Rev. B* **2**, 4005 (1970).

• Refractive index

Table 13.10.7 *Refractive index n near the fundamental absorption edge of w-CdSe for $\boldsymbol{E}\perp c$ at 300 K [10.13].*

E (eV)	λ (μm)	n	E (eV)	λ (μm)	n
0.1	12.40	2.4440	0.775	1.599	2.4818
0.31	3.998	2.4491	0.885	1.401	2.4929
0.326	3.802	2.4498	1.03	1.203	2.5132
0.344	3.603	2.4509	1.24	1.000	2.552
0.365	3.396	2.4518	1.3	0.953	2.572
0.387	3.203	2.4532	1.35	0.918	2.590
0.413	3.001	2.4522	1.4	0.885	2.612
0.443	2.798	2.4562	1.45	0.855	2.632
0.477	2.599	2.4590	1.5	0.826	2.656

Table 13.10.7 *Continued.*

E (eV)	λ (μm)	n	E (eV)	λ (μm)	n
0.516	2.402	2.4612	1.55	0.800	2.685
0.563	2.202	2.4642	1.6	0.775	2.722
0.62	1.999	2.4682	1.65	0.751	2.764
0.689	1.799	2.4732	1.7	0.729	2.805

[10.13] See, S. Adachi, *Optical Constants of Crystalline and Amorphous Semiconductors: Numerical Data and Graphical Information* (Kluwer Academic, Boston, 1999).

Table 13.10.8 *Refractive index n near the fundamental absorption edge of w-CdSe for* $\boldsymbol{E} \parallel \boldsymbol{c}$ *at 300 K [10.14].*

E (eV)	λ (μm)	n	E (eV)	λ (μm)	n
0.1	12.3950	2.4530	0.775	1.5994	2.5008
0.31	3.9984	2.4685	0.885	1.4006	2.5133
0.326	3.8021	2.4694	1.03	1.2034	2.5331
0.344	3.6032	2.4702	1.24	0.9996	2.5696
0.365	3.3959	2.4714	1.3	0.9535	2.592
0.387	3.2028	2.4726	1.35	0.9181	2.604
0.413	3.0012	2.4741	1.4	0.8854	2.619
0.443	2.7980	2.4757	1.45	0.8548	2.636
0.477	2.5985	2.4784	1.5	0.8263	2.657
0.516	2.4021	2.4798	1.55	0.7997	2.687
0.563	2.2016	2.4840	1.6	0.7747	2.722
0.62	1.9992	2.4873	1.65	0.7512	2.755
0.689	1.7990	2.4930	1.7	0.7291	2.793

[10.14] See, S. Adachi, *Optical Constants of Crystalline and Amorphous Semiconductors: Numerical Data and Graphical Information* (Kluwer Academic, Boston, 1999).

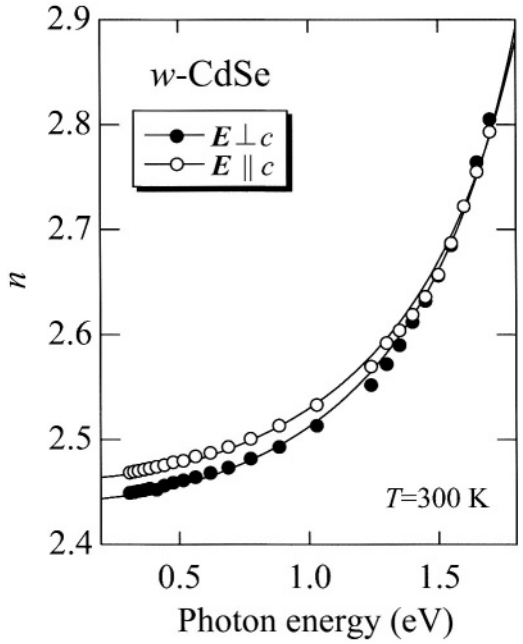

Fig. 13.10.4 Refractive index dispersion in *w*-CdSe at T=300 K. The experimental data are taken from S. Adachi [*Optical Constants of Crystalline and Amorphous Semiconductors: Numerical Data and Graphical Information* (Kluwer Academic, Boston, 1999)]. The solid lines represent the calculated results using $n^2=4.46+[1.50\lambda^2/(\lambda^2-0.292)]$ for $\boldsymbol{E}\perp\boldsymbol{c}$ and $n^2=4.56+[1.50\lambda^2/(\lambda^2-0.284)]$ for $\boldsymbol{E} \parallel \boldsymbol{c}$ with λ in μm.

● **Refractive index: Temperature dependence**

Table 13.10.9 *Temperature coefficient of the refractive index,* $n^{-1}(dn/dT)$*, in the long-wavelength limit for w-CdSe [10.15].*

$\frac{1}{n}\frac{dn}{dT}$ (10^{-5} K^{-1})	Comment
4	$\boldsymbol{E}\perp c$, $\boldsymbol{E}\parallel c$

[10.15] See, S. Adachi, *Optical Properties of Crystalline and Amorphous Semiconductors: Materials and Fundamental Properties* (Kluwer Academic, Boston, 1999).

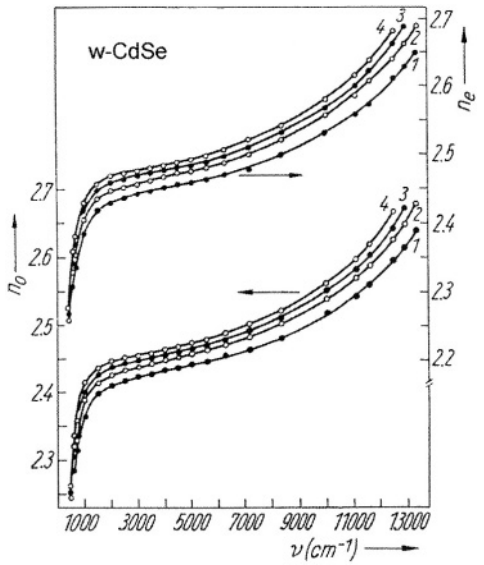

Fig. 13.10.5 Refractive index in *w*-CdSe for $\boldsymbol{E}\perp c$ (n_o) and $\boldsymbol{E}\parallel c$ (n_e) measured at four different temperatures, T=100 (1), 300 (2), 450 (3), and 600 K (4). [From M. P. Lisitsa, L. F. Gudymenko, V. N. Malinko, and S. F. Terekhova, *Phys. Status Solidi* **31**, 389 (1969).]

● **Refractive index: Pressure dependence**

Refractive index change due to uniaxial stress has been reported by M. Grynberg [*Phys. Status Solidi* **27**, 255 (1968)].

● **Fundamental absorption edge: Temperature dependence**

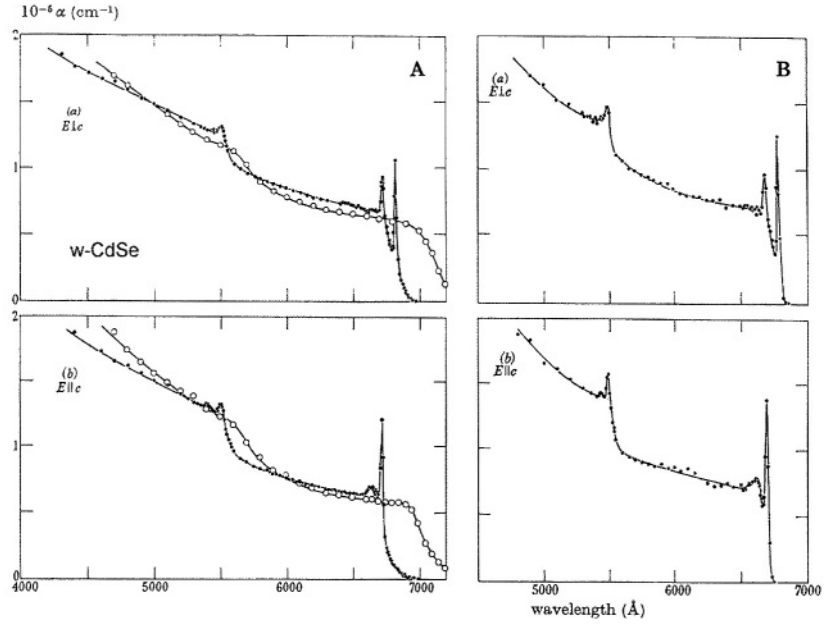

Fig. 13.10.6 (A) Absorption coefficient α for *w*-CdSe at T=77 K (solid circles) and 300 K (open circles). (B) As for (A) at T=4.2 K. (a) $\boldsymbol{E}\perp c$; (b) $\boldsymbol{E}\parallel c$. [From R. B. Parsons, W. Wardzynski, and A. D. Yoffe, *Proc. Roy. Soc. A* **262,** 120 (1961).]

13.10.4 The Interband Transition Region

• **Fundamental optical spectra**

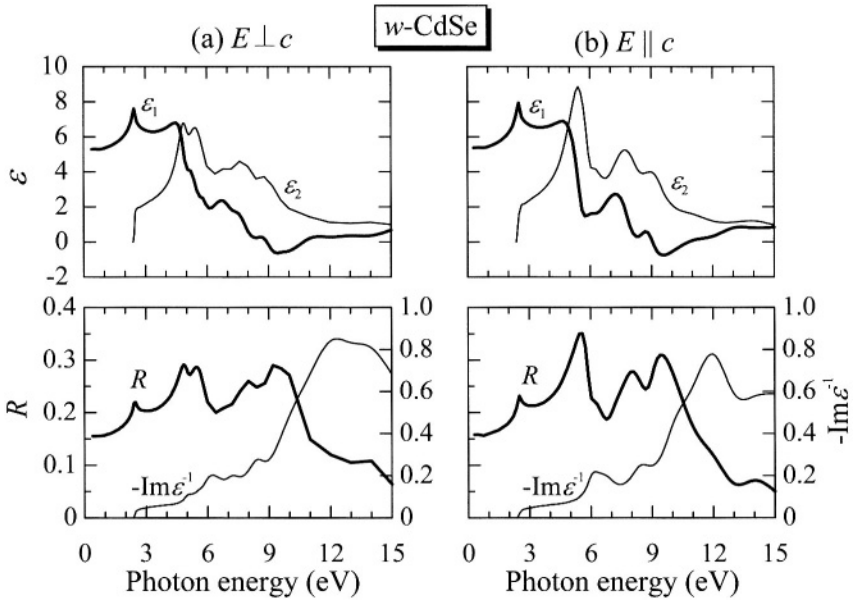

Fig. 13.10.7 Complex dielectric function, $\varepsilon(E)=\varepsilon_2(E)+i\varepsilon_2(E)$, fundamental reflectivity, $R(E)$, and energy-loss function, $-\mathrm{Im}\varepsilon^{-1}(E)$, for *w*-CdSe at 300 K. The experimental data are taken from tabulation by S. Adachi [*Optical Constants of Crystalline and Amorphous Semiconductors: Numerical Data and Graphical Information* (Kluwer Academic, Boston, 1999)].

• $\varepsilon(E)$ **spectrum: External perturbation and/or doping effects**

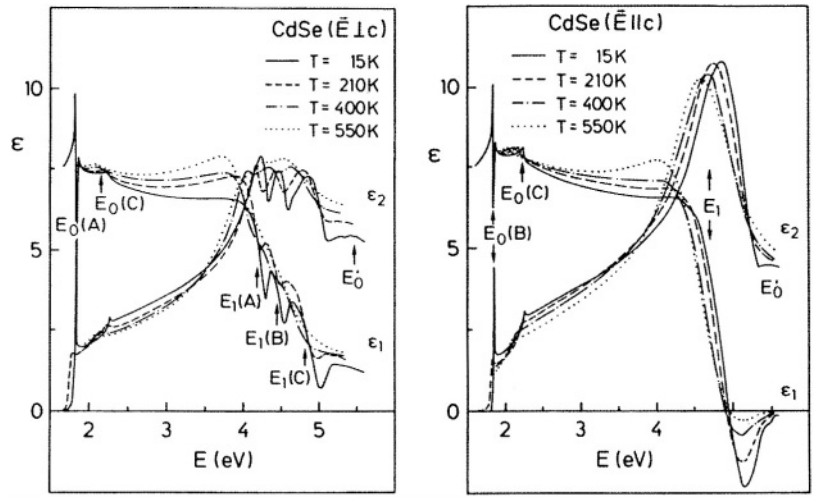

Fig. 13.10.8 Real and imaginary parts of the dielectric function $\varepsilon(E)=\varepsilon_1(E)+i\varepsilon_2(E)$ of *w*-CdSe measured at several temperatures for $\boldsymbol{E}\perp\boldsymbol{c}$ (left-hand side) and $\boldsymbol{E}\parallel\boldsymbol{c}$ (right-hand side). [From S. Logothetidis, M. Cardona, P. Lautenschlager, and M. Garriga, *Phys. Rev. B* **34**, 2458 (1986).]

13.10.5 Free-Carrier Absorption and Related Phenomena

No detailed data are available for *w*-CdSe.

13.11 ELASTOOPTIC, ELECTROOPTIC, AND NONLINEAR OPTICAL PROPERTIES

13.11.1 Elastooptic Effect

• **Photoelastic constant**

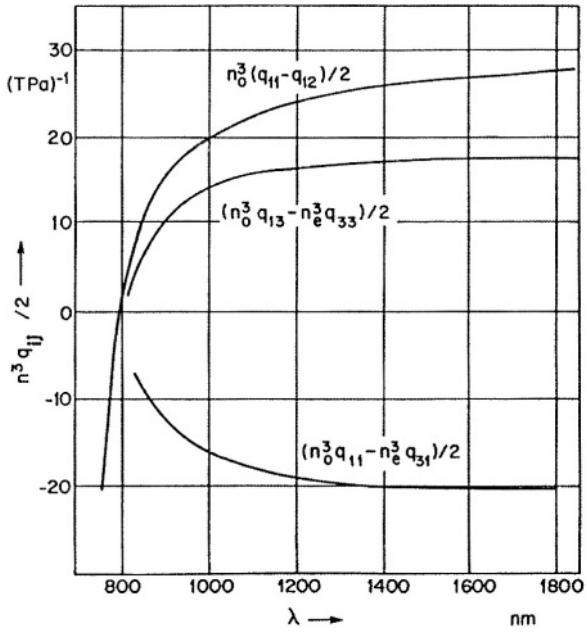

Fig. 13.11.1 Dispersion of the photoelastic coefficient, $n_o^3 q_{ij}/2$ [n_0=refractive index; $q_{ij}=p_{ij}S_{ij}$ (S_{ij}: elastic compliance constant)], in *w*-CdSe. [From A. A.Reza and G. A. Babonas, *Sov. Phys. Solid State* **16**, 909 (1974); see also, *Numerical Data and Functional Relationships in Science and Technology,* edited by K.-H. Hellwege and A. M. Hellwege, Landolt–Börnstein, New Series, Group III, Vol. 18 (Springer, Berlin, 1984), p. 393.]

13.11.2 Linear Electrooptic Constant

Table 13.11.1 *Linear electrooptic constant r_{ij} for w-CdSe.*

Wavelength (μm)	r_{ij} (pm/V)			Comment
	r_{13}	r_{33}	r_{42}	
3.39	1.8	4.3		Clamped value (T) [11.1]

[11.1] See, I. P. Kaminow and E. H. Turner, in *Handbook of Lasers,* edited by R. J. Pressley (Chemical Rubber, Cleveland, 1971), Chap. 15.

13.11.3 Quadratic Electrooptic Constant

No detailed data are available for *w*-CdSe.

13.11.4 Franz–Keldysh Effect

No detailed data are available for *w*-CdSe.

13.11.5 Nonlinear Optical Constant

- **Second-order nonlinear optical susceptibility**

Table 13.11.2 *Experimental second-order nonlinear optical susceptibility d_{ij} for w-CdSe.*

d_{ij} (pm/V)			Comment
d_{15}	d_{31}	d_{33}	
		+65	λ=2.12 μm [11.2]
31	–29	+55	λ=10.6 μm [11.2]
	–18	+36	λ=10.6 μm [11.3]

[11.2] *Numerical Data and Functional Relationships in Science and Technology,* edited by K.-H. Hellwege and A. M. Hellwege, Landolt–Börnstein, New Series, Group III, Vol. 11 (Springer, Berlin, 1979).
[11.3] D. A. Roberts, *IEEE J. Quantum Electron.* **28**, 2057 (1992).

- **Two-photon optical absorption**

Table 13.11.3 *Two-photon absorption coefficient β for w-CdSe.*

Wavelength (μm)	β (cm/GW)	Comment
1.064	160	$\boldsymbol{E}\perp c\parallel\boldsymbol{k}$, T=300 K [11.4]
	160	$\boldsymbol{E}\perp c\perp\boldsymbol{k}$, T=300 K [11.4]
	80	$\boldsymbol{E}\parallel c\perp\boldsymbol{k}$, T=300 K [11.4]
	50	$\boldsymbol{E}\perp c\parallel\boldsymbol{k}$, T=300 K [11.5]
1.15	1.99	$\boldsymbol{E}\parallel c\perp\boldsymbol{k}$, T=300 K [11.6]
1.22	2.15	$\boldsymbol{E}\parallel c\perp\boldsymbol{k}$, T=300 K [11.6]
1.30	3.04	$\boldsymbol{E}\parallel c\perp\boldsymbol{k}$, T=300 K [11.6]
1.37	3.55	$\boldsymbol{E}\parallel c\perp\boldsymbol{k}$, T=300 K [11.6]
1.42	0.0763	$\boldsymbol{E}\parallel c\perp\boldsymbol{k}$, T=300 K [11.6]
1.46	0.0546	$\boldsymbol{E}\parallel c\perp\boldsymbol{k}$, T=300 K [11.6]
1.50	0.102	$\boldsymbol{E}\parallel c\perp\boldsymbol{k}$, T=300 K [11.6]

[11.4] V. S. Dneprovskii and S. M. Ok, *Sov. J. Quantum Electron.* **6**, 298 (1976).
[11.5] M. Bass, E. W. Van Stryland, and A. F. Stewart, *Appl. Phys. Lett.* **34**, 142 (1979).
[11.6] I.. B. Zotova and Y. J. Ding, *Appl. Opt.* **40**, 6654 (2001).

13.12 CARRIER TRANSPORT PROPERTIES

13.12.1 Low-Field Mobility: Electrons

Table 13.12.1 *300-K (μ_{300K}) and peak Hall mobilities (μ_{peak}) for electrons in w-CdSe.*

Mobility	Value (cm^2/V s)	Comment
μ_{300K}	900	$\boldsymbol{j}\perp c$, n=3.7×10^{17}, 8.1×10^{17} cm^{-3} [12.1]
μ_{peak}	2.0×10^4	T~23 K [12.2]

[12.1] D. M. Heinz and E. Banks, *J. Phys. Chem.* **24**, 391 (1956).
[12.2] R. S. Krupyshev, S. A. Abagyan, A. A. Davydov, and A. A. Kartushina, *Sov. Phys.–Semicond.* **6**, 1422 (1973).

• **Temperature dependence**

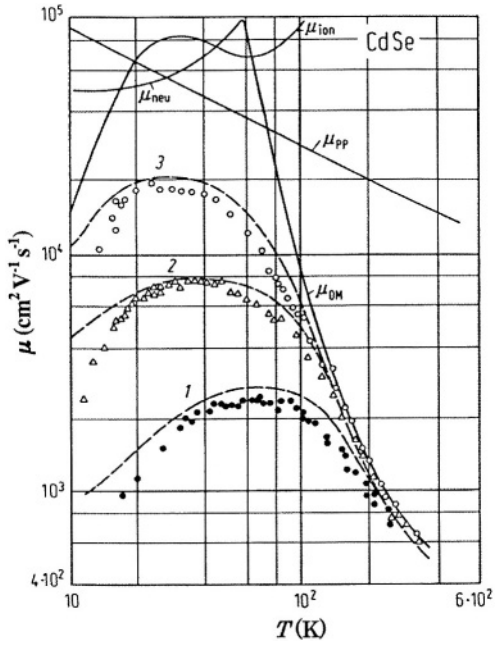

Fig. 13.12.1 Electron Hall mobility μ versus temperature T for three different *w*-CdSe samples. 1: N_A=5.4×10^{15} cm^{-3}; 2: N_A=4×10^{14} cm^{-3}; 3: N_A=1.5×10^{14} cm^{-3}. The solid lines show the calculated mobilities limited for optical mode scattering (μ_{OM}), piezoelectric potential scattering (μ_{pp}), and scattering by charged (μ_{ion}) and neutral impurities (μ_{neu}). The dashed lines take into account all these scattering processes. [From R. S. Krupyshev, S. A. Abagyan, A. A. Davydov, and A. A. Kartushina, *Sov. Phys.–Semicond.* **6**, 1422 (1973).]

• **Donor concentration (free-carrier) dependence**

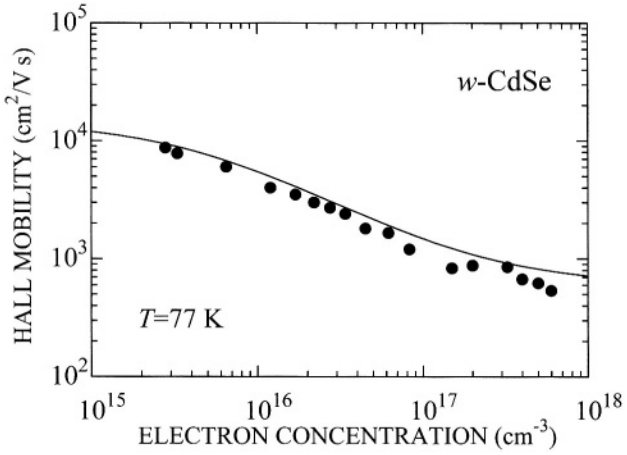

Fig. 13.12.2 Electron Hall mobility μ versus electron concentration n in *n*-type *w*-CdSe at 77 K. The experimental data are gathered from various sources. The solid line represents the calculated result with $\mu = 600 + 14000/[1 + (n/5\times10^{15})^{0.90}]$, where n is in cm^{-3} and μ is in cm^2/V s.

• **Hall factor**

The Hall factor for *w*-CdSe has been obtained theoretically by D. L. Rode [*Phys. Status Solidi B* **55**, 687 (1973)], and its value is reported to be $\gamma \sim 1.07$ at T=300 K.

13.12.2 Low-Field Mobility: Holes

Table 13.12.2 *300-K (μ_{300K}) and peak mobilities (μ_{peak}) for holes in w-CdSe.*

Mobility	Value (cm^2/V s)	Comment
μ_{300K}	50	Hall mobility [12.3]
	75	Drift mobility [12.4]
μ_{peak}		

[12.3] See, *Numerical Data and Functional Relationships in Science and Technology,* edited by O. Madelung, New Series, Group III, Vol. 17 (Springer, Berlin, 1982).
[12.4] C. Canali, F. Nava, G. Ottaviani, and C. Paorici, *Solid State Commun.* **11**, 105 (1972).

13.12.3 High-Field Transport: Electrons

- **Electron drift velocity–field characteristic**

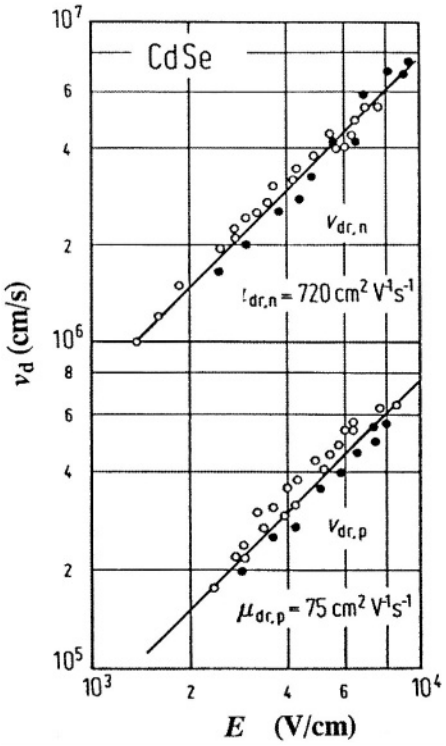

Fig. 13.12.3 Electron ($v_{dr,n}$) and hole drift velocity ($v_{dr,p}$) versus electric field E in *w*-CdSe measured at room temperature by time-of-flight method. [From C. Canali, F. Nava, G. Ottaviani, and C. Paorici, *Solid State Commun.* **11**, 105 (1972).]

13.12.4 High-Field Transport: Holes

- **Hole drift velocity–field characteristic**

See Sec. 13.12.3.

13.12.5 Minority-Carrier Transport: Electrons in *p*-Type Materials

No detailed data are available for *w*-CdSe.

13.12.6 Minority-Carrier Transport: Holes in *n*-Type Materials

- **Minority-hole diffusion length**

Table 13.12.3 *Minority-hole diffusion length L in w-CdSe at room temperature.*

L (μm)	Comment
4.59±1.01	n~10^{14} cm^{-3} [12.5]
4.98±0.34	n~10^{16} cm^{-3} [12.5]
0.124	n=2.5×10^{18} cm^{-3} [12.6]
0.12	n=2×10^{18} cm^{-3} [12.7]

[12.5] S. Mora, N. Romeo, and L. Tarricone, *Nuovo Cimento* **60B**, 97 (1980).
[12.6] A. Etchebery, M. Etman, B. Fotouhi, J. Gautron, J.-L. Sculfort, and P. Lemasson, *J. Appl. Phys.* **53**, 8867 (1982).
[12.7] J. Gautron and P. Lemasson, *J. Cryst. Growth* **59**, 332 (1982).

13.12.7 Impact Ionization Coefficient

No detailed data are available for *w*-CdSe.

Chapter 14

Cadmium Telluride (CdTe)

14.1 STRUCTURAL PROPERTIES

14.1.1 Ionicity

Table 14.1.1 *Phillips's ionicity f_i for CdTe [1.1].*

f_i
0.717

[1.1] J. C. Phillips, *Bonds and Bands in Semiconductors* (Academic, New York, 1973).

14.1.2 Elemental Isotopic Abundance and Molecular Weight

- **Isotopic abundance**

Table 14.1.2 *Isotopic abundance in percent for cadmium and tellurium [1.2].*

Isotope	% nat. abundance	Isotope	% nat. abundance
^{106}Cd	1.25	^{120}Te	0.096
^{108}Cd	0.89	^{122}Te	2.603
^{110}Cd	12.49	^{123}Te	0.908
^{111}Cd	12.80	^{124}Te	4.816
^{112}Cd	24.13	^{125}Te	7.139
^{113}Cd	12.22	^{126}Te	18.95
^{114}Cd	28.73	^{128}Te	31.69
^{116}Cd	7.49	^{130}Te	33.80

[1.2] D. R. Lide, *CRC Handbook of Chemistry and Physics,* 78th Edition (CRC Press, Boca Raton, 1997).

• **Molecular weight**

Table 14.1.3 *Molecular (average atomic) weight M for CdTe.*

M (amu)
240.01

14.1.3 Crystal Structure and Space Group

Table 14.1.4 *Crystal structure and its space andpint groupsfor CdTe.*

Crystal structure	Space group	Point group
Zincblende (Cubic)	$F\bar{4}3m$	T_d

14.1.4 Lattice Constant and Its Related Parameters

• **Lattice constant, near-neighbor distance, etc.**

Table 14.1.5 *Lattice constant (a), near-neighbor distance (d), unit cube volume (a^3), and molecular density (d_M) for CdTe at 300 K.*

Parameter	Value
Lattice constant a (Å)	6.481 [1.3]
d (Cation–Anion) (Å)	2.806*
d (Cation–Cation) (Å)	4.583*
Unit cube volume a^3 (10^{-22} cm^3)	2.722*
Molecular density d_M (10^{22} cm^{-3})	1.469*

[1.3] D. J. Williams, in *Properties of Narrow Gap Cadmium-based Compounds,* EMIS Datareviews Series No. 10, edited by P. Capper (INSPEC, London, 1994), p. 399.
*Calculated.

• **Crystal density**

Table 14.1.6 *Crystal density g for CdTe at 300 K.**

g (g/cm^3)
5.856

*Calculated using a=6.481 Å.

14.1.5 Structural Phase Transition

Table 14.1.7 *Structural phase transition in CdTe at high pressures.**

Structure	Transition pressure (GPa)
Zincblende ($F\bar{4}3m$)	Normal pressure
Cinnabar	3.53 [1.4]
Rocksalt (NaCl)	3.80 [1.4]
Orthorhombic (*Cmcm*)	10.1 [1.5]

[1.4] M. I. McMahon, R. J. Nelmes, N. G. wright, and D. R. Allan, *Phys. Rev. B* **48**, 16246 (1993).
[1.5] R. J. Nelmes, M. I. McMahon, N. G. wright, and D. R. Allan, *Phys. Rev. B* **51**, 15723 (1995).
*The basic sequence for structural phase transition in CdTe has been well documented for some 30 years, with the zincblende→rocksalt transition occurring at 3.5 GPa [A. N. Mariano and E. P. Warekois, *Sci-*

ence **142**, 672 (1963); N. B. Owen, P. L. Smith, J. E. Martin, and A. J. Wright, *J. Phys. Chem. Solids* **24**, 1519 (1963); I. Y. Borg and D. K. Smith, Jr., *J. Phys. Chem. Solids* **28**, 49 (1967)], and the rock-salt→β-Sn transition at ~10 GPa N. B. Owen, P. L. Smith, J. E. Martin, and A. J. Wright, *J. Phys. Chem. Solids* **24**, 1519 (1963); I. Y. Borg and D. K. Smith, Jr., *J. Phys. Chem. Solids* **28**, 49 (1967)]. A further transition, to an orthorhombic structure (*Pmm*2), has also been reported at ~12 GPa [J. Z. Hu, *Solid State Commun.* **63**, 471 (1987)].

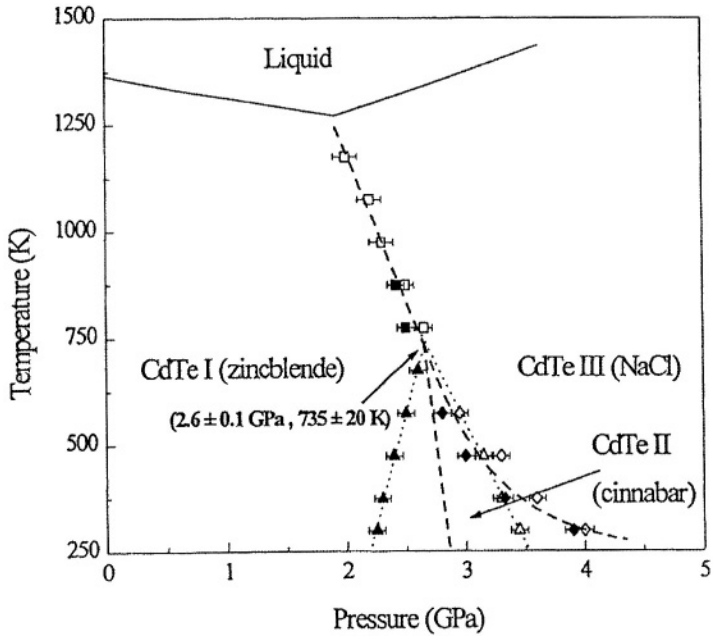

Fig. 14.1.1 Phase diagram of CdTe. The open and solid symbols refer to the transition observed on the upstroke and downstroke, respectively. Triangles: zincblende–cinnabar transformation; diamonds: cinnabar–NaCl (rocksalt) transformation; squares: zincblende–rocksalt direct transformation; dashed lines: upstroke/downstroke average lines. [From D. Martínez-García, Y. Le Godec, M. Mézouar, G. Syfosse, J. P. Itié, and J. M. Besson, *Phys. Status Solidi B* **211**, 461 (1999).]

14.1.6 Cleavage Plane

Table 14.1.8 *Crystallographic plane most readily cleaved for CdTe.*

Cleavage plane
(110)

- **Surface energy**

Table 14.1.9 *Surface energy for CdTe (in J/m^2).*

Plane				Comment
(100)	(110)	(111)	$(\bar{1}\,\bar{1}\,\bar{1})$	
	0.794	0.725	0.650	Calc. [1.6]
0.85	0.18	0.58		Calc. [1.7]

[1.6] B. N. Oshcherin, *Phys. Status Solidi A* **34**, K181 (1976).
[1.7] M. A. Berding, S. Krishnamurthy, A. Sher, and A.-B. Chen, *J. Appl. Phys.* **67**, 6175 (1990).

14.2 THERMAL PROPERTIES

14.2.1 Melting Point and Its Related Parameters

Table 14.2.1 *Melting point T_m and its related parameter for CdTe.*

Parameter	Value
Melting point T_m (K)	1365 [2.1]
Entropy of fusion ΔS_m (cal/mol K)	16.10 [2.2]

[2.1] See, M. R. Lorenz, in *Physics and Chemistry of II–VI Compounds,* edited by M. Aven and J. S. Prener (North-Holland, Amsterdam, 1967), p. 73.
[2.2] See, B. R. Nag, *J. Electron. Mater.* **26**, 70 (1997).

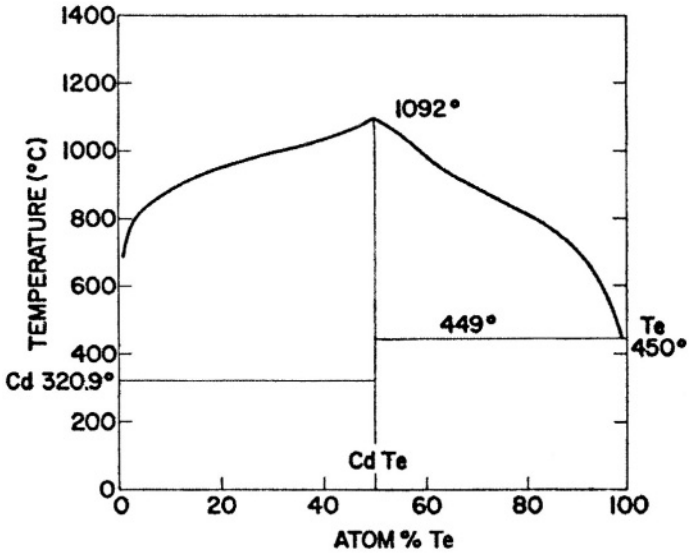

Fig. 14.2.1 *T–x* project of the II–VI binary system Cd–Te. [From M. R. Lorenz, in *Physics and Chemistry of II–VI Compounds,* edited by M. Aven and J. S. Prener (North-Holland, Amsterdam, 1967), p. 73.]

14.2.2 Specific Heat

Table 14.2.2 *Experimental specific heat C_p (at constant pressure) for CdTe [2.3].*

Temperature (K)	C_p (mJ/g K)	Temperature (K)	C_p (mJ/g K)
1.748	0.0226	9.098	8.17
2.111	0.0409	10.14	11.1
2.439	0.0637	11.10	14.4
2.961	0.121	12.49	19.0
3.104	0.145	14.22	24.6
4.042	0.351	15.33	27.5
4.347	0.463	16.45	31.4
4.926	0.779	18.82	38.2
5.916	1.67	20.66	42.9
6.984	3.32	22.27	46.4
7.632	4.49	24.82	51.9
8.272	5.96		

[2.3] J. A. Birch, *J. Phys. C: Solid State Phys.* **8**, 2043 (1975).

Table 14.2.3 *Experimental specific heats C_p (at constant pressure) and C_v (at constant volume) for CdTe (in J/gK) [2.4].*

Temperature (K)	C_p	C_v	Temperature (K)	C_p	C_v
55	0.1174	0.1174	190	0.1990	0.1987
60	0.1257	0.1257	200	0.2002	0.1998
70	0.1403	0.1402	210	0.2012	0.2009
80	0.1518	0.1517	220	0.2021	0.2018
90	0.1616	0.1615	230	0.2030	0.2027
100	0.1688	0.1687	240	0.2041	0.2037
110	0.1749	0.1747	250	0.2050	0.2046
120	0.1800	0.1798	260	0.2059	0.2055
130	0.1840	0.1839	270	0.2069	0.2064
140	0.1876	0.1874	273.16	0.2070	0.2065
150	0.1906	0.1904	280	0.2073	0.2069
160	0.1934	0.1932	290	0.2078	0.2074
170	0.1957	0.1954	300	0.2082	0.2078
180	0.1975	0.1972			

[2.4] A. F. Demidenko, *Inorg. Mater.* **5**, 210 (1969).

- **Functional expression**

Table 14.2.4 *Specific heat C_p (at constant pressure) as a function of temperature T for CdTe.**

C_p (J/g K)	Comment
$0.206+3.59\times10^{-5}T$	[2.5]
$0.167+1.37\times10^{-4}T$	T=298–1000 K [2.6]
$0.1915+5.97\times10^{-5}T+0.11360T^{-2}$	T=360–760 K [2.7]
$-2.2111\times10^{-2}+3.57776T-21.12T^{2}+53.761T^{3}-48.317T^{4}$ (T in kilokelvins)	T=5–300 K [2.8]

[2.5] P. Goldfinger and M. Jeunehomme, *Trans. Faraday Soc.* **59,** 2851 (1963).
[2.6] K. C. Mills, *Themodynamic Date for Inorganic Sulphides, Selenides and Tellurides* (Butterworths, London, 1974).
[2.7] A. S. Malkova, V. V. Zharov, G. I. Shmoilova, and A. S. Pashinkin, *Russ. J. Phys. Chem.* **63**, 2 (1989).
[2.8] M. Gambino, V. Vassiliev, and J. P. Bros, *J. Alloys Compounds* **176,** 13 (1991) [see also, H. Maleki and L. R. Holland, in *Properties of Narrow Gap Cadmium-based Compounds,* EMIS Datareviews Series No. 10, edited by P. Capper (INSPEC, London, 1994), p. 408].
*These expressions give an average value of C_p~0.211 J/g K at T=300 K.

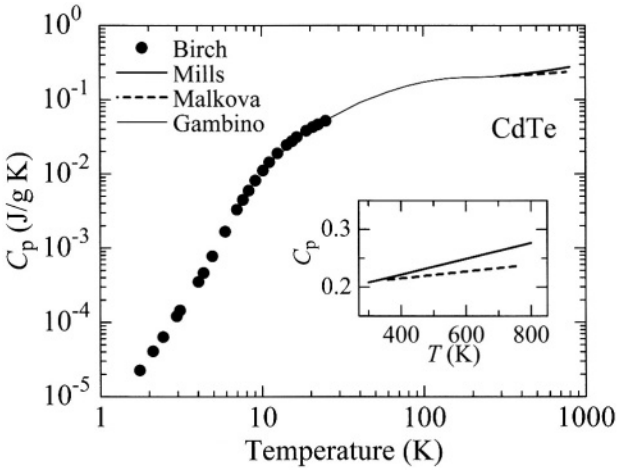

Fig. 14.2.2 Specific heat C_p (at constant pressure) versus temperature for CdTe. The experimental data are taken from J. A. Birch [*J. Phys. C: Solid State Phys.* **8**, 2043 (1975); solid circles], from K. C. Mills [*Themodynamic Date for Inorganic Sulphides, Selenides and Tellurides* (Butterworths, London, 1974); heavy solid line], from A. S. Malkova, V. V. Zharov, G. I. Shmoilova, and A. S. Pashinkin [*Russ. J. Phys. Chem.* **63**, 2 (1989); dashed line], and from M. Gambino, V. Vassiliev, and J. P. Bros [*J. Alloys Compounds* **176,** 13 (1991); light solid line].

14.2.3 Debye Temperature

Table 14.2.5 *Debye temperature θ_D for CdTe [2.9].*

Temperature (K)	θ_D (K)	Temperature (K)	θ_D (K)
0*	158	55	198
1.6	156	60	201
2.4	154	70	205
3.4	151	80	208
4.2	143	90	208
5.0	134	100	210
5.8	126	110	210
6.8	121	120	207
7.6	117	130	206
8.4	114	140	202
9.4	113	150	201
10.4	115	160	197
11.5	116	170	193
12.4	117	180	186
14	121	190	182
15.2	124	200	177
16	127	210	172
18.4	134	220	167
20.4	139	230	160
22.2	144	240	150
24.8	154	250	138
29.8	166	260	122
35.2	178	270	105

Table 14.2.5 *Continued.*

Temperature (K)	θ_D (K)	Temperature (K)	θ_D (K)
40	185	273.16	96
44.8	189	280	81
50	195	290	44

[2.9] The experimental data are taken for $T \leq 50$ K from D. Bagot, R. Granger, and S. Rolland [*Phys. Status Solidi B* **177,** 295 (1993)] and for $T < 50$ K from A. F. Demidenko [*Inorg. Mater.* **5**, 210 (1969)].

*In the low-temperature (0 K) limit [see, H. Siethoff and K. Ahlborn, *Phys. Status Solidi B* **190**, 179 (1995)].

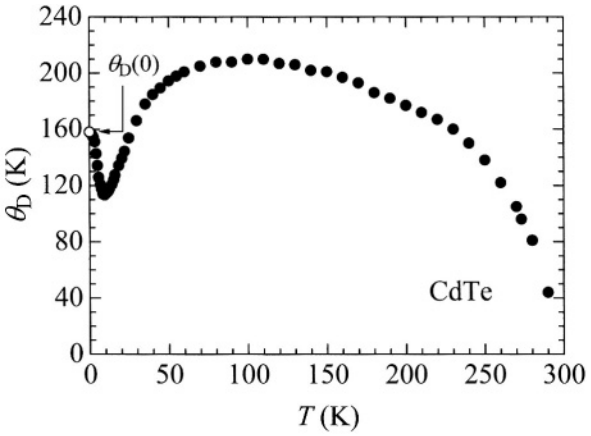

Fig. 14.2.3 Debye temperature θ_D for CdTe. The experimental data are taken for $T \leq 50$ K from D. Bagot, R. Granger, and S. Rolland [*Phys. Status Solidi B* **177**, 295 (1993)] and for $T > 50$ K from A. F. Demidenko [*Inorg. Mater.* **5**, 210 (1969)]. The low-temperature limit value $\theta_D(0)$ is from H. Siethoff and K. Ahlborn [*Phys. Status Solidi B* **190**, 179 (1995)].

14.2.4 Thermal Expansion Coefficient

Table 14.2.6 *Thermal expansion coefficient α_{th} for CdTe [2.10]. Note that the expansion coefficient shows a minimum at T~28 K.*

Temperature (K)	α_{th} (10^{-6} K^{-1})	Temperature (K)	α_{th} (10^{-6} K^{-1})
2	–0.0014	18	–2.39
3	–0.0048	19	–2.54
4	–0.0142	20	–2.65
5	–0.0450	22	–2.83
6	–0.112	24	–2.95
7	–0.222	25	–3.00
8	–0.380	26	–3.03
9	–0.573	28	–3.04
10	–0.790	30	–3.00
11	–1.010	32	–2.94
12	–1.245	57.5	–0.40
13	–1.481	65	0.15
14	–1.700	75	0.92
15	–1.890	85	1.57
16	–2.065	283	4.70
17	–2.238		

[2.10] T. F. Smith and G. K. White, *J. Phys. C: Solid State Phys.* **8**, 2031 (1975).

Table 14.2.7 *Thermal expansion coefficient α_{th} for CdTe [2.11].*

Temperature (K)	α_{th} (10^{-6} K^{-1})	Temperature (K)	α_{th} (10^{-6} K^{-1})
40	–2.66	160	3.78
50	–1.58	180	4.09
60	–0.56	200	4.28
70	0.372	220	4.37
80	0.930	240	4.47
90	1.40	260	4.54
100	2.01	280	4.61
120	2.83	300	4.67*
140	3.35		

[2.11] D. Bagot, R. Granger, and S. Rolland, *Phys. Status Solidi B* **177**, 295 (1993).
*Estimated.

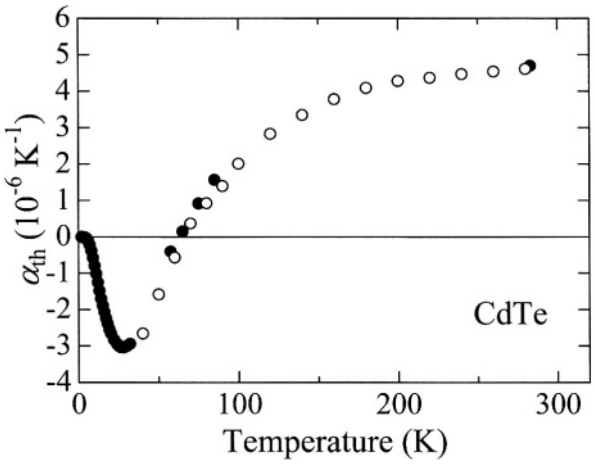

Fig. 14.2.4 Thermal expansion coefficient α_{th} versus temperature for CdTe. The experimental data are taken from T. F. Smith and G. K. White [*J. Phys. C: Solid State Phys.* **8**, 2031 (1975); solid circles] and from D. Bagot, R. Granger, and S. Rolland [*Phys. Status Solidi B* **177**, 295 (1993); open circles].

14.2.5 Thermal Conductivity and Diffusivity

Table 14.2.8 *Thermal conductivity K for CdTe [2.12]. Thermal diffusivity can be calculated from a relation $D=K/(C_p \cdot g)$, where C_p is the specific heat at constant pressure and g is the crystal density.*

Temperature (K)	K (W/cm K)	Temperature (K)	K (W/cm K)
3.5	4.2	25	2.2
4.3	5.1	29	2.0
5.7	6.1	33	1.6
7.3	6.3	39	1.3
8.8	5.8	53	0.77
10	5.0	65	0.55
12	4.1	80	0.41
14	3.6	130	0.22
16	3.2	190	0.12
21	2.5	300	0.075

[2.12] G. A. Slack and S. Galginaitis, *Phys. Rev.* **133**, A253 (1964).

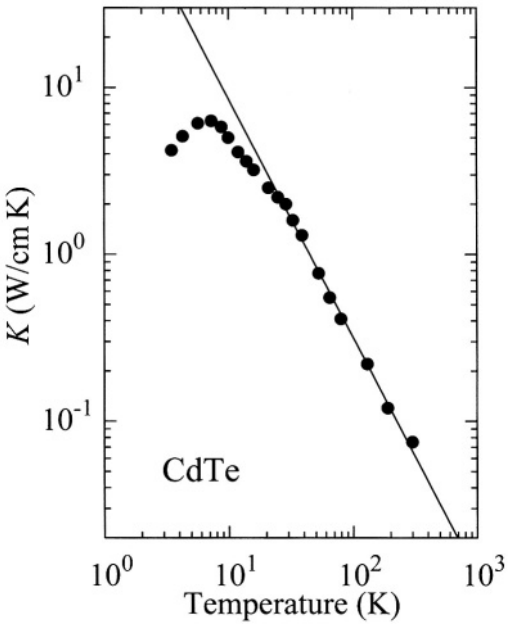

Fig. 14.2.5 Thermal conductivity K for CdTe. The experimental data are taken from G. A. Slack and S. Galginaitis [*Phys. Rev.* **133**, A253 (1964)]. The solid line is calculated from $K=AT^n$ with A=230 $Wcm^{-1}K^{0.43}$ and n= –1.43.

14.3 ELASTIC PROPERTIES

14.3.1 Elastic Constant

- **Room-temperature value and its temperature and pressure derivatives**

Table 14.3.1 *Elastic constant and its temperature and pressure derivatives for CdTe at 300 K.*

Parameter	Value
Stiffness (10^{11} dyn/cm^2) [3.1]	
C_{11}	5.35
C_{12}	3.69
C_{44}	2.02
Compliance (10^{-12} cm^2/dyn) [3.1]	
S_{11}	4.27
S_{12}	–1.74
S_{44}	4.95
dC_{ij}/dT (10^7 dyn/cm^2 K) [3.1]	
C_{11}	–10.7
C_{12}	–8.5
C_{44}	–1.9
dC_{ij}/dp	
C_{11}	
C_{12}	
C_{44}	

[3.1] *Numerical Data and Functional Relationships in Science and Technology,* edited by K.-H. Hellwege and A. M. Hellwege, Landolt–Börnstein, New Series, Group III, Vol. 11 (Springer, Berlin, 1979).

14.3.2 Third-Order Elastic Constant

No detailed data are available for CdTe.

14.3.3 Young's Modulus, Poisson's Ratio, and Similar

• Young's modulus

Table 14.3.2 *Young's modulus Y for CdTe at 300K.**

Crystallographic plane	Y (10^{11} dyn/cm^2)
(100) plane	
[001] direction	2.34
[011] direction	4.00
(110) plane	
[001] direction	2.34
[111] direction	5.23
(111) plane	4.00

*Calculated using S_{11}=4.27, S_{12}=−1.74, and S_{44}=4.95 (all in 10^{-12} cm^2/dyn).

• Poisson's ratio

Table 14.3.3 *Poisson's ratio P for CdTe at 300 K.**

Crystallographic plane	P
(100) plane	
m=[010], n=[001]	0.407
m=[011], n=[0$\bar{1}$1]	−0.011
(110) plane	
m=[001], n=[1$\bar{1}$0]	0.407
m=[1$\bar{1}$1], n=[11$\bar{2}$]	0.294
(111) plane	0.460

*Calculated using S_{11}=4.27, S_{12}= −1.74, and S_{44}=4.95 (all in 10^{-12} cm^2/dyn).

• Bulk modulus, shear modulus, etc.

Table 14.3.4 *Bulk modulus, B_u, pressure derivative of B_u, dB_u/dp, shear modulus, C_s, isotropy factor, A, linear compressibility, C_o, Caucy ratio, C_a, and Born ratio, B_o, for CdTe at 300 K.*

Parameter	Value
B_u (10^{11} dyn/cm^2)	4.24 [3.2]
dB_u/dp	3.6–4.36 [3.3]
	6.4±0.6 [3.4]
C_s (10^{10} dyn/cm^2)	8.30 [3.2]
A	0.411 [3.2]
C_o (10^{-13} cm^2/dyn)	7.86 [3.2]
C_a	1.83 [3.2]
B_o	1.15 [3.2]

[3.2] Calculated using C_{11}=5.35, C_{12}=3.69, and C_{44}=2.02 (all in 10^{11} dyn/cm^2).

[3.3] Theor. [see, M. B. Kanoun, W. Sekkal, H. Aourag, and G. Merad, *Phys. Lett. A* **272**, 113 (2000)].

[3.4] Exper. [K.Strössner, S. Ves, W. Dieterich, W. Gebhardt, and M. Cardona, *Solid State Commun.* **56**, 563 (1985)].

14.3.4 Microhardness

Table 14.3.5 *Microhardness H for CdTe.*

H (GPa)	Ref.
0.45–0.60	[3.5], [3.6]

[3.5] See, L. Garbato and A. Rucci, *Phil. Mag.* **35**, 1681 (1977).
[3.6] A. M. Andrukhiv, V. I. Ivanov–Omskiĭ, and P. G. Sidorchuk, *Sov. Phys. Solid State* **34**, 1934 (1992).

14.3.5 Sound Velocity

Table 14.3.6 *Sound velocity propagating in CdTe at 300 K.* LA=longitudinal acoustic; TA1, TA2=transverse acoustic.*

Propagation direction	Mode	Sound velocity (10^5 cm/s)
[100]	LA	3.02
[100]	TA1, TA2	1.86
[110]	LA	3.34
[110]	TA1	1.19
[110]	TA2	1.86
[111]	LA	3.44
[111]	TA1, TA2	1.45

*Calculated using $C_{11}=5.35\times10^{11}$ dyn/cm^2, $C_{12}=3.69\times10^{11}$ dyn/cm^2, $C_{44}=2.02\times10^{11}$ dyn/cm^2, and $g=5.856$ g/cm^3.

14.4 PHONONS AND LATTICE VIBRONIC PROPERTIES

14.4.1 Phonon Dispersion Relation

- **Dispersion curve**

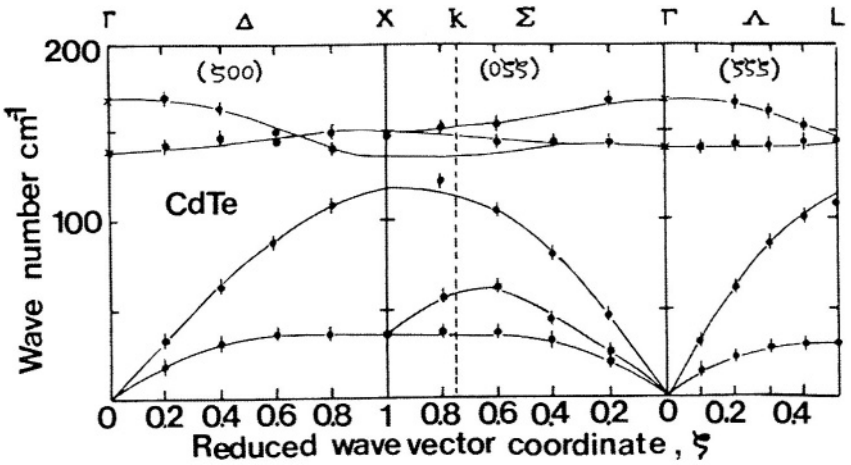

Fig. 14.4.1 Dispersion curves for the acoustic and optical branch phonons in CdTe at 300 K. The solid lines are calculated from a rigid ion model. The symbols represent the neutron data measured by J. M. Rowe, R. M. Nicklow, D.L. Price, and K. Zanio [*Phys. Rev. B* **10**, 671 (1974)]. [From D. N. Talwar and M. Vandevyver, *J. Appl. Phys.* **56**, 1601 (1984).]

• **Phonon density of states**

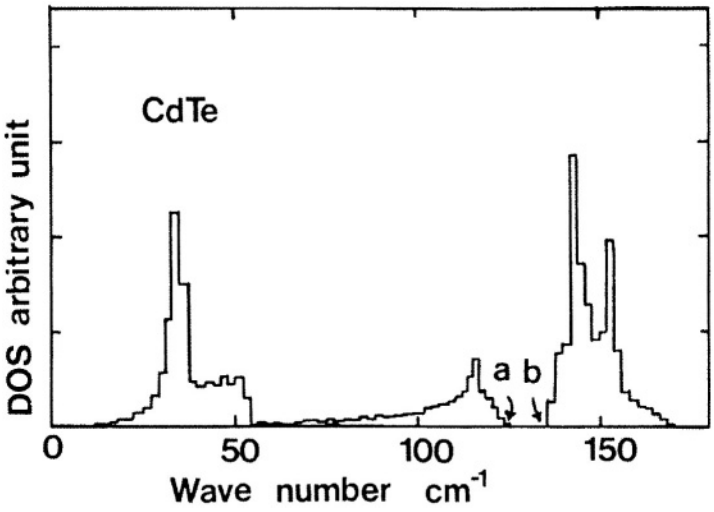

Fig. 14.4.2 Calculated one-phonon density of states (DOS) for CdTe based on a rigid ion model. The terms *a* and *b* represent the limits of the calculated gap in the one-phonon density of states. [From D. N. Talwar and M. Vandevyver, *J. Appl. Phys.* **56**, 1601 (1984).]

14.4.2 Phonon Frequency

• **Room-temperature value**

Table 14.4.1 *Long-wavelength ($q \to 0$) and zone-boundary phonon frequencies for CdTe [4.1].*

Critical point	Phonon	Phonon frequency (cm^{-1})
Γ	TO	140
		143 [4.2]
		139 [4.3]
	LO	169
		168 [4.2]
		167 [4.3]
X	TA	35
	LA	
	TO	148
	LO	
L	TA	29
	LA	108
	TO	144
	LO	144

[4.1] J. M. Rowe, R. M. Nicklow, D. L. Price, and K. Zanio, *Phys. Rev. B* **10**, 671 (1974).
[4.2] M. Górska and W. Nazarewicz, *Phys. Status Solidi B* **65**, 193 (1974).
[4.3] D. N. Talwar and M. Vandevyver, *J. Appl. Phys.* **56**, 1601 (1984).

• **Temperature dependence**

It has been reported that the TO (LO) phonon frequency in CdTe shows a decrease (increase) of about 3 (4) cm^{-1} in going from 100 to 300 K [A. Manabe, A. Mitsuishi, and H. Yoshinaga, *Jpn. J. Appl. Phys.* **6**, 593 (1967)].

Table 14.4.2 *Temperature dependence of the TO phonon frequency ω_{TO} for CdTe.*

$$\omega_{TO}(T) = A + B\left(\frac{T}{\theta}\right) + C\left(\frac{T}{\theta}\right)^2$$

Parameter				Comment
A (THz)	B (THz)	C (THz)	θ(K)	
4.361	–0.0298	–0.0348	207	T=10–300 K [4.4]

[4.4] M. Schall, M. Walther, and P. U. Jepsen, *Phys. Rev. B* **64**, 94301 (2001).

- **Pressure dependence**

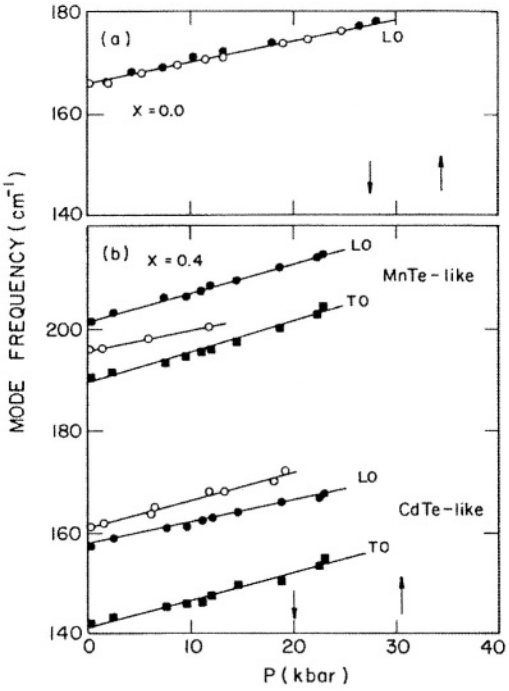

Fig. 14.4.3 Hydrostatic-pressure dependence of the zone-center phonon frequencies in (a) CdTe (x=0.0). and (b) $Cd_{1-x}Mn_xTe$ (x=0.4) at 300 K. [From A. K. Arora, D. U. Bartholomew, D. L. Peterson, and A. K. Ramdas, *Phys. Rev. B* **35**, 7966 (1987).]

14.4.3 Mode Grüneisen Parameter

Table 14.4.3 *Mode Grüneisen parameter for phonons at a number of critical points in CdTe [4.5].*

Critical point	Phonon	Mode Grüneisen parameter
Γ	TO	1.61±0.06*
	LO	1.01±0.03
X	TA	–1.8±0.1*
	LA	
	TO	
	LO	

[4.5] A. K. Arora, D. U. Bartholomew, D. L. Peterson, and A. K. Ramdas, *Phys. Rev. B* **35**, 7966 (1987).
*Value of $Cd_{1-x}Mn_xTe$ with x=0.2.

14.4.4 Phonon Deformation Potential

Table 14.4.4 *Long-wavelength phonon deformation potential (PDP) for CdTe [4.6].*

PDP	TO	LO
K_{11}	−3.25±0.57	−1.08±0.12
K_{12}	−3.20±0.22	−2.49±0.11
K_{44}	−2.1±1.0	−4.54±0.44
$K_{11}-K_{12}$	−0.05	1.41

[4.6] V. C. Stergiou, Y. S. Raptis, E. Anastassakis, N. T. Pelekanos, A. Nahmani, and J. Cibert, *Phys. Status Solidi B* **223**, 237 (2001).

14.5 COLLECTIVE EFFECTS AND RELATED PROPERTIES

14.5.1 Piezoelectric Constant

Table 14.5.1 *Piezoelectric stress (e_{14}), strain (d_{14}), and electromechanical coupling constants ($K_{[110]}^2$) for CdTe [5.1].*

Parameter	Value
e_{14} (C/m^2)	0.0335
d_{14} (10^{-12} m/V)	1.68
$K_{[110]}^2$	6.0×10^{-5} *

[5.1] T=77 K [D. Berlincourt, H. Jaffe, and L. R. Shiozawa, *Phys. Rev.* **129**, 1009 (1963)].
*Calculated.

14.5.2 Fröhlich Coupling Constant

Table 14.5.2 *Fröhlich coupling constant α_F of CdTe.*

α_F	Ref.
0.40±0.03	[5.2]
0.315	[5.3]
0.35±0.03	[5.4]

[5.2] C. W. Litton, K. J. Button, and J. Waldman, *Phys. Rev. B* **13**, 5392 (1976).
[5.3] E. Kartheuser, in *Polarons in Ionic Crystals and Polar Semiconductors,* edited by J. T. Devreese (North-Holland, Amsterdam, 1972), p. 717.
[5.4] M. Helm, W. Knap, W. Seidenbusch, R. Lassnig, E.Gornik, R. Triboulet, and L. L. Taylor, *Solid State Commun.* **53**, 547 (1985).

14.6 ENERGY-BAND STRUCTURE: ENERGY-BAND GAPS

14.6.1 Basic Properties

• **Electronic energy-band structure**

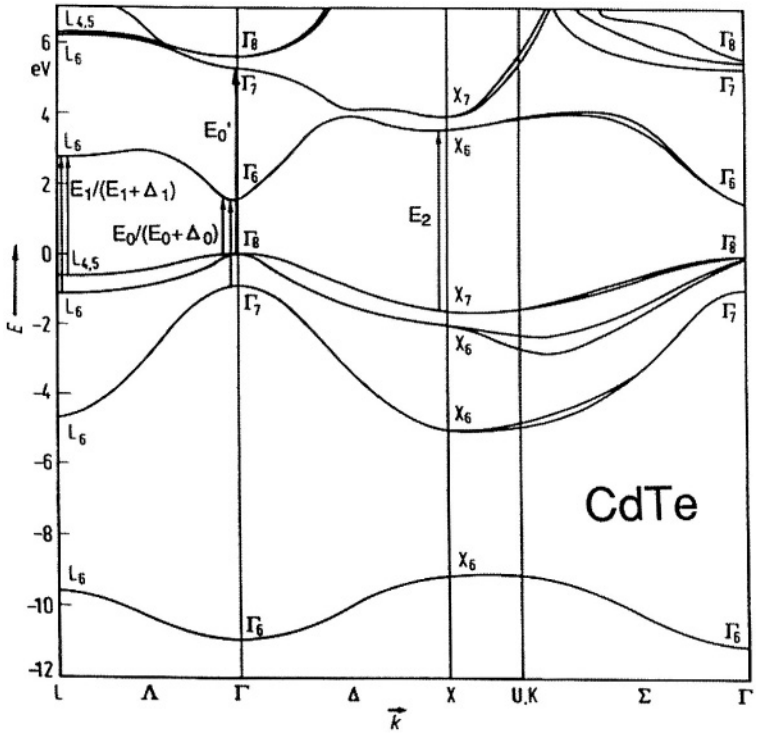

Fig. 14.6.1 Electronic energy-band structure of CdTe as calculated by an empirical nonlocal pseudopotential method. The electronic states are labeled using the notation for the representations of the double group of the zinc-blende structure. [From J. R. Chelikowsky and M. L. Cohen, *Phys. Rev. B* **14**, 556 (1976).] The main interband transitions are indicated by the vertical arrows.

• **Electronic density of states**

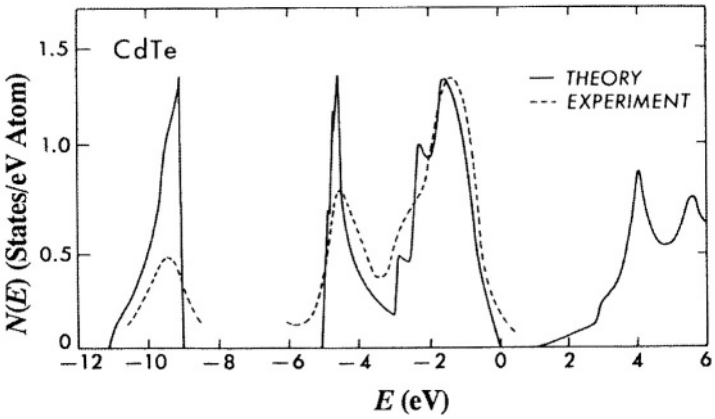

Fig. 14.6.2 Theoretical and experimental electronic density of states $N(E)$ for CdTe. The experimental data are from D. E. Eastman, W. D. Grobman, J. L. Freeouf, and M. Erbudak [*Phys. Rev. B* **9**, 3473 (1974)]. [From J. R. Chelikowsky and M. L. Cohen, *Phys. Rev. B* **14**, 556 (1976).]

• **Energy eigenvalue**

Table 14.6.1 *Energy eigenvalues at the Γ, X, and L points for the valence and first few conduction bands of CdTe [6.1].*

Critical point	Level	Value (eV)	
		Calc.	Exper.*
Γ	Γ_6^v (Γ_1^v)	−11.07	
	Γ_7^v (Γ_{15}^v)	−0.89	−0.90
	Γ_8^v	0.00	0.00
	Γ_6^c (Γ_1^c)	1.59	1.59–1.607
	Γ_7^c (Γ_{15}^c)	5.36	4.80–5.34
	Γ_8^c	5.61	
X	X_6^v (X_1^v)	−9.12	−8.8
	X_6^v (X_3^v)	−5.05	−4.7, −5.1
	X_6^v (X_5^v)	−1.98	−1.8
	X_7^v	−1.60	
	X_6^c (X_1^c)	3.48	
	X_7^c (X_3^c)	3.95	
L	L_6^v (L_1^v)	−9.64	−8.8, −9.1
	L_6^v (L_1^v)	−4.73	−4.4, −4.7
	L_6^v (L_3^v)	−1.18	
	$L_{4,5}^v$	−0.65	−0.7, −0.9
	L_6^c (L_1^c)	2.82	
	L_6^c (L_3^c)	6.18	
	$L_{4,5}^c$	6.35	

[6.1] J. R. Chelikowsky and M. L. Cohen, *Phys. Rev. B* **14**, 556 (1976).
The data are gathered from various sources.

14.6.2 E_0-Gap Region

• **Temperature dependence**

Table 14.6.2 *E_0- (excitonic), $E_0+\Delta_0$-, and Δ_0-gap energies for CdTe determined at various temperatures.*[1]*

Temperature (K)	E_0 (eV)	$E_0+\Delta_0$ (eV)	Δ_0 (eV)
1.6	1.6063		
	1.607		
2	1.590		
4.2	1.602		
	1.6063		
	1.6065		
	1.606		
6	1.5949		
77	1.59	2.4	0.8
80	1.578		
90	1.55		
294	1.504	2.432	0.928

Table 14.6.2 *Continued.*

Temperature (K)	E_0 (eV)	$E_0+\Delta_0$ (eV)	Δ_0 (eV)
296	1.493	2.412	0.919
300	1.475		
	1.483		
	1.49	2.41	0.92
	1.493		
	1.495		
	1.501		
	1.506		
	1.5067		
	1.511		
	1.513		
	1.514		
	1.516		
	1.517		
	1.529		
	1.54	2.43	0.89
		2.45	
	1.51*[2]		
332	1.476	2.397	0.921
389	1.456	2.360	0.904
446	1.436	2.339	0.903
503	1.416	2.320	0.904
558		2.308	
615		2.301	
671		2.281	
			0.90 (Mean value)

*[1] The data are gathered from various sources.
*[2] Mean value at T~300 K.

Table 14.6.3 *Spin–orbit–splitoff energy Δ_0 for CdTe**

Δ_0 (eV)
0.90

*Note that Δ_0 may not vary with temperature if one supposes the valence-band rigidity of the II–VI compounds.

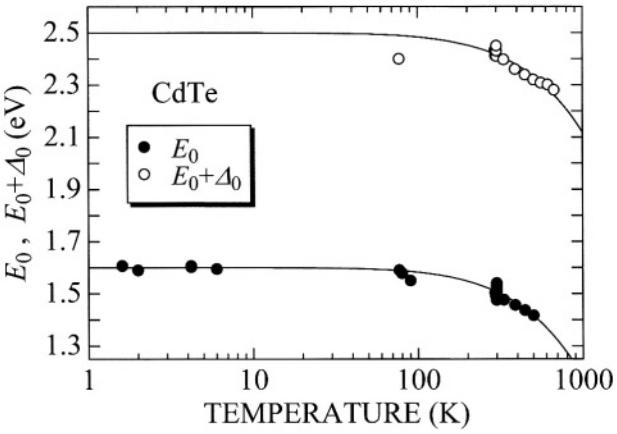

Fig. 14.6.3 E_0- and $E_0+\Delta_0$-gap energies versus temperature for CdTe. The experimental data are gathered from various sources. The solid lines show the calculated results of $E_g(T)=E_g(0)-[\alpha T^2/(T+\beta)]$ with $E_g(0)=1.600$ eV, $\alpha=5.0\times10^{-4}$ eV/K, and $\beta=180$ K (E_0); $E_g(0)=2.500$ eV, $\alpha=4.5\times10^{-4}$ eV/K, and $\beta=180$ K ($E_0+\Delta_0$).

Table 14.6.4 *Empirical equation for the E_0- and $E_0+\Delta_0$-gap energy variations with temperature T for CdTe.*

$$E_g(T) = E_g(0) - \frac{\alpha T^2}{T+\beta}$$

Band gap	Parameter			Comment
	$E_g(0)$ (eV)	α (10^{-4} eV/K)	β (K)	
E_0	1.597	4.35	126.8	T=10–300 K [6.2]
	1.590	3.7	28.95	T=296–503 K [6.3]
	1.565	4.06	180	T=296–503 K [6.4]
$E_0+\Delta_0$	2.547	4.35	126.8	T=10–300 K [6.2]
	2.493	3.4	28.95	T=296–671 K [6.3]
	2.478	3.51	100	T=296–671 K [6.4]

[6.2] D. J. Olego and J. P. Faurie, *Phys. Rev. B* **33**, 7357 (1986).
[6.3] C. C. Kim and S. Sivananthan, *J. Electron. Mater.* **26**, 561 (1997).
[6.4] C. C. Kim, M. Daraselia, J. W. Garland, and S. Sivananthan, *Phys. Rev. B* **56**, 4786 (1997).

Table 14.6.5 *Empirical equation for the E_0- and $E_0+\Delta_0$-gap energy variation with temperature T for CdTe [6.5]. 3D-CP=three-dimensional critical point.*

$$E_g(T) = E_B - 2a_B\left(\frac{1}{2} + \frac{1}{e^{\Theta/T}-1}\right)$$

Band gap	Parameter			Comment
	E_B (eV)	a_B (meV)	Θ (K)	
E_0	1.617	21.5	115	Excitonic transition
	1.615	19.3	106	3D-CP
$E_0+\Delta_0$	2.563	25	117	Excitonic transition
	2.560	22	107	3D-CP

[6.5] J. T. Benhlal, K. Strauch, R. Granger, and R. Triboulet, *Opt. Mater.* **12**, 143 (1999).

Table 14.6.6 *Empirical equation for the E_0-gap energy variation with temperature T for CdTe [6.6].*

$$E_0(T) = E_0(0) - S\langle\hbar\Omega\rangle\left[\coth\left(\frac{\langle\hbar\Omega\rangle}{2kT}\right) - 1\right]$$

$E_0(0)$ (eV)	S	$\langle\hbar\Omega\rangle$ (meV)
1.608	1.68	5.8

[6.6] K. P. O'Donnell and P. G. Middleton, in *Properties of Wide Bandgap II–VI Semiconductors,* EMIS Datareviews Series No. 17, edited by R. Bhargava (INSPEC, London, 1997), p. 33.

Table 14.6.7 *Empirical equation for the E_0-gap energy variation with temperature T for CdTe [6.7].*

$$E_0(T) = E_0(0) - \frac{\alpha\Theta_p}{2}\left[\sqrt[p]{1+\left(\frac{2T}{\Theta_p}\right)^p} - 1\right]$$

$E_0(0)$ (eV)	p	α (meV/K)	Θ_p (K)	Comment
1.606	1.97	0.310	108	T=2–300 K [6.7]

[6.7] R. Pässler, *Phys. Status Solidi B* **216**, 975 (1999).

Table 14.6.8 *Empirical equation for the E_0-gap energy variation with temperature T for CdTe.*

$$E_0(T) = E_0(0) - \alpha \sum_{i=1,2} \frac{W_i\Theta_i}{\exp(\Theta_i/T) - 1}$$

$E_0(0)$ (eV)	α (10^{-4} eV/K)	Θ_1 (K)	Θ_2 (K)	W_1	W_2	Comment
1.606	3.08	40	177	0.52	0.48	T=2–300 K [6.8]

[6.8] R. Pässler, *J. Appl. Phys.* **89,** 6235 (2001).

- **Pressure dependence**

Table 14.6.9 *Empirical equation for the E_0-gap energy variation with pressure p for CdTe.*

$$E_0(p) = E_0(0) + ap + bp^2$$

Parameter			Comment
$E_0(0)$ (eV)	a (10^{-2} eV/GPa)	b (10^{-4} eV/GPa^2)	
1.501	8.0	–34	T=300 K [6.9]
1.483	8.3	–40	T=300 K [6.10]
1.594	7.59±0.19	–29±7	T=15 K [6.11]
1.578	8.57	–47.8	T=80 K [6.12]
1.529	8.40	–39.6	T=300 K [6.13]

[6.9] J. R. Mei and V. Lemos, *Solid State Commun.* **52**, 785 (1984).
[6.10] W. Shan, S. C. Shen, and H. R. Zhu, *Solid State Commun.* **55**, 475 (1985).
[6.11] M. Prakash, M. Chandrasekhar, H. R. Chandrasekhar, I. Miotkowski, and A. K. Ramdas, *Phys. Rev. B* **42**, 3586 (1990).
[6.12] H. M. Cheong, J. H. Burnett, and W. Paul, *Solid State Commun.* **77**, 565 (1991).
[6.13] J. González, R V. Pérez, E. Moya, and J. C. Chervin, *J. Phys. Chem. Solids* **56**, 335 (1995).

- **Temperature and/or pressure coefficient**

Table 14.6.10 *Linear temperature and pressure coefficients of the E_0- and $E_0+\Delta_0$-gap energies for CdTe.*

Band gap	Coefficient	Value	Comment
E_0	dE_g/dT (10^{-4} eV/K)	–3.6	T=77–300 K [6.14]
		–3.0	T=77–300 K [6.15]
		–3.6±0.1[a]	T=100–370 K [6.16]

Table 14.6.10 *Continued.*

Band gap	Coefficient	Value	Comment
	dE_g/dT (10^{-4} eV/K)	–3.5±0.1[b]	T=100–370 K [6.16]
	dE_g/dp (10^{-2} eV/GPa)	7.9±0.2	T=300 K [6.17]
		6.5±0.2	T=2 K [6.18]
		7.9±0.2	T=80 K [6.19]
$E_0+\Delta_0$	dE_g/dT (10^{-4} eV/K)	–3.3	T=77–300 K [6.14]
		–3.0	T=77–300 K [6.15]
	dE_g/dp (10^{-2} eV/GPa)	8.7±0.2	T=300 K [6.17]

[6.14] C. C. Kim and S. Sivananthan, *J. Electron. Mater.* **26**, 561 (1997).
[6.15] C. C. Kim, M. Daraselia, J. W. Garland, and S. Sivananthan, *Phys. Rev. B* **56**, 4786 (1997).
[6.16] J. T. Benhlal, K. Strauch, R. Granger, and R. Triboulet, *Opt. Mater.* **12**, 143 (1999).
[6.17] G. A. Babonas, R. A. Bendoryus, and A. Yu. Shileika, *Sov. Phys. –Semicond.* **5**, 392 (1971).
[6.18] D. J. Dunstan, B. Gil, and K. P. Homewood, *Phys. Rev. B* **38**, 7862 (1988).
[6.19] H. M. Cheong, J. H. Burnett, and W. Paul, *Solid State Commun.* **77**, 565 (1991).
[a] Assuming excitonic transitions.
[b] Assuming three-dimensional critical point.

- **Doping dependence**

No detailed data are available for CdTe. However, the band-gap shrinkage in the presence of a dense electron-hole plasma has been observed in an MBE-grown CdTe thin layer [J. H. Collet, M. Pugnet, W. W. Rühle, L. Nardo, and R. Sirvin, *J. Appl. Phys.* **68**, 1815 (1990)].

14.6.3 Higher-Lying Direct Gap

- **Room-temperature value**

Table 14.6.11 *Higher-lying direct-gap energies for CdTe at room temperature.*

Band gap	Value (eV)
E_1	3.36 *[1]
$E_1+\Delta_1$	3.95 *[1]
Δ_1	0.59 *[1],*[2]
E_0'	4.80–5.34
E_2	4.96–5.56
$E_2+\delta$	5.77–5.9
E_1'	6.4–6.76

*[1] Mean value obtained from various sources.
*[2] Note that Δ_1 may not vary with temperature if one supposes the valence-band rigidity of the II–VI compounds.

- **Temperature dependence**

Table 14.6.12 *E_1-, $E_1+\Delta_1$-, and Δ_1-gap energies for CdTe determined at various temperatures [6.20].*

Temperature (K)	E_1 (eV)	$E_1+\Delta_1$ (eV)	Δ_1 (eV)
6	3.563	4.147	0.584
20	3.53	4.07	0.54
77	3.53		

Table 14.6.12 *Continued.*

Temperature (K)	E_1 (eV)	$E_1+\Delta_1$ (eV)	Δ_1 (eV)
77	3.44	4.01	0.57
78	3.49	4.05	0.56
90	3.490	4.06	0.57
97	3.52		
100	3.485	4.06	0.58
110	3.475	4.06	0.59
117	3.51		
120	3.465	4.05	0.59
127	3.479		
130	3.46	4.04	0.58
140	3.45	4.02	0.57
150	3.46	4.02	0.56
162	3.48		
173	3.455		
180	3.43	4.02	0.59
200	3.44	4.02	0.58
201	3.46		
203	3.443		
210	3.43	4.01	0.58
240	3.42	3.98	0.56
241	3.42		
270	3.38	3.97	0.59
293	3.351	3.937	0.586
295	3.32	3.88	0.56
296	3.363	3.959	0.596
297	3.38	3.96	0.58
297	3.38		
300	3.28	3.89	0.61
300	3.31	3.91	0.60
300	3.393	3.9686	0.576
300	3.423		
300	3.37	3.95	0.58
324	3.371		
332	3.338	3.939	0.601
389	3.297	3.904	0.607
446	3.253	3.870	0.617
503	3.209	3.827	0.618
558	3.163	3.790	0.627
615	3.101	3.743	0.642
671	3.055	3.735	0.680

[6.20] See, A. Kaneta and S. Adachi, *J. Appl. Phys.* **87**, 7360 (2000).

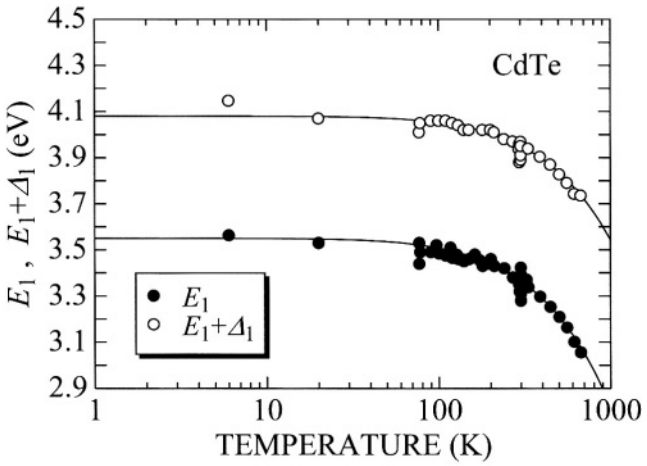

Fig. 14.6.4 E_1- and $E_1+\Delta_1$-gap energies versus temperature for CdTe. The experimental data are gathered from various sources [see, A. Kaneta and S. Adachi, *J. Appl. Phys.* **87**, 7360 (2000)]. The solid lines show the calculated results of $E_g(T)=E_g(0)-[\alpha T^2/(T+\beta)]$ with $E_g(0)=3.55$ eV, $\alpha=8.0\times10^{-4}$ eV/K, and $\beta=90$ K (E_1); $E_g(0)=4.08$ eV, $\alpha=6.0\times10^{-4}$ eV/K, and $\beta=120$ K ($E_1+\Delta_1$).

Table 14.6.13 *Empirical equation for the higher-lying direct-gap energy variation with temperature T for CdTe.*

$$E_g(T) = E_g(0) - \frac{\alpha T^2}{T+\beta}$$

Band gap	Parameter			Ref.
	$E_g(0)$ (eV)	α (10^{-4} eV/K)	β (K)	
E_1	3.55	8.3	140	[6.21]
	3.594	8.3	28.95	[6.22]
	3.467	14.68	924	[6.23]
	3.51	7.0	150	[6.24]
	3.55	8.0	90	*
$E_1+\Delta_1$	4.133	6.4	28.95	[6.22]
	4.068	7.53	300	[6.23]
	4.08	6.0	150	[6.24]
	4.08	6.0	120	*
$E_2(X)$	5.229	9.2	28.95	[6.22]
	5.124	11.54	382	[6.23]
$E_2(\Sigma)$	5.462	4.5	28.95	[6.22]
	5.447	4.56	80	[6.23]

[6.21] A. Ksendzov, F. H. Pollak, and O. K. Wu, *Solid State Commun.* **70**, 963 (1989).
[6.22] C. C. Kim and S. Sivananthan, *J. Electron. Mater.* **26**, 561 (1997).
[6.23] C. C. Kim, M. Daraselia, J. W. Garland, and S. Sivananthan, *Phys. Rev. B* **56**, 4786 (1997).
[6.24] A. Kaneta and S. Adachi, *J. Appl. Phys.* **87**, 7360 (2000).
*See figure, above.

Table 14.6.14 *Empirical equation for the higher-lying direct-gap energy variation with temperature T for CdTe. 2D-CP=two-dimensional critical point.*

$$E_g(T) = E_B - 2a_B\left(\frac{1}{2} + \frac{1}{e^{\Theta/T} - 1}\right)$$

Band gap	Parameter			Comment
	E_B (eV)	a_B (meV)	Θ (K)	
E_1	3.568	43	115	Excitonic transition [6.25]
	3.580	65	169	2D-CP [6.25]
	3.55	45	150	Excitonic transition [6.26]
$E_1+\Delta_1$	4.126	28	83	Excitonic transition [6.25]
	4.171	97	244	2D-CP [6.25]
	4.12	40	150	Excitonic transition [6.26]
E_2	5.152	27	144	2D-CP [6.25]

[6.25] J. T. Benhlal, K. Strauch, R. Granger, and R. Triboulet, *Opt. Mater.* **12**, 143 (1999).
[6.26] A. Kaneta and S. Adachi, *J. Appl. Phys.* **87**, 7360 (2000).

- **Temperature and/or pressure coefficient**

Table 14.6.15 *Linear temperature and pressure coefficients of the higher-lying band-gap energy for CdTe.*

Band gap	Coefficient	Value	Comment
E_1	dE_g/dT (10^{-4} eV/K)	–5.5	T=77–300 K [6.27]
		–5.7	T=127–324 K [6.28]
		–2.3	T=90–300 K [6.29]
		–6.8	T=77–297 K [6.30]
		–8.1	T=77–300 K [6.31]
		–4.5	T=77–300 K [6.32]
		–7.2±0.3	T=100–370 K, excitonic transition [6.33]
		–7.3±0.3	T=100–370 K, 2D-CP [6.33]
		–6.2	T~300 K [6.34]
		–5.9	T~300 K [6.34]
	dE_g/dp (10^{-2} eV/GPa)	7.4	T=90 K [6.29]
		6.0	[6.35]
$E_1+\Delta_1$	dE_g/dT (10^{-4} eV/K)	–6.0	T=77–300 K [6.27]
		–1.7	T=90–300 K [6.29]
		–6.2	T=77–300 K [6.31]
		–4.5	T=77–300 K [6.32]
		–5.3	T~300 K [6.34]
		–5.2	T~300 K [6.34]
	dE_g/dp (10^{-2} eV/GPa)	8.9	T=90 K [6.29]
	dE_g/dT (10^{-4} eV/K)	–3.6±0.3	T=100–370 K, 2D-CP [6.33]
	dE_g/dp (10^{-2} eV/GPa)	3.1	Calc. [6.36]
		–1.0	Calc. [6.37]

Table 14.6.15 *Continued.*

Band gap	Coefficient	Value	Comment
$E_2(X)$	dE_g/dT (10^{-4} eV/K)	–9.0	T=77–300 K [6.31]
		–6.2	T=77–300 K [6.32]
$E_2(\Sigma)$	dE_g/dT (10^{-4} eV/K)	–4.4	T=77–300 K [6.31]
		–4.1	T=77–300 K [6.32]

[6.27] M. Cardona and D. L. Greenaway, *Phys. Rev.* **131**, 98 (1963).
[6.28] S. Antosi, E.Reguzzoni, and G. Samoggia, *Solid State Commun.* **9**, 1081 (1971).
[6.29] A. D. Brothers and J. B. Brungardt, *Phys. Status Solidi B* **99**, 291 (1980).
[6.30] A. Ksendzov, F. H. Pollak, and O. K. Wu, *Solid State Commun.* **70**, 963 (1989).
[6.31] C. C. Kim and S. Sivananthan, *J. Electron. Mater.* **26**, 561 (1997).
[6.32] C. C. Kim, M. Daraselia, J. W. Garland, and S. Sivananthan, *Phys. Rev. B* **56**, 4786 (1997).
[6.33] J. T. Benhlal, K. Strauch, R. Granger, and R. Triboulet, *Opt. Mater.* **12**, 143 (1999).
[6.34] A. Kaneta and S. Adachi, *J. Appl. Phys.* **87**, 7360 (2000).
[6.35] See, Y. F. Tsay, S. S. Mitra, and B. Bendow, *Phys. Rev. B* **10**, 1476 (1974).
[6.36] D. L. Camphausen, G. A. N. Connell, and W. Paul, *Phys. Rev. Lett.* **26**, 184 (1971).
[6.37] Y. F. Tsay, S. S. Mitra, and B. Bendow, *Phys. Rev. B* **10**, 1476 (1974).

14.6.4 Lowest Indirect Gap

• Theoretical value

Table 14.6.16 *Theoretically obtained lowest indirect-gap energy for CdTe (in eV).*

E_g^{L} *1	E_g^{X} *2	Ref.
2.82	3.48	[6.38]
2.36	2.88	[6.39]
3.02	3.5	[6.40]
2.84	3.46	[6.41]

[6.38] J. R. Chelikowsky and J. L. Cohen, *Phys. Rev. B* **14**, 556 (1976).
[6.39] M.-Z. Huang and W. Y. Ching, *J. Phys. Chem. Solids* **46**, 977 (1985).
[6.40] Y. Li and P. J. Lin-Chung, *Phys. Status Solidi B* **153**, 215 (1989).
[6.41] O. Zakharov, A. Rubio, X. Blase, M. L. Cohen, and S. L. Louie, *Phys. Rev. B* **50**, 10780 (1994).
*1 Γ_8^v (Γ_{15}^v)→L_6^c(L_1^c).
*2 Γ_8^v (Γ_{15}^v)→X_6^c(X_1^c).

• Temperature and/or pressure coefficient

Table 14.6.17 *Linear pressure coefficient of the lowest indirect-gap energy for CdTe.*

Coefficient	Value	Comment
dE_g^{L}/dp (10^{-2} eV/GPa)	1.9	Calc. [6.42]
	0.5	Calc. [6.43]
	4.98	Calc. [6.44]
	4.2	Calc. [6.45]
dE_g^{X}/dp (10^{-2} eV/GPa)	–1.9	Calc. [6.42]
	–4.3	Calc. [6.43]
	–1.99	Calc. [6.44]
	–3.2	Calc. [6.45]

[6.42] D. L. Camphausen, G. A. N. Connell, and W. Paul, *Phys. Rev. Lett.* **26**, 184 (1971).
[6.43] Y. F. Tsay, S. S. Mitra, and B. Bendow, *Phys. Rev. B* **10**, 1476 (1974).
[6.44] P. E. Van Camp and V. E. Van Doren, *Solid State Commun.* **91**, 607 (1994).
[6.45] S.-H. Wei and A. Zunger, *Phys. Rev. B* **60**, 5404 (1999).

14.6.5 Conduction-Valley Energy Separation

No detailed data are available for CdTe.

14.6.6 Direct–Indirect-Gap Transition Pressure

No direct–indirect-gap crossing occurs in CdTe for pressures up to the first phase transition (p~3.5 GPa).

14.7 ENERGY-BAND STRUCTURE: ELECTRON AND HOLE EFFECTIVE MASSES

14.7.1 Electron Effective Mass: Γ Valley

Table 14.7.1 *Effective polaron (m_{ep}*) and band masses (m_e^{Γ}) for electrons at the Γ-conduction band in CdTe. α_F=Fröhlich coupling constant.*

m_{ep}^*/m_0	m_e^{Γ}/m_0	Comment
0.11±0.01		[7.1]
0.096±0.005		T=4.2 K [7.2]
0.0963±0.0008		T=11–63 K [7.3]
0.09794	0.090	T<20 K, α_F=0.40 [7.4]
0.096±0.003		T=1.5 K [7.5]
0.094±0.004	0.088±0.004	T=1.8 K, $\boldsymbol{B}$ || <100>, α_F=0.4 [7.6]
0.093±0.005		T=1.8 K [7.7]
	0.0920 (0.0898)	α_F=0.3 (α_F=0.4) [7.8]
	0.09±0.005	T=4.2 K, α_F=0.35 [7.9]
0.099±0.003		T=4.2 K [7.10]
	0.0909	T=4.2 K, α_F=0.4 [7.11]
	0.090 (Mean value)	

[7.1] D. T. F. Marple, *Phys. Rev.* **129**, 2466 (1963).
[7.2] K. K. Kanazawa and F. C. Brown, *Phys. Rev.* **135**, A1757 (1964).
[7.3] A. L. Mears and R. A. Stradling, *Solid State Commun.* **7**, 1267 (1969).
[7.4] C. W. Litton, K. J. Button, and J. Waldman, *Phys. Rev. B* **13**, 5392 (1976).
[7.5] R. Romestain and C. Weisbuch, *Phys. Rev. Lett.* **45**, 2067 (1980).
[7.6] Le Si Dang, G. Neu, and R. Romestain, *Solid State Commun.* **44**, 1187 (1982).
[7.7] E. Molva and Le Si Dang, *Phys. Rev. B* **27**, 6222 (1983).
[7.8] F. M. Peeters and J. T. Devreese, *Solid State Commun.* **127B**, 408 (1984).
[7.9] M. Helm, W. Knap, W. Seidenbusch, R. Lassnig, E.Gornik, R. Triboulet, and L. L. Taylor, *Solid State Commun.* **53**, 547 (1985).
[7.10] Ch. Neumann, A. Nöthe, and N. O. Lipari, *Phys. Rev. B* **37**, 922 (1988).
[7.11] H. Kobori, T. Ohyama, and E. Otsuka, *Solid State Commun.* **84**, 383 (1992).

14.7.2 Electron Effective Mass: Satellite Valley

No detailed data are available for CdTe.

14.7.3 Hole Effective Mass

• Luttinger's valence-band parameter

Table 14.7.2 *Luttinger's valence-band parameter γ_i for CdTe (in $\hbar^2/2m_0$).*

γ_1	γ_2	γ_3	Technique
5.29	1.89	2.46	Five-level $\boldsymbol{k \cdot p}$ calculation [7.12]
5.98	2.18	2.48	Excited acceptor-state analysis [7.13]
5.3±0.5	1.7±0.3	2.0±0.3	Cyclotron resonance [7.14]
4.11	1.08	1.95	Two-photon magnetoabsorption [7.15]
5.30	1.62	2.10	Excited acceptor-state analysis [7.16]
4.14	1.09	1.62	Zeeman splitting [7.17]

[7.12] P.Lawaetz, *phys. Rev. B* **4**, 3460 (1971).
[7.13] L. Svob, Y. Marfaing, M.Hoclet, P. Plumelle, and M. Vandevyver, *Solid State Commun.* **28**, 895 (1978).
[7.14] Le Si Dang, G. Neu, and R. Romestain, *Solid State Commun.* **44**, 1187 (1982).
[7.15] Ch. Neumann, A. Nöthe, and N. O. Lipari, *Phys. Rev. B* **37**, 922 (1988).
[7.16] M. Said and M.A. Kanehisa, *Phys. Status Solidi B* **157**, 311 (1990).
[7.17] T. Friedrich, J. Kraus, G. Schaack, and W. O. G. Schmitt, *J. Phys.: Condens. Matter* **6**, 4307 (1994).

• Band mass, cyclotron mass, etc.

Table 14.7.3 *Band (m_{HH}, m_{LH}), density-of-states heavy-hole (m_{HH}*), averaged light-hole (m_{LH}*), and spherically-averaged heavy-hole (m_{HH}^s) and light-hole masses (m_{LH}^s) in CdTe.*

Mass	Value (m_0)
m_{HH} ([001] direction)	0.51*
m_{LH} ([001] direction)	0.158*
m_{HH} ([111] direction)	1.11*
m_{LH} ([111] direction)	0.136*
m_{HH}*	0.82*
	0.81±0.05 [7.18]
	0.60±0.01 (<100>), 0.69±0.02 (<111>) [7.19]
	0.63±0.06 [7.20]
m_{LH}*	0.145*
	0.12±0.02 [7.18]
	0.12±0.01 (<100>), 0.11±0.01 (<111>) [7.19]
m_{HH}^s	0.76*
m_{LH}^s	0.144*

[7.18] R. Romestain and C. Weisbuch, *Phys. Rev. Lett.* **45**, 2067 (1980).
[7.19] Le Si Dang, G. Neu, and R. Romestain, *Solid State Commun.* **44**, 1187 (1982).
[7.20] S. Yamada, *J. Phys. Soc. Jpn* **15**, 1940 (1980). .

*Calculated using a set of the Luttinger's parameters, γ_1=4.14, γ_2=1.09, and γ_3=1.62.

• **Spin–orbit–splitoff hole effective mass**

Table 14.7.4 *Spin–orbit–splitoff hole effective mass* m_{SO} *for CdTe.*

m_{SO}/m_0	Technique
0.37	$k \cdot p$ method [7.21]
0.28	$k \cdot p$ method [7.22]
0.26	Linear-muffin-tin-orbitals calculation [7.23]
0.218	$k \cdot p$ method [7.24]
0.24	*

[7.21] M. Cardona, *J. Phys. Chem. Solids* **24**, 1543 (1963).
[7.22] P. Lawaetz, *Phys. Rev. B* **4**, 3460 (1971).
[7.23] M. Cardona, N. E. Christensen, and G. Fasol, *Phys. Rev. B* **38**, 1806 (1988).
[7.24] N. P. Belov, V. T. Prokopenko, and A. D. Yas'kov, *Sov. Phys. Semicond.* **23**, 1296 (1989).
*Obtained from the Luttinger's parameter ($m_{SO}=1/\gamma_1$).

14.8 ELECTRONIC DEFORMATION POTENTIAL

14.8.1 Intravalley Deformation Potential: Γ Point

• **Conduction band**

Table 14.8.1 *Γ-conduction-band intravalley deformation potential* a_c^{Γ} $(=E_1^{\Gamma})$ *for CdTe.*

a_c^{Γ} (eV)	Comment
–5.45	Calc. [8.1]
–9.9	Calc. [8.2]
–3.7	Calc. [8.3]
–3.96	Calc. [8.4]

[8.1] J. H. Lee and G. Myers, *Phys. Status Solidi B* **77**, K81 (1976).
[8.2] A. Blacha, H. Presting, and M. Cardona, *Phys. Status Solidi B* **126**, 11 (1984).
[8.3] M. Cardona and N. E. Christensen, *Phys. Rev. B* **35**, 6182 (1987); erratum, *ibid.* **36**, 2906 (1987).
[8.4] C. G. Van de Walle, *Phys. Rev. B* **39**, 1871 (1989).

Table 14.8.2 *Γ-conduction-band acoustic deformation potential* E_1 *for CdTe obtained from transport data analysis.*

E_1 (eV)	Ref.
9.5	[8.5]
4.0	[8.6]

[8.5] D. L. Rode, *Phys. Rev. B* **2**, 4036 (1970).
[8.6] D. L. Rode, in *Semiconductors and Semimetals,* edited by R. K. Willardson and A. C. Beer (Academic, New York, 1975), Vol. 10, p. 1.

• **Valence band**

Table 14.8.3 *Γ-valence-band deformation potentials a, b, and d for CdTe.*

Deformation potential (eV)			Comment
a	*b*	*d*	
–4.8	1.2	–2.9	Calc. [8.7]
–1.0			Calc. [8.8]
0.55	–1.10		Calc. [8.9]
–0.09	–1.25		Calc. [8.10]
	–1.1		Calc. [8.11]
	–1.13		Calc. [8.12]
	0.9		Calc. [8.13]
	–1.18	–4.83	Exper. [8.14]
	–1.1	–5.45	Exper. [8.15]
	–0.74	–2.97	Exper. [8.16]
	–1.0	–4.4	Mean value (Exper.)

[8.7] A. Blacha, H. Presting, and M. Cardona, *Phys. Status Solidi B* **126**, 11 (1984).
[8.8] M. Cardona and N. E. Christensen, *Phys. Rev. B* **35**, 6182 (1987); erratum, *ibid.* **36**, 2906 (1987).
[8.9] C. G. Van de Walle, *Phys. Rev. B* **39**, 1871 (1989).
[8.10] A. Qteish and R. J. Needs, *Phys. Rev. B* **45**, 1317 (1992).
[8.11] M. Silver, W. Batty, A. Ghiti, and E. P. O'Reilly, *Phys. Rev. B* **46**, 6781 (1992).
[8.121] T. Nakayama, *Solid-State Electron.* **37**, 1077 (1994).
[8.13] B. Koopmans, P. V. Santos, and M. Cardona, *Phys. Status Solidi B* **205**, 419 (1998).,
[8.14] D. G. Thomas, *J. Appl. Phys.* **32** (Suppl.), 2298 (1961).
[8.15] A. Gavini and M. Cardona, *Phys. Rev. B* **1**, 672 (1970).
[8.16] D. J. Dunstan, B. Gil, and K. P. Homewood, *Phys. Rev. B* **38**, 7862 (1988).

• E_0 **gap**

Table 14.8.4 *Hydrostatic deformation potential* a_0^Γ *for the* E_0 *gap of CdTe.*

a_0^Γ (eV)	Comment
–5.1	Calc. [8.17]
–4.52	Calc. [8.18]
–4.13	Calc. [8.19]
–3.70	Calc. [8.20]
–2.74±0.09	Exper. [8.21]
–3.1	Exper. *
–2.9	Mean value (Exper.)

[8.17] A. Blacha, H. Presting, and M. Cardona, *Phys. Status Solidi B* **126**, 11 (1984).
[8.18] C. G. Van de Walle, *Phys. Rev. B* **39**, 1871 (1989).
[8.19] T. Nakayama, *Solid-State Electron.* **37**, 1077 (1994).
[8.20] S.-H. Wei and A. Zunger, *Phys. Rev. B* **60**, 5404 (1999).
[8.21] D. J. Dunstan, B. Gil, and K. P. Homewood, *Phys. Rev. B* **38**, 7862 (1988).
*Estimated from dE_0/dp value.

• **Optical-phonon deformation potential**

Table 14.8.5 *Optical-phonon deformation potential d_0 at the Γ-valence band of CdTe.*

d_0 (eV)	Comment
30.5	Calc. [8.22]
22.8	Calc. [8.23]
22	Exper. (see [8.22])

[8.22] W. Pötz and P. Vogl, *Phys. Rev. B* **24**, 2025 (1981).
[8.23] A. Blacha, H. Presting, and M. Cardona, *Phys. Status Solidi B* **126**, 11 (1984).

14.8.2 Intravalley Deformation Potential: High-Symmetry Points

• **Optical-phonon deformation potential: L point**

Table 14.8.6 *Optical-phonon deformation potentials $d_{1o}(c)$, $d_{1o}(v)$, and d_{3o} at the L point of CdTe.*

Deformation potential	Value (eV)	Comment
$d_{1o}(c)$	−27.5	Calc. [8.24]
$d_{1o}(v)$	−17.4	Calc. [8.24]
d_{3o}	42.5	Calc. [8.24]

[8.24] W. Pötz and P. Vogl, *Phys. Rev. B* **24**, 2025 (1981).

14.8.3 Intervalley Deformation Potential

• **Absolute value**

Table 14.8.7 *Intervalley deformation potential D_{ij} for electrons in CdTe [8.25].*

D_{ij}	Phonon	Value (eV/Å)
$D_{\Gamma L}$	LA	1.68
	LO	1.76
$D_{\Gamma X(1)}$	LA	1.23
	LO	0
$D_{\Gamma X(3)}$	LA	0
	LO	0.40

[8.25] Calculated [D. Olguín, M. Cardona, and A. Cantarero, *Solid State Commun.* **122**, 575 (2002)].

14.9 ELECTRON AFFINITY AND SCHOTTKY BARRIER HEIGHT

14.9.1 Electron Affinity

Table 14.9.1 *Electron affinity χ_s for CdTe.*

χ_s (eV)	Ref.
4.28	[9.1]

[9.1] A. G. Milnes and D. L. Feucht, *Heterojunctions and Metal-Semiconductor Junctions* (Academic, New York, 1972).

14.9.2 Schottky Barrier Height

Table 14.9.2 *Summary of the Schottky barrier height ϕ_n for metal/n-CdTe contacts at 300 K.**

Metal	ϕ_n (eV)	Metal	ϕ_n (eV)
Ag	0.5–0.88	Mg	0.4
Al	0.35–0.93	Ni	0.4–0.53
Au	0.59–1.0	Pb	0.62
Bi	0.78–0.83	Pd	0.65–0.86
Cd	0.45–0.56	Pt	0.58–0.89
Co	0.74	Sb	0.76
Cu	0.48–0.82	Sn	0.48
Fe	0.78–0.85		

*The data are gathered from various sources.

Table 14.9.3 *Summary of the Schottky barrier height ϕ_p for metal/p-CdTe contacts at 300 K [9.2].*

Metal	ϕ_p (eV)
Au	0.6
Cd	1.0

[9.2] R. T. Collins and T. C. McGill, *J. Vac. Sci. Technol. A* **1**, 1633 (1983).

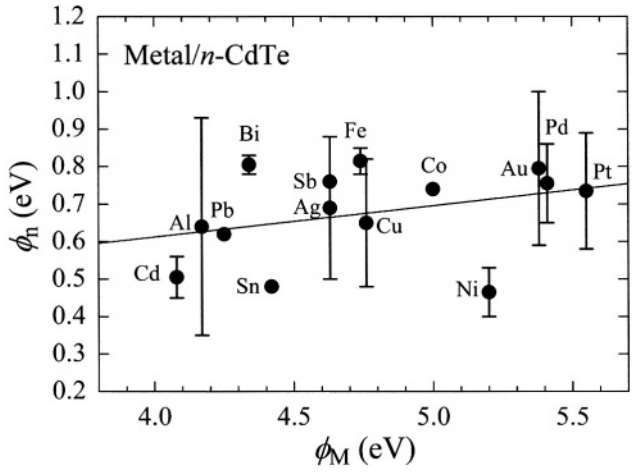

Fig. 14.9.1 Schottky barrier height ϕ_n versus metal work function ϕ_M observed for metal/*n*-CdTe contacts. Values of the metal work function were taken from H. P. R. Frederikse [in *CRC Handbook of Chemistry and Physics,* 78th Edition, edited by D. R. Lide (CRC Press, Boca Raton, 1997), p. 12-115]. The solid line represents the least-squares-fit result with ϕ_n=0.084ϕ_M+0.278 (ϕ_M and ϕ_n in eV).

14.10 OPTICAL PROPERTIES

14.10.1 Summary of Optical Dispersion Relations

• **$\varepsilon(E)$ and $n^*(E)$ spectra**

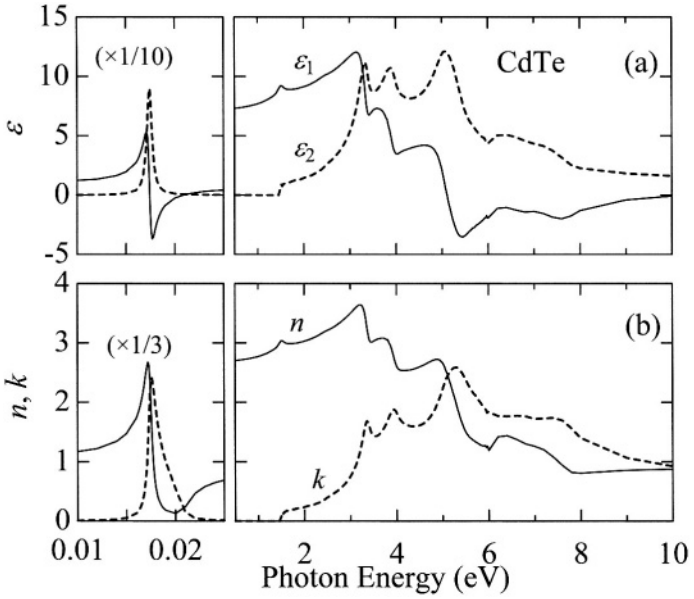

Fig. 14.10.1 (a) Complex dielectric-constant $[\varepsilon(E)=\varepsilon_1(E)+i\varepsilon_2(E)]$ and (b) complex refractive-index spectra $[n^*(E)=n(E)+ik(E)]$ for CdTe at 300 K. The numerical data are taken from tabulation by S. Adachi [*Optical Constants of Crystalline and Amorphous Semiconductors: Numerical Data and Graphical Information* (Kluwer Academic, Boston, 1999)].

• **$\alpha(E)$ and $R(E)$ spectra**

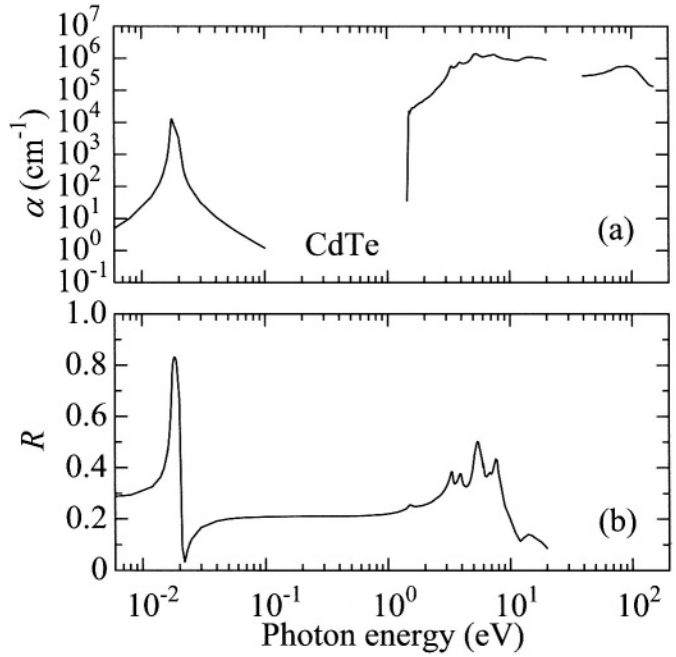

Fig. 14.10.2 (a) Absorption $[\alpha(E)]$ and (b) normal-incidence reflectivity spectra $[R(E)]$ for CdTe at 300 K. The numerical data are taken from tabulation by S. Adachi [*Optical Constants of Crystalline and Amorphous Semiconductors: Numerical Data and Graphical Information* (Kluwer Academic, Boston, 1999)].

14.10.2 The Reststrahlen Region

- **Static and high-frequency dielectric constants**

Table 14.10.1 *Static and high-frequency dielectric constants ε_s and ε_∞ for CdTe.*

ε_s	ε_∞	Comment
9.65		T=77 K [10.1]
10.6		T=300 K [10.2]
	7.21	T=300 K [10.3]
10.60±0.15	7.05±0.05	T=300 K [10.4]
9.4	7.1	T=100 K [10.5]
10.2	7.1	T=300 K [10.5]
9.0±0.4	6.7±0.3	T=8 K [10.6]
9.4±0.4	6.7±0.3	T=300 K [10.6]
10.294±0.01	7.194±0.008	T=300 K [10.7]
10.2	7.1	T=300 K [10.8]
10.5	7.3	T=293 K [10.9]
10.31±0.08		T=0 K [10.10]
11.00		T=296 K [10.10]
10.7	7.1	T=300 K [10.11]
	7.21	T=300 K [10.12]
10.4	7.1	Mean value at T~300 K

[10.1] D. Berlincourt, H. Jaffe, and L. R. Shiozawa, *Phys. Rev.* **129**, 1009 (1963).
[10.2] B. Segall, M. R. Lorenz, and R. E. Halsted, *Phys. Rev.* **129**, 2471 (1963).
[10.3] D. T. F. Marple, *J. Appl. Phys.* **35**, 539 (1964).
[10.4] O. G. Lorimor and W. G. Spitzer, *J. Appl. Phys.* **36**, 1841 (1965).
[10.5] A. Manabe, A. Mitsuishi, and H. Yoshinaga, *Jpn. J. Appl. Phys.* **6**, 593 (1967).
[10.6] C. J. Johnson, G. H. Sherman, and R. Weil, *Appl. Opt.* **8**, 1667 (1969).
[10.7] E. J. Danieleweicz and P. D. Coleman, *Appl. Opt.* **13**, 1164 (1974).
[10.8] S. Perkowitz and R. H. Thorland, *Phys. Rev. B* **9**, 545 (1974).
[10.9] L. K. Vodopop'yanov, E. A. Vinogradov, V. V. Kolotkov, and Y. A. Mityagin, *Sov. Phys. Solid State* **16**, 912 (1974).
[10.10] I. Strzalkowski, S. Joshi, and C. R. Crowell, *Appl. Phys. Lett.* **28**, 350 (1976).
[10.11] A. N. Pikhtin and A. D. Yas'kov, *Sov. Phys. Semicond.* **12**, 622 (1978).
[10.12] S. Adachi and T. Kimura, *Jpn. J. Appl. Phys.* **32**, 3866 (1993).

Table 14.10.2 *Temperature dependence of the static dielectric constant ε_s for CdTe.*

$$\varepsilon_s(T) = A + B\left(\frac{T}{\theta}\right) + C\left(\frac{T}{\theta}\right)^2$$

Parameter				Comment
A	B	C	θ(K)	
9.808	0.1719	0.1414	207	T=10–300 K [10.13]

[10.13] M. Schall, M. Walther, and P. U. Jepsen, *Phys. Rev. B* **64**, 94301 (2001).

Table 14.10.3 *Linear temperature and pressure coefficients of the static (ε_s) and high-frequency dielectric constants (ε_∞) for CdTe.*

Coefficient	Value
$d\varepsilon_s/dT$ (10^{-3} K^{-1})	2.34±0.02 [10.14]
$d\varepsilon_\infty/dT$ (10^{-4} K^{-1})	
$d\varepsilon_s/dp$ (GPa^{-1})	
$d\varepsilon_\infty/dp$ (GPa^{-1})	

[10.14] I. Strzalkowski, S. Joshi, and C. R. Crowell, *Appl. Phys. Lett.* **28**, 350 (1976).

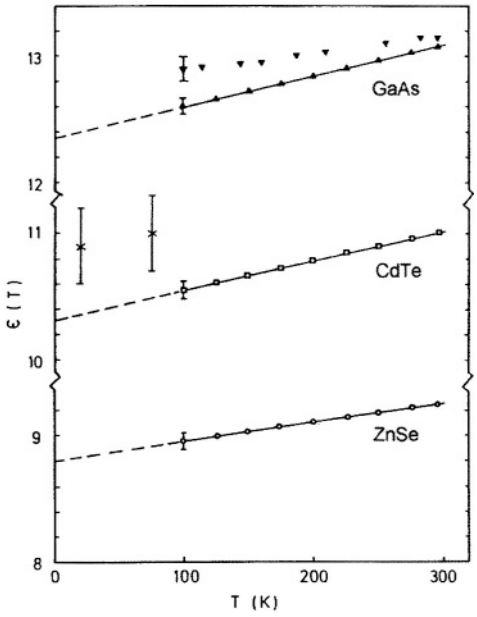

Fig. 14.10.3 Temperature dependence of the static dielectric constant ε_s (ε) for CdTe (□), together with those for GaAs (△) and ZnSe (○). The symbols are: (×) from D. de Nobel [*Philips Res. Rep.* **14**, 361 (1959)]; (▼) from K. S. Champlin and G. H. Glover [*Appl. Phys. Lett.* **12**, 23 (1968)]. [From I. Strzalkowski, S. Joshi, and C. R. Crowell, *Appl. Phys. Lett.* **28**, 350 (1976).]

- **Reststrahlen parameter**

Table 14.10.4 *A set of the reststrahlen parameters for CdTe.*

$$\varepsilon(\omega) = \varepsilon_\infty \left(1 + \frac{\omega_{LO}^2 - \omega_{TO}^2}{\omega_{TO}^2 - \omega^2 - i\omega\gamma} \right)$$

ε_∞	ω_{LO} (cm^{-1})	ω_{TO} (cm^{-1})	γ (cm^{-1})	Comment
7.1	165	144	2.2	T=100 K [10.15]
7.1	169	141	6.6	T=300 K [10.15]
7.1	168.6	140.7	8.7	T=300 K [10.16]
7.3	167.5	140.5	5	T=293 K [10.17]

[10.15] A. Manabe, A. Mitsuishi, and H. Yoshinaga, *Jpn. J. Appl. Phys.* **6**, 593 (1967).
[10.16] S. Perkowitz and R. H. Thorland, *Phys. Rev. B* **9**, 545 (1974).
[10.17] L. K. Vodopop'yanov, E. A. Vinogradov, V. V. Kolotkov, and Y. A. Mityagin, *Sov. Phys. Solid State* **16**, 912 (1914).

- **Multiphonon optical absorption spectra**

Several two-photon combination bands have been identified in the multiphonon absorption band region of CdTe by E. J. Danieleweicz and P. D. Coleman [*Appl. Opt.* **13**, 1164 (1974)].

14.10.3 At or Near the Fundamental Absorption Edge

• Free-exciton binding energy and related parameters

Table 14.10.5 *Free-exciton binding (Rydberg) energy G for CdTe.*

G (meV)	Comment
11	T=1.6–20 K [10.18]
10	[10.19]
10.5	T=1.64 K [10.20]
9.05	T=2 K [10.21]
10.4	T=10 K [10.22]

[10.18] D. G. Thomas, *J. Appl. Phys.* **32** (Suppl.), 2298 (1961).
[10.19] See, B. Segall and D. T. F. Marple, in *Physics and Chemistry of II–VI Compounds,* edited by M. Aven and J. S. Prener (North-Holland, Amsterdam, 1967), p. 317.
[10.20] M. Nawrocki and A. Twardowski, *Phys. Status Solidi B* **97**, K61 (1980).
[10.21] M. A. Abdullaev, S. I. Kokhanovskiĭ, O. S. Koshchug, and R. P. Seĭsyan, *Sov. Phys. Semicond.* **23**, 726(1989).
[10.22] G. N. Aliev, N. P. Gavaleshko, O. S. Koshchug, V. I. Pleshko, R. P. Seĭsyan, and K. D. Sushkevich, *Sov. Phys. Solid State* **34**, 1286 (1992).

Table 14.10.6 *Free-exciton parameters (G=binding energy; a_B=1st-orbital Bohr radius; μ=reduced mass) at the fundamental absorption edge of CdTe [10.23].*

G (meV)	a_B (Å)	μ (m_0)	Comment
10.5	65	0.085	Direct exciton

[10.23] From tabulation by S. Adachi [*Optical Properties of Crystalline and Amorphous Semiconductors: Materials and Fundamental Properties* (Kluwer Academic, Boston, 1999)].

Table 14.10.7 *Spin-exchange interaction constant j for CdTe [10.24].*

j (meV)
0.045

[10.24] See, M. Julier, J. Campo, B. Gil, J. P. Lascaray, and S. Nakamura, *Phys. Rev. B* **57**, R6791 (1998); D. W. Langer, R. N. Euwema, K. Era, and T. Koda, *Phys. Rev. B* **2**, 4005 (1970).

• Refractive index

Table 14.10.8 *Refractive index n near the fundamental absorption edge of CdTe at 300 K [10.25].*

E (eV)	λ (μm)	n	E (eV)	λ (μm)	n
0.1	12.395	2.683	0.9	1.377	2.752
0.2	6.198	2.697	0.95	1.305	2.762
0.3	4.132	2.700	1	1.240	2.773
0.4	3.099	2.701	1.05	1.180	2.785
0.5	2.479	2.703	1.1	1.127	2.798
0.55	2.254	2.707	1.15	1.078	2.813
0.6	2.066	2.712	1.2	1.033	2.830
0.65	1.907	2.717	1.254	0.988	2.852
0.7	1.771	2.723	1.304	0.951	2.874
0.75	1.653	2.729	1.354	0.915	2.898
0.8	1.549	2.736	1.405	0.882	2.932
0.85	1.458	2.744	1.455	0.852	2.989

[10.25] See, S. Adachi, *Optical Constants of Crystalline and Amorphous Semiconductors: Numerical Data and Graphical Information* (Kluwer Academic, Boston, 1999).

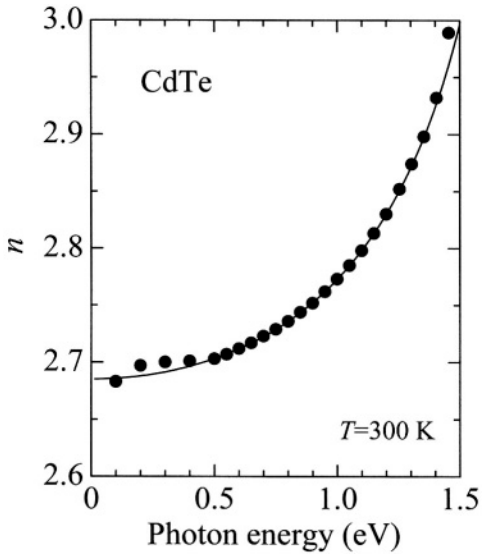

Fig. 14.10.4 Refractive index n for CdTe. The experimental data are taken from S. Adachi [*Optical Constants of Crystalline and Amorphous Semiconductors: Numerical Data and Graphical Information* (Kluwer Academic, Boston, 1999)]. The solid line represents the calculated result using $n^2=5.68+[1.53\lambda^2/(\lambda^2-0.366)]$ with λ in μm.

• Refractive index: Temperature dependence

Table 14.10.9 *Temperature coefficient of the refractive index* $n^{-1}(dn/dT)$ *in the long-wavelength limit for CdTe [10.26].*

$\frac{1}{n}\frac{dn}{dT}$ $(10^{-5}\ K^{-1})$
4.4

[10.26] See, S. Adachi, *Optical Properties of Crystalline and Amorphous Semiconductors: Materials and Fundamental Properties* (Kluwer Academic, Boston, 1999).

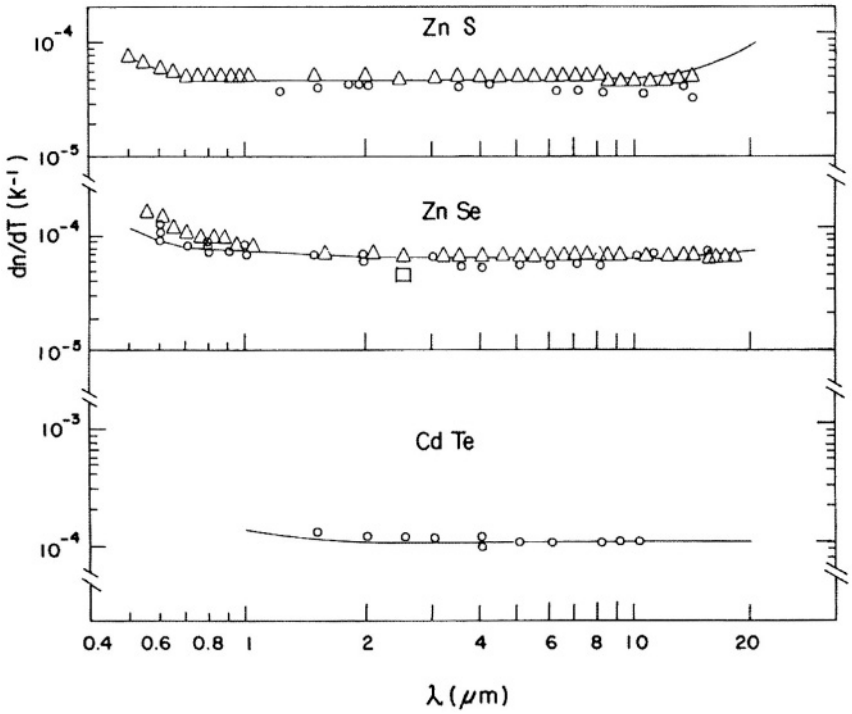

Fig. 14.10.5 Temperature coefficient of the refractive index dn/dT for CdTe, together with those for β-ZnS and ZnSe. [From M. Bertolotti, V. Bogdanov, A. Ferrari, A. Jascow, N. Nazorova, A. Pikhtin, and L. Schirone, *J. Opt. Soc. Am. B* **7**, 918 (1990).]

• **Fundamental absorption edge: Temperature dependence**

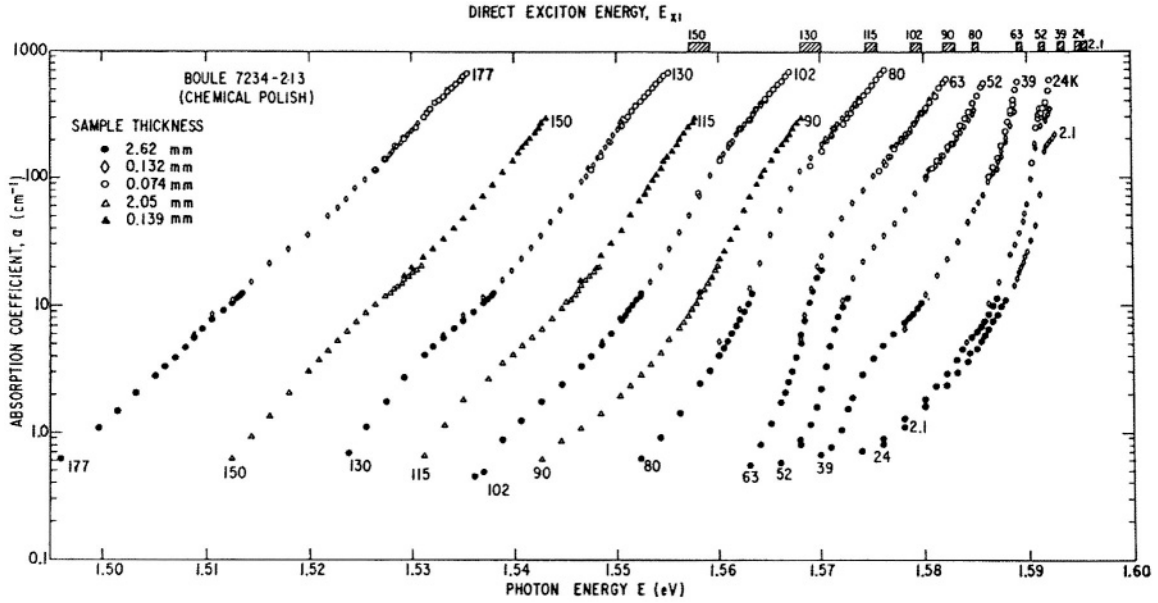

Fig. 14.10.6 Absorption coefficient α for the purest section of a zone-refined CdTe ingot as a function of photon energy E and temperature T. The samples were prepared by chemical polishing. [From D. T. F. Marple, *Phys. Rev.* **150**, 728 (1966).]

• **Fundamental absorption edge: Urbach tail**

The Urbach tail in CdTe has been investigated by J. T. Mullins, J. Carles, and A. W. Brinkman [*J. Appl. Phys.* **81**, 6374 (1997)].

• **Fundamental absorption edge: Pressure dependence**

The shift in the fundamental absorption edge with hydrostatic pressure for CdTe has been studied by J. González, F. V. Pérez, E. Moya, and J. C. Chervin [*J. Phys. Chem. Solids* **56**, 335 (1995)].

14.10.4 The Interband Transition Region

• **Fundamental optical spectra**

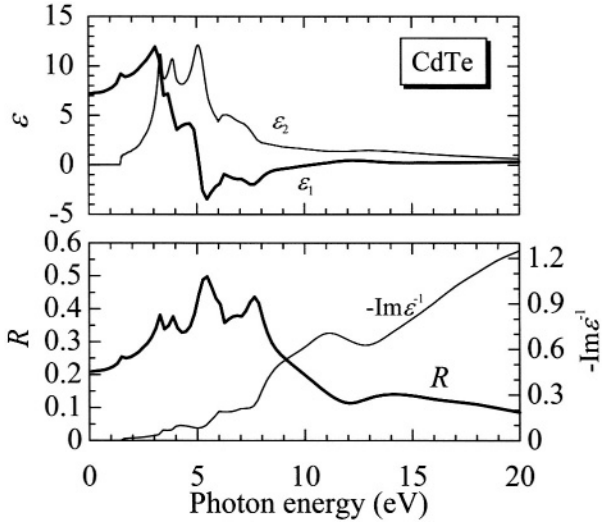

Fig. 14.10.7 Complex dielectric function, $\varepsilon(E)=\varepsilon_2(E)+i\varepsilon_2(E)$, fundamental reflectivity, $R(E)$, and energy-loss function, $-\mathrm{Im}\varepsilon^{-1}(E)$, for CdTe at 300 K. The experimental data are taken from tabulation by S. Adachi [*Optical Constants of Crystalline and Amorphous Semiconductors: Numerical Data and Graphical Information* (Kluwer Academic, Boston, 1999)].

• **$\varepsilon(E)$ spectrum: External perturbation and/or doping effects**

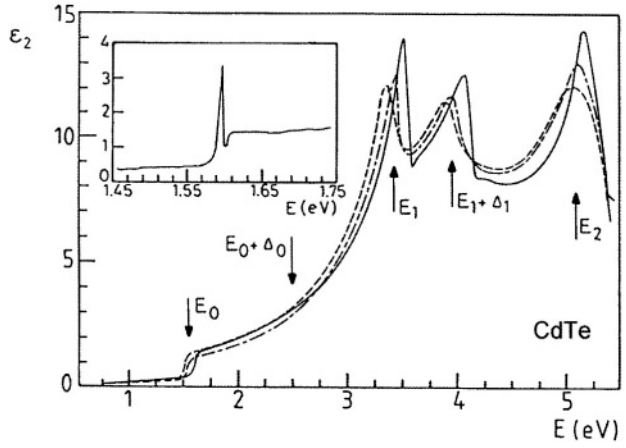

Fig. 14.10.8 Imaginary part $\varepsilon_2(E)$ of the dielectric function of CdTe measured at T=20 K (—), 208 K (–·–), and 294 K (- - -) obtained with a spectral width of 10 meV. The inset shows a magnified view of $\varepsilon_2(E)$ around the fundamental gap as obtained with a spectral width of 1 meV (T=20 K). [From J. T. Benhlal, K. Strauch, R.Granger, and R. Triboulet, *Opt. Mater.* **12**, 143 (1999).]

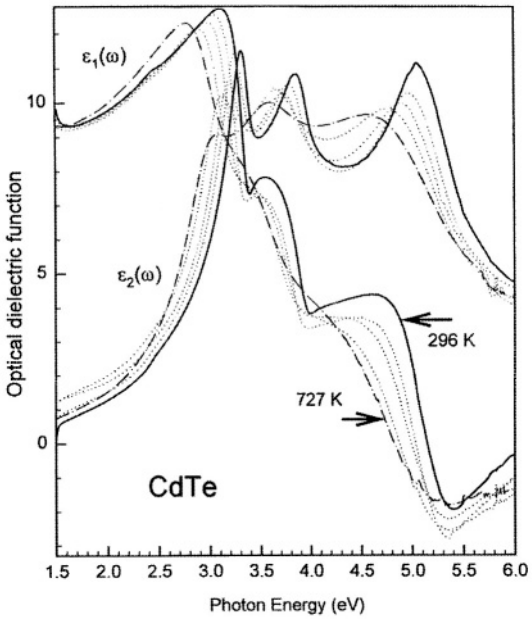

Fig. 14.10.9 Real $\varepsilon_1(\omega)$ and imaginary parts $\varepsilon_2(\omega)$ of the dielectric function of CdTe measured at temperatures T=296, 389, 503, 615, and 727 K. Note that the intermediate-temperature data are shown by the dotted lines. [From C. C. Kim, M. Daraselia, J. W. Garland, and S. Sivananthan, *Phys. Rev. B* **56**, 4786 (1997).]

14.10.5 Free-Carrier Absorption and Related Phenomena

No detailed data are available for CdTe.

14.11 ELASTOOPTIC, ELECTROOPTIC, AND NONLINEAR OPTICAL PROPERTIES

14.11.1 Elastooptic Effect

• **Photoelastic constant**

Table 14.11.1 *Photoelastic constant p_{ij} in the static limit ($E \to 0$ eV) for CdTe.*

$p_{11}-p_{12}$	p_{44}
–0.135	–0.057

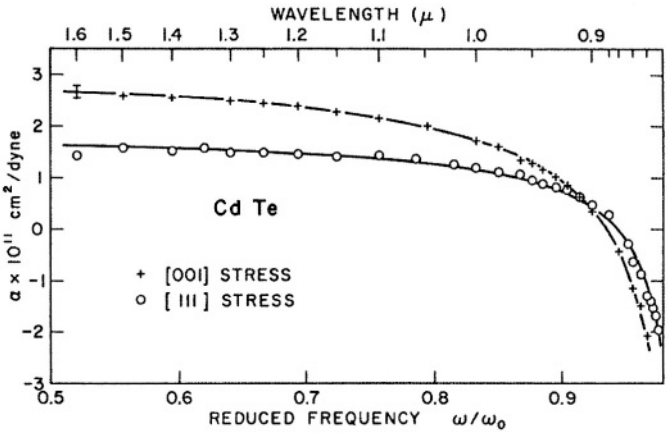

Fig. 14.11.1 Dispersion of the photoelastic coefficient α (α_{pe}) for CdTe with [100] and [111] compressive stresses at 300 K. The solid lines represent the theoretically obtained dispersion curves. [From P. Y. Yu and M. Cardona, *J. Phys. Chem. Solids* **34**, 29 (1973).]

14.11.2 Linear Electrooptic Constant

Table 14.11.2 *Free (r_{41}^T) and clamped values (r_{41}^S) of the linear electrooptic constant for CdTe.*

Wavelength (μm)	$\lvert r_{41}^T \rvert$ (pm/V)	$\lvert r_{41}^S \rvert$ (pm/V)	Ref.
1.0	4.5		[11.1]
1.5	5.4	4.0	[11.2]
3.39	6.8		[11.3]
10.6	6.8		[11.3]
	5.5	4.1	[11.4]
23.35	5.47		[11.5]
27.95	5.04		[11.5]

[11.1] See, K. Tada and M. Aoki, *Jpn. J. Appl. Phys.* **10**, 998 (1971).
[11.2] A. Zappettini, L. Cerati, A.Milani, S. M. Pietralunga, P. Boffi, and M. Martinelli, *J. Electron. Mater.* **30**, 743 (2001).
[11.3] J. E. Kiefer and A. Yariv, *Appl. Phys. Lett.* **15**, 26 (1969).
[11.4] G. L. Herrit and H.E. Reedy, *Mat. Res. Soc. Symp. Proc.* **152**, 169 (1989).
[11.5] C. J. Johnson, *Proc. IEEE* **56**, 1719 (1968).

• Temperature dependence

Table 14.11.3 *Temperature coefficient of the linear electrooptic constant $(1/r_{41})(dr_{41}/dT)$ for CdTe.*

$\frac{1}{r_{41}}\frac{dr_{41}}{dT}$ (10^{-4} K^{-1})	Comment
<<3	λ=0.6328, 1.0 μm [11.6]

[11.6] T. G. Okroashvili, *Opt. Spectrosc.* **47**, 442 (1979).

14.11.3 Quadratic Electrooptic Constant

No detailed data are available for CdTe.

14.11.4 Franz–Keldysh Effect

No detailed data are available for CdTe.

14.11.5 Nonlinear Optical Constant

• Second-order nonlinear optical susceptibility

Table 14.11.4 *Experimental second-order nonlinear optical susceptibility d_{14} for CdTe.*

Wavelength, in μm (Energy, in eV)	d_{14} (pm/V)*	Ref.
1.064 (1.165)	109	[11.7]
1.548 (0.8007)	73	[11.7]
1.9 (0.65)	71	[11.8]
10.6 (0.117)	170	[11.9]
28.0 (0.044)	59	[11.10]

[11.7] I. Shoji, T. Kondo, A. Kitamoto, M. Shirane, and R. Ito, *J. Opt. Soc. Am. B* **14**, 2268 (1997).
[11.8] A. Zappettini, S. M. Pietralunga, A. Milani, D. Piccinin, M. Feré, and M. Martinelli, *J. Electron. Mater.* **30**, 738 (2001).
[11.9] C. K. N. Patel, *Phys. Rev. Lett.* **16,** 613 (1966).
[11.10] G. H. Sherman and P. D. Coleman, *J. Appl. Phys.* **44**, 238 (1973).
*1 m/V=$3\times10^4/4\pi$ esu.

• Third-order nonlinear optical susceptibility

Table 14.11.5 *Experimental third-order nonlinear optical susceptibility $\chi^{(3)}(\omega)$ observed in CdTe [11.11].*

Wavelength (μm)	$\lvert\chi^{(3)}(\omega)\rvert$ (10^{-11} esu)*
1.064	72±21

[11.11] E. J. Canto-Said, D. J. Hagan, J. Young, and E. W. Van Stryland, *IEEE Quantum Electron.* **27**, 2274 (1991).
*1 $m^2/V^2=9\times10^8/4\pi$ esu.

Table 14.11.6 *Theoretical third-order nonlinear optical susceptibility $\chi^{(3)}_{ijkl}(-3\omega;\omega,\omega,\omega)$ in the static limit ($\hbar\omega\to0$ eV) for CdTe.*

$\chi^{(3)}_{ijkl}$ (10^{-11} esu)*		Ref.
$\chi^{(3)}_{1111}$	$\chi^{(3)}_{1212}$	
0.03	0.67	[11.12]
5.41	4.02	[11.13]

[11.12] Ed Ghahramani, D. J. Moss, and J. E. Sipe, *Phys. Rev. B* **43**, 9700 (1991).
[11.13] W.Y. Ching and M.-Z. Huang, *Phys. Rev. B* **47**, 9479 (1993).
*1 $m^2/V^2=9\times10^8/4\pi$ esu.

• Two-photon optical absorption

Table 14.11.7 *Two-photon absorption coefficient β for CdTe.*

Wavelength (μm)	β (cm/GW)	Ref.
1.064	130	[11.14]
	170	[11.15]
	22	[11.16]
	26	[11.17]

[11.14] M. Bass, E. W. Van Stryland, and A. F. Stewart, *Appl. Phys. Lett.* **34**, 142 (1979).
[11.15] I. M. Catalano and A. Cingolani, *Solid State Commun.* **43**, 213 (1982).

[11.16] E. W. Van Stryland, H. Vanherzeele, M. A. Woodall, M. J. Soileau, A. L. Smirl, S. Guha, and T. F. Boggess, *Opt. Eng.* **24**, 613 (1985).
[11.17] A. A. Said, M. Sheik-Bahae, D. J. Hagan, T. H. Wei, J. Wang, J. Young, and E. W. Van Stryland, *J. Opt. Soc. Am. B* **9**, 405 (1992).

14.12 CARRIER TRANSPORT PROPERTIES

14.12.1 Low-Field Mobility: Electrons

Table 14.12.1 *300-K (μ_{300K}) and peak Hall mobilities (μ_{peak}) for electrons in CdTe.*

Mobility	Value (cm^2/V s)	Comment
μ_{300K}	1050	[12.1]
μ_{peak}	1×10^5	T~30 K [12.2]

[12.1] B. Segall, M. R. Lorenz, and R. E. Halsted, *Phys. Rev.* **129**, 2471 (1963).
[12.2] See, D. L. Rode, in *Semiconductors and Semimetals,* edited by R. K. Willardson and A. C. Beer (Academic, New York, 1975), Vol. 10, p. 1.

- **Temperature dependence**

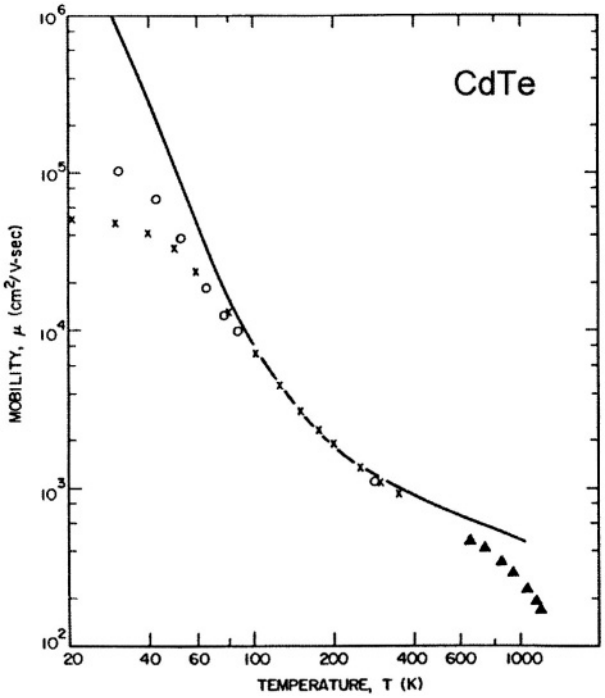

Fig. 14.12.1 Theoretical electron drift mobility μ versus temperature T for pure CdTe. The various symbols represent the experimental Hall mobility data. [From D. L. Rode, in *Semiconductors and Semimetals,* edited by R. K. Willardson and A. C. Beer (Academic, New York, 1975), Vol. 10, p. 1.]

- **Hall factor**

The Hall factor for CdTe has been obtained theoretically by D. L. Rode [*Phys. Status Solidi B* **55**, 687 (1973)], and its value is reported to be $\gamma \sim 1.04$ at T=300 K.

14.12.2 Low-Field Mobility: Holes

Table 14.12.2 *300-K (μ_{300K}) and peak Hall mobilities (μ_{peak}) for holes in CdTe.*

Mobility	Value (cm^2/V s)	Comment
μ_{300K}	104	Epilayer on GaAs(100) substrate, p=2.2×10^{15} cm^{-3} [12.3]
μ_{peak}	1200	T=170 K [12.4]

[12.3] K. Yasuda, M. Ekawa, N. Matsui, S. Sone, Y. Sugiura, A. Tanaka, and M. Saji, *Jpn. J. Appl.* Phys. **29**, 479(1990).
[12.4] D. de Nobel, *Philips Res. Rep.* **14**, 361 (1959); **14**, 430 (1959).

- **Temperature dependence**

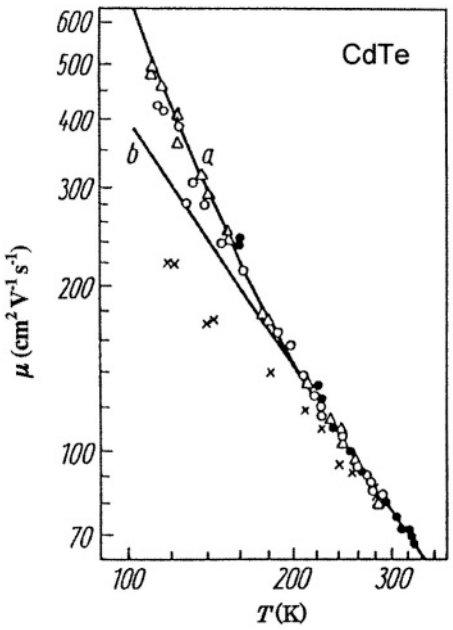

Fig. 14.12.2 Hole Hall mobility μ versus temperature T for CdTe. (a) $\mu(T)=57[\exp(252/T)-1]$; (b) $\mu(T)=4\times10^5 T^{-3/2}$. [From S. Yamada, *J. Phys. Soc. Jpn* **15**, 1940 (1960).]

14.12.3 High-Field Transport: Electrons

- **Electron drift velocity–field characteristic**

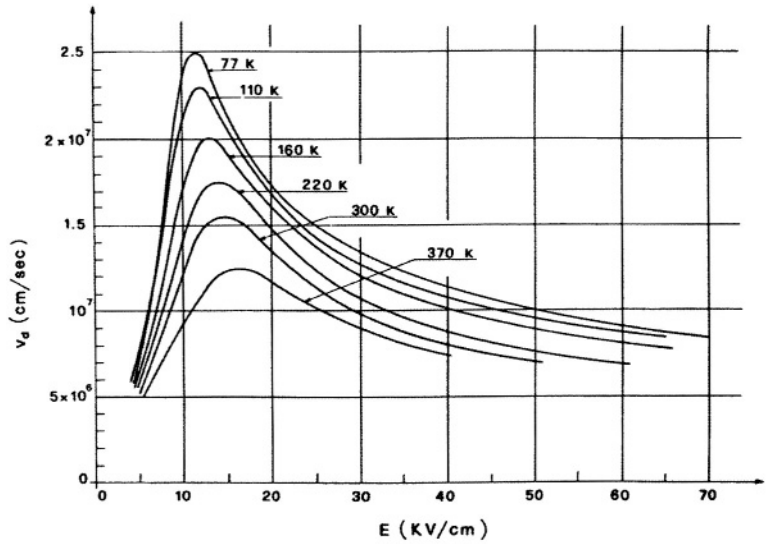

Fig. 14.12.3 Electron drift velocity v_d (v_e) in high-resistivity CdTe as a function of electric field E at different temperatures. [From C. Canali, M. Martini, G. Ottaviani, and K. R. Zanio, *Phys. Rev. B* **4**, 422 (1971).]

• **LO-phonon-scattering-limited electron saturation drift velocity**

Table 14.12.3 *Calculated LO-phonon-scattering-limited electron saturation drift velocity* $v_{e,sat}$ *in the lowest-conduction-band valley* α *for CdTe at 300 K.**

$$v_{e,sat}^{\alpha} = \left(\frac{8\hbar\omega_{LO}}{3\pi m_c^{\alpha}} \right)^{1/2}$$

Valley	$v_{e,sat}$ (10^7 cm/s)
Γ	1.9

*Calculated with $m_c^{\Gamma} = 0.090 m_0$ and $\omega_{LO} = 167$ cm^{-1}.

14.12.4 High-Field Transport: Holes

• **Hole drift velocity–field characteristic**

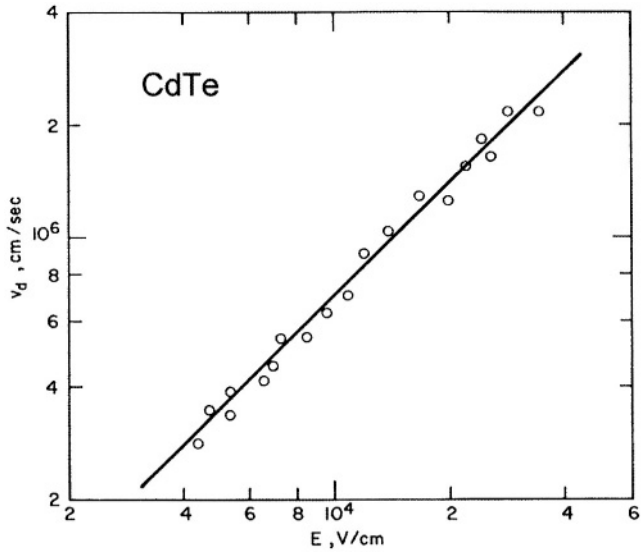

Fig. 14.12.4 Hole drift velocity v_d (v_h) in CdTe as a function of electric field E at room temperature. [From C. Canali, G. Ottaviani, M. Martini, and K. Zanio, *Appl. Phys. Lett.* **19**, 51 (1971).]

14.12.5 Minority-Carrier Transport: Electrons in *p*-Type Materials

• **Minority-electron diffusion length**

Table 14.12.4 *Minority-electron diffusion length L in p-type CdTe at room temperature.*

L (μm)	Comment
0.87	$p = 5\times10^{14}$ cm^{-3} [12.5]
0.58	$p = 2\times10^{15}$ cm^{-3} [12.5]
0.6	$p = 2\times10^{15}$ cm^{-3} [12.5]
0.74	$p = 7\times10^{15}$ cm^{-3} [12.5]
1.6	$p = 4\times10^{15}$ cm^{-3} [12.6]

[12.5] P. Gaugash and A. G. Milnes, *J. Electrochem. Soc.* **128**, 921 (1981).
[12.6] J. Gautron and P. Lemasson, *J. Cryst. Growth* **59**, 332 (1982).

14.12.6 Minority-Carrier Transport: Holes in *n*-Type Materials

● **Minority-hole diffusion length**

Table 14.12.5 *Minority-hole diffusion length L in n-type CdTe at room temperature.*

L (μm)	Comment
1.6	$n=3\times10^{16}$ cm^{-3}, $\rho=10$ Ω·cm [12.7]
2.8	$n=7\times10^{16}$ cm^{-3}, $\rho\sim10$ Ω·cm [12.7]
1.05	$n=1\times10^{17}$ cm^{-3}, $\rho\sim0.1$ Ω·cm [12.7]
2.8	$n=2\times10^{17}$ cm^{-3}, $\rho\sim0.1$ Ω·cm [12.7]
1.3–2.4	$\rho=0.01$ Ω·cm [12.7]
0.14	$n=8.5\times10^{17}$ cm^{-3} [12.8]
5.0	$n=2\times10^{13}$ cm^{-3} [12.9]
1.75	$n=8\times10^{14}$ cm^{-3} [12.9]
0.74	$n=4\times10^{15}$ cm^{-3} [12.9]
0.13	$n=8\times10^{17}$ cm^{-3} [12.9]

[12.7] P. Gaugash and A. G. Milnes, *J. Electrochem. Soc.* **128**, 921 (1981).
[12.8] A. Etchebery, M. Etman, B. Fotouhi, J. Gautron, J.-L. Sculfort, and P. Lemasson, *J. Appl. Phys.* **53**, 8867 (1982).
[12.9] J. Gautron and P. Lemasson, *J. Cryst. Growth* **59**, 332 (1982).

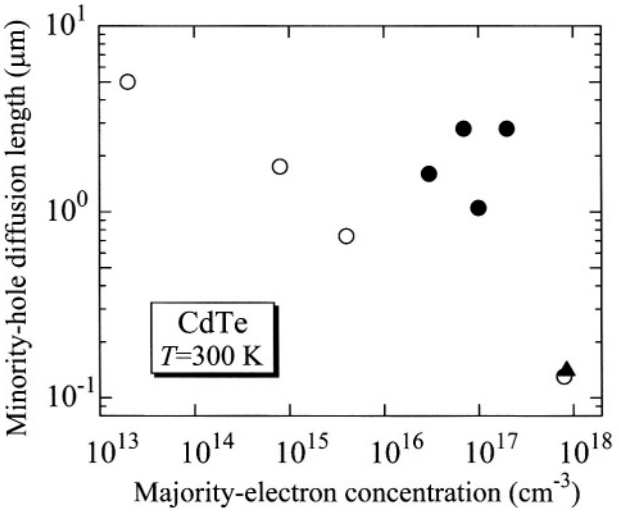

Fig. 14.12.5 Minority-hole diffusion length L versus majority-electron concentration n in n-type CdTe at room temperature. (○) J. Gautron and P. Lemasson, *J. Cryst. Growth* **59**, 332 (1982); (▲) A. Etchebery, M. Etman, B. Fotouhi, J. Gautron, J.-L. Sculfort, and P. Lemasson, *J. Appl. Phys.* **53**, 8867 (1982); (●) P. Gaugash and A. G. Milnes, *J. Electrochem. Soc.* **128**, 921 (1981).

14.12.7 Impact Ionization Coefficient

No detailed data are available for CdTe.

Chapter 15

Cubic Mercury Sulphide (β-HgS)

15.1 STRUCTURAL PROPERTIES

15.1.1 Ionicity

Table 15.1.1 *Phillips's ionicity f_i for β-HgS [1.1].*

f_i
0.790

[1.1] J. C. Phillips, *Bonds and Bands in Semiconductors* (Academic, New York, 1973).

15.1.2 Elemental Isotopic Abundance and Molecular Weight

- **Isotopic abundance**

Table 15.1.2 *Isotopic abundance in percent for mercury and sulfur [1.2].*

Isotope	% nat. abundance	Isotope	% nat. abundance
^{196}Hg	0.15	^{32}S	95.02
^{198}Hg	9.97	^{33}S	0.75
^{199}Hg	16.87	^{34}S	4.21
^{200}Hg	23.10	^{36}S	0.02
^{201}Hg	13.18		
^{202}Hg	29.86		
^{204}Hg	6.87		

[1.2] D. R. Lide, *CRC Handbook of Chemistry and Physics,* 78th Edition (CRC Press, Boca Raton, 1997).

• **Molecular weight**

Table 15.1.3 *Molecular (average atomic) weight M for β-HgS.*

M (amu)
232.66

15.1.3 Crystal Structure and Space Group

Table 15.1.4 *Crystal structure and its space and pint groups for β-HgS.*

Crystal structure	Space group	Point group
Zincblende (Cubic)	$F\bar{4}3m$	T_d

*Note that under atmospheric pressure HgS crystallizes in the trigonal cinnabar structure (α-HgS).

15.1.4 Lattice Constant and Its Related Parameters

• **Lattice constant, near-neighbor distance, etc.**

Table 15.1.5 *Lattice constant (a), near-neighbor distance (d), unit cube volume (a^3), and molecular density (d_M) for β-HgS at 300 K.*

Parameter	Value
Lattice constant a (Å)	5.8514±0.0003 [1.3]
d (Cation–Anion) (Å)	2.534*
d (Cation–Cation) (Å)	4.138*
Unit cube volume a^3 (10^{-22} cm^3)	2.003*
Molecular density d_M (10^{22} cm^{-3})	1.997*

[1.3] T. Ohmiya, *J. Appl. Cryst.* **7**, 396 (1974).
*Calculated.

• **Crystal density**

Table 15.1.6 *Crystal density g for β-HgS at 300 K.**

g (g/cm^3)
7.713

*Calculated using a=5.8514 Å.

15.1.5 Structural Phase Transition

Table 15.1.7 *Structural phase transition in β-HgS at high pressures.*

Structure	Transition pressure (GPa)
Zincblende ($F\bar{4}3m$)	Normal pressure
Trigonal (cinnabar, α-HgS)	* [1.4]

[1.4] A. N. Mariano and E. P. Warekois, *Science* **142**, 672 (1963).
*No attempt was made to accurately determine the transition pressure.

Table 15.1.8 *Structural phase transition in β-HgS at high temperatures [1.5].*

Transition	Temperature (°C)
β-HgS (zincblende)→α-HgS (trigonal)	100
α-HgS (trigonal)→β-HgS (zincblende)	362

[1.5] T. Ohmiya, *J. Appl. Cryst.* **7**, 396 (1974).

15.1.6 Cleavage Plane

Table 15.1.9 *Crystallographic plane most readily cleaved for β-HgS.**

Cleavage plane
(100)

*Expected.

• **Surface energy**

Table 15.1.10 *Surface energy for β-HgS (in J/m^2).*

Plane			Comment
(110)	(111)	$(\bar{1}\,\bar{1}\,\bar{1})$	
1.13	1.00	0.73	Calc. [1.6]

[1.6] B. N. Oshcherin, *Phys. Status Solidi A* **34**, K181 (1976).

15.2 THERMAL PROPERTIES

15.2.1 Melting Point and Its Related Parameters

Table 15.2.1 *Melting point T_m and its related parameters for HgS.*

Parameter	Value
Melting point T_m (K)	1723 [2.1]
Entropy of fusion ΔS_m (cal/mol K)	14.2 [2.2]

[2.1] P. H. Hamilton, *Semicond. Prod. Solid State Technol.* **7**, 15 (1964).
[2.2] A. Pajaczkowska and Z. Dziuba, *J. Cryst. Growth* **11**, 21 (1971).

15.2.2 Specific Heat

No detailed data are available for β-HgS.

15.2.3 Debye Temperature

Table 15.2.2 *Debye temperature θ_D for β-HgS.*

θ_D (K)	Comment
178	T=0 K [2.3]

[2.3] In the low-temperature (0 K) limit [see, H. Siethoff and K. Ahlborn, *Phys. Status Solidi B* **190**, 179 (1995)].

15.2.4 Thermal Expansion Coefficient

Table 15.2.3 *Thermal expansion coefficient α_{th} for β-HgS.*

α_{th} (10^{-6} K^{-1})	T (K)	Ref.
4.3±1.4	484–621	[2.4]

[2.4] T. Ohmiya, *J. Appl. Cryst.* **7**, 396 (1974).

15.2.5 Thermal Conductivity and Diffusivity

No detailed data are available for β-HgS.

15.3 ELASTIC PROPERTIES

15.3.1 Elastic Constant

- **Room-temperature value**

Table 15.3.1 *Elastic stiffness and compliance constants for β-HgS at 300 K.*

Parameter	Value
Stiffness (10^{11} dyn/cm^2) [3.1]	
C_{11}	8.13
C_{12}	6.22
C_{44}	2.64
Compliance (10^{-12} cm^2/dyn) [3.1]	
S_{11}	3.65
S_{12}	−1.58
S_{44}	3.79

[3.1] *Numerical Data and Functional Relationships in Science and Technology,* edited by K.-H. Hellwege and A. M. Hellwege, Landolt–Börnstein, New Series, Group III, Vol. 11 (Springer, Berlin, 1979).

15.3.2 Third-Order Elastic Constant

No detailed data are available for β-HgS.

15.3.3 Young's Modulus, Poisson's Ratio, and Similar

- **Young's modulus**

Table 15.3.2 *Young's modulus Y for β-HgS at 300 K.**

Crystallographic plane	Y (10^{11} dyn/cm^2)
(100) plane	
[001] direction	2.74
[011] direction	5.04
(110) plane	
[001] direction	2.74
[111] direction	7.01
(111) plane	5.04

*Calculated using S_{11}=3.65, S_{12}=−1.58, and S_{44}=3.79 (all in 10^{-12} cm^2/dyn).

- **Poisson's ratio**

Table 15.3.3 *Poisson's ratio P for β-HgS at 300 K.**

Crystallographic plane	*P*
(100) plane	
m=[010], n=[001]	0.433
m=[011], n=[0$\bar{1}$1]	–0.044
(110) plane	
m=[001], n=[1$\bar{1}$0]	0.433
m=[1$\bar{1}$1], n=[1$\bar{1}\bar{2}$]	0.328
(111) plane	0.517

*Calculated using S_{11}=3.65, S_{12}= –1.58, and S_{44}=3.79 (all in 10^{-12} cm^2/dyn).

- **Bulk modulus, shear modulus, etc.**

Table 15.3.4 *Bulk modulus, B_u, pressure derivative of B_u, dB_u/dp, shear modulus, C_s, isotropy factor, A, linear compressibility, C_o, Caucy ratio, C_a, and Born ratio, B_o, for β-HgS at 300 K.*

Parameter	Value
B_u (10^{11} dyn/cm^2)	6.86 [3.2]
dB_u/dp	5.0 [3.3]
C_s (10^{10} dyn/cm^2)	9.55 [3.2]
A	0.362 [3.2]
C_o (10^{-13} cm^2/dyn)	4.86 [3.2]
C_a	2.36 [3.2]
B_o	1.15 [3.2]

[3.2] Calculated using C_{11}=8.13, C_{12}=6.22, and C_{44}=2.64 (all in 10^{11} dyn/cm^2).
[3.3] Theor. [S.-H. Wei and A. Zunger, *Phys. Rev. B* **60**, 5404 (1999)].

15.3.4 Microhardness

The variation of microhardness H with ionicity in HgSe nad HgTe suggests a very small value of H for β-HgS [L. Garbato and A. Rucci, *Phil. Mag.* **35**, 1681 (1977)].

15.3.5 Sound Velocity

Table 15.3.5 *Sound velocity propagating in β-HgS at 300 K.* LA=longitudinal acoustic; TA1, TA2=transverse acoustic.*

Propagation direction	Mode	Sound velocity (10^5 cm/s)
[100]	LA	3.25
[100]	TA1, TA2	1.85
[110]	LA	3.57
[110]	TA1	1.11
[110]	TA2	1.85
[111]	LA	3.67
[111]	TA1, TA2	1.40

*Calculated using C_{11}=8.13×10^{11} dyn/cm^2, C_{12}=6.22×10^{11} dyn/cm^2, C_{44}=2.64×10^{11} dyn/cm^2, and g=7.713 g/cm^3.

15.4 PHONONS AND LATTICE VIBRONIC PROPERTIES

15.4.1 Phonon Dispersion Relation

• **Dispersion curve**

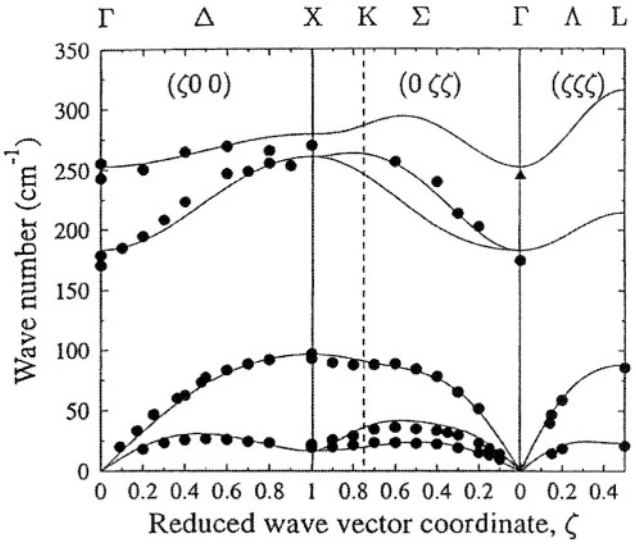

Fig. 15.4.1 Phonon dispersion curves along the high symmetry directions in the Brillouin zone for β-HgS at low temperature. The experimental results are represented by the solid circles and triangles, while the solid lines show the theoretical results obtained by the non-central version of the rigid ions model. [From W. Szuszkiewicz, K. Dybko, B.Hennion, M. Jouanne, C. Julien, E. Dynowska, J. Górecka, and B. Witkowska, *J. Cryst. Growth* **184/185**, 1204 (1998).]

15.4.2 Phonon Frequency

Table 15.4.1 *Long-wavelength ($q \to 0$) and zone-boundary phonon frequencies for β-HgS.*

Critical point	Phonon	Phonon frequency (cm^{-1})	
		Low temperature [4.1]	T=300 K [4.2]
Γ	TO	175	177.0±0.5
	LO	250	224±1
X	TA	21	
	LA	95	
	TO		
	LO		
L	TA	21	
	LA	85	
	TO		
	LO		

[4.1] W. Szuszkiewicz, K. Dybko, B.Hennion, M. Jouanne, C. Julien, E. Dynowska, J. Górecka, and B. Witkowska, *J. Cryst. Growth* **184/185**, 1204 (1998).
[4.2] H. D. Riccius and K. J. Siemsen, *J. Chem. Phys.* **52**, 4090 (1970).

15.4.3 Mode Grüneisen Parameter

No detailed data are available for β-HgS.

15.4.4 Phonon Deformation Potential

No detailed data are available for β-HgS.

15.5 COLLECTIVE EFFECTS AND RELATED PROPERTIES

15.5.1 Piezoelectric Constant

Table 15.5.1 *Piezoelectric stress (e_{14}), strain (d_{14}), and electromechanical coupling constants ($K_{[110]}^2$) for β-HgS [5.1].*

Parameter	Value
e_{14} (C/m^2)	+0.14
d_{14} (10^{-12} m/V)	+5.3 *
$K_{[110]}^2$	4.6×10^{-4} *

[5.1] Theor. [K. Hübner, *Phys. Status Solidi B* **57**, 627 (1973)].
*Calculated.

15.5.2 Fröhlich Coupling Constant

No detailed data are available for β-HgS.

15.6 ENERGY-BAND STRUCTURE: ENERGY-BAND GAPS

15.6.1 Basic Properties

- **Energy eigenvalue**

Table 15.6.1 Energyeigenvalues at the *Γ, X, and L points for the valence and first few conduction bands of β-HgS.*

Critical point	Level	Value (eV)	
		Calc. [6.1]	Exper.*
Γ	Γ_{15}^v	0.0	0.0, –0.07
	Γ_1^c	1.5	–(0.04~0.54)
	Γ_{15}^c	9.3	
X	X_3^v	–2.0	
	X_5^v	–0.8	
	X_1^c	4.3	
	X_3^c	8.3	
L	L_1^v	–2.7	
	L_3^v	–0.1	
	L_1^c	5.0	
	L_3^c	9.2	

[6.1] F. Herman, R. L. Kortum, C. D. Kuglin, and J. L. Shay, in *II–VI Semiconducting Compounds,* edited by D. G. Thomas (Benjamin, New York, 1967), p. 503.
*Obtained from various sources.

15.6.2 E_0-Gap Region

• General remark

The band structure of β-HgS is considered to be of the inverted type. The lowest-conduction-band minimum and the top of the valence band in β-HgS are degenerate at the center of the Brillouin zone (Γ point; k=0). The Γ_8 level is the fourfold component of the spin–orbit–split valence band. The Γ_6 level, which for most cubic semiconductor is the conduction-band minimum with an energy larger than the Γ_8 state, is locate below the Γ_8 state (i.e., *"negative"* energy gap, *"inverted"* band structure).

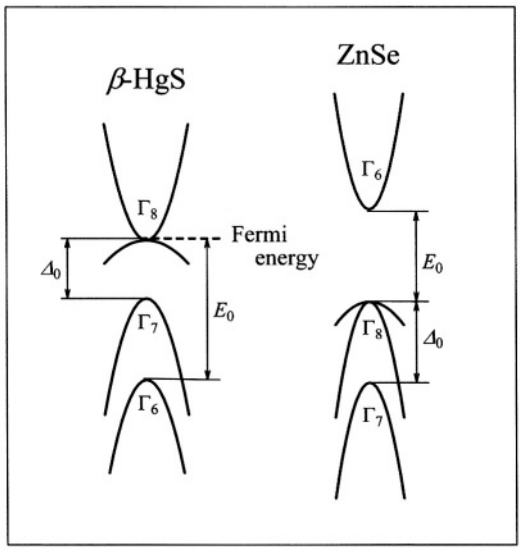

Fig. 15.6.1 Schematic diagram of the electronic energy-band structure of β-HgS and ZnSe at k=0. The bands are labeled in the double-group representation. In β-HgS, the band-gap energy between the Γ_8 conduction and valence bands is zero (semimetal). Note also that the diagram for β-HgS in the figure corresponds to the case at low temperatures (i.e., $|E_0|>|\Delta_0|$).

• E_0- and Δ_0-gap value

Table 15.6.2 *E_0-gap energy for β-HgS.*

E_0 (eV)	Comment
–0.2	T=300 K [6.2]
–0.54	Exper. (T=300 K) [6.3]
–0.22 *	T=4.2 K
–0.04 *	T=300 K

[6.2] Estimated from an E_0 versus x plot for $Zn_{1-x}Hg_xS$ [see, K. J. Siemsen and H. D. Riccius, *Phys. Status Solidi* **37**, 445 (1970)].
[6.3] K. J. Siemsen and H. D. Riccius, *Phys. Status Solidi* **37**, 445 (1970).
*Estimated from a plot of E_0 versus a (lattice constant) for β-HgS, HgSe, and HgTe (see figure, below).

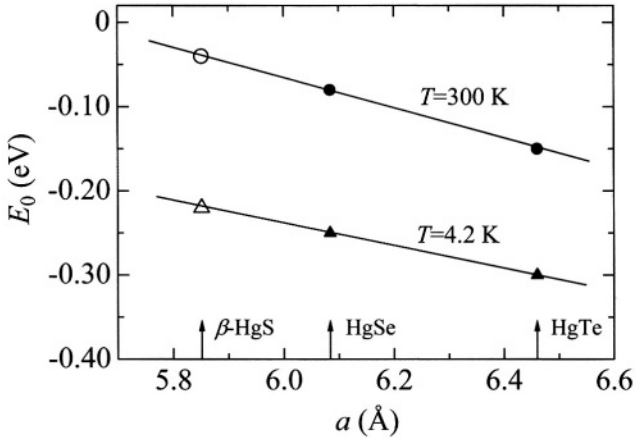

Fig. 15.6.2 Plot of E_0 versus a for HgSe and HgTe. From this plot, we can estimate E_0 value for β-HgS to be –0.22 eV at T=4.2 K and –0.04 eV at T=300 K.

Table 15.6.3 *Spin–orbit–splitoff energy Δ_0 for β-HgS.*

Δ_0 (eV)	Comment
0.11	Calc. [6.4]
0.07	*

[6.4] M. Willatzen, M. Cardona, and N. E. Christensen, *Phys. Rev. B* **51**, 17992 (1995).
* Estimated from Δ_0 values of the II–VI common-anion materials (see figure, below).

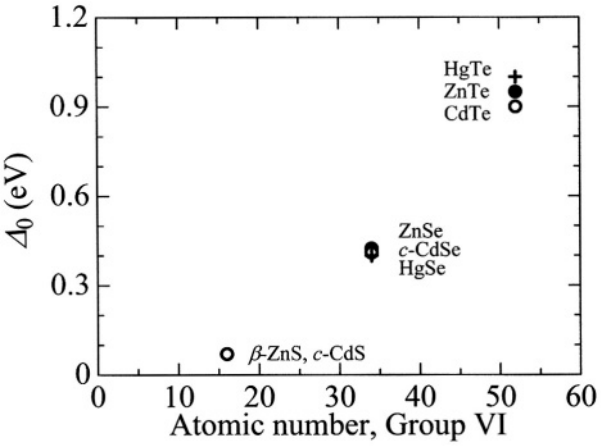

Fig. 15.6.3 Variation of Δ_0 for some II–VI binary semiconductors with respect to the corresponding group-VI (anion) atomic numbers. From this plot, we can estimate Δ_0 value for β-HgS to be 0.07 eV.

15.6.3 Higher-Lying Direct Gap

- **Theoretical and experimental values**

Table 15.6.4 *Theoretically and experimentally obtained higher-lying direct-gap energies for β-HgS.*

Band gap	Theoretical (eV) [6.5]	Experimental (eV) [6.6]
E_1 ($\Lambda_3^v \rightarrow \Lambda_1^c$)		3.54
($L_3^v \rightarrow L_1^c$)	5.1	4.62
		5.76
E_2 ($X_5^v \rightarrow X_1^c$)	5.1	6.43
$E_2+\delta$ ($X_5^v \rightarrow X_3^c$)	9.1	7.01, 8.05
E_0' ($\Gamma_{15}^v \rightarrow \Gamma_{15}^c$)	9.3	
E_1' ($L_3^v \rightarrow L_3^c$)	9.3	8.95

[6.5] F. Herman, R. L. Kortum, C. D. Kuglin, and J. L. Shay, in *II–VI Semiconducting Compounds,* edited by D. G. Thomas (Benjamin, New York, 1967), p. 503.
[6.6] H. D. Riccius and K. J. Siemsen, in *The Physics of Semimetals and Narrow-Gap Semiconductors,* edited by D. L. Carter and R.T. Bate (Pergamon, Oxford, 1971), p. 493.

15.6.4 Lowest Indirect Gap

- **Theoretical value**

Table 15.6.5 *Theoretically obtained lowest indirect-gap energy for β-HgS [6.7].*

Band gap	Value (eV)
E_g^L ($\Gamma_{15}^v \rightarrow L_1^c$)	5.0
E_g^X ($\Gamma_{15}^v \rightarrow X_1^c$)	4.3

[6.7] F. Herman, R. L. Kortum, C. D. Kuglin, and J. L. Shay, in *II–VI Semiconducting Compounds,* edited by D. G. Thomas (Benjamin, New York, 1967), p. 503.

• **Temperature and/or pressure coefficient**

Table 15.6.6 *Linear temperature and pressure coefficients of the lowest indirect-gap energy for β-HgS.*

Coefficient	Value	Comment
dE_g^L/dp (10^{-2} eV/GPa)	1.6	Calc. [6.8]
dE_g^X/dp (10^{-2} eV/GPa)	−1.9	Calc. [6.8]

[6.8] S.-H. Wei and A. Zunger, *Phys. Rev. B* **60**, 5404 (1999).

15.6.5 Conduction-Valley Energy Separation

No detailed data are available for β-HgS.

15.6.6 Direct–Indirect-Gap Transition Pressure

No detailed data are available for β-HgS.

15.7 ENERGY-BAND STRUCTURE: ELECTRON AND HOLE EFFECTIVE MASSES

15.7.1 Electron Effective Mass: Γ Valley

• **Theoretical value**

Table 15.7.1 *Theoretical electron effective mass m_e^Γ at the Γ_6 valley for β-HgS.*

m_e^Γ/m_0	Technique
−0.006*	Five-level $\boldsymbol{k}\cdot\boldsymbol{p}$ calculation [7.1]

[7.1] P. Lawaetz, *Phys. Rev. B* **4**, 3460 (1971).

*The sign is chosen positive for a normal band structure like that of CdTe (i.e., "−" means that free carriers behave like holes, not electrons).

15.7.2 Electron Effective Mass: Satellite Valley

No detailed data are available for β-HgS.

15.7.3 Hole Effective Mass

• **Luttinger's valence-band parameter**

Table 15.7.2 *Luttinger's valence-band parameter γ_i for β-HgS (in $\hbar^2/2m_0$).*

γ_1	γ_2	γ_3	Technique
−41.28	−21.00	−20.73	Five-level $\boldsymbol{k}\cdot\boldsymbol{p}$ calculation [7.2]

[7.2] P. Lawaetz, *Phys. Rev. B* **4**, 3460 (1971).

• **Band mass, cyclotron mass, etc.**

Table 15.7.3 *Band (m_{HH}, m_{LH}), density-of-states heavy-hole (m_{HH}*), averaged light-hole (m_{LH}*), and spherically-averaged heavy-hole (m_{HH}^s) and light-hole masses (m_{LH}^s) in β-HgS.*

Mass	Value (m_0)
m_{HH} ([001] direction)	1.39*[1]
m_{LH} ([001] direction)	–0.012*[1, *2]
m_{HH} ([111] direction)	5.56*[1]
m_{LH} ([111] direction)	–0.012*[1, *2]
m_{HH}*	–0.012*[1, *2]
	–0.055*[2] [7.3]
m_{LH}*	2.22*[1]
m_{HH}^s	2.53*[1]
m_{LH}^s	–0.012*[1, *2]

[7.3] n=7×10^{17} cm^{-3} [K. J. Siemsen and H. D. Riccius, *Phys. Status Solidi* **37**, 445 (1970)].
*[1] Calculated using a set of the Luttinger's parameters, γ_1=–41.28, γ_2=–21.00, and γ_3=–20.73.
*[2] The sign is chosen positive for a normal band structure like that of CdTe (i.e., "–" means that free carriers behave like electrons, not holes).

• **Spin–orbit–splitoff hole effective mass**

Table 15.7.4 *Spin–orbit–splitoff hole effective mass m_{SO} for β-HgS.*

m_{SO}/m_0	Technique
–0.013*	Five-level $\boldsymbol{k}\cdot\boldsymbol{p}$ calculation [7.4]

[7.4] P. Lawaetz, *Phys. Rev. B* **4**, 3460 (1971).
* The sign is chosen positive for a normal band structure like that of CdTe (i.e., "–" means that free carriers behave like electrons, not holes).

• **Doping dependence**

Table 15.7.5 *Doping-dependent electron effective mass m_n at the Γ_8-valence band in β-HgS [7.5].**

Functional expression
$\left(\frac{m_n}{m_0 - m_n}\right)^2 = 32.5\times10^{-32}\frac{E_g^2}{P^4} + 8.27\times10^{-30}\frac{n^{2/3}}{P^2}$
with E_g=–0.43 eV, P=3.5×10^{-8} eV cm, and n in cm^{-3}

[7.5] K. J. Siemsen and H. D. Riccius, *Phys. Status Solidi* **37**, 445 (1970).
*Note that the Γ_8-valence band in β-HgS (semimetal) behaves like conduction band. Thus, the free carriers at this band are electrons, not holes.

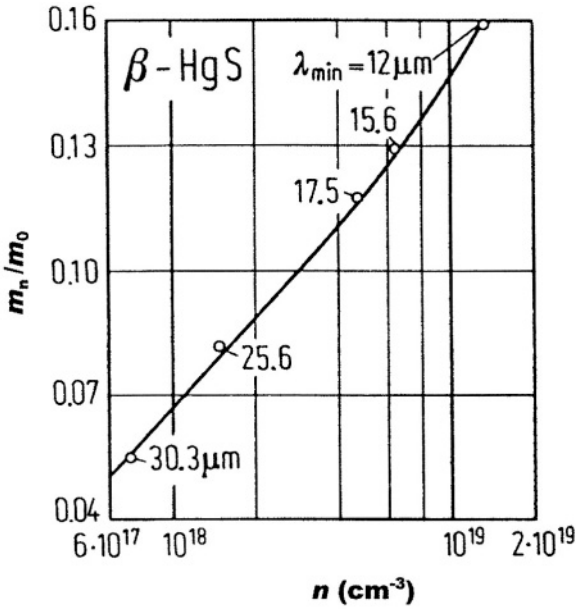

Fig. 15.7.1 Electron effective mass, m_n/m_0, at the "Γ_8-valence band" in β-HgS at T=293 K determined from reflectivity measurements. Plasma reflection minima depending on carrier density are observed at the wavelengths λ_{min}. [From K. J. Siemsen and H. D. Riccius, *Phys. Status Solidi* **37**, 445 (1970).]

15.8 ELECTRONIC DEFORMATION POTENTIAL

15.8.1 Intravalley Deformation Potential: Γ Point

- **Valence band**

Table 15.8.1 *Γ-valence-band deformation potentials a, b, and d for β-HgS.*

Deformation potential (eV)			Comment
a	*b*	*d*	
	−1.24		Calc. [8.1]

[8.1] T. Nakayama, *Solid-State Electron.* **37**, 1077 (1994).

- **E_0 gap**

Table 15.8.2 *Hydrostatic deformation potential a_0^Γ for the E_0 gap of β-HgS.*

a_0^Γ (eV)	Comment
−4.64	Calc. [8.2]
−2.16	Calc. [8.3]

[8.2] T. Nakayama, *Solid-State Electron.* **37**, 1077 (1994).
[8.3] S.-H. Wei and A. Zunger, *Phys. Rev. B* **60**, 5404 (1999).

15.8.2 Intravalley Deformation Potential: High-Symmetry Points

No detailed data are available for β-HgS.

15.8.3 Intervalley Deformation Potential

No detailed data are available for β-HgS.

15.9 ELECTRON AFFINITY AND SCHOTTKY BARRIER HEIGHT

15.9.1 Electron Affinity

No detailed data are available for β-HgS.

15.9.2 Schottky Barrier Height

No detailed data are available for β-HgS.

15.10 OPTICAL PROPERTIES

15.10.1 Summary of Optical Dispersion Relations

No detailed data are available for β-HgS.

15.10.2 The Reststrahlen Region

• Static and high-frequency dielectric constants

Table 15.10.1 *Static and high-frequency dielectric constants ε_s and ε_∞ for β-HgS.*

ε_s	ε_∞	Comment
30.6		T=300 K [10.1]
18.2	11.36	T=300 K [10.2]

[10.1] Z. I. Kir'iashkina, F. M. Popov, D. N. Bilenko, and V. I. Kir'iashkin, *Sov. Phys.–Tech. Phys.* **2**, 69 (1957).
[10.2] H. D. Riccius and K. J. Siemsen, *J. Chem. Phys.* **52**, 4090 (1970).

• Reststrahlen parameter

A complete set of the reststrahlen parameter for β-HgS have not yet been determined; however, far-infrared reflectivity spectra of $Hg_{1-x}Mn_xS$ alloy (x=0.02–0.33) have been reported by Z. V. Popović, N. Tomić, and A. Milutinović [*Phys. Statsus Solidi B* **197**, 315 (1996)].

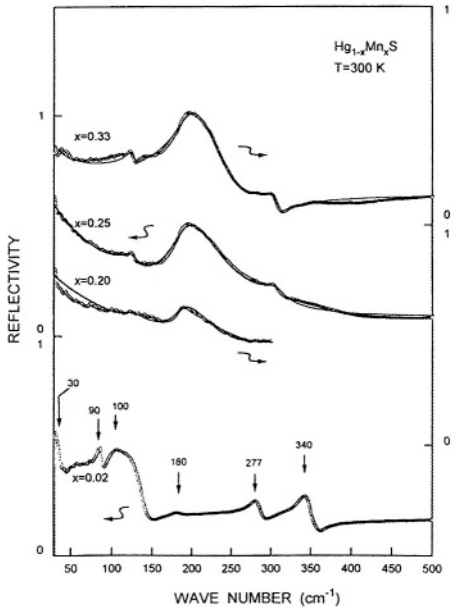

Fig. 15.10.1 Far-infrared reflectivity spectra of $Hg_{1-x}Mn_xS$ alloy (x=0.02–0.33) at 300 K. The experimental data are represented by the open circles, while the solid lines are calculated from a harmonic oscillator model including a term of the plasmon–phonon interaction. The oscillators of α-HgS around 30, 90, 100, 277, and 340 cm^{-1} are clearly seen (x=0.02), in complete agreement with the oscillators of this modification given by R. Zallen, G. Lucovsky, W. Taylor, A. Pinczuk, and E. Burstein [*Phys. Rev. B* **1**, 4058 (1970)]. Besides, an oscillator of β-HgS with highest intensity around 180 cm^{-1} is noticeable, too. [From Z. V. Popović, N. Tomić, and A. Milutinović, *Phys. Statsus Solidi B* **197**, 315 (1996).]

15.10.3 At or Near the Fundamental Absorption Edge

- **Fundamental absorption edge: Electron concentration/temperature dependence**

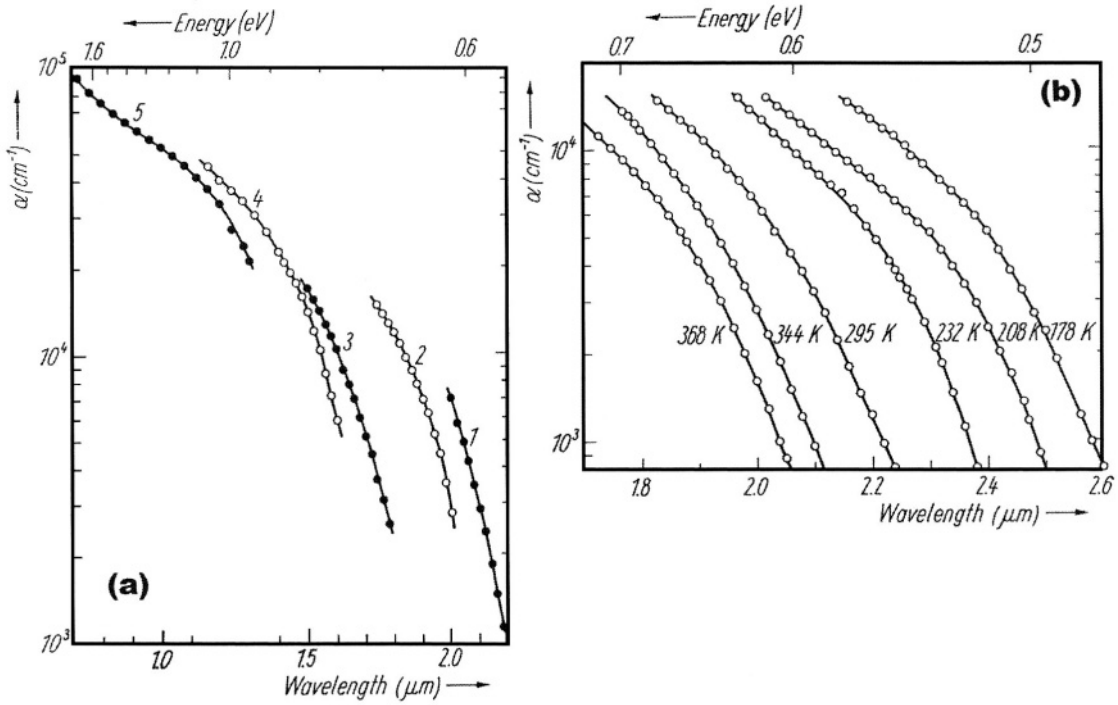

Fig. 15.10.2 (a) Absorption coefficient α as a function of wavelength for various β-HgS films with different thickness and electron concentration (T=300 K). 1: d=6.00 μm, n=1.46×10^{18} cm^{-3}; 2: d=2.46 μm, n=6.18×10^{18} cm^{-3}; 3: d=1.72 μm, n=1.05×10^{19} cm^{-3}; 4: d=0.69 μm, n=1.30×10^{19} cm^{-3}; 5: d=0.23 μm, n=2.92×10^{19} cm^{-3}. (b) Shift of the absorption edge of β-HgS with temperature from 178 to 368 K (d=6.00 μm, n=1.46×10^{18} cm^{-3}). [From K. J. Siemsen and H. D. Riccius, *Phys. Status Solidi* **37**, 445 (1970).]

15.10.4 The Interband Transition Region

- **Fundamental optical spectra**

Fundamental reflectivity measurements have been carried out on thin evaporated layers of β-HgS in the photon-energy range 0.5–10 eV at 295 K [H. D. Riccius and K. J. Siemsen, in *The Physics of Semimetals and Narrow-Gap Semiconductors,* edited by D. L. Carter and R.T. Bate (Pergamon, Oxford, 1971), p. 493].

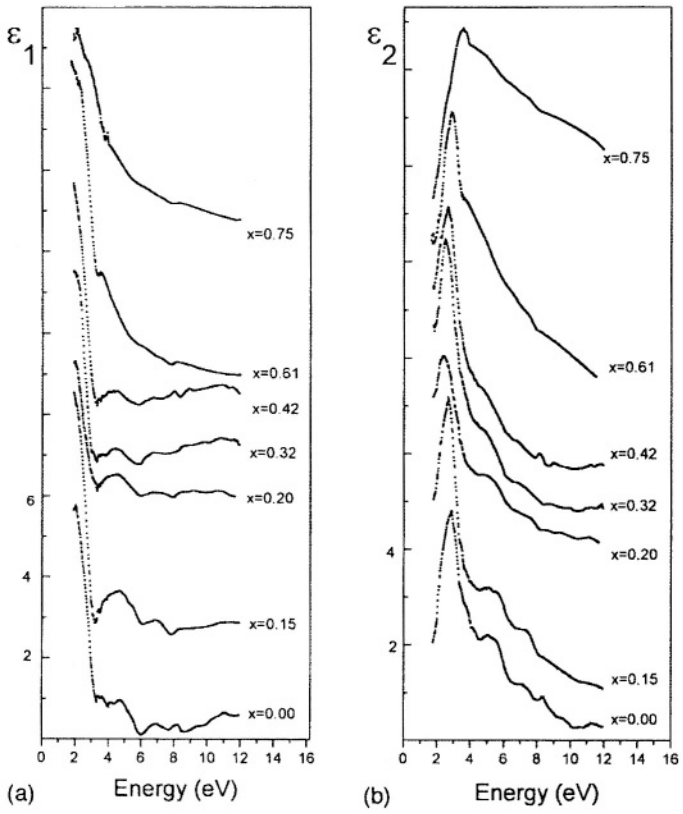

Fig. 15.10.3 (a) Real and (b) imaginary parts of the dielectric function, $\varepsilon(E)=\varepsilon_1(E)+i\varepsilon_2(E)$, for $HgSe_{1-x}S_x$ alloy (x=0–0.75) at 300 K. The samples measured were cut from $HgSe_{1-x}S_x$ crystals grown by a modified Bridgman method, and had a sphalerite crystal structure. [From E. Guziewicz, B. J. Kowalski, K. Szamota-Sadowska, W. Szuszkiewicz, and B. A. Orlowski, *Phys. Rev. B* **55**, 4405 (1997).]

15.10.5 Free-Carrier Absorption and Related Phenomena

No detailed data are available for β-HgS.

15.11 ELASTOOPTIC, ELECTROOPTIC, AND NONLINEAR OPTICAL PROPERTIES

15.11.1 Elastooptic Effect

No detailed data are available for β-HgS.

15.11.2 Linear Electrooptic Constant

No detailed data are available for β-HgS.

15.11.3 Quadratic Electrooptic Constant

No detailed data are available for β-HgS.

15.11.4 Franz–Keldysh Effect

No detailed data are available for β-HgS.

15.11.5 Nonlinear Optical Constant

No detailed data are available for β-HgS.

15.12 CARRIER TRANSPORT PROPERTIES

15.12.1 Low-Field Mobility: Electrons

Table 15.12.1 *300-K (μ_{300K}) and peak Hall mobilities (μ_{peak}) for electrons in β-HgS.*

Mobility	Value (cm^2/V s)	Comment
μ_{300K}	230	[12.1]
μ_{peak}	580	T~4.2 K [12.1]

[12.1] K. J. Siemsen and H. D. Riccius, *Phys. Status Solidi* **37**, 445 (1970).

- **Temperature dependence**

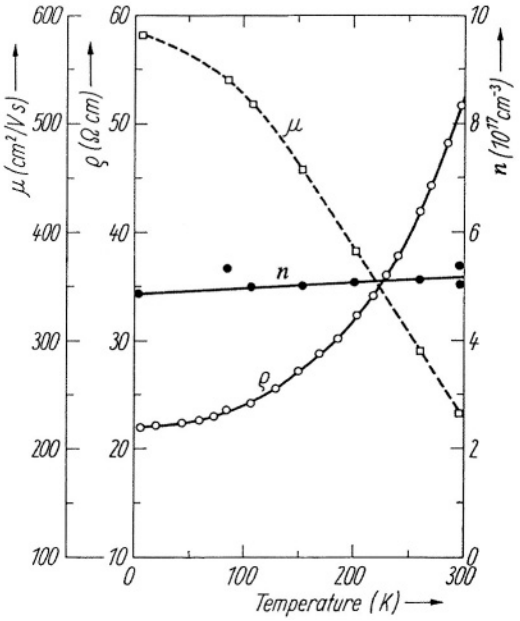

Fig. 15.12.1 Temperature variation of the Hall mobility μ, electrical resistivity ρ, and electron concentration n for β-HgS film grown by a modified vacuum deposition. [From K. J. Siemsen and H. D. Riccius, *Phys. Status Solidi* **37**, 445 (1970).]

15.12.2 Low-Field Mobility: Holes

No detailed data are available for β-HgS.

15.12.3 High-Field Transport: Electrons

No detailed data are available for β-HgS.

15.12.4 High-Field Transport: Holes

No detailed data are available for β-HgS.

15.12.5 Minority-Carrier Transport: Electrons in p-Type Materials

No detailed data are available for β-HgS.

15.12.6 Minority-Carrier Transport: Holes in n-Type Materials

No detailed data are available for β-HgS.

15.12.7 Impact Ionization Coefficient

No detailed data are available for β-HgS.

Chapter 16

Mercury Selenide (HgSe)

16.1 STRUCTURAL PROPERTIES

16.1.1 Ionicity

Table 16.1.1 *Phillips's ionicity f_i for HgSe [1.1].*

f_i
0.680

[1.1] J. C. Phillips, *Bonds and Bands in Semiconductors* (Academic, New York, 1973).

16.1.2 Elemental Isotopic Abundance and Molecular Weight

- **Isotopic abundance**

Table 16.1.2 *Isotopic abundance in percent for mercury and selenium [1.2].*

Isotope	% nat. abundance	Isotope	% nat. abundance
^{196}Hg	0.15	^{74}Se	0.89
^{198}Hg	9.97	^{76}Se	9.36
^{199}Hg	16.87	^{77}Se	7.63
^{200}Hg	23.10	^{78}Se	23.78
^{201}Hg	13.18	^{80}Se	49.61
^{202}Hg	29.86	^{82}Se	8.73
^{204}Hg	6.87		

[1.2] D. R. Lide, *CRC Handbook of Chemistry and Physics,* 78th Edition (CRC Press, Boca Raton, 1997).

• **Molecular weight**

Table 16.1.3 *Molecular (average atomic) weight M for HgSe.*

M (amu)
279.55

16.1.3 Crystal Structure and Space Group

Table 16.1.4 *Crystal structure and its space and pint groups for HgSe.*

Crystal structure	Space group	Point group
Zincblende (Cubic)	$F\bar{4}3m$	T_d

16.1.4 Lattice Constant and Its Related Parameters

• **Lattice constant, near-neighbor distance, etc.**

Table 16.1.5 *Lattice constant (a), near-neighbor distance (d), unit cube volume (a^3), and molecular density (d_M) for HgSe at 300 K.*

Parameter	Value
Lattice constant a (Å)	6.084 [1.3]
d (Cation–Anion) (Å)	2.634*
d (Cation–Cation) (Å)	4.302*
Unit cube volume a^3 (10^{-22} cm^3)	2.252*
Molecular density d_M (10^{22} cm^{-3})	1.776*

[1.3] T.-L. Huang and A. L. Ruoff, *Phys. Rev. B* **31**, 5976 (1985).
*Calculated.

• **Crystal density**

Table 16.1.6 *Crystal density g for HgSe at 300 K.**

g (g/cm^3)
8.245

*Calculated using a=6.084 Å.

16.1.5 Structural Phase Transition

Table 16.1.7 *Structural phase transition in HgSe at high pressures.*

Structure	Transition pressure (GPa)
Zincblende ($F\bar{4}3m$)	Normal pressure
Cinnabar	0.75 (see [1.4])
	0.7–0.75 [1.5]
Rocksalt (NaCl)	16 (see [1.4])
Body-centered tetragonal*	28 [1.4]

[1.4] T. Huang and A. L. Ruoff, *Phys. Rev. B* **27**, 7811 (1983).
[1.5] A. Jayaraman, W. Klement, Jr., and G. C. Kennedy, *Phys. Rev.* **130**, 2277 (1963).
*T. Huang and A. L. Ruoff, *Phys. Rev. B* **31**, 5976 (1985).

16.1.6 Cleavage Plane

Table 16.1.8 *Crystallographic plane most readily cleaved for HgSe.*

Cleavage plane
(100)

16.2 THERMAL PROPERTIES

16.2.1 Melting Point and Its Related Parameters

Table 16.2.1 *Melting point T_m and its related parameter for HgSe.*

Parameter	Value
Melting point T_m (K)	1072±1 [2.1]
Entropy of fusion ΔS_m (cal/mol K)	11.0 [2.2]

[2.1] T. C. Harman, in *Physics and Chemistry of II–VI Compounds,* edited by M. Aven and J. S. Prener (North-Holland, Amsterdam, 1967), p. 767.
[2.2] A. Pajaczkowska and Z. Dziuba, *J. Cryst. Growth* **11**, 21 (1971).

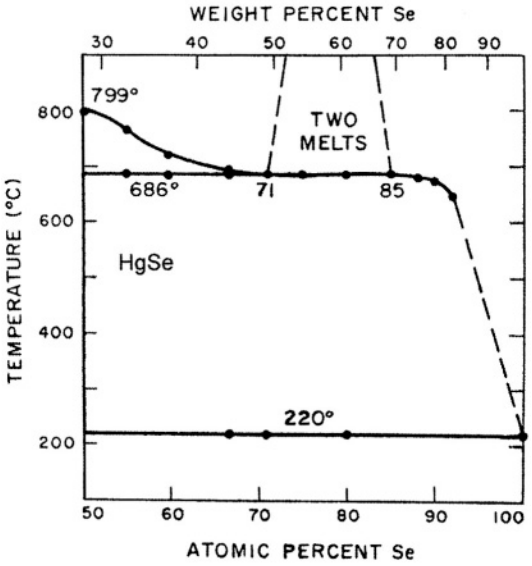

Fig. 16.2.1 Hg–Se binary liquid phase diagram. [From T. C. Harman, in *Physics and Chemistry of II–VI Compounds,* edited by M. Aven and J. S. Prener (North-Holland, Amsterdam, 1967), p. 767.]

16.2.2 Specific Heat

Table 16.2.2 *Experimental specific heats C_p (at constant pressure) and C_v (at constant volume) for HgSe (in J/g K) [2.3].*

Temperature (K)	C_p	C_v	Temperature (K)	C_p	C_v
80	0.258	0.256	200	0.341	0.333
90	0.271	0.269	220	0.345	0.336
100	0.283	0.280	240	0.349	0.339
120	0.301	0.297	260	0.352	0.341
140	0.315	0.310	280	0.354	0.342

Table 16.2.2 *Continued.*

Temperature (K)	C_p	C_v	Temperature (K)	C_p	C_v
160	0.326	0.320	300	0.355	0.343
180	0.334	0.328			

[2.3] P. V. Gul'tyaev and A. V. Petrov, *Sov. Phys. –Solid State* **1**, 330 (1959).

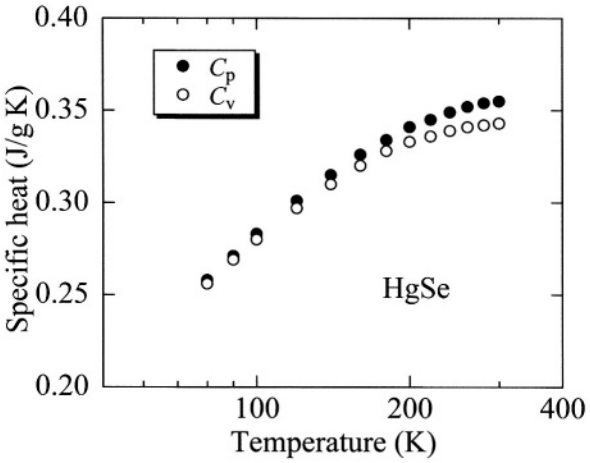

Fig. 16.2.2 Specific heats, C_p (at constant pressure) and C_v (at constant volume), versus temperature for HgSe. The experimental data are taken from P. V. Gul'tyaev and A. V. Petrov [*Sov. Phys. –Solid State* **1**, 330 (1959)].

16.2.3 Debye Temperature

Table 16.2.3 *Debye temperature θ_D for HgSe [2.4].*

Temperature (K)	θ_D (K)	Temperature (K)	θ_D (K)
0*	157	180	235
80	212	200	232
90	220	220	235
100	225	240	233
120	231	260	231
140	235	280	235
160	235	300	242

[2.4] P. V. Gul'tyaev and A. V. Petrov, *Sov. Phys. –Solid State* **1**, 330 (1959).
*In the low-temperature (0 K) limit [see, H. Siethoff and K. Ahlborn, *Phys. Status Solidi B* **190**, 179 (1995)].

16.2.4 Thermal Expansion Coefficient

Table 16.2.4 *Thermal expansion coefficient α_{th} for HgSe [2.5].*

Temperature (K)	α_{th} (10^{-6} K^{-1})	Temperature (K)	α_{th} (10^{-6} K^{-1})
25	–7.01	175	0.30
33	–7.15	200	0.73
42	–6.55	225	1.03
52	–5.82	250	1.20
61	–5.04	275	1.33
71	–4.03	300	1.41

Table 16.2.4 *Continued.*

Temperature (K)	α_{th} (10^{-6} K^{-1})	Temperature (K)	α_{th} (10^{-6} K^{-1})
80	–3.26	350	1.51
90	–2.56	400	1.61
100	–2.01	450	1.69
125	–1.05	500	1.77
150	–0.40		

[2.5] V. V. Zhdanova, V. I. Lukina, and S. I. Novikova, *Phys. Status Solidi* **13**, K19 (1966).

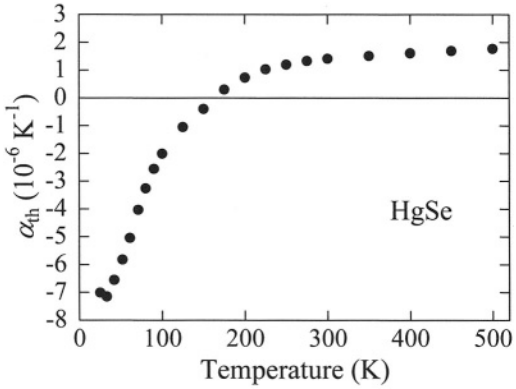

Fig. 16.2.3 Thermal expansion coefficient α_{th} versus temperature for HgSe. The experimental data are taken from V. V. Zhdanova, V. I. Lukina, and S. I. Novikova [*Phys. Status Solidi* **13**, K19 (1966)].

16.2.5 Thermal Conductivity and Diffusivity

Table 16.2.5 *Thermal conductivity for HgSe at 300 K [2.6]. Thermal diffusivity can be calculated from a relation* $D=K/(C_p g)$, *where* C_p *is the specific heat at constant pressure and g is the crystal density.*

K (W/cm K)
0.001–0.035*

[2.6] C. R. Whitsett, D. A. Nelson, J. G. Broerman, and E. C. Paxhia, *Phys. Rev. B* **7**, 4625 (1973).
*The large spread of *K* values is due to the substantial electronic contribution to the total thermal conductivity.

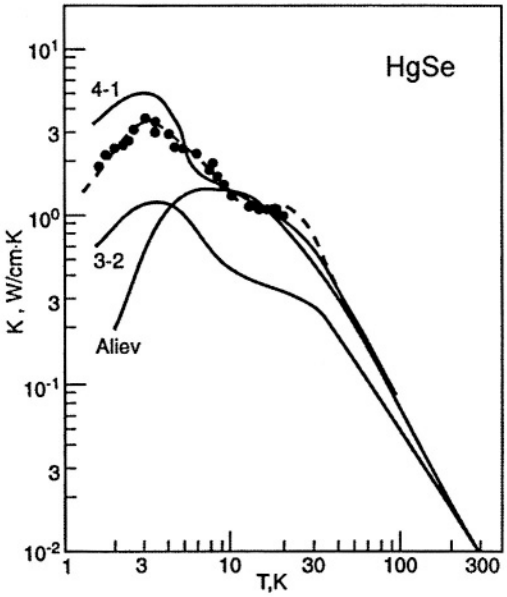

Fig. 16.2.4 Thermal conductivity *K* for HgSe. The dashed line represents the fit to the experimental data (solid circles). The curves denoted 4-1 and 3-2 are from C. R. Whitsett, D. A. Nelson, J. G. Broerman, and E. C. Paxhia [*Phys. Rev. B* **7**, 4625 (1973)]. The curve denoted "Aliev" is from S. A. Aliev, L. L. Korenblit, and S. S. Shalyt [*Sov. Phys.–Solid State* **8**, 565 (1966)]. [From S. M. Wasim, B. Fernández, and R. Aldana, *Phys. Status Solidi A* **76**, 743 (1983).]

16.3 ELASTIC PROPERTIES

16.3.1 Elastic Constant

• Room-temperature value and its temperature and pressure derivatives

Table 16.3.1 *Elastic constant and its temperature and pressure derivatives for HgSe at 300 K.*

Parameter	Value
Stiffness (10^{11} dyn/cm^2) [3.1]	
C_{11}	6.08
C_{12}	4.46
C_{44}	2.23
Compliance (10^{-12} cm^2/dyn) [3.1]	
S_{11}	4.34
S_{12}	−1.84
S_{44}	4.49
dC_{ij}/dT (10^7 dyn/cm^2 K) [3.2]	
C_{11}	−30
C_{12}	−27
C_{44}	−4.5
dC_{ij}/dp [3.1]	
C_{11}	1.8
C_{12}	2.9
C_{44}	−0.56

[3.1] *Numerical Data and Functional Relationships in Science and Technology,* edited by K.-H. Hellwege and A. M. Hellwege, Landolt–Börnstein, New Series, Group III, Vol. 18 (Springer, Berlin, 1984).

[3.2] *Numerical Data and Functional Relationships in Science and Technology,* edited by K.-H. Hellwege and A. M. Hellwege, Landolt–Börnstein, New Series, Group III, Vol. 11 (Springer, Berlin, 1979).

16.3.2 Third-Order Elastic Constant

Table 16.3.2 *Third-order elastic constant of HgSe [3.3].**

Modulus	Value (10^{12} dyn/cm^2)
C_{111}	−2.12
C_{112}	−1.27
C_{123}	−0.91
C_{144}	−0.071
C_{166}	−0.43
C_{456}	+0.006

[3.3] P. J. Ford, A. J. Miller, G. A. Saunders, Y. K. Yuğurtçu, J. K. Furdyna, and M. Jaczynski, *J. Phys. C: Solid State Phys.* **15**, 657 (1982).

*Theoretical values.

16.3.3 Young's Modulus, Poisson's Ratio, and Similar

- **Young's modulus**

Table 16.3.3 *Young's modulus Y for HgSe at 300K.**

Crystallographic plane	Y (10^{11} dyn/cm^2)
(100) plane	
[001] direction	2.30
[011] direction	4.22
(110) plane	
[001] direction	2.30
[111] direction	5.83
(111) plane	4.22

*Calculated using S_{11}=4.34, S_{12}= –1.84, and S_{44}=4.49 (all in 10^{-12} cm^2/dyn).

- **Poisson's ratio**

Table 16.3.4 *Poisson's ratio P for HgSe at 300 K.**

Crystallographic plane	P
(100) plane	
m=[010], n=[001]	0.424
m=[011], n=[0$\bar{1}$1]	–0.054
(110) plane	
m=[001], n=[1$\bar{1}$0]	0.424
m=[1$\bar{1}$1], n=[1$\bar{1}\bar{2}$]	0.308
(111) plane	0.499

*Calculated using S_{11}=4.34, S_{12}= –1.84, and S_{44}=4.49 (all in 10^{-12} cm^2/dyn).

- **Bulk modulus, shear modulus, etc.**

Table 16.3.5 *Bulk modulus, B_u, pressure derivative of B_u, dB_u/dp, shear modulus, C_s, isotropy factor, A, linear compressibility, C_o, Caucy ratio, C_a, and Born ratio, B_o, for HgSe at 300 K.*

Parameter	Value
B_u (10^{11} dyn/cm^2)	5.00 [3.4]
dB_u/dp	2.53 [3.5]
C_s (10^{10} dyn/cm^2)	8.10 [3.4]
A	0.363 [3.4]
C_o (10^{-13} cm^2/dyn)	6.67 [3.4]
C_a	2.00 [3.4]
B_o	1.19 [3.4]

[3.4] Calculated using C_{11}=6.08, C_{12}=4.46, and C_{44}=2.23 (all in 10^{11} dyn/cm^2).
[3.5] Calculated from dC_{ij}/dp data [*Numerical Data and Functional Relationships in Science and Technology,* edited by K.-H. Hellwege and A. M. Hellwege, Landolt–Börnstein, New Series, Group III, Vol. 18 (Springer, Berlin, 1984)].

16.3.4 Microhardness

Table 16.3.6 *Microhardness H for HgSe [3.6].*

H (GPa)
0.23

[3.6] See, L. Garbato and A. Rucci, *Phil. Mag.* **35**, 1681 (1977).

16.3.5 Sound Velocity

Table 16.3.7 *Sound velocity propagating in HgSe at 300 K.* LA=longitudinal acoustic; TA1, TA2=transverse acoustic.*

Propagation direction	Mode	Sound velocity (10^5 cm/s)
[100]	LA	2.72
[100]	TA1, TA2	1.64
[110]	LA	3.02
[110]	TA1	0.99
[110]	TA2	1.64
[111]	LA	3.11
[111]	TA1, TA2	1.25

*Calculated using $C_{11}=6.08\times10^{11}$ dyn/cm^2, $C_{12}=4.46\times10^{11}$ dyn/cm^2, $C_{44}=2.23\times10^{11}$ dyn/cm^2, and $g=8.245$ g/cm^3.

16.4 PHONONS AND LATTICE VIBRONIC PROPERTIES

16.4.1 Phonon Dispersion Relation

- **Dispersion curve**

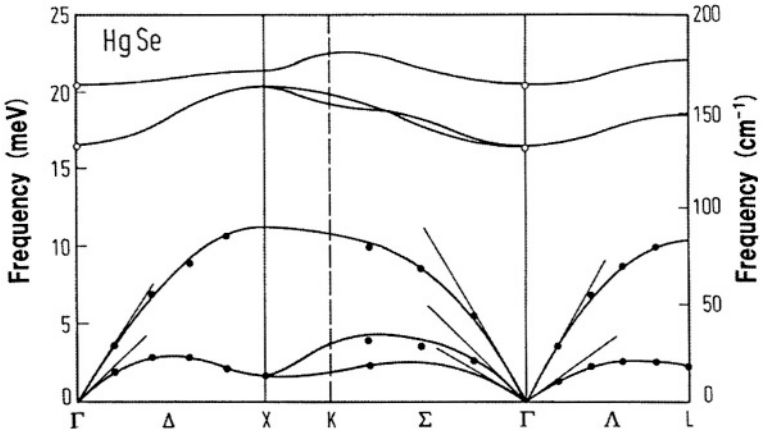

Fig. 16.4.1 Dispersion curves for the acoustic and optical branch phonons in HgSe. The solid lines are calculated from a rigid ion model. The symbols represent the experimental data at 300 K. [From H. Kępa, T. Giebultowicz, B. Buras, B. Lebech, and K. Clausen, *Phys. Scripta* **25**, 807 (1982).]

- **Phonon density of states**

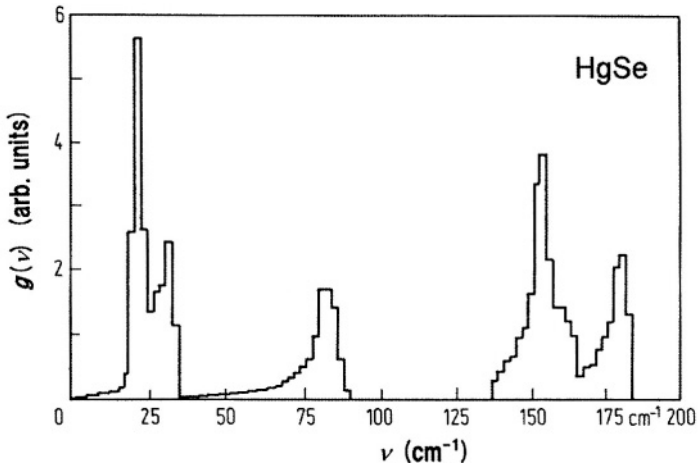

Fig. 16.4.2 One-phonon density of states $g(\nu)$ for HgSe. [From H. Kępa, T. Giebultowicz, B. Buras, B. Lebech, and K. Clausen, *Phys. Scripta* **25**, 807 (1982).]

16.4.2 Phonon Frequency

Table 16.4.1 *Long-wavelength ($q \to 0$) and zone-boundary phonon frequencies for HgSe.*

Critical point	Phonon	Phonon frequency (cm^{-1})				
		T=300 K [4.1]	T=300 K [4.2]	T=300 K [4.3]	T=300 K [4.4]	T=90 K [4.5]
Γ	TO	132±1	132±1		132	133
	LO		164±5		174	
X	TA			14		
	LA					
	TO					
	LO					
L	TA			19		21.5
	LA					
	TO					
	LO					

[4.1] A. Manabe and A. Mitsuishi, *Solid State Commun.* **16**, 743 (1975).
[4.2] A. M. Witowski and M. Grynberg, *Phys. Status Solidi B* **100**, 389 (1980).
[4.3] H. Kępa, T. Giebultowicz, B. Buras, B. Lebech, and K. Clausen, *Phys. Scripta* **25**, 807 (1982).
[4.4] K. Kumazaki, *Phys. Status Solidi B* **160**, K173 (1990).
[4.5] W. Szuszkiewicz, E. Dynowska, J. Górecka, B. Witkowska, M. Jouanne, J. F. Morhange, C. Julien, and B. Hennion, *Phys. Status Solidi B* **215**, 93 (1999).

- **Temperature and/or pressure dependence**

It has been reported that the TO phonon frequency in HgSe shows a decrease of about $3\ cm^{-1}$ in going from 6 to 300 K [A. M. Witowski and M. Grynberg, *Phys. Status Solidi B* **100**, 389 (1980); see also, A. Manabe, H. Noguchi, and A. Mitsuishi, *Phys. Status Solidi B* **90**, 157 (1978)].

16.4.3 Mode Grüneisen Parameter

No detailed data are available for HgSe.

16.4.4 Phonon Deformation Potential

No detailed data are available for HgSe.

16.5 COLLECTIVE EFFECTS AND RELATED PROPERTIES

16.5.1 Piezoelectric Constant

Table 16.5.1 *Piezoelectric stress (e_{14}), strain (d_{14}), and electromechanical coupling constants ($K_{[110]}^2$) for HgSe [5.1].*

Parameter	Value
e_{14} (C/m^2)	+0.058
d_{14} (10^{-12} m/V)	+2.6 *
$K_{[110]}^2$	6.6×10^{-5} *

[5.1] Theor. [K. Hübner, *Phys. Status Solidi B* **57**, 627 (1973)].
*Calculated.

16.5.2 Fröhlich Coupling Constant

No detailed data are available for HgSe.

16.6 ENERGY-BAND STRUCTURE: ENERGY-BAND GAPS

16.6.1 Basic Properties

- **Electronic energy-band structure**

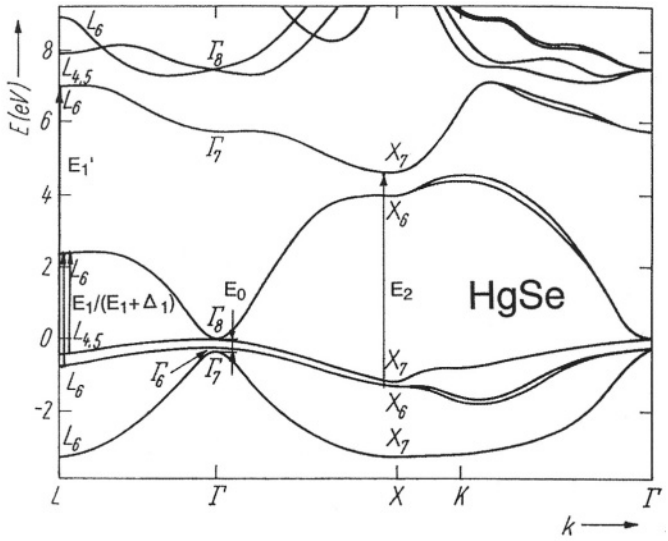

Fig. 16.6.1 Electronic energy-band structure of HgSe as calculated by an empirical pseudopotential method. The electronic states are labeled using the notation for the representations of the double group of the zinc-blende structure. [From S. Bloom and T. K. Bergstresser, *Phys. Status Solidi* **42**, 191 (1970).] The locations of several interband transitions are included by the vertical arrows.

• **Energy eigenvalue**

Table 16.6.1 *Energy eigenvalues at the Γ, X, and L points for the valence and first few conduction bands of HgSe [6.1].*

Critical point	Level	Value (eV)	
		Calc. [6.1]	Exper.*
Γ	Γ_{15}^{v}	0.0	0.0, –(0.38–0.45)
	Γ_{1}^{c}	0.0	–(0.19–0.274)
	Γ_{15}^{c}	8.2	
X	X_{3}^{v}	–2.5	
	X_{5}^{v}	–0.3	
	X_{1}^{c}	4.2	
	X_{3}^{c}	5.5	
L	L_{1}^{v}	–2.8	
	L_{3}^{v}	0.0	
	L_{1}^{c}	3.0	
	L_{3}^{c}	8.2	

[6.1] F. Herman, R. L. Kortum, C. D. Kuglin, and J. L. Shay, in *II–VI Semiconducting Compounds,* edited by D. G. Thomas (Benjamin, New York, 1967), p. 503.
*Obtained from various sources.

16.6.2 E_0-Gap Region

• **General remark**

The band structure of HgSe is considered to be of the inverted type. The lowest-conduction-band minimum and the top of the valence band in HgSe are degenerate at the center of the Brillouin zone (Γ point, k=0). The Γ_8 level is the fourfold component of the spin–orbit–split valence band. The Γ_6 level, which for most cubic semiconductor is the conduction-band minimum with an energy larger than the Γ_8 state, is locate below the Γ_8 state (i.e., "*negative*" energy gap, "*inverted*" band structure).

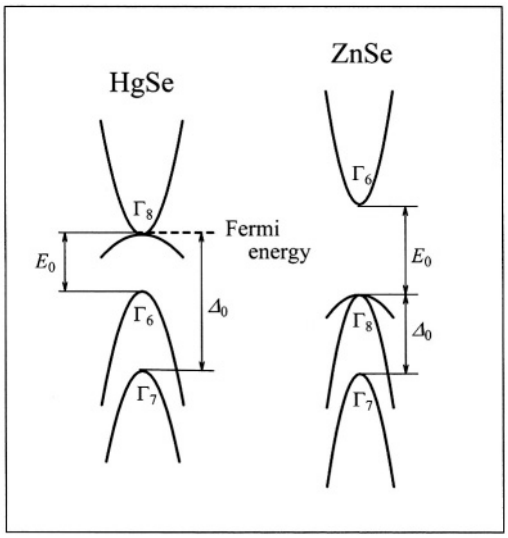

Fig. 16.6.2 Schematic diagram of the electronic energy-band structure of HgSe and ZnSe at k=0. The bands are labeled in the double-group representation. In HgSe, the band-gap energy between the Γ_8 conduction and valence bands is zero (semimetal).

● **Temperature dependence**

Table 16.6.2 *E_0- and Δ_0-gap energies for HgSe determined at various temperatures.*

Temperature (K)	E_0 (eV)	Δ_0 (eV)	Ref.
0	–0.2733	0.387±0.002	[6.2]
1.3	–0.22	0.45	[6.3]
4.2	–0.19	0.38	[6.4]
	–0.220		[6.5]
	–0.274±0.002	0.39±0.01	[6.6]
	–0.272	0.383	[6.7]
5	–0.274	0.387	[6.8]
6	–0.270	0.387	[6.9]
10	–0.268±0.001	0.387±0.002	[6.2]
	–0.216		[6.5]
	–0.26	0.40	[6.10]
20	–0.260±0.001	0.387±0.002	[6.2]
	–0.208		[6.5]
30	–0.206		[6.5]
40	–0.246±0.001	0.387±0.002	[6.2]
	–0.206		[6.5]
50	–0.204		[6.5]
58	–0.227±0.001	0.387±0.002	[6.2]
60	–0.203		[6.5]
70	–0.199		[6.5]
77	–0.20±0.01		[6.11]
77.3	–0.197		[6.5]
80	–0.205±0.001	0.387±0.002	[6.2]
	–0.202	0.40	[6.10]
90	–0.187		[6.5]
100	–0.188		[6.5]
	–0.18		[6.12]
	–0.20		[6.13]
120	–0.177		[6.5]
140	–0.159		[6.5]
160	–0.147		[6.5]
180	–0.136		[6.5]
200	–0.128		[6.5]
220	–0.116		[6.5]
240	–0.106		[6.5]
260	–0.091		[6.5]
270	–0.084		[6.5]
280	–0.076		[6.5]
290	–0.068		[6.5]

Table 16.6.2 *Continued.*

Temperature (K)	E_0 (eV)	Δ_0 (eV)	Ref.
293	–0.13		[6.12]
300	–0.061		[6.5]
	–0.03	0.40	[6.10]
	–0.10		[6.13]
Recommended value (T~300 K): E_0= –0.08 eV; Δ_0=0.4 eV			

[6.2] M. Dobrowolska, W. Dobrowolski, and A. Mycielski, *Solid State Commun.* **34**, 441 (1980).
[6.3] D. G. Seiler, R. R. Galazka, and W. M. Becker, *Phys. Rev. B* **3**, 4274 (1971).
[6.4] L. M. Bliek and G. Landwehr, *Phys. Status Solidi* **33**, K67 (1969).
[6.5] S. L. Lehoczky, J. G. Broerman, D. A. Nelson, and C. R. Whitsett, *Phys. Rev. B* **9**, 1598 (1974).
[6.6] Y. Guldner, C. Rigaux, M. Dobrowolska, A. Mycielski, and W. Dobrowolski, in *Physics of Narrow-Gap Semiconductors*, edited by J. Rauluszkiewicz, M. Gorska, and E. Kaczmarek (Elsevier, Amsterdam, 1978), p. 87.
[6.7] A. Mycielski, J. Kossut, M. Dobrowolska, and W. Dobrowolski, *J. Phys. C: Solid State Phys.* **15**, 3293 (1982).
[6.8] M. von Truchseß, A. Pfeuffer-Jeschke, C. R. Becker, G. Landwehr, and E. Batke, *Phys. Rev. B* **61**, 1666(2000).
[6.9] I. Stolpe, O. Portugall, N. Puhlmann, H.-U. Mueller, M. von Ortenberg, M. von Truchsess, C. R. Becker, A. Pfeuffer-Jeschke, and G. Landwehr, *Physica B* **294-295**, 459 (2001).
[6.10] W. Szuszkiewicz, *Phys. Status Solidi B* **91**, 361 (1979).
[6.11] P. Byszewski, J. Kowalski, and R. R. Gałązka, *Phys. Status Solidi B* **78**, 477 (1976).
[6.12] V. V. Volkov, L. V. Volkova, and P. S. Kireev, *Sov. Phys. Semicond.* **7**, 420 (1973).
[6.13] T. Dietl and A. Jędrzejczak, *Phys. Status Solidi B* **71**, K39 (1975).

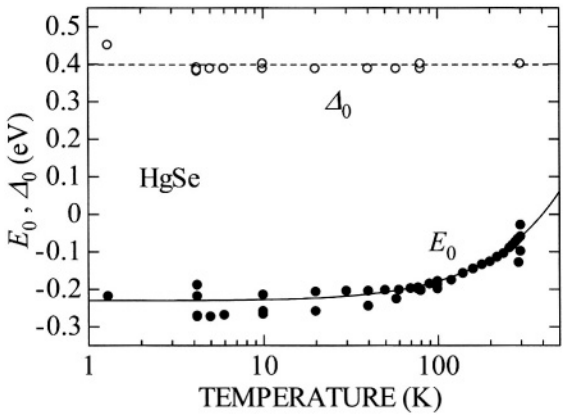

Fig. 16.6.3 E_0- and Δ_0-gap energies versus temperature for HgSe. The experimental data are gathered from various sources. The solid line represents the calculated result of an expression, $E_0(T) = -0.23 + (6.0\times10^{-4}T^2)/(T+16)$, while the dashed line indicates a value of Δ_0=0.4 eV.

Table 16.6.3 *Empirical equation for the E_0-gap energy variation with temperature T for HgSe.*

$$E_0(T) = E_0(0) - \frac{\alpha T^2}{T+\beta}$$

Parameter			Comment
$E_0(0)$ (eV)	α (10^{-4} eV/K)	β (K)	
–0.2733	–10.2	16	T=10–80 K [6.14]
–0.23	–6.0	16	*

[6.14] M. Dobrowolska, W. Dobrowolski, and A. Mycielski, *Solid State Commun.* **34**, 441 (1980)

*See figure, above.

• **Temperature and/or pressure coefficient**

Table 16.6.4 *Linear temperature and pressure coefficients of the E_0-gap energy for HgSe.*

Coefficient	Value	Comment
dE_0/dT (10^{-4} eV/K)	+2.6	T=100–293 K [6.15]
	+5	T=100–300 K [6.16]
	+8.3±1.1	T=10–295 K [6.17]
	+7.4±0.4	T=5–200 K [6.18]
dE_0/dp (10^{-2} eV/GPa)	~0	p<7.5 GPa [6.19]
	−15.9	p>7.5 GPa [6.19]

[6.15] V. V. Volkov, L. V. Volkova, and P. S. Kireev, *Sov. Phys. Semicond.* **7**, 420 (1973).
[6.16] T. Dietl and A. Jędrzejczak, *Phys. Status Solidi B* **71**, K39 (1975).
[6.17] W. Szuszkiewicz, *Phys. Status Solidi B* **91**, 361 (1979).
[6.18] S. Einfeldt, F. Goschenhofer, C. R. Becker, and G. Landwehr, *Phys. Rev. B* **51**, 4915 (1995).
[6.19] A. Ohtani, T. Seike, M. Motobayashi, and A. Onodera, *J. Phys. Chem. Solids* **43**, 627 (1982).

• **Doping dependence**

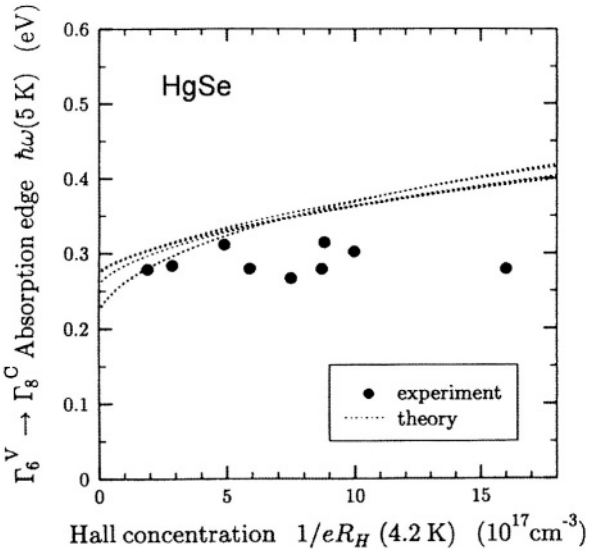

Fig. 16.6.4 $\Gamma_6^v \rightarrow \Gamma_8^c$ absorption-edge shift at 5 K versus Hall carrier concentration at 4.2 K in HgSe. The solid circles and dotted lines represent the experimental and theoretical results, respectively. [From S.Einfeldt, F. Goschenhofer, C. R. Becker, and G. Landwehr, *Phys. Rev. B* **51**, 4915 (1995).]

16.6.3 Higher-Lying Direct Gap

• **Room-temperature value**

Table 16.6.5 *E_1-, $E_1+\Delta_1$-, and Δ_0-gap energies for HgSe at room temperature.*

E_1 (eV)	$E_1+\Delta_1$ (eV)	Δ_1 (eV)	Ref.
2.82	3.13	0.31	[6.20]
2.87	3.20	0.33	[6.21]
2.85	3.15	0.30	[6.22]
2.90	3.15	0.25	[6.23]
2.88	3.21	0.33	[6.24]
2.85	3.17	0.32	[6.25]
2.781	3.120	0.339	[6.26]
2.797	3.159	0.362	[6.27]

Table 16.6.5 *Continued.*

E_1 (eV)	$E_1+\Delta_1$ (eV)	Δ_1 (eV)	Ref.
2.86	3.06	0.20	[6.28]
2.80	3.05	0.25	[6.29]
2.84	3.14	0.30	Mean value

[6.20] M. Cardona, *J. Appl. Phys.* **32** (Suppl.), 2151 (1961).
[6.21] M. Cardona and G. Harbeke, *J. Appl. Phys.* **34**, 813 (1963).
[6.22] M. Cardona, K. L. Shaklee, and F. H. Pollak, *Phys. Rev.* **154**, 696 (1967).
[6.23] A. Moritani, H. Sekiya, K. Taniguchi, C. Hamaguchi, J. Nakai, and R. Makabe, *Jpn. J. Appl. Phys.* **10**, 1410 (1971).
[6.24] I. N. Borisov, V. V. Mikhailin, P. S. Kireev, and V. M. Bezborodova, *Sov. Phys–Semicond.* **5**, 728 (1971).
[6.25] A. Moritani, C. Hamaguchi, and J. Nakai, *J. Phys. Soc. Jpn* **32**, 1151 (1972).
[6.26] K. Kumazaki, L. Viña, C. Umbach, and M. Cardona, *Solid State Commun.* **68**, 591 (1988).
[6.27] K. Kumazaki, L. Viña, C. Umbach, and M. Cardona, *Phys. Status Solidi B* **156**, 371 (1989).
[6.28] Y. Lansari, J. W. Cook, Jr., and J. F. Schetzina, *J. Electron. Mater.* **22**, 809 (1993).
[6.29] S.Einfeldt, F. Goschenhofer, C. R. Becker, and G. Landwehr, *Phys. Rev. B* **51**, 4915 (1995).

Table 16.6.6 *Higher-lying interband transition energies in HgSe at room temperature.*

Peak	Value (eV)		
	a	b	c
E_0'	5.08	5.01	5.00
B	5.7	5.83 (E_2)	5.50
$B+\Delta_2$	6.0	6.11 ($E_2+\Delta_2$)	
		6.21 ($E_2+\delta$)	
C	6.45	6.49 ($E_2+\delta+\Delta_2$)	6.95
$C+\Delta_2$	6.75		
E	7.6	7.45 (E_3)	7.10
A	8.3	8.20 (E_1')	8.36
$A+\delta_1$	8.6	8.51 (E_1'+Δ_1)	
d_1	9.7		9.50
d_2	11.1		11.24

[a] H. Overhof, *Phys. Status Solidi B* **43**, 221 (1971).
[b] I. N. Borisov, V. V. Mikhailin, P. S. Kireev, and V. M. Bezborodova, *Sov. Phys–Semicond.* **5**, 728 (1971).
[c] E. Guziewicz, B. J. Kowalski, K. Szamota-Sadowska, W. Szuszkiewicz, and B. A. Orlowski, *Phys. Rev. B* **55**, 4405 (1997).

- **Temperature dependence**

Table 16.6.7 *Empirical equation for the higher-lying direct-gap energy variation with temperature T for HgSe [6.30].*

$$E_g(T) = E_g(0) - \frac{\alpha T^2}{T+\beta}$$

Band gap	Parameter		
	$E_g(0)$ (eV)	α (10^{-4} eV/K)	β (K)
E_1	2.949	5.8	60
$E_1+\Delta_1$	3.219	5.8	60

[6.30] S.Einfeldt, F. Goschenhofer, C. R. Becker, and G. Landwehr, *Phys. Rev. B* **51**, 4915 (1995).

Table 16.6.8 *Empirical equation for the higher-lying direct-gap energy variation with temperature T for HgSe [6.31].*

$$E_g(T) = E_B - 2a_B\left(\frac{1}{2} + \frac{1}{e^{\Theta/T} - 1}\right)$$

Band gap	Parameter		
	E_B (eV)	a_B (meV)	Θ(K)
E_1	2.971	24	87
$E_1+\Delta_1$	3.241	24	87

[6.31] S.Einfeldt, F. Goschenhofer, C. R. Becker, and G. Landwehr, *Phys. Rev. B* **51**, 4915 (1995).

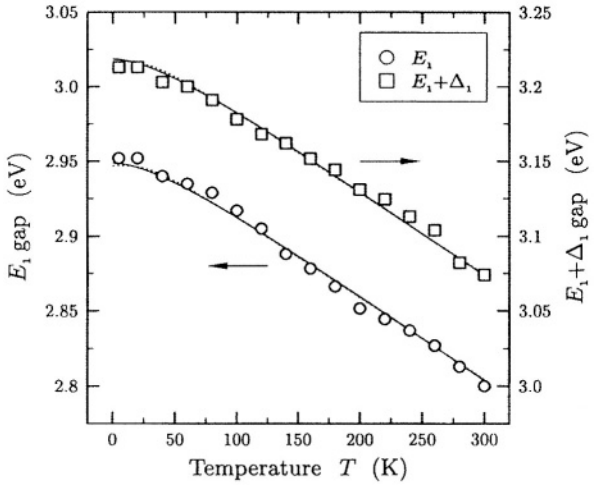

Fig. 16.6.5 Temperature dependence of E_1 and $E_1+\Delta_1$ gaps for HgSe. The solid and dotted lines represent the least squares fits to the experimental data using the empirical expressions. [From S.Einfeldt, F. Goschenhofer, C. R. Becker, and G. Landwehr, *Phys. Rev. B* **51**, 4915 (1995).]

- **Temperature and/or pressure coefficient**

Table 16.6.9 *Linear temperature coefficient of the higher-lying band-gap energy for HgSe.*

Band gap	Coefficient	Value	Comment
E_1	dE_g/dT (10^{-4} eV/K)	–4.3±0.6	Exper. [6.32]
		–4.6±0.2	Exper. [6.33]
	dE_g/dp (10^{-2} eV/GPa)	5.9	Calc. [6.34]
$E_1+\Delta_1$	dE_g/dT (10^{-4} eV/K)	–4.3±0.6	Exper. [6.32]
		–3.8±0.3	Exper. [6.33]
E_2	dE_g/dp (10^{-2} eV/GPa)	3.9	Calc. [6.34]

[6.32] M. Cardona, *J. Appl. Phys.* **32** (Suppl.), 2151 (1961).
[6.33] M. Cardona and G. Harbeke, *J. Appl. Phys.* **34**, 813 (1963).
[6.34] D. L. Camphausen, G. A. N. Cornell, and W. Paul, *Phys. Rev. Lett.* **26**, 184 (1971).

16.6.4 Lowest Indirect Gap

- **Theoretical value**

Table 16.6.10 *Theoretically obtained lowest indirect-gap energy for HgSe [6.35].*

Band gap	Value (eV)
E_g^L ($\Gamma_{15}^v \rightarrow L_1^c$)	3.0
E_g^X ($\Gamma_{15}^v \rightarrow X_1^c$)	4.2

[6.35] F. Herman, R. L. Kortum, C. D. Kuglin, and J. L. Shay, in *II–VI Semiconducting Compounds,* edited by D. G. Thomas (Benjamin, New York, 1967), p. 503.

- **Temperature and/or pressure coefficient**

Table 16.6.11 *Linear temperature and pressure coefficients of the lowest indirect-gap energy for HgSe.*

Coefficient	Value	Comment
dE_g^L/dp (10^{-2} eV/GPa)	1.8	Calc. [6.36]
dE_g^X/dp (10^{-2} eV/GPa)	–3.1	Calc. [6.36]

[6.36] S.-H. Wei and A. Zunger, *Phys. Rev. B* **60**, 5404 (1999).

16.6.5 Conduction-Valley Energy Separation

No detailed data are available for HgSe.

16.6.6 Direct–Indirect-Gap Transition Pressure

No detailed data are available for HgSe.

16.7 ENERGY-BAND STRUCTURE: ELECTRON AND HOLE EFFECTIVE MASSES

16.7.1 Electron Effective Mass: Γ Valley

- **Theoretical value**

Table 16.7.1 *Theoretical electron effective mass m_e^Γ at the Γ_6 valley for HgSe*

m_e^Γ/m_0	Technique
–0.042*	Five-level $\boldsymbol{k}\cdot\boldsymbol{p}$ calculation [7.1]

[7.1] P. Lawaetz, *Phys. Rev. B* **4**, 3460 (1971).

*The sign is chosen positive for a normal band structure like that of CdTe (i.e.,"–" means that free carriers behave like holes, not electrons).

16.7.2 Electron Effective Mass: Satellite Valley

No detailed data are available for HgSe.

16.7.3 Hole Effective Mass

- **Luttinger's valence-band parameter**

Table 16.7.2 *Luttinger's valence-band parameter γ_i for HgSe ($in\ \hbar^2/2m_0$).*

γ_1	γ_2	γ_3	Technique
–25.96	–13.69	–13.20	Five-level $\boldsymbol{k}\cdot\boldsymbol{p}$ calculation [7.2]

[7.2] P. Lawaetz, *Phys. Rev. B* **4**, 3460 (1971).

• **Band mass, cyclotron mass, etc.**

Table 16.7.3 *Band (m_{HH}, m_{LH}), density-of-states heavy-hole (m_{HH}*), averaged light-hole (m_{LH}*), and spherically-averaged heavy-hole (m_{HH}^s) and light-hole masses (m_{LH}^s) in HgSe.*

Mass	Value (m_0)
m_{HH} ([001] direction)	0.70*[1]
m_{LH} ([001] direction)	–0.019*[1,*2]
m_{HH} ([111] direction)	2.27*[1]
m_{LH} ([111] direction)	–0.019*[1,*2]
m_{HH}*	–0.019*[1,*2]
	–0.03*[2] [7.3]
m_{LH}*	1.07*[1]
m_{HH}^s	1.20*[1]
m_{LH}^s	–0.019*[1,*2]

[7.3] n~2×10^{17} cm^{-3} [D. G. Seiler, R. R. Galazka, and W. M. Becker, *Phys. Rev. B* **3**, 4274 (1971)].
*[1] Calculated using a set of the Luttinger's parameters, $\gamma_1=-25.96$, $\gamma_2=-13.69$, and $\gamma_3=-13.20$.
*[2] The sign is chosen positive for a normal band structure like that of CdTe (i.e., "–" means that free carriers behave like electrons, not holes).

• **Spin–orbit–splitoff hole effective mass**

Table 16.7.4 *Spin–orbit–splitoff hole effective mass m_{SO} for HgSe.*

m_{SO}/m_0	Technique
0.031	Five-level $\boldsymbol{k\cdot p}$ calculation [7.4]

[7.4] P. Lawaetz, *Phys. Rev. B* **4**, 3460 (1971).

• **Doping dependence**

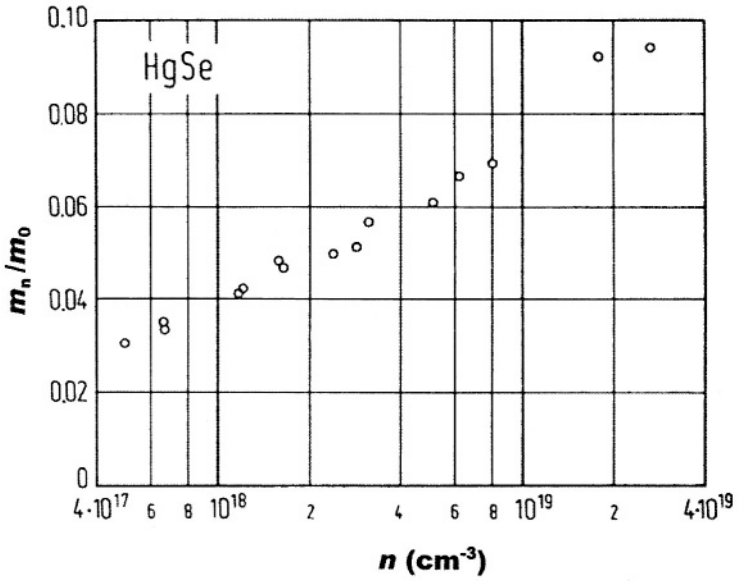

Fig. 16.7.1 Electron effective mass, m_n/m_0, at the "Γ_8-valence band" in HgSe at T=300 K determined from magnetoreflectivity measurements. [From G. B. Wright, A. J. Strauss, and T. C. Harman, *J. Appl. Phys.* **125**, 1534 (1962).]

16.8 ELECTRONIC DEFORMATION POTENTIAL

16.8.1 Intravalley Deformation Potential: Γ Point

- **Conduction band**

Table 16.8.1 *Intravalley acoustic deformation potential E_1 for HgSe used in the electron transport analysis.*

E_1 (eV)	Ref.
4	[8.1]

[8.1] D. L. Rode, in *Semiconductors and Semimetals,* edited by R. K. Willardson and A. C. Beer (Academic, New York, 1975), Vol. 10, p. 1.

- **Valence band**

Table 16.8.2 *Γ-valence-band deformation potentials a, b, and d for HgSe.*

Deformation potential (eV)			Comment
a	*b*	*d*	
	−1.16		Calc. [8.2]

[8.2] T. Nakayama, *Solid-State Electron.* **37**, 1077 (1994).

- **E_0 gap**

Table 16.8.3 *Hydrostatic deformation potential a_0^Γ for the E_0 gap of HgSe.*

a_0^Γ (eV)	Comment
−3.66	Calc. [8.3]
−2.15	Calc. [8.4]

[8.3] T. Nakayama, *Solid-State Electron.* **37**, 1077 (1994).
[8.4] S.-H. Wei and A. Zunger, *Phys. Rev. B* **60**, 5404 (1999).

16.8.2 Intravalley Deformation Potential: High-Symmetry Points

No detailed data are available for HgSe.

16.8.3 Intervalley Deformation Potential

No detailed data are available for HgSe.

16.9 ELECTRON AFFINITY AND SCHOTTKY BARRIER HEIGHT

16.9.1 Electron Affinity

No detailed data are available for HgSe.

16.9.2 Schottky Barrier Height

No detailed data are available for HgSe.

16.10 OPTICAL PROPERTIES

16.10.1 Summary of Optical Dispersion Relations

- **$\varepsilon(E)$ and $n^*(E)$ spectra**

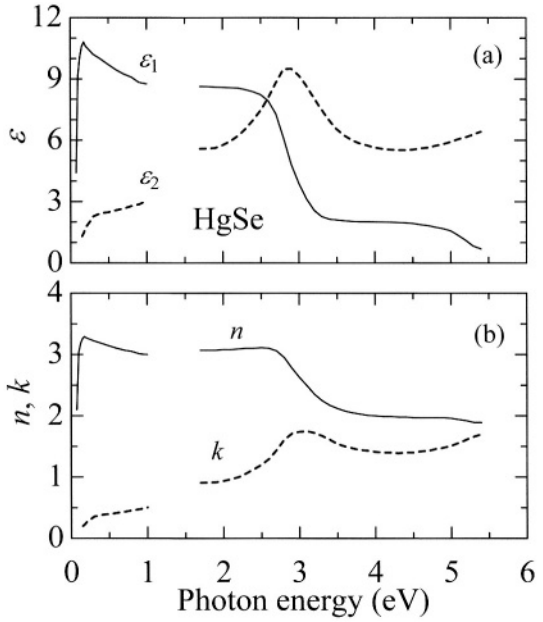

Fig. **16.10.1** (a) Complex dielectric-constant [$\varepsilon(E)=\varepsilon_1(E)+i\varepsilon_2(E)$] and (b) complex refractive-index spectra [$n^*(E)=n(E)+ik(E)$] for HgSe at 300 K. The numerical data are taken from tabulation by S. Adachi [*Optical Constants of Crystalline and Amorphous Semiconductors: Numerical Data and Graphical Information* (Kluwer Academic, Boston, 1999)].

- **$\alpha(E)$ and $R(E)$ spectra**

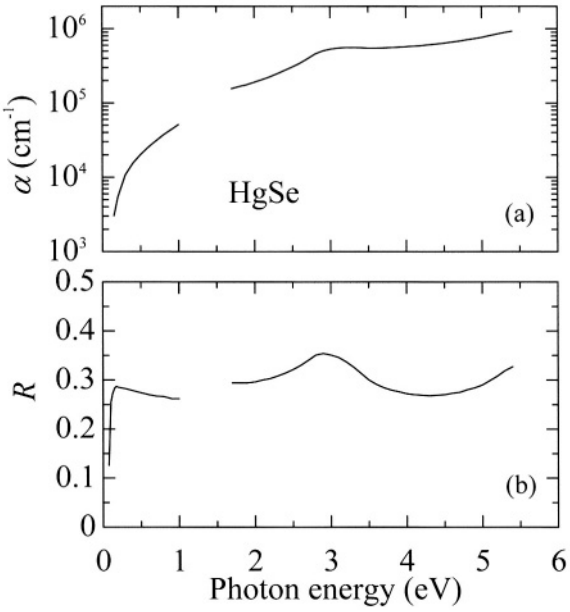

Fig. 16.10.2 (a) Absorption [$\alpha(E)$] and (b) normal-incidence reflectivity spectra [$R(E)$] for HgSe at 300 K. The numerical data are taken from tabulation by S. Adachi [*Optical Constants of Crystalline and Amorphous Semiconductors: Numerical Data and Graphical Information* (Kluwer Academic, Boston, 1999)].

16.10.2 The Reststrahlen Region

- **Static and high-frequency dielectric constants**

Table 16.10.1 *Static and high-frequency dielectric constants ε_s and ε_∞ for HgSe.*

ε_s	ε_∞	Comment
25.6		T=300 K [10.1]
	12±1*	T=300 K [10.2]
	9±1*	T=350 K [10.3]
	8.25±1	T=300 K [10.4]
	11±1	T=2–300 K [10.5]
	5.8–7.2	T=10–295 K [10.6]
	6.5–7.5	T=6–300 K [10.7]
25.7	11	T=300 K [10.8]
	7.5±1	T=300 K [10.9]
26	7.5	Recommended value (T=300 K)

[10.1] Z. I. Kir'iashkina, F. M. Popov, D. N. Bilenko, and V. I. Kir'iahkina, *Sov. Phys.–Tech. Phys.* **2**, 69 (1957).
[10.2] G. B. Wright, A. J. Strauss, and T. C. Harman, *J. Appl. Phys.* **125**, 1534 (1962).
[10.3] V.V. Volkov, L. V. Volkova, and P. S. Kireev, *Sov. Phys.–Semicond.* **4**, 1230 (1971).
[10.4] S. L. Lehoczky, J. G. Broerman, D. A. Nelson, and C. R. Whitsett, *Phys. Rev. B* **9**, 1598 (1974).
[10.5] A. Manabe, H. Noguchi, and A. Mitsuishi, *Phys. Status Solidi B* **90**, 157 (1978).
[10.6] W. Szszkiewicz, A. M. Witowski, and M. Grynberg, *Phys. Status Solidi B* **87**, 637 (1978).
[10.7] A. M. Witowski and M. Grynberg, *Phys. Status Solidi B* **100**, 389 (1980).
[10.8] K. Kumazaki, *Phys. Status Solidi B* **160**, K173 (1990).
[10.9] S.Einfeldt, F. Goschenhofer, C. R. Becker, and G. Landwehr, *Phys. Rev. B* **51**, 4915 (1995).
*The interband contribution was included in the analysis.

- **Reststrahlen parameter**

Fundamental reflectivity spectra in the reststrahlen region of HgSe have been analyzed at T=2, 95, and 300 K by A. Manabe, H. Noguchi, and A. Mitsuishi [*Phys. Status Solidi B* **90**, 157 (1978)] and at T=6, 80, and 300 K by A. M. Witowski and M. Grynberg [*Phys. Status Solidi B* **100**, 389 (1980)].

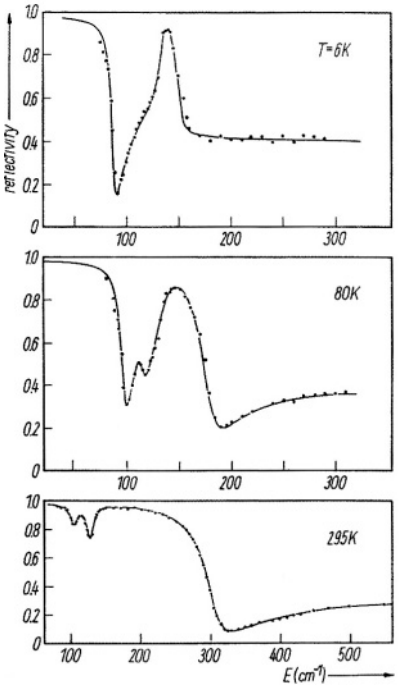

Fig. 16.10.3 Far-infrared reflectivity spectra of HgSe at T=6, 80, and 295 K. The dots show the experimental points, while the solid lines represent the theoretical dispersion curves. [From A. M. Witowski and M. Grynberg, *Phys. Status Solidi B* **100**, 389 (1980).]

16.10.3 At or Near the Fundamental Absorption Edge

- **Refractive index**

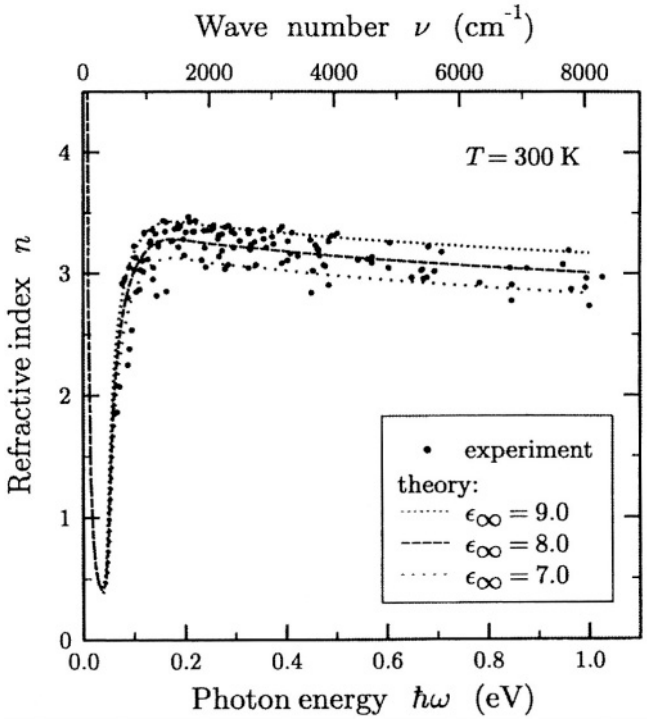

Fig. 16.10.4 Refractive index n for HgSe at 300 K. [From S.Einfeldt, F. Goschenhofer, C. R. Becker, and G. Landwehr, *Phys. Rev B* **51**, 4915 (1995).]

- **Fundamental absorption edge: Temperature dependence**

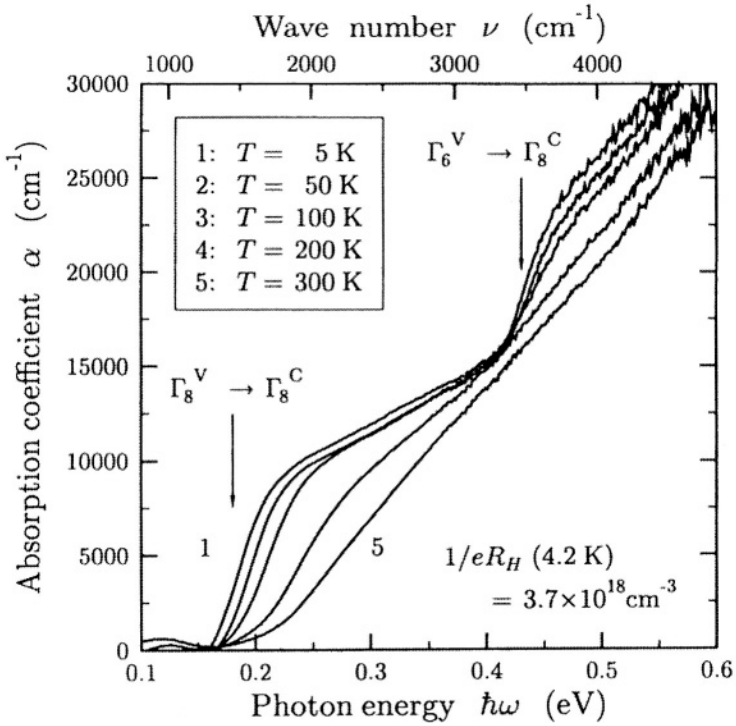

Fig. 16.10.5 Absorption coefficient α for HgSe at temperatures from T=5 to 300 K. The van der Pauw measurement for this sample resulted in $1/eR_H$=3.7×10^{18} cm^{-3} (at 4.2 K). [From S.Einfeldt, F. Goschenhofer, C. R. Becker, and G. Landwehr, *Phys. Rev. B* **51**, 4915 (1995).]

16.10.4 The Interband Transition Region

- **Fundamental optical spectra**

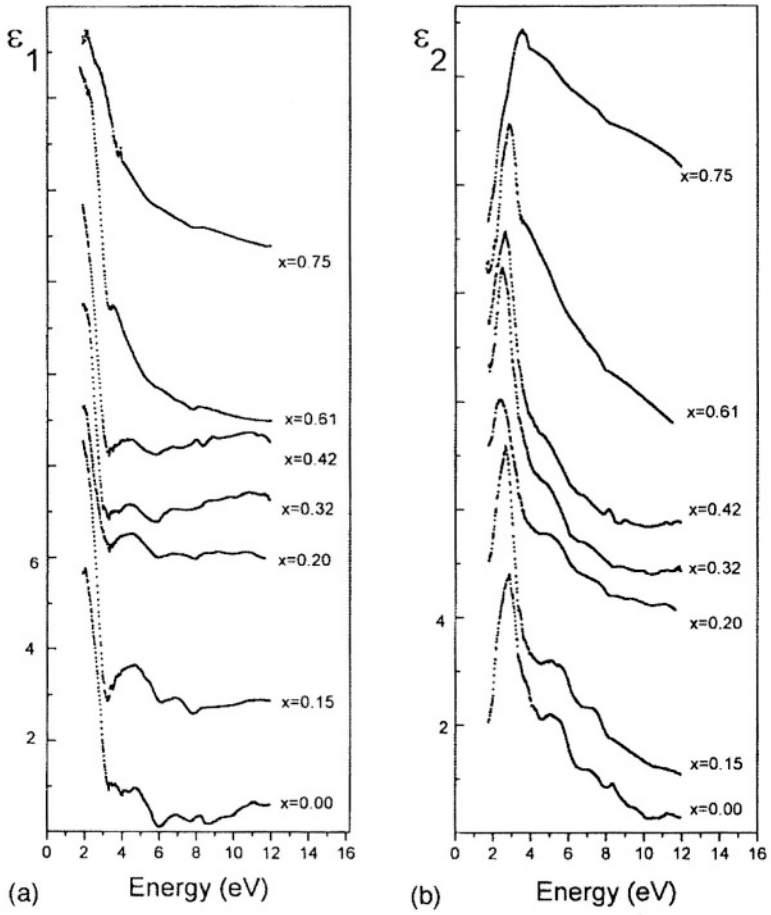

Fig. 16.10.6 (a) Real and (b) imaginary parts of the dielectric function, $\varepsilon(E)=\varepsilon_1(E)+i\varepsilon_2(E)$, for $HgSe_{1-x}S_x$ alloy (x=0–0.75) at 300 K. The samples measured were cut from $HgSe_{1-x}S_x$ crystals grown by a modified Bridgman method, and had a sphalerite crystal structure. [From E. Guziewicz, B. J. Kowalski, K. Szamota-Sadowska, W. Szuszkiewicz, and B. A. Orlowski, *Phys. Rev. B* **55**, 4405(1997).]

16.10.5 Free-Carrier Absorption and Related Phenomena

No detailed data are available for HgSe.

16.11 ELASTOOPTIC, ELECTROOPTIC, AND NONLINEAR OPTICAL PROPERTIES

16.11.1 Elastooptic Effect

No detailed data are available for HgSe.

16.11.2 Linear Electrooptic Constant

No detailed data are available for HgSe.

16.11.3 Quadratic Electrooptic Constant

No detailed data are available for HgSe.

16.11.4 Franz–Keldysh Effect

No detailed data are available for HgSe.

16.11.5 Nonlinear Optical Constant

No detailed data are available for HgSe.

16.12 CARRIER TRANSPORT PROPERTIES

16.12.1 Low-Field Mobility: Electrons

Table 16.12.1 *300-K (μ_{300K}) and peak Hall mobilities (μ_{peak}) for electrons in HgSe.*

Mobility	Value (cm^2/V s)	Comment
μ_{300K}	2.2×10^4	[12.1]
μ_{peak}	1.7×10^5	T~20–30 K [12.2]

[12.1] A. M. Witowski and M. Grynberg, *Phys. Status Solidi B* **100**, 389 (1980).
[12.2] S. L. Lehoczky, J. G. Broerman, D. A. Nelson, and C. R. Whitsett, *Phys. Rev. B* **9**, 1598 (1974).

- **Temperature dependence**

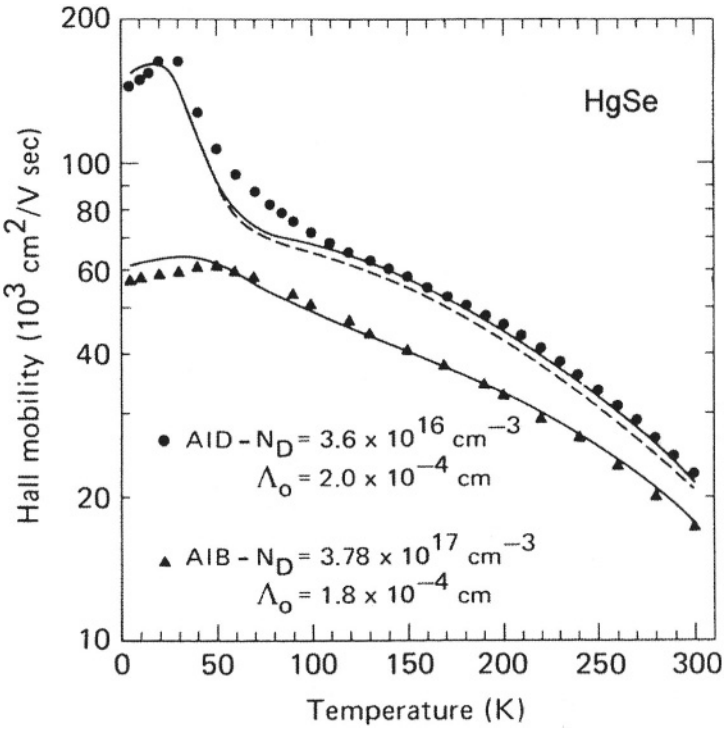

Fig. 16.12.1 Experimental (symbols) and calculated Hall mobilities as a function of temperature in HgSe. The dashed line for sample AID is calculated for electron–hole scattering in the flat-band approximation and the solid line for the approximation of a $p^{3/2}$-hole pocket. The rapid decrease in the mobility of sample AID between 30 and 50 K is due to interband scattering. [From S. L. Lehoczky, J. G. Broerman, D. A. Nelson, and C. R. Whitsett, *Phys. Rev. B* **9**, 1598 (1974).]

- **Donor concentration (free-carrier) dependence**

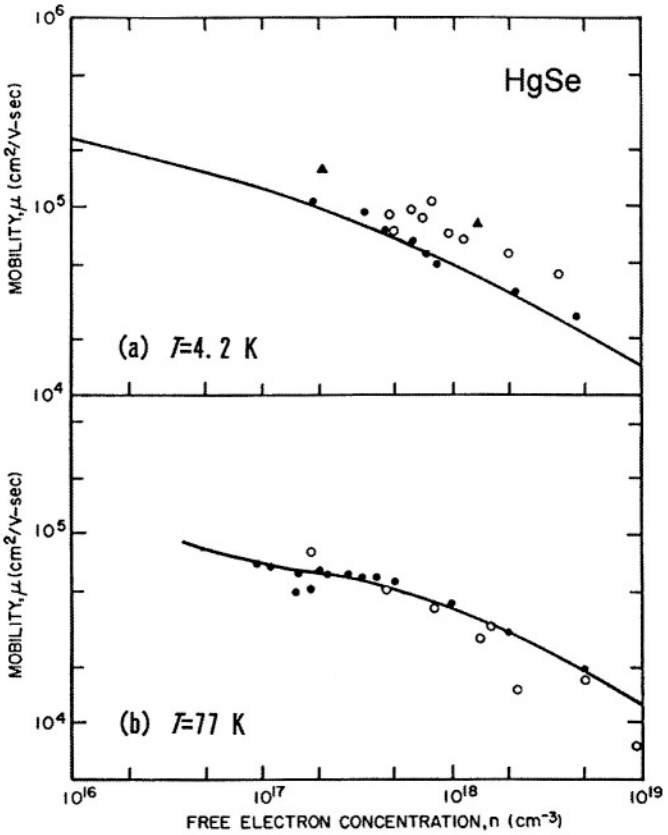

Fig. 16.12.2 Electron drift mobility μ versus electron concentration n in HgSe at (a) T=4.2 K and (b) 77 K. The solid lines represent the theoretical results. [From D. L. Rode, in *Semiconductors and Semimetals,* edited by R. K. Willardson and A. C. Beer (Academic, New York, 1975), Vol. 10, p. 1.]

- **Hall factor**

The Hall factor for HgSe has been obtained theoretically by D. L. Rode [*Phys. Status Solidi B* **55**, 687 (1973)], and its value is reported to be $\gamma \sim 1.02$ at T=200 K.

16.12.2 Low-Field Mobility: Holes

No detailed data are available for HgSe.

16.12.3 High-Field Transport: Electrons

No detailed data are available for HgSe.

16.12.4 High-Field Transport: Holes

No detailed data are available for HgSe.

16.12.5 Minority-Carrier Transport: Electrons in *p*-Type Materials

No detailed data are available for HgSe.

16.12.6 Minority-Carrier Transport: Holes in *n*-Type Materials

No detailed data are available for HgSe.

16.12.7 Impact Ionization Coefficient

No detailed data are available for HgSe.

Chapter 17

Mercury Telluride (HgTe)

17.1 STRUCTURAL PROPERTIES

17.1.1 Ionicity

Table 17.1.1 *Phillips's ionicity f_i for HgTe [1.1].*

f_i
0.650

[1.1] J. C. Phillips, *Bonds and Bands in Semiconductors* (Academic, New York, 1973).

17.1.2 Elemental Isotopic Abundance and Molecular Weight

- **Isotopic abundance**

Table 17.1.2 *Isotopic abundance in percent for mercury and tellurium [1.2].*

Isotope	% nat. abundance	Isotope	% nat. abundance
^{196}Hg	0.15	^{120}Te	0.096
^{198}Hg	9.97	^{122}Te	2.603
^{199}Hg	16.87	^{123}Te	0.908
^{200}Hg	23.10	^{124}Te	4.816
^{201}Hg	13.18	^{125}Te	7.139
^{202}Hg	29.86	^{126}Te	18.95
^{204}Hg	6.87	^{128}Te	31.69
		^{130}Te	33.80

[1.2] D. R. Lide, *CRC Handbook of Chemistry and Physics,* 78th Edition (CRC Press, Boca Raton, 1997).

• **Molecular weight**

Table 17.1.3 *Molecular (average atomic) weight M for HgTe.*

M (amu)
328.19

17.1.3 Crystal Structure and Space Group

Table 17.1.4 *Crystal structure and its space and pint groups for HgTe.*

Crystal structure	Space group	Point group
Zincblende (Cubic)	$F\bar{4}3m$	T_d

17.1.4 Lattice Constant and Its Related Parameters

• **Lattice constant, near-neighbor distance, etc.**

Table 17.1.5 *Lattice constant (a), near-neighbor distance (d), unit cube volume (a^3), and molecular density (d_M) for HgTe at 300 K.*

Parameter	Value
Lattice constant a (Å)	6.4603 [1.3]
d (Cation–Anion) (Å)	2.7974*
d (Cation–Cation) (Å)	4.5681*
Unit cube volume a^3 (10^{-22} cm^3)	2.6962*
Molecular density d_M (10^{22} cm^{-3})	1.4835*

[1.3] J. P. Schwartz, T. Tung, and R. F. Brebrick, *J. Electrochem. Soc.* **128**, 438 (1982).
*Calculated.

• **Crystal density**

Table 17.1.6 *Crystal density g for HgTe at 300 K.**

g (g/cm^3)
8.0849

*Calculated using a=6.4603 Å.

17.1.5 Structural Phase Transition

Table 17.1.7 *Structural phase transition in HgTe at high pressures.*

Structure	Transition pressure (GPa)
Zincblende ($F\bar{4}3m$)	Normal pressure
Cinnabar	1.4 [1.4]
Rocksalt (NaCl)	8 [1.4]
Orthorhombic ($Cmcm$)*	12 (β-Sn) [1.4]
	12.0 (body-centered tetragonal) [1.5]
	10.2 [1.6]
Distorted CsCl	38.1 [1.5]

[1.4] A. Werner, H. D. Hockheimer, K. Strössner, and A. Jayaraman, *Phys. Rev. B* **28**, 3330 (1983).

[1.5] T. Huang and A. L. Ruoff, *Phys. Rev. B* **31**, 5976 (1985).
[1.6] M. I. McMahon, N. G. Wright, D. R. Allan, and R. J. Nelmes, *Phys. Rev. B* **53**, 2163 (1996).
*M. I. McMahon, N. G. Wright, D. R. Allan, and R. J. Nelmes, *Phys. Rev. B* **53**, 2163 (1996).

17.1.6 Cleavage Plane

Table 17.1.8 *Crystallographic plane most readily cleaved for HgTe.*

Cleavage plane
(100)

- **Surface energy**

Table 17.1.9 *Surface energy for HgTe (in J/m^2).*

Plane				Comment
(100)	(110)	(111)	$(\bar{1}\,\bar{1}\,\bar{1})$	
	0.820	0.725	0.675	Calc. [1.7]
0.05	0.12	0.09		Calc. [1.8]

[1.7] B. N. Oshcherin, *Phys. Status Solidi A* **34**, K181 (1976).
[1.8] M. A. Berding, S. Krishnamurthy, A. Sher, and A.-B. Chen, *J. Appl. Phys.* **67**, 6175 (1990).

17.2 THERMAL PROPERTIES

17.2.1 Melting Point and Its Related Parameters

Table 17.2.1 *Melting point T_m and its related parameter for HgTe.*

Parameter	Value
Melting point T_m (K)	943±1 [2.1]
Entropy of fusion ΔS_m (cal/mol K)	14.2 [2.2]
	9.24 [2.3]

[2.1] T. C. Harman, in *Physics and Chemistry of II–VI Compounds,* edited by M. Aven and J. S. Prener (North-Holland, Amsterdam, 1967), p. 767.
[2.2] A. Pajaczkowska and Z. Dziuba, *J. Cryst. Growth* **11**, 21 (1971).
[2.3] J. Steininger, *J. Electron. Mater.* **5**, 299 (1976).

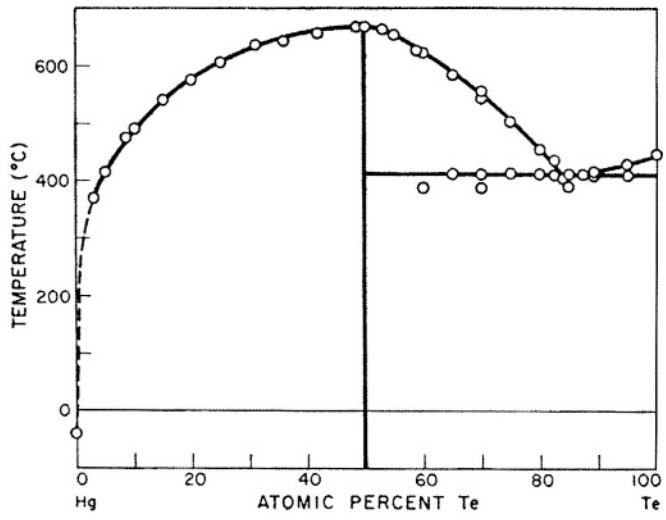

Fig. 17.2.1 Hg–Te binary liquid phase diagram. [From T. C. Harman, in *Physics and Chemistry of II–VI Compounds,* edited by M. Aven and J. S. Prener (North-Holland, Amsterdam, 1967), p. 767.]

17.2.2 Specific Heat

Table 17.2.2 *Experimental specific heat C_p (at constant pressure) for HgTe.**

Temperature (K)	C_p (mJ/g K)	Temperature (K)	C_p (mJ/g K)
2	0.035	18	39.0
2.5	0.082	20	42.7
3	0.192	22	46.0
4	0.853	24	48.8
5	2.53	26	51.2
6	5.18	293	163.3
7	8.44	333	162.6
8	12.0	373	162.7
10	19.5	413	163.3
12	25.3	453	163.7
14	31.4	503	165.6
16	34.4		

*The experimental data are taken for $T \leq 26$ K from J. G. Collins, G. K. White, J. A. Birch, and T. F. Smith [*J. Phys. C: Solid State Phys.* **13**, 1649 (1980)] and for $T \geq 293$ K from F. Kelemen, E. Cruceanu, and D. Niculescu [*Phys. Status Solidi* **11**, 865 (1965)].

- **Functional expression**

Table 17.2.3 *Specific heat C_p (at constant pressure) as a function of temperature T for HgTe.*

C_p (J/g K)	Comment
$0.136+7.5\times10^{-5}T$ [2.a]*	[2.4]
$0.15503+2.478\times10^{-5}T$ *	T=300–523 K [2.5]

[2.4] P. Goldfinger and M. Jeunehomme, *Trans. Faraday Soc.* **59**, 2851 (1963).
[2.5] M. Gambino, V. Vassiliev, and J. P. Bros, *J. Alloys Compounds* **176,** 13 (1991).
*This expression gives a value of C_p~0.162 J/g K at T=300 K.

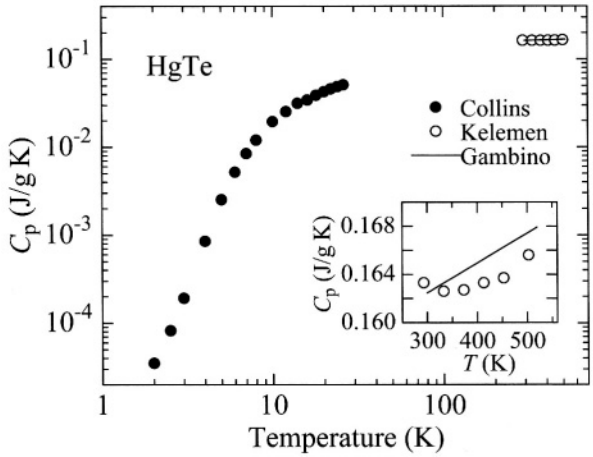

Fig. 17.2.2 Specific heat C_p (at constant pressure) versus temperature T for HgTe. The experimental data are taken from J. G. Collins, G. K. White, J. A. Birch, and T. F. Smith [*J. Phys. C: Solid State Phys.* **13**, 1649 (1980); solid circles], from F. Kelemen, E. Cruceanu, and D. Niculescu [*Phys. Status Solidi* **11**, 865 (1965); open circles], and from an empirical expression obtained by M. Gambino, V. Vassiliev, and J. P. Bros [*J. Alloys Compounds* **176,** 13 (1991); solid line].

17.2.3 Debye Temperature

Table 17.2.4 *Debye temperature θ_D for HgTe.*

θ_D (K)	Comment
145	T=0 K [2.6]

[2.6] In the low-temperature (0 K) limit [see, H. Siethoff and K. Ahlborn, *Phys. Status Solidi B* **190**, 179 (1995)].

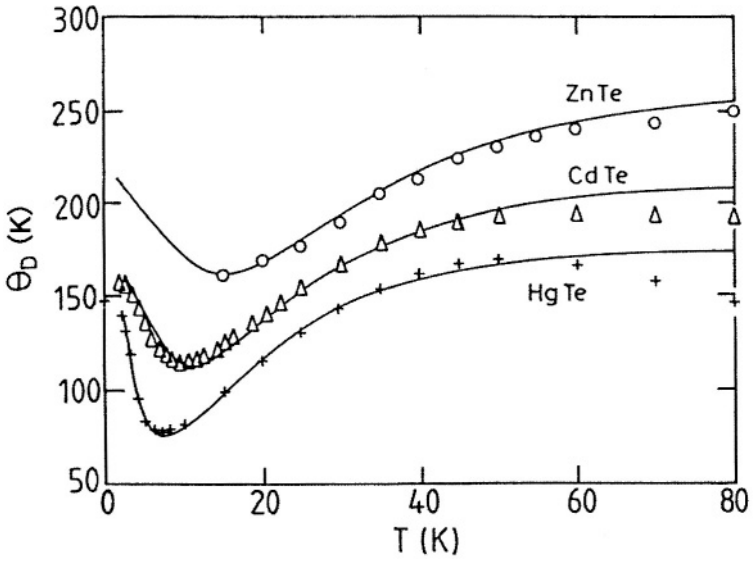

Fig. 17.2.3 Debye temperature θ_D for HgTe, together with those for ZnTe and CdTe. The symbols represent the experimental data. [From D. Bagot, R. Granger, and S. Rolland, *Phys. Status Solidi B* **177,** 295 (1993).]

17.2.4 Thermal Expansion Coefficient

Table 17.2.5 *Thermal expansion coefficient α_{th} for HgTe [2.7]. Note that the expansion coefficient shows a minimum at T~22 K.*

Temperature (K)	α_{th} (10^{-6} K^{-1})	Temperature (K)	α_{th} (10^{-6} K^{-1})
2	–0.0028	18	–3.79
2.5	–0.0069	20	–3.87
3	–0.0220	22	–3.90
4	–0.1165	24	–3.86
5	–0.345	26	–3.78
6	–0.69	28	–3.64
7	–1.10	30	–3.48
8	–1.52	57.5	–0.33
10	–2.29	65	0.32
12	–2.87	75	1.22
14	–3.33	85	1.90
16	–3.60	283	4.75

[2.7] J. G. Collins, G. K. White, J. A. Birch, and T. F. Smith, *J. Phys. C: Solid State Phys.* **13**, 1649 (1980).

Table 17.2.6 *Thermal expansion coefficient α_{th} for HgTe [2.8].*

Temperature (K)	α_{th} (10^{-6} K^{-1})	Temperature (K)	α_{th} (10^{-6} K^{-1})
24	–4.00	200	4.49
40	–2.05	220	4.65
60	–0.20	240	4.70
80	1.27	260	4.70
100	2.24	280	4.70
120	3.00	300	4.70
140	3.63	320	4.70
160	4.00	340	4.70
180	4.29		

[2.8] S. N. Novikova and N. Kh. Abrikosov, *Sov. Phys. –Solid State* **5**, 1558 (1964).

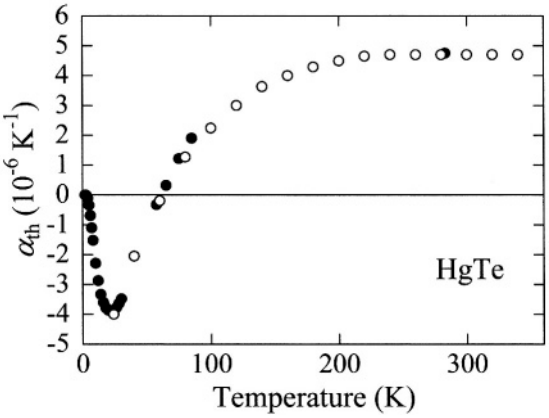

Fig. 17.2.4 Thermal expansion coefficient α_{th} versus temperature for HgTe. The experimental data are taken from J. G. Collins, G. K. White, J. A. Birch, and T. F. Smith [*J. Phys. C: Solid State Phys.* **13**, 1649 (1980); solid circles] and from S. N. Novikova and N. Kh. Abrikosov [*Sov. Phys.–Solid State* **5**, 1558 (1964); open circles].

17.2.5 Thermal Conductivity and Diffusivity

Table 17.2.7 *Thermal conductivity K for HgTe.* Thermal diffusivity can be calculated from a relation $D=K/(C_p \cdot g)$, where C_p is the specific heat at constant pressure and g is the crystal density.*

Temperature (K)	*K* (W/cm K)	Temperature (K)	*K* (W/cm K)
1.75	0.153	43.5	0.60
1.80	0.175	47.5	0.47
1.95	0.21	54	0.37
2.15	0.29	63	0.285
2.45	0.415	72	0.22
2.60	0.47	81	0.175
2.85	0.6	95	0.14
3.05	0.72	102	0.12
3.15	0.9	125	0.085
3.6	1.05	145	0.066
3.8	1.15	165	0.051
4.2	1.38	185	0.042
4.8	1.65	220	0.031

Table 17.2.7 *Continued.*

Temperature (K)	K (W/cm K)	Temperature (K)	K (W/cm K)
5.6	1.9	294	0.0242
6.0	2.1	300	0.0238
6.8	2.2	303	0.024
8.1	2.4	313	0.0232
9.6	2.6	323	0.0226
11.0	2.7	333	0.0222
12.5	2.7	345	0.0218
14.0	2.65	357	0.0213
15.5	2.52	370	0.0209
16.5	2.45	385	0.0206
18.5	2.3	400	0.0203
21.5	2.08	417	0.0200
23.5	1.8	435	0.0197
27	1.5	455	0.0196
30	1.25	476	0.0195
32	1.05	500	0.0194
38	0.76	526	0.0194

*The experimental data are taken for $T \leq 220$ K from C. R. Whitsett and D. A. Nelson [*Phys. Rev. B* **5**, 3125 (1972)] and for $T \geq 294$ K from F. Kelemen, E. Cruceanu, and D. Niculescu [*Phys. Status Solidi* **11**, 865 (1965)].

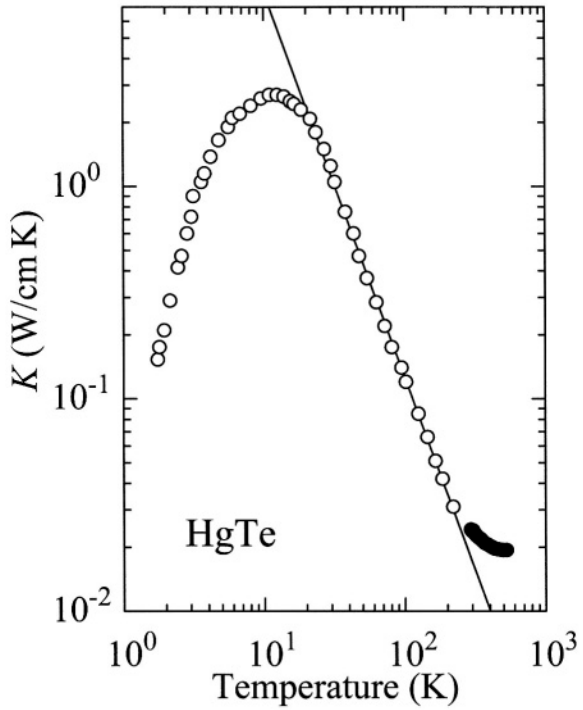

Fig. 17.2.5 Thermal conductivity K for HgTe. The experimental data are taken from C. R. Whitsett and D. A. Nelson [*Phys. Rev. B* **5**, 3125 (1972); open circles] and from F. Kelemen, E. Cruceanu, and D. Niculescu [*Phys. Status Solidi* **11,** 865 (1965)]. The solid line is calculated from $K=AT^n$ with $A=550$ W/cm K$^{-0.82}$ and $n=-1.82$.

17.3 ELASTIC PROPERTIES

17.3.1 Elastic Constant

- **Room-temperature value and its temperature and pressure derivatives**

Table 17.3.1 *Elastic constant and its temperature and pressure derivatives for HgTe at 300 K.*

Parameter	Value
Stiffness (10^{11} dyn/cm^2) [3.1]	
C_{11}	5.32
C_{12}	3.68
C_{44}	2.08
Compliance (10^{-12} cm^2/dyn) [3.1]	
S_{11}	4.33
S_{12}	–1.77
S_{44}	4.80
dC_{ij}/dT (10^7 dyn/cm^2 K) [3.1]	
C_{11}	–22
C_{12}	–16
C_{44}	–5.6
dC_{ij}/dp [3.2]	
C_{11}	3.3
C_{12}	4.1
C_{44}	–0.12

[3.1] *Numerical Data and Functional Relationships in Science and Technology,* edited by K.-H. Hellwege and A. M. Hellwege, Landolt–Börnstein, New Series, Group III, Vol. 11 (Springer, Berlin, 1979).

[3.2] *Numerical Data and Functional Relationships in Science and Technology,* edited by K.-H. Hellwege and A. M. Hellwege, Landolt–Börnstein, New Series, Group III, Vol. 18 (Springer, Berlin, 1984).

17.3.2 Third-Order Elastic Constant

Table 17.3.2 *Third-order elastic constant of HgTe [3.3].*

Modulus	Value (10^{12} dyn/cm^2)
C_{111}	–2.60
C_{112}	–1.70
C_{123}	–0.77
C_{144}	–0.17
C_{166}	–0.57
C_{456}	–0.01

[3.3] *Numerical Data and Functional Relationships in Science and Technology,* edited by K..-H. Hellwege and A. M. Hellwege, Landolt–Börnstein, New Series, Group III, Vol. 18 (Springer, Berlin, 1984).

17.3.3 Young's Modulus, Poisson's Ratio, and Similar

- **Young's modulus**

Table 17.3.3 *Young's modulus Y for HgTe at 300 K.**

Crystallographic plane	Y (10^{11} dyn/cm^2)
(100) plane	
[001] direction	2.31
[011] direction	4.03
(110) plane	
[001] direction	2.31
[111] direction	5.37
(111) plane	4.03

*Calculated using S_{11}=4.33, S_{12}=−1.77, and S_{44}=4.80 (all in 10^{-12} cm^2/dyn).

- **Poisson's ratio**

Table 17.3.4 *Poisson's ratio P for HgTe at 300 K.**

Crystallographic plane	P
(100) plane	
m=[010], n=[001]	0.409
m=[011], n=[0$\bar{1}$1]	−0.032
(110) plane	
m=[001], n=[1$\bar{1}$0]	0.409
m=[1$\bar{1}$1], n=[1$\bar{1}\bar{2}$]	0.288
(111) plane	0.465

*Calculated using S_{11}=4.33, S_{12}=−1.77, and S_{44}=4.80 (all in 10^{-12} cm^2/dyn).

- **Bulk modulus, shear modulus, etc.**

Table 17.3.5 *Bulk modulus, B_u, pressure derivative of B_u, dB_u/dp, shear modulus, C_s, isotropy factor, A, linear compressibility, C_o, Caucy ratio, C_a, and Born ratio, B_o, for HgTe at 300 K.*

Parameter	Value
B_u (10^{11} dyn/cm^2)	4.23 [3.4]
dB_u/dp	2.1 [3.5]
	3.8 [3.6]
C_s (10^{10} dyn/cm^2)	8.20 [3.4]
A	0.394 [3.4]
C_o (10^{-13} cm^2/dyn)	7.89 [3.4]
C_a	1.77 [3.4]
B_o	1.18 [3.4]

[3.4] Calculated using C_{11}=5.32, C_{12}=3.68, and C_{44}=2.08 (all in 10^{11} dyn/cm^2).

[3.5] Exper. [A. Werner, H. D. Hochheimer, K. Strössner, and A. Jayaraman, *Phys. Rev. B* **28**, 3330 (1983)].

[3.6] Calculated from dC_{ij}/dp data [*Numerical Data and Functional Relationships in Science and Technology,* edited by K.-H. Hellwege and A. M. Hellwege, Landolt–Börnstein, New Series, Group III, Vol. 18 (Springer, Berlin, 1984)].

17.3.4 Microhardness

Table 17.3.6 *Microhardness H for HgTe.*

H (GPa)	Ref.
0.37	[3.7]
0.23–0.37	[3.8]

[3.7] See, L. Garbato and A. Rucci, *Phil. Mag.* **35**, 1681 (1977).
[3.8] A. M. Andrukhiv, V. I. Ivanov–Omskiĭ, and P. G. Sidorchuk, *Sov. Phys. Solid State* **34**, 1934 (1992).

17.3.5 Sound Velocity

Table 17.3.7 *Sound velocity propagating in HgTe at 300 K.* LA=longitudinal acoustic; TA1, TA2=transverse acoustic.*

Propagation direction	Mode	Sound velocity (10^5 cm/s)
[100]	LA	2.57
[100]	TA1, TA2	1.60
[110]	LA	2.85
[110]	TA1	1.01
[110]	TA2	1.60
[111]	LA	2.94
[111]	TA1, TA2	1.24

*Calculated using $C_{11}=5.32\times10^{11}$ dyn/cm^2, $C_{12}=3.68\times10^{11}$ dyn/cm^2, $C_{44}=2.08\times10^{11}$ dyn/cm^2, and $g=8.0849$ g/cm^3.

17.4 PHONONS AND LATTICE VIBRONIC PROPERTIES

17.4.1 Phonon Dispersion Relation

- **Dispersion curve**

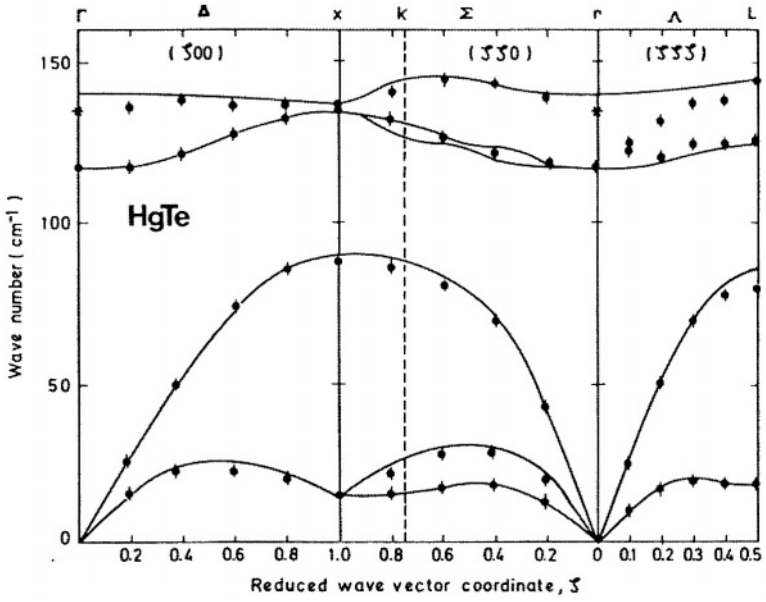

Fig. 17.4.1 Dispersion curves for the acoustic and optical branch phonons in HgTe at 300 K. The solid lines are calculated from a rigid ion model. The symbols represent the neutron data measured by H. Kępa, T. Giebultowicz, B. Buras, B. Lebech, and K. Clausen [*Phys. Scripta* **25**, 807 (1982)]. [From D. N. Talwar and M. Vandevyver, *J. Appl. Phys.* **56**, 1601 (1984).]

- **Phonon density of states**

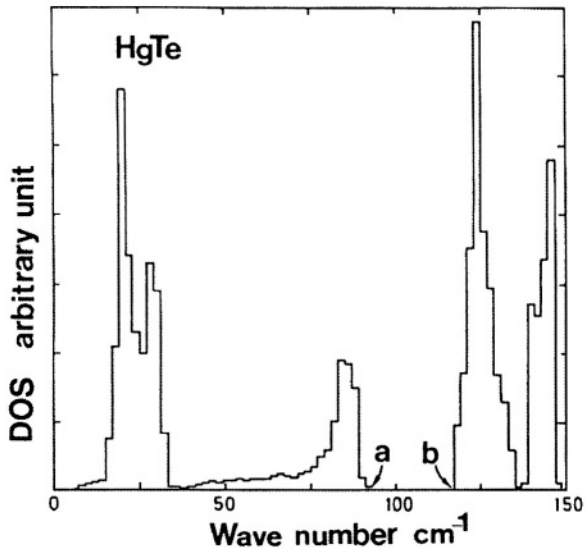

Fig. 17.4.2 Calculated one-phonon density of states (DOS) for HgTe based on a rigid ion model. The terms *a* and *b* represent the limits of the calculated gap in the one-phonon density of states. [From D. N. Talwar and M. Vandevyver, *J. Appl. Phys.* **56**, 1601 (1984).]

17.4.2 Phonon Frequency

- **Room-temperature value**

Table 17.4.1 *Long-wavelength ($q \to 0$) and zone-boundary phonon frequencies for HgTe [4.1].*

Critical point	Phonon	Phonon frequency (cm^{-1})
Γ	TO	118
		117 [4.2]
		116 [4.3]
	LO	136
		137 [4.2]
		135 [4.3]
X	TA	15.9
	LA	85.2
	TO	134.2
	LO	136.0
L	TA	18.4
	LA	80.4
	TO	127.9
	LO	145.7

[4.1] H. Kępa, T. Giebultowicz, B. Buras, B. Lebech, and K. Clausen, *Phys. Scripta* **25**, 807 (1982).
[4.2] A. Ingale, M. L. Bansal, and A. P. Roy, *Phys. Rev. B* **40**, 12353 (1989).
[4.3] M. Rösch, R. Atzmüller, G. Schaack, and C. R. Becker, *Phys. Rev. B* **49**, 13460 (1994).

- **Temperature dependence**

It has been reported that the TO phonon frequency in HgTe shows an increase of about 2 to 3 cm^{-1} in going from 10 to ~290 K [M. Grynberg, R. Le Toullec, and M. Balkanski, *Phys. Rev. B* **9**, 517 (1974); M. L. Bansal, A. Ingale, and A. P. Roy, *Phys. Rev. B* **43**, 7020 (1991)].

17.4.3 Mode Grüneisen Parameter

No detailed data are available for HgTe.

17.4.4 Phonon Deformation Potential

No detailed data are available for HgTe.

17.5 COLLECTIVE EFFECTS AND RELATED PROPERTIES

17.5.1 Piezoelectric Constant

Table 17.5.1 *Piezoelectric stress (e_{14}), strain (d_{14}), and electromechanical coupling constants ($K_{[110]}^2$) for HgTe [5.1].*

Parameter	Value
e_{14} (C/m^2)	+0.029
d_{14} (10^{-12} m/V)	+1.4 *
$K_{[110]}^2$	2.2×10^{-5} *

[5.1] Theor. [K. Hübner, *Phys. Status Solidi B* **57**, 627 (1973)].
*Calculated.

17.5.2 Fröhlich Coupling Constant

No detailed data are available for HgTe.

17.6 ENERGY-BAND STRUCTURE: ENERGY-BAND GAPS

17.6.1 Basic Properties

- **Electronic energy-band structure**

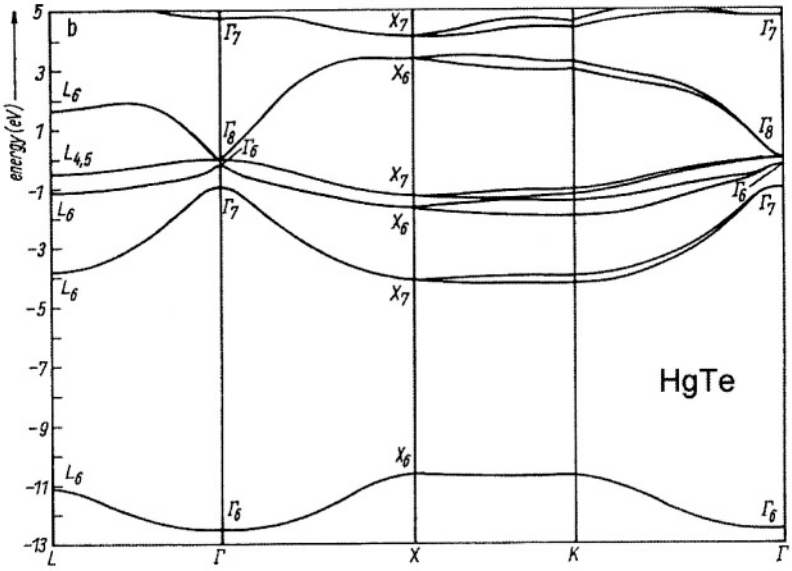

Fig. 17.6.1 Electronic energy-band structure of HgTe as calculated by the tight-binding model. The electronic states are labeled using the notation for the representations of the double group of the zinc-blende structure. [From M. T. Czyżyk and M. Podgórny, *Phys. Status Solidi B* **98**, 507 (1980).]

- **Energy eigenvalue**

Table 17.6.1 *Energy eigenvalues at the Γ, X, and L points for the valence and first few conduction bands of HgTe [6.1].*

Critical point	Level	Value (eV)	
		Calc. [6.1]	Exper.*
Γ	Γ_{15}^{v}	0.0	0.0, –(0.896–1.08)
	Γ_{1}^{c}	0.0	–0.3
	Γ_{15}^{c}	6.0	
X	X_{3}^{v}	–3.1	
	X_{5}^{v}	–0.9	
	X_{1}^{c}	2.9	
	X_{3}^{c}	3.6	
L	L_{1}^{v}	–3.2	
	L_{3}^{v}	–0.1	
	L_{1}^{c}	2.4	
	L_{3}^{c}	6.2	

[6.1] F. Herman, R. L. Kortum, C. D. Kuglin, and J. L. Shay, in *II–VI Semiconducting Compounds,* edited by D. G. Thomas (Benjamin, New York, 1967), p. 503.
*Obtained from various sources.

17.6.2 E_0-Gap Region

- **General remark**

The band structure of HgTe is considered to be of the inverted type. The lowest-conduction-band minimum and the top of the valence band in HgTe are degenerate at the center of the Brillouin zone (Γ point, k=0). The Γ_8 level is the fourfold component of the spin–orbit–split valence band. The Γ_6 level, which for most cubic semiconductor is the conduction-band minimum with an energy larger than the Γ_8 state, is locate below the Γ_8 state (i.e., "*negative*" energy gap, "*inverted*" band structure).

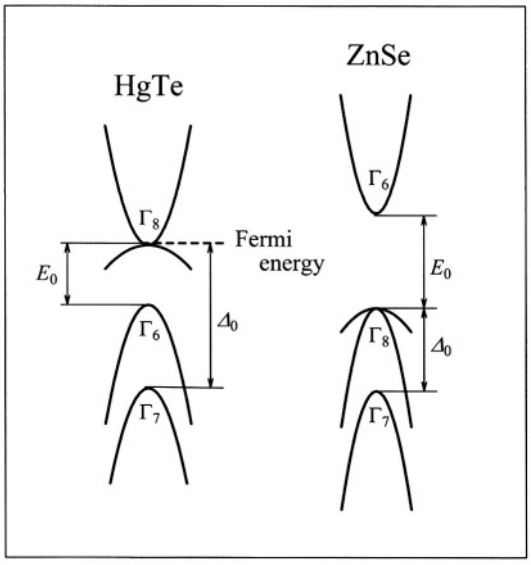

Fig. 17.6.2 Schematic diagram of the electronic energy-band structure of HgTe and ZnSe at k=0. The bands are labeled in the double-group representation. In HgTe, the band-gap energy between the Γ_8 conduction and valence bands is zero (semimetal).

• **Temperature dependence**

Table 17.6.2 *E_0- and Δ_0-gap energies for HgTe determined at various temperatures.*

Temperature (K)	E_0 (eV)	Δ_0 (eV)	Ref.
4.2	–0.283±0.001		[6.2]
	–0.30		[6.3]
	–0.30		[6.4]
4.4	–0.3025		[6.5]
10	–0.3	1.08	[6.6]
40	–0.29±0.02	0.91±0.02	[6.7]
77	–0.25		[6.4]
80	–0.259		[6.8]
95	–0.22		[6.9]
292	–0.146		[6.8]
300	–0.16		[6.3]
	–0.15		[6.4]
	–0.32±0.03	0.91±0.02	[6.7]
	–0.12		[6.9]
	–0.146	0.896	[6.10]
Recommended value (T~300 K): E_0= –0.15 eV; Δ_0=1.0 eV			

[6.2] S. H. Groves, R. N. Brown, and C. R. Pidgeon, *Phys. Rev.* **161**, 779 (1967).
[6.3] R. R. Galazka, *Phys. Lett.* **32A**, 101 (1970).
[6.4] See, A. Rogalski, *Prog. Quantum Electron.* **13**, 299 (1989).
[6.5] Y. Guldner, C. Rigaux, M. Grynberg, and A. Mycielski, *Phys. Rev. B* **8**, 3875 (1973).
[6.6] W. Szuszkiewicz, *Phys. Status Solidi B* **79**, 691 (1977).
[6.7] N. Orlowski, J. Augustin, Z. Gołacki, C. Janowitz, and R. Manzke, *Phys. Rev. B* **61**, R5058 (2000).
[6.8] B. Toulouse, R. Granger, S. Rolland, and R. Triboulet, *J. Phys. (Paris)* **48**, 247 (1987).
[6.9] V. G. Sredin, V. G. Savitskiĭ, Yu. V. Danilyuk, M. V. Miliyanchuk, and I. V. Petrovich, *Sov. Phys. Semicond* **15**, 249 (1981).
[6.10] O. Castaing, J. T. Benhlal, R. Granger, and R. Triboulet, *J. Phys. IFrance* **6**, 907 (1996).

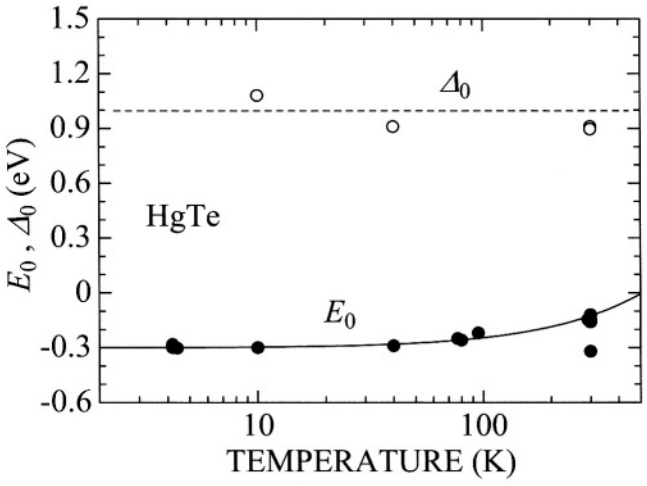

Fig. 17.6.3 E_0- and Δ_0-gap energies versus temperature for HgTe. The experimental data are gathered from various sources. The solid line represents the calculated result of an expression, $E_0(T) = -0.30 + (6.0\times10^{-4}T^2)/(T+10)$, while the dashed line indicates a value of Δ_0=1.0 eV.

Table 17.6.3 *Expression of $E_0(T)$ for HgTe (T in kelvin).*

$E_0(T)$ (eV)	Ref.
$-0.303+5.6\times10^{-4}T$	[6.11]
$-0.25+5.233\times10^{-4}T$	[6.12]
$-0.30+5.0\times10^{-4}T$	[6.13]
$-0.304+5.0\times10^{-4}T$	[6.14]
$-0.302+5.35\times10^{-4}T$	[6.15]
$-0.30+5.30\times10^{-4}T$	[6.16]
$-0.303+\frac{6.3\times10^{-4}T^2}{11+T}$	[6.17]
$-0.295+6.0\times10^{-4}T$	[6.18]
$-0.2854-1.15\times10^{-4}T$	[6.19]
$-0.30+\frac{6.0\times10^{-4}T^2}{10+T}$	*

[6.11] M. W. Scott, *J. Appl. Phys.* **40**, 4077 (1969).
[6.12] J. L. Schmit and E. L. Stelzer, *J. Appl. Phys.* **40**, 4865 (1969).
[6.13] A. D. Shneider and D. I. Tsiutsiura, *Phys. Status Solidi A* **5**, K39 (1971).
[6.14] R. S. Kim and S. Narita, *Phys. Status Solidi B* **73**, 741 (1976).
[6.15] G. L. Hansen, J. L. Schmit, and T. N. Casselman, *J. Appl. Phys.* **53**, 7099 (1982).
[6.16] B. Toulouse, R. Granger, S. Rolland, and R. Triboulet, *J. Phys. (Paris)* **48**, 247 (1987); O. Castaing, J. T. Benhlal, R. Granger, and R. Triboulet, *J. Phys. I France* **6**, 907 (1996).
[6.17] J. P. Laurenti, J. Camassel, A. Bouhemadou, B. Toulouse, R.Legros, and A. Lusson, *J. Appl. Phys.* **67**,6454(1990).
[6.18] J. Chu, Z. Mi, and D. Tang, *Infrared Phys.* **32**, 195 (1991).
[6.19] $T\geq40$ K [N. Orlowski, J. Augustin, Z. Gołacki, C. Janowitz, and R. Manzke, *Phys. Rev. B* **61**, R5058 (2000)].
*See figure, above.

- **Pressure coefficient**

Table 17.6.4 *Linear pressure coefficient of the E_0-gap energy for HgTe.*

Coefficient	Value	Technique
dE_0/dp (10^{-2} eV/GPa)	−10±2	[6.20]
	−15.3	Transport [6.21]

[6.20] See, N. B. Brandt, O. N. Belousova, L. A. Bovina, V. I. Stafeev, and Ya. G. Ponomarev, *Sov. Phys.–JETP* **39**,157 (1974).
[6.21] A. Ohtani, T. Seike, M. Motobayashi, and A. Onodera, *J. Phys. Chem. Solids* **43**, 627 (1982).

17.6.3 Higher-Lying Direct Gap

- **Room-temperature value**

Table 17.6.5 *E_1-, $E_1+\Delta_1$-, and Δ_0-gap energies for HgTe at room temperature.*

E_1 (eV)	$E_1+\Delta_1$ (eV)	Δ_1 (eV)	Ref.
2.08	2.77	0.69	[6.22]
2.14	2.78	0.64	[6.23]
2.09	2.71	0.62	[6.24]
2.12	2.78	0.66	[6.25]

Table 17.6.5 *Continued.*

E_1 (eV)	$E_1+\Delta_1$ (eV)	Δ_1 (eV)	Ref.
2.06±0.1	2.73±0.1	0.67±0.02	[6.26]
2.18	2.80	0.62	[6.27]
2.11	2.72	0.61	[6.28]
2.068	2.73	0.66	[6.29]
2.11	2.74	0.63	[6.30]
2.147±0.005	2.778±0.005	0.631±0.001	[6.31]
2.114±0.002	2.756±0.012	0.642	[6.32]
2.109±0.002	2.741±0.009	0.632	[6.33]
2.106±0.003	2.736±0.010	0.630	[6.34]
2.11	2.75	0.64	Mean value

[6.22] M. Cardona, *J. Appl. Phys.* **32** (Suppl.), 2151 (1961).
[6.23] M. Cardona and G. Harbeke, *J. Appl. Phys.* **34**, 813 (1963).
[6.24] M. Cardona and D. L. Greenaway, *Phys. Rev.* **131**, 98 (1963).
[6.25] M. Cardona, K. L. Shaklee, and F. H. Pollak, *Phys. Rev.* **154**, 696 (1967).
[6.26] R. R. Gałązka and A. Kisiel, *Phys. Status Solidi* **34**, 63 (1969).
[6.27] A. Moritani, H. Sekiya, K. Taniguchi, C. Hamaguchi, J. Nakai, and R. Makabe, *Jpn. J. Appl. Phys.* **10**,1410 (1971).
[6.28] I. N. Borisov, V. V. Mikhailin, P. S. Kireev, and V. M. Bezborodova, *Sov. Phys.–Semicond* **5**, 728 (1971).
[6.29] A. Kisiel, M. Podgórny, A. Rodzik, and W. Giriat, *Phys. Status Solidi B* **71**, 457 (1975).
[6.30] V. G. Sredin, V. G. Savitskiĭ, Yu. V. Danilyuk, M. V. Miliyanchuk, and I. V. Petrovich, *Sov. Phys. Semicond.* **15**, 249 (1981).
[6.31] L. Viña, C. Umbach, M. Cardona, and L. Vodoyanov, *Phys. Rev. B* **29**, 6752 (1984).
[6.32] H. Arwin and D. E. Aspnes, *J. Vac. Sci. Technol. A* **2**, 1316 (1984).
[6.33] Assuming two-dimensional critical point [O. Castaing, J. T. Benhlal, R. Granger, and R. Triboulet, *J. Phys. I France* **6**, 907 (1996)].
[6.34] Assuming excitonic transition [O. Castaing, J. T. Benhlal, R. Granger, and R. Triboulet, *J. Phys. I France* **6**, 907 (1996)].

Table 17.6.6 *Higher-lying interband transition energies in HgTe at room temperature.*

Peak	Value (eV)	
	a	b
E_0'	4.1	4.19
		4.65 (E_0'+Δ_0')
B	5.0	4.96 (E_2)
$B+\Delta_2$	5.1	5.19 ($E_2+\Delta_2$)
C	5.4	5.49 ($E_2+\delta+\Delta_2$)
$C+\Delta_2$	5.6	
E	6.55	6.40 (E_3)
		6.72 (E_3')
A	7.5	7.50 (E_1')
$A+\delta_1$	8.25	8.21 (E_1'+Δ_1)
d_1	9.55	
d_2	11.1	

[a] H. Overhof, *Phys. Status Solidi B* **43**, 221 (1971).
[b] I. N. Borisov, V. V. Mikhailin, P. S. Kireev, and V. M. Bezborodova, *Sov. Phys.–Semicond.* **5**, 728 (1971).

• **Temperature and/or pressure coefficient**

Table 17.6.7 *Linear temperature coefficient of the higher-lying band-gap energy for HgTe.*

Band gap	Coefficient	Value	Comment
E_1	dE_g/dT (10^{-4} eV/K)	–4.5±0.2	Exper. [6.35]
		–5.5	Exper. [6.36]
		–6.13	Exper. [6.37]
	dE_g/dp (10^{-2} eV/GPa)	5.4	Calc. [6.38]
$E_1+\Delta_1$	dE_g/dT (10^{-4} eV/K)	–3.8±0.3	Exper. [6.35]
		–6.4	Exper. [6.36]
		–6.45	Exper. [6.37]
E_0'	dE_g/dT (10^{-4} eV/K)	~–3	Exper. [6.36]
		–6.66	Exper. [6.37]
E_2	dE_g/dT (10^{-4} eV/K)	–(5.1–6.0)	Exper. [6.36]
		–6.97	Exper. [6.37]
	dE_g/dp (10^{-2} eV/GPa)	3.4	Calc. [6.38]

[6.35] M. Cardona and G. Harbeke, *J. Appl. Phys.* **34**, 813 (1963).
[6.36] M. Cardona and D. L. Greenaway, *Phys. Rev.* **131,** 98 (1963).
[6.37] A. Rodzik and A. Kisiel, *J. Phys. C: Solid State Phys.* **16,** 203 (1983).
[6.38] D. L. Camphausen, G. A. N. Connell, and W. Paul, *Phys. Rev. Lett.* **26**, 184 (1971).

17.6.4 Lowest Indirect Gap

• **Theoretical value**

Table 17.6.8 *Theoretically obtained lowest indirect-gap energy for HgTe [6.39].*

Band gap	Value (eV)
E_g^L ($\Gamma_{15}^v \rightarrow L_1^c$)	2.4
E_g^X ($\Gamma_{15}^v \rightarrow X_1^c$)	2.9

[6.39] F. Herman, R. L. Kortum, C. D. Kuglin, and J. L. Shay, in *II–VI Semiconducting Compounds,* edited by D. G. Thomas (Benjamin, New York, 1967), p. 503.

• **Temperature and/or pressure coefficient**

Table 17.6.9 *Linear temperature and pressure coefficients of the lowest indirect-gap energy for HgTe.*

Coefficient	Value	Comment
dE_g^L/dp (10^{-2} eV/GPa)	1.8	Calc. [6.40]
dE_g^X/dp (10^{-2} eV/GPa)	–4.7	Calc. [6.40]

[6.40] S.-H. Wei and A. Zunger, *Phys. Rev. B* **60**, 5404 (1999).

17.6.5 Conduction-Valley Energy Separation

No detailed data are available for HgTe.

17.6.6 Direct–Indirect-Gap Transition Pressure

No detailed data are available for HgTe.

17.7 ENERGY-BAND STRUCTURE: ELECTRON AND HOLE EFFECTIVE MASSES

17.7.1 Electron Effective Mass: Γ Valley

- **Theoretical value**

Table 17.7.1 *Theoretical electron effective mass m_e^Γ at the Γ_6 valley for HgTe*

m_e^Γ/m_0	Technique
–0.031*	Five-level $\boldsymbol{k}\cdot\boldsymbol{p}$ calculation [7.1]

[7.1] P. Lawaetz, *Phys. Rev. B* **4**, 3460 (1971).
*The sign is chosen positive for a normal band structure like that of CdTe (i.e., "–" means that free carriers behave like holes, not electrons).

- **Experimental value**

Table 17.7.2 *Experimental electron effective mass m_e^Γ at the Γ_6 valley for HgTe*

m_e^Γ/m_0	Technique
–0.028±0.001*	Magnetoabsorption, T=4.4 K [7.2]

[7.2] Y. Guldner, C. Rigaux, M. Grynberg, and A. Mycielski, *Phys. Rev. B* **8**, 3875 (1973).
*The sign is chosen positive for a normal band structure like that of CdTe (i.e., "–" means that free carriers behave like holes, not electrons).

17.7.2 Electron Effective Mass: Satellite Valley

No detailed data are available for HgTe.

17.7.3 Hole Effective Mass

- **Luttinger's valence-band parameter**

Table 17.7.3 *Luttinger's valence-band parameter γ_i for HgTe (in $\hbar^2/2m_0$).*

γ_1	γ_2	γ_3	Technique
–18.3	–11.2	–10.0	Magnetoreflectivity, T=4.2K [7.3]
–18.68	–10.19	–9.56	Five-level $\boldsymbol{k}\cdot\boldsymbol{p}$ calculation [7.4]
–12.8±0.5	–8.4±0.1	–8.4±0.1	Magnetoabsorption, T=4.4 K [7.5]
–14.8	–9.0	–8.2	Magnetooptics, T=4.2 K [7.6]
–15.6	–9.6	–8.6	Magnetoabsorption, T=4.2 K [7.7]
–16.8±0.2	–10.6±0.1	–8.8±0.1	Magnetoabsorption, T=4.2 K [7.8]
–14.8	–9.5	–8.0	Magnetophonon resonance, T=4.2 K [7.9]
–17.3	–10.7	–8.5	Magnetoreflectivity, T=12–300 K [7.10]
–18.3±0.8	–11.8±0.6	–9.9±0.5	Magnetophonon resonance, T=4.2 K [7.11]

[7.3] S. H. Groves, R. N. Brown, and C. R. Pidgeon, *Phys. Rev.* **161,** 779 (1967).
[7.4] P. Lawaetz, *Phys. Rev. B* **4**, 3460 (1971).
[7.5] Y. Guldner, C. Rigaux, M. Grynberg, and A. Mycielski, *Phys. Rev. B* **8**, 3875 (1973).
[7.6]S. Uchida and S. Tanaka, *J. Phys. Soc. Jpn* **40**, 118 (1976).
[7.7] K. Shimizu, S. Narita, Y. Nisida, and V. I. Ivanov-Omskii, *Solid State Commun.* **32**, 327 (1979).
[7.8] R. Stępniewski, K. Pastor, and M. Grynberg, *J. Phys. C: Solid State Phys.* **13,** 5783 (1980).
[7.9] K. Takita, T. Ippōshi, and K. Masuda, *Solid State Commun.* **52**, 1021 (1984).

[7.10] S. Tanana, S. Takeyama, N. Miura, and S. Uchida, *J. Phys. Soc. Jpn* **56**, 788 (1987).
[7.11] M. V. Yakunin, *Sov. Phys. Semicond.* **22**, 918 (1988).

- **Band mass, cyclotron mass, etc.**

Table 17.7.4 *Band (m_{HH}, m_{LH}), density-of-states heavy-hole (m_{HH}*), averaged light-hole (m_{LH}*), and spherically-averaged heavy-hole (m_{HH}^s) and light-hole masses (m_{LH}^s) in HgTe.*

Mass	Value (m_0)
m_{HH} ([001] direction)	0.28*[1]
m_{LH} ([001] direction)	–0.029*[1,*2]
m_{HH} ([111] direction)	0.63*[1]
m_{LH} ([111] direction)	–0.030*[1,*2]
m_{HH}*	–0.030*[1,*2]
	–0.031±0.001*[2] [7.12]
	–0.0272*[2] [7.13]
	–0.032±0.001*[2] [7.14]
m_{LH}*	0.38*[1]
m_{HH}^s	0.42*[1]
m_{LH}^s	–0.030*[1,*2]

[7.12] Y. Guldner, C. Rigaux, M. Grynberg, and A. Mycielski, *Phys. Rev. B* **8**, 3875 (1973).
[7.13] L. P. Zverev, V. V. Krushaev, G. M. Min'kov, and O. E. Rut, *Sov. Phys. JETP* **53**, 595 (1981).
[7.14] A. Sh. Mekhtiev, *Sov. Phys. Semicond.* **17**, 953 (1983).
*[1] Calculated using a set of the Luttinger's parameters, $\gamma_1=-15.6$, $\gamma_2=-9.6$, and $\gamma_3=-8.6$.
*[2] The sign is chosen positive for a normal band structure like that of CdTe (i.e., "–" means that free carriers behave like electrons, not holes).

Table 17.7.5 *Γ_8-valence-band hole effective mass m_{HH} in HgTe determined by magnetoreflectivity at T=4.2 K [7.15].*

Direction	m_{HH}/m_0
<100>	0.320
<110>	0.406
<111>	0.445

[7.15] S. H. Groves, R. N. Brown, and C. R. Pidgeon, *Phys. Rev.* **161,** 779 (1967).

- **Spin–orbit–splitoff hole effective mass**

Table 17.7.6 *Spin–orbit–splitoff hole effective mass m_{SO} for HgTe.*

m_{SO}/m_0	Technique
0.102	Five-level $\boldsymbol{k}\cdot\boldsymbol{p}$ calculation [7.16]

[7.16] P. Lawaetz, *Phys. Rev. B* **4**, 3460 (1971).

17.8 ELECTRONIC DEFORMATION POTENTIAL

17.8.1 Intravalley Deformation Potential: Γ Point

• Conduction band

Table 17.8.1 *Γ-conduction-band intravalley deformation potential* a_c^{Γ} $(=E_1^{\Gamma})$ *for HgTe.*

a_c^{Γ} (eV)	Technique
–4.60	Calc. [8.1]

[8.1] C. G. Van de Walle, *Phys. Rev. B* **39**, 1871 (1989).

Table 17.8.2 *Intravalley acoustic deformation potential* E_1 *for HgTe used in the electron transport analysis.*

E_1 (eV)	Ref.
4	[8.2]

[8.2] D. L. Rode, in *Semiconductors and Semimetals,* edited by R. K. Willardson and A. C. Beer (Academic, New York, 1975), Vol. 10, p. 1.

• Valence band

Table 17.8.3 *Γ-valence-band deformation potentials a, b, and d for HgTe.*

Deformation potential (eV)			Technique
a	*b*	*d*	
–2.0			Calc. [8.3]
–0.13	–1.15		Calc. [8.4]
–0.92	–1.21		Calc. [8.5]
	–1.22		Calc. [8.6]
	–1.3±0.4	–2.1±0.2	Magnetooptics [8.7]
	–1.5±0.2		Magnetoresistivity [8.8]
	–1.5±0.1	–8.0±0.5	Magnetophonon resonance [8.9]

[8.3] M. Cardona and N. E. Christensen, *Phys. Rev. B* **35**, 6182 (1987); erratum, *ibid.* **36**, 2906 (1987).
[8.4] C. G. Van de Walle, *Phys. Rev. B* **39**, 1871 (1989).
[8.5] A. Qteish and R. J. Needs, *Phys. Rev. B* **45**, 1317 (1992).
[8.6] T. Nakayama, *Solid-State Electron.* **37,** 1077 (1994).
[8.7] R. Yoshizaki and S. Tanaka, *J. Phys. Soc. Jpn* **42,** 1601 (1977).
[8.8] K. Takita, K. Onabe, and S. Tanaka, *Phys. Status Solidi B* **92**, 297 (1979).
[8.9] M. V. Yakunin, *Sov. Phys. Semicond.* **22,** 918 (1988).

• E_0 gap

Table 17.8.4 *Hydrostatic deformation potential* a_0^{Γ} *for the* E_{0gap} *of HgTe.*

a_0^{Γ} (eV)	Comment
–4.48	Calc. [8.10]
–4.22	Calc. [8.11]
–3.19	Calc. [8.12]

[8.10] C. G. Van de Walle, *Phys. Rev. B* **39**, 1871 (1989).

[8.11] T. Nakayama, *Solid-State Electron.* **37**, 1077 (1994).
[8.12] S.-H. Wei and A. Zunger, *Phys. Rev. B* **60**, 5404 (1999).

17.8.2 Intravalley Deformation Potential: High-Symmetry Points

- **Optical-phonon deformation potential: L point**

Table 17.8.5 *Optical-phonon deformation potentials* $d_{1o}(c)$, $d_{1o}(v)$, *and* d_{3o} *at the L point of HgTe.*

Deformation potential	Value (eV)	Technique
d_{1o}	24 ($\|d_{1o}\|$)	Raman scattering [8.13]
	−19.9	Raman scattering [8.14]
d_{3o}	21.6 ($\|d_{3o}\|$)	Raman scattering [8.13]
	14.7	Raman scattering [8.14]

[8.13] A. Ingale, M. L. Bansal, and A. P. Roy, *Phys. Rev. B* **40**, 12353 (1989).
[8.14] M. Rösch, R. Atzmüller, G. Schaack, and C. R. Becker, *Phys. Rev. B* **49**, 13460 (1994).

17.8.3 Intervalley Deformation Potential

No detailed data are available for HgTe.

17.9 ELECTRON AFFINITY AND SCHOTTKY BARRIER HEIGHT

17.9.1 Electron Affinity

No detailed data are available for HgTe.

17.9.2 Schottky Barrier Height

No detailed data are available for HgTe.

17.10 OPTICAL PROPERTIES

17.10.1 Summary of Optical Dispersion Relations

• **$\varepsilon(E)$ and $n^*(E)$ spectra**

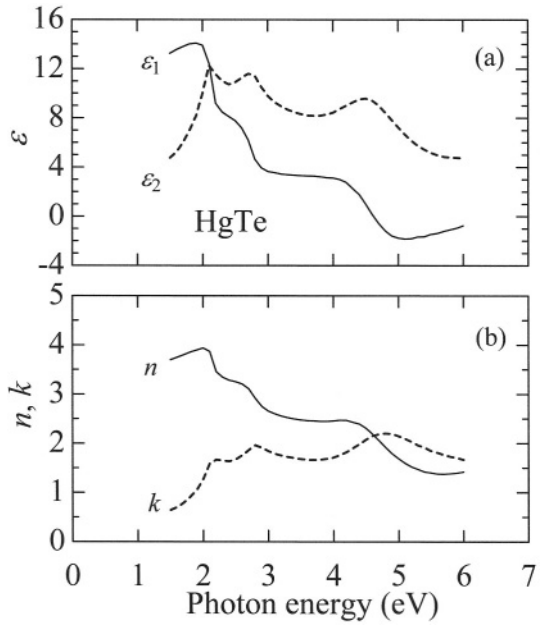

Fig. 17.10.1 (a) Complex dielectric-constant [$\varepsilon(E)=\varepsilon_1(E)+i\varepsilon_2(E)$] and (b) complex refractive-index spectra [$n^*(E)=n(E)+ik(E)$] for HgTe at 300 K. The numerical data are taken from tabulation by S. Adachi [*Optical Constants of Crystalline and Amorphous Semiconductors: Numerical Data and Graphical Information* (Kluwer Academic, Boston, 1999)].

• **$\alpha(E)$ and $R(E)$ spectra**

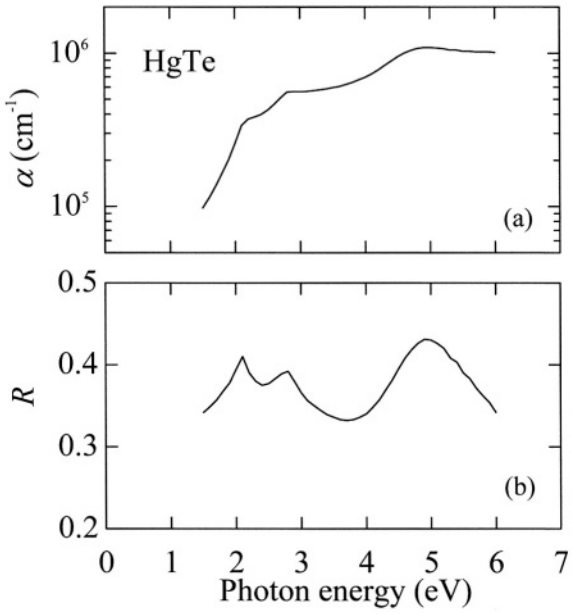

Fig. 17.10.2 (a) Absorption [$\alpha(E)$] and (b) normal-incidence reflectivity spectra [$R(E)$] for HgTe at 300 K. The numerical data are taken from tabulation by S. Adachi *[Optical Constants of Crystalline and Amorphous Semiconductors: Numerical Data and Graphical Information* (Kluwer Academic, Boston, 1999)].

17.10.2 The Reststrahlen Region

• Static and high-frequency dielectric constants

Table 17.10.1 *Static and high-frequency dielectric constants ε_s and ε_∞ for HgTe.*

ε_s	ε_∞	Comment
21.0	15.2*	T=77 K [10.1]
	7 (14*)	T=300 K [10.2]
	7.1±0.5	T=295 K [10.3]
	13.2*	T=295 K [10.4]
21	7	Recommended value (T=300 K)

[10.1] J. Baars and F. Sorger, *Solid State Commun.* **10,** 875 (1972).
[10.2] M. Grynberg, R. Le Toullec, and M. Balkanski, *Phys. Rev. B* **9**, 517 (1974).
[10.3] W. Szszkiewicz, A. M. Witowski, and M. Grynberg, *Phys. Status Solidi B* **87**, 637 (1978).
[10.4] M. P. Volz, F. R. Szofran, S. L. Lehoczky, and C.-H. Su, *Solid State Commun.* **75**, 943 (1990).
*The interband contribution was included in the analysis.

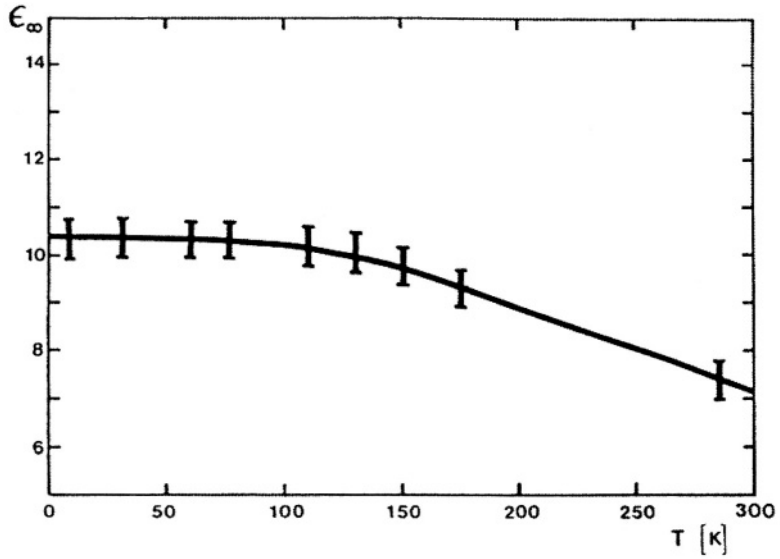

Fig. 17.10.3 Temperature dependence of the high-frequency dielectric constant ε_∞ for HgTe as determined from the far-infrared reflectivity spectra. [From M. Grynberg, R. Le Toullec, and M. Balkanski, *Phys. Rev. B* **9**, 517 (1974).]

• Reststrahlen parameter

Fundamental reflectivity spectra in the reststrahlen region of HgTe have been analyzed at T=8–300 K by M. Grynberg, R. Le Toullec, and M. Balkanski [*Phys. Rev. B* **9**, 517 (1974)] and at T=295 K by M. P. Volz, F. R. Szofran, S. L. Lehoczky, and C.-H. Su [*Solid State Commun.* **75,** 943 (1990)].

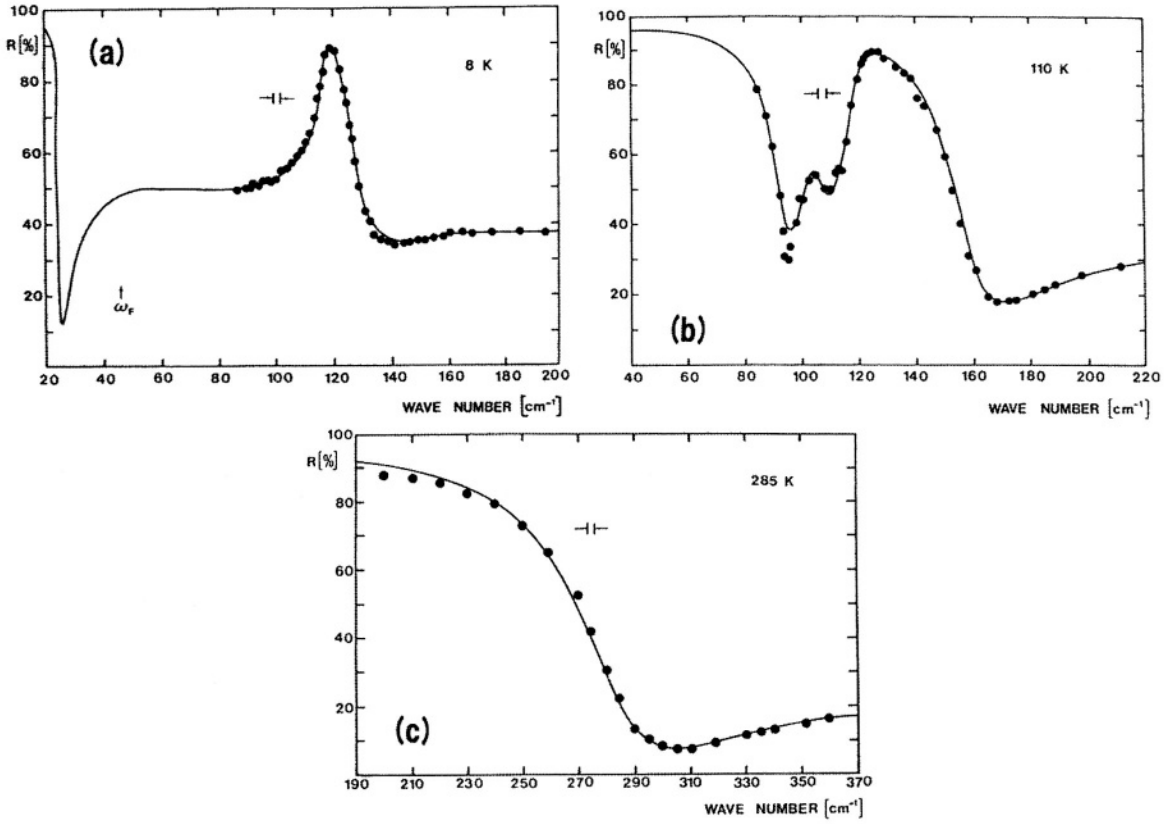

Fig. 17.10.4 Far-infrared reflectivity spectra of HgTe measured at (a) T=8 K, (b) 110 K, and (c) 285 K. The solid lines represent the theoretical dispersion curves. In (c), the position of the Fermi level is shown as ω_F. [From M. Grynberg, R. Le Toullec, and M. Balkanski, *Phys. Rev. B* **9**, 517 (1974).]

17.10.3 At or Near the Fundamental Absorption Edge

- **Refractive index**

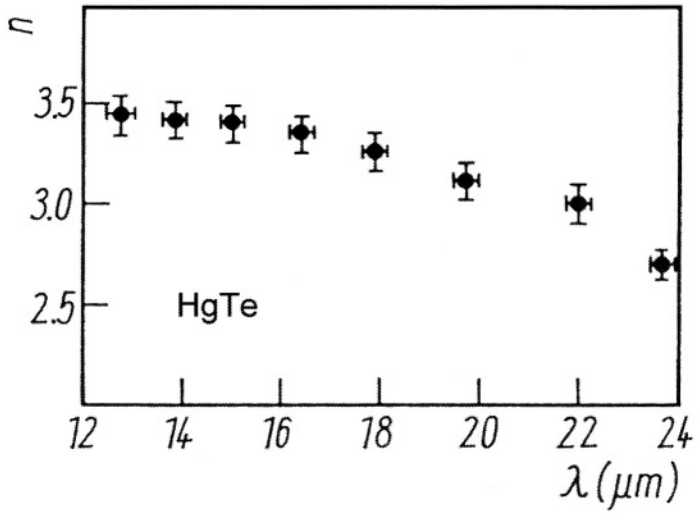

Fig. 17.10.5 Refractive index n for HgTe as a function of wavelength λ at T=295 K. [From W. Szszkiewicz, A. M. Witowski, and M. Grynberg, *Phys. Status Solidi B* **87**, 637 (1978).]

• **Fundamental absorption edge**

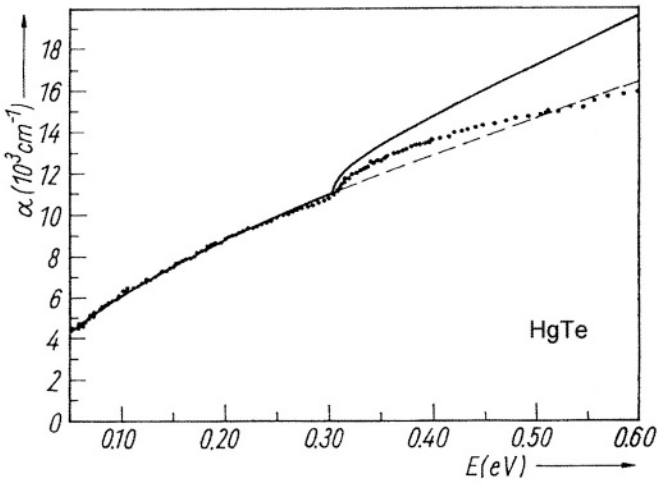

Fig. 17.10.6 Absorption coefficient α versus photon energy E for HgTe at 10 K. The dots represent the experimental points. The solid and dashed lines show the theoretical spectra using numerical parameter values, E_0=–0.3 eV, Δ_0=1.08 eV, P=8.0×10^{-8} eV·cm, etc. (*P*: momentum matrix element). [From W. Szuszkiewicz, *Phys. Status Solidi B* **79,** 691 (1977).]

17.10.4 The Interband Transition Region

• **Fundamental optical spectra**

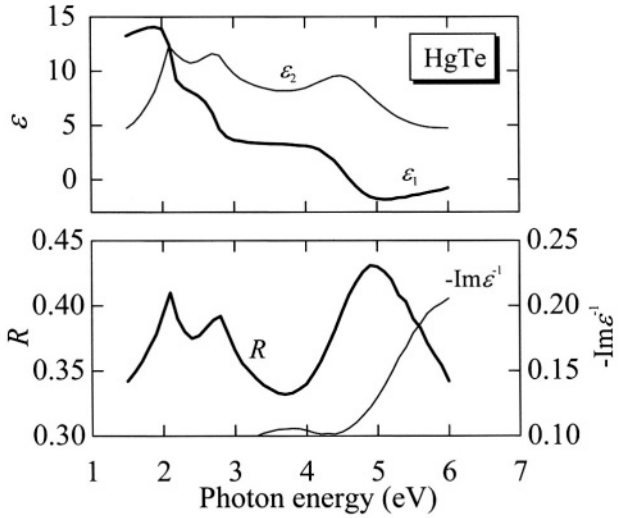

Fig. 17.10.7 Complex dielectric function $\varepsilon(E)=\varepsilon_2(E)+i\varepsilon_2(E)$ and energy-loss function $-\mathrm{Im}\varepsilon^{-1}(E)$ for HgTe at 300 K. The numerical data are taken from tabulation by S. Adachi [*Optical Constants of Crystalline and Amorphous Semiconductors: Numerical Data and Graphical Information* (Kluwer Academic, Boston, 1999)].

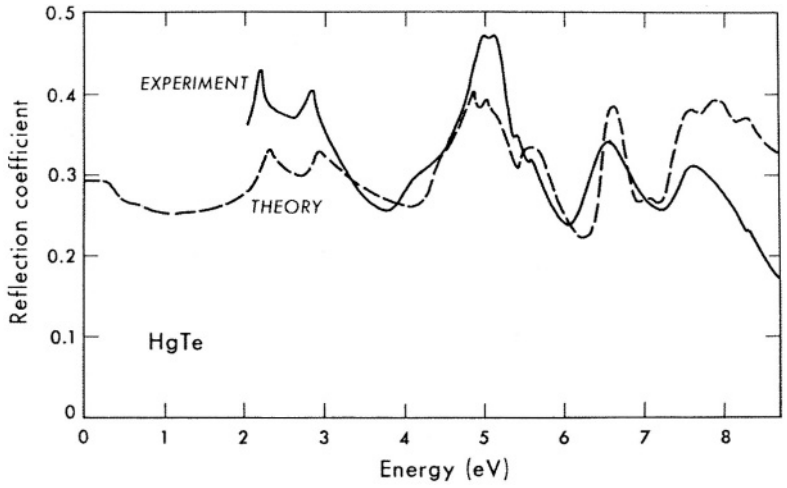

Fig. 17.10.8 Experimental and theoretical reflectivity spectra in the infrared region of HgTe. The experimental spectrum was obtained at 10 K. [From D. J. Chadi, J. P. Walter, M. L. Cohen, Y. Petroff, and M. Balkanski, *Phys. Rev. B* **5**, 3058 (1972).]

17.10.5 Free-Carrier Absorption and Related Phenomena

No detailed data are available for HgTe.

17.11 ELASTOOPTIC, ELECTROOPTIC, AND NONLINEAR OPTICAL PROPERTIES

17.11.1 Elastooptic Effect

No detailed data are available for HgTe.

17.11.2 Linear Electrooptic Constant

No detailed data are available for HgTe.

17.11.3 Quadratic Electrooptic Constant

No detailed data are available for HgTe.

17.11.4 Franz–Keldysh Effect

No detailed data are available for HgTe.

17.11.5 Nonlinear Optical Constant

No detailed data are available for HgTe.

17.12 CARRIER TRANSPORT PROPERTIES

17.12.1 Low-Field Mobility: Electrons

Table 17.12.1 *300-K (μ_{300K}) and peak Hall mobilities (μ_{peak}) for electrons in HgTe.*

Mobility	Value ($cm^2/V\,s$)	Comment
μ_{300K}	2.65×10^4	[12.1]
μ_{peak}	1.4×10^6	T=4.2 K [12.2]

[12.1] R. R. Galazka, *Phys. Lett.* **32A**, 101 (1970).
[12.2] M. V. Yakunin, *Sov. Phys. Semicond.* **22**, 918 (1988).

• **Temperature dependence**

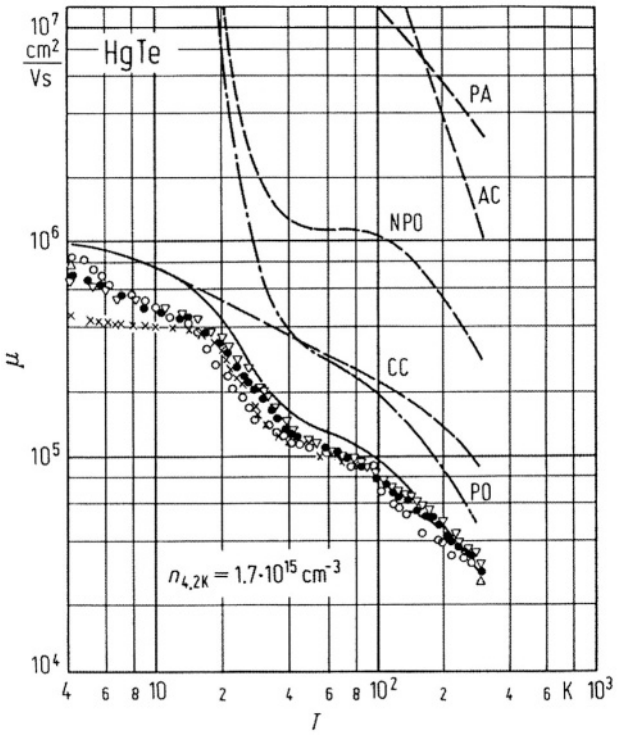

Fig. 17.12.1 Temperature variation of electron mobility μ for undoped HgTe. The dashed lines represent contributions from charged center (CC), polar optical (PO), nonpolar optical (NPO), acoustic (AC), and piezo-acoustic (PA) scattering modes. The combined Hall mobility is shown by the solid line. The experimental data are gathered from various sources. [From J. J. Dubowski, T. Dietl, W. Szymańska, and R. R. Gałazka, *J. Phys. Chem. Solids* **42**, 351 (1981).]

• **Pressure dependence**

Low-field transport properties in *n*-type HgTe have been studied for pressures up to 14 kbar in the temperature range 77–300 K by S. Otmezguine, F. Raymond, G. Weill, and C. Vérié [in *Proc. 10th Int. Conf. Phys. Semicond.,* Cambridge, USA (1970), p. 536] and for pressures up to 9 kbar in the temperature range 1.6–300 K at magnetic fields up to 14 kG by J. Stankiewicz and W. Giriat [*Phys. Rev. B* **13**, 665 (1976)].

• **Donor concentration (free-carrier) dependence**

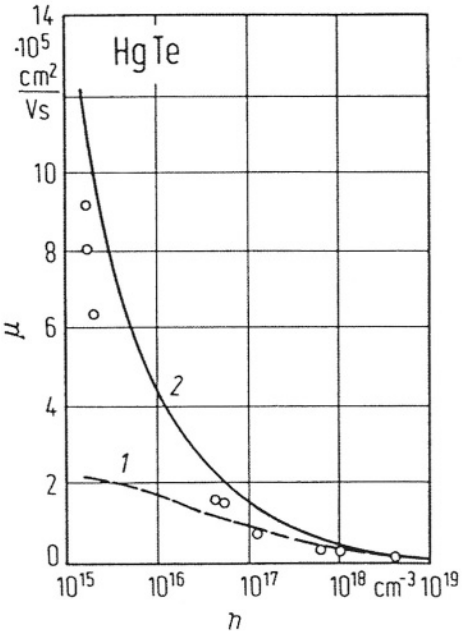

Fig. 17.12.2 Electron mobility μ versus electron concentration n in HgTe at T=4.2 K. The open circles denote the experimental data. Curves 1 and 2 are calculated without and with considereing the interband screening of the scattered centers, respectively. [From B. L. Gel'mont, V. I. Ivanov-Omskii, B. T. Kolomiets, V. K. Ogorodnikov, and K. P. Smekalova, *Sov. Phys. –Semicond.* **5,** 228 (1971).]

• **Hall factor**

The Hall factor for HgTe has been obtained theoretically by D. L. Rode [*Phys. Status Solidi B* **55**, 687 (1973)], and its value is reported to be $\gamma \sim 1.00$ at $T = 100$ K.

17.12.2 Low-Field Mobility: Holes

Table 17.12.2 *300-K (μ_{300K}) and peak Hall mobilities (μ_{peak}) for holes in HgTe.*

Mobility	Value (cm^2/V s)	Comment
μ_{300K}	320	[12.3]
μ_{peak}	4.5×10^4	T~10 K [12.4]

[12.3] P. Byszewski, E. Z. Dziuba, R. R. Gałązka, K. Szlenk, K. Szymborski, and W. Walukiewicz, *Phys. Status Solidi B* **71**, 117 (1975).
[12.4] Z. Dziuba and J. Wróbel, *Phys. Status Solidi B* **100,** 379 (1980).

• **Temperature dependence**

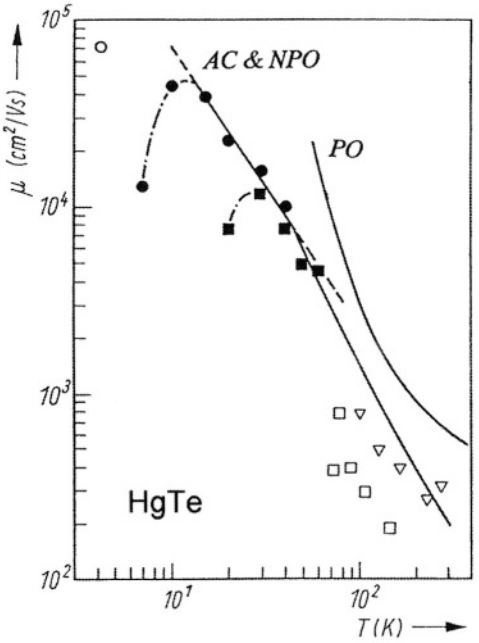

Fig. 17.12.3 Temperature variation of hole Hall mobility in HgTe. The theoretical lines denote contributions from acoustic (AC, dashed line), polar optical (PC), and acoustic and nonpolar optical (AC & NPO). The experimental data are taken from various sources. [From Z. Dziuba and J. Wróbel, *Phys. Status Solidi B* **100**, 379 (1980).]

17.12.3 High-Field Transport: Electrons

No detailed data are available for HgTe.

17.12.4 High-Field Transport: Holes

No detailed data are available for HgTe.

17.12.5 Minority-Carrier Transport: Electrons in *p*-Type Materials

No detailed data are available for HgTe.

17.12.6 Minority-Carrier Transport: Holes in *n*-Type Materials

No detailed data are available for HgTe.

17.12.7 Impact Ionization Coefficient

No detailed data are available for HgTe.